

SURAT - TUGAS

Nomor : 158/PL.01.11 /FTI-STD/I/2025

- Dasar :
- bahwa Fakultas Teknologi Industri Universitas Trisakti (FTI-Usakti) adalah lembaga yang mengemban tugas menyelenggarakan Tri Dharma Perguruan Tinggi yaitu Pendidikan, Penelitian dan Pengabdian kepada Masyarakat, dimana ketiganya menjadi poin penting dalam mewujudkan visi dari perguruan tinggi.
 - bahwa sesuai dengan Tri Dharma Perguruan Tinggi, tugas dosen selain tugas pokok sebagai pengajar juga harus melaksanakan kegiatan penelitian dan pengabdian kepada masyarakat, maka perlu dilaksanakan penelitian strategis bagi dosen tetap dalam lingkup FTI-Usakti
 - bahwa hasil penelitian perlu dipublikasikan agar semua proses dan hasilnya dapat dikenal oleh masyarakat luas, maka dipandang perlu menugaskan seluruh dosen tetap dalam lingkup FTI-Usakti untuk melaksanakan kegiatan tersebut.
 - bahwa agar pelaksanaan proses penelitian dan publikasi karya ilmiah dapat berjalan dengan baik dan memperoleh hasil yang maksimal, maka Dekan FTI-Usakti dengan ini :

MENUGASKAN

K e p a d a : Dosen Tetap Fakultas Teknologi Industri Universitas Trisakti

U n t u k : Melaksanakan kegiatan penelitian dan publikasi karya ilmiah pada jurnal nasional terakreditasi atau jurnal internasional bereputasi.

Periode : Tahun Akademik 2024/2025

Demikian surat tugas ini untuk dilaksanakan dengan sebaik-baiknya dan penuh tanggung jawab.

Jakarta, 9 Januari 2025

D e k a n,



Prof. Dr. Ir. Rianti Dewi Sulamet-Ariobimo, ST, M.Eng, IPM

Lecture Notes in Mechanical Engineering

Mohamad Rusydi Mohamad Yasin
Zulhelmi Ismail
Cucuk Nur Rosyidi
Mohammad Osman Tokhi *Editors*

Proceedings of the 7th Asia Pacific Conference on Manufacturing Systems and 6th International Manufacturing Engineering Conference— Volume 2

iMEC-APCOMS 2024, Melaka, Malaysia

Lecture Notes in Mechanical Engineering

Series Editors

Fakher Chaari, National School of Engineers, University of Sfax, Sfax, Tunisia

Francesco Gherardini^{iD}, Dipartimento di Ingegneria “Enzo Ferrari”, Università di Modena e Reggio Emilia, Modena, Italy

Vitalii Ivanov, Department of Manufacturing Engineering, Machines and Tools, Sumy State University, Sumy, Ukraine

Mohamed Haddar, National School of Engineers of Sfax (ENIS), Sfax, Tunisia

Editorial Board

Francisco Cavas-Martínez^{iD}, Departamento de Estructuras, Construcción y Expresión Gráfica Universidad Politécnica de Cartagena, Cartagena, Spain

Francesca di Mar^{iD}, Institute of Energy Technology, Ruhr-Universität Bochum, Bochum, Germany

Young W. Kwon, Department of Manufacturing Engineering and Aerospace Engineering, Graduate School of Engineering and Applied Science, Monterey, USA

Tullio A. M. Tolidi, Department of Mechanical Engineering, Politecnico di Milano, Milano, Italy

Justyna Trojanowska, Poznan University of Technology, Poznan, Poland

Robert Schmitt, RWTH Aachen University, Aachen, Germany

Jinyang Xu, School of Mechanical Engineering, Shanghai Jiao Tong University, Shanghai, China

Lecture Notes in Mechanical Engineering (LNME) publishes the latest developments in Mechanical Engineering—quickly, informally and with high quality. Original research or contributions reported in proceedings and post-proceedings represents the core of LNME. Volumes published in LNME embrace all aspects, subfields and new challenges of mechanical engineering.

To submit a proposal or request further information, please contact the Springer Editor of your location:

Europe, USA, Africa: Leontina Di Cecco Leontina.dicecco@springer.com

China: Ella Zhang ella.zhang@cn.springernature.com

India, Rest of Asia, Australia, New Zealand: Swati Meherishi swati.meherishi@springer.com

Topics in the series include:

- Engineering Design
- Machinery and Machine Elements
- Mechanical Structures and Stress Analysis
- Automotive Engineering
- Engine Technology
- Aerospace Technology and Astronautics
- Nanotechnology and Microengineering
- Control, Robotics, Mechatronics
- MEMS
- Theoretical and Applied Mechanics
- Dynamical Systems, Control
- Fluid Mechanics
- Engineering Thermodynamics, Heat and Mass Transfer
- Manufacturing Engineering and Smart Manufacturing
- Precision Engineering, Instrumentation, Measurement
- Materials Engineering
- Tribology and Surface Technology

Indexed by SCOPUS, EI Compendex, and INSPEC.

All books published in the series are evaluated by Web of Science for the Conference Proceedings Citation Index (CPCI).

To submit a proposal for a monograph, please check our Springer Tracts in Mechanical Engineering at <https://link.springer.com/bookseries/11693>.

Mohamad Rusydi Mohamad Yasin ·
Zulhelmi Ismail · Cucuk Nur Rosyidi ·
Mohammad Osman Tokhi
Editors

Proceedings of the 7th Asia Pacific Conference on Manufacturing Systems and 6th International Manufacturing Engineering Conference—Volume 2

iMEC-APCOMS 2024, Melaka, Malaysia

Editors

Mohamad Rusydi Mohamad Yasin
Faculty of Manufacturing and Mechatronic
Engineering Technology
Universiti Malaysia Pahang Al-Sultan
Abdullah
Pekan, Malaysia

Zulhelmi Ismail
Faculty of Manufacturing and Mechatronic
Engineering Technology
Universiti Malaysia Pahang Al-Sultan
Abdullah
Pekan, Malaysia

Cucuk Nur Rosyidi
Program Studi Teknik Industri
Universitas Sebelas Maret
Surakarta, Indonesia

Mohammad Osman Tokhi
Department of Electrical and Electronic
Engineering
London South Bank University
London, Middlesex, UK

ISSN 2195-4356

ISSN 2195-4364 (electronic)

Lecture Notes in Mechanical Engineering

ISBN 978-981-96-5689-9

ISBN 978-981-96-5690-5 (eBook)

<https://doi.org/10.1007/978-981-96-5690-5>

© The Editor(s) (if applicable) and The Author(s), under exclusive license to Springer Nature Singapore Pte Ltd. 2025

This work is subject to copyright. All rights are solely and exclusively licensed by the Publisher, whether the whole or part of the material is concerned, specifically the rights of translation, reprinting, reuse of illustrations, recitation, broadcasting, reproduction on microfilms or in any other physical way, and transmission or information storage and retrieval, electronic adaptation, computer software, or by similar or dissimilar methodology now known or hereafter developed.

The use of general descriptive names, registered names, trademarks, service marks, etc. in this publication does not imply, even in the absence of a specific statement, that such names are exempt from the relevant protective laws and regulations and therefore free for general use.

The publisher, the authors and the editors are safe to assume that the advice and information in this book are believed to be true and accurate at the date of publication. Neither the publisher nor the authors or the editors give a warranty, expressed or implied, with respect to the material contained herein or for any errors or omissions that may have been made. The publisher remains neutral with regard to jurisdictional claims in published maps and institutional affiliations.

This Springer imprint is published by the registered company Springer Nature Singapore Pte Ltd. The registered company address is: 152 Beach Road, #21-01/04 Gateway East, Singapore 189721, Singapore

If disposing of this product, please recycle the paper.

Preface

We are delighted to present the proceedings of the fourth edition of the 6th International Manufacturing Engineering Conference and the 7th Asia-Pacific Conference on Manufacturing System (iMEC-APCOMS 2024), hosted by Universiti Malaysia Pahang Al-Sultan Abdullah through its Faculty of Manufacturing and Mechatronic Engineering Technology. Held on September 11th and 12th, 2024, the conference embraced the theme of “Sustainable Development Goals through Innovative Manufacturing Engineering.”

iMEC-APCOMS 2024 has attracted a remarkable 99 submissions, all of which underwent a rigorous single-blind review process. Based on the recommendations of our dedicated reviewers, 41 papers were selected for publication in Volume 2 of the conference proceedings. We are immensely grateful to all contributing authors whose research has added great value to this collection. Each paper in this volume was thoughtfully evaluated by our esteemed technical review committee, comprised of leading experts in manufacturing engineering.

The conference served as a vibrant forum for the exchange of pioneering ideas and insights, highlighted by keynote presentations from distinguished speakers, including Prof. Ir. Dr. Nik Mohd Zuki Nik Mohamed (Universiti Malaysia Pahang Al-Sultan Abdullah, Malaysia), Prof. Dr. Cucuk Nur Rosyidi (Universitas Sebelas Maret, Indonesia), and Prof. Dr. Ir. Anas Ma'ruf (Institut Teknologi Bandung, Indonesia).

In closing, we hope that readers find this volume insightful and enriching. Our sincere appreciation goes to Springer Lecture Notes of Mechanical Engineering for their invaluable support in bringing this publication to life. Additionally, we extend our heartfelt thanks to the conference organizers and the dedicated members of the Conference Committee, whose tireless efforts made iMEC-APCOMS 2024 a resounding success.

Pekan, Malaysia
Pekan, Malaysia
Surakarta, Indonesia
London, UK

Mohamad Rusydi Mohamad Yasin
Zulhelmi Ismail
Cucuk Nur Rosyidi
Mohammad Osman Tokhi

Contents

Effect of Coolant Conditions on Machining Performance and Surface Quality in Ball End Milling of AISI 1040 Steel	1
Ahmad Saifuddin Azraie and Faiz Mohd Turan	
Enhancing Sustainability in Manufacturing Processes: A Comprehensive Study on Sustainability Index and Assessment Methods in a Malaysia Electronic Industry.....	11
Khairil Izhan Anuar and Amiril Sahab Abdul Sani	
Enhancing Agricultural Efficiency with GIS and TSP-Optimized Drone Pathways	25
Antonio Passaka Adi Wijaya, Rayinda Pramuditya Soesanto, and Fandi Achmad	
Experimental Investigation of the Effect and Optimization of FDM Process Parameters on Build Time and Compressive Strength of Printed Bone Screws Using Taguchi Method.....	35
Sugoro Bhakti Sutono, Cucuk Nur Rosyidi, Pringgo Widyo Laksono, and Eko Pujiyanto	
Microporous of Magnesium/Hydroxyapatite Coatings on Oxidized High Carbon Co–Cr–Mo Medium-Entropy Alloy for Biocompatibility Improvement.....	47
M. N. Amir Akmal, H. Mas Ayu, Rosdi Daud, Juliawati Alias, and M. S. Dambatta	
Influence of Different Materials on Inductance Values of Vitroperm 500 at High Temperature Annealing	57
Murshidi Mdzuki, H. Mas Ayu, S. Mohd Mawardi, and Rosdi Daud	
Investigating the Impact of Lean Practices and Industry 4.0 Technologies Towards Operational Performance.....	65
Sharah Qistina Shari Fuzzaman, Noraini Mohd Razali, and Kartina Johan	

Recycling Methods for Effective Circular Economy: Bibliometric Analysis and Research Trends.....	75
Iwan Roswandi, Eko Pujiyanto, Cucuk Nur Rosyidi, and Wakhid Ahmad Jauhari	
Review of the Design and Concept of the Double Pipe Heat Exchanger	85
R. N. Syafiq, Mohd Fadzil Ali Ahmad, Deevikthiran Jeevaraj, and Ibnu Kasir Ahmad Nadzri	
Enhancing Benchmark Optimization with Evolutionary Random Approach: A Comparative Analysis of Modified Adaptive Bats Sonar Algorithm (MABSA)	95
Nor Shuhada Ibrahim, Nafrizuan Mat Yahya, Saiful Bahri Mohamed, and Mohd Ismail Yusof	
Leveraging Explainable AI for Accurate Production Forecasting in the Bag Manufacturing Industry.....	105
Rayinda Pramuditya Soesanto and Fandi Achmad	
Tool Condition Monitoring in Milling Machining Process via IOT Communications	115
Mohd Azfar Afiq Azhar, Ismayuzri Ishak, and Ahmad Razlan Yusoff	
Classification of <i>Capsicum Annum</i> L. Var. Kulai Through Object Detection Using Deep Learning Models.....	123
Nur Aliya Syahirah Badrol Hisam, Yin Jun Chan, Amir FakarullIsroq Abdul Razak, Muhammad Nur Aiman Shapiee, Mohd Izzat Mohd Rahman, and Mohd Azraai Mohd Razman	
Multi-objective Optimization Modeling in 3D Printing Process of PLA+ Using Response Surface Methodology and NSGA.II	135
Saufik Luthfianto, Eko Pujiyanto, Cucuk Nur Rosyidi, and Pringgo Widyo Laksono	
Predicting Sustainability in SMEs Through Knowledge Factors Using Decision Tree Analysis.....	149
Amelia Kurniawati, Artamevia Salsabila Rizaldi, and Mia Amelia	
The Improvement of Procurement Process for Promotional Goods Using Value Stream Mapping and Multi-Criteria Decision Making..	159
Sekar Zaneta Amirul Putri, Wakhid Ahmad Jauhari, and Cucuk Nur Rosyidi	
The Compressive Strength and Failure Behaviours of the Alporas Foam—Effect of Different Geometric Sizes	171
A. N. Md Idriss, S. Kasolang, M. A. Maleque, and M. A. Mohd Azhari	

Autonomous Mobile Robot for Obstacle Avoidance with Vision System	181
Yoganraj Ravi, Mohd Rais Hakim Bin Ramlee, and Ismail Mohd Khairuddin	
Knowledge Management for Developing Disability-Friendly Criteria in SME.....	191
Luciana Andrawina, Mia Amelia, and Artamevia Salsabila Rizaldi	
Solving Sustainable Supplier Selection Problems Based on FAHP and FTOPSIS for Textile Industry	203
Feri Ancen Pakpahan, Mohammad Mi'radj Isnaini, Abdul Hakim Halim, and Shih-Che Lo	
Vendor Managed Inventory Model Considering Degree of Component Commonality and Quality Inspection Policies	215
Yosi Agustina Hidayat and Nadin Fadilla	
A Hybrid Multi-Criteria Decision-Making Model for Evaluating Energy Efficiency Practices in Indonesia's Textile Industry.....	227
Mulia Hendra, Muhammad Akbar, Shi-Woei Lin, and Dradjad Irianto	
Barrier Model Development for Industry 4.0 Technologies Adoption in Small-to-Medium Food and Beverage Industry in Indonesia.....	239
Arif Nurrahman, Nur Faizatus Sa'idah, Hui-Chih Hung, and Iwan Inrawan Wiratmadja	
Study of Sintering Effects on Grain Size of Al-Doped/Graphene Nanoparticles via Microwave-Assisted Sol-Gel Method....	249
Karthikraj A. L. Nithyanantham, Suraya Sulaiman, Wan Fahmin Faiz Wan Ali, Izman Sudin, and Ramli Junid	
The Classification of Tennis Strokes Through Machine Learning....	259
Pavithran Selvaraju, Risshidaran Nair Kumar, and Muhammad Amirul Abdullah	
A Systematic Mapping Study of Sustainability Assessment in the Mining Industry: A Perspective of Manufacturing Performance	269
Elfritia Wiratmani, Dadan Umar Daihani, Emelia Sari, Rahmi Maulidya, and Mohd Yazid Abu	
Experimental Study of Parameters Effects on Dimensional Accuracy and Surface Integrity of the HDPE Substrate Using the Hot Embossing Process	281
Muhammad Syahrir, Ahmad Rosli Bin Abdul Manaf, Wan Hamdi, and Khair Khalil	

Sustainable Value Stream Mapping Application in the Furnace Process at a Large Nickle Company.....	293
Cristin Angel, Cucuk Nur Rosyidi, and Wakhid Ahmad Jauhari	
Green Strategy Implementation and Innovativeness in SMEs: A Pathway Towards Sustainable Development Goals.....	305
Iwan Inrawan Wiratmadja, Fandi Achmad, and Afrin Fauzya Rizana	
Development Model of Organizational Learning, Innovation and Performance: A Case Study on Disabled MSMEs in Bandung .	315
Hanifah Widyarani Sinatrya, Luciana Andrawina, and Sri Martini	
Health Diagnostics for Lithium-Ion Batteries Using Convolutional Neural Network Model	327
Ikhsan Romli, Mohammad Mi'radj Isnaini, Rachmawati Wangsaputra, and Bermawi Priyatna Iskandar	
Design and Fabrication of a New Replaceable Nozzle for Abrasive Water Jet Application.....	339
Nuraini Lusi, Mebrahitom Gebremariam, Abdur-Rasheed Alao, Kushendarsyah Saptaji, and Azmir Azhari	
Measurement of Operational Risk Management Using the AS/NZS ISO 31000:2009 in the Outsourcing Start-Up Company.....	351
Tiena Gustina Amran, Annisa Dewi Akbari, Ellyana Amran, Adinda Aniza, Emelia Sari, and Mohd Yazid Abu	
The Reliability and Effectiveness of Sensors in IoT-Enabled Solar Drying System	377
Thevanesveeran Aso Kumar, Nur Najmiyah Jaafar, Sarah 'Atifah Saruchi, Nafrizuan Mat Yahya, and Suraya Sulaiman	
Thermodynamic Analysis of Microstructural Evolution in Aluminum Alloys.....	389
Mohamad Rusydi Mohamad Yasin and Dongke Liu	
Studies on pH Effects on ZnO Nanoparticles via Microwave-Assisted Sol-Gel Method.....	399
Suraya Sulaiman, Wan Fahmin Faiz Wan Ali, Izman Sudin, Muhammad Firdaus Omar, and Nadhrah Md. Yatim	
Real Time Simulation of Optimal Control-Based Flow Control for Continuous Production System	411
Rachmawati Wangsaputra and Fariz Muharram Hasby	
Solving the Capacitated Vehicle Routing Problem (CVRP) with the Simulated Annealing Method: A Case Study.....	423
Parwadi Moengin, Elvania Rivanda Dantjie, and Fani Puspitasari	

Designing the Flexible Jig and Fixture to Reduce the Production Time of the Excavator Buckets.....	433
Rahmi Maulidya, Nora Azmi, Soni Iskandar, and Docki Saraswati	
Tensile Properties and Characterization of Tamarind Powder Reinforced Epoxy-Jute Fiber Hybrid Polymer Composites.....	443
Dewan Muhammad Nuruzzaman, Noor Mazni Ismail, A. K. M. Parvez Iqbal, Nayem Hossain, A. K. M. Asif Iqbal, and Md. Jobaed Hossen	
Microstructure and Hardness Distribution of Seven-Layered Al-Al₂O₃ Graded Composite Material Prepared Through Pressureless Sintering.....	455
Maziyana Marzuki, Noor Mazni Ismail, and Dewan Muhammad Nuruzzaman	

Effect of Coolant Conditions on Machining Performance and Surface Quality in Ball End Milling of AISI 1040 Steel



Ahmad Saifuddin Azraie and Faiz Mohd Turan 

Abstract The role of cutting fluids in machining operations is crucial, impacting productivity, tool lifespan, and work quality. An experimental investigation was conducted on ball end milling of AISI 1040 steel using uncoated HSS tools under various coolant conditions and milling modes. The study encompassed four coolant conditions: dry, mist, 4% coolant concentration, and 8% coolant concentration, with constant cutting parameters. Machining performance was assessed based on tool wear and surface roughness. Results indicate a significant influence of coolant conditions on machining performance and surface quality. Mist coolant in down milling mode exhibited superior performance in terms of tool wear and average surface roughness (0.09 mm and 0.462 μm , respectively). Following closely was mist coolant in up milling mode, then 8% coolant concentration, and lastly 4% coolant concentration under up milling mode. This research sheds light on the importance of coolant selection and milling mode in optimizing machining outcomes.

Keywords Machining performance · Cutting fluids · Surface quality

1 Introduction

Milling involves feeding a workpiece past a rotating tool with multiple cutting edges. The tool, known as a milling cutter, has teeth along its edges. Plain-carbon steel, an alloy of iron and carbon with additional elements like manganese and silicon, varies in properties based on its carbon content. Cutting fluids, which cool and lubricate tools during machining, come in various forms like oils and emulsions [1–3]. High

A. S. Azraie · F. Mohd Turan (✉)

Faculty of Manufacturing and Mechatronic Engineering Technology, Universiti Malaysia Pahang
Al-Sultan Abdullah, 26600 Pekan, Pahang, Malaysia
e-mail: faizmt@ump.edu.my

A. S. Azraie

Institut Kemahiran Tinggi Belia Negara Temerloh, 28500 Lanchang, Pahang, Malaysia

© The Author(s), under exclusive license to Springer Nature Singapore Pte Ltd. 2025
M. R. Mohamad Yasin et al. (eds.), *Proceedings of the 7th Asia Pacific Conference on Manufacturing Systems and 6th International Manufacturing Engineering Conference—Volume 2*, Lecture Notes in Mechanical Engineering,
https://doi.org/10.1007/978-981-96-5690-5_1

Speed Steel (HSS) cutting tools, containing carbon, chromium, and other elements, maintain hardness up to 600 °C, making them suitable for machining mild steel. This study explores different cooling conditions' impact on tool wear and surface finish during ball milling of AISI 1040 steel using HSS ball mills, considering various milling modes and coolant options [4, 5].

Recent studies related to the scope of this research may include research exploring novel cutting fluid formulations aimed at enhancing machining performance and environmental sustainability [6–8]. Studies focusing on advanced machining techniques, such as high-speed machining or cryogenic machining, and their interactions with cutting fluids could also be relevant [9, 10]. Additionally, investigations into the influence of cutting parameters, such as cutting speed, feed rate, and depth of cut, on the effectiveness of different coolant conditions may provide insights into optimizing machining processes further [11, 12]. Furthermore, studies examining the use of alternative coolant delivery methods, such as minimum quantity lubrication (MQL) or near-dry machining, and their effects on tool wear and surface quality could contribute valuable findings to this area of research [13, 14].

Another significant aspect lies in its potential to contribute to the development of more sustainable machining practices [14]. By assessing the impact of various coolant conditions on machining performance and surface quality, insights are offered into optimising coolant selection and usage to minimise environmental impact while maintaining productivity [15–17]. This can inform the machining industry about the importance of considering environmental factors in coolant selection and encourage the adoption of more eco-friendly machining practices [18, 19]. Furthermore, by identifying coolant conditions that offer superior performance in terms of tool wear and surface roughness, material waste and energy consumption associated with machining processes can be reduced, thereby promoting sustainability in manufacturing operations [20]. Additionally, investigating the interactions between advanced machining techniques and cutting fluids can uncover opportunities for further reducing environmental footprint while improving machining efficiency [21, 22].

The study aims to assess how different cooling conditions affect the machining performance of an uncoated HSS tool during ball milling of AISI 1040 steel. The project focuses on specific areas: utilising AISI 1040 steel as the workpiece, employing an 8 mm diameter 2-flute HSS uncoated ball end mill as the cutting tool, and utilising a HASS VF 1D CNC machine for experimentation. Various coolant conditions will be examined, including dry cutting, mist coolant, and coolant concentrations of 4 and 8%. Cutting speed, feed, and depth of cut will remain constant throughout the experiments. The investigation stems from concerns about excessive coolant usage impacting operator health and the environment. Furthermore, the study aims to explore the effects of different cooling conditions and milling modes on tool wear, with surface roughness serving as an additional criterion for coolant performance evaluation.

Table 1 Composition of HSS ball end mill

Carbon, C	1.1%
Chromium, Cr	4%
W	1.5%
Molybdenum, Mo	9.5%
Vanadium, V	1%
Cobalt, Co	8%

Table 2 Mechanical properties of HSS ball end mill

Diameter, d	8 mm
Diameter, d1	10 mm
No of flute	2
Milling mode	Up and down milling
Overall length, l1	88 mm
Cutting length, l2	19 mm
Hardness	66–68.5 HRC
Product code	3,350,800

2 Methodology

2.1 Cutting Tools

For this study, a Somta Ball End Mill, identified by code 335, made of uncoated High-Speed Steel (HSS) with M42 grade, was utilised. Details regarding the composition and mechanical properties of this tool are provided in Tables 1 and 2, respectively.

2.2 Workpiece Materials

The workpiece comprises medium carbon steel (AISI 1040), measuring 160 mm × 50 mm × 10 mm. Details regarding the chemical composition and mechanical properties of the workpiece are provided in Tables 3 and 4, respectively.

Table 3 Nominal chemical composition (%) of AISI 1040 steel

Carbon (C)	Mangan (Mn)	Sulfur (S)	Phosphorus (P)
0.37–0.44	0.60–0.90	0.05 (max)	0.04 (max)

Table 4 Physical and mechanical properties of work material AISI 1040

Properties		Conditions	
		T (°C)	Treatment
Density ($\times 1000 \text{ kg/m}^3$)	7.845	25	
Poisson's ratio	0.27–0.30		
Elastic modulus (GPa)	190–210	25	
Tensile strength (Mpa)	518.8	25	Annealed at 790°C
Yield strength (Mpa)	353.4		
Elongation (%)	30.2		
Reduction in area (%)	57.2		
Hardness (HB)	149	25	Annealed at 790°C
Impact strength (J) (<i>Izod</i>)	44.3	25	Annealed at 790°C

2.3 Measurement and Observation

Coolant concentration and surface roughness were assessed using specific equipment. Surface roughness was measured using the Mahr Perthometer M2, with calibration performed before each measurement. The Mahr Perthometer M2 specifications include a cut-off length of 2.5 mm and a sample length of 25 mm. Coolant concentration was determined using a hand refractometer model ATAGO Master—T. Tool wear was observed under the Zeiss Video Microscope at 50 \times magnification, with specifications including a magnification range from 6.5 \times to 50 \times and a voltage of 240 V. These measurements and observations were essential for evaluating machining performance and surface quality.

2.4 Machining Conditions

In this study, an uncoated HSS Somta End Mill Ball Nose 2 Flute was employed across four distinct coolant conditions, maintaining consistent cutting speed, feed rate, and axial depth of cut. Up milling mode was selected for profile cutting with dimensions of 32 mm \times 32 mm using the Haas CNC Machine. Each coolant condition underwent machining for a total of five cutting profiles, resulting in a cumulative cutting length of 5424 mm. Detailed cutting parameters for the experiment can be found in Table 5.

Table 5 The cutting conditions

	Cutting parameters	HSS uncoated carbide tool
1	Cutting speed, V_c (mm/min)	52
2	Spindle speed, N (rpm)	856
3	Axial depth of cut, a_p (mm)	0.8
4	Step over (mm)	1
5	Coolant condition	Mist, Dry, CC 4%, CC 8%

3 Experimental Results

3.1 Surface Roughness

Surface roughness (R_a) values were measured for each coolant condition after cutting at specified intervals. These R_a values are then graphically represented in Fig. 1 to observe the trend for each coolant condition. From the graph, comparisons between coolant conditions can be made. The surface roughness profile for various coolant conditions during up milling operation is displayed in Fig. 1, showing a similar trend among all conditions. A slight increase in surface roughness was observed towards the end of cutting compared to the initial cutting phase.

The overall results presented in Table 6 indicate that mist coolant resulted in the lowest surface roughness values, with a minimum of $0.265\text{ }\mu\text{m}$, an average of $0.462\text{ }\mu\text{m}$, and a maximum of $0.689\text{ }\mu\text{m}$. Following closely was the 8% coolant concentration, which exhibited a minimum surface roughness of $0.502\text{ }\mu\text{m}$. The 4% coolant concentration came next with a minimum value of $0.928\text{ }\mu\text{m}$, while dry cutting performed the worst, yielding a minimum surface roughness of $1.279\text{ }\mu\text{m}$.

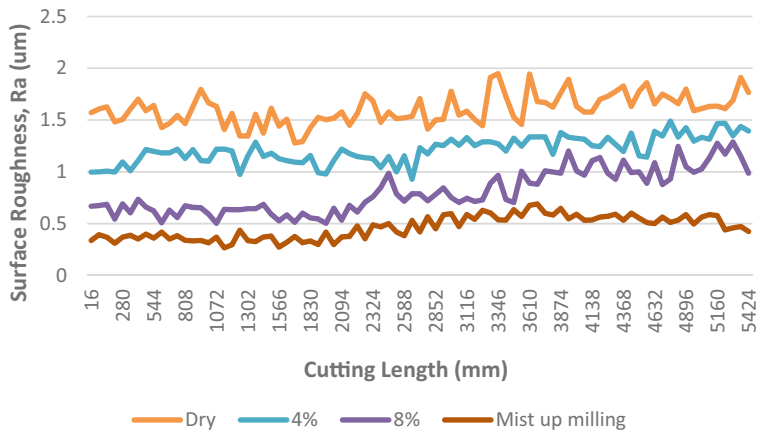


Fig. 1 Surface roughness curve against of cut length for various coolant conditions in up milling mode

Mist coolant showed superior performance, as noted by previous studies. Dry cutting resulted in the highest surface roughness due to increased heat generation and tool wear, with observed sparks during experimentation indicating high friction. The temperature rise during dry cutting affects part accuracy and can cause expansion. Additionally, high coolant concentration led to lower surface roughness by reducing friction and tool wear, enhancing machining quality.

In the majority of cases, there was a slight increase in the surface roughness value observed after 30 min of cutting (Fig. 2), likely attributable to the expansion of the wear land on the cutting edge.

Table 6 and Figure 3 present the average surface roughness values for various coolant conditions under up milling mode. The results demonstrate a linear increase in average surface roughness values across different coolant conditions, starting with mist coolant, followed by 8% coolant concentration, 4% coolant concentration, and dry cutting. The smoother surface obtained from mist coolant is visibly apparent, contrasting with the rougher surface resulting from dry cutting. Mist coolant penetrates the cutting zone, providing cooling, lubrication, and chip removal. Overall, the surface roughness values range from 0.42 to 1.76 μm , significantly better than the typical range of 0.8–6.3 μm observed in average milling applications.

Table 6 Surface roughness value at cutting length 5424 mm under various coolant condition with up milling mode

Surface roughness, Ra (μm)	Dry cutting	4% cc	8% cc	Mist
Average value	1.607	1.213	0.804	0.462
Max value	1.947	1.490	1.289	0.689
Minimum value	1.279	0.928	0.502	0.265

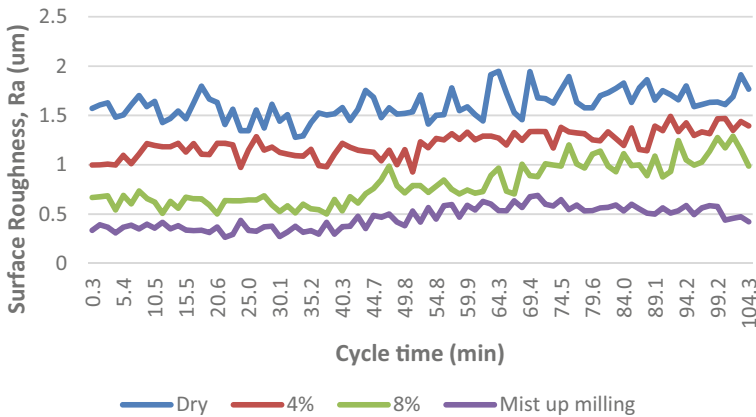


Fig. 2 Surface roughness curve against cutting time for various cooling condition—up milling

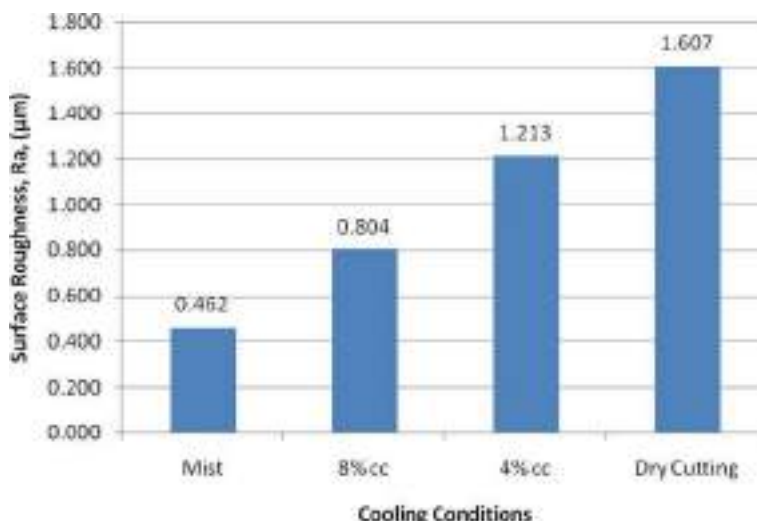


Fig. 3 Average surface roughness at various coolant conditions at cutting length of 5424 mm—up milling

3.2 Comparison of Up Milling and Down Milling Modes

A comparison study was conducted to analyse the performance of mist coolant condition in both up milling and down milling modes during ball end milling of AISI steel using uncoated HSS tools. Figure 4 illustrates the surface roughness profile between the two milling modes under mist coolant condition. Results indicate that down milling demonstrates superior surface roughness compared to up milling mode. This finding aligns with previous research on surface finish visualization in high-speed ball nose milling applications. Down milling, known to extend cutter life by up to 50%, proves effective across various milling applications. The cutter teeth in down milling prevent chips from being carried into the workpiece, reducing the risk of surface damage. Furthermore, chips are directed behind the cutter, facilitating easier chip removal and resulting in improved surface finish.

3.3 Tool Wear

Apart from assessing surface roughness, an evaluation of the effectiveness of different coolant conditions was conducted by examining the tool wear progression. Flank wear (V_b) of the cutting edge was measured using an optical microscope, at the conclusion of the experiment for each condition. The flank wear data for all coolant conditions are presented in Table 7.

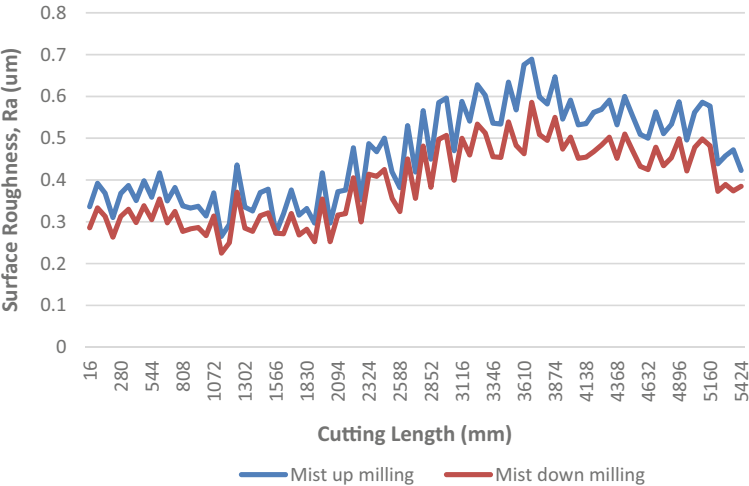


Fig. 4 Surface roughness between up milling (um) and down milling (dm) under mist coolant condition

Table 7 Flank wear at cutting length 5424 mm or 106 min of cutting time-up milling

Condition	Flank wear (mm)					
	Cutting edge 1		Cutting edge 2		Average wear	
	Vb ave 1	Vb max 1	Vb ave 2	Vb max 2	Vb ave	Vb max
Mist	0.08	0.08	0.09	0.09	0.085	0.085
8% cc	0.1	0.14	0.11	0.17	0.105	0.155
4% cc	0.11	0.19	0.15	0.2	0.13	0.195
Dry	0.31	0.56	0.21	0.37	0.26	0.465

Results indicated that, except for dry cutting, the flank wear values were well below the standard tool life criteria of $Vb\ ave < 0.3\ mm$ and $Vb\ max < 0.5\ mm$, which is typical for tool wear and does not significantly impair tool functionality until it reaches levels causing cutting edge failure. The tool used in dry cutting failed after machining 5424 mm for 106 min, while mist coolant showed the lowest tool wear compared to other conditions. This aligns with findings by López de Lacalle et al. [23] and Kishawy et al. [24], highlighting mist coolant’s effective penetration into the cutting zone and its lubrication properties, which reduce cutting temperatures and enhance chip-tool interaction, thus maintaining cutting edge sharpness. Therefore, mist coolant is recommended for ball milling AISI 1040 steel using uncoated HSS tools, particularly when surface roughness and tool wear are primary concerns. Furthermore, beyond enhancing machining performance in terms of tool life and surface finish, mist coolant also offers environmental, health, and economic benefits to the machining industry.

4 Conclusion

In conclusion, this research successfully achieved its objective of evaluating the impact of coolant conditions on machining performance, focusing on surface roughness and tool wear in ball milling AISI 1040 steel with uncoated HSS tools. The study revealed several key findings:

- i. Coolant condition significantly affects both surface roughness and tool wear, with mist coolant showing the best performance in up milling, followed by 8% coolant concentration, 4% coolant concentration, and dry conditions.
- ii. Mist coolant consistently outperformed other conditions in terms of surface finish and tool wear.
- iii. Down milling with mist coolant produced the lowest surface roughness value at 0.246 μm .

As a recommendation, further investigations could explore down milling operations with different cutting tools and evaluate the performance of various lubricants such as palm oil or seed oil.

Acknowledgements This research was funded by a grant from Universiti Malaysia Pahang Al-Sultan Abdullah (RDU233016).

References

1. Kim D-H, Lee C-M (2021) Experimental investigation on machinability of titanium alloy by laser-assisted end milling. *Metals* (Basel) 11:1552. <https://doi.org/10.3390/met11101552>
2. Chen Z, Yue C, Liu X et al (2021) Surface topography prediction model in milling of thin-walled parts considering machining deformation. *Materials* 14:7679. <https://doi.org/10.3390/ma14247679>
3. Wu Y, Chen N, Bian R et al (2020) Investigations on burr formation mechanisms in micro milling of high-aspect-ratio titanium alloy ti-6al-4 v structures. *Int J Mech Sci* 185:105884. <https://doi.org/10.1016/j.ijmecsci.2020.105884>
4. Nayak M, Sehgal R, Kumar R (2021) Investigating machinability of AISI D6 tool steel using CBN tools during hard turning. *Mater Today Proc* 47:3960–3965. <https://doi.org/10.1016/j.matpr.2021.04.020>
5. Wang Z, Li H, Yu T (2022) Study on surface integrity and surface roughness model of titanium alloy TC21 milling considering tool vibration. *Appl Sci* 12:4041. <https://doi.org/10.3390/app12084041>
6. Mohd Turan F, Johan K (2016) Assessing sustainability framework of automotive related industry in the Malaysia context based on GPM P5 standard. *ARPN J Eng Appl Sci* 11:7606–7611
7. Mohd Turan F, Johan K, Nor NHM (2016) Criteria assessment model for sustainable product development. *IOP Conf Ser: Mater Sci Eng* 160:0124. <https://doi.org/10.1088/1757-899X/160/1/012004>
8. Selamat SN, Nor NHM, Rashid MHA et al (2017) Review of CO₂ reduction technologies using mineral carbonation of iron and steel making slag in Malaysia. *J Phys: Conf Ser* 914:012012. <https://doi.org/10.1088/1742-6596/914/1/012012>

9. Çakır Şencan A, Şirin Ş, Selayet Saraç EN et al (2024) Evaluation of machining characteristics of SiO₂ doped vegetable based nanofluids with Taguchi approach in turning of AISI 304 steel. *Tribol Int* 191:109122. <https://doi.org/10.1016/j.triboint.2023.109122>
10. Hegab H, Damir A, Attia H (2021) Sustainable machining of Ti-6Al-4V using cryogenic cooling: an optimized approach. *Proc CIRP* 101:346–349. <https://doi.org/10.1016/j.procir.2021.02.036>
11. Zha X, Qin H, Yuan Z et al (2024) Effect of cutting feed rate on machining performance and surface integrity in cutting process of Ti-6Al-4V alloy. *Int J Adv Manuf Technol* 131:2791–2809. <https://doi.org/10.1007/s00170-023-12458-y>
12. Altaf SF, Parray MA, Khan MJ et al (2024) Machining with minimum quantity lubrication and nano-fluid MQL: a review. *Tribol Online* 19:209–217. <https://doi.org/10.2474/trol.19.209>
13. Niu Q, Rong J, Jing L et al (2023) Study on force-thermal characteristics and cutting performance of titanium alloy milled by ultrasonic vibration and minimum quantity lubrication. *J Manuf Process* 95:115–130. <https://doi.org/10.1016/j.jmapro.2023.04.002>
14. Mohd Said J, Mohd Turan F (2022) Optimising MIG weld bead geometry of hot rolled carbon steel using response surface method. In *Enabling industry 4.0 through advances in manufacturing and materials: selected articles from iM3F 2021, Malaysia*, pp 179–188. https://doi.org/10.1007/978-981-19-2890-1_18
15. Aikhuele DO, Turan FM (2016) A hybrid fuzzy model for lean product development performance measurement. *IOP Conf Ser: Mater Sci Eng* 114:012048. <https://doi.org/10.1088/1757-899X/114/1/012048>
16. Aikhuele DO, Turan FM (2016) Proposal for a conceptual model for evaluating lean product development performance: a study of LPD enablers in manufacturing companies. *IOP Conf Ser: Mater Sci Eng* 114:012047. <https://doi.org/10.1088/1757-899X/114/1/012047>
17. Sahimi NS, Turan FM, Johan K (2017) Development of sustainability assessment framework in hydropower sector. *IOP Conf Ser: Mater Sci Eng* 226:012048. <https://doi.org/10.1088/1757-899X/226/1/012048>
18. Magar SR, Singh G, Goyal KK (2023) A review on minimum quantity lubrication for sustainable machining of titanium alloy. *Mater Today Proc* 80:258–263. <https://doi.org/10.1016/j.matpr.2023.01.096>
19. Sahimi NS, Turan FM, Johan K (2018) Framework of sustainability assessment (FSA) method for manufacturing industry in Malaysia. *IOP Conf Ser: Mater Sci Eng* 342:012079. <https://doi.org/10.1088/1757-899X/342/1/012079>
20. Ghatge D, Ramanujam R (2023) Sustainable machining: a review. *Mater Today Proc* <https://doi.org/10.1016/j.matpr.2023.08.275>
21. Bag R, Panda A, Kumar Sahoo A (2022) A concise review on environmental sustainable machining conditions of hard part materials. *Mater Today Proc* 62:3724–3728. <https://doi.org/10.1016/j.matpr.2022.04.433>
22. Said JM, Turan FM, Sazali N (2023) Integrated assessment of MIG welding parameters on carbon steel using RSM optimisation. *J Adv Res Appl Mech* 111:16–29. <https://doi.org/10.37934/aram.111.1.1629>
23. López de Lacalle LN, Angulo C, Lamikiz A, Sánchez JA (2006) Experimental and numerical investigation of the effect of spray cutting fluids in high speed milling. *J Mater Process Technol* 172:11–15. <https://doi.org/10.1016/j.jmatprotec.2005.08.014>
24. Kishawy HA, Dumitrescu M, Ng E-G, Elbestawi MA (2005) Effect of coolant strategy on tool performance, chip morphology and surface quality during high-speed machining of A356 aluminum alloy. *Int J Mach Tools Manuf* 45:219–227. <https://doi.org/10.1016/j.ijmachtools.2004.07.003>

Enhancing Sustainability in Manufacturing Processes: A Comprehensive Study on Sustainability Index and Assessment Methods in a Malaysia Electronic Industry



Khairil Izhan Anuar and Amiril Sahab Abdul Sani

Abstract This paper addresses the challenges in balancing environmental, economic, and societal concerns in Malaysia's electronic industry by proposing an integrated sustainability assessment method. The method combines quantitative and qualitative indicators, weighted for relevance to the industry, to create a unit-less sustainability index. Using real data from Malaysian electronic manufacturing companies, the index highlights strengths and weaknesses in sustainability performance across environmental, economic, and societal dimensions. The findings reveal opportunities for improvement, such as reducing emissions, mitigating wastewater pollution, and enhancing working conditions, providing actionable insights for decision-makers to drive sustainable practices.

Keywords Sustainability index · Manufacturing process · Energy efficiency

1 Introduction

Sustainable manufacturing is vital for addressing Malaysia's electronic industry's environmental and socio-economic challenges, which struggles with high energy use, resource depletion, and waste. Historically, sustainability assessments in this sector have focused mainly on environmental and economic factors, often neglecting social dimensions. Previous sustainability indices for industries like automotive and textile have primarily addressed environmental and economic aspects without fully integrating social factors [1]. Our proposed method addresses this gap by using a Triple Bottom Line (TBL) approach to incorporate environmental, financial, and

K. I. Anuar · A. S. Abdul Sani (✉)

Faculty of Manufacturing and Mechatronic Engineering Technology, Universiti Malaysia Pahang
Al-Sultan Abdullah, 26600 Pekan, Pahang, Malaysia

e-mail: amiril@umpsa.edu.my

social aspects. Employing Monte Carlo simulation and fuzzy logic, and tools such as Crystal Ball and the Fuzzy Logic Toolbox, this method offers a comprehensive assessment [2]. A case study in Malaysia demonstrates its practical application and potential to enhance sustainability in developing nations.

2 Methodology

The proposed sustainability assessment method for Malaysia's electronic industry combines quantitative and qualitative indicators to address uncertainties. Quantitative metrics, including environmental, economic, and social aspects, are treated as stochastic variables and analyzed through Monte Carlo simulation. Social indicators, examined as fuzzy variables, are utilized [3]. Fuzzy Inference Systems (FISs) with the Mamdani method for fuzzy modeling. The final Total Sustainability Index is derived from the weighted contributions of both subsystems.

The methodology involves defining the study's objective and scope, identifying relevant sustainability indicators through expert consultation, and selecting small electronic manufacturing firms in Malaysia for case studies [4]. The approach focuses on developing a practical and applicable sustainability assessment tailored to the needs of smaller entities in the industry (cf. Fig. 1).

Focused on the collection and normalization of data from the selected case study companies. The data were normalized to ensure comparability across different indicators, despite the variations in measurement units [5]. The normalization process was crucial, and it involved using specific formulas for indicators with positive and negative signs. This normalization allowed for a consistent analysis of the indicators.

$$\tilde{x}_{mn} = (\frac{f_{mn}^1}{C_n^+}, \frac{f_{mn}^2}{C_n^+}, \frac{f_{mn}^3}{C_n^+}) \quad (1)$$

$$\tilde{x}_{mn} = (\frac{f_{mn}^1}{C_n^-}, \frac{f_{mn}^2}{C_n^-}, \frac{f_{mn}^3}{C_n^-}) \quad (2)$$

$$\tilde{c}_{mn} = w_n \cdot \tilde{x}_{mn} \quad (3)$$

To quantify qualitative indicators into a singular real value $P(\tilde{m})$, derived from three fuzzy estimates, the graded mean integration [6] representation method was employed. Equation (4) outlines the formula utilized for this purpose.

$$P(\tilde{m}) = \frac{1}{6}(a + 4b + c) \quad (4)$$

The study evaluated qualitative indicators by focusing on nine social indicators categorized under labor rights, working conditions, and customer well-being [7]. A

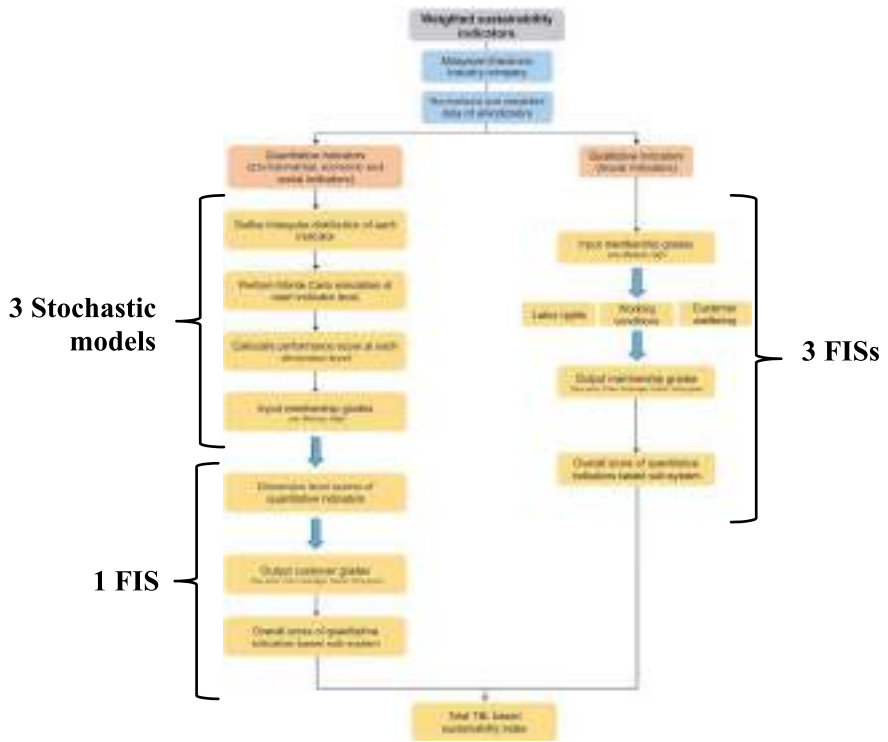


Fig. 1 Flow chart of the proposed in sustainability assessment research

fuzzy logic approach was employed to handle the qualitative nature of these indicators. For each category, Fuzzy Inference Systems (FISs) were developed, which utilized triangular membership functions for input variables and output results [8]. The study crafted rules within these FISs to assess the social indicators, ultimately producing scores for each category.

$$R = n^v$$

(5)

The study used Monte Carlo simulation to analyze quantitative indicators, addressing stochastic uncertainties, while fuzzy logic was applied to handle varying sustainability impacts. Environmental and economic dimensions, with negative-oriented indicators, were assessed differently from the social dimension, leading to the creation of an additional Fuzzy Inference System (FIS) for comprehensive scoring [8]. The final step involved calculating a Triple Bottom Line (TBL)-based sustainability index, combining weighted scores from both qualitative and quantitative indicators [9]. This index provided a holistic measure of sustainability [3], categorizing companies into five levels, particularly benefiting small manufacturing firms in Malaysia’s electronic industry [10]. This final sustainability index allows for

Table 1 Fuzzy membership grades for environmental and economic dimensions

Number	Membership grades			Description
1	0.0	0.0	0.5	Low
2	0.0	0.5	1.0	Medium
3	0.5	1.0	1.0	High

Table 2 Overall triple-bottom-line (TBL) based sustainability performance levels

Number	Membership grades			Description
1	0.0	0.0	0.25	Very poor
2	0.0	0.25	0.50	Poor
3	0.25	0.50	0.75	Average
4	0.50	0.75	1.0	Good
5	0.75	1.0	1.0	Very good

the categorization of the electronic company's sustainability performance into one of the five levels provided in Tables 1 and 2.

3 Result and Discussion

To demonstrate the methodology's effectiveness, it was tested at "E-Tech Innovations," a small electronic manufacturing company in Penang, Malaysia. Established in 1997, the facility specializes in high-quality electronic components. The sustainability evaluation covered the entire production process, focusing on environmental impact and resource use. Data was collected through on-site inspections and interviews, with manufacturing and packaging processes standardized into 'per unit' metrics. Quantitative and qualitative metrics were measured using standard units and a Likert scale, as outlined in Table 3 [11].

Table 3 Linguistic variables and their values for quantitative indicators

Number	Linguistic variable	Measuring scale
1	Very low (VL)	1
2	Low (L)	2
3	Medium (M)	3
4	High (H)	4
5	Very high (VH)	5

3.1 Normalization and Weighting of the Data

Normalization was carried out using Eqs. (1) and (2). The weight of each indicator was multiplied by its normalized value to derive its normalized weighted value, as shown in Eq. (3). Tables 4 and 5 display example the quantitative and qualitative indicator data [5]. For the qualitative indicators, a single real value $P(\tilde{m})$ was computed using Eq. (4).

3.2 Evaluation of Sub-system Using Qualitative Indicators

In Sect. 2, qualitative indicators were evaluated using a fuzzy logic approach with membership grades and linguistic terms from Tables 1 and 2. Fuzzy rule bases were developed for each aspect category labor rights, working conditions, and customer well-being resulting in three Fuzzy Inference Systems (FISs) [7]. Matlab's fuzzy logic toolbox was used for simulation, with Fig. 2 showcasing an example configuration of the Mamdani-type FISs.

After executing the FISs, defuzzified scores for each category were obtained. The overall score for the qualitative indicators was 0.518, calculated by summing the equally weighted scores of the three aspect categories as given in Table 6.

3.3 Evaluation of Sub-system Using Quantitative Indicators

Quantitative indicators were analyzed using Monte Carlo simulation followed by fuzzy logic. Triangular distributions and three-point normalized data were used, with simulations run 1000 times for each indicator [12]. Average scores from these simulations were aggregated to assess performance at the dimension level, and applied similarly to environmental, economic, and social dimensions [13]. Figure 3 illustrates the stochastic simulation results [11].

The sustainability assessment evaluated the performance across three dimensions: environmental, economic, and social [13]. Each dimension's performance was determined by averaging the simulated scores of relevant quantitative indicators [14]. You can find the scores for all three dimensions in Table 7.

Another FIS was constructed utilizing the performance scores at the dimension level for quantitative indicators, aiming to derive a score for the sub-system based on quantitative indicators [15]. As previously stated, FIS was employed to address the issue of varying impacts among sustainability dimensions [16]. The resulting overall performance score for the sub-system based on quantitative indicators stood at 0.947.

Table 4 Environmental indicator data

Category	Indicators	Units	Indicators' ID	±	Indicators' scores	C _n ⁺	C _n ⁻	Normalized scores	Indicators' weights	Normalized weighted scores
Waste management	Recycling and reusing water	L	E1	+	Min: 2.0 Likely: 3.75 Max: 5.0	5.0	N/A	Min. 0.4 Likely 0.75 Max. 1	0.759	Min. 0.304 Likely 0.569 Max. 0.759
	Wastewater disposal	L	E2	-	Min: 3.0 Likely: 4.31 Max: 5.0	N/A	3.0	Min. 0.6 Likely 0.69 Max. 1	0.823	Min. 0.494 Likely 0.568 Max. 0.823
	Non-renewable resources and Renewable resources	Tons/kWh	E3	-	Min: 3.0 Likely: 3.81 Max: 5.0	N/A	3.0	Min. 0.6 Likely 0.79 Max. 1	0.967	Min. 0.580 Likely 0.764 Max. 0.967
	Chemical reused or recovered	Tons/L	E4	+	Min: 2.0 Most Likely: 3.75 Max: 5.0	5.0	N/A	Min. 0.4 Likely 0.75 Max. 1	0.901	Min. 0.360 Likely 0.676 Max. 0.901
Environmental impact	Noise level	dB	F1	-	Min: 3.0 Likely: 4.18 Max: 5.0	N/A	3.0	Min. 0.6 Likely 0.72 Max. 1	0.953	Min. 0.572 Likely 0.686 Max. 0.953
	Greenhouse gases	tCO ₂ e	F2	-	Min: 3.0 Likely: 4.12 Max: 5.0	N/A	3.0	Min. 0.6 Likely 0.73 Max. 1	0.927	Min. 0.556 Likely 0.677 Max. 0.927
	Water pollution	Mg/L	F3	-	Min: 2.0 Likely: 3.75 Max: 5.0	N/A	2.0	Min. 0.4 Likely 0.53 Max. 1	0.943	Min. 0.377 Likely 0.500 Max. 0.943

(continued)

Table 4 (continued)

Category	Indicators	Units	Indicators' ID	±	Indicators' scores	C _n ⁺	C _n ⁻	Normalized scores	Indicators' weights	Normalized weighted scores
	Air pollution	ppm	F4	–	Min:2.0 Likely: 4.25 Max:5.0	N/A	2.0	Min. 0.4 Likely 0.47 Max. 1	0.967	Min. 0.387 Likely 0.454 Max. 0.967
	Land pollution and soil protection	mg/kg	F5	–	Min: 1.0 Likely:2.25 Max:5.0	N/A	1.0	Min. 0.2 Likely 0.44 Max. 1	0.751	Min. 0.150 Likely 0.330 Max. 0.751

Table 5 Social inventory data for qualitative indicators

Category	Indicators	Units	Indicators' ID	\pm	Indicators' scores	C_n^+	C_n^-	Normalized scores	Indicators' weights	Normalized weighted scores	Single value
Labor rights	Competitive compensation	VL to VH	S-1	+	Min: 3 Likely: 5 Max: 5	5		Min: 0.6 Likely: 1 Max: 1	0.045	Min: 0.027 Likely: 0.045 Max: 0.045	0.042
	Equal opportunity employment or anti-discrimination	VL to VH	S-2	+	Min: 3 Likely: 5 Max: 5	5		Min: 0.6 Likely: 1 Max: 1	0.440	Min: 0.264 Likely: 0.0440 Max: 0.0440	0.042
	Right to unionize or freedom of assembly	VL to VH	S-3	+	Min: 3 Likely: 4 Max: 4	4		Min: 0.75 Likely: 1 Max: 1	0.038	Min: 0.029 Likely: 0.038 Max: 0.038	0.037
Working conditions	Reasonable working hours (regulatory compliance)	VL to VH	S-4	+	Min: 4 Likely: 4 Max: 5	5		Min: 0.8 Likely: 0.8 Max: 1	0.047	Min: 0.038 Likely: 0.038 Max: 0.047	0.039
	Manageable workload (regulatory compliance)	VL to VH	S-5	+	Min: 4 Likely: 4 Max: 5	5		Min: 0.8 Likely: 0.8 Max: 1	0.044	Min: 0.035 Likely: 0.035 Max: 0.044	0.037
Customer wellbeing	Ethically sourced materials	VL to VH	S-6	+	Min: 2 Likely: 4 Max: 4	4		Min: 0.5 Likely: 1 Max: 1	0.042	Min: 0.021 Likely: 0.042 Max: 0.042	0.039
	Safe components	VL to VH	S-7	+	Min: 3 Likely: 4 Max: 4	4		Min: 0.75 Likely: 1 Max: 1	0.044	Min: 0.033 Likely: 0.044 Max: 0.044	0.042

(continued)

Table 5 (continued)

Category	Indicators	Units	Indicators' ID	±	Indicators' scores	C_n^+	C_n^-	Normalized scores	Indicators' weights	Normalized weighted scores	Single value
	Eco-friendly and non-toxic materials	VL to VH	S-8	+	Min: 3 Likely: 5 Max: 5	5		Min: 0.6 Likely: 1 Max: 1	0.036	Min: 0.022 Likely: 0.036 Max: 0.036	0.034
	Transparent documentation	VL to VH	S-9	+	Min: 3 Likely: 5 Max: 5	5		Min: 0.6 Likely: 1 Max: 1	0.045	Min: 0.027 Likely: 0.045 Max: 0.045	0.042

VL to VH = Very Low to Very High, N/A = not applicable

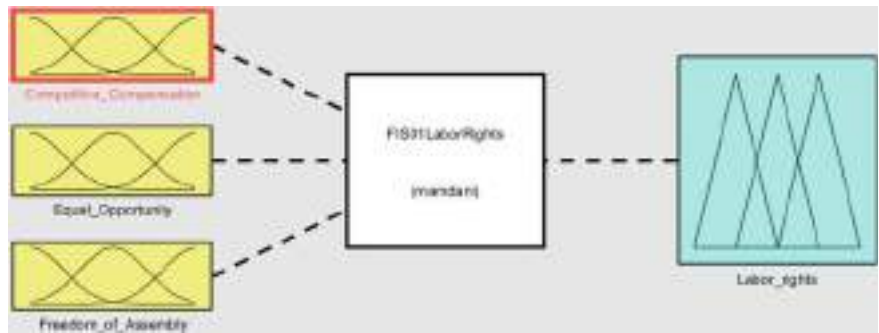
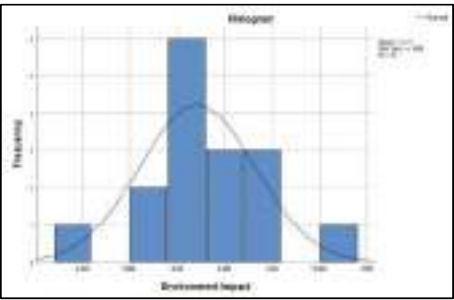


Fig. 2 Fuzzy modeling and assessment

Table 6 Aspect category performance based on FISs [7]

Number	Aspect category	Score
1	Labor rights	0.175
2	Working conditions	0.171
3	Customer wellbeing	0.172

Statistic	Fit: Beta	Forecast Values
Mean	3.7125	0.15162
95% Confidence Interval for Mean		
Lower Bound	3.3893	
Upper Bound	4.0357	
5% Trimmed Mean	3.7139	
Median	3.6000	
Variance	0.368	
Std. Deviation	0.60649	
Minimum	2.40	
Maximum	5.00	
Range	2.60	
Interquartile Range	0.75	
Skewness	0.102	0.564
Kurtosis	0.999	1.091



(a)

(b)

Fig. 3 Simulation outputs (based on indicator level). **a** Simulated environmental impact; **b** Distribution fitting of performance outputs

Table 7 Dimension-level performance based on Monte Carlo simulation

Number	Sustainability dimension	Score
1	Environmental	0.79
2	Economic	0.85
3	Social	0.80

Table 8 Total TBL-based sustainability index

Sub-system name	Modeling approach	Model name	Model score	Sub-system level score	Weight	Total TBL sustainability index	
Qualitative indicators based sub-system	Fuzzy logic (three models)	Labor rights	0.175	0.518	0.163	0.65	
		Working conditions	0.171				
		Customer wellbeing	0.172				
Quantitative indicators based sub-system	Monte Carlo simulation (three models)	Environmental	0.79	0.947	0.592		
		Economic	0.85				
		Social	0.80				

3.4 Total TBL Based Sustainability Index

The comprehensive sustainability index, rooted in the Triple Bottom Line (TBL) framework [13] was derived by summing the weighted evaluations of two key subsystems: one grounded in qualitative indicators and the other in quantitative measures. This holistic index illustrates the proportional significance of each subsystem [17]. The weighting factors for the quantitative (0.592) and qualitative (0.163) subsystems were determined based on the relative importance of their respective indicators [5]. Table 8 provides a breakdown of the total sustainability index for the referenced company [18].

As previously noted, sustainability performance was measured on a scale from 0 to 1. We categorized the performance into five ranges [5] as outlined in Table 4 as well Table 5. For instance, if the index falls between 0.0 and 0.19, the performance is deemed very poor. The overall sustainability index for the case company stood at 0.65, placing it within the “Good” sustainability performance category.

3.5 Discussion

This segment reviews the fuzzy and stochastic model findings, focusing on the total sustainability index and uncertainties. Labor rights scored highest at 0.175, followed by customer well-being (0.172) and working conditions (0.171), with room for improvement in working hours and workload. The social dimension had the highest combined score (0.678), while the economic and environmental dimensions scored 0.85 and 0.79, respectively, due to challenges like air emissions and wastewater. The overall TBL sustainability index was 0.65, indicating average performance with potential for improvement. Further analysis explored how each dimension contributed to result variability.

4 Conclusion

Contemporary sustainability assessments struggle with finding comprehensive indicators, handling uncertainties, incorporating the Triple Bottom Line (TBL), and assessing sustainability in data-scarce developing nations. This article developed and validated a novel methodology using Monte Carlo simulation and fuzzy logic to address these challenges. A case study of a Malaysian food manufacturing company showed an average sustainability performance with a TBL index of 0.65, identifying areas for improvement, such as reducing air emissions, managing wastewater, and enhancing working conditions.

References

1. Utne IB (2009) Improving the environmental performance of the fishing fleet by use of Quality Function Deployment (QFD). *J Clean Prod* 17(8):724–731
2. Zhang H, Haapala KR (2015) Integrating sustainable manufacturing assessment into decision making for a production work cell. *J Clean Prod* 105(Oct):52–63
3. de Vries M, de Boer IJM (2010) Comparing environmental impacts for livestock products: a review of life cycle assessments 128(1–3):1–11
4. Ahmad S, Daddi T, Iraldo F (2024) Integration of open innovation, circularity and sustainability: a systematic mapping of connections, analysis of indicators and future prospects. *Creativity Innov Manage* 33(3):414–437
5. Ahmad S, Wong KY (2019) Development of weighted triple-bottom line sustainability indicators for the Malaysian food manufacturing industry using the Delphi method. *J Clean Prod* 229(May):1167–1182
6. Ahmad S, Wong KY, Rajoo S (2019) Sustainability indicators for manufacturing sectors: a literature survey and maturity analysis from the triple-bottom line perspective. *J Manuf Technol Manag* 30(2):312–334
7. Ahmad S, Wong KY, Zaman B (2019) A comprehensive and integrated stochastic-fuzzy method for sustainability assessment in the Malaysian food manufacturing industry. *Sustainability* 11(4):948
8. Tilman D, Clark M (2014) Global diets link environmental sustainability and human health. *Nature* 515(7528):518–522
9. Linke BS, Corman GJ, Dornfeld DA, Tönissen S (2013) Sustainability indicators for discrete manufacturing processes applied to grinding technology. *J Manuf Syst* 32(4):556–563
10. Rosen MA, Kishawy HA (2012) Sustainable manufacturing and design: concepts, practices and needs. *Sustainability* 4(2):154–174
11. Seuring S, Müller M (2008) From a literature review to a conceptual framework for sustainable supply chain management. *J Clean Prod* 16(15):1699–1710
12. Bonilla Hernandez AE, Lu T, Beno T, Fredriksson C, Jawahir IS (2019) Process sustainability evaluation for manufacturing of a component with the 6R application. *Proc Manuf* 33:546–553
13. Huang A, Badurdeen F (2018) Metrics-based approach to evaluate sustainable manufacturing performance at the production line and plant levels. *J Clean Prod* 192(August):462–476
14. Hetland ML (2009) The basic principles of metric indexing. In: Coello CAC, Dehuri S, Ghosh S (eds) *Swarm intelligence for multi-objective problems in data mining*. SCI, vol 242. Springer, Berlin, Heidelberg, pp 199–232
15. Gani A, James AT, Asjad M, Talib F (2022) Development of a manufacturing sustainability index for MSMEs using a structural approach management. *J Clean Prod* 353(June):131687

16. Böhringer C, Jochem PEP (2007) Measuring the immeasurable—a survey of sustainability indices. *Ecol Econ* 63(1):1–8
17. Egilmez G, Kucukvar M, Tatari O (2013) Sustainability assessment of U.S. manufacturing sectors: an economic input output-based frontier approach. *J Clean Prod* 53(Aug):91–102
18. Jayal AD, Badurdeen F, Dillon OW, Jawahir IS (2010) Sustainable manufacturing: modelling and optimization challenges at the product, process and system levels. *CIRP J Manuf Sci Technol* 2(3):144–152

Enhancing Agricultural Efficiency with GIS and TSP-Optimized Drone Pathways



Antonio Passaka Adi Wijaya, Rayinda Pramuditya Soesanto,
and Fandi Achmad

Abstract This study addresses soil and leaf quality scanning challenges using detection drones in crop fields, focusing on limited drone battery life and inefficient route planning. It aims to devise an integrated solution by leveraging Geographic Information System (GIS) technology with the Traveling Salesman Problem (TSP) algorithm. GIS provides spatial data access and enables complex analyses, while the TSP algorithm optimizes drone route planning. This combined approach optimizes battery usage, reduces operational costs, and enhances mapping capabilities for accurate land management decisions. Moreover, GIS facilitates visual route planning, enhancing decision-making processes based on real-time data and environmental conditions. The integration of GIS and the TSP algorithm streamlines workflows, improves efficiency, and enhances data accuracy in agricultural monitoring, contributing to better resource utilization, cost reduction, and productivity in agricultural practices.

Keywords Drone route optimization · Geographic information system · Traveling salesman problem · Agricultural monitoring

1 Introduction

This paper addresses the challenges in agricultural monitoring due to limited drone battery power, which hampers the efficiency of scanning crop fields and tea plantations. By collaborating with third-party drone operators and integrating Geographic Information System (GIS) with the Traveling Salesman Problem (TSP) algorithm, the study aims to optimize routes, reduce costs, and enhance mapping precision.

A. P. A. Wijaya · R. P. Soesanto (✉) · F. Achmad
Telkom University, Bandung, Indonesia
e-mail: raysoesanto@telkomuniversity.ac.id

R. P. Soesanto
The University Center of Excellence for Intelligent Sensing-IoT, Telkom University, Bandung, Indonesia

GIS allows for precise mapping, efficient route planning, and real-time monitoring, minimizing the risk of drones depleting their power mid-operation [1]. The TSP algorithm is adapted to account for battery limitations, optimizing operational efficiency [2]. Applied to the Pusat Penelitian Teh dan Kina (PPTK) Gambung, this approach reduces operational costs, extends equipment lifespan, and improves agricultural productivity through data-driven decision-making [3–6].

Leveraging advanced technology, this study integrates TSP and GIS for optimized drone route design, enhancing agricultural productivity and sustainability. Focusing on PPTK Gambung as a case study, it aligns with Sustainable Development Goal 2 (SDG 2)—Zero Hunger, particularly target 2.4, by promoting sustainable food production systems and resilient agricultural practices to increase productivity, maintain ecosystems, and strengthen climate change adaptation [7–9]. Additionally, the study supports target 2.a, emphasizing the importance of investment in rural infrastructure, agricultural research, and technology development to boost productivity, especially in developing countries [8, 10, 11]. By optimizing drone routes and incorporating GIS for precise planning and real-time data analysis, the research enhances monitoring efficiency, reduces operational costs, and supports the sustainability and resilience of agricultural systems, contributing significantly to achieving SDG 2 targets [12–14].

2 Methodology

The research methodology in this study employs quantitative methods, primarily utilizing the Travelling Salesman Problem (TSP) algorithm to optimize drone flight routes for soil and leaf quality detection. The integration of Geographic Information System (GIS) with TSP aims to streamline route optimization, minimize costs, and enhance mapping accuracy. Data collection involved field surveys, researcher interviews, collaboration with drone operators, and literature studies [1, 12]. Insights from these sources guided the evaluation of variables, facilitating the integration of the TSP algorithm into GIS. The GIS system features a layer menu allowing users to toggle various spatial data layers, including plantation blocks, soil quality zones, and drone flight paths [11]. Route visualization utilizes arrows indicating direction and sequence of drone travel. Essential spatial attributes such as latitude and longitude coordinates are used for accurate mapping and analysis. For enhanced user interaction and visualization, the GIS system leverages Leaflet, an open-source JavaScript library for mobile-friendly interactive maps, which allows for efficient handling of map tiles and markers, thus providing a seamless experience in visualizing drone routes and spatial data [6, 11]. The Haversine formula calculates the great-circle distance between two points on Earth's surface using their latitude and longitude coordinates [15]. This mathematical expression is formulated as follows:

$$distance(p1, p2) = R \cdot c \quad (1)$$

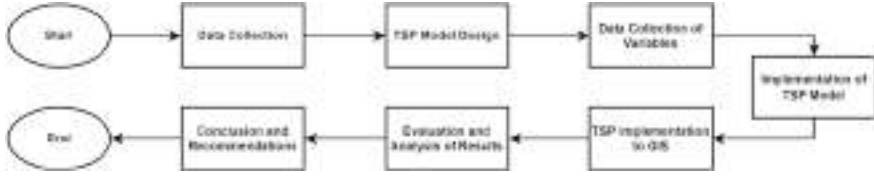


Fig. 1 Research flow evaluation

$$c = 2 \cdot \text{atan2}(\tilde{a}, \sqrt{1 - \tilde{a}^2}) \quad (2)$$

$$a = \left(\left(\sin\left(\frac{\Delta \text{lat}}{2}\right) \right)^2 + \cos(\text{lat}1) \cdot \cos(\text{lat}2) \cdot \left(\left(\sin\left(\frac{\Delta \text{lat}}{2}\right) \right)^2 \right) \right) \quad (3)$$

The TSP algorithm is adapted to account for drone battery limitations and recharging needs, optimizing operational efficiency [2, 16–21]. Implemented in Pseudocode, the algorithm initializes coordinates, defines the Haversine formula, constructs initial routes, optimizes routes, and visualizes the optimized route on GIS. This study optimizes drone flight routes for efficient soil and leaf quality detection. The research begins with data collection through field surveys, interviews, and literature studies, followed by the design of a TSP model tailored for agricultural monitoring. Key variables such as geographical coordinates, battery life, and terrain characteristics are used. The TSP model is implemented in Python and integrated with GIS for route visualization, utilizing Leaflet for interactive mapping. The evaluation assesses the optimized routes based on cost savings, mapping precision, and operational efficiency, concluding with insights and recommendations for future agricultural monitoring (Fig. 1).

3 Result and Discussion

3.1 Data Collection

The calculations for the TSP and GIS visualization for the drone are grounded in the following data presented in Table 1. This includes key constraints and operational capabilities for drone flights, ensuring comprehensive and realistic modeling for route optimization.

In addition to the field data, detailed GIS attributes are essential for accurate mapping and visualization. Table 2 lists the GIS data attributes that include spatial information about the plantation blocks, pathways, and access points.

Furthermore, GIS will incorporate data reports for review by researchers, providing detailed insights into drone flight paths, scanned areas, and operational metrics. These reports will facilitate thorough examination and validation of the

Table 1 Field data and assumptions

Constraints	Information
Drone flight capability	15 minutes
Scanning capability per existing day	4 blocks
Drone batteries carried by the operator	4 batteries
Drone scanning time per block	10 minutes
Travel time	Not taken into account
Scanning activity flow	Can be resumed after recharging

Table 2 GIS data attributes

Attribute	Description
Plantation block coordinates	Latitude and longitude coordinates of each block
Block boundaries	Geospatial boundaries of each plantation block
Pathway and access points	Coordinates of pathways and access points for drone operations

collected data, ensuring accurate and reliable information is available for analysis. This comprehensive data collection effort ensures that all relevant factors are considered in the TSP model and GIS visualization, facilitating effective optimization of drone flight routes for soil and leaf quality detection in agricultural monitoring.

3.2 TSP and GIS Model Design

This section outlines two algorithms that optimize drone flight routes for soil and leaf quality detection using the Traveling Salesman Problem (TSP) model and Geographic Information Systems (GIS). The process begins by initializing location coordinates and calculating distances using the Haversine formula. An initial route is constructed with the nearest neighbor method and then optimized using the TSP algorithm. The optimized route is visualized with GIS, displaying directional arrows for better operational planning, and the final output includes the route and cost savings. The pseudocode details each step of this process, from route generation to optimization. The following is the pseudocode for Algorithm 1.

Algorithm 1 Pseudocode for generating the flight route and optimizing it:

```

1: Initialize drone at starting point, i, and pickup point, k
2: For each block i in block_coordinates do
3:   For each block j in block_coordinates \ {i} do
4:     For each block k in block_coordinates \ {i, j} do
5:       Set c_drone to the distance between block_coordinates[i] and block_coordinates[j]
6:       While c(drone)  $\leq$  battery_limit do
7:         Insert the nearest unvisited node to the last inserted drone node (h)
8:         Update c_drone to the duration of new drone route including h
9:       End while
10:    End for
11:    Keep the last generated operation
12:    Insert the nearest unvisited node to the last inserted drone node
13:    Compute the travel time of the new drone route
14:    Keep the new operation
15:  End for
16: End for

```

Algorithm 1 is designed to optimize drone flight routes for agricultural monitoring by leveraging the TSP model and considering practical constraints like battery limits. The algorithm begins by initializing the drone's starting position and iterates through all possible block combinations to generate a route. Using the Haversine formula, it calculates distances between blocks, ensuring that the drone's path stays within its battery capacity. The TSP algorithm is applied to find the most efficient route, allowing the drone to visit each block once before returning to the starting point. The algorithm continuously updates and refines the route to minimize travel time and energy consumption, ensuring an optimized flight path. The final output is an optimized route, which is then visualized using Geographic Information Systems (GIS) to provide a clear operational plan. Integrating GIS allows for real-time visualization and potential adjustments to the drone's route based on live data, enhancing the system's robustness in various scenarios. This integration is crucial for effective operational planning, enabling operators to anticipate obstacles and manage the mission efficiently. The algorithm significantly improves operational efficiency by optimizing battery usage, ultimately lowering maintenance costs. By optimizing the route, the drone allocates more resources to accurate data collection, which is crucial for agricultural settings where time, resources, and precision are key.

3.3 Simulation Methods and Results

The simulation methods employed in this study are based on variations of the Flying Sidekick Traveling Salesman Problem with Pick-Up and Delivery (FSTSP-PDP) and Drone Energy Optimization [22]. Two distinct approaches are compared to optimize drone routes and energy consumption in agricultural monitoring scenarios. Figure 2 illustrates the first simulation method, where the drone’s starting point is determined by the operator. In this method, the drone sequentially visits each block, completes its task, returns to the starting point, and swap its battery before moving on to the next block. Consequently, the drone always initiates its route with a fully charged battery for each new block. This battery swapping method is more efficient compared to traditional charging, as it minimizes downtime and maximizes operational efficiency [18, 19, 22]. The simulation results indicate that all six blocks are scanned, with a total battery usage of six units.

Figure 3 depicts the second simulation method, which utilizes the centroid of predetermined block coordinates as the starting point. In this approach, the drone visits blocks until its battery duration nears depletion then returns to the centroid to swap the battery and resumes scanning from the last visited block. This method optimizes battery usage by minimizing unnecessary return trips to the starting point. Simulation results reveal that all six blocks are scanned with only four units of battery utilized.

In Method 2, the TSP calculation is employed, utilizing the centroid of predetermined block coordinates as the starting point. This approach allows the drone to visit blocks until its battery duration expires. If sufficient time has been spent in one block, the drone can move to another without needing to recharge first. However, if the battery is depleted, the drone returns to the centroid and continues its progress from the previously visited block. This systematic approach ensures efficient coverage of the surveyed area while optimizing battery usage. The drone follows a predetermined route, visiting blocks in sequence before returning to the starting point. This route is generated based on the TSP algorithm. The algorithm then identifies the nearest unvisited block from the drone’s position and generates a flight route prioritizing

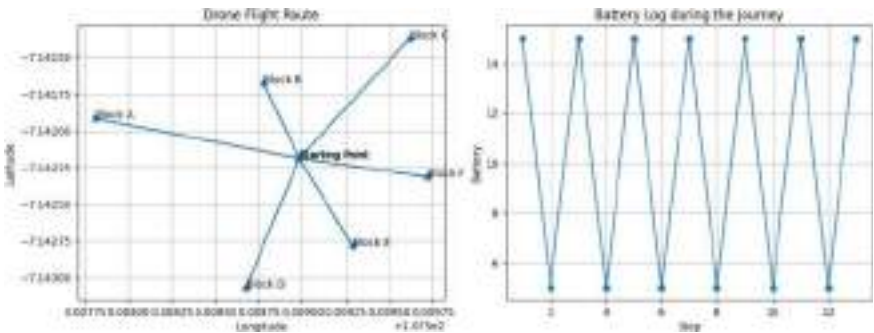


Fig. 2 Method 1 drone flight route and battery consumption simulation

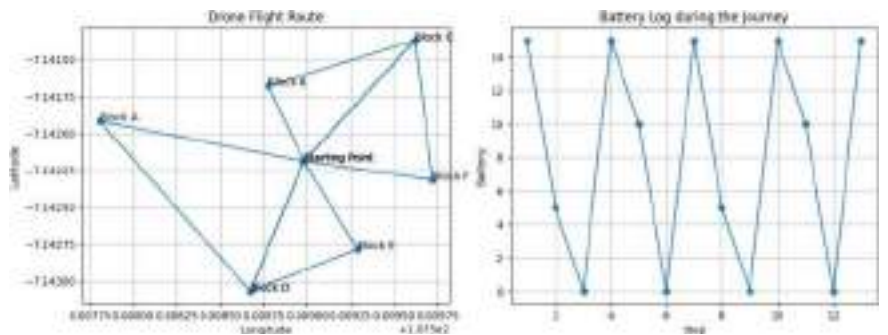


Fig. 3 Method 2 drone flight route and battery consumption simulation

proximity. Battery usage is managed during flight, with the drone returning for swap its battery if levels drop below a threshold. Constraints like battery capacity and route optimization are integrated to ensure effective coverage and operational reliability.

The algorithm aims to optimize route efficiency and scanning coverage in tea and cinchona plantations, enhancing agricultural monitoring. This method builds upon previous research by Cokyasar et al. [18], which investigated designing a drone delivery network with automated battery swapping machines [19, 22]. The flexible swapping strategy employed in Method 2 aligns with their findings, contributing to enhanced operational efficiency and coverage. These methods optimize drone routes and scanning coverage, summarized in Table 3 for route optimization, scanning coverage, and operational efficiency comparison.

Table 3 compares simulation results of two methods: Method 1, with operator-determined starting points, and Method 2, which uses the centroid of block coordinates. Method 1 swaps the drone’s battery after scanning each block, using a total of 6 battery units for 6 blocks. In contrast, Method 2 adopts a flexible battery swap strategy, using only 4 battery units, representing a 33.3% reduction in consumption compared to Method 1. This highlights Method 2’s greater efficiency, allowing for more extensive scanning within the same battery limits. These results align with studies by Cokyasar et al. [18], Zhang and Cao [4], Budiharto et al. [7], and Yilmazer et al. [5], which also focus on GIS and TSP optimization in agriculture, supporting the potential for improved operational efficiency and coverage in drone-based agricultural monitoring.

Table 3 Simulation summary

Method	Starting point determination	Charging strategy	Blocks scanned	Battery used
Method 1	Operator-determined	After each block	6	6
Method 2	Centroid of block coordinates	As needed	6	4

3.4 TSP Implementation to GIS

In Fig. 4, the processed information from the TSP is translated into a comprehensive visualization, encompassing the selected routes, identifying the starting point, depicting the battery consumption, and incorporating feedback from operators regarding the smooth execution or any encountered challenges during the sampling operations. This visualization serves as a valuable tool for researchers and drone operators, facilitating efficient data interpretation and operational assessment. Additionally, the GIS visualization includes spatial data layers representing the terrain conditions to be traversed by the drone. These layers enable operators to plan drone routes effectively by identifying scanned areas and planning which blocks to scan next. This feature enhances the operational efficiency of agricultural monitoring by providing real-time insights into scanned areas and facilitating strategic planning for future scans. By integrating spatial data layers with TSP implementation, the GIS visualization optimizes route planning and resource allocation for drone-based monitoring operations. Moreover, the system allows drone operators to provide operational reports to researchers, detailing the scanning history and any relevant observations during the flight missions. The use of GIS for agricultural monitoring is supported by research such as that by Zhang and Cao [6], which discusses the application and research progress of Geographic Information Systems (GIS) in agriculture. Their findings underscore the significance of efficient drone operations in agricultural monitoring, aligning with the objective of integrating TSP into GIS to optimize drone routes in agriculture.

4 Conclusion

In conclusion, this study underscores the efficacy of drone technology in agricultural surveying tasks, particularly within tea and cinchona plantations. Leveraging advanced algorithms like the Traveling Salesman Problem (TSP) alongside Geographic Information System (GIS), drones can efficiently navigate through designated blocks, maximizing coverage while conserving battery power. The integration of GIS provides crucial spatial intelligence, enabling precise route planning and real-time monitoring of drone operations. Results from the comparative analysis between Method 1 and Method 2 reveal the superior battery efficiency of the latter, attributed to centroid-based starting point determination and an adaptive charging strategy. This emphasizes the significance of strategic algorithm design in optimizing drone-based agricultural surveying. Moving forward, continued advancements in drone technology and GIS integration promise to further enhance agricultural monitoring and management, boosting productivity. Future research could explore additional constraints like travel distance and refined centroid selection based on terrain to further optimize drone operations.



Fig. 4 TSP implementation to GIS

Acknowledgements The researchers extend their gratitude to the PPTK Gambung and Drone Operator for their invaluable assistance in providing access to necessary data and for their cooperation as respondents in this study.

References

1. Puspita IA, Soesanto RP, Muhammad F (2019) Designing mobile geographic information system for disaster management by utilizing wisdom of the crowd. In: 2019 IEEE 6th international conference on industrial engineering and applications (ICIEA), pp 496–500. <https://doi.org/10.1109/IEA.2019.8715031>
2. Dienstknecht M, Boysen N, Briskorn D (2022) The traveling salesman problem with drone resupply. OR Spectr 44(4). <https://doi.org/10.1007/s00291-022-00680-1>
3. Gataullin RI (2024) Using geographic information systems for unmanned aerial vehicles task management. In: 2024 conference of young researchers in electrical and electronic engineering (ElCon), pp 155–157. <https://doi.org/10.1109/ElCon61730.2024.10468535>
4. Zhang F, Cao N (2019) Application and research progress of geographic information system (GIS) in agriculture. In: 2019 8th international conference on agro-geoinformatics (agro-geoinformatics), pp 1–5. <https://doi.org/10.1109/Agro-Geoinformatics.2019.8820476>
5. Yilmazer M, Karakose E, Karakose M (2021) Multi-package delivery optimization with drone. In: 2021 international conference on data analytics for business and industry, ICDABI 2021. <https://doi.org/10.1109/ICDABI53623.2021.9655791>
6. Zhang H (2021) Research on UAV route optimization method based on double target of confidence and ambiguity. Front Neurorobot 15. <https://doi.org/10.3389/fnbot.2021.694899>

7. Budiharto W, Chowanda A, Gunawan AAS, Irwansyah E, Suroso JS (2019) A review and progress of research on autonomous drone in agriculture, delivering items and geographical information systems (GIS). In: Proceedings of 2019 2nd world symposium on communication engineering, WSCE 2019. <https://doi.org/10.1109/WSCE49000.2019.9041004>
8. sdgs.bappenas.go.id, SDGs BAPPENAS (2022)
9. Tian S, Lin L, Li Y (2019) Modeling of big data database based on agricultural basic geographic information. In: Proceedings—2019 Chinese automation congress, CAC 2019. <https://doi.org/10.1109/CAC48633.2019.8996592>
10. Butora A, Soloniewicz B, Schwartz C, Aziz C, Su S, Mahmoud M (2022) The practical use of GIS in agriculture. In: Proceedings—2022 international conference on computational science and computational intelligence, CSCI 2022. <https://doi.org/10.1109/CSCI58124.2022.00270>
11. Clifford J, Curry D (2021) Inherently spatial: GIS in agriculture [Online]. <https://www.esri.com/arcgis-blog/products/apps/field-mobility/inherently-spatial-gis-in-agriculture/>
12. Ouchra H, Belangour A, Erraissi A (2022) Spatial data mining technology for GIS: a review. In: 2022 international conference on data analytics for business and industry, ICDABI 2022. <https://doi.org/10.1109/ICDABI56818.2022.10041574>
13. Al-Mulla Y, Al-Ruehelli A (2020) Use of drones and satellite images to assess the health of date palm trees. In: International geoscience and remote sensing symposium (IGARSS). <https://doi.org/10.1109/IGARSS39084.2020.9324065>
14. Guo Y et al (2019) A drone-based sensing system to support satellite image analysis for rice farm mapping. In: International geoscience and remote sensing symposium (IGARSS). <https://doi.org/10.1109/IGARSS.2019.8898638>
15. Prasetya DA, Nguyen PT, Faizullin R, Iswanto I, Armay EF (2020) Resolving the shortest path problem using the haversine algorithm. *J Crit Rev* 7(1):62–64. <https://doi.org/10.22159/jcr.07.01.11>
16. Dell’Amico M, Montemanni R, Novellani S (2020) Matheuristic algorithms for the parallel drone scheduling traveling salesman problem. *Ann Oper Res* 289(2). <https://doi.org/10.1007/s10479-020-03562-3>
17. Huang H, Savkin AV, Huang C (2020) Round trip routing for energy-efficient drone delivery based on a public transportation network. *IEEE Trans Transp Electr* 6(3). <https://doi.org/10.1109/TTE.2020.3011682>
18. Cokyasar T, Dong W, Jin M, Verbas İÖ (2021) Designing a drone delivery network with automated battery swapping machines. *Comput Oper Res* 129. <https://doi.org/10.1016/j.cor.2020.105177>
19. Es Yurek E, Ozmutlu HC (2021) Traveling salesman problem with drone under recharging policy. *Comput Commun* 179:35–49. <https://doi.org/10.1016/j.comcom.2021.07.013>
20. Schermer D, Moeini M, Wendt O (2020) A branch-and-cut approach and alternative formulations for the traveling salesman problem with drone. *Networks* 76(2). <https://doi.org/10.1002/net.21958>
21. Kim S, Moon I (2019) Traveling salesman problem with a drone station. *IEEE Trans Syst Man Cybern Syst* 49(1). <https://doi.org/10.1109/TSMC.2018.2867496>
22. Gacal JB, Urera MQ, Cruz DE (2020) Flying sidekick traveling salesman problem with pick-up and delivery and drone energy optimization. In: IEEE international conference on industrial engineering and engineering management. <https://doi.org/10.1109/IEEM45057.2020.9309960>

Experimental Investigation of the Effect and Optimization of FDM Process Parameters on Build Time and Compressive Strength of Printed Bone Screws Using Taguchi Method



Sugoro Bhakti Sutono , Cucuk Nur Rosyidi , Pringgo Widyo Laksono , and Eko Pujiyanto

Abstract This paper analyzes the effect and optimization of fused deposition modeling process parameters on the build time and compressive strength of printed bone screws. The improved polylactic acid (PLA+) bone screws were designed and printed following the ASTM F543 standard. The Taguchi method was employed to examine the effects of six process parameters, namely layer height, wall thickness, infill density, nozzle temperature, bed temperature, and printing speed, on both build time and compressive strength. The effect of each parameter on outputs and optimal values for the minimum build time and maximum compressive strength were determined. The findings indicated that layer height, infill density, and printing speed significantly influence the build time. Additionally, infill density and wall thickness significantly affected the compressive strength. The optimum process parameter settings were determined to minimize the build time and maximize the compressive strength. To reduce build time, the optimal process parameter settings were a layer height of 0.14 mm, a wall thickness of 0.6 mm, an infill density of 20%, a nozzle temperature of 195 °C, a bed temperature of 55 °C, and a printing speed of 60 m/s. On the other hand, the optimal process parameter settings for maximizing compressive strength were a layer height of 0.1 mm, a wall thickness of 0.6 mm, an infill density of 100%, a nozzle temperature of 200 °C, a bed temperature of 50 °C, and a printing speed of 30 m/s.

S. B. Sutono (✉) · C. N. Rosyidi · P. W. Laksono · E. Pujiyanto
Department of Industrial Engineering, Universitas Sebelas Maret, Surakarta, Central Java 57126, Indonesia
e-mail: sugoro@umk.ac.id

S. B. Sutono
Department of Mechanical and Industrial Engineering, Universitas Muria Kudus, Kudus, Central Java 59327, Indonesia

Keywords Fused deposition modeling · Additive manufacturing · Process parameters · Bone screw · Taguchi method

1 Introduction

Additive Manufacturing (AM), or 3D printing, is a manufacturing process that involves producing components layer by layer utilizing 3D model data. This differs from subtractive manufacturing methods, which include removing material to create the desired shape [1]. The main advantages of AM include cost reduction in production, minimizing material waste, the capability to produce complex geometry with lower weight, and decreased production time.

Fused Deposition Modeling (FDM) is a popular AM technique widely used in 3D printing in biomedical applications, particularly in producing customized orthopedic implants. The flexibility of 3D printing enables the creation of complex geometries that can closely correspond to the individual anatomical features of each patient, potentially improving the fit and functionality of the implants. In orthopedics, FDM has been explored for the fabrication of various components, such as bone screws, which are essential for the fixation and stabilization of fractures [2]. 3D printing offers more options for material selection compared to traditional manufacturing methods. This allows for the use of biocompatible and biodegradable polymers, such as polylactic acid (PLA). PLA is widely used in orthopedics for the production of 3D-printed medical products due to its excellent biocompatibility, mechanical properties, and biodegradability [3]. However, the mechanical performance of FDM-printed parts is strongly influenced by the process parameters, which must be optimized to meet the required specifications. The impact of various FDM process parameters on the mechanical properties of printed parts has been studied in the literature [4, 5].

Design of experiments (DoE) is a systematic method for determining the influence of process parameters. DoE, like the Taguchi Method (TM) and Response Surface Methodology (RSM), was used to reduce the number of experimental trials and identify the optimal combination of process parameters that improved the mechanical properties [6]. Researchers widely employed the Taguchi method (TM) to reduce the number of experiments required for optimizing 3D printing process parameters [7]. Kechagias et al. [8] used the TM to investigate the impact of different process parameters in FDM on the mechanical characteristics of 3D-printed PLA parts. These characteristics were considerably influenced by infill density, raster deposition angle, nozzle temperature, printing speed, layer thickness, and bed temperature. Similarly, Camposeco-Negrete et al. [9] investigated the effects of infill pattern, build orientation, and infill percentage on the mechanical properties of PLA parts printed by FDM using the TM and analysis of variance (ANOVA). Pachauri et al. [10] employed TM and ANOVA to determine the optimal combination of process parameters for producing FDM 3D-printed PLA parts with the highest tensile strength. The study indicated that the proposed method may help optimize printing parameters to produce high-strength PLA parts. TM and ANOVA have also been employed in other studies

to determine the optimal process parameters for making the PLA parts using FDM with improved performance characteristics [11, 12]. However, previous research indicates that no study has been conducted on investigating or optimizing FDM process parameters for printing bone screws using the Taguchi method.

This study aims to empirically investigate the effect and optimization of FDM process parameters, including layer height, wall thickness, infill density, nozzle temperature, bed temperature, and printing speed, on the build time and compressive strength of 3D-printed bone screws using the Taguchi method.

2 Material and Methods

The filament used for printing the 3D bone screws was the improved polylactic acid (PLA+), with a diameter of 1.75 mm, and was commercially available from eSUN Manufacturer (Shenzhen, China). PLA+ is a modified version of PLA with excellent impact resistance and adherence between printed layers, making it suitable for 3D printing functional products. The material properties of PLA+ are given in Table 1.

The 3D model of bone screws was initially designed in Solidworks software, with geometric dimensions based on the ASTM F543 Type HA screw specification outlined in Table 2. Figure 1 presents the 3D model of the bone screw. This 3D model was subsequently converted to an STL file format and imported into Ultimaker Cura 5.5.0 software. In this program, G-codes were generated, process parameters were set, and the 3D model was sliced for 3D printing. The designed bone screws were ultimately fabricated using the Creality Ender 6 FDM 3D printer, with a nozzle diameter of 0.2 mm.

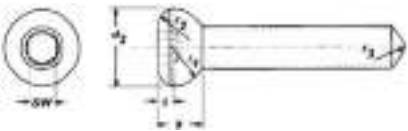
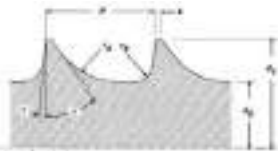
The FDM process involves numerous parameters that are specific to 3D printing. Six process parameters that affect the performance of FDM-printed bone screws were used as input/control factors in this investigation. These include layer height (L_h), wall thickness (W_t), infill density (I_d), nozzle temperature (N_t), bed temperature (B_t), and printing speed (P_s). These parameters were selected based on the relevant literature [5, 8, 15]. During the experiment, all other parameters were kept constant.

This study used the TM to design experiments and optimize FDM process parameters. The TM is a robust design approach that uses orthogonal arrays (OA) to study the entire parameter space with fewer experiments. With minimum experimentation, it can efficiently find the optimal process parameter settings for the desired product quality characteristics [16].

Table 1 Improved polylactic acid (PLA+) filament properties [13]

Density (g/cm ³)	Melt flow index (°C/kg)	Tensile strength (MPa)	Elongation at break (%)	Flexural strength (MPa)	Izod impact strength (kJ/m ²)	Recyclability
1.23	190/2.16	60	20	74	6	Yes

Table 2 Dimensions for HA screw design based on ASTM F543 (in mm) [14]

Bone screw type and size								
HA 5.0 × 30 mm	d_2	k	r_1	r_2	r_3	Screwdriver size	SW	t
	8.0	4.6	4.250	2.5	1.0	3.5	3.510	2.8
								
	d_1	d_5	e	P	r_4	r_5	α	β
	5.0	3.50	0.1	1.75	1.0	0.3	35	3

Note: d_1 is thread diameter, d_2 is head diameter, d_5 is core diameter, r_1 is bottom head radius, r_2 is top head radius, r_3 is tip radius, r_4 is leading-edge radius, r_5 is trailing-edge radius, k is head height, e is crest width, P is thread pitch, α is leading-edge angle, β is trailing-edge angle, t is screwdriver thickness, and SW is key or wrench width

Fig. 1 Design of bone screw



This study used six process parameters and a five-level parameter set adapted to the L_{25} (5^6) OA. The process parameters and their levels are shown in Table 3. Employing the TM reduced the number of experiments from 15,625 to 25 and from 46,875 to 75 due to the experiments being performed in three repetitions. Table 4 presents the DoE for the L_{25} OA. The compressive strength of the printed bone screws was evaluated using a universal testing machine following ASTM D695 standards. Compression

tests were performed on a Zwick/Roell Z020 Universal Testing Machine with a 1.5 mm/min test speed. Additionally, each specimen's build time during manufacturing was recorded and calculated by 3D printing slicing software. Figure 2 illustrates the equipment used in the various processes, from producing the test specimens to breaking specimens during the compression test. The experimental results for the average build time (B_T) and compressive strength (C_S) values are presented in Table 4.

The experimental data was analyzed using the TM to examine how the process parameters affected build time and compressive strength and the optimal parameter settings for minimizing build time and maximizing compressive strength. The influence of process parameters on responses was investigated using the Taguchi experimental design method. The signal-to-noise (S/N) ratio was calculated for each response characteristic, and the mean S/N ratio response table and main effects plots were generated to identify the optimal parameter levels. The process parameter with the highest S/N ratio indicates the optimal level.

The TM uses different formulas to calculate the S/N ratio, depending on whether the experiment target minimizes or maximizes the response. For minimization problems, the minimum response is computed using the S/N ratio with the smaller-the-better (STB) response characteristic. Conversely, for maximization problems, the S/N ratio with the larger-the-better (LTB) response characteristic is used. In this study, the objective is to minimize the build time and maximize the compressive strength of the 3D-printed bone screws. The formula for the STB (Eq. 1) and the LTB (Eq. 2) is as follows:

$$S/N_{STB} = -10\log_{10} \left[\frac{1}{n} \sum_{i=1}^n y_{ij}^2 \right] \quad (1)$$

$$S/N_{LTB} = -10\log_{10} \left[\frac{1}{n} \sum_{i=1}^n \frac{1}{y_{ij}^2} \right] \quad (2)$$

where y_{ij} is the collected response data of the 3D printing process parameters for a given test condition, and n is the number of replications.

Table 3 Process parameters and their levels

Process parameters	Symbol	Levels				
		1	2	3	4	5
Layer height (mm)	A	0.06	0.08	0.10	0.12	0.14
Wall thickness (mm)	B	0.2	0.4	0.6	0.8	1.0
Infill density (%)	C	20	40	60	80	100
Nozzle temperature (°C)	D	195	200	205	210	215
Bed temperature (°C)	E	40	45	50	55	60
Printing speed (mm/s)	F	20	30	40	50	60

Table 4 The experimental layout used $L_{25} (5^6)$ OA, experimental results, and S/N ratio

Exp. no	Input parameters						Response variables		S/N ratio of responses	
	A	B	C	D	E	F	B _T (min)	C _S (MPa)	B _T (min)	C _S (MPa)
1	1	1	1	1	1	1	53.42	11.518	−34.554	21.227
2	1	2	2	2	2	2	59.60	23.581	−35.505	27.451
3	1	3	3	3	3	3	64.58	36.969	−36.202	31.357
4	1	4	4	4	4	4	64.75	37.978	−36.225	31.591
5	1	5	5	5	5	5	66.00	35.919	−36.391	31.107
6	2	1	2	3	4	5	42.93	17.027	−32.656	24.623
7	2	2	3	4	5	1	53.95	30.801	−34.640	29.771
8	2	3	4	5	1	2	53.78	37.613	−34.613	31.507
9	2	4	5	1	2	3	50.75	45.669	−34.109	33.192
10	2	5	1	2	3	4	42.92	24.127	−32.653	27.650
11	3	1	3	5	2	4	38.97	25.510	−31.814	28.134
12	3	2	4	1	3	5	42.60	40.614	−32.588	32.174
13	3	3	5	2	4	1	48.48	51.575	−33.712	34.249
14	3	4	1	3	5	2	33.60	20.270	−30.527	26.137
15	3	5	2	4	1	3	36.67	27.219	−31.285	28.697
16	4	1	4	2	5	3	36.30	38.596	−31.198	31.731
17	4	2	5	3	1	4	37.53	41.720	−31.488	32.407
18	4	3	1	4	2	5	28.45	19.725	−29.082	25.900
19	4	4	2	5	3	1	33.67	22.914	−30.544	27.202
20	4	5	3	1	4	2	33.60	35.637	−30.527	31.038
21	5	1	5	4	3	2	33.90	43.545	−30.604	32.779
22	5	2	1	5	4	3	23.53	12.220	−27.434	21.742
23	5	3	2	1	5	4	27.03	25.102	−28.638	27.994
24	5	4	3	2	1	5	27.20	28.958	−28.691	29.235
25	5	5	4	3	2	1	33.32	32.390	−30.453	30.208

Additionally, analysis of variance (ANOVA) was used to determine how statistically significant the optimized process parameters were and how they contributed to the response characteristics [4]. Following the Taguchi methodology, the experimental design, calculations, and graphical analysis were conducted using Minitab 21 software.

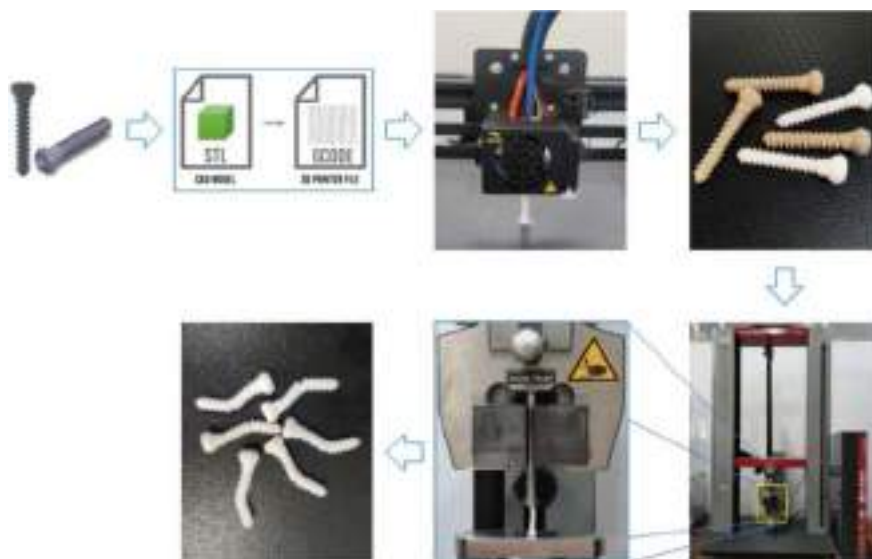


Fig. 2 Experimental steps and devices used

3 Results and Discussion

TM converts the experimental results into S/N ratios. The S/N ratio is utilized to optimize the quality characteristics of responses in Taguchi-based optimization. This study analyzed the S/N ratio to identify the optimal process parameters that minimize B_T and maximize C_S . The smaller-the-better characteristic was selected as the target to minimize B_T , and Eq. (1) was applied to calculate the S/N ratio. The larger-the-better characteristic was chosen to maximize C_S , and Eq. (2) was applied. The experimental results were transformed into S/N ratios, as presented in Table 4. The mean S/N ratio response table is used to analyze each parameter level. It shows which parameter has the most significant effect on the final response, as well as the highest and lowest values of the response characteristics that are associated with it [16]. The highest S/N ratio value indicates the best parameter settings. The optimum values for each parameter in this table are used to determine the optimal combination of process parameters that minimize B_T and maximize C_S .

3.1 Build Time Analysis

The TM was first employed to analyze the effect of printing process parameters on each response individually. Table 5 presents the mean S/N ratio response table for B_T . The bold values indicate the highest mean S/N at each level of the process parameters.

Table 5 Mean S/N ratio response table for build time

Process parameters	Levels					Delta	Rank
	1	2	3	4	5		
Layer height	−35.775	−33.734	−31.985	−30.568	−29.164	6.611	1
Wall thickness	−32.165	−32.331	−32.449	−32.019	−32.262	0.430	4
Infill density	−30.850	−31.726	−32.375	−33.015	−33.261	2.411	2
Nozzle temperature	−32.083	−32.352	−32.265	−32.367	−32.159	0.284	6
Bed temperature	−32.126	−32.192	−32.518	−32.111	−32.279	0.408	5
Printing speed	−32.780	−32.355	−32.046	−32.164	−31.882	0.899	3

A high S/N ratio value indicates that the responses provide the desired result, and for B_T , the smaller-the-better characteristic is preferable. Figure 3a displays the main effects plots, illustrating the mean S/N ratios for build time. It shows that the highest S/N values for B_T are obtained with L_h (A) at the 1st level, W_t (B) at the 3rd level, I_d (C) at the 5th level, N_t (D) at the 4th level, B_t (E) at the 3rd level, and P_s (F) at the 1st level. These correspond to process parameters with a layer height of 0.14 mm, a wall thickness of 0.6 mm, an infill density of 20%, a nozzle temperature of 195 °C, a bed temperature of 55 °C, and a printing speed of 60 m/s. Additionally, the delta value, which represents the difference between the highest and lowest average S/N ratios, indicates the effect of each process parameter on the response. The optimum printing conditions were determined as $A_1B_3C_5D_4E_3F_1$. This combination of process parameters has been identified as the optimal combination of process parameters for reducing the build time of the 3D-printed bone screws.

3.2 Compressive Strength Analysis

The mean S/N ratio response table analysis for C_s , which considers the factors L_h , W_t , I_d , N_t , B_t , and P_s , is presented in Table 6. The bold values represent the highest mean S/N at each level of the process parameters. This analysis employed an approach where larger values are favored to calculate the S/N ratios for maximizing C_s . Figure 3b also displays the main effects plots, illustrating the mean S/N ratios for C_s . According to Table 6, I_d is the most influential process parameter among the other five parameters for C_s , while P_s is the least influential parameter. Similarly, L_h has a minimal impact on C_s . The maximum S/N ratios correspond to the optimum levels for the process parameters. Based on this analysis, the optimal process parameter values to achieve maximum compressive strength for 3D-printed bone screws are a layer height of 0.1 mm, a wall thickness of 0.6 mm, an infill density of 100%, a

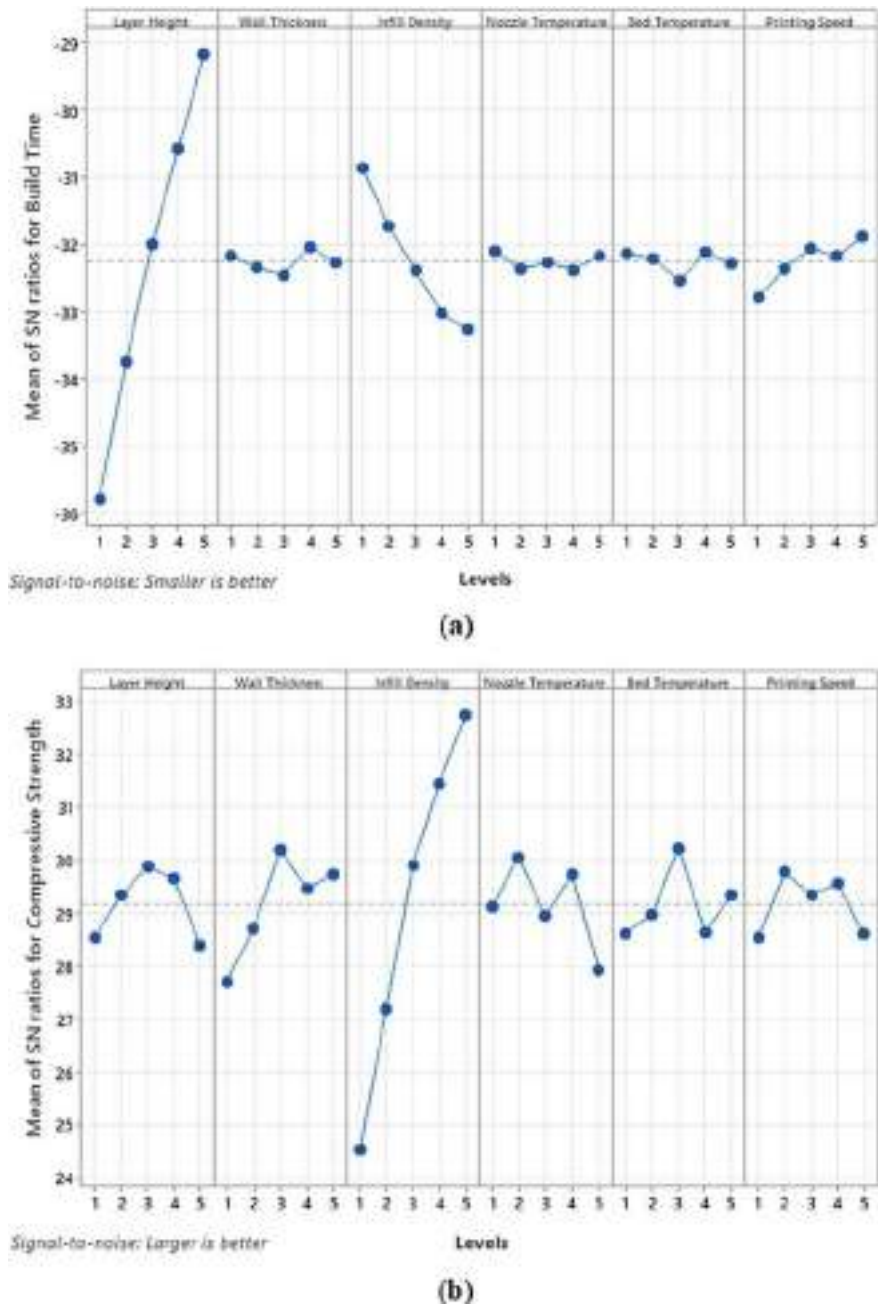


Fig. 3 Mean effect for S/N ratio of a build time and b compressive strength

Table 6 Mean S/N ratio response table for compressive strength

Process parameters	Levels					Delta	Rank
	1	2	3	4	5		
Layer height	28.546	29.349	29.878	29.656	28.392	1.487	5
Wall thickness	27.699	28.709	30.201	29.472	29.740	2.503	2
Infill density	24.531	27.194	29.907	31.442	32.747	8.215	1
Nozzle temperature	29.125	30.063	28.946	29.748	27.938	2.125	3
Bed temperature	28.615	28.977	30.232	28.648	29.348	1.618	4
Printing speed	28.532	29.782	29.344	29.555	28.608	1.251	6

nozzle temperature of 200 °C, a bed temperature of 50 °C, and a printing speed of 30 m/s.

3.3 Analysis of Variance

An analysis of variance (ANOVA) was conducted to evaluate the statistical significance of the process parameters and their contribution to the variation in build time and compressive strength. The ANOVA results for build time and compressive strength are presented in Table 7.

The ANOVA results indicate that layer height, infill density, and printing speed have a statistically significant effect on the build time of the 3D-printed bone screws, as evidenced by their *p*-values below 0.05. Conversely, wall thickness, nozzle, and bed temperature do not significantly affect build time. Layer height exhibits the highest contribution at 84.82%, followed by infill density at 11.8% and printing speed at 1.25%. These findings are consistent with the Taguchi analysis, which identified layer height as the most influential parameter in minimizing build time, while infill density and printing speed ranked second and third, respectively, in Taguchi's factor rank order.

According to the ANOVA results, infill density and wall thickness are the most critical process parameters for compressive strength, while layer height, nozzle temperature, bed temperature, and printing speed have no significant effect. Infill density is the dominant parameter, contributing 77.33% to the variation in compressive strength, followed by wall thickness at 4.25%. These findings are consistent with the Taguchi analysis, which identified infill density and wall thickness as the most influential parameters in maximizing compressive strength. The results from both the ANOVA and Taguchi methods are aligned.

Table 7 ANOVA of build time and compressive strength

Source	DoF	Adj SS	Adj MS	F-value	p-value	% contribution
<i>ANOVA for build time</i>						
Layer height	4	134.295	134.295	724.330	0.000	84.82
Wall thickness	4	0.007	0.007	0.040	0.848	0.00
Infill density	4	18.679	18.679	100.740	0.000	11.80
Nozzle temperature	4	0.014	0.014	0.080	0.786	0.01
Bed temperature	4	0.025	0.025	0.130	0.719	0.02
Printing speed	4	1.979	1.979	10.670	0.004	1.25
Total	24	154.998				97.89
<i>ANOVA for compressive strength</i>						
Layer height	4	0.000	0.000	0.000	0.999	0.00
Wall thickness	4	11.738	11.738	4.530	0.047	4.25
Infill density	4	213.817	213.817	82.470	0.000	77.33
Nozzle temperature	4	3.616	3.616	1.390	0.253	1.31
Bed temperature	4	0.647	0.647	0.250	0.623	0.23
Printing speed	4	0.003	0.003	0.000	0.974	0.00
Total	24	229.820				83.12

4 Conclusions

Using the Taguchi method, this study investigated the effect and optimization of FDM 3D printing parameters on bone screws' build time and compressive strength. These settings included layer height, wall thickness, infill density, nozzle temperature, bed temperature, and printing speed. The results showed that layer height, infill density, and printing speed were the significant parameters affecting the build time, while infill density and wall thickness significantly affected compressive strength. The optimum process parameter settings were determined to minimize build time and maximize compressive strength. The optimal parameter settings for minimizing build time were identified as a layer height of 0.14 mm, a wall thickness of 0.6 mm, an infill density of 20%, a nozzle temperature of 195 °C, a bed temperature of 55 °C, and a printing speed of 60 m/s. On the other hand, the optimal parameter settings for maximizing compressive strength were a layer height of 0.1 mm, a wall thickness of 0.6 mm, an infill density of 100%, a nozzle temperature of 200 °C, a bed temperature of 50 °C, and a printing speed of 30 m/s.

This optimization approach can contribute to the development of high-performance and cost-effective bone screws fabricated using FDM 3D printing. By minimizing build time and maximizing compressive strength, the findings of this study provide valuable insights to guide the design and manufacturing of 3D-printed bone screws for orthopedic applications. Further research could explore the impact

of other factors, such as print orientation and post-processing treatments, on the performance characteristics of 3D-printed bone screws.

References

1. Alafaghani A, Qattawi A (2018) Investigating the effect of fused deposition modeling processing parameters using Taguchi design of experiment method. *J Manuf Process* 36:164–174
2. Lough C, Bezold W, Feltz K, Middleton K, Skelley N, Gieg S (2020) Mechanical comparison of 3D-printed plates and screws for open reduction and internal fixation of fractures. *Orthop J Sport Med* 8. <https://doi.org/10.1177/2325967120S00389>
3. Joseph TM, Kallingal A, Suresh AM, Mahapatra DK, Hasanin MS, Haponiuk J, Thomas S (2023) 3D printing of polylactic acid: recent advances and opportunities. *Int J Adv Manuf Technol* 125:1015–1035
4. Popescu D, Zapciu A, Amza C, Baciuc F, Marinescu R (2018) FDM process parameters influence over the mechanical properties of polymer specimens: a review. *Polym Test* 69:157–166
5. Darji V, Singh S, Mali HS (2023) Mechanical characterization of additively manufactured polymer composites: a state-of-the-art review and future scope. *Polym Compos* 44:4370–4419
6. Junid R, Siregar JP, Endot NA, Razak JA, Wilkinson AN (2021) Optimization of glass transition temperature and pot life of epoxy blends using Response Surface Methodology (RSM). *Polymers (Basel)* 13:3304
7. Mohamed OA, Masood SH, Bhowmik JL (2015) Optimization of fused deposition modeling process parameters: a review of current research and future prospects. *Adv Manuf* 3:42–53
8. Kechagias JD, Vidakis N, Petousis M, Mountakis N (2023) A multi-parametric process evaluation of the mechanical response of PLA in FFF 3D printing. *Mater Manuf Process* 38:941–953
9. Camposeco-Negrete C, Varela-Soriano J, Rojas-Carreón JJ (2021) The effects of printing parameters on quality, strength, mass, and processing time of polylactic acid specimens produced by additive manufacturing. *Prog Addit Manuf* 6:821–840
10. Pachauri S, Gupta NK, Gupta A (2023) Influence of 3D printing process parameters on the mechanical properties of polylactic acid (PLA) printed with fused filament fabrication: experimental and statistical analysis. *Int J Interact Des Manuf* 1–19
11. Elkaseer A, Schneider S, Scholz SG (2020) Experiment-based process modeling and optimization for high-quality and resource-efficient FFF 3D printing. *Appl Sci* 10:2899
12. Giri J, Sunheriya N, Sathish T, Kadu Y, Chadge R, Giri P, Parthiban A, Mahatme C (2024) Optimization of process parameters to improve mechanical properties of fused deposition method using Taguchi method. *Interactions* 245:87
13. eSUN PLA+ filament. <https://www.esun3d.com/pla-pro-product/>. Accessed 26 Feb 2024
14. ASTM Standard (2009) ASTM F 543: standard specification and test methods for metallic medical bone screws
15. Agarwal R, Gupta V, Singh J (2022) Mechanical and biological behaviour of additive manufactured biomimetic biodegradable orthopaedic cortical screws. *Rapid Prototyp J* 28:1690–1705
16. Mia M, Dhar NR (2017) Optimization of surface roughness and cutting temperature in high-pressure coolant-assisted hard turning using Taguchi method. *Int J Adv Manuf Technol* 88:739–753

Microporous of Magnesium/ Hydroxyapatite Coatings on Oxidized High Carbon Co–Cr–Mo Medium-Entropy Alloy for Biocompatibility Improvement



M. N. Amir Akmal , H. Mas Ayu , Rosdi Daud , Juliawati Alias ,
and M. S. Dambatta

Abstract In this work, sol–gel dip coating technique was used to coat magnesium/hydroxyapatite (Mg/HA) slurry with incorporating 10 and 30% of epoxy as binder on high carbon Co–Cr–Mo medium-entropy alloy (MEA). High carbon Co–Cr–Mo MEA which priory have been treated via thermal oxidation at 850 and 1050 °C for 2 h under controlled furnace atmosphere which to create an oxide layer for surface modification purposes. The coating of Mg/HA on oxidized substrate were then investigated by using Field Emission Scanning Electron Microscopy (FESEM) with Energy Dispersive X-ray spectroscopy (EDX) and X-ray Diffraction (XRD) to evaluate the optimum substrate surface condition for further investigation. Findings from this study revealed that oxidation at 1050 °C on high carbon Co–Cr–Mo MEA demonstrates good anchorage for Mg/HA coating layer to adhere on the substrate surface and the presence of magnesium cobalt oxide indicate that substrate surface advantageous to act as antifungal agent to human body. Furthermore, by incorporating 30% of epoxy to Mg/HA slurry has improved the coating morphology. The results showed absent of microcracks and high microporous of Mg/HA with dominating sizes range from 27.9 to 188.5 μm which is believed can promote greater biocompatibility on high carbon Co–Cr–Mo MEA.

M. N. Amir Akmal · H. Mas Ayu (✉)

Faculty of Manufacturing and Mechatronics Engineering Technology (FTKPM), Universiti Malaysia Pahang Al-Sultan Abdullah, 26600 Pekan, Pahang, Malaysia
e-mail: masszee@umpsa.edu.my

R. Daud · J. Alias

Faculty of Mechanical and Automotive Engineering Technology (FTKMA), Universiti Malaysia Pahang Al-Sultan Abdullah, 26600 Pekan, Pahang, Malaysia

M. S. Dambatta

Faculty of Engineering, Kano University of Science and Technology, Wudil, Kano State, Nigeria

Keywords HC Co–Cr–Mo MEA • Thermal oxidation • Magnesium/
Hydroxyapatite slurry • Biomaterial • Sol–gel dip coating

1 Introduction

In order to satisfy the expectations of the medical industry going forward, there is a growing need for a new generation of metallic biomaterials with excellent mechanical and biocompatibility features [1]. The use of Co–Cr–Mo medium-entropy alloy (MEA) in the fabrication of orthopedic and dental implants has grown in popularity recently [2]. The Co–Cr–Mo MEA surfaces are reported in scientific literature to form passive oxide layers that are more stable than the metallic components themselves. This successfully stops the toxicity of the metallic elements from dissolving in the human body by forming a barrier between the implant surface and the abrasive aqueous environment [3]. Although several other research have been published on this subject, their conclusions are still unclear. Specifically, the thermal oxidation effect of high carbon Co–Cr–Mo medium-entropy alloy (HC Co–Cr–Mo MEA) for surface modification prior to biocompatible coatings, such as hydroxyapatite (HA) coating needs serious investigations.

HA is the primary component present in human bone tissue, with a Ca/P ratio of 1.67 and a hexagonal crystal shape. It can be created and applied to orthopedic implants to improve their bioactivity, resistance to corrosion, and osteoconductivity—the capacity to stimulate the formation of new bone [4]. Beside of having excellent biocompatibility and many other potential effectiveness, it is well established that HA coating alone is limited for loading implant applications due to its inherent brittleness [5]. Therefore, many researchers have reported that by incorporating HA with Mg powders can potentially reduce the brittleness as well as enhance healing, thus leading to a more functionally desirable of metallic implant [6, 7].

Despite the literature showing publications associating Mg/HA coating for biomaterial implants such as regeneration of bone tissue and speed up bone ingrowth, so far, no study has been found associating Mg/HA slurry with incorporating epoxy as binder on HC Co–Cr–Mo MEA to enhance biocompatibility as proposed in this study. Furthermore, the effect of surface modification via thermal oxidation on HC Co–Cr–Mo MEA prior to Mg/HA coating was not yet evidenced. Therefore, the objective of this study was to obtain optimum slurry of Mg/HA with epoxy before deposited on thermally treated HC Co–Cr–Mo MEA via sol–gel dip coating technique, to enhance biocompatibility properties of this metallic implant. The following clarifies the study's specifics.

2 Materials and Methods

The material utilized in this study was a 14 mm diameter round bar of high carbon Cobalt-Chromium-Molybdenum medium-entropy alloy (HC Co–Cr–Mo MEA) biomedical grade (ASTM F1537). Carpenter Technology Asia Pacific provided the following material compositions (in weight percentage): Cr: 29.6, Mo: 6.5, Si: 0.7, Ni: 0.1, Fe: 0.12, Mn: 0.7, C: 0.24, N: 0.16 and Co: equilibrium. A Buehler, Isomet 4000 precision cutter was used to cut the bar into a 2 mm thick disk. The disk cylinder faces were cleaned ultrasonically with acetone after being wet ground through a 1000 mesh screen. $R_a = 0.1 \pm 0.02 \mu\text{m}$ is the initial average of substrate surface roughness. Thermal oxidation was used to modify the surface in a muffle furnace for two hours at 850 and 1050 °C, which is below the HC Co–Cr–Mo MEA substrate's annealing temperature of 1121 °C [8, 9].

Magnesium (Mg) and hydroxyapatite (HA) micron-sized powders with respective purity levels of 99 and 90% were purchased from Sigma Aldrich. Diglycidyl ether of bisphenol A (DGEBA) resin (Araldite LY556) was utilized as epoxy resin and was purchased from Huntsman. Triethylenetetramine (HY951), a hardener, was acquired from Permula Chemical. The slurry mixture of Mg:HA followed the 1:1 ratio (10 g:10 g) to ensure a homogeneous and well-dispersed of 28 mL ethanol with epoxy binder mediums were prepared. The mixing ratio of epoxy resin solution is 2:1 epoxy to hardener comprising the weight of epoxy-saturated resin of 10 and 30%. The Mg/HA slurry consists of an epoxy binder magnetically stirred for 3 h 30 min at a speed of 2000 rpm to avoid particle aggregation. The oxidized substrate of HC Co–Cr–Mo MEA were then dipped in the Mg/HA slurry coating at fixed dipping and withdrawal speeds of 200 mm.min⁻¹ using HTWL-01 Desktop Dip Coater (MT1 Cooperation, USA) at room temperature. Once dried at room temperature, the next layer of coating takes place to produce the desired coating thickness. The coating deposition process was repeated for 5 times.

HC Co–Cr–Mo MEA and Mg/HA coatings on oxidized substrate were subjected to surface morphology analysis using a Field Emission Scanning Electron Microscope (FESEM, JEOL JSM-7800F, JEOL, Japan) that was operated at a 5 kV accelerating voltage. Energy Dispersive X-ray Spectroscopy (EDX, LSM880-FESEM, Carl Zeiss AG, Germany) was used to analyze elements. Using Cu K α radiation ($\theta = 1.54060 \text{ \AA}$) operated at 45 kV and 40 mA in the angle range of 20°–70° of 2θ , X-ray diffraction (XRD, Bruker D8 Model 2016, Berlin, Germany) was used to examine the crystal structure of the coated substrate. A 2° incident angle was used to gather all of the patterns in order to reduce substrate interference.

3 Results and Discussion

Structural and morphological characteristics. Figure 1 shows the corresponding EDX spectra and the FESEM images of thermally oxidized HC Co–Cr–Mo MEA. It is thought that the metallic element that reacts at a specific temperature and the thermal oxidation process control the variety in the formed shapes, sizes, and surface textures. The topographies micrographs revealed that microporous of HC Co–Cr–Mo MEA at 1050 °C surface differed significantly from the HC Co–Cr–Mo MEA at 850 °C. The thermally treated substrate at 850 °C (Fig. 1a—left) exhibited like prismatic crystallites that can be seen with oriented characteristic of chromium oxide (Cr_2O_3), indicating the formation of chromia scale (dark green) takes place predominantly by outward growth. The ImageJ software is used to calculate the average grain sizes which is 1.753 μm and the dominating sizes range from 0.967 to 2.394 μm (data not presented). The EDX mapping of the oxidized surface at 850 °C is also presented in Fig. 1a—right as a qualitative estimate, due to it does not represent the entire substrate surface. The presence of dominating element of chromium (Cr), manganese (Mn), oxygen (O) and cobalt (Co) with weight percentages of 37.96, 28.50, 26.08 and 5.82, respectively, confirmed the high amount of chromium oxide (Cr_2O_3) compared to manganese cobalt oxide (MnCo_2O_4) (XRD data not presented) [10].

This phenomenon occurred due to chromium and manganese has high reactivity and easily react with oxygen during thermal oxidation process above 500 °C [11, 12]. Conversely, the preferential development across grain boundaries cannot continue indefinitely because the oxygen diffusion distance in the Cr_2O_3 protrusions eventually grows to a size that promotes growth at the ridge bases. Since the height of these ridges is constrained, this may be the cause of the absence of pores in the majority of the oxide layer [13, 14].

Meanwhile, at 1050 °C (Fig. 1b—left), the oxide layer appeared to have smaller particle sizes and more interconnected micropores with adjacent spherical structures. Naturally, porous structure is preferable because of better anchorage for coating adhesion on the substrate surface. Further inspection observed that the average particle sizes vary between 0.323 and 0.621 μm , but smaller particles are also observed, with sizes from 0.149 to 0.281 μm (data not presented). It is worth to note that at high temperature of oxidation, these oxide scales have an enormous ability to deform from prismatic crystallites into smaller spherical grains with micropores. It is believed that at this stage, inward diffusion of oxygen takes place and perforate the ridges, leading to the formation of small gaps and micropores [14]. However, given the previously stated substrate color and oxide temperature, neither spallation nor cracking of the oxide scale was seen.

The corresponding EDX in the selected sites for oxidized substrates at 1050 °C is also shown in Fig. 1b—right. The mapping images revealed a significant difference of weight percentage compared to oxidize substrate at 850 °C. The spectra display the corresponding peaks dominant by cobalt (36.00 wt.%) followed by oxygen (28.08 wt.%), chromium (26.03 wt.%) and lastly, manganese (4.69%). This scenario clearly reflects that oxidation at higher temperature has donate sufficient energy to excite

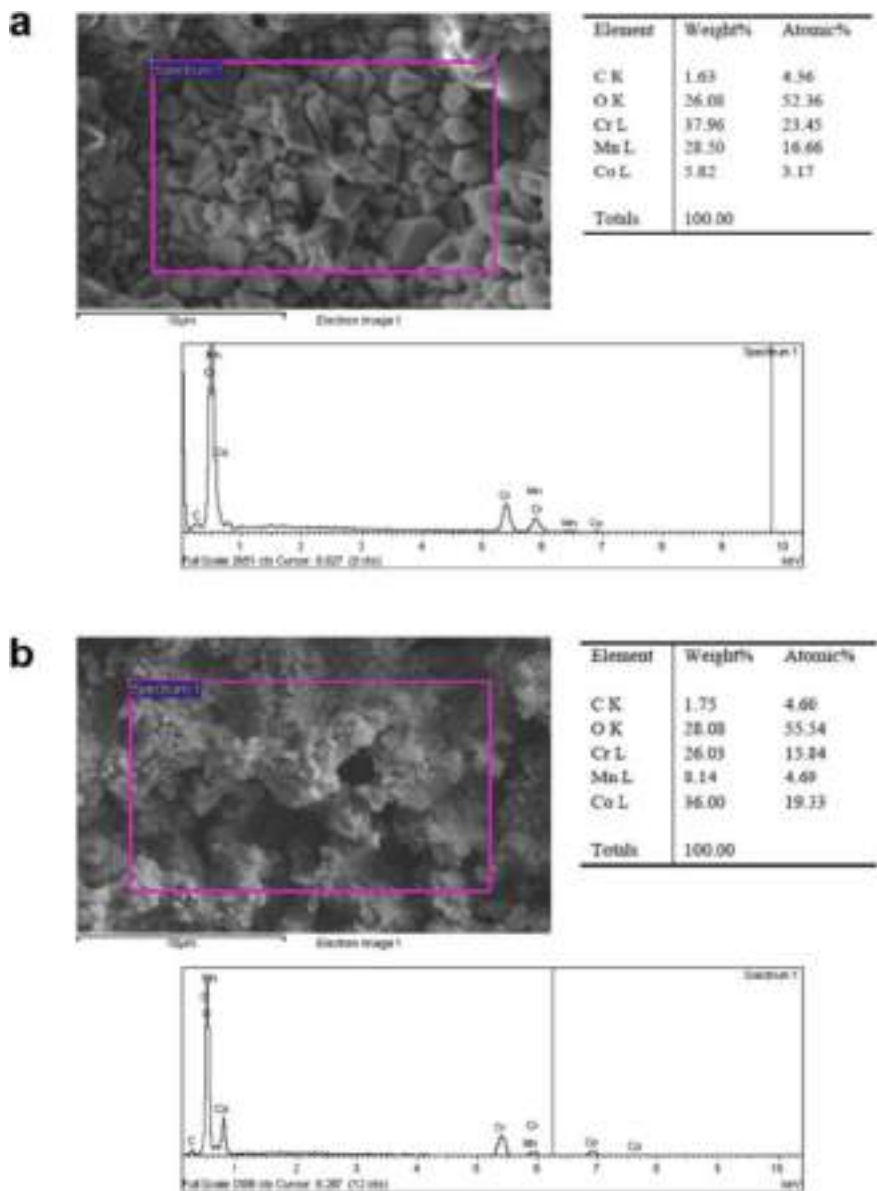


Fig. 1 FESEM micrographs of thermally oxidized of HC Co–Cr–Mo MEA indicating morphology at **a** 850 °C and **b** 1050 °C for 2 h with their corresponding EDX spectrum of element present. The images were recorded at the magnification of 10,000x (left)

cobalt element to form into cobalt chromate (CoCr_2O_4). Beside that, Cr_2O_3 and $\text{Mn}_{1.5}\text{Cr}_{1.5}\text{O}_4$ oxide were also detected in XRD results (data not presented) [10]. These findings in line with elements discovered in EDX results.

The FESEM micrographs demonstrate how the oxidation temperature has an impact on the oxide layer's size and form, as was previously mentioned. It is believed that the formation of the hexagonal phase at lower oxidation temperature is the initial stage of chromium crystallization which also enhanced by adsorption of atomic oxygen. It is well established that free energy of the hexagonal chromium is lower than the cubic chromium [12]. As a result, the hexagonal structure becomes stable and tightly-packed structure as shown in Fig. 1a—right. While the temperature increase, chromia scale (Cr_2O_3) become unstable and evolves into small-sized crystallites resulting in the transformation of hcp chromium into bcc chromium [15, 16]. Change of the chromium phase structure by the specified temperature is also accompanied by a change of the substrate surface such as increment of surface roughness and emergence of micropores (Fig. 1b—left).

Figure 2 presents the image of Mg/HA coatings on oxidized HC Co–Cr–Mo MEA revealing the formation of microporous structures and by incorporating 30% of epoxy no microcracks are visible. The EDX results also confirm the deposition of Mg/HA coatings on all oxidized substrates. As shown in Fig. 2a and c—left, microcracks were evident on the coating surface. It can be noted, despite incorporating 10% of epoxy, the coating still shows breakdown outspread on the surface. The present of severe cracks on coating surface can interfere with the sustainability of the coating for further biocompatibility testing. Even though microporous are desirable for bone ingrowth and cell adhesion, yet these defects is not tolerable under rigorous environment in human body due to delamination of coatings will occurs [7].

Meanwhile, the addition of 30% of epoxy into Mg/HA slurry significantly improve the coating quality which can be attributed to the absence of microcracks as shown in Fig. 2b and d—left. In Fig. 2b, it can be noted that Mg/HA coating has average of micropores that vary between 54.7 and 108.3 μm . While in Fig. 2d, the micropores having an average size between 27.9 and 186.5 μm which are greater number of porosities in the range scattered on the oxidized of HC Co–Cr–Mo MEA at 1050 °C compared to 850 °C.

XRD analysis in Fig. 3 showed the phases of cobalt oxide (CoO), magnesium oxide (MgO), magnesium (V) oxide (MgO_2), chromium (VI) oxide (Cr_1O_3), cobalt molybdenum (Co_3Mo_1), magnesium cobalt oxide (MgCoO) and cobalt chromium (CoCr) on HC Co–Cr–Mo MEA after 5 layers of Mg/HA coating deposition. All samples showed similar XRD spectra after Mg/HA coating on HC Co–Cr–Mo MEA, which suggested a consistent formation of highly crystallized magnesium and cobalt on the substrate surface. Although both coated substrates have the favorable characteristics which believed can accelerate osteoconduction and osteointegration processes in bone tissues [1, 10] but further investigation revealed that only coated substrate that oxidized at 1050 °C have formation of magnesium cobalt oxide (MgCoO), as observed in the XRD pattern (Fig. 3). It is believed that MgCoO have advantageous to prevent cell cancer and act as antifungal agent to human body [17]. Previous researchers also reported that when magnesium and cobalt were present in the same

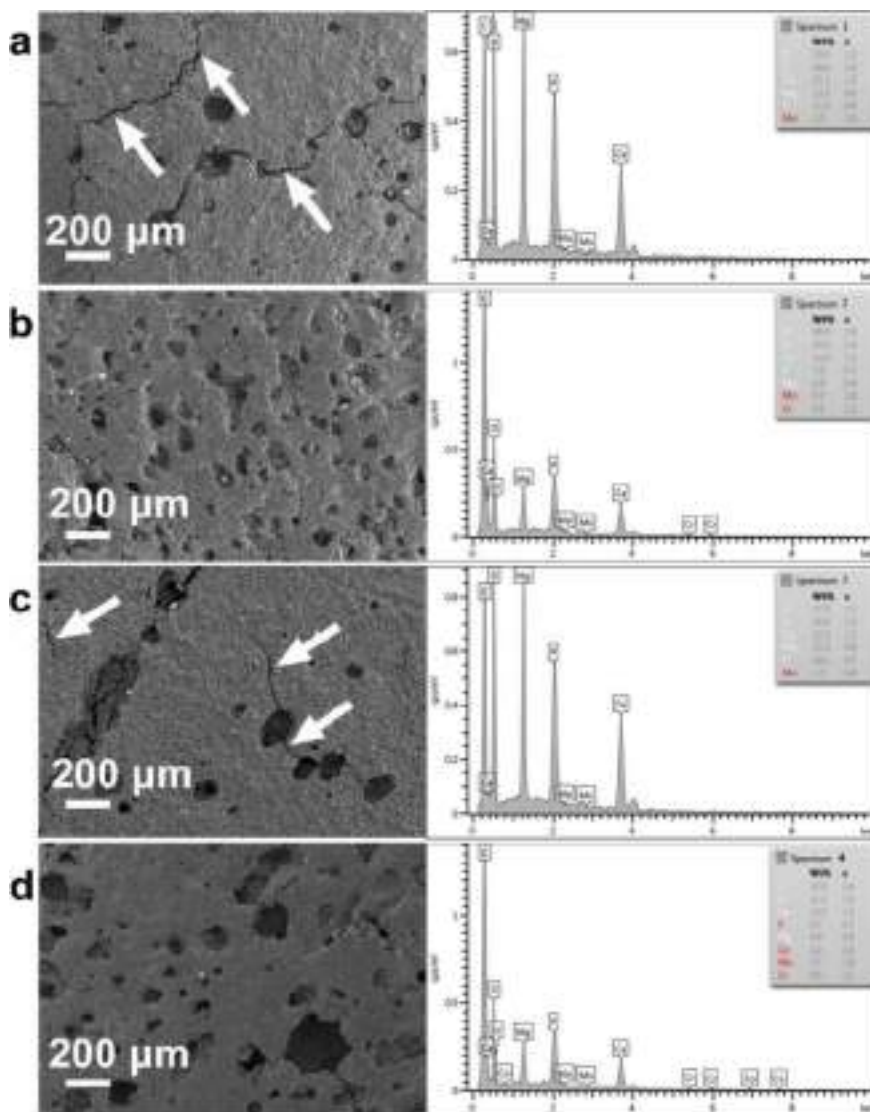


Fig. 2 The FESEM micrographs and EDX spectrum of Mg/HA coating on oxidized HC Co–Cr–Mo MEA alloy **a** 850 °C with 10% epoxy, **b** 850 °C with 30% epoxy, **c** 1050 °C with 10% epoxy and **d** 1050 °C with 30% epoxy

reaction mixture, they behaved competitively toward each other, and the competition profile altered depending on the relative concentrations of the metals [5]. Therefore, both elements were concluded to combine and react at high temperature oxidation and formed into magnesium and cobalt phases which believed can promote greater

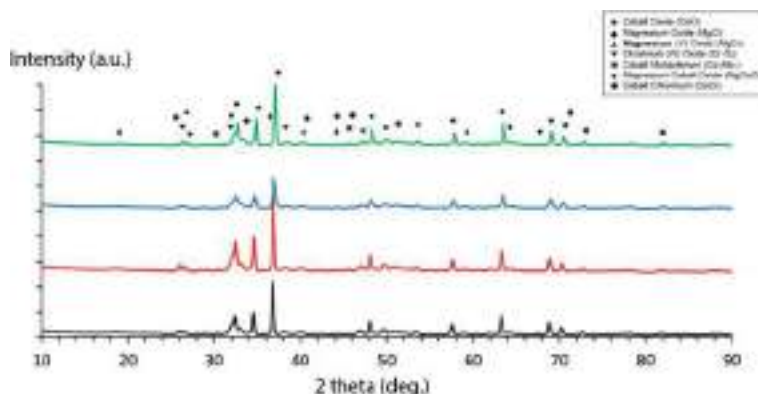


Fig. 3 The XRD pattern of Mg/HA coating on oxidized HC Co–Cr–Mo MEA alloy **a** 850 °C with 10% epoxy, **b** 850 °C with 30% epoxy, **c** 1050 °C with 10% epoxy and **d** 1050 °C with 30% epoxy

biocompatibility and improve the properties of the HC Co–Cr–Mo MEA in this study [18].

4 Conclusions

In this study, magnesium/hydroxyapatite (Mg/HA) slurry with incorporating 10 and 30% of epoxy as binder was coated on oxidized high carbon Co–Cr–Mo medium-entropy alloy (MEA) at 850 and 1050 °C. The presence of Cr_2O_3 layer was observed in all oxidized substrates with no evidence of oxide scale spallation or cracking occurred. However, it is worth noting that best Mg/HA coating was on oxidized substrate at 1050 °C with incorporating of 30% epoxy. The reasons are due to variation sizes of microporous and formation of magnesium cobalt oxide (MgCoO) on the substrate. It has been suggested that MgCoO advantageous to act as antifungal agent to human body. These findings allow for further thorough research to confirm the relationship between these oxide layers and the in-vitro testing's release of hazardous ions. All things considered, the published results can offer pertinent information on the HC Co–Cr–Mo MEA, which can be used as a secure implant material in biological applications.

Acknowledgements Universiti Malaysia Pahang Al-Sultan Abdullah (UMPSA) fully supports the facilities and resources for this research. The authors would like to acknowledge the financial support of the internal grants of Universiti Malaysia Pahang Al-Sultan Abdullah (RDU230317 and RDU230345).

References

1. da Luz Belo F et al (2023) Additive manufacturing of poly (lactic acid)/hydroxyapatite/carbon nanotubes biocomposites for fibroblast cell proliferation. *Sci Rep* 13(1):20387
2. Gurel S et al (2022) From corrosion behavior to radiation response: a comprehensive biocompatibility assessment of a CoCrMo medium entropy alloy for utility in orthopedic and dental implants. *Intermetallics* 149:107680
3. Mas Ayu H et al (2019) Improving biocompatibility of cobalt based alloy using chemical etching and mechanical treatment. *Materialwiss Werkstofftech* 50(3):254–259
4. Sheykholeslami SOR et al (2024) Innovative hydroxyapatite/submicron mesoporous SiO₂/HA particles composite coatings for enhanced osteogenic activity of NiTi bone implants: a comprehensive investigation of materials and biological interactions. *Ceram Int* 50(12):21289–21303
5. Tian Q et al (2019) Nano-to-submicron hydroxyapatite coatings for magnesium-based biore-sorbable implants—deposition, characterization, degradation, mechanical properties, and cytocompatibility. *Sci Rep* 9(1):810
6. Wan P et al (2021) Construction of bio-functional Mg/HA composite layered coating for orthopedic application. *Sci China Technol Sci* 64(11):2541–2550
7. Xue ZY et al (2024) Greatly enhanced corrosion/wear resistances of epoxy coating for Mg alloy through a synergistic effect between functionalized graphene and insulated blocking layer. *J Magnes Alloys* 12(1):332–344
8. Baddar BI et al (2020) Hydroxyapatite and thermal oxidation as intermediate layer on metallic biomaterial for medical implant: a review. *J Adv Res Fluid Mech Therm Sci* 62(1):138–150
9. Hassan MA et al (2017) In-vitro biocompatibility study of hydroxyapatite coated on Co–Cr–Mo with oxide interlayer. *Jurnal Teknologi* 80
10. Matula G et al (2021) Structure and properties of Co–Cr–Mo alloy manufactured by powder injection molding method. *Materials* 14(8):2010
11. Hallström S et al (2013) High temperature oxidation of chromium: kinetic modeling and microstructural investigation. *Solid State Ionics* 240:41–50
12. Latu-Romain L et al (2017) Towards the growth of stoichiometric chromia on pure chromium by the control of temperature and oxygen partial pressure. *Corros Sci* 126:238–246
13. Li H et al (2020) Microstructural features of biomedical cobalt–chromium–molybdenum (CoCrMo) alloy from powder bed fusion to aging heat treatment. *J Mater Sci Technol* 45:146–156
14. Sun L, Fu Q-G, Sun J (2020) Effect of SiO₂ barrier scale prepared by pre-oxidation on hot corrosion behavior of MoSi₂-based coating on Nb alloy. *Corros Sci* 176:109051
15. Bedolla-Hernández M et al (2022) Electrodeposition mechanism of chromium nanoparticle coatings: modeling and experimental validation. *Chem Eng Sci* 252:117291
16. Basha M et al (2023) The effect of Si addition on the microstructure, mechanical properties, and wear rate of the Co–Cr–Mo-based biomedical alloys. *SILICON* 15(16):6963–6969
17. Luque-Agudo V et al (2020) The role of magnesium in biomaterials related infections. *Colloids Surf B* 191:110996
18. Zhang Y et al (2023) Enhancing the mechanical property of laser powder bed fusion CoCrMo alloy by tailoring the microstructure and phase constituent. *Mater Sci Eng A* 862:144449

Influence of Different Materials on Inductance Values of Vitroperm 500 at High Temperature Annealing



Murshidi Mdzuki, H. Mas Ayu, S. Mohd Mawardi, and Rosdi Daud

Abstract The purpose of this study is to evaluate the effect of mild steel as dummy with various heights on the inductance value of core. The experiment is performed according to standard operation procedure used in VACUUMSCHMELZE (M) SDN. BHD. (VAC) production line and all parameters such as core weight, tension of core and temperature process are controlled based on the actual practice for specific core production. The VITROPERM 500 (Fe–Cu–Si–X) strip was used as the main material and the magnetic field annealing process was carried out using magnetic field annealing furnace. As for the inductance value measurement, a UNITESTER test machine which developed by VAC was used to measure the inductance value for each core after the heat treatment process for 12 h duration. Prior to the annealing process, a test on the magnetic field strength inside the furnace was done to check the strength of magnetic field where the data indicate a non-linear strength along the furnace, which is the strength will be greater at the middle (1.85 kA/cm) and lowest at the bottom of the furnace (1.70 kA/cm) where the cores is placed. Quantitative analyses showed the inductance value of bottom core decreased greater than 10% as compared to the neighboring core with the absence of the mild steel. One should keep in mind that the value for the tested cores is not specified, only the deviation of the inductance value of bottom core will be considered. This phenomenon occurred due to the attraction strength of bottom dummy towards the magnetic field. Further

M. Mdzuki · H. Mas Ayu (✉)

Faculty of Manufacturing and Mechatronics Engineering Technology (FTKPM), Universiti Malaysia Pahang Al-Sultan Abdullah, 26600 Pekan, Pahang, Malaysia
e-mail: masszee@umpsa.edu.my

M. Mdzuki

Department of Engineering, Vacuumschmelze (M) Sdn. Bhd., 26600 Pekan, Pahang, Malaysia

S. Mohd Mawardi

Faculty of Electrical and Electronics Engineering Technology (FTKEE), Universiti Malaysia Pahang Al-Sultan Abdullah, 26600 Pekan, Pahang, Malaysia

R. Daud

Faculty of Mechanical and Automotive Engineering Technology (FTKMA), Universiti Malaysia Pahang Al-Sultan Abdullah, 26600 Pekan, Pahang, Malaysia

experiment was done to evaluate the effect of different height of mild steel and it is worth to note that various height of mild steel does not gives any significant effect on the inductance value of core.

Keywords Magnetic heat treatment • Transverse field • Inductance value • Mild steel • Vitroperm 500

1 Introduction

Fe-based nanocrystalline have been reported to have excellent properties of soft magnetic, including low core loss value (P_{core}), which include hysteresis loss and eddy current loss, and high effective permeability (μ_e) at high frequencies which can satisfy the development of electronic devices [1]. From the previous studies, increased of Fe content effectively will increases the magnetization flux density (B_s) of pure Fe-based amorphous alloys [2–4]. Nanocrystalline VITROPERM 500 (VP500) has been used recently to produce inductive components and cores which including common mode of chokes, gate drive transformers, current transformers, amorphous and nanocrystalline cores.

The standard procedures are VP500 strip will undergo several processes such as winding process and tools setup before convey to next process such as heat treatment (HT). The HT process is crucial as it can affect the magnetic value of the core (nanocrystalline alloy) after thermally treated for several hours [5, 6]. The presence of a transverse field during HT process can modify the magnetic properties of VP500 by inducing anisotropies and softening the Fe-rich nanocrystalline into soft magnetic alloys which give the inductance value to the individual core. Nevertheless, the transverse field strength inside the furnace may be varies during HT process due to the design of the furnace and the characteristic of the induced magnetic field [7–9]. However, the effect of the magnetic field strength on the microstructure of VP500 before and after HT process was not yet evidenced.

In the light of the background provided herein, an investigation on the influence of different height of mild steel and alloy steel used as dummy on VP500 core after undergone a magnetic field annealing process will be conducted. Details of the study are elucidated as follow.

2 Materials and Methods

In this study, a comparison of inductance values of bottom core using different types of material as dummy such as mild steel (ST37), ceramic and stainless steel (SS304) to stack the nanocrystalline VITROPERM 500 (VP500) core will be carried out. The current design and practice at VAC production line required the use of ST37 dummy. Initial experiment was done to see any influence of the material that touching the

bottom core without concerning the shape or height of the material. The experiment using combination of three small ceramics to hold the core in position is to make sure the bottom surface of bottom core does not touch any metal and to make a comparison with the standard practice. This small type of ceramics is used as it is common at VAC production line. No single cylinder ceramics is used due to non-availability and the high manufacturing cost for new size ceramic. This experiment also shows the importance of suitable material which can influence the deviation of inductance value of the bottom core. Annealing tools which also made up from stainless steel needle and pipe (SS304) are needed for each dummy material to hold the VP500 core vertically in rack. The diameter of the pipe is 1 mm smaller than the internal diameter of the cores to hold and to make sure a good alignment of the stacking cores. The needle was designed with a 12 mm step diameter near the bottom end to place a washer on top of it to act as a base for the bottom dummy. The dummy was placed at the bottom of the annealing needle with at least 90 pieces of VP500 core on top of it. The setup for the annealing tool and cores is illustrate in Fig. 1. The annealing needle was then placed on the annealing rack before undergone a magnetic field annealing process for 12 h with 1 h holding time at 570 °C and then 3 h holding time at 395 °C. A transverse field is turned on for 3 h 43 min before the process end. This procedure is based on the instructional card and the guideline provided by the production line (instructional card not provided).



Fig. 1 The setup for annealing tools and the position of bottom core and dummy

In order to identify the inductance value of individual cores at 10 kHz, each core was tested using unitester machine and the data was plotted in point graph. UNITESTER is a tester that was developed and used only by VAC in their production line. It uses the 4-wire principle for the measurement where the core will be fitted with a primary winding for feeding in the measuring current (drive) and a separate secondary plug-in winding for sensing the measuring voltage (sense). Both measuring connections are located and connected in the immediate vicinity of the winding ends. Before the evaluation of the inductance value, predetermined values of 10 kHz frequency, and 26.2 mA current must be specified (VAC Technical Data Sheet). The inductance value will be generated based on the formulae programmed inside the UNITESTER. The core setup during measurement using UNITESTER is shown in the Fig. 2. The value of inductance was measured from the top core to the bottom core along the annealing tool. The dummy material that shows the lowest value of variation for the bottom core is chosen for further analysis.

In this case, the material dummies of mild steel (ST37) are chosen to further investigate the effect of dummy material with different heights on the inductance value of core. The dummy with hollow round bar, having same dimension of outer and inner diameter, which is 40 mm and 25 mm respectively, but different in heights such as 15 and 45 mm were used. Another experiment with alloy steel (AISI4140) dummies is made as a comparison. The selection of alloy steel is due its low cost and are known as a common material in heavy engineering industries [10]. It is widely used for its high compressive strength and favorable mechanical characteristics [11].

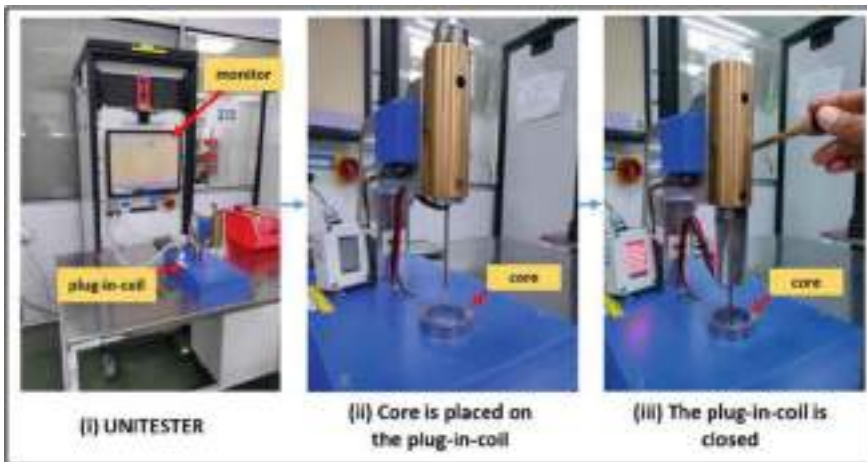


Fig. 2 The UNITESTER unit and the core setup. The inductance value will be displayed on the monitor when the plug-in-coil is closed

3 Results and Discussion

Result from the experimental works indicated a significant effect of different materials on the inductance value of core. However, it is worth to note that regardless of any material, that height of dummy does not affect on the inductance value. Therefore, for further investigation, only 15 mm of dummy height was applied on both materials. The average deviation of inductance value of individual core as compared to the top position core is around 1%. Despite that, the ST37 showed the lowest variation of inductance value which is about 10%, followed by SS304 up to 25%, and lastly, ceramic which approximately 50% as shown in Fig. 3. This phenomenon happened due to the dummy material which have its own attraction strength towards magnetic force, yet the strength of the magnetic attraction which can give the least deviation of inductance value of bottom core is not defined.

The magnetic field strength inside the furnace may affect the inductance value of individual cores along the annealing needle. A magnetic strength test using 2000 A current was done with the reading taken from the bottom to the top of the furnace, at different radius point. The graph showed in Fig. 4 reveled a curvature shape of magnetic field strength inside the furnace during annealing process. It is believed that due to the design of the furnace, the magnetic strength is higher in the middle and significantly reducing at the bottom and top of the furnace. The graph also indicates the greater magnetic strength observed at the outside of the rack (to hold the needle and core) and decreasing towards the center. According to on the magnetic field strength formula, this was true as the value decrease inversely with the radial distance [12]. Based on the results obtained, the magnetic field strength at the bottom,

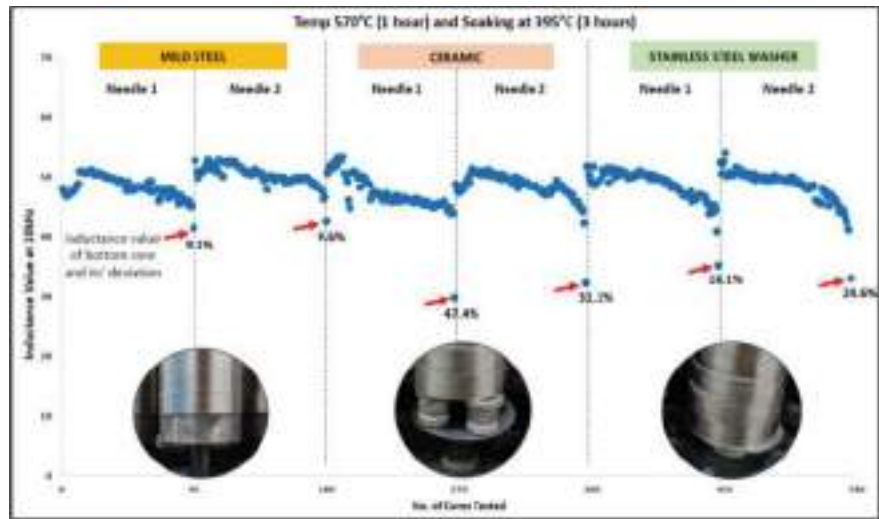


Fig. 3 Inductance value of test core after heat treatment process using different types of dummy material

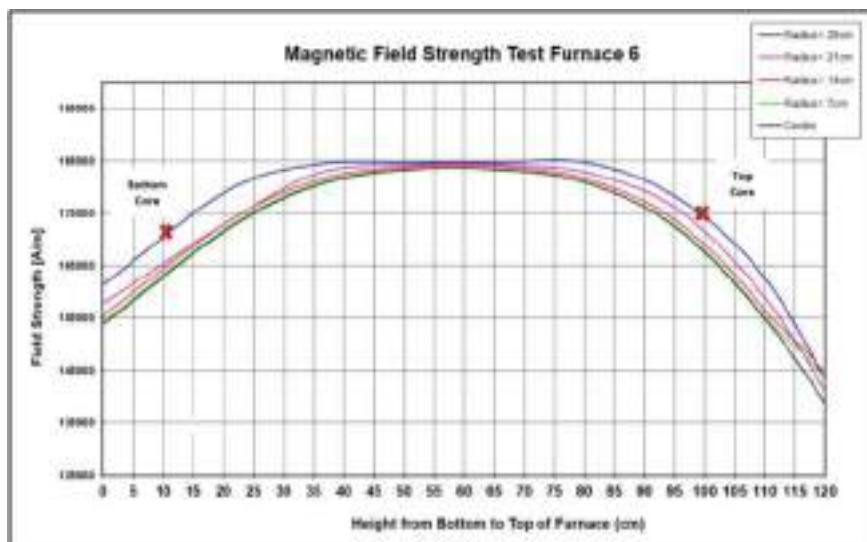


Fig. 4 The magnetic field strength test reveals a variation in field intensity along the vertical axis of the furnace. Here, X represents the measurement position, and the field is applied at both the top and bottom cores

middle and top position was recorded around 1.70 kA/cm, 1.85 kA/cm and 1.76 kA/cm respectively.

It is also confirmed that by applying different height of mild steel dummy, it shows no evident of deviation of inductance value of the bottom core and neighboring core as shown in Fig. 5. The inductance value of both cores at the bottom showed a deviation value more than 10% as compared to other cores which is less than 2%. The value for both cores is around 68 μH which is out of specification limit. These results strengthen the initial theory that material plays the important role that affect the value of bottom core as it can result in substantial distortion in the uniformity of the magnetic field [13].

Further experiment using alloy steel and mild with 15 cm height was done and the inductance value is recorded as shown in Fig. 6. The value for bottom cores both is around 77 μH and 75 μH for alloy steel and indicates the deviation of bottom core values of 10.1% and 7.5% respectively. The value for bottom cores for mild steel is 71.2 and 78.6 μH and indicates the deviation of 15.7 and 16.8%. The deviation with alloy steel is reduced as compared to mild steel dummy but still high when compared to the average deviation of other cores measurement which is less than 2%. The better attraction of alloy steel towards magnetic field may improves the inductance value and the deviation of inductance value based on result shown in Fig. 5. From the findings, it is noted that the similar pattern of inductance value after magnetic field annealing process where the values are decreasing towards the bottom of the needle. This reveals the influence of the mechanical stress on the individual core might impact the inductance values.

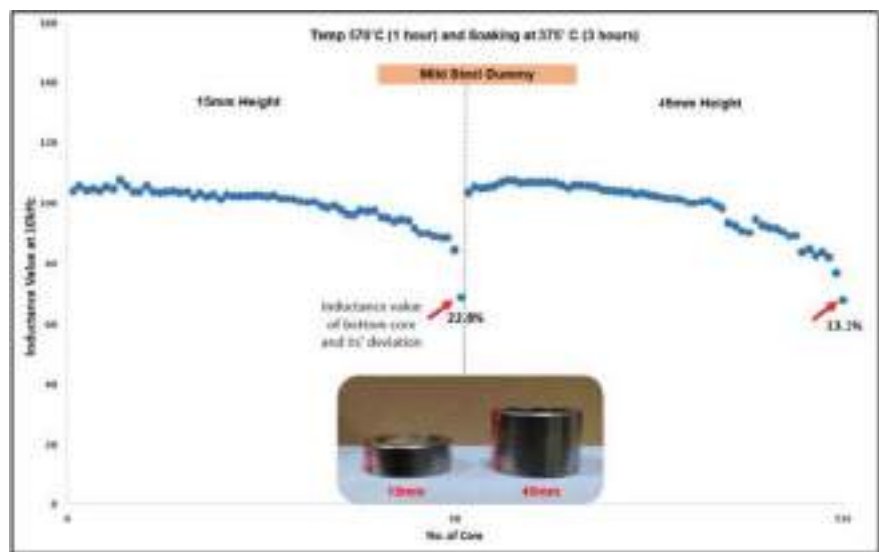


Fig. 5 Inductance value of test core after HT process using different height of mild steel dummy

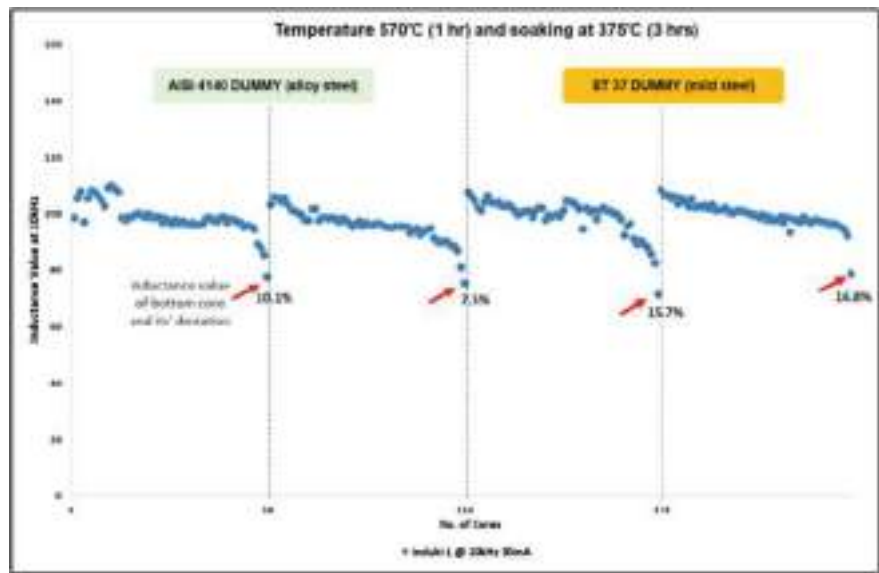


Fig. 6 Inductance value of test core deviations after annealing process on AISI 4140 and ST37 as dummy material under conditions of 570 °C for 1 hour and soaking at 375 °C for 3 hours. Indicated with red arrows, are the inductance value measured at the bottom core dummy.

4 Conclusion

In this study, the inductance value of the bottom core after magnetic field annealing process reveals the importance of suitable material for the dummy in order to reduce rejected core after HT process. The different of dummy height gives no advantage to reduce the variation of the inductance value. The weight exert on the core may affect the inductance value of individual cores but did not show any direct relation with the high deviation at the bottom core. These results enable additional extensive investigations to validate the elements of mild steel material with the inductance value of bottom core.

Acknowledgements Universiti Malaysia Pahang Al-Sultan Abdullah (UMPSA) fully supports the facilities and resources for this research. The authors would like to acknowledge the financial support from the industrial grants (UIC240802) collaboration between Vacuumschmelze (M) Sdn. Bhd. and Universiti Malaysia Pahang Al-Sultan Abdullah.

References

1. Silveyra JM et al (2018) Soft magnetic materials for a sustainable and electrified world. *Science* 362(6413):eaao0195
2. Makino A et al (2008) FeSiBP bulk metallic glasses with high magnetization and excellent magnetic softness. *J Magn Magn Mater* 320(20):2499
3. Luborsky F, Becker J (1980) Origin of magnetic properties in amorphous metals. DTIC Document
4. Yue SQ et al (2019) Magnetic and thermal stabilities of FeSiB eutectic amorphous alloys: compositional effects. *J Alloys Compd* 77:833
5. Li HX et al (2019) Fe-based bulk metallic glasses: glass formation, fabrication, properties and applications. *Prog Mater Sci* 103:235
6. Suryanarayana C, Inoue A (2013) Iron-based bulk metallic glasses. *Int Mater Rev* 58(3):131
7. Zhao CL et al (2021) Nano-heterogeneity-stabilized and magnetic-interaction-modulated metallic glasses. *Sci China Mater* 64(7):1813
8. Zhao CL et al (2018) Significant improvement of soft magnetic properties for Fe(Co) BPSiC amorphous alloys by magnetic field annealing. *J Alloys Compd* 742:220
9. Wang F et al (2017) Soft magnetic Fe–Co-based amorphous alloys with extremely high saturation magnetization exceeding 1.9 T and low coercivity of 2 A/m. *J Alloys Compd* 723:376
10. Pinder LW et al (2010) High temperature corrosion of low alloy steels. *Ref Module Mater Sci Mater Eng*. Elsevier
11. Sathish T et al (2022) Experimental investigation on tribological behaviour of AA6066: HSS-Cu hybrid composite in dry sliding condition. *Adv Mater Sci Eng*, p 1
12. Filippopoulos G, Tsanakas D (2005) Analytical calculation of the magnetic field produced by electric power lines. *IEEE Trans Power Deliv* 20(2):1474
13. Roy SB (2017) Chapter 21—Materials in a high magnetic field, materials under extreme conditions, pp 755–789. ISBN 9780128013007
14. Ogawa Y et al (2006) Magnetic properties of high Bs Fe-based amorphous material. *J Magn Magn Mater* 304(2):e675
15. Wang AD et al (2015) Fe-based amorphous alloys for wide ribbon production with high Bs and outstanding amorphous forming ability. *J Alloy Compd* 630:209

Investigating the Impact of Lean Practices and Industry 4.0 Technologies Towards Operational Performance



Sharah Qistina Shari Fuzzaman, Noraini Mohd Razali, and Kartina Johan

Abstract The integration of Industry 4.0 technologies and Lean practices in Malaysia's manufacturing industry is the subject of this study. The primary objective is to investigate how incorporating these practices might enhance operational effectiveness, lower expenses, and enhance product quality. A survey was developed and distributed to various manufacturing firms, collecting both qualitative and quantitative data on the application and perceived benefits of Lean Practices such as 5S, Kanban, and Just-in-Time (JIT), as well as Industry 4.0 technologies including the Internet of Things (IoT), Big Data Analytics and Cloud Computing. Data analysis was performed using Excel to identify patterns and correlations. The findings show that the combined use of Lean Practices and Industry 4.0 Technology leads to a significant increase in operational efficiency, cost reduction and product quality improvement with a percentage of response to the perceived impact of 75%, 89% and 96%, respectively. It was also found that 5S and system integration are the most frequently implemented practices in the industry compared to other practices. However, challenges such as integration strategies and infrastructure limitations were also identified. The study concludes that although the integration between Lean and Industry 4.0 offers great benefits, addressing the challenges highlighted is essential to maximize their potential in the manufacturing sector.

Keywords Lean practices · Industry 4.0 · Manufacturing · Operational performance

S. Q. S. Fuzzaman · N. Mohd Razali (✉) · K. Johan
Faculty of Manufacturing and Mechatronic Engineering Technology, Universiti Malaysia Pahang
Al-Sultan Abdullah, Kuantan, Pahang, Malaysia
e-mail: noraininmr@gmail.com

© The Author(s), under exclusive license to Springer Nature Singapore Pte Ltd. 2025
M. R. Mohamad Yasin et al. (eds.), *Proceedings of the 7th Asia Pacific Conference on Manufacturing Systems and 6th International Manufacturing Engineering Conference—Volume 2*, Lecture Notes in Mechanical Engineering,
https://doi.org/10.1007/978-981-96-5690-5_7

1 Introduction

This study investigates the impact of Lean Practices and Industry 4.0 Technologies on the operational performance within the manufacturing sector in Malaysia. Through a comprehensive survey questionnaire, we collected data to analyze the impact and implementation of these methodologies. The survey was distributed primarily via LinkedIn, utilizing direct messages and public posts, with additional dissemination through direct email. Out of approximately 350 targeted respondents, we successfully obtained 53 responses from a diverse range of manufacturing companies, including both multinational corporations (MNC) and small and medium enterprises (SME). The collected data was meticulously analyzed using Excel, providing insights into how Lean Practices and Industry 4.0 Technologies are employed to optimize operational performance.

1.1 *Lean Practices and Industry 4.0 Technologies*

Originating from the Toyota Production System, Lean practices, which incorporate ideas and methods for waste reduction, continuous improvement, and overall efficiency, have developed into a comprehensive operational philosophy. This methodology, often referred to as Lean, extends beyond the manufacturing sector, gaining widespread acceptance across various industries in recent years [1, 2].

At its core, Lean is a set of management concepts created to reduce waste in the production process and maximize the flow of activities deemed important to the final product. This approach has witnessed significant acknowledgement in the manufacturing sector and has progressively expanded its influence into diverse industries [1, 2].

The implementation of Lean Practices is intricately linked to process enhancement, playing a pivotal role in achieving sustainable supply chain and organizational performance. Das [3] and Sajan et al. [4] collectively highlight the transformative impact of Lean Practices on operational efficiency and overall performance. By emphasizing waste elimination, continuous improvement, and workflow optimization, Lean Practices contributes to streamlined processes that are not only cost-effective but also inherently resilient. This lean approach fosters a culture of efficiency, responsiveness, and adaptability, enabling organizations to navigate dynamic business landscapes effectively.

The sustainable supply chain and organizational performance outcomes associated with Lean Practices emanate from their ability to instill operational discipline, reduce lead times, enhance product quality, and cultivate a mindset of continuous improvement throughout the organizational ecosystem. In essence, the implementation of Lean Practices serves as a cornerstone for organizations seeking enduring excellence in both their supply chain and overall operational endeavors. The multifaceted benefits of Lean Practices position them as a strategic imperative

for organizations striving for efficiency, quality, and sustained competitiveness in the contemporary business environment.

Industry 4.0 represents a transformative shift from centralized to highly adaptable and self-controlled production processes. This pattern involves the comprehensive digitization and interconnection of products, systems, and engineering processes, enabling the whole sharing and transmission of information throughout both horizontal and vertical value chains and wide-ranging networks [5]. Central to Industry 4.0 is the capacity to rapidly gather, process, examine, and exchange vast datasets among machines, forming the backbone of its operational framework. The main objective is to fully automate and integrate industrial systems, thereby altering traditional relationships between suppliers, manufacturers, and customers and improving operations throughout the whole value chain [6].

Modern technologies like Cyber Physical Systems (CPS) and the Internet of Things (IoT) play instrumental roles in Industry 4.0, enabling swift and flexible responses to challenges and streamlining value-creation processes to reduce costs [7, 8], three pivotal Industry 4.0 tools include the Cloud Computing, Big Data, and IoT, particularly sensors and radio frequency identification (RFID). These tools enhance the capacity to capture and leverage data, facilitating more informed decision-making throughout the production lifecycle.

The implementation of integrated systems featuring autonomous and collaborative robots represents a significant facet of Industry 4.0. Beyond mere automation, this integration has the potential to elevate production quality, redefine the impact of labor on product costs, and influence decisions related to outsourcing for supply chain optimization and lead time minimization [9]. In essence, Industry 4.0 signifies a paradigm shift that goes beyond technological integration, reshaping the very dynamics of manufacturing and supply chain management.

Recent research highlights the complementary nature of Lean Manufacturing and Industry 4.0 technologies. Lean's focus on waste reduction aligns with Industry 4.0's capabilities in real-time data collection and process optimization. For instance, Goh et al. (2021) argue that Industry 4.0 technologies can enhance Lean practices by providing advanced analytics and real-time insights that support more informed decision-making and process improvements [10]. Similarly, Saldaña et al. (2020) find that the integration of Industry 4.0 tools, such as IoT and AI, with Lean practices can lead to significant improvements in production efficiency and quality by enabling predictive maintenance and reducing downtime [11].

2 Research Methodology

The first stage of the study involved designing a comprehensive survey questionnaire to investigate the impact of Lean Practices and Industry 4.0 Technologies on operational performance in the Malaysian manufacturing sector. The questionnaire was crafted to capture both qualitative and quantitative data, focusing on key areas such as process improvement, efficiency gains, cost reduction, and quality enhancement.

Demographic questions were included to categorize respondents by company size, industry type, and role, ensuring a diverse and comprehensive analysis.

Pilot testing was conducted with a small group from the target population to ensure the questionnaire's clarity and effectiveness. Feedback from this phase led to necessary adjustments, improving the survey's overall quality and reliability. Once the questionnaire met the desired standards, it was distributed to a broader audience of manufacturing companies across Malaysia using digital channels. Follow up reminders were sent to maximize response rates, resulting in a total of 53 completed responses from approximately 350 targeted respondents.

Data collection was systematically monitored to ensure a sufficient number of high-quality responses. Each survey was reviewed for completeness and consistency, with follow-up communication initiated when necessary. The collected data was meticulously analyzed using Microsoft Excel, which facilitated organizing, interpreting, and visualizing the survey results. Excel's functionalities allowed for a comprehensive examination of the data, revealing key trends, correlations, and significant findings. Weighted averages were computed to evaluate the contributions of Industry 4.0 technology and Lean tools to different operational performance metrics. Each aspect, rated on a scale from 1 to 5, was analyzed to provide a nuanced view of the perceived effectiveness of each tool and technology in areas such as cost effectiveness, resource efficiency, energy consumption, waste reduction, worker well-being, and community impact.

In conclusion, the methodology adhered to a structured approach, from survey design to results interpretation, ensuring a thorough investigation into the impact of Lean Practices and Industry 4.0 Technologies. The systematic process provided valuable insights into how these methodologies are being implemented in the Malaysian manufacturing sector and their effectiveness in enhancing operational performance. This methodical approach offers guidance for manufacturing organizations aiming to implement these strategies for maximum impact, ultimately improving efficiency, productivity, and overall operational outcomes.

3 Results and Discussion

The assessment of both the most and least utilized Lean practices shows in Fig. 1 reveals a consistent pattern of high effectiveness across various operational performance measures. Across practices such as 5S, Kaizen, Poka Yoke, Kanban, and TPM, which are extensively employed, there is strong performance in critical areas like cost effectiveness, resource efficiency, energy consumption, waste reduction, workforce well-being, and community impact. These practices consistently achieve high weighted averages, indicating their robust contributions to enhancing organizational efficiency and sustainability. Similarly, the less commonly utilized Lean practices, including Six Sigma, Hoshin Kanri, Heijunka, Jidoka, and SMED, also demonstrate significant effectiveness in these same operational metrics, albeit with slightly lower

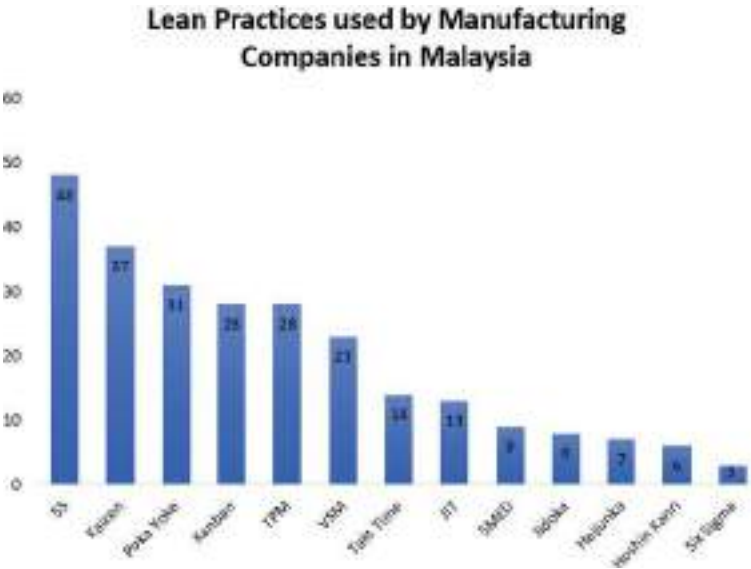


Fig. 1 Lean practices used by manufacturing companies in Malaysia

adoption rates. This indicates that while these tools may not be as widely implemented, they still offer substantial benefits in improving operational processes and outcomes across diverse dimensions. Together, both sets of Lean practices underscore the comprehensive impact of Lean methodologies in driving operational excellence and fostering positive organizational performance across various industries and sectors.

The evaluation of both the most and least utilized Industry 4.0 technologies shows in Fig. 2 reveals their consistent and significant impact across various operational performance measures. Widely adopted technologies include cloud computing, big data analytics, cyber security, system integration, and the Internet of Things (IoT), demonstrate exemplary performance in critical areas including cost effectiveness, resource efficiency, energy consumption, waste reduction, workforce well-being, and community impact. These technologies consistently achieve high weighted averages, highlighting their transformative role in optimizing operational processes and enhancing organizational sustainability. Similarly, the less frequently utilized Industry 4.0 technologies such as Augmented Reality, Additive Manufacturing, Advanced Materials, Autonomous Robots, and Artificial Intelligence also exhibit strong effectiveness across these operational metrics, albeit with lower adoption rates. This underscores their potential to significantly contribute to operational efficiency and effectiveness, suggesting that despite varying levels of deployment, these technologies offer substantial benefits in advancing organizational performance across diverse operational dimensions.

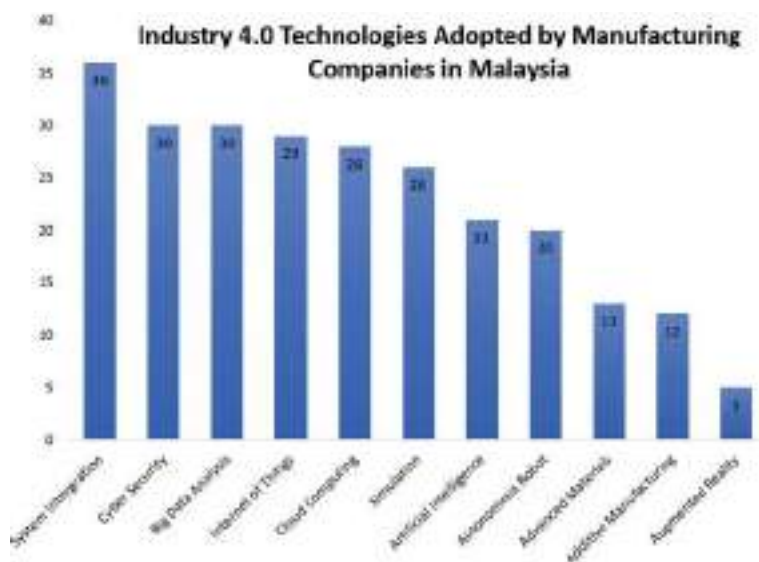


Fig. 2 Industry 4.0 technologies adopted by manufacturing companies in Malaysia

The results of the survey indicate a significant positive impact of combining Lean Practices and Industry 4.0 Technologies on the operational performance of manufacturing companies in Malaysia. Companies that adopted both practices reported improvements in efficiency, cost reduction, and product quality. Figures 3, 4, and 5 show the responses percentage on the perceived impact of Lean Practices and Industry 4.0 Technologies on Operational Efficiency, Cost Reduction and Quality Enhancement, respectively. The use of IoT and Big Data Analytics facilitated real time data collection and analysis, permitting more informed decision making and process optimization. Lean tools such as 5S and Kanban complemented these technologies by streamlining workflows and reducing waste. However, the study also identified several challenges, including integration difficulties and the need for substantial infrastructure investment. These findings underscore the importance of a strategic approach to implementing these methodologies to maximize their benefits.

4 Conclusion and Recommendation

This study highlighted the significant role that both Lean Practices and Industry 4.0 Technologies play in enhancing manufacturing operation. Survey responses indicated that system integration, cybersecurity, big data analytics, Internet of Things (IoT), and cloud computing are the most commonly used Industry 4.0 technologies. These technologies complement Lean Practices by providing real-time data, improving process integration, and enabling more informed decision-making.

Impact of Integrating Lean Practices and Industry 4.0 on Operational Efficiency

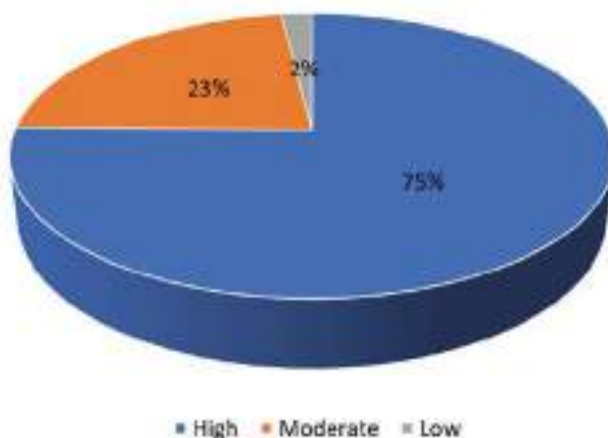


Fig. 3 Responses percentage on the perceived impact of lean practices and industry 4.0 technologies on operational efficiency

Impact of Integrating Lean Practices and Industry 4.0 on Cost Reduction

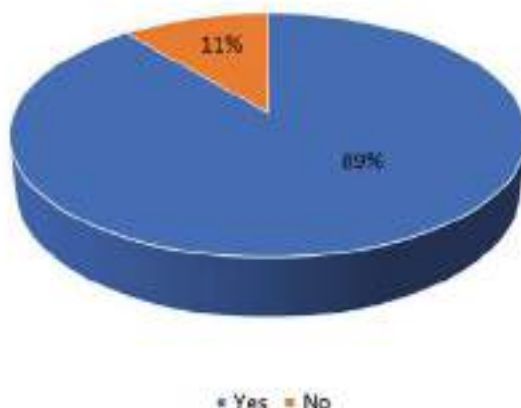


Fig. 4 Responses percentage on the perceived impact of lean practices and industry 4.0 technologies on cost reduction

Impact of Integrating Lean Practices and Industry 4.0 on Quality Enhancement

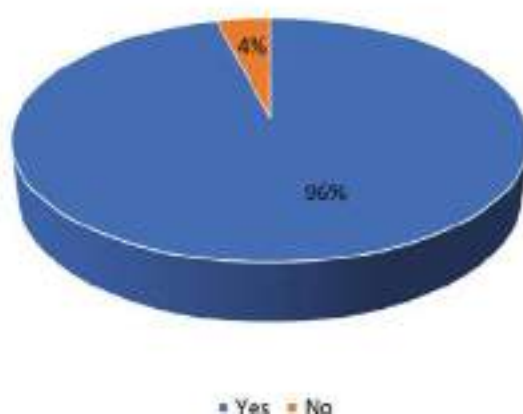


Fig. 5 Responses percentage on the perceived impact of lean practices and industry 4.0 technologies on quality enhancement

Lean Practices and Industry 4.0 Technologies are both widely adopted across various manufacturing sectors in Malaysia. The integration of these methodologies has led to notable improvements in operational efficiency, cost reduction, and quality enhancement. System integration and big data analytics were particularly noted for their roles in optimizing processes and facilitating real-time decision-making. Cybersecurity is essential for protecting data integrity and ensuring compliance with regulatory standards.

The combined application of Lean Practices and Industry 4.0 Technologies has led to significant improvements in visibility, coordination, and overall operational performance. Respondents reported substantial cost savings, reduced downtime, and enhanced product quality. According to a study by Kuo et al. (2022), the adoption of Industry 4.0 technologies in Lean environments results in notable improvements in production efficiency and reduction in cycle times [12]. Their research demonstrates that real-time data and automated systems enhance Lean practices by reducing process variability and improving throughput. Another study by Ahmed et al. (2021) highlights that the combination of Lean and Industry 4.0 leads to significant reductions in defect rates and material waste, contributing to higher overall product quality [13].

Despite the valuable insights obtained, the study faced several limitations. The sample size, while adequate, could be expanded to provide a more comprehensive

view of the manufacturing sector in Malaysia. Additionally, the reliance on self-reported data may introduce biases, as respondents might overestimate the effectiveness of their practices and technologies. The survey distribution methods, predominantly digital, may have excluded potential respondents who are less active on social media platforms.

In order to overcome these limitations and reach a broader audience, future research should entail larger sample sizes and a wider variety of distribution strategies. Deeper understanding of the long-term effects of combining Industry 4.0 technologies and lean practices may be obtained through longitudinal research. Furthermore, case studies of specific companies could offer detailed examples of best practices and lessons learned. Exploring the specific challenges and success factors associated with implementing these methodologies in different manufacturing environments would also be beneficial.

In conclusion, this study emphasizes the critical importance of merging Lean Practices with Industry 4.0 Technologies to attain optimal operational performance in the manufacturing sector. The findings suggest that these methodologies are not only complementary but also mutually reinforcing, leading to significant improvements in efficiency, quality, and cost-effectiveness. By addressing the identified limitations and building on the insights gained, future research can further elucidate the full potential of these transformative approaches in the manufacturing industry.

Acknowledgements The author would like to express their gratitude to the manufacturing companies in Malaysia that participated in this study and provided valuable insights through their survey responses. We also thank Universiti Malaysia Pahang Al-Sultan Abdullah for their support in facilitating the research process.

References

1. Womack JP, Jones DT (2003) *Lean thinking banish waste and create wealth in your corporation*. Free Press, New York
2. Taj S (2008) Lean manufacturing performance in China: assessment of 65 manufacturing plants. *J Manuf Technol Manag* 19(2):217–234
3. Das K (2018) Integrating lean systems in the design of a sustainable supply chain model. *Int J Prod Econ* 198:177–190
4. Sajan MP, Shalij PR, Ramesh A, Augustine BP (2017) Lean manufacturing practices in Indian manufacturing SMEs and their effect on sustainability performance. *J Manuf Technol Manag* 28(6):772–793
5. Leyh C, Martin S, Schäffer T (2017) Industry 4.0 and lean production—a matching relationship? An analysis of selected industry 4.0 models. In: *Proceedings of the federated conference on computer science and information systems*, pp 989–993
6. Rüßmann et al (2015) *Industry 4.0: the future of productivity and growth in manufacturing industries*, pp 1–14. Boston Consulting Group (BCG)
7. Oztemel E, Gursev S (2018) Literature review of industry 4.0 and related technologies. *J Intell Manuf* 31:127–182
8. Dombrowski U, Richter T, Krenkel P (2017) Interdependencies of industrie 4.0 & lean production systems: a use cases analysis. *Proc Manuf* 11:1061–1068

9. Baines et al (2017) Servitization: revisiting the state-of-the-art and research priorities. *Int J Oper Prod Manag* 37:256–278
10. Goh M, Lee S, Zhang X (2021) The integration of lean and industry 4.0 technologies: implications for operational efficiency. *J Manuf Process* 64:1–14
11. Saldaña J, López M, Ramirez A (2020) Enhancing lean manufacturing with industry 4.0 technologies: a case study in the automotive industry. *Int J Prod Econ* 228:107693
12. Kuo YF, Kuo LY (2022) Impact of industry 4.0 technologies on lean manufacturing performance: a systematic review. *J Clean Prod* 321:129136
13. Ahmed M, Shah M, Ahmed I (2021) Operational performance improvement through lean and industry 4.0 integration: an empirical study in automotive sector. *Proc CIRP* 99:432–437

Recycling Methods for Effective Circular Economy: Bibliometric Analysis and Research Trends



Iwan Roswandi, Eko Pujiyanto, Cucuk Nur Rosyidi,
and Wakhid Ahmad Jauhari

Abstract This research paper examines the evolution of recycling in support of a circular economy. The research utilized a literature review of 1058 articles published on Scopus between 2001 and 2023. The analysis focused on the main topics of scientific journals, authors, research findings and keywords. The results are presented in the form of graphs outlining the relationships between the various links. This research shows a marked increase in publications on this topic from 2018 to 2023. From the selection made based on the keywords recycling, circular economy, tires, 24 relevant articles were obtained. The research was conducted in four stages, starting with data collection from journals and ending with data visualization. The main sub-sub topics covered in the literature review were circular economy, recycling, sustainable development, waste management, and sustainability. The trending research data is the processing of used waste into environmentally friendly products using several approaches ranging from raw material manufacturing processes, production processes, distribution, customers, consumables processing, reuse, recycling, for all products that can be reprocessed, including the LCA approach, laboratory simulations, mathematical models, TMM, and combining the two methods as appropriate to the case.

Keywords Circular economy · Recycling · Waste · Bibliometric analysis

1 Introduction

Waste is a problem that every country can deal with by disposing of it, storing it, or reusing it. However, waste is not only waste from cities but also raw materials used in production that come from nature and will be depleted over time, so resources will

I. Roswandi (✉) · E. Pujiyanto · C. N. Rosyidi · W. A. Jauhari
Department of Industrial Engineering, Faculty of Engineering, Sebelas Maret University,
Surakarta, Indonesia
e-mail: iwan.roswandi@student.uns.ac.id

be reduced. The ideal way to treat such waste is to recycle and reuse it in another form. Waste prevention is best achieved by recycling, but its life cycle needs to be addressed if it still generates waste in the production process. The current economic model of society is essentially linear. We extract natural resources and bring them to different parts of the world and make products and goods derived from those natural resources, then the finished products are distributed to different parts of the world, where consumers buy, use and dispose of the products for various reasons. This is how the waste process occurs from raw materials to finished products and after the end of life, the products end up in landfills, incinerators, or are littered in the surrounding environment. However, according to some of the research that has been done, a circular model is necessary, in addition to a stable and sustainable economy, it will also have an impact on a healthy environment [1]. The circular economy is one of the latest concepts promoted as a pathway for greener and more sustainable development [2]. Where waste materials or garbage are converted into valuable resources, it is gaining more and more attention from society [3]. Due to the growing population, the demand for resources is increasing exponentially and therefore it is necessary to measure the consumption of resources to meet the demand. Due to the limited availability of resources, it is important to adopt reuse strategies to address resource depletion [4]. Overall, companies and industries can be forced to reorganize their industrial value chains so that resource reuse and waste treatment can be effectively implemented in the production process [5]. Circular economy the policy package covers various aspects, such as waste treatment waste, plastic recycling, food waste reduction, and remanufacturing, basically an employment promotion policy and policy [6]. In the design process stage of product manufacturing, the integration of product functionality should be considered, so as to avoid adding additional materials at the manufacturing stage, which may cause problems in the process of recycling or reusing materials from the product. Choosing the type of rubber to which certain additives are applied can have a positive effect on the environment if the rubber can be recycled more easily. Example, to improve and reduce waste tire, it is important for certain parts of the structure, which remain functional and valuable, to be recovered for reuse or reconfigured into useful products [7].

2 Methods

Previous research is an important way of conducting research to find out the gaps between previously conducted research and future research.. The steps in this study, namely planning the topic to be researched by collecting literature review from the Scopus database for the period 2001–2023. Figure 1. shows the literature search and screened.

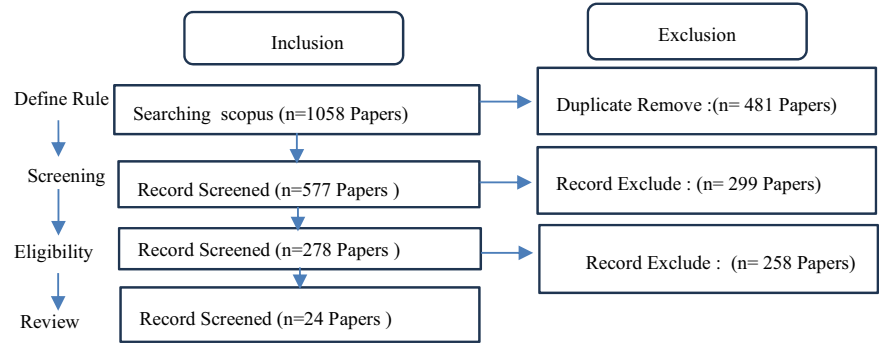


Fig. 1 Literature search and screened

3 Results and Discussion

For discussion and conclusion, it consists of define rule, screening, eligibility and review, all stages are done sequentially and structured.

3.1 Define Rule

The first step defines rule is four topics data collection, namely circular, economy, redesign, recycle, for each topic several keywords we used as presented in Table 1.

Initial Search In the process of searching for keywords on the search menu in Scopus, by entering a combination of keywords (Rule 1 OR Rule 2 AND Rule 3 OR Rule 4) in the search query field and searching for “Article title, Abstract, keywords” in the scopus database. Documents searched for publication year “All years”, All subject areas, document type using the category “All” (article, survey, book, short survey, note, conference review, retratcted), keyword “all”, Language “all”, and access type “All” (including open access). Initial search efforts yielded 1058 articles from 2001 to 2023 for topics related to redesigning, recycle, circular economy.

Figure 2 explains the increase in the number of articles on redesigning, recycle, circular economy until 2023, for a decade this research is still in a minimal amount, but the most significant is starting in the last 5 years with the achievement of continuing to increase with the highest articles in 2022.

Table 1 Define rule searching

No	Topic	Keywords
1	Circular economy	(TITLE-ABS-KEY (redesigning) OR TITLE-ABS-KEY (recycle) AND TITLE-ABS-KEY (circular) AND TITLE-ABS-KEY (economy)

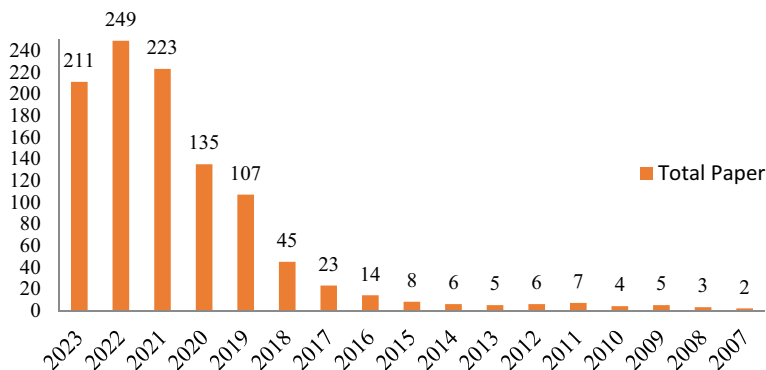
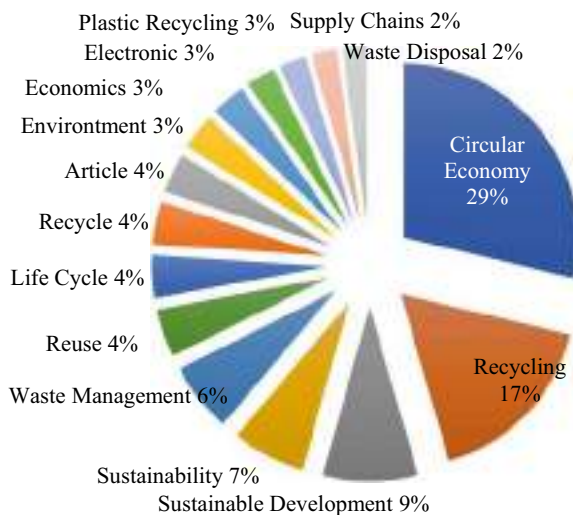


Fig. 2 Trend related circular economy, redesigning and recycled

3.2 Research Classification

Analysis of keyword visualization of 1058 articles based on keywords can be seen there are 20 dominant topics based on color, namely circular economy 650 times, recycling 379 times, sustainable development 199 times, sustainability 154 times, waste management 146 times, reuse 101 times, life cycle 90 times and recycle 90 times, article 84 times, environment impact 76 times, economics 72 times, electronic waste 60 times (Fig. 3) [8].

Fig. 3 Author keyword



3.2.1 Screening

From the 1058 articles at the initial screening stage, most scientific articles appeared in various categories, so we filtered by document type “article” (excluding conference papers, books, book chapters, reviews, letters, notes, etc.), publication year “2001–2023” and source type “journal” and language “English”. This filtered the articles and left a total of 577 articles.

3.2.2 Eligibility

From the 577 screened articles, more papers still appeared in categories, so we screened by document type “article” (excluding conference papers, books, book chapters, reviews, letters, notes, etc.), publication year “2001–2023” and source type “journal” and language “English”. This filtered out the articles and left a total of 278 articles.

3.2.3 Review

From the total number of articles 1058 after going through the screening process, eligibility and finally screening with the keywords redesigning, recycle, circular economy, tyres or tire, until it was narrowed down to 24 Articles as shown in Table 2.

3.3 Conceptual Framework

Bibliometric analysis and visualization using Vost viewer by number of papers from 2001 to 2023, selected based on the number of papers published. Keywords represent specific characteristics or fields of the study documents associated in the information.

In a system, it is divided into two parts of keywords: author and index. Author keywords are created by authors in the journal system and index keywords are created by the Scopus database system. The author keywords that frequently appear in the selected articles and are presented in the form of circles are visualized in Fig. 4. The network as a keyword in this study has a minimum threshold of 5 occurrences. The retrieved data shows that 1058 articles have 4940 different keywords. The size of the circles represents the keyword network based on the total occurrences. The size of the circles in each cluster depicts the number of articles captured by the primary keywords and the clusters are depicted with yellow, blue, green, red, and orange colors. Figure 4 presents a visual report of the keywords that appear 5 times or more. The top five author keywords were “circular economy,” which appeared 540 times, “recycling” 63 times, “sustainable development” 54 times, “sustainability” 41 times, and “waste management” 41 times. This group of keywords is commonly found in articles on green logistics, sustainable supply chains, and technology in inventory

Table 2 Review article

Step	Query	Selection	Total article
1	Rule 1 OR Rule 2 AND Rule 3 AND Rule 4	(TITLE-ABS-KEY (redesigning) OR TITLE-ABS-KEY (recycle) AND TITLE-ABS-KEY (circular) AND TITLE-ABS-KEY (economy)	1058
2	Rule 1 OR Rule 2 AND Rule 3 AND Rule 4 OR Rule 5 AND	(redesigning) OR TITLE-ABS-KEY (recycle) AND TITLE-ABS-KEY (circular) AND TITLE-ABS-KEY (economy) OR TITLE-ABS-KEY (tyres)) AND PUBYEAR > 2017 AND PUBYEAR < 2023	577
3	Rule 1 OR Rule 2 AND Rule 3 AND Rule 4 OR Rule 5 AND Rule 6 AND	Your query: ((TITLE-ABS-KEY (redesigning) OR TITLE-ABS-KEY (recycle) AND TITLE-ABS-KEY (circular) AND TITLE-ABS-KEY (economy) OR TITLE-ABS-KEY (tyres)) AND PUBYEAR > 2017 AND PUBYEAR < 2023 AND (LIMIT-TO (PUBSTAGE,"final")) AND (LIMIT-TO (SUBJAREA))	278
4	Rule 1 OR Rule 2 AND Rule 3 AND Rule 4 AND Rule 5 OR	(TITLE-ABS-KEY (redesigning) OR TITLE-ABS-KEY (recycle) AND TITLE-ABS-KEY (circular) AND TITLE-ABS-KEY (economy) AND TITLE-ABS-KEY (tyres) OR TITLE-ABS-KEY (tire))	24

management. Previously conducted circular economy research methods can be seen in the Table 3.

From several stages of screening the research conducted on recycling has a wide variety of products that are used to support the circular economy, the last screening we focused on tyre recycling. The 24 articles that have been screened can be seen that the tyre recycling system is carried out in several ways including 7 articles with recycling, 2 articles recycling and reuse, 2 articles reduce, recycle, reuse, for recycling used tyres there are 2 methods used namely devulcanisation and pyrolysis besides that there are several methods used as in Table 3 namely Lab test, LCA, PLS, SEM and several methods combined with other methods, besides that there are also circular economy methods.

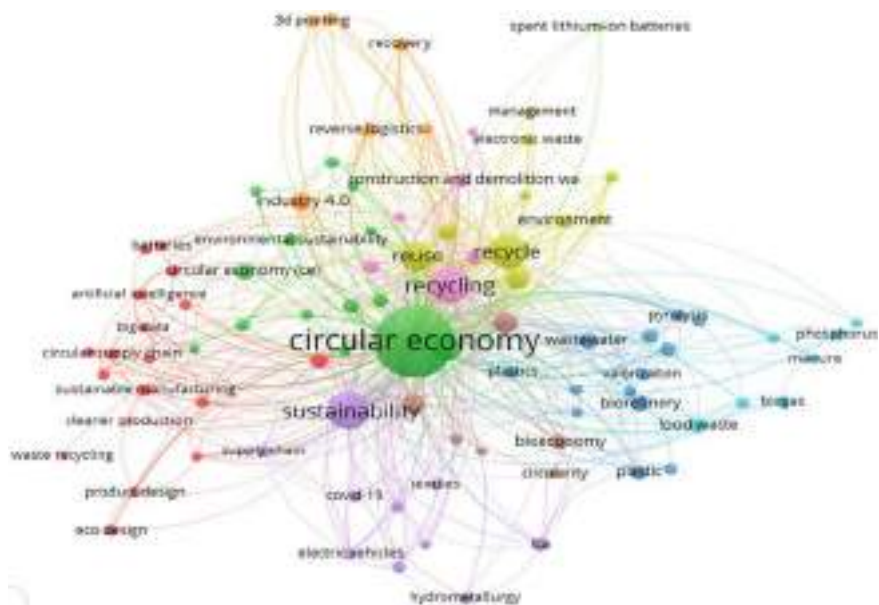


Fig. 4 Vos viewer base on keyword

Table 3 Research analysis method

No	Authors	Year	System developed	Type of method
1	Dobrota et al. [9]	2019	Recycling	CBA, NPV, IRR Models
2	Roy et al. [10]	2023	Recycling	Interview stakeholders
3	Schyns et al. [11]	2023	Recycling	LAB Test simulation
4	Mohammadhosseini et al. [12]	2021	Recycling	Statistical analysis dan investigasi
5	Tavares et al. [13]	2022	Recycling	Pyrolysis
6	Handrikse et al. [14]	2023	Recycling	LAB test
7	Thongphang et al. [15]	2023	Recycling	LAB Test
8	Landi et al. [16]	2019	Recycling dan reuse	LCA
9	Vitale et al. [17]	2021	Recycling dan reuse	LCA
10	Boesen et al. [18]	2019	Qualitative interviews	LCA
11	Ceceres-mendoza et al. [7]	2023	Recycling dan additive manufacturing	LCA and DRAM
12	Wang et al. [19]	2021	Reduce reuse recycle	LCA dan EMA
13	Nguyen et al. [20]	2022	Recycle dan waste manajemen	Mathematic models
14	Guo et al. [21]	2023	Recycling Policies	PLS-SEM modeling
15	Wolfel et al. [22]	2020	Recycling and reprosesing	Lab test dan mathematic model
16	Vilniskis et al. [23]	2023	Devulcanisation	Transfer matrix method (TMM Models)
17	Undas et al. [24]	2023	Reduce reuse recycle	NIAS dan IAS
18	Symeonides et al. [25]	2019	Pyrolysis	SWOT and PESTEL
19	Bockstal et al. [26]	2019	Devulcanisation	Waste tire manajemen
20	Saputra et al. [27]	2021	Devulcanisation	Thermo mechanical process
21	Martinez [28]	2021	Pyrolysis	Atomation machine system
22	Araujo-Morera et al. [29]	2021	Devulcanisation	7 Rs circular economy
23	Formela et al. [8]	2021	Devulcanisation	Grinding and treatment method
24	Feraandez et al. [30]	2023	Rubber recovery	Measuring equipment tool

4 Conclusion

In this literature study, it can be seen that the circular economy is carried out to utilize used products into useful products so that they can be useful for a sustainable economy, using several approaches starting from the process of making raw materials, production processes, distribution, customers, processing consumables,

reuse, recycling. The circular economy is not limited to specific products but all products. The recycling of scrap tires and other products has the effect of reducing environmental pollution (both through reducing the amount of waste and the level of gases discharged into the atmosphere as a result of combustion or used as fuel used in various industries, especially in the cement industry that supports the circular economy process, and ensures the sustainability of the entire scrap tire waste recovery process, the methods often used in research include recycling, reuse, reduction, reprocessing, devulcanization, recovery with LCA approach, laboratory simulation, mathematical models, TMM, and the combination of two methods according to the theme to be studied.

References

1. Tauberova R, Marticek M, Knapcikova L (2022) Selected innovative approaches in the waste tyres management. *Acta Logistica* 9(4):411–415
2. Uvarova I, Atstaja D, Volkova T, Grasis J, Ozolina-Ozola I (2023) The typology of 60R circular economy principles and strategic orientation of their application in business. *J Clean Prod* 409
3. Stamm C, Binder CR, Frossard E, Haygarth PM, Oberson A, Richardson AE et al (2022) Towards circular phosphorus: the need of inter- and transdisciplinary research to close the broken cycle. *Ambio* 51(3):611–622
4. Kirchherr J, Reike D, Hekkert M. Conceptualizing the circular economy: an analysis of 114 definitions. *Resour Conserv Recycl* 127:221–232. Elsevier B.V.
5. Barbaritano M, Bravi L, Savelli E (2019) Sustainability and quality management in the Italian luxury furniture sector: a circular economy perspective. *Sustainability (Switzerland)* 11(11)
6. Umeda Y, Kitagawa K, Hirose Y, Akaho K, Sakai Y, Ohta M (2020) Potential impacts of the European Union's circular economy policy on Japanese manufacturers. *Int J Autom Technol* 14(6):857–866
7. Caceres-Mendoza C, Santander-Tapia P, Cruz Sanchez FA, Troussier N, Camargo M, Boudaoud H (2023) Life cycle assessment of filament production in distributed plastic recycling via additive manufacturing. *Clean Waste Syst* 1:5
8. Formela K (2021) Sustainable development of waste tires recycling technologies—recent advances, challenges and future trends. *Adv Indus Eng Polym Res* 4(3):209–222
9. Dobrota D, Dobrota G, Dobrescu T, Mohora C (2019) The redesigning of tires and the recycling process to maintain an efficient circular economy. *Sustainability (Switzerland)* 11(19)
10. Roy D, Berry E, Orr K, Dempster M (2023) Barriers to recycling plastics from the perspectives of industry stakeholders: a qualitative study. *J Integr Environ Sci* 20(1)
11. Schyns ZOG, Patel AD, Shaver MP (2023) Understanding poly (ethylene terephthalate) degradation using gas-mediated simulated recycling. *Resour Conserv Recycl* 198
12. Mohammadhosseini H, Alyousef R, Tahir MM (2021) Towards sustainable concrete composites through waste valorisation of plastic food trays as low-cost fibrous materials. *Sustainability (Switzerland)* 13(4):1–23
13. Tavares T, Leon F, Vaswani J, Peñate B, Ramos-Martín A (2022) Study for recycling water treatment membranes and components towards a circular economy—case of Macaronesia Area. *Membranes (Basel)* 12(10)
14. Hendrikse HC, El Khallabi H, Hartog T, Varveri A, Tolboom A (2023) Characterization and design of circular binders. *Sustainability (Switzerland)* 15(17)
15. Thongphang C, Namphonsane A, Thanawan S, Chia CH, Wongsagonsup R, Smith SM et al (2023) Toward a circular bioeconomy: development of pineapple stem starch composite as a plastic-sheet substitute for single-use applications. *Polymers (Basel)* 15(10)

16. Landi D, Germani M, Marconi M (2019) Analyzing the environmental sustainability of glass bottles reuse in an Italian wine consortium. *Proc CIRP* 399–404. Elsevier B.V.
17. Vitale P, Napolitano R, Colella F, Menna C, Asprone D (2021) Cement-matrix composites using CFRP waste: a circular economy perspective using industrial symbiosis. *Materials* 14(6)
18. Boesen S, Bey N, Niero M (2019) Environmental sustainability of liquid food packaging: Is there a gap between Danish consumers' perception and learnings from life cycle assessment? *J Clean Prod* 210:1193–1206
19. Wang Q, Zhang Y, Tian S, Yuan X, Ma Q, Liu M et al (2021) Evaluation and optimization of a circular economy model integrating planting and breeding based on the coupling of emergy analysis and life cycle assessment. *Environ Sci Pollut Res* 28(44):62407–62420
20. Nguyen TTA, Ta YT, Dey PK (2022) Developing a plastic cycle toward circular economy practice. *Green Process Synth* 11(1):526–535
21. Guo M, Huang W (2023) Consumer willingness to recycle the wasted batteries of electric vehicles in the era of circular economy. *Sustainability (switzerland)* 15(3)
22. Wölfel B, Seefried A, Allen V, Kaschta J, Holmes C, Schubert DW (2020) Recycling and reprocessing of thermoplastic polyurethane materials towards nonwoven processing. *Polymers (Basel)* 12(9)
23. Vilniškis T, Januševičius T (2023) Experimental research and transfer matrix method for analysis of transmission loss in multilayer constructions with devulcanized waste rubber. *Sustainability (Switzerland)* 15(17)
24. Undas AK, Groenen M, Peters RJB, van Leeuwen SPJ (2023) Safety of recycled plastics and textiles: review on the detection, identification and safety assessment of contaminants. *Chemosphere* 312
25. Symeonides D, Loizia P, Zorpas AA (2019) Tire waste management system in Cyprus in the framework of circular economy strategy. *Environ Sci Pollut Res* 26(35):35445–35460
26. Bockstal L, Berchem T, Schmetz Q, Richel A (2019) Devulcanisation and reclaiming of tires and rubber by physical and chemical processes: a review. *J Clean Prod* 236:117574
27. Saputra R, Walvekar R, Khalid M, Mubarak NM, Sillanpää M (2021) Current progress in waste tire rubber devulcanization. *Chemosphere* 265:129033
28. Martínez JD (2021) An overview of the end-of-life tires status in some Latin American countries: proposing pyrolysis for a circular economy. *Renew Sustain Energy Rev* 144:111032
29. Araujo-Morera J, Verdejo R, López-Manchado MA, Hernández SM (2021) Sustainable mobility: the route of tires through the circular economy model. *Waste Manage* 126:309–322
30. Ferrández D, Yedra E, Recalde-Esnoz I, del Castillo H (2023) Reuse of end-of-life tires and their impact on the setting time of mortars: experimental study using a new measuring equipment. *J Build Eng* 15:69

Review of the Design and Concept of the Double Pipe Heat Exchanger



R. N. Syafiq, Mohd Fadzil Ali Ahmad, Deevikthiran Jeevaraj,
and Ibnu Kasir Ahmad Nadzri

Abstract The heat exchanger, a crucial device in numerous industrial processes, is responsible for transferring heat from a high-temperature fluid to a low-temperature fluid. There is a growing demand to further enhance the efficiency of heat exchangers, explore various methods to increase heat transfer rates, and minimize the size and cost of industrial equipment. This comprehensive review delves into literature related to the different types of double pipe heat exchangers and the myriad factors that impact heat transfer rates and pressure drops. The versatile double pipe heat exchanger finds widespread use across various industries due to its efficiency and reliability. Research studies have proposed several models of double pipe heat exchangers and have explored their applications in industrial processes, cooling technology, refrigeration, sustainable energy, and more. Further classification of double pipe heat exchangers includes parallel, counter, and cross flow configurations. To optimize the effectiveness of double pipe heat exchangers, extensive research has been conducted, exploring methods such as turbulators, inserts, modifications to channel geometry, and innovative fluid injection approaches. This in-depth study presents a thorough overview of the extensive research available on double pipe heat exchangers, with a specific focus on determining the most suitable effectiveness parameters.

Keywords Double pipe · Heat exchanger · Sustainable energy · Cooling technology

R. N. Syafiq · M. F. A. Ahmad (✉) · D. Jeevaraj · I. K. A. Nadzri
Faculty of Manufacturing and Mechatronic Engineering Technology, Universiti Malaysia Pahang
Al-Sultan Abdullah, 26600 Pekan, Pahang, Malaysia
e-mail: fadzilali@ump.edu.my

© The Author(s), under exclusive license to Springer Nature Singapore Pte Ltd. 2025
M. R. Mohamad Yasin et al. (eds.), *Proceedings of the 7th Asia Pacific Conference on Manufacturing Systems and 6th International Manufacturing Engineering Conference—Volume 2*, Lecture Notes in Mechanical Engineering,
https://doi.org/10.1007/978-981-96-5690-5_9

1 Introduction

Heat exchangers allow thermal energy to be transferred between two fluids without causing any mixing into the mixture. Although they are often kept apart by a solid wall with a high heat conductivity to prevent mixing, the fluids can be in close contact with one another. While the secondary flow of gas containing the free water is directed into the annular chamber using a dehydration method like a supersonic separator, the primary inflow material continues to the main pipeline [1]. The first type of heat exchanger is called a parallel-flow arrangement. In a parallel flow setup, hot and cold fluids enter at the same end, flow in the same direction, and exit at the same end. The other type of heat exchanger is called a counter-flow arrangement. The fluids enter at opposite ends, flow in opposite directions, and exit at opposite ends when they are arranged in a counterflow configuration. A number of designs would be used to categorize heat exchangers. The first kind is determined by the direction of flow (cross, counter, and parallel fluids) [2]. The second kind is determined by how the heat exchangers are built (such as plate or tubular heat exchangers) [3]. Additionally, the third types are dependent on whether there is direct or indirect fluid contact [4]. Heat exchangers are used in many different kinds of activities [5] in the commercial [6], residential, and industrial domains to regulate the transformation [7] and retrieval of thermal energy. Some examples of universal applications are waste heat recapture, sensible heating, production of steam generation in power plants, products of various agricultural, chemical, and pharmaceutical scopes, condensation enforcement, cooling of sustainable energy implementation, and fluid heating mode in manufacturing [8]. Enhance heat exchanger performance to create more cost-effective heat exchanger designs that help to enhance thermal energy exchange, choose the best component to raise thermal exchange rate, and lower costs associated with the thermal exchange process [9].

2 Design and Construction of Double Pipe Heat Exchangers

The enhancement of heat exchange processes has been the focus of extensive research, with the primary objectives being the improvement of heat exchanger efficiency, reduction of size, and cost minimization [10]. Research in this field has predominantly centered on three main types of enhancement techniques [11]. The first category encompasses active enhancement methods, which necessitate external power input to optimize heat transfer processes. Examples of these techniques include mechanical aids, surface vibration, fluid vibration, electrostatic fields, injection suction, and jet impingement [12]. Passive enhancement methods constitute the second category, requiring no additional external power input. These techniques aim to enhance thermal exchange by increasing the surface area effectiveness and residence time of thermal fluids. Various types of inserts, such as baffles, twisted tape, ribs, wire coils, plates, helical inserts, and convergent–divergent conical rings,

are employed to enhance the heat transfer rate [13]. Lastly, compound enhancement techniques involve the simultaneous use of two or more techniques from the active and passive categories. This approach aims to surpass the results achieved by using any individual technique alone, ultimately enhancing the rate of heat energy transformation for any device [14].

The enhancement of thermal energy transformation in heat exchangers is a topic of considerable significance, involving the utilization of various modes of heat transfer performance. This technique aims to improve the convective mode by reducing thermal resistance in a double pipe heat exchanger [15]. Employing augmentation techniques for thermal energy transformation increases the convective coefficient mode, albeit with an associated increase in pressure drop. Over the past decade, different techniques have been developed to achieve a high rate of heat exchange while considering the rise in power consumption [16]. In recent years, industries have increasingly utilized swirl flow modes to enhance heat energy exchange [17]. This paper aims to present the different methods used to enhance thermal energy transformation between different fluids. Specifically, the paper will provide an overview of several turbulators, including coil pipes, extended objects on surfaces (fins, strips, winglets), rugged surfaces (outer or inner corrugated pipes, Ribs), and devices that induce swirl flow, such as twisted tape, conical rings, entry snail turbulators, vortex rings, and coiled wires (Table 1).

3 Section of the Test with a Changed Geometry

See Table 2.

4 New Technology (Industrial Application)

4.1 Solar Energy Systems

Numerous industries employ double-pipe heat exchangers for diverse purposes. Radiators for automobiles, heat pipes, cooling systems, solar collectors, nuclear reactors, and many other sectors use them extensively. Additionally, they help reduce air pollution and have significant economic benefits when they are utilized in the recovery of low temperature waste heat. The low hydraulic and thermal resistance, steady heat transfer fluid flow, and almost isothermal absorption surfaces of solar collectors utilizing HP technology have led to a great deal of research into this technology [25]. A unique flat-plate heat pipe solar collector was created and tested in the UK by Joughara et al. [26] in order to evaluate its performance. The solar/thermal energy conversion efficiency for a collector without PV was roughly 64%, whereas the system with a PV layer obtained about 50%. The performance of the solar/thermal,

Table 1 Investigation of variable flow in double-pipe heat exchanger

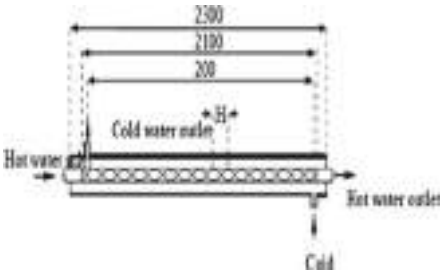
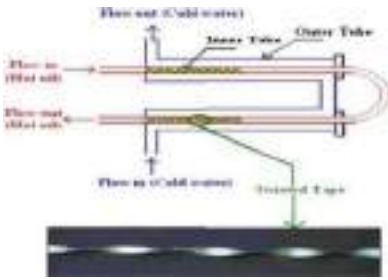

Authors	Procedures	Findings
Gao et al. [18]	The established thermal dynamic model uses numerical methods to predict the transient response of an unmixed-unmixed cross flow heat exchanger. An analysis is conducted on the transient response at varying mass flow rates and intake temperatures, subject to different transient conditions	Basic understandings gained from this study have the potential to enhance the heat exchanger's cooling operation
Milani Shirvam et al. [19]	To achieve exchanger influences and heat transfer mode, the turbulent models K— ϵ and Darcy—Brinkman—Forchheimer are used. Analysis is done on the porous substrate thickness, Reynolds number, Darcy number, and boundary parameters	At a Reynolds number of 5000, Darcy number of 10–5, and porous substrate thickness of one-third, higher average Nusselt numbers are needed for maximum efficiency
Liu et al. [20]	Designing a non-contacted double-walled-straight-tube heat exchanger for Lead–Bismuth Eutectic (LBE) loop KYLIN-II	It has been determined that the heat exchanger's performance is influenced by the temperature distribution and flow rate. The findings of the numerical simulation show that the heat exchanger packed with powder in the space between the tubes is not affected thermally by non-uniform LBE flow
Roy and Majumder [21]	Using simulation modelling to assess the shell and tube heat exchanger's (STHX) performance characteristics. The energetic plant effectiveness, energetic cycle efficiency, and electric power are among the performance parameters. The feed forward back propagation network (FFBN) algorithm is used to analyse the fouling factor and cost	Several training algorithms are utilized to train the network structure during the validation phase. According to the outcome, the suggested system maximizes electrical power, energetic cycle efficiency, and energetic plant efficiency by 98.11%, 97.4%, and 96.35%, respectively

uncooled PV, and PV/T was compared. Examining the effect of cooling on solar/electrical energy conversion efficiency, it was found that the uniform cooling offered by the cooling system increased efficiency by 15% for the cooled PV system.

4.2 Nuclear Energy Systems

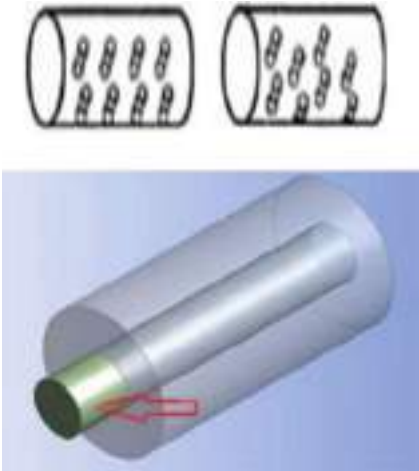
Alkali-metal HP radiators were suggested by Zhang et al. [27] for the TOPAZ-II space nuclear reactor's power system in Russia in order to improve heat transfer efficiency and safety while avoiding the single-point failure issue with the original

Table 2 A different experimental test area within a double pipe heat exchanger

No			
(1)	Authors Naphon [22]	Formation (T.T.) Twisted tape, straight type	Structure 
	Hot side Water	Cold side Water	Outcome The heat exchange rate at greater twist ratios will be lower than at lower twist ratios at different Reynolds number values. The temperature of the hot water at the inflow has a significant impact on the rate of heat exchange
(2)	Authors Singh Yadav [23]	Formation Half-length twisted tapes, U- type	Structure 
	Hot side Oil	Cold side Water	Outcome It is observed that the half-length twisted tape insert increases the pressure coefficient when compared to the plain version. Half-length twisted tape performs better than smooth pipe at the same mass flow rate for heat exchange rate, and vice versa at the same pressure drop
(3)	Authors Naphon [22]	Formation Inner pipe in straight type with added coil-wire	Structure 

(continued)

Table 2 (continued)

No			
	Hot side	Cold side	Outcome
	Water	Water	The effect of adding coil wire to a laminar flow to increase heat exchange rate tends to increase with Reynolds number
(4)	Authors	Formation	Structure
	Akpinar and Bicer [24]	Inner pipe of straight type has elements make swirl as utilized in entry section	
	Hot side	Cold side	Outcome
	Water	Water	When the number of holes increases and the diameters decreases, the rates of heat transfer will likewise increase. When the swirl element was applied, the greatest rate of heat transfer rose in comparison to the smooth pipe. Five holes with a diameter of 3 mm each comprise the zigzag arrangement of the swirl element

pumped loop radiators. They conducted a steady-state examination of the planned HP radiators using numerical simulations, forecasted their heat dissipation properties, and contrasted the pump loop radiators’ and HP radiators’ heat transfer efficiency. The findings showed that, under typical operating conditions, the intended HP radiators satisfied the TOPAZ-II power system’s waste heat rejection standards.

4.3 HVAC Systems

A thermosyphon heat exchanger was suggested by Zhang et al. [27] as a replacement for conventional air conditioning systems in communication base station cooling during the winter and transitional seasons. Moreover, there is virtually no cross-leakage between the supply and exhaust air in HPHXs due to the complete separation

of hot and cold fluids, which makes them appropriate for systems in which two airflows shouldn't mix. For example, Sukarno et al. [28] coupled the HVAC system with HPHXs to meet the regulations for Airborne Infection Isolation (AII) rooms since the intake and return air in hospitals should not be mingled.

5 Conclusion

To enhance thermal energy exchange through the forced convective mode that occurs in double pipe heat exchangers, this review study presents experimental and theoretical survey. It is demonstrated that this type of heat exchanger was widely utilized in the industrial process, engineering sector, and application of sustainable energy. Heat exchangers that can transport heat more effectively while occupying less space are still in demand. Researchers continue to hunt for the ideal heat exchanger design that satisfies known input requirements while producing an efficient output. Numerous researchers have sought to boost the rate of heat transfer by various techniques, such as creating inserts, utilizing heat exchangers with varied core configurations, and employing nanofluids. Numerous studies support the idea that thermal energy exchange can occur, and that friction can be reduced. This is nearly directly related to the passive enhancement technique. When compared to smooth tubes, the thermal energy exchange is found to nearly treble in several of the studied scenarios, while the pressure loss is kept to a minimum. The active technique that is intended to improve thermal energy exchange in double pipe heat exchangers is not widely implemented or propagated, so researchers should be sure to identify it specifically. Numerous studies have demonstrated the application of nanofluids and related techniques in various types of heat exchangers, a development that has attracted significant attention in the current period.

Acknowledgements The valuable feedback provided by our reviewers has greatly enhanced the caliber of our study, which we sincerely appreciate. Under Grant No. RDU230326, Universiti Malaysia Pahang Al-Sultan Abdullah (UMPSA) is funding this research project.

References





1. Hashim FM, Ahmad MFA (2014) Numerical simulation of supersonic subsea compact wet gas separator for gas transmission pipeline. *Appl Mech Mater* 298–302. Trans Tech Publications Ltd. <https://doi.org/10.4028/www.scientific.net/AMM.607.298>
2. Jafarzad A, Heyhat MM (2020) Thermal and exergy analysis of air-nanofluid bubbly flow in a double-pipe heat exchanger. *Powder Technol* 372:563–577. <https://doi.org/10.1016/j.powtec.2020.06.046>
3. Sivalakshmi S, Raja M, Gowtham G (2020) Effect of helical fins on the performance of a double pipe heat exchanger. *Mater Today Proc* 1128–1131. Elsevier Ltd. <https://doi.org/10.1016/j.matpr.2020.08.563>

4. Vaisi A, Moosavi R, Lashkari M, Mohsen Soltani M (2020) Experimental investigation of perforated twisted tapes turbulator on thermal performance in double pipe heat exchangers. In: Chemical engineering and processing—process intensification, vol 154. <https://doi.org/10.1016/j.cep.2020.108028>
5. Chennu R, Veeredhi VR (2020) Measurement of heat transfer coefficient and pressure drops in a compact heat exchanger with lance and offset fins for water based Al_2O_3 nano-fluids. *Heat Mass Transfer/Waerme- und Stoffuebertragung* 56(1):257–267. <https://doi.org/10.1007/s00231-019-02707-w>
6. Akyürek EF, Geliş K, Şahin B, Manay E (2018) Experimental analysis for heat transfer of nanofluid with wire coil turbulators in a concentric tube heat exchanger. *Results Phys* 9:376–389. <https://doi.org/10.1016/j.rinp.2018.02.067>
7. Jassim EI, Ahmed F (2020) Experimental assessment of Al_2O_3 and Cu nanofluids on the performance and heat leak of double pipe heat exchanger. *Heat Mass Transfer/Waerme- und Stoffuebertragung* 56(6):1845–1858. <https://doi.org/10.1007/s00231-020-02826-9>
8. Patil AS, Kore SS, Sane NK (2020) Thermal performance of tube exchanger enhanced with hexagonal ring turbulators. *Exp Heat Transf* 33(5):455–470. <https://doi.org/10.1080/08916152.2019.1656302>
9. Chen T, Wu D (2018) Enhancement in heat transfer during condensation of an HFO refrigerant on a horizontal tube with 3D fins. *Int J Therm Sci* 124:318–326. <https://doi.org/10.1016/j.ijthermalsci.2017.10.022>
10. Salem MR, Eltoukhey MB, Ali RK, Elshazly KM (2018) Experimental investigation on the hydrothermal performance of a double-pipe heat exchanger using helical tape insert. *Int J Therm Sci* 124:496–507. <https://doi.org/10.1016/j.ijthermalsci.2017.10.040>
11. Raei B, Shahraki F, Jamialahmadi M, Peyghambarzadeh SM (2017) Experimental study on the heat transfer and flow properties of $\gamma\text{-Al}_2\text{O}_3$ /water nanofluid in a double-tube heat exchanger. *J Therm Anal Calorim* 127(3):2561–2575. <https://doi.org/10.1007/s10973-016-5868-x>
12. Barzegarian R, Aloueyan A, Yousefi T (2017) Thermal performance augmentation using water based Al_2O_3 -gamma nanofluid in a horizontal shell and tube heat exchanger under forced circulation. *Int Commun Heat Mass Transfer* 86:52–59. <https://doi.org/10.1016/j.icheatmasstransfer.2017.05.021>
13. Liu S, Sakr M (2013) A comprehensive review on passive heat transfer enhancements in pipe exchangers. <https://doi.org/10.1016/j.rser.2012.11.021>
14. Sheikholeslami M, Ganji DD (2016) Heat transfer improvement in a double pipe heat exchanger by means of perforated turbulators. *Energy Convers Manag* 127:112–123. <https://doi.org/10.1016/j.enconman.2016.08.090>
15. Raj R, Shankar Lakshman N, Mukkamala Y (2015) Single phase flow heat transfer and pressure drop measurements in doubly enhanced tubes. *Int J Therm Sci* 88:215–227. <https://doi.org/10.1016/j.ijthermalsci.2014.10.004>
16. Naphon P, Suchana T (2011) Heat transfer enhancement and pressure drop of the horizontal concentric tube with twisted wires brush inserts. *Int Commun Heat Mass Transfer* 38(2):236–241. <https://doi.org/10.1016/j.icheatmasstransfer.2010.11.018>
17. Yu W, France DM, Timofeeva EV, Singh D, Routbort JL (2012) Comparative review of turbulent heat transfer of nanofluids. <https://doi.org/10.1016/j.ijheatmasstransfer.2012.06.034>
18. Gao T, Sammakia B, Geer J (2015) Dynamic response and control analysis of cross flow heat exchangers under variable temperature and flow rate conditions. *Int J Heat Mass Transf* 81:542–553. <https://doi.org/10.1016/j.ijheatmasstransfer.2014.10.046>
19. Milani Shirvan K, Ellahi R, Mirzakanlari S, Mamourian M (2016) Enhancement of heat transfer and heat exchanger effectiveness in a double pipe heat exchanger filled with porous media: numerical simulation and sensitivity analysis of turbulent fluid flow. *Appl Therm Eng* 109:761–774. <https://doi.org/10.1016/j.applthermaleng.2016.08.116>
20. Liu S, Jin M, Lyu K, Zhou T, Zhao Z (2018) Flow and heat transfer behaviors for double-walled-straight-tube heat exchanger of HLM loop. *Ann Nucl Energy* 120:604–610. <https://doi.org/10.1016/j.anucene.2018.06.016>

21. Roy U, Majumder M (2019) Evaluating heat transfer analysis in heat exchanger using NN with IGWO algorithm. *Vacuum* 161:186–193. <https://doi.org/10.1016/j.vacuum.2018.12.042>
22. Naphon P (2006) Heat transfer and pressure drop in the horizontal double pipes with and without twisted tape insert. *Int Commun Heat Mass Transfer* 33(2):166–175. <https://doi.org/10.1016/j.icheatmasstransfer.2005.09.007>
23. Singh Yadav A (2009) Effect of half length twisted-tape turbulators on heat transfer and pressure drop characteristics inside a double pipe U-bend heat exchanger [Online]. <https://www.researchgate.net/publication/237250067>
24. Akpinar EK, Bicer Y (2005) Investigation of heat transfer and exergy loss in a concentric double pipe exchanger equipped with swirl generators. *Int J Therm Sci* 44(6):598–607. <https://doi.org/10.1016/j.ijthermalsci.2004.11.001>
25. Rassamakin B, Khairnasov S, Zaripov V, Rassamakin A, Alforova O (2013) Aluminum heat pipes applied in solar collectors. *Sol Energy* 94:145–154. <https://doi.org/10.1016/j.solener.2013.04.031>
26. Jouhara H et al (2016) The performance of a novel flat heat pipe based thermal and PV/T (photovoltaic and thermal systems) solar collector that can be used as an energy-active building envelope material. *Energy* 108:148–154. <https://doi.org/10.1016/j.energy.2015.07.063>
27. Zhang W, Wang C, Chen R, Tian W, Qiu S, Su GH (2016) Preliminary design and thermal analysis of a liquid metal heat pipe radiator for TOPAZ-II power system. *Ann Nucl Energy* 97:208–220. <https://doi.org/10.1016/j.anucene.2016.07.007>
28. Sukarno R, Putra N, Hakim II, Rachman FF, Indra Mahlia TM (2021) Utilizing heat pipe heat exchanger to reduce the energy consumption of airborne infection isolation hospital room HVAC system. *J Build Eng* 35. <https://doi.org/10.1016/j.jobbe.2020.102116>

Enhancing Benchmark Optimization with Evolutionary Random Approach: A Comparative Analysis of Modified Adaptive Bats Sonar Algorithm (MABSA)



Nor Shuhada Ibrahim , Nafrizuan Mat Yahya ,
Saiful Bahri Mohamed , and Mohd Ismail Yusof 

Abstract Optimization algorithms play as a crucial role in solving complex real-world problems, where achieving global optimal in high-dimensional spaces remains challenging. This article presents a novel hybrid algorithm, which combining the Modified Adaptive Bats Sonar Algorithm (MABSA) with the Squirrel Search Algorithm (SSA). This synergistic approach is designed to improve conjunction speed and solution accuracy, particularly in high-dimensional in solving optimization problems using evolutionary algorithms. To evaluate the performance of this enhanced MABSA, experimental evaluations are conducted using a comprehensive suite of seven single objective benchmark test functions to assess the performance of MABSA-SSA against the original MABSA. Notably, the SSA component enhances the capability and improves their exploration diversity. The results demonstrate that MABSA-SSA consistently better solution quality compared to the original MABSA alone. The comparative analysis demonstrates that the enhancement of MABSA exhibits superior performance in avoiding local optima and maintaining solution diversity. As conclusion, the enhancement of MABSA-SSA approach represent a significant advancement in benchmark optimization fields, providing a foundation for future developments in metaheuristic optimization and potential addressing the complex optimization challenges.

N. S. Ibrahim · N. M. Yahya (✉)

Faculty on Manufacturing and Mechatronic Engineering Technology, UMPsa, Pekan, Pahang, Malaysia

e-mail: nafrizuanmy@umpsa.edu.my

S. B. Mohamed

Faculty of Innovative Design and Technology, UniSZA, Kuala Terengganu, Terengganu, Malaysia

M. I. Yusof

Instrumentation and Control Engineering Section, Institute of Industrial Technology, UniKL, Johor Bahru, Malaysia

Keywords Evolutionary algorithm · Optimization · Benchmark test function · Swarm intelligent · MABSA · Squirrel search algorithm · Single objective optimization

1 Introduction

Quick development in science and technology lead the new studies to figure out the novelty in optimization. To solve the optimization problems, the implementation of metaheuristic evolutionary algorithms gained attention in recent decades [1]. Basically, these algorithms are inspired by biological behaviours or physical phenomena that grouped into three categories, whereby: swarm intelligence (SI), evolutionary algorithms (EA), and physical-based (PB) algorithms. SI is inspired based on the simulation of collective behaviour of a social group of a living species of animals such as birds, fish, insects, and more [2]. The algorithms are inspired based on collective behaviour of swarm which in complex interaction between individuals and its neighbourhoods with nature-based. The recent implementation of SI in solving optimization problems are particle swarm optimization (PSO) [3, 4], artificial bee colony [5], cuckoo search (CS) [6], and whale optimization (WO) [7]. Evolutionary algorithms (EAs) imitate the evolutionary behaviours of creatures based on nature that have stochastic behaviour. The searching algorithm begins with randomly generated solutions, called population. The most familiar EA that been used widely is genetic algorithm (GA), particularly in solving optimization problems [8]. Next is physical-based algorithms, which are based on the basic physical law in universe such gravitational force, and inertia force. Most of the well-known algorithms related is simulated annealing [9] and gravitational search algorithm [10]. Even though, in reality recent studies are more focused implemented on swarm intelligence [5–7, 10–18] which more studies found used the SI algorithms to solve single objective optimization problems.

Single objective optimization more basic than complex optimization such as multi objectives, niching and so on but single objective still appropriate to solve real-parameter optimization problems. Besides that, the single objective optimization problems able to focus on optimizing a specific metric, which allows to streamline the algorithm development process. In order to solve an engineering problems, single objective benchmark test function can be applied as validation platforms. Single objective benchmark test functions provided a common language for discussion between researchers and practitioners in the optimization field. They provide a way of benchmarking different optimization algorithms with standard test cases, which helps to advance the field of optimization by providing a standardized approach to algorithm development and evaluation. Overall, the use of single objective benchmark test functions is crucial in the development of optimization algorithms, ensuring that they perform reliably and effectively in solving practical optimization problems. The significant of single objective benchmark test functions lies in the fact

that it provided a standard comparison tool for evaluating the performance of algorithms. Benchmark test functions have specific characteristic such as multiple optima, convexity or non-convexity, different levels of difficulty and dimensionality. These properties making the idealist for testing and comparing in optimization algorithms.

In development of algorithms, single objective benchmark test function is a significant platform that involves to designing, optimizing and evaluating that able to attracted the attention from the researchers in developing an efficient and robust algorithms. The process of algorithm development entails identifying the objective function that able to be optimized, selecting appropriate search algorithms, tuning algorithmic parameters and evaluation their performance, even some of the problems with complexity, the development of algorithms may remain as it facing with several challenges that require further exploration.

Generally, there are various types of algorithm that commonly used in algorithm development which include Genetic Algorithm [19]. This algorithm is a searching techniques to optimize the problems by simulating natural evolution processes. This situation need to selecting the individuals from a population of solutions and then generating a new generation by applying genetic operators such as crossover, mutation and selection. Besides that, PSO also one of the familiar algorithm that used in development algorithm. These algorithms are used based on the optimization problem under consideration. Each algorithms has their own strengths and weakness in optimization process therefore, it is very important to select the appropriate algorithm for every specific optimization problems before developing the algorithms. The recently various modification are also proposed in the basic version of existing nature-inspired algorithms for solving complex optimization problems [20].

This article discussed about the effectiveness of combination MABSA with Squirrel Search Algorithm (SSA), which termed as MABSA-SSA using single objective benchmark test functions. Modified adaptive bats sonar algorithm (MABSA) is one recently introduced nature-inspired algorithm which an improved version after refining modification from adaptive bats sonar algorithm (ABSA) [21]. MABSA and SSA has their special characteristic that can be merge in order to find a better solution. This algorithm is proposed to replace the jumping strategies from SSA into bats echolocation in both local and global search phase.

2 Modified Adaptive Bats Sonar Algorithm (MABSA)

MABSA was formulated by Mat Yahya and Tokhi [22] and being applied as solving an unconstrained single objective optimization problem. This algorithm was created to generate a good solution which satisfied into all of the constraints. Basically, the original MABSA formulated by modifying three search actions which are creating a way to set the *beam length* (L), *determining the starting angle* (θ_m), and *the angle between beams* (θ_i) and last one is *calculating the end point position* (pos_i). In previous MABSA, the value of *beam length* (L) are obtained based on random value which to make real variation of beam lengths. The original formulation for L are

calculated as in Eq. (1):

$$L = Rand \times \left(\frac{SSsize}{10\% \times Bats} \right) \quad (1)$$

The *solution range* of (*SSsize*) is the limit value between the upper search space which is (*SSMax*) and lower search space (*SSMin*). The solution range divided into micron scales, such as low as 10% of the overall population of bats in the search space. The percentage is marked as the conceivable search space size of each bat to emit sound without colliding with one another. In MABSA, this random *L* is ready to make a real variation of beam length of each *number of beams* (*NBeam*) at every dimension. Each *NBeam* with *L* emitted from a specific angle location. The bounce-back strategy has been applied and not considering to clarify in this paper. In original MABSA, the pos_i for each transmitted beam is designed as in Eq. (2):

$$pos_i = \alpha \times pos_{sp} + \beta \times L(\cos[\theta_m + (i - 1)\theta])^\omega \quad (2)$$

According to the equation, there are two random variables and one fixed. The first random variable in this equation was declared as the *position adaptability factor* (α). This factor are same indicative as the random walk concept. The value of α is selected from range 0 and 1. The second random variable is the *collision avoidance factor* (β) whereby is essential to prevent the beam from overlapping with other beams. The value of (β) also comes in ranges between 0 and 1 using random factors. The only constant in this equation is the *beam-turning constant* (ω) which 2. However, these $\alpha\beta$ and ω components will not be further discussed in this article since it is similar to the previous MABSA. This part will only describe the details improvement of *beam length* (*L*). The new mechanism implemented in this *L* is to create a new exploration component in calculating the end point position generated based on squirrel search optimization. This concept will be a new component in MABSA.

3 Squirrel Search Algorithm (SSA)

The searching mechanism begin once the squirrels are foraging. These squirrels will search for their food resources by gliding from one tree to others on autumn session. Their change the location and explore new areas in the forest. As the climatic conditions are hot, they meet their regularly daily energy which required to be more quickly on the diet of acorns available abundance. Therefore, they consume acorns immediately upon finding them. After completing their daily energy, they will start searching for an optimal food source for the winter season by searching for hickory nuts. The storage of this nut will encourage them to maintain the energy that's needed in extremely harsh weather while reducing the costly foraging trips and increasing the probability of survival. On winters, all of the squirrels become less active due to

the increase in of risk predation but after the end of this season, they will become active again [20].

Therefore, this repetitive life will continue until their lifespan then forming the foundation of the squirrel search algorithm. The random initial location searching of flying squirrels is represented the same as familiar other algorithms. Their location is represented in vector, in d dimensional search point. So, the flying squirrels can glide in 1-D, 2-D, 3-D, or hyperdimensional search space and change their location vectors. The initialize population formula was described in the following Eq. (3):

$$FS_i = FS_L + rand(1, D) \times (FS_U - FS_L) \quad (3)$$

The number of the population was assumed as N (FS_i). The upper and lower bounds value of search spaces are represented as FS_U and FS_L . FS_i represents the i -th individual, ($i = 1 \dots N$); $rand(0,1)$ is a uniformly distributed random number in the range (0,1). Recently, SSA has been used in various applications, especially to solve unconstrained optimization problems. The implementation of SSA in optimization gained more attention from researchers in various fields. SSA has been used to resolve many real-world problems such as in the medication [23], heat flow [20], and traveling schedule [24]. All these variations proved the effectiveness of the algorithm in their particular cases but in order to get better global convergence ability, it is recommended to combine it with others optimization algorithms.

4 Proposed Approach MABSA with SSA

This proposed a novelty of MABSA with SSA which implemented to increase the exploration in finding a new search space and consequently diversity the population. The proposed optional is an alternative way from the original MABSA to achieve better performance and higher velocity of convergence. In previous MABSA, the way to setting up the *solution range* or the minimum and maximum values of the search space are based on [25]. In order to achieve the requirement in optimization, the significant points to preserve the diversity of the population, then develop the new search space effectively.

In this MABSA-SSA, the new L is described in the following Eq. (4);

$$L = SSMin + (levy \times Bats) \times (SSSize) \quad (4)$$

where the *solution range* ($SSSize$) is the value of upper search space limit ($SSMax$) and lower search space ($SSMin$) limit as in Eq. (5);

$$SSSize = SSMax - SSMin \quad (5)$$

The representing of *Levy* is distributed encouragement of better and more structured search space exploration. According to previous studies, Levy flight is one of the

powerful mathematical tools used by researchers for improving global exploration [9, 26, 27].

From the modification, it will make a guidance mechanism to improvise the transmitted bats to the new directional based on [28]. To improvise the searchability of the algorithm, it assumed that each of the bats emits pulses in two different directions. One direction belongs to the best individual and the other is the direction to randomly chosen bats. To simplify the calculation, eliminate velocity terms in the basic bats by Eq. (5). Thus, this can be said that the combination of MABSA and SSA fulfilled the requirements of global convergence and hence a global solution is guaranteed for most of the situation.

For validation purpose and performance of developed algorithms, we employed (7) seven different benchmark test problems with varying number of objectives and dimensionality in the experiments. These benchmark test problems included seven of well-known benchmarks, i.e., Easom function, Beale function [29], Eggholder function [30], Alphine function [31], Cross-in-tray function [32], Storn's function [33] and Levy's N.13 function. This research used four dimension which $D = 2$, $D = 5$, $D = 10$ and $D = 12$ as a benchmarking and comparison standards based on study [6]. The variation dimensions (D) being used to validate the new algorithm is crucial for ensuring the robustness, scalability and also generalization ability. Aside from that, it also helps to identifying how well algorithms can handle the complex, high-dimensional problems which is an essential for solving real-world applications. By systematically testing the algorithm across various dimensions, the future study and practitioners may optimize in term of their performance, tune their parameters effectively, and ensure consistent results across different problems spaces [34].

5 Result and Discussion

This section, consist of the results from simulation MABSA-SSA are presented. The experiments are performed 30 times for a variables dimension (D) size of 2, 5, 10 and 12. For performance evaluation, simulation are performed on Matlab r2016b. Here, seven (7) well-known single objective benchmark test functions are used whereby *Easom function*, *Beale function*, *Eggholder function*, *Alphine function*, *cross-in-tray function*, *Storn's function* and *Levy's N.13 function* are used. The resultant from this MABSA-SSA was compared into original MABSA.

Figure 1 shown the bar plot of statistical results among MABSA-SSA with original MABSA. The results of comparison are presented using different size of dimension (D) which are $D = 2$, $D = 5$, $D = 10$ and $D = 12$ as refers based on [6]. The results in this bar plot are based on one single objective benchmark test function which is Easom function, according to their *best* value. The optimum global value for this function is (-1) . From this result, as can see starting from $D = 5$, $D = 10$ and $D = 12$, the new developed MABSA-SSA gives good increment which better minimum point that global which obtained (-3.84) , (-3.85) and (-3.77) , respectively. This finding shown that higher dimension enable the algorithm to capture better and exploit

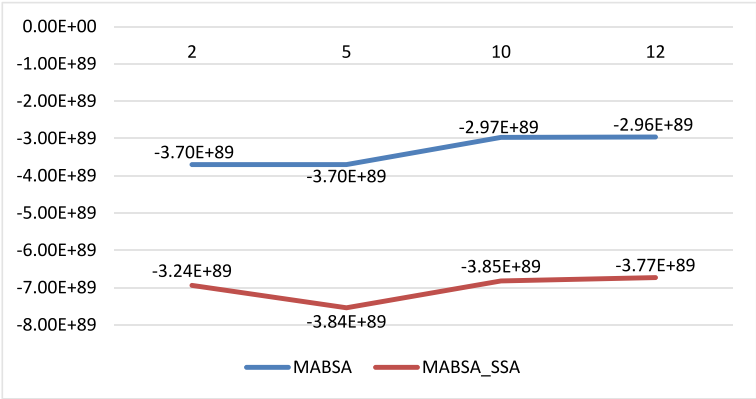


Fig. 1 A figure shown the bar plot of statistical results comparing MABSA-SSA with original MABSA

intricate features of the data, lead to more reliable and accurate results when it used to solve complex optimization problems. To sum up, all simulation results indicate the improved hybrid of MABSA is very helpful in improving the efficiency of new approach in MABSA with SSA in terms of result quality.

The important of using this variation of dimension in this development of the algorithm are for creating robustness, efficient and more scalable optimization methods. Addressing the challenges posed by high-dimensional spaces requires innovative strategies that balance exploration, manage computational complexity, and adapt dynamically to varying problem scales. By focusing on these aspects, the study can enhance the performance and applicability of optimization algorithms across a huge scope of real-world problems.

6 Conclusion

The study was introduced a novel hybrid optimization algorithm, which integrated the strength of MABSA with SSA. The hybrid approach aims to enhance benchmark optimization performance by combining MABSA’s adaptive frequency with SSA’s dynamic foraging strategy. Our extensive comparative analysis demonstrates that the MABSA-SSA hybrid consistently outperforms the original MABSA across a range of benchmark functions. The finding shown that the mechanisms of MABSA combined with the seasonal behavior of SSA developed a robust balance between exploration. This been proof when evaluated in *Easom Function* (F01) using $D = 12$, the global minimum value for this function is (-1) . The percentage increment in this function using original MABSA with MABSA-SSA shown 41.33% improves over than original MABSA when considering the global value as a reference point. To calculate the percentage of increment in this context, where the performance

values are negative, it's important to consider the improvement in performance in terms of their absolute values, especially since the performance metric might imply that a lower (more negative) value indicates better performance. Additionally, the global value serves as a reference point to understand the scale of improvement. In conclusion, the MABSA-SSA algorithm represents a substantial advancement in the field of optimization. Its integration of evolutionary random mechanisms and adaptive search strategies offers a powerful tool for addressing complex and high-dimensional problems. Future research could explore further hybridizations and real-world optimization applications, potentially extending the algorithm's versatility and effectiveness. This study lays a solid foundation for continued innovation in optimization algorithm development, emphasizing the benefits of hybrid approaches in achieving superior performance.

Acknowledgements This paper would not have been possible without the financial support given by the Internal Grant No.RDU240309 from University Malaysia Pahang Al-Sultan Abdullah (UMPSA).

References

1. Zheng T, Luo W (2019) An improved squirrel search algorithm for global function optimization. *Algorithms* 12(4):31. <https://doi.org/10.1155/2019/6291968>
2. Abdullah JM, Rashid TA, Member I (2019) Fitness dependent optimizer: inspired by the bee swarming reproductive process. *IEEE Access*. <https://doi.org/10.1109/ACCESS.2019.2907012>
3. Mat Yahya N, Nor Azlan NA, Tokhi MO (2019) Parametric study of dual-particle swarm optimisation-modified adaptive bats sonar algorithm on multi-objective benchmark test functions. *Mekatronika* 1(2):72–80. <https://doi.org/10.15282/mekatronika.v1i2.4988>
4. Jahandideh-Tehrani M, Bozorg-Haddad O, Loáiciga HA (2020) Application of particle swarm optimization to water management: an introduction and overview. *Environ Monit Assess* 192(5). <https://doi.org/10.1007/s10661-020-8228-z>
5. Azlan NA, Yahya NM (2019) Modified adaptive bats sonar algorithm with doppler effect mechanism for solving single objective unconstrained optimization problems. In: *Proceedings—2019 IEEE 15th international colloquium on signal processing and its applications, CSPA 2019*, no March, pp 27–30. <https://doi.org/10.1109/CSPA.2019.8696057>
6. Salgotra R, Singh U, Saha S, Gandomi AH (2020) Improving cuckoo search: incorporating changes for CEC 2017 and CEC 2020 benchmark problems. In: *2020 IEEE congress on evolutionary computation, CEC 2020—conference proceedings*. <https://doi.org/10.1109/CEC48606.2020.9185684>
7. Soleimani Gharehchopogh F, Gholizadeh H (2019) A comprehensive survey: whale optimization algorithm and its applications. *Swarm Evol Comput* 48(March):1–24. <https://doi.org/10.1016/j.swevo.2019.03.004>
8. Han S, Xiao L (2022) An improved adaptive genetic algorithm. *SHS Web Conf* 140:01044. <https://doi.org/10.1051/shsconf/202214001044>
9. Bozorg-Haddad O (2018) *Studies in computational intelligence—advanced optimization by nature-inspired algorithms*
10. Xiaobing Y, Xianrui Y, Hong C (2019) An improved gravitational search algorithm for global optimization. *J Intell Fuzzy Syst* 37(4):5039–5047. <https://doi.org/10.3233/JIFS-182779>

11. Tawhid MA, Dsouza KB (2020) Hybrid binary bat enhanced particle swarm optimization algorithm for solving feature selection problems. *Appl Comput Inform.* <https://doi.org/10.1016/j.aci.2018.04.001>
12. Sharifi MR, Akbarifard S, Madadi MR, Qaderi K, Akbarifard H (2022) Application of MOMSA algorithm for optimal operation of Karun multi objective multi reservoir dams with the aim of increasing the energy generation. *Energy Strateg Rev* 42(May):100883. <https://doi.org/10.1016/j.esr.2022.100883>
13. Bahrami M, Bozorg-Haddad O, Chu X (2018) Application of cat swarm optimization algorithm for optimal reservoir operation. *J Irrig Drain Eng* 144(1):1–10. [https://doi.org/10.1061/\(ASCE\)IR.1943-4774.0001256](https://doi.org/10.1061/(ASCE)IR.1943-4774.0001256)
14. Zhang X, Yu X, Qin H (2016) Optimal operation of multi-reservoir hydropower systems using enhanced comprehensive learning particle swarm optimization. *J Hydro-Environ Res* 10:50–63. <https://doi.org/10.1016/j.jher.2015.06.003>
15. Jing Niu W, Kai Feng Z, Tian Cheng C, Yu Wu X (2018) A parallel multi-objective particle swarm optimization for cascade hydropower reservoir operation in southwest China. *Appl Soft Comput J* 70:562–575. <https://doi.org/10.1016/j.asoc.2018.06.011>
16. Neshat M, Adeli A, Sepidnam G, Sargolzaei M, Toosi AN (2012) A review of artificial fish swarm optimization methods and applications. *Int J Smart Sens Intell Syst* 5(1):107–148. <https://doi.org/10.21307/ijssis-2017-474>
17. Hebala A, Hebala O, Ghoneim WAM, Ashour HA (2018) Multi-objective particle swarm optimization of wind turbine directly connected PMSG. In: 2017 19th international middle-east power systems conference MEPCON 2017—Proceedings, pp 1075–1080. <https://doi.org/10.1109/MEPCON.2017.8301315>
18. Scheepers C, Engelbrecht AP, Cleghorn CW (2019) Multi-guide particle swarm optimization for multi-objective optimization: empirical and stability analysis. *Swarm Intell* 13(3–4):245–276. <https://doi.org/10.1007/s11721-019-00171-0>
19. Maghawry A, Hodhod R, Omar Y, Kholief M (2021) An approach for optimizing multi-objective problems using hybrid genetic algorithms. *Soft Comput* 25(1):389–405. <https://doi.org/10.1007/s00500-020-05149-3>
20. Jain M, Singh V, Rani A (2019) A novel nature-inspired algorithm for optimization: squirrel search algorithm. *Swarm Evol Comput* 44(February):148–175. <https://doi.org/10.1016/j.swevo.2018.02.013>
21. Yahya NM, Tokhi MO (2017) A modified bats echolocation-based algorithm for solving constrained optimisation problems. *Int J Bio-Inspired Comput* 10(1):12–23. <https://doi.org/10.1504/IJBIC.2017.085335>
22. Mat Yahya N, Tokhi MO (2017) A modified bats echolocation-based algorithm for solving constrained optimisation problems. *Inderscience* 10(1):12–23
23. Deb D, Roy S (2021) Brain tumor detection based on hybrid deep neural network in MRI by adaptive squirrel search optimization. *Multimed Tools Appl* 80(2):2621–2645. <https://doi.org/10.1007/s11042-020-09810-9>
24. Liu Z et al (2021) A discrete squirrel search optimization based algorithm for Bi-objective TSP. *Wirel Netw* 8. <https://doi.org/10.1007/s11276-021-02653-8>
25. Tawfeeq MA (2012) Intelligent algorithm for optimum solutions based on the principles of bat sonar 10(10):11–19
26. Chawla M, Duhan M (2018) Levy flights in metaheuristics optimization algorithms—a review. *Appl Artif Intell* 32(9–10):802–821. <https://doi.org/10.1080/08839514.2018.1508807>
27. Liu Y, Cao B (2020) A novel ant colony optimization algorithm with levy flight. *IEEE Access* 8:67205–67213. <https://doi.org/10.1109/ACCESS.2020.2985498>
28. Shan X, Cheng H (2018) Modified bat algorithm based on covariance adaptive evolution for global optimization problems. *Soft Comput* 22(16):5215–5230. <https://doi.org/10.1007/s00500-017-2952-5>
29. Omae Y (2024) Gaussian process-based Bayesian optimization and shape transformation of benchmark functions. *J Phys Conf Ser* 2701(1). <https://doi.org/10.1088/1742-6596/2701/1/012022>

30. Demidova A (2016) Global optimization software and evolutionary algorithms, vol 02009, pp 1–4
31. Jensi R, Jiji GW (2016) An enhanced particle swarm optimization with levy flight for global optimization. *Appl Soft Comput J* 43:248–261. <https://doi.org/10.1016/j.asoc.2016.02.018>
32. Khari M, Kumar P (2017) An effective meta-heuristic cuckoo search algorithm for test suite optimization. *Inform* 41(3):363–377
33. Storn R, Price K (1997) Differential evolution—a simple and efficient heuristic for global optimization over continuous spaces. *J Glob Optim* 11(4):341–359. <https://doi.org/10.1023/A:1008202821328>
34. Nguyen BH, Xue B, Zhang M (2020) A survey on swarm intelligence approaches to feature selection in data mining. *Swarm Evol Comput* 54(February):100663. <https://doi.org/10.1016/j.swevo.2020.100663>

Leveraging Explainable AI for Accurate Production Forecasting in the Bag Manufacturing Industry



Rayinda Pramuditya Soesanto and Fandi Achmad

Abstract The use of Explainable AI (XAI) to improve the accuracy and transparency of production forecasts in the bag manufacturing business is investigated in this study. Historical production data, such as material types, lead times, vendor capacity, and seasonal demand fluctuations, were used to create prediction models with machine learning algorithms. The Gradient Boosting Machines was chosen as the best-performing model. The SHAP (SHapley Additive Explanations) analysis revealed that “Units_Produced” and “Season_Demand” were the most influential elements in predicting demand. XAI substantially increased the model’s transparency, allowing stakeholders to understand the rationale behind forecasts and promoting trust in AI-driven decision making. The findings show the importance of production volume and seasonal modifications in accurate forecasting, resulting in improved inventory management and production planning. This study expands the fields of AI, manufacturing analytics, and production planning by showing the practical benefits of implementing XAI into industrial processes. The inclusion of SHAP analysis allowed for a detailed interpretation of the model’s predictions, revealing that “Units_Produced” and “Season_Demand” were the most influential factors. Limitations include data quality and industry specificity, indicating that future studies should focus on various data sources and broader XAI applications. The findings highlight XAI’s potential to transform production forecasting while improving operational efficiency and strategic planning in manufacturing.

R. P. Soesanto (✉)

The University Center of Excellence for Intelligent Sensing-IoT, Telkom University,
Bandung 40257, Indonesia

e-mail: raysoesanto@telkomuniversity.ac.id

F. Achmad

The University Center of Excellence for Digital Business Ecosystem, Telkom University,
Bandung 40257, Indonesia

R. P. Soesanto · F. Achmad

Telkom University, Bandung 40527, Indonesia

Keywords Bag manufacturing · Demand forecasting · Explainable AI · Production planning · SHAP analysis

1 Introduction

The bag manufacturing industry is a vibrant and diverse sector that manufactures a wide variety of bags, including tote bags, backpacks, luxury handbags, and travel luggage. Bag manufacture has grown significantly in recent years, due to rising customer demand for both functionality and style. According to Grand View Research, the global bag market is expected to grow at a CAGR of 5.9% from 2021 to 2028 [1]. The development of e-commerce has accelerated this expansion by allowing manufacturers to reach a global audience, with Kompas reporting 3% increase in sales through online platforms in Indonesia [2]. However, the industry has significant challenges, such as unpredictable raw material prices, growing labour costs, and the requirement for environmentally friendly procedures. The demand for customization, combined with sudden shifts in customer tastes, requires adaptability and creativity in organizations. In this unpredictable environment, precise production prediction is critical for successful inventory management, supply chain optimization, and satisfying market demand.

Accurate production forecasting is critical in the bag manufacturing industry since it directly influences a company's capacity to successfully meet market demand while keeping prices low. Manufacturers can optimize production schedules, manage inventory levels efficiently, and reduce the risks of overproduction and stockouts by precisely estimating future demand [3–8]. This not only ensures quick delivery to clients, increasing happiness and loyalty but also improves the utilization of resources, including raw materials and people, resulting in increased operational efficiency and cost savings. In a competitive business with continuously changing consumer tastes, the ability to accurately estimate demand is a huge advantage, allowing companies to remain ahead of market trends and respond quickly to customer wants.

Advanced prediction techniques, such as machine learning, can help businesses better understand and forecast demand, increasing their overall competitiveness. In the context of production planning, the importance of transparent and explainable AI models has grown. As manufacturers use AI-powered methodologies to forecast demand and optimize production, the complexity of these models frequently distorts their decision-making processes. This lack of transparency might cause mistrust among stakeholders. Explainable AI (XAI) addresses this issue by providing insights into how models make predictions, emphasizing the role of diverse variables, and making the AI's reasoning processes easier to understand and understandable [9–12]. Specifically, SHAP (Shapley Additive Explanations) provides a robust method for interpreting complex models by quantifying the contribution of each

feature to the predictions [13]. This improves transparency and trust, allowing stakeholders to understand the underlying factors influencing demand forecasts. Implementing Explainable AI (XAI) in production forecasts has significant benefits for manufacturers, notably in terms of cost savings and efficiency.

Despite the growing adoption of AI and XAI in various industries, there is a lack of study specifically addressing the application of SHAP in the context of the bag manufacturing industry. This study aims to fill this gap by investigating how SHAP can enhance the interpretability and accuracy of demand forecasting models in this sector. By implementing and analysing the impact of SHAP-based XAI models, this study seeks to provide manufacturers with more reliable and transparent tools for decision-making, ultimately improving operational efficiency and responsiveness to market demands. By offering clear insights into demand factors, XAI allows for more informed inventory management, production scheduling, and resource allocation. Furthermore, XAI makes complex AI models interpretable, increasing trust and adoption of AI technology.

2 Methodology

The primary objective of this study is to enhance the accuracy and transparency of production forecasting in the bag manufacturing industry through the application of Explainable AI (XAI) techniques. The method used for this study begins with thorough data collecting and preparation. Figure 1 show the proposed methodology for prediction using explainable AI in bag manufacturer. From Fig. 1 it is known that the bag manufacturing company's records contain historical production data, such as batch information, material types, lead times, vendor capacities, seasonal demand changes, SKUs, units produced, and actual sales. This dataset provides a solid foundation for building predictive models. The acquired data is subsequently pre-processed to remove missing values and outliers while ensuring consistency, resulting in a clean and reliable dataset for analysis. The next phase includes developing prediction models with machine learning techniques. Five separate techniques are used: linear regression, decision trees, random forest, support vector regression (SVR), and gradient boosting machines (GBMs).

Linear regression is one of the most basic and widely used algorithms for predictive modelling. It models the link between a dependent variable and one or more independent variables by fitting a linear equation to the observed data. Previous studies that use linear regression for forecasting are from El Jaouhari et al. [14] and Markuryeva et al. [15]. Decision trees are nonlinear predictive models that use a tree-like structure to represent decisions and their potential outcomes. Previous studies that use decision trees are [16, 17]. Random Forest is an ensemble learning method that constructs several decision trees during training and outputs the class that is the mode of the classes (classification) or the mean prediction (regression) of each tree.

Previous studies shows that the error from this is minimum [18, 19]. Support Vector Regression (SVR) is a regression-specific version of Support Vector Machines

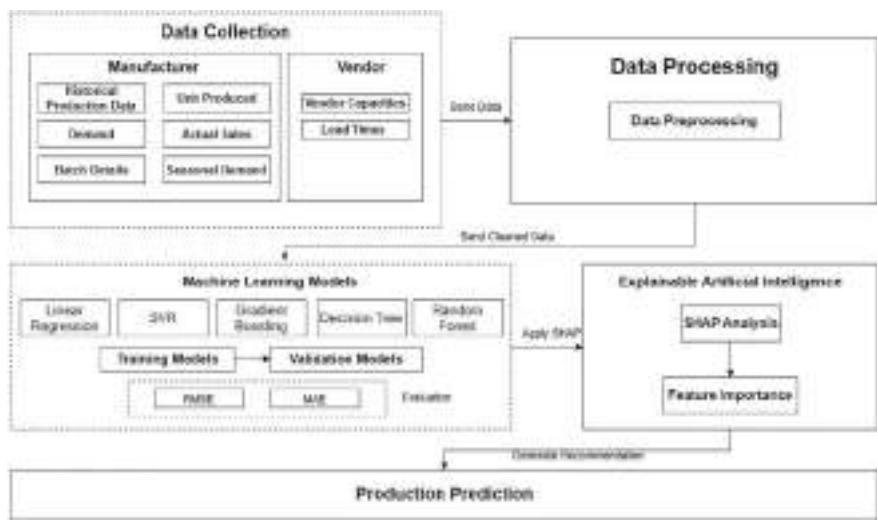


Fig. 1 Proposed model for explainable AI prediction

(SVM). SVR works well in high-dimensional domains and when there are more dimensions than samples. Previous studies that use SVR for forecasting are from Fradinata et al. [20], Guo et al. [21], and Kamal et al. [22]. Gradient Boosting Machines (GBMs) are a strong ensemble learning technology that constructs a predictive model by incrementally adding predictors, often decision trees. Each new model tries to fix the mistakes caused by prior models. GBMs can perform a variety of predictive modelling tasks and are noted for their accuracy and ability to handle complex data structures. Previous studies that uses SVR for forecasting are from Panarese et al. [23], Han et al. [24], and Metawa [25].

The models use the pre-processed dataset to anticipate future demand based on past trends and influencing factors. To enhance model performance, hyperparameter tuning is applied to each algorithm, adjusting their settings to attain the highest predicted accuracy. Cross-validation techniques are used to validate the models, assuring accuracy and applicability to new data. Each model’s predictive accuracy is assessed using metrics such as Mean Absolute Error (MAE), Mean Squared Error (MSE), and Root Mean Squared Error (RMSE). Furthermore, visuals are made to compare the error rates of the various algorithms, emphasizing the most effective model.

Explainable AI (XAI) approaches are used during the model construction process to ensure the predictions’ transparency and interpretability. In this study SHAP (SHapley Additive Explanations) is used for explaining the output of the model, SHAP is widely used to explain the output. Previous study from Yang et al. [26] focused on using SHAP for explaining cooperative AI workers. Previous study from Lee and Roh [27] use the benefit of SHAP in semiconductor manufacturing. Previous study from Li et al. [28] use SHAP to explain the machine learning model

for transportation. For this study, SHAP values are used to explain the output of the best-performing models. SHAP values give extensive information about how each element contributes to the model’s predictions, allowing stakeholders to understand the impact of factors like material type, lead time, and seasonal demand. This transparency aids in identifying important drivers of demand and enables educated decision-making based on the AI model’s explanations.

The final stage is to evaluate the performance of the developed models. The impact of lead time and seasonal demand on demand forecasting is examined using the insights provided by XAI methodologies. This thorough examination guarantees that the most accurate and interpretable model is chosen for practical use, hence improving the production forecasting process in the bag manufacturing business.

3 Result and Discussion

The object of this study is one bag manufacturing company in Bandung, Indonesia. The data collection approach for this study includes obtaining significant historical data from the bag manufacturing company. The data that is used in this study is taken from historical data from 2022 to 2023. Table 1 shows the variables that are used in this study.

Data preprocessing is essential for accurate predictive models. It includes handling missing data, addressing outliers, standardizing variable formats and units, and encoding categorical variables like Material Type and SKU. Specifically, missing

Table 1 Variable for predicting production

Variables	Description
Batch	Represents a specific production run within a given time frame, identified by a unique batch code
Material type	Specifies the type of material used in the production of bags
Lead time	The time in days from ordering materials to their arrival at the vendor, influencing production schedules
Vendor capacity	The maximum number of units a vendor can produce within a given period, reflecting the vendor’s production capabilities
Season demand	A multiplier that adjusts demand forecasts based on seasonal variations
SKU (stock keeping unit)	A unique identifier for each product variant, including different colors and designs
Units produced	The actual number of units manufactured during the batch
Demand	The forecasted demand for each SKU, predicting the number of units expected to be sold
Actual sales	The real number of units sold during the period, used to measure the accuracy of demand forecasts

data was addressed through median imputation, outliers were managed using IQR methods, and categorical variables were encoded using One-Hot Encoding. The dataset is then split into training and testing sets to develop and validate the models. The predictive model is developed using Python. The predictive model development provided significant insight into the accuracy and efficacy of several machine learning algorithms in estimating production demand in the bag manufacturing business. Five distinct models were tested: Linear Regression, Decision Trees, Random Forest, Support Vector Regression (SVR), and Gradient Boosting Machines (GBM). Table 2 shows the comparison results of MAE and RMSE between the algorithms. The Gradient Boosting Regressor is the most accurate model, with an R-squared (R^2) value of 0.99, explaining 99% of the variance in demand data. The MAE and RMSE measurements also revealed that the Gradient Boosting model outperformed the other models, with much-reduced error rates.

The use of Explainable AI (XAI) approaches, notably SHAP (SHapley Additive Explanations), provides useful insights into the model’s decision-making process. The SHAP analysis results, as shown in Fig. 2, give a clear picture of the relative importance of various characteristics in the Random Forest Regressor model used for demand forecasting in the bag manufacturing industry.

The graphic shows the mean absolute SHAP values, which show the average effect of each feature on the model’s output. The study shows that “Units_Produced” is the most impactful attribute, with a much higher SHAP value than the others. This indicates that the number of units produced contributes a critical role in predicting demand, probably because it directly correlates with the actual sales and inventory

Table 2 Comparison results of MAE and RMSE between algorithms

	MAE	RMSE
Linear regression	5.478	10.697
Decision tree regressor	0	0
Random forest regressor	1.473	5.695
Gradient boosting regressor	0.039	0.084
Support vector regressor	26.562	78.556

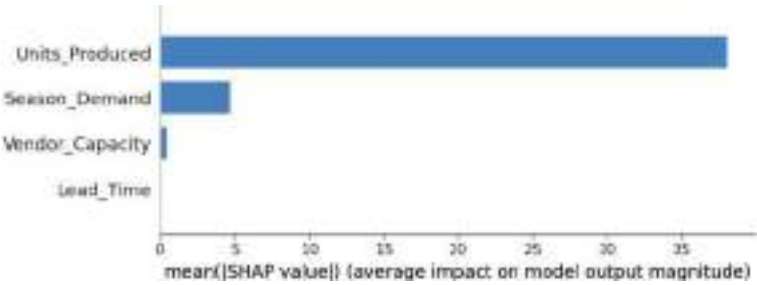


Fig. 2 Global feature importance

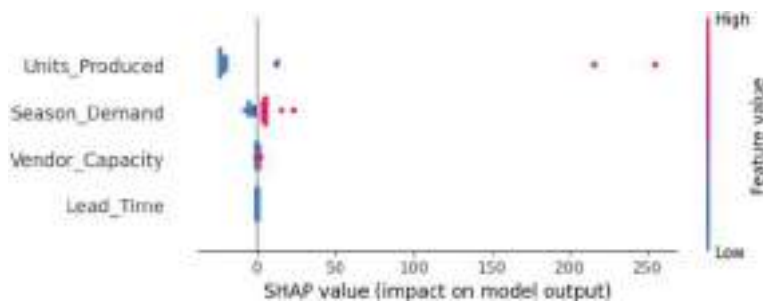


Fig. 3 SHAP summary

levels. “Season_Demand” is the second most effective element, emphasizing the significance of accounting for seasonal fluctuations in demand forecasting. This is consistent with the frequent business observation that demand for products varies dramatically depending on the time of year. “Vendor_Capacity” and “Lead_Time” have lower SHAP values, showing that, although they have an impact on demand estimates, it is less evident than “Units_Produced” and “Season_Demand”. This study indicates that production capacity and the time necessary to get supplies are crucial, but they may not be as strongly related to immediate demand variations as the other components.

Figure 3 shows the SHAP summary, the graphic shows the influence and distribution of each feature’s contribution to the model’s predictions in Gradient Boosting Machines, that is used to estimate demand in the bag manufacturing industry. This map shows the size and direction of feature impacts on model output, with each dot indicating a SHAP value for a specific prediction.

“Units_Produced” is the most important feature, with a large range of SHAP values suggesting its strong and different impact on the model’s predictions. High feature values for “Units_Produced” (shown in pink) correlate with high positive SHAP values, implying that larger production volumes are closely connected with higher demand forecasts. This emphasizes the direct relationship between production output and anticipated demand. “Season_Demand” also has a significant impact, although slightly less than “Units_Produced”. The dots for “Season_Demand” are clustered, showing that this feature regularly influences the model’s output, with higher seasonal demand values (in pink) leading to more accurate demand projections. This highlights the significance of updating estimates based on seasonal variations to appropriately reflect demand fluctuations. “Vendor_Capacity” and “Lead_Time” have lower SHAP values, suggesting less influence on the model’s predictions. The range of SHAP values for these variables is rather small, indicating that changes in vendor capacity and lead time have a more consistent but minor impact on demand forecasting. This shows that, though these operational characteristics are important, their fluctuation has no substantial impact on demand forecasts when compared to production volume and seasonality.

Explainable AI (XAI) considerably improves the forecasting model's transparency and trustworthiness, as shown by the findings. SHAP provides deep insights into each feature's contribution to the model's projections, allowing stakeholders to better understand the underlying drivers of predicted demand. For example, the SHAP analysis found that "Units_Produced" and "Season_Demand" are the most influential elements, with a clear impact on demand estimates. This level of transparency helps to explain the AI model's decision-making process, allowing production planners and management to trust and rely on the model's results. SHAP values let stakeholders assess the model's logic by displaying how different variables affect predictions, ensuring that it matches their domain expertise and operational expectations. This transparency not only increases confidence in the AI-powered forecasting system, but also allows for improved collaboration across departments because everyone can see and understand how and why certain decisions are made. Overall, XAI, through SHAP, provides manufacturers with clear, interpretable, and actionable data, resulting in more informed and trustworthy decisions about production planning and inventory management.

The findings of this study have important consequences for the bag manufacturing industry, especially in terms of inventory management and production planning. Manufacturers can improve demand forecasting accuracy by using Explainable AI (XAI), allowing them to optimize production plans and inventory levels. The insights offered by SHAP analysis highlight the importance of production volume and seasonal demand in forecasting, allowing manufacturers to better anticipate market needs and adjust operations accordingly.

4 Conclusion

This study shows the significant advantages of implementing Explainable AI (XAI) to improve production forecasting accuracy and transparency in the bag manufacturing industry. The Gradient Boosting Machines model had a high R-squared value of 0.99, and SHAP analysis showed that "Units_Produced" and "Season_Demand" were the most influential components. These findings highlight the importance of production volume and seasonal modifications in accurate demand forecasting, resulting in better production planning and inventory management.

XAI, particularly SHAP, improves the model's transparency and trustworthiness by explaining how each feature contributes to the predictions. This transparency enables stakeholders to understand and trust the AI model's outputs, resulting in more informed decision-making and improved collaboration across departments. The study has limitations in terms of data quality and bag manufacturing-specificity. Future studies should investigate integrating other data sources, using XAI in different manufacturing contexts, and undertaking longitudinal studies to determine the long-term impact of AI-driven forecasting on operational efficiency and financial performance.

References

1. Grand View Research (2023) Handbag market size, share & trends analysis report by raw material (leather, fabric), by product (tote bag, clutch), by distribution channel, by region, and segment forecasts, 2023–2030
2. Kompas (2023) Kompas market insight: Indonesian FMCG E-commerce report 2023
3. Pal S (2023) Advancements in AI-enhanced just-in-time inventory: elevating demand forecasting accuracy. *Int J Res Appl Sci Eng Technol* 11(11):282–289. <https://doi.org/10.22214/ijraset.2023.56503>
4. Tang Y-M, Ho GTS, Lau Y-Y, Tsui S-Y (2022) Integrated smart warehouse and manufacturing management with demand forecasting in small-scale cyclical industries. *Machines* 10(6):472. <https://doi.org/10.3390/machines10060472>
5. Terrada L, El Khaili M, Ouajji H (2022) Demand forecasting model using deep learning methods for supply chain management 4.0. *Int J Adv Comput Sci Appl* 13(5). <https://doi.org/10.14569/IJACSA.2022.0130581>
6. Dou Z, Sun Y, Zhang Y, Wang T, Wu C, Fan S (2021) Regional manufacturing industry demand forecasting: a deep learning approach. *Appl Sci* 11(13):6199. <https://doi.org/10.3390/app11136199>
7. Lorente-Leyva LL et al (2019) Artificial neural networks in the demand forecasting of a metal-mechanical industry. *J Eng Appl Sci* 15(1):81–87. <https://doi.org/10.36478/jeasci.2020.81.87>
8. Achmad F, Wiratmadja II (2024) Driving sustainable performance in SMEs through frugal innovation: the nexus of sustainable leadership, knowledge management, and dynamic capabilities. *IEEE Access* 12:103329–103347. <https://doi.org/10.1109/ACCESS.2024.3433474>
9. Gade K, Geyik SC, Kenthapadi K, Mithal V, Taly A (2019) Explainable AI in industry. In: *Proceedings of the 25th ACM SIGKDD international conference on knowledge discovery & data mining*, pp 3203–3204. ACM, New York, NY, USA. <https://doi.org/10.1145/3292500.3332281>
10. Branco R et al (2023) Explainable AI in manufacturing: an analysis of transparency and interpretability methods for the XMANAI platform. In: *2023 IEEE international conference on engineering, technology and innovation (ICE/ITMC)*, pp 1–8. IEEE. <https://doi.org/10.1109/ICE/ITMC58018.2023.10332373>
11. Gade K, Geyik S, Kenthapadi K, Mithal V, Taly A (2020) Explainable AI in industry: practical challenges and lessons learned. In: *Companion proceedings of the web conference 2020*, pp 303–304. ACM, New York, NY, USA. <https://doi.org/10.1145/3366424.3383110>
12. Miltiadou D, Perakis K, Sesana M, Calabresi M, Lampathaki F, Biliri E (2023) A novel explainable artificial intelligence and secure artificial intelligence asset sharing platform for the manufacturing industry. In: *2023 IEEE international conference on engineering, technology and innovation (ICE/ITMC)*, pp 1–8. IEEE. <https://doi.org/10.1109/ICE/ITMC58018.2023.10332346>
13. Nohara Y, Matsumoto K, Soejima H, Nakashima N (2019) Explanation of machine learning models using improved shapley additive explanation. In: *Proceedings of the 10th ACM international conference on bioinformatics, computational biology and health informatics*, pp 546–546. ACM, New York, NY, USA. <https://doi.org/10.1145/3307339.3343255>
14. El Jaouhari A, Alhilali Z, Arif J, Fellaki S, Amejwal M, Azzouz K (2022) Demand forecasting application with regression and IoT based inventory management system: a case study of a semiconductor manufacturing company. *Int J Eng Res Afr* 60:189–210. <https://doi.org/10.4028/p-8ntq24>
15. Merkuryeva G, Valberga A, Smirnov A (2019) Demand forecasting in pharmaceutical supply chains: a case study. *Proc Comput Sci* 149:3–10. <https://doi.org/10.1016/j.procs.2019.01.100>
16. Irmalasari I, Dwiyantri L (2023) Algorithm analysis of decision tree, gradient boosting decision tree, and random forest for classification (Case study: west java house of representatives election 2019). In: *2023 international conference on electrical engineering and informatics (ICEEI)*, pp 1–5. IEEE. <https://doi.org/10.1109/ICEEI59426.2023.10346727>

17. Luo H, Cheng F, Yu H, Yi Y (2021) SDTR: soft decision tree regressor for tabular data. *IEEE Access* 9:55999–56011. <https://doi.org/10.1109/ACCESS.2021.3070575>
18. Chaoura C, Lazar H, Jarir Z (2022) Predictive system of traffic congestion based on machine learning. In: 2022 9th international conference on wireless networks and mobile communications (WINCOM), pp 1–6. IEEE. <https://doi.org/10.1109/WINCOM55661.2022.9966448>
19. Yao B (2023) Walmart sales prediction based on decision tree, random forest, and K neighbors regressor. *Highlights Bus Econ Manage* 5:330–335. <https://doi.org/10.54097/hbem.v5i.5100>
20. Fradinata E, Kesuma ZM, Rusdiana S, Zaman N (2019) Forecast analysis of instant noodle demand using support vector regression (SVR). *IOP Conf Ser Mater Sci Eng* 506:012021. <https://doi.org/10.1088/1757-899X/506/1/012021>
21. Guo L, Fang W, Zhao Q, Wang X (2021) The hybrid PROPHET-SVR approach for forecasting product time series demand with seasonality. *Comput Ind Eng* 161:107598. <https://doi.org/10.1016/j.cie.2021.107598>
22. Kamal E, Abdel-Gawad AFA, Ibraheem B, Zaki S (2023) Machine learning fusion and data analytics models for demand forecasting in the automotive industry: a comparative study. *Fusion Pract Appl* 12(1):24–37. <https://doi.org/10.54216/FPA.120102>
23. Panarese A, Settanni G, Vitti V, Galiano A (2022) Developing and preliminary testing of a machine learning-based platform for sales forecasting using a gradient boosting approach. *Appl Sci* 12(21):11054. <https://doi.org/10.3390/app122111054>
24. Han X, Zhang R, Li Z (2023) Research on construction and contribution analysis of demand forecasting model based on GBDT-LightGBM algorithm. In: 2023 IEEE international conference on image processing and computer applications (ICIPCA), pp 359–364. IEEE. <https://doi.org/10.1109/ICIPCA59209.2023.10257726>
25. Metawa N (2019) Forecasting business demand to enhance supply chain financial optimization: a predictive modeling approach. *Am J Bus Oper Res* 0(2):75–82. <https://doi.org/10.54216/AJBOR.000201>
26. Yang M et al (2022) Design and implementation of an explainable bidirectional LSTM model based on transition system approach for cooperative AI-workers. *Appl Sci* 12(13):6390. <https://doi.org/10.3390/app12136390>
27. Lee Y, Roh Y (2023) An expandable yield prediction framework using explainable artificial intelligence for semiconductor manufacturing. *Appl Sci* 13(4):2660. <https://doi.org/10.3390/app13042660>
28. Li M, Wang Y, Sun H, Cui Z, Huang Y, Chen H (2023) Explaining a machine-learning lane change model with maximum entropy shapley values. *IEEE Trans Intell Veh* 8(6):3620–3628. <https://doi.org/10.1109/TIV.2023.3266196>

Tool Condition Monitoring in Milling Machining Process via IOT Communications



Mohd Azfar Afiq Azhar, Ismayuzri Ishak, and Ahmad Razlan Yusoff

Abstract This study develops an IoT-based Tool Condition Monitoring (TCM) system for milling operations, aiming to enhance product quality through real-time tool wear detection. Utilizing an ESP-32 microcontroller and a vibration sensor positioned near the cutting tool, the system captures and analyzes vibration signals during the milling process. Advanced signal processing techniques extract relevant features to assess tool condition. Experimental trials demonstrate the system's effectiveness, with a strong correlation (Pearson's $r = 0.77$) between vibration-based predictions and actual tool wear measurements. This IoT-enabled TCM system offers a cost-effective solution for industrial milling applications, potentially improving product quality, reducing downtime, and optimizing tool replacement schedules. The research contributes to the advancement of smart manufacturing technologies, providing a practical approach to integrating IoT communications in machining processes for enhanced operational efficiency and product quality control.

Keywords Tool condition · Monitoring · Tool wear length · Milling process · IOT communications

1 Introduction

Tool Condition Monitoring (TCM) has emerged as a critical component in modern manufacturing processes, particularly in machining operations such as milling, turning, grinding, and drilling. TCM systems serve as preventive measures against

M. A. A. Azhar · I. Ishak · A. R. Yusoff (✉)

Faculty of Manufacturing and Mechatronic Engineering Technology, Universiti Malaysia Pahang Al-Sultan Abdullah, 26600 Pekan, Pahang, Malaysia
e-mail: razlan@umpsa.edu.my

I. Ishak · A. R. Yusoff

Centre for Advanced Industrial Technology, Universiti Malaysia Pahang Al-Sultan Abdullah, 26600 Pekan, Pahang, Malaysia

cutting tool damage and play a crucial role in maintaining product quality [1, 2]. These systems utilize various sensors and data analysis techniques to continuously assess the condition of cutting tools during operation, enabling real-time decision-making and process control [3, 4].

The primary motivation for this research stems from the increasing demand for automated and unmanned manufacturing processes. Traditional methods rely heavily on operator experience to detect tool wear, often leading to unexpected downtime and quality issues. By implementing advanced TCM systems, manufacturers can significantly reduce machine downtime, prevent tool failure, and optimize the overall machining process [1–5]. Furthermore, the integration of TCM with Internet of Things (IoT) technologies aligns with the broader Industry 4.0 paradigm, promising enhanced operational efficiency and predictive maintenance capabilities [6].

Recent literature in the field of TCM has focused on developing multi-sensor approaches and advanced signal processing techniques. Researchers have explored various sensor types, including vibration, acoustic emission, and current sensors, to capture tool wear indicators [7, 8]. Machine learning algorithms have been increasingly employed for feature extraction and wear classification, improving the accuracy and reliability of TCM systems [6]. Additionally, there is a growing trend towards the development of IoT-based TCM solutions that enable remote monitoring and data-driven decision-making in manufacturing environments [8, 9].

Despite these advancements, there remains a need for cost-effective, easily implementable TCM solutions for small to medium-scale manufacturing operations, particularly in milling processes. This paper addresses this gap by presenting the development and implementation of an IoT-based TCM system for milling machines. The primary objectives of this research are to design and implement a TCM system using vibration sensors and for real-time tool wear monitoring in milling operations.

2 Experiments Details

TCM system's software component is developed using C programming language in the Arduino IDE, tailored for ESP32 compatibility [4]. A Graphical User Interface (GUI) is created using the Blynk platform, facilitating real-time monitoring and user interaction. The software architecture integrates IoT capabilities, aligning with current trends in smart manufacturing [6]. Iterative testing and debugging ensure robust performance and seamless integration with hardware components.

Machining Experiment and Sensor Arrangement as shown in Figs. 1 and 2: The experimental setup employs a milling machine equipped with an indexable end mill (BAP300R121S16). Spheroidal graphite cast iron (FCD 450) is selected as the workpiece material due to its durability, low cost, and high machinability. An MPU6050 accelerometer sensor is strategically positioned on a non-rotary part of the milling machine to capture tri-axial vibration signals during the machining process [9]. This multi-sensor approach follows recent advancements in TCM research [7].

The NodeMCU ESP32 microcontroller, integrated with the MPU6050, forms the core of the data acquisition system, shown in Fig. 1.

Real-time data acquisition is facilitated by the ESP32’s Wi-Fi capability, which transmits vibration data to the Blynk cloud [6]. The system collects time-domain vibration signals across three axes during the milling operation (Fig. 2). Data analysis involves signal processing techniques to convert raw time-domain signals into

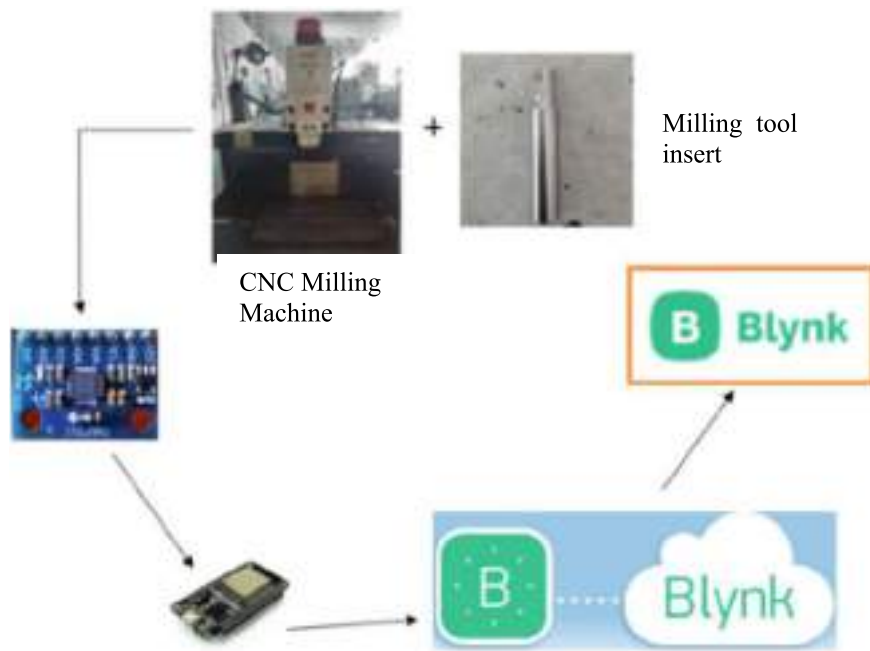


Fig. 1 Data collection during machining

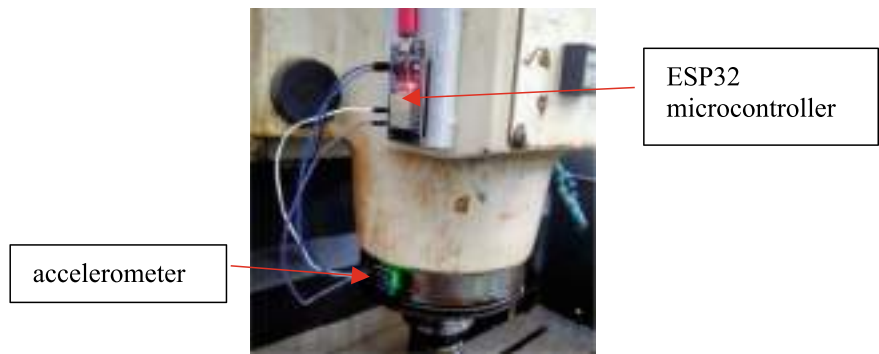


Fig. 2 Sensor arrangement on CNC machine

meaningful information. Kurtosis analysis is applied to identify changes in vibration patterns associated with tool wear [8]. The processed data is used to classify tool condition into five states: perfect, good, small wear, large wear, and fracture. This classification is displayed in real-time on the Blynk GUI, enabling operators to make informed decisions about tool replacement and process optimization. The integration of real-time monitoring and data-driven analysis contributes to the development of predictive maintenance strategies in CNC machine as shown in Fig. 2 [5, 6].

3 Result and Discussions

The experimental phase of this study involved data collection using an indexable end mill with a single insert. The MPU6050 sensor was strategically placed on a non-rotary surface near the tool, enabling the capture of vibration data across three axes (x, y, and z), as shown in Fig. 3. This placement was crucial for obtaining comprehensive vibration profiles during the milling process [9]. Data acquisition was accomplished using two parallel methods using the Blynk app for real-time graphical representation and Excel DataStream for numerical data collection. The Blynk app provided instantaneous visual feedback, allowing for immediate assessment of vibration patterns. In Fig. 3, typical experiment 11 demonstrated notable variations in vibration amplitudes across all three axes during the machining process, indicating potential tool wear progression.

For in-depth analysis, 131 data points were collected for each axis in each experiment using Excel DataStream. These datasets were subsequently processed using Origin Lab software to generate detailed graphical representations, facilitating a more nuanced understanding of vibration characteristics throughout the milling operation. The study encompassed 27 experiments, with results summarized in Table 1, correlating kurtosis values with tool wear length. A clear trend emerged, showing that higher kurtosis values generally corresponded to larger tool wear lengths. The maximum observed tool wear length was 0.4727 mm, associated with a kurtosis value of 2.233. These findings align with previous research indicating the effectiveness of kurtosis analysis in tool wear detection [8]. Based on these experimental results, a classification system for tool condition was developed and implemented in the Blynk-based GUI, as shown in Fig. 4. The system categorizes tool condition into five states of Perfect: $\text{Kurtosis} < 0.75$; Good: $0.76 \leq \text{Kurtosis} \leq 1.50$; Small wear: $1.51 \leq \text{Kurtosis} \leq 2.25$; Large wear: $2.26 \leq \text{Kurtosis} \leq 3.00$; Fracture: $\text{Kurtosis} > 3.00$, as tabulated in Table 2.

Based on the classification system, it is integrated into the GUI, provides real-time feedback on tool condition, enabling operators to make informed decisions about tool replacement and process optimization, as shown in Fig. 4. The developed TCM system demonstrates the potential for IoT-based solutions in enhancing predictive maintenance strategies for CNC machines [6]. The integration of real-time data acquisition, kurtosis-based analysis, and a user-friendly GUI represents a significant step towards implementing cost-effective, easily deployable TCM solutions in small

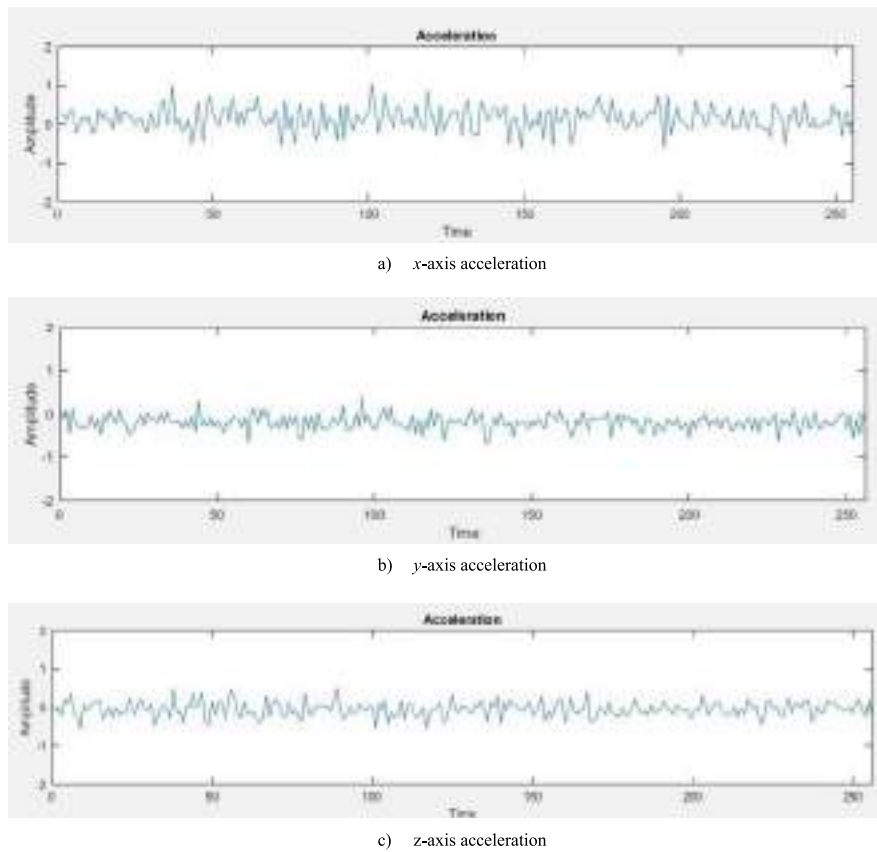


Fig. 3 Sample acceleration in experiment 11 during cutting process in Blynk environment

to medium-scale manufacturing environments. This approach aligns with the growing trend of smart manufacturing and Industry 4.0 principles [6, 8], offering a practical tool for improving machining efficiency and product quality.

Table 1 Mapping for Kurtosis value and tool wear length

Experiment	Kurtosis value	Wear length (mm)
1	0.043096448	0.090474
2	0.301342478	0.279432
3	0.232129028	0.200631
4	0.246975578	0.286959
5	0.701135233	0.167123
6	0.714218765	0.217752
7	0.853004344	0.283027
8	0.309418815	0.251106
9	0.367930002	0.280462
10	0.357399879	0.135162
11	0.198931332	0.256077
12	0.358292603	0.192442
13	0.187149477	0.294071
14	1.379460646	0.106415
15	0.467287141	0.261582
16	0.154103745	0.161238
17	0.295610459	0.105113
18	0.479910193	0.056248
19	0.087068374	0.128229
20	0.278852595	0.317750
21	0.818261418	0.072892
22	2.233727067	0.472703
23	0.264178500	0.086199
24	0.624546012	0.093685
25	0.653602292	0.138668
26	1.315160243	0.231532
27	0.569922713	0.100811

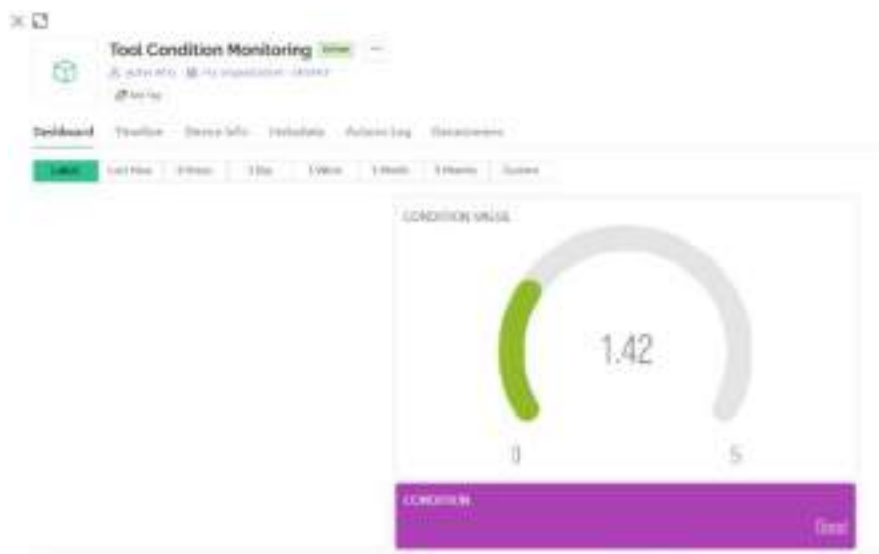


Fig. 4 Tool condition monitoring using Blynk app

Table 2 Kurtosis classification for tool conditions

Kurtosis value	Condition
<0.75	Perfect
0.76–1.50	Good
1.51–2.25	Small wear
2.26–3.00	Large wear
>3	Fracture

4 Conclusion

This study successfully developed a Tool Condition Monitoring (TCM) system for milling operations using vibration signal analysis. Several conclusions can be made:

- The system, comprising an MPU6050 sensor, ESP32 microcontroller, and Blynk app interface, effectively captured and analyzed tri-axial vibration data during the machining of FCD 450 with an indexable endmill.
- Kurtosis statistical analysis proved instrumental in determining tool condition from the vibration signals. The Blynk app provided an intuitive GUI for real-time monitoring, enhancing user accessibility. The strong correlation between kurtosis values and tool wear length, indicated by a Pearson’s r value of 0.77, demonstrates the system’s reliability in predicting tool wear.

This IoT-based TCM system offers a practical solution for improving machining efficiency and product quality in industrial applications.

Acknowledgements The authors would like to thank the Faculty of Manufacturing and Mechatronics Engineering Technology in Universiti Malaysia Pahang Al-Sultan Abdullah (UMPSA) and University Malaysia Pahang Al-Sultan Abdullah for financial support under UIC231517.

References

1. Li X, Djordjevich A, Venuvinod PK (2000) Current-sensor-based feed cutting force intelligent estimation and tool wear condition monitoring. *IEEE Trans Industr Electron* 47(3):697–702
2. Failing JM et al (2023) A tool condition monitoring system based on low-cost sensors and an IoT platform for rapid deployment. *Processes* 11:668
3. Lara de Leon MA, Kolarik J, Byrtus R, Koziorek J, Zmij P, Martinek R (2024) Tool condition monitoring methods applicable in the metalworking process. *Arch Comput Methods Eng* 31:221–242
4. Xiqing M, Chuangwen X (2009) Tool wear monitoring of acoustic emission signals from milling processes. In: 2009 first international workshop on education technology and computer science
5. Kandilli I, Sonmez M, Ertunc HM, Cakir B (2007) Online monitoring of tool wear in drilling and milling by multi-sensor neural network fusion. In: 2007 international conference on mechatronics and automation
6. Al-Naggar YM, Jamil N, Hassan MF, Yusoff AR (2021) Condition monitoring based on IoT for predictive maintenance of CNC machines. *Proc CIRP* 102:314–318
7. Ambhore N, Kamble D, Chinchani S, Wayal V (2015) Tool condition monitoring system: a review. *Mater Today Proc* 2(4–5):3419–3428
8. Serin G, Sener B, Ozbayoglu AM, Unver HO (2020) Review of tool condition monitoring in machining and opportunities for deep learning. *Int J Adv Manuf Technol* 109(3–4):953–974
9. Zhou C, Guo K, Sun J (2021) An integrated wireless vibration sensing tool holder for milling tool condition monitoring with singularity analysis. *Measurement* 174:109038

Classification of *Capsicum Annum* L. Var. Kulai Through Object Detection Using Deep Learning Models



Nur Aliya Syahirah Badrol Hisam , Yin Jun Chan,
Amir Fakarullisroq Abdul Razak , Muhammad Nur Aiman Shapiee ,
Mohd Izzat Mohd Rahman , and Mohd Azraai Mohd Razman

Abstract This research project aims to implement deep learning models for large-scale agricultural crop detection. The study investigates the performance of YOLOv8, Detection Transformer (DETR), Neural network, and Support Vector Machine (SVM) models in terms of mean average precision (mAP), precision, recall, F1-score, and detection time. The dataset used for training and evaluation comprises 684 images with a total of 27,852 bounding boxes, including 2542 instances of *Capsicum Annum* L. Var Kulai (Chilli Kulai) crops. The dataset is split into training, validation, and test sets. All machine learning and deep learning models are trained with 200 iterations. The results indicate that YOLOv8 achieves the highest mean average precision of 96.2% and an average recall of 92.6%. The neural network shows good performance, with a mean average precision of 90.5% and a recall of 90.5%. The SVM model also performs well, with a mean average precision of 89.0% and a recall of 89.1%, providing a good balance between accuracy and detection speed. DETR has the lowest mean average precision of 71.9% and a recall of 45.0%. In conclusion, this research shows that YOLOv8 is the leader in performance. It was found that the model for yolov8 is the best. The study demonstrates the potential for further development in the automation of the local agricultural sector, highlighting the benefits of using advanced machine learning models to enhance crop management techniques.

Keywords Deep learning · Agriculture crops · Chilli · Object detection · Classification

N. A. S. Badrol Hisam · Y. J. Chan · A. F. Abdul Razak · M. N. A. Shapiee ·
M. I. Mohd Rahman · M. A. Mohd Razman (✉)

Faculty of Manufacturing and Mechatronic Engineering Technology, Universiti Malaysia Pahang
Al-Sultan Abdullah, 26600 Pekan, Pahang, Malaysia
e-mail: mohdazraai@umpsa.edu.my

1 Introduction

The Department of Statistics Annual Economic Statistics (AES) for the Agriculture Sector in 2023 reveals the economic performance of four sub-sectors: crops, live-stock, forestry and logging, and fisheries [1]. Overall, the gross output value for the agriculture sector surged from RM82.2 billion in 2020 to RM101.3 billion in 2021, marking a growth rate of 23.2%. The key contributors to this increase were Sarawak (30.2%), Sabah (20.3%), and Johor (12.3%). Conversely, the value of intermediate input experienced a faster growth of 26.5% during the same period. Among the sub-sectors, crops took the lead in contributing to the gross output value at RM75.8 billion, followed by livestock (RM18.7 billion), forestry and logging (RM4.4 billion), and fisheries (RM2.4 billion). This statistic emphasized how crucial the agriculture sector is for Malaysia's economic progress. As a result, it's vital to carefully manage and monitor both the quality and quantity of harvested crops.

Detection systems has been developed for the purpose of identifying diseases in paddy crops [2]. This enables farmers with limited resources to identify plant diseases in their early stages and avoid the improper use of fertilizers, which could be detrimental to both the soil and the plants. The system's performance and classification accuracy were evaluated through various experiments, particularly focusing on classification and processing times. The machine learning model demonstrated an impressive accuracy of 99.48%, using a customized Convolutional Neural Network (CNN) model. This model effectively classifies images into categories such as Healthy, Leaf Blast, Leaf Scald, Neck Blast, and False Smut. In other study, to classify the maturity stage of large green *Capsicum Annum L. Var Kulai* (Chilli Kulai) by using convolutional neural networks (CNN) based deep learning and computer vision [3]. The best result for the maturity stage of large green *Capsicum Annum L. Var Kulai* (Chilli Kulai) is into three maturity, maturity 1 (maturity index 1/34 days after anthesis (DAA)), maturity 2 (maturity index 3/47 DAA), and maturity 3 (maturity index 5/60 DAA).

A comprehensive comparison was conducted among various cutting-edge CNN-based object detection algorithms, with a focus on the latest models in various fields [2]. A finding was revealed that Yolo-v3 emerged as the fastest, closely followed by Single Shot Detector (SSD), while Faster Region based Convolutional Neural Networks (RCNN) lagged behind. For small datasets without real-time requirements, Faster RCNN is recommended. Yolo-v3 is advantageous for live video feed analysis, while SSD offers a balance between speed and accuracy. Yolo-v3, being the most recent, benefits from active open-source contributions and demonstrates superior overall performance. The field is dynamic, with ongoing advancements and new algorithms or updates introduced yearly, catering to applications in aviation, autonomous vehicles, and industrial machinery. In another study, Very Deep Convolutional Networks (VGG) were used to achieve good results of 89.8% and 86.1% using transfer learning models VGG16 and VGG18, respectively, to extract features from Diabetic Retinopathy (DR) images for classifying the disease via SVM [4]. A study by investigated the use of VGG16, VGG19, and ResNet50 for detecting heart

murmurs, which are unusual heartbeat sounds that may indicate a serious heart condition and can only be identified by trained specialists using a stethoscope [5]. The study showed promising results, with classification accuracies of 83.95%, 83.95%, and 87.65% for VGG16, VGG19, and ResNet50, respectively. A study by Amjad, suggests that using deep learning in agriculture could significantly enhance agricultural practices [6]. By using CNN (Convolutional Neural Networks), ResNet, VGG, and EfficientNet, their results were 70%, 87%, 87%, and 91%, respectively. It was shown that by applying CNN on various application could provide good detection. The choice of an object detection algorithm depends on the specific use case.

This paper is organized as follows: Sect. 2 offers a brief overview of recent research on deep learning object detection models in agriculture. Section 3 describes the methodology for preparing a custom dataset. Section 4 details the experimental setup and discusses the results. Section 5 concludes with the findings of the study.

2 Related Works

Several studies have used either Deep Learning or Machine Learning to classify crops for category detection, disease and type. A study, on the development of a skill performance test for talent identification in amateur skateboarding sport used a machine learning model with PCA, achieving good results with loading factors equal to 0.80 [7]. This value, being greater than the threshold, implies that the machine learning model can be used in various fields. In a study, which aims to improve eggplant development and production using a machine learning model, it was found that the random forest algorithm achieved 100% classification accuracy [8]. The support vector machine (SVM) reached 99.7% accuracy, while the Naïve Bayes algorithm achieved 97.0% accuracy. In other study, Electromyography (EMG) signals are extensively utilized for predicting human motor intention, an essential element in human–robot collaboration platforms that use machine learning [9]. These studies achieved classification accuracies of 100%, 99%, and 99% on training, testing, and validation datasets, respectively, based on the identified features. According to Alzubaidi et al. (2021), deep learning, a branch of machine learning uses large datasets to find relationships between input data and labels without relying on predefined rules [10]. It consists of multiple layers of artificial neural networks (ANNs), each providing a unique interpretation of the input data. The key advantage of deep learning is its capacity to autonomously learn and identify patterns from data.

In their 2021 study, Ishengoma et al., created a dataset of 11,280 images of maize, evenly split between infected and uninfected samples [11]. They divided the dataset into training (7896 images), validation (1692 images), and test sets (1692 images) using a 70:15:15 ratio. Using the TensorFlow 2.0 framework, they trained various architectures, including VGG16, VGG19, InceptionV3, and MobileNetV2, along with their modified versions. InceptionV3 and MobileNetV2 performed the best, achieving 100% accuracy, sensitivity, specificity, precision, and F1-score, surpassing other models. The experiments were conducted using the Phantom 4 pro v2 hardware.

In Zhou et al.'s (2020) study, a system Kiwi Detector was developed to identify kiwifruits in images with a resolution of 3968×2976 pixels [12]. Four models (SSD with MobileNetV2, quantized MobileNetV2, InceptionV3, and quantized InceptionV3) were tested on a HUAWEI P20 smartphone using 100 field images. MobileNetV2 had the highest True Detection Rate (TDR) at 90.8%, while quantized MobileNetV2 had the fastest detection speed at 103 ms per image.

Dang et al. (2023), conducted a study that involved the creation of a dependable weed identification dataset, encompassing 5648 images representing 12 weed classes and featuring 9370 bounding boxes of weeds [13]. Utilizing YOLO-based deep learning algorithms, various detection systems were developed, incorporating models such as YOLOv3, YOLOv4, Scaled-YOLOv4, YOLOR, YOLOv5, YOLOv6, and YOLOv7. The experiment's outcomes highlighted the significant potential of all YOLO models for real-time weed detection. Notably, YOLOv5s exhibited exceptional performance, achieving a mAP of 94.10% following the implementation of data augmentation.

In their 2023 study, MacEachern et al., trained six YOLO convolutional neural network models to identify ripeness stages in wild blueberries [14]. YOLOv4 achieved the highest accuracy, with mAP50 scores of 79.79% for the 3-class model and 88.12% for the 2-class model. YOLOv4-Tiny excelled in inference time (7.8 ms) and memory usage (1.63 GB), making it ideal for smartphone app integration. Additionally, regression equations were developed, with YOLOv4-Small showing the lowest absolute mean error (24.1%) among 2-class models. These findings lay the groundwork for a smartphone app, facilitating real-time ripeness detection and yield estimation, thus aiding blueberry growers in their management practices.

3 Methodology

3.1 *Image Dataset for Chilli Crops Detection*

In Fig. 1 collecting data for training a deep learning model to recognize chilli plants involves gathering a diverse set of images from public datasets, online repositories, or by capturing new images manually or automatically. The dataset should include various chilli plant varieties, growth stages, and environmental conditions to ensure it is comprehensive and representative. Adhering to best practices during data collection is crucial to avoid issues like inaccurate, missing, or imbalanced data, which can negatively impact the model's performance. The objective is to create a robust dataset that enables the model to accurately identify and classify chilli plant images.



Fig. 1 Image chillies datasets

3.2 Image Annotation

Before using images for bounding box object recognition and classification, they are labelled and annotate with an image labelling or annotation tool in Fig. 2. This tool helps identify objects within an image by allowing users to highlight or mark specific items. There are various types of image annotation, including bounding box, polygonal segmentation, semantic segmentation, 3D cuboid segmentation, keypoint landmarks, and line splines. In this research, we used Roboflow as a platform to annotate images. In Annotation image we classified two categories of image chilli which is red chilli and green chilli which is a fundamental step in creating image recognition algorithms and training deep learning models. The goal is to create reliable datasets for the models to train on, ultimately leading to the development of better and more accurate machine learning models. Common techniques for image annotation include image classification, object detection, and image segmentation, each serving specific purposes in training computer vision models.

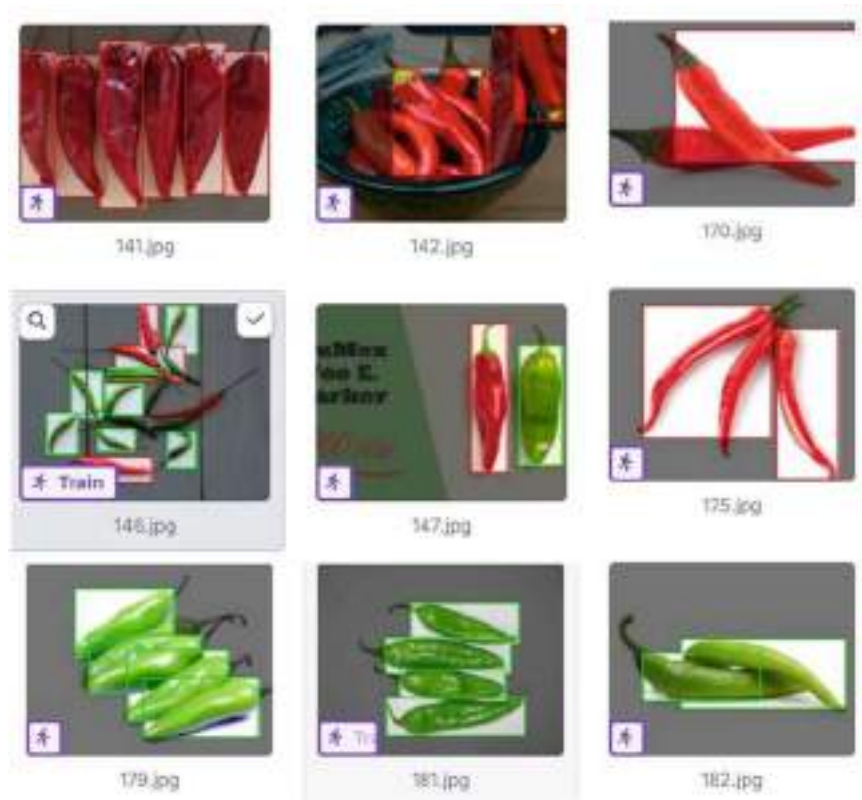


Fig. 2 Annotate of chillies

3.3 Image Augmentation

Image augmentation is a crucial method in deep learning for enhancing model performance. It involves creating new training examples from existing ones to diversify the dataset, thus preventing overfitting, and improving generalization. The example techniques include flip, 90° rotate, rotation, saturation and exposure (Table 1).

3.4 Software Configuration

The model was train through YOLOv8, Neural Network, SVM and Detection Transformer (DETR) compared to another advanced YOLOv4-based deep learning model, YOLOv4-tiny. The experiment was conducted on Google Colab, an online GPU service featuring a 12 GB Nvidia K80, running Ubuntu 20.04 LTS, Python 3.9, Cuda 12, and Cudnn 11.8 [15].

Table 1 Augmentation setup that has been applied to the dataset

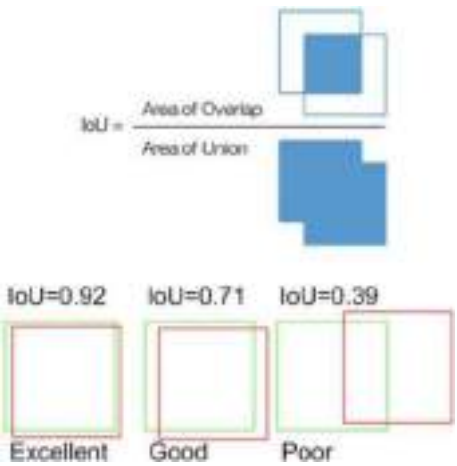
Augmentation	Direction	Functions
Flip	Horizontal and vertical	Help model be insensitive to subject orientation
90° rotate	Clockwise, counterclockwise, upside down	Help model be insensitive to camera orientation
Rotation	−45° to 45°	Help your model be more resilient to camera roll
Saturation	−45% to 45%	Randomly adjust the vibrancy of the colors in the images
Exposure	−30% to 30%	Help your model be more resilient to lighting and camera setting changes

3.5 Performance Evaluation

The AP and mAP are metrics for evaluating object detection models in Fig. 3. AP measures the agreement between predicted and ground truth bounding boxes using precision and recall, with precision calculated based on the IoU threshold. mAP is the average AP across all classes and IoU thresholds, balancing precision, and recall. It is computed by finding the area under the precision-recall curve for each class. In some evaluations, AP is calculated for each class and then averaged for mAP, while in others, like COCO, AP and mAP are used interchangeably.

“Precision” measures the accuracy of your predictions, indicating the percentage of correct predictions made by the model. “Recall” assesses how well the model identifies all true positive detections, representing the percentage of actual positive cases that were found [16]. The F1 score combines the precision and recall scores to provide an overall performance evaluation. Intersection Over Union (IoU) quantifies

Fig. 3 Performance evaluation of model



the overlap between two bounding boxes, indicating the extent to which the predicted box aligns with the actual box in object identification and segmentation tasks.

4 Result and Discussion

Table 2 show the performance details of four models (Yolov8, Neural Network, SVM, and DETR) based on their mAP@0.5 (%), Recall (%), F1 Score (%), and Speed of detection (ms). YOLOv8 is the best choice among the models for high accuracy and speed, while Neural Network offers good balance, SVM lags in both accuracy and speed, and DETR is the least favorable for real-time applications. They both emphasize the importance of selecting the right model based on specific needs and application requirements.

Based on the observation in Figs. 4 and 5, above it compares four machine learning models—YOLOv8, SVM, Neural Network, and DETR—evaluating their performance based on mean Average Precision at 0.5 IoU (mAP@0.5), Recall, F1 Score, and Detection Speed. YOLOv8 excels across all metrics, achieving the highest mAP@0.5 (96.2%), Recall (92.6%), F1 Score (92.0%), and the fastest detection speed (101.8 ms), making it ideal for real-time applications. The Neural Network also performs well with a mAP@0.5 of 90.5%, matching Recall and F1 Scores of 90.5%, and a detection speed of 112.5 ms, offering a good balance of accuracy and speed. SVM shows a slight decline with an mAP@0.5 of 89.1%, Recall and F1 Scores around 89%, and a slower detection speed of 152.4ms. DETR faces the most challenges, with the lowest mAP@0.5 (71.9%), Recall (45.0%), and the slowest detection speed (231.4 ms), indicating it is less suitable for accurate and timely detections.

In conclusion, YOLOv8 is the best choice among the four models, offering the highest accuracy and speed. A study by Md Sadid showed a high mAP in disease detection [17]. While YOLOv8 is used for detecting chili types in this paper, the high mAP offered by the model suggests it is likely robust enough to handle some degree of structural defects, such as those caused by diseases. Although specific accuracy metrics for detecting defects are not provided, the high overall accuracy implies that minor structural defects due to disease are unlikely to significantly affect the model’s ability to detect chilies. The Neural Network model, while slightly less accurate, still provides reliable performance with good detection speed. SVM lags in both accuracy and speed, making it less suitable for critical tasks. DETR, with the lowest scores and

Table 2 Performance details of the 4 models

Models	mAp@0.5 (%)	Recall (%)	F1 score (%)	Speed of detection (ms)
Yolov8	96.2	92.6	92.0	101.8
Neural network	90.5	90.5	90.4	112.5
SVM	89.0	89.1	89.0	152.4
DETR	71.9	45.0	70.2	231.4

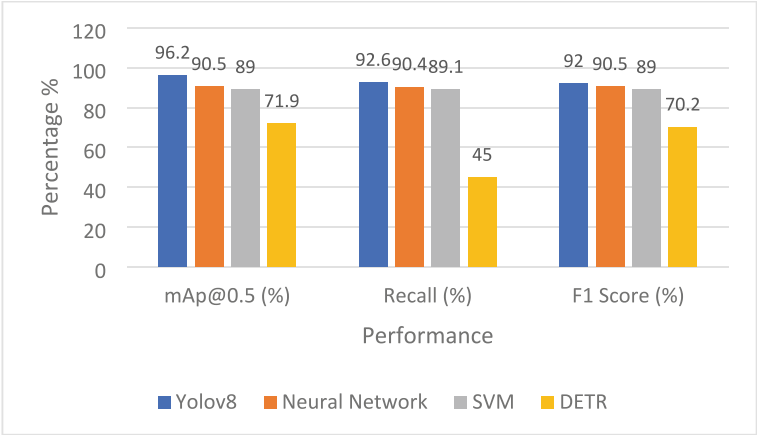


Fig. 4 Performance analysis of each models



Fig. 5 Model’s speed performance

slowest detection speed, is the least favorable for real-time detection. These findings underscore the importance of choosing the right model based on application-specific needs, balancing accuracy, and speed accordingly.

5 Conclusion

In summary, this study compared YOLOv8, SVM, Neural Network, and DETR deep learning models for detecting chilli plants. YOLOv8 proved most effective, with a mean average precision (mAP@0.5) of 96.2% and a detection speed of 101.8 ms, making it suitable for real-time crop detection. This integration marks a significant advancement in precision agriculture, providing accessible tools for optimizing crop yields and enhancing productivity

References

1. Ministry of Economy Department of Statistic Malaysia Official Portal (2023) Department of statistics Malaysia official portal agriculture. In: Ministry of economy department of statistic Malaysia official portal
2. Srivastava S, Divekar AV, Anilkumar C et al (2021) Comparative analysis of deep learning image detection algorithms. *J Big Data* 8. <https://doi.org/10.1186/s40537-021-00434-w>
3. Hendrawan Y, Rohmatulloh B, Prakoso I et al (2021) Classification of large green chilli maturity using deep learning. *IOP Conf Ser Earth Environ Sci* 924:012009. <https://doi.org/10.1088/1755-1315/924/1/012009>
4. Noor FNM, Mohd Isa WH, Khairuddin IM et al (2021) The diagnosis of diabetic retinopathy: a transfer learning with support vector machine approach. In: Mat Jizat JA, Khairuddin IM, Mohd Razman MA et al (eds) *Advances in robotics, automation and data analytics*. Springer International Publishing, Cham, pp 391–398
5. Almanifi ORA, Ab Nasir AF, Mohd Razman MA et al (2022) Heartbeat murmurs detection in phonocardiogram recordings via transfer learning. *Alex Eng J* 61:10995–11002. <https://doi.org/10.1016/j.aej.2022.04.031>
6. Amjad SA, Anuradha T, Datta TM, Babu UM (2024) Chilli leaf disease detection using deep learning. In: Garg D, Rodrigues JJPC, Gupta SK, et al (eds) *Advanced computing*, pp 81–89. Springer Nature Switzerland, Cham
7. Rasid AMA, Kamarudin NA, Abdullah MA et al (2021) Development of skill performance test for talent identification in amateur skateboarding sport. In: Mat Jizat JA, Khairuddin IM, Mohd Razman MA et al (eds) *Advances in robotics, automation and data analytics*. Springer International Publishing, Cham, pp 385–390
8. Shapiee MNA, Shapari MASM, Rahman MIM, et al (2024) Unsupervised learning of time-series classification using machine learning through fertigation system. In: Tan A, Zhu F, Jiang H et al (eds) *Advances in intelligent manufacturing and robotics*, pp 81–89. Springer Nature Singapore, Singapore
9. Mohd Khairuddin I, Sidek SN, Abdul Majeed APP et al (2021) The classification of movement intention through machine learning models: the identification of significant time-domain EMG features. *PeerJ Comput Sci* 7:e379. <https://doi.org/10.7717/peerj-cs.379>
10. Alzubaidi L, Zhang J, Humaidi AJ et al (2021) Review of deep learning: concepts, CNN architectures, challenges, applications, future directions. *J Big Data* 8. <https://doi.org/10.1186/s40537-021-00444-8>
11. Ishengoma FS, Rai I, Said R (2021) Identification of maize leaves infected by fall armyworms using UAV-based imagery and convolutional neural networks. *Comput Electron Agric* 184:106124. <https://doi.org/10.1016/j.compag.2021.106124>
12. Fu L (2020) Real-time kiwifruit detection in orchard using deep learning on Android™ smartphones for yield estimation. *Comput Electron Agric* 2020:105856. <https://doi.org/10.1016/j.compag.2020.105856>

13. Dang F, Chen D, Lu Y, Li Z (2023) YOLOWeeds: a novel benchmark of YOLO object detectors for multi-class weed detection in cotton production systems. *Comput Electron Agric* 205:107655. <https://doi.org/10.1016/j.compag.2023.107655>
14. MacEachern CB, Esau TJ, Schumann AW et al (2023) Detection of fruit maturity stage and yield estimation in wild blueberry using deep learning convolutional neural networks. *Smart Agric Technol* 3:100099. <https://doi.org/10.1016/j.atech.2022.100099>
15. Raja P (2023) What is Google Colab? In: androidpolice
16. Kukil (2022) Intersection over Union (IoU) in Object Detection & Segmentation. In: learnopencv
17. Uddin MS, Mazumder MKA, Prity AJ et al (2024) Cauli-Det: enhancing cauliflower disease detection with modified YOLOv8. *Front Plant Sci* 15. <https://doi.org/10.3389/fpls.2024.1373590>

Multi-objective Optimization Modeling in 3D Printing Process of PLA+ Using Response Surface Methodology and NSGA II



Saufik Luthfianto , Eko Pujiyanto , Cucuk Nur Rosyidi ,
and Pringgo Widyo Laksono

Abstract 3D printing manufactures products layer by layer, promoting the conservation of natural resources while offering an economical and safe choice for workers, communities, and consumers. Certain features can be integrated into the 3D printing process by developing mathematical models that determine the optimal parameters for achieving optimal printing outcomes. This research creates a mathematical model for multi-objective optimization aimed at identifying the best 3D printing process parameters. The study's findings on Multi-Objective Optimization Modeling in 3D Printing of PLA+ using Response Surface Methodology (RSM) and NSGA II have significant practical implications. By integrating RSM and NSGA II, the study enables a more precise and efficient optimization of key 3D printing parameters, such as print speed, temperature, and layer height. This leads to enhanced print quality, reduced material waste, and optimized mechanical properties of the printed parts. This study involved several decision variables, such as infill density, nozzle temperature, printing speed, layer thickness, and bed temperature. This study has two objective functions, such as maximizing tensile strength and minimizing surface roughness. The Gamultiobj algorithm (MATLAB) and the non-dominated sorting genetic algorithm II method have the specific advantage of simultaneously searching for optimal values for the four objective functions. The study found that the best level setting for the infill density was 99.992%, 214.998 °C for the nozzle temperature, 70.000 mm/s for the printing speed, 0.151 mm for the layer thickness, and 48.390 °C. The optimal response is a tensile strength of 31.399 MPa and a surface roughness of 10.290 μm .

Keywords 3D printing · Multi objective optimization

S. Luthfianto (✉) · E. Pujiyanto · C. N. Rosyidi · P. W. Laksono
Department of Industrial Engineering, Universitas Sebelas Maret, Surakarta, Indonesia
e-mail: saufik@student.uns.ac.id

© The Author(s), under exclusive license to Springer Nature Singapore Pte Ltd. 2025
M. R. Mohamad Yasin et al. (eds.), *Proceedings of the 7th Asia Pacific Conference on Manufacturing Systems and 6th International Manufacturing Engineering Conference—Volume 2*, Lecture Notes in Mechanical Engineering,
https://doi.org/10.1007/978-981-96-5690-5_14

135

1 Introduction

Since ancient times, humans have created items essential for everyday life, demonstrating a practical understanding of materials to develop tools for their purposes. During manufacturing, the tools employed subtractive techniques, systematically removing excess material from the original components until they formed the desired final product. The subtractive method of production has significantly advanced over time, with new techniques constantly emerging. A new manufacturing paradigm, known as additive manufacturing, emerged in the early 1990s [1]. It has proven to be a very successful technique for creating shapes of any complexity or form.

Additive manufacturing (AM) is an innovative production method that constructs objects layer by layer based on digital designs created with computer-aided design software. It provides numerous benefits compared to conventional manufacturing techniques [2]. AM enables the creation of intricate geometries that are difficult or impossible to produce using traditional methods. It provides design flexibility, allowing for customization, quick prototyping, and on-demand manufacturing. As technology progresses, AM is poised to revolutionize the manufacturing sector, fostering innovation and generating fresh prospects in product development and production [3, 4].

The industry widely favors fused deposition modeling (FDM) among AM technologies due to its cost-effectiveness, user-friendliness, diverse material choices, and wide range of applications. The FDM process uses various thermoplastic materials to print diverse objects with complex shapes. One of the materials used in the FDM process is polylactic acid [5]. PLA comes from sustainable sources and is compostable. 3D printing highly prefers PLA due to its low melting point, biodegradability, and ease of use during printing [6–8]. Furthermore, the ability to print PLA without a heated bed reduces energy requirements [9]. Because process parameters influence PLA more than other materials, researchers are particularly interested in it [10].

These technologies typically generate smoother surfaces owing to their distinct printing methods and higher resolutions [11]. Multiple factors, such as process parameters, material characteristics, and geometric aspects, affect tensile strength and surface roughness in FDM printing [12–14]. In FDM printing, various systematic approaches use statistical methods to optimize tensile and surface roughness. This includes tuning process variables like infill density, nozzle temperature, printing speed, layer thickness, bed temperature, and more to discover the ideal combination that achieves a balance between surface quality and other operational needs.

Researchers have created a mathematical model to study how different 3D printing process parameters impact the strength of PLA plastic products [15, 16]. Researchers [17] have developed another mathematical model that describes the extrusion process in 3D printing with FFF material. Researchers [18–20] have conducted several mathematical theories related to the 3D printing process. However, these researchers have not considered two objective functions together to achieve an optimal solution. Some of these mathematical models focus exclusively on either tensile strength or surface

roughness, rather than considering both simultaneously to determine the optimal solution.

The previously mentioned studies have the potential to develop a multi-objective optimization framework that aims to identify optimal parameters for 3D printing processes, taking into account assessments of both tensile strength and surface roughness. This study utilizes tensile strength and surface roughness tests within the 3D printing process, employing a mathematical model to determine the best printing parameters based on the critical studies mentioned earlier. This study involved several decision variables, such as infill density, nozzle temperature, printing speed, layer thickness, and bed temperature. This study has two objective functions, such as maximizing tensile strength and minimizing surface roughness. The search for optimal values for the four objective functions is conducted simultaneously using the Gamultiobj algorithm (MATLAB) and the non-dominated sorting genetic algorithm II method.

2 Material and Methods

This research utilized a 3D printer based on the fused deposition modeling technique. A “Creality Ender 3 Pro” 3D printer was used to print Polylactic Acid Plus (PLA+) specimens for the experimental work. The printer features a build volume of 220 * 220 * 250 mm and operates on a Cartesian system, with each of the three axes moving independently via stepper motors. The experiment utilized a 1.75 mm diameter PLA+ filament, securely stored on its spool mount. All samples were designed using the CAD software SolidWorks and generated in the Stereolithography (STL) file format. The file was then processed in Ultimaker Cura slicing software according to specified parameters, generating the G-Code “machine code for the printer,” which was subsequently loaded into the 3D printer (see Fig. 1).

The study started with a Taguchi experiment using MINITAB. Next, the data were analyzed using the Response Surface Methodology to determine how the decision variables related to the objective function. Subsequently, the function was optimized using NSGA II, yielding multiple alternative solutions. The TOPSIS method was then applied to determine a single solution. Several experimental variables were investigated, including infill density, nozzle temperature, printing speed, layer thickness, and bed temperature. The study focuses on two objectives: maximizing tensile strength and minimizing surface roughness. The research utilized the Taguchi L_{16} orthogonal array, selecting five factors, namely: infill density, nozzle temperature, printing speed, layer thickness, and bed temperature. Each with four levels, as shown in Table 1.

Using PLA+ filament with a diameter of 1.75 mm, 3D printing machines manufactured Type I tensile specimens for ASTM D638 testing and surface roughness tests in accordance with ISO 21920 procedures. STL files were generated from 3D images of the ASTM D638 specimens. The ZWICK Roell Z020 machine conducted

Fig. 1 Creality ender 3 pro printer



Table 1 Factors and level in Taguchi experiment

Parameter	Level			
	1	2	3	4
Infill density (%)	85	90	95	100
Nozzle temperature (°C)	200	205	210	215
Printing speed (mm/s)	40	50	60	70
Layer thickness (mm)	0.15	0.20	0.25	0.30
Bed temperature (°C)	45	50	55	60

tensile tests, and a Mitutoyo SJ-201 surface roughness tester using the stylus method conducted surface roughness measurements (Ra).

An ASTM D638 sample, with dimensions of 165 mm in length, 19 mm in width, and 7 mm in thickness, was selected for the tensile testing. Figure 2 illustrates the dimensions of the dumbbell-shaped specimens, while the third Fig. 3 shows the printed tensile test samples. Figure 4 depicts the ZWICK Roell Z020 machine, which was used for conducting the tensile tests. The specimen was produced in accordance with the experimental design by adjusting the process parameters. The printed samples were carefully packaged to protect them from environmental exposure and moisture. Tensile testing was conducted using the ZWICK Roell Z020 machine, which has a maximum load capacity of 100 kN. The specimen was gripped securely,

and testing was initiated. The cross-head velocity and strain rate were maintained at 5 mm/min throughout the test.

A Mitutoyo surface roughness tester SJ-201 from Mitutoyo Corporation in Kana-gawa, Japan, was used to measure Ra using the stylus method, as shown in Fig. 5. The measurement procedure adhered to the guidelines outlined in ISO 21920 [21]. The Mitutoyo surface roughness tester was configured with specific parameters, including an evaluation length of 4 mm, a tip angle of 90°, a tip radius of 2 μm, a tracing speed of 0.25 mm/s, and a cut-off wavelength of 0.8 mm. These settings were standardized to ensure uniformity and precision in all measurements (Fig. 6).

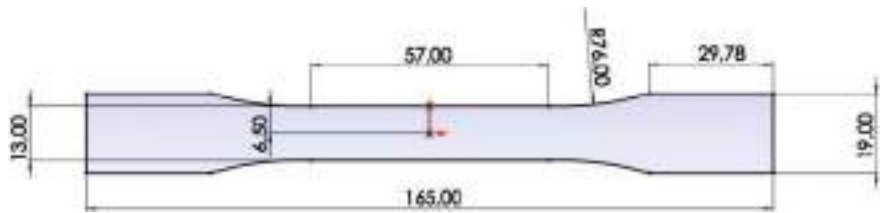


Fig. 2 ASTM D638 specimen for tensile testing (mm)

Fig. 3 Printed specimens for tensile test



Fig. 4 Tensile tests using ZWICH Roell Z020



Fig. 5 Surface roughness measurement using a Mitutoyo surface roughness tester



Fig. 6 A printed specimen using a Mitutoyo surface roughness tester



3 Results and Discussion

The specimens undergo the tensile strength test of ASTM D638 and the surface roughness test of ISO 21920. Tables 2 present the experimental data.

The analysis of variance and percent contribution of the factors influencing surface roughness as well as tensile strength are calculated from Tables 3 and 4. Infill density is one of the main factors in increasing the percentage contribution to tensile strength and surface roughness. This indicates that the infill density influences the tensile strength and surface roughness values by 50.310% and 47.110%, respectively. At 26.680% and 31.160%, respectively, bed temperature is the component that contributes the second most to tensile strength and surface roughness. The nozzle temperature is the third factor that influences tensile strength. It contributes 3.500% of its value to the tensile strength. Layer thickness is the third component that influences surface roughness. Make a 3.000% contribution. Printing speed and layer thickness have the least impact on the tensile strength value when compared to other parameters. When considering other aspects, printing speed and nozzle temperature have the least impact on the surface roughness value.

Table 2 Tensile strength and surface roughness data

Run	ID (%)	NT (°C)	PS (mm/s)	LT (mm)	BT (°C)	Tensile strength (MPa)				Surface roughness (µm)			
						1	2	3	4	1	2	3	4
1	85	200	40	0.15	45	29.257	29.365	27.853	23.137	9.200	9.300	8.300	6.300
2	85	205	50	0.20	50	30.305	30.54	30.179	26.242	10.660	10.880	9.880	11.880
3	85	210	60	0.25	55	32.131	32.535	31.080	28.469	11.840	11.240	10.240	12.240
4	85	215	70	0.30	60	35.174	34.511	34.095	30.179	13.990	13.550	12.550	14.550
5	90	200	50	0.25	60	35.902	36.426	35.100	31.143	14.550	14.880	13.880	15.880
6	90	205	40	0.30	55	35.030	34.281	33.886	29.772	13.780	13.340	12.330	14.330
7	90	210	70	0.15	50	30.115	29.255	28.666	31.282	9.760	9.230	10.440	12.440
8	90	215	60	0.20	45	30.695	31.306	29.815	27.248	10.700	10.100	9.270	11.270
9	95	200	60	0.30	50	35.220	34.352	33.212	27.948	13.070	13.450	12.440	10.440
10	95	205	70	0.25	45	34.097	33.22	32.159	26.955	12.290	12.870	11.760	13.760
11	95	210	40	0.20	60	37.133	38.081	36.545	31.306	15.900	15.240	14.220	12.220
12	95	215	50	0.15	55	34.162	35.361	33.993	31.296	13.060	13.580	12.550	13.550
13	100	200	70	0.20	55	41.853	41.238	40.631	37.751	18.310	18.980	17.950	15.950
14	100	205	60	0.15	60	42.865	43.332	41.122	42.463	19.280	19.560	18.440	15.440
15	100	210	50	0.30	45	35.053	34.514	34.025	28.711	13.190	13.870	12.880	15.880
16	100	215	40	0.25	50	38.811	38.491	37.379	34.588	16.760	16.120	15.320	12.320

Table 3 Anova and percentage contribution of tensile strength

Factors	DF	SumSqr	MeanSqr	F value	Prob F	% Contribution
Infill density	3	731.200	243.735	50.210	0.000	50.310
Nozzle temperature	3	50.840	16.948	3.490	0.023	3.500
Printing speed	3	34.500	11.500	2.370	0.082	2.370
Layer thickness	3	16.190	5.398	1.110	0.354	1.110
Bed temp	3	387.720	129.240	26.620	0.000	26.680
Error	48	233.000	4.854			16.030
Total	63					100

Table 4 Anova and percentage contribution of surface roughness

Factors	DF	SumSqr	MeanSqr	F Value	Prob F	% Contribution
Infill density	3	4.444	1.481	49.900	0.000	47.110
Nozzle temperature	3	0.209	0.070	2.350	0.084	2.220
Printing speed	3	0.132	0.044	1.480	0.231	1.400
Layer thickness	3	0.283	0.094	3.180	0.320	3.000
Bed temperature	3	2.939	0.980	33.000	0.000	31.160
Error	48	1.425	0.030			15.110
Total	63					100

Figure 7a and b illustrates the contour plots for the tensile test results and surface roughness. The contour plots highlight the significant influence of infill density and bed temperature, among other parameters. To achieve higher tensile strength, the contour plots show that infill density and bed temperature should be 90% and 65 °C, respectively. To achieve lower surface roughness, the contour plots show that bulk density and bed temperature should be greater than 105% and less than 65 °C, respectively.

According to [22] demonstrates the significant influence of bed temperature on various responses, including tensile strength, tensile force, impact energy, and flexural strength of PLA. The temperature of the bed gradually alters a number of mechanical properties. It predicts increased mechanical properties from the influence of bed temperature because it helps ensure the first layer of filament adheres well to the print surface. Good adhesion of the first layer is very important to prevent warping (curving of the printed part) and ensure stability during printing [23, 24]. Warping occurs when the mold’s bottom cools too quickly, causing uneven shrinkage and warping. A warm bed temperature helps to keep the mold’s bottom hot longer, preventing rapid shrinkage and reducing the risk of warping. A proper bed temperature ensures that the filament remains in optimal condition when in contact with the print surface. This helps maintain a consistent mold size and shape from start to finish. The correct bed temperature can also impact the quality of the mold’s bottom

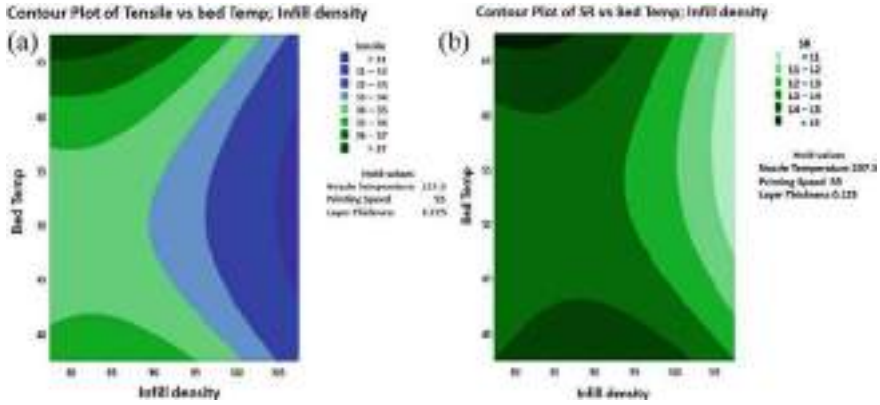


Fig. 7 **a** Contour plot of tensile strength. **b** Contour plot of surface roughness

surface. A surface that is too cool can cause irregularities and a lack of smoothness, whereas the right surface can produce a smoother, neater result.

The response surface methodology generated the regression equation from the experimental data in Table 2. Equations 1 and 2, respectively, display the regression equations for tensile strength and surface roughness.

$$\begin{aligned}
 Ts = & 507 - 2.63 \sim ID - 3.69 \sim NT + 0.77 \sim PS - 148 \sim LT \\
 & + 1.67 \sim BT - 0.0061 \sim ID^2 + 0.0082 \sim NT^2 + 0.00027 \sim PS^2 - 174 \sim LT^2 \\
 & + 0.0102 \sim BT^2 + 0.0143 \sim ID \sim NT + 0.01019 \sim ID \sim PS + 0.93 \sim ID \sim LT \\
 & - 0.0021 \sim ID \sim BT - 0.01116 \sim NT \sim PS + 0.85 \sim NT \sim LT - 0.0136 \sim NT \sim BT \\
 & + 0.297 \sim PS \sim LT + 0.00944 \sim PS \sim BT - 0.93 \sim LT \sim BT
 \end{aligned} \quad (1)$$

$$\begin{aligned}
 Sr = & 163 + 0.20 \sim ID - 1.82 \sim NT - 0.26 \sim PS - 159 \sim LT + 2.50 \sim BT \\
 & - 0.00617 \sim ID^2 + 0.00494 \sim NT^2 - 0.00066 \sim PS^2 - 20.1 \sim LT^2 \\
 & + 0.00687 \sim BT^2 + 0.00355 \sim ID \sim NT + 0.00337 \sim ID \sim PS + 0.584 \sim ID \sim LT \\
 & - 0.00386 \sim ID \sim BT - 0.00036 \sim NT \sim PS + 0.527 \sim NT \sim LT - 0.01389 \sim NT \sim BT \\
 & + 0.269 \sim PS \sim LT + 0.00044 \sim PS \sim BT - 0.107 \sim LT \sim BT
 \end{aligned} \quad (2)$$

where

Ts Tensile Strength (MPa)
 Sr Surface Roughness (μm)
 ID Infill Density (%)
 NT Nozzle Temperature ($^{\circ}\text{C}$)
 PS Printing Speed (mm/s)
 LT Layer Thickness (mm)
 BT Bed Temperature ($^{\circ}\text{C}$)

The next step is to optimize simultaneously using Matlab's NSGA II. According to the model development for 3D printing machine parameters, the objective functions for the proposed model are tensile strength (f1; Eq. 1) and surface roughness (f2; Eq. 2). The optimal 3D printing machine parameters must be appropriate for the constraint functions. The constraint functions used in this study are infill density, nozzle temperature, printing speed, layer thickness, and bed temperature. The 3D printing process applies each of these constraints. These parameter relationship constraints are suitable for our model. Equations 3, 4, 5, 6, 7 and 8 display the objective function and constraints.

$$\text{Objective function (Max Ts, Min Sr)} \quad (3)$$

Subject to

$$85 \leq \text{ID} \leq 100 \quad (4)$$

$$200 \leq \text{NT} \leq 215 \quad (5)$$

$$40 \leq \text{PS} \leq 70 \quad (6)$$

$$0.15 \leq \text{LT} \leq 0.30 \quad (7)$$

$$45 \leq \text{BT} \leq 60 \quad (8)$$

The Pareto point, which forms the Pareto front. Figure 7 displays examples of Pareto fronts for the objective functions Ts and Sr, and Table 5 displays all 20 Pareto front points, representing potential solutions. The twenty points correspond to the decision variables' values and the objective function's values. TOPSIS is utilized to determine the optimal single solution. Table 6 presents the single optimal solution, corresponding to alternative 19 in Tables 2 (Fig. 8).

After the Gamultiobj algorithm identifies a non-dominated solution (Pareto front), the next step is to use the TOPSIS approach to find the best solution. TOPSIS finds the best solution, revealing 20 points related to the non-dominated solution (Pareto front). This study bases the TOPSIS approach on research [25]. The TOPSIS approach consists of seven steps to find a single optimal solution. Table 6 shows the results of the optimal solution using the TOPSIS approach. Below are the seven steps to finding the optimal solution.

1. Create an evaluation matrix, (a_{ij}) $A * f$, consisting of A alternatives and f criteria. In this case, A are 20 points corresponding to non-dominated solutions and f are objective functions.
2. Use this formula to normalize the evaluation matrix, $a_{ij} = \frac{a_{ij}}{\sqrt{\sum_{i=1}^{20} (a_{ij})^2}}$

Table 5 Pareto points correspond to the values of decision variables and objective functions

Pareto point	Decision variables					Objective functions	
	Infill density (%)	Nozzle temperature (°C)	Printing speed (mm/s)	Layer thickness (mm)	Bed temperature (°C)	Tensile strength (MPa)	Surface roughness (μm)
1	99.995	214.997	69.999	0.150	50.076	31.489	9.980
2	99.997	214.998	69.998	0.150	49.348	31.431	10.10
3	99.993	214.998	69.999	0.150	51.740	31.649	9.720
4	99.994	214.998	69.999	0.150	48.812	31.402	10.20
5	99.996	214.997	69.996	0.150	55.561	32.219	9.252
6	99.995	214.997	69.998	0.151	54.056	31.955	9.410
7	99.994	214.997	69.999	0.150	55.170	32.153	9.290
8	99.995	214.996	69.999	0.150	51.326	31.609	9.780
9	99.991	214.998	69.999	0.151	48.390	31.399	10.290
10	99.993	214.998	69.998	0.150	50.432	31.521	9.920
11	99.999	214.994	69.995	0.150	58.964	32.984	9.010
12	99.994	214.996	69.997	0.150	54.553	32.042	9.350
13	99.996	214.998	69.998	0.150	51.071	31.572	9.820
14	99.994	214.998	69.996	0.151	51.929	31.698	9.700
15	99.993	214.997	69.998	0.150	50.558	31.527	9.890
16	99.996	214.996	69.998	0.150	49.649	31.452	10.05
17	99.995	214.997	69.997	0.150	56.743	32.475	9.160
18	99.997	214.995	69.997	0.150	53.678	31.900	9.460
19	99.998	214.995	69.997	0.150	58.162	32.787	9.060
20	99.990	214.999	69.999	0.150	48.295	31.369	10.290

Table 6 The single optimal solution

Decision variables				
Infill density (%)	Nozzle temperature (°C)	Printing speed (mm/s)	Layer thickness (mm)	Bed temperature (°C)
99.992	214.998	70.000	0.151	48.390
Optimal value of objective function				
Tensile strength (MPa)		Surface roughness (μm)		
31.399		10.290		

- Where a_{ij} is normalized the evaluation matrix value.
3. Determine the normalized weighted decision matrix, $x_{ij} = a_{ij} \sim \omega_j$
- Where $\omega_j = \frac{\omega_j}{\sum_{j=1}^2 \omega_j}$, $\sum_{j=1}^2 \omega_j = 1$, where weight for $f_1 = 0.60$ and $f_2 = 0.40$.

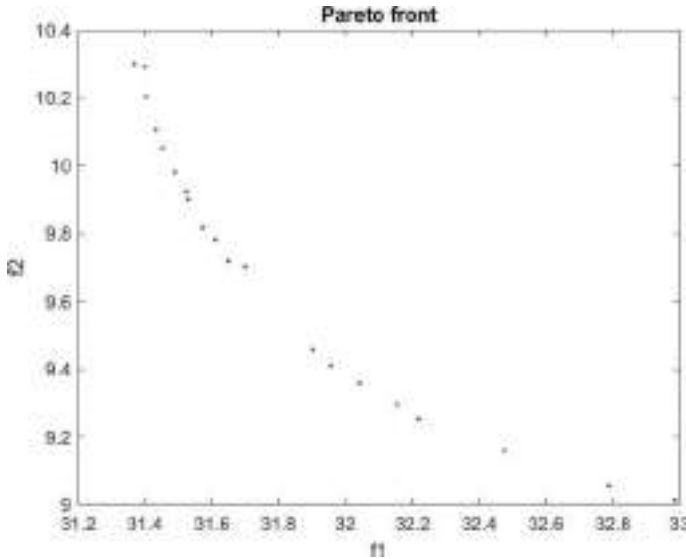


Fig. 8 Pareto fronts for Ts and Sr

Where x_{ij} is normalized weighted, a_{ij} is normalized the evaluation matrix value, ω_j is the individual weighted of response j .

4. Determine the maximum (A_j^+) and the minimum (A_j^-) alternative for each criterion: $A_j^+ = \max_{i=1}^{20} x_{ij}$, $A_j^- = \min_{i=1}^{20} x_{ij}$

Where A_j^+ is maximum alternative for each criterion, A_j^- is minimum alternative for each criterion.

5. Calculate the Euclidean distance between the target alternative and the maximum (d_i^+) and minimum (d_i^-) alternative: $d_i^+ = \sqrt{\sum_{j=1}^2 (x_{ij} - x_j^+)^2}$, $d_i^- = \sqrt{\sum_{j=1}^2 (x_{ij} - x_j^-)^2}$

Where d_i^+ is The distance of the i -th experiment from the ideal solution (positive ideal solution) has been calculated, d_i^- is The distance of the i -th experiment from the ideal solution (negative ideal solution) has been calculated.

6. For each alternative calculate the similarity to the minimum alternative using $S_i = \frac{d_i^-}{d_i^- + d_i^+}$, the result are TOPSIS scores.

Where S_i is TOPSIS value.

7. Identify the maximum TOPSIS score. In A9, the maximum TOPSIS scores are 31.399 and 10.290. The maximum TOPSIS score corresponds to the optimal single solution.

An additional combination of parameter settings and the number of roughing passes (n) is performed using a comparable procedure and step. The first stage

involves finding the Pareto front, while the second stage aims to identify a single optimal solution using TOPSIS.

The Taguchi method can only optimize the data in Table 2 for one objective function at a time, experimenting with the values of the decision variables (level factors). This research not only optimizes concurrently, but also expands from discrete to continuous solutions. For example, the nozzle temperature and bed temperature decision variables have values of 214.998 °C and 48.390 °C, respectively.

4 Conclusion

To determine the 3D printing process parameters, this work uses the Taguchi technique to construct a multi-objective optimization mathematical model that takes tensile strength and surface roughness from experimentation into account. Several choice factors, including infill density, nozzle temperature, printing speed, layer thickness, and bed temperature, were examined in this study. Two goals are being pursued by this research: increasing tensile strength, and minimizing surface roughness. The Non-dominated Sorting Genetic Algorithm II technique and the Gamultiobj algorithm (MATLAB) are utilized to simultaneously search for the ideal values for the four objective functions. The ideal level setting for the infill density of 99.992%, 214.990 °C nozzle temperature, 70.000 mm/s printing speed, 0.151 mm layer thickness, and 48.390 °C was determined by the study's findings. The tensile strength of 31.399 MPa, and the 10.290 µm of surface roughness are the best response values.

References

1. Gao W, Zhang Y, Ramanujan D, Ramani K, Chen Y, Williams CB, Whang CCL, Shin YC, Zhang S (2015) The status, challenges, and future of additive manufacturing in engineering. *CAD Comput Aided Des* 69(12):65–89
2. Pereira T, Kennedy JV, Potgieter J (2019) A comparison of traditional manufacturing vs additive manufacturing, the best method for the job. In: Yarlagadda PKDV, Xavier AM, Gibson I, Zhu Y (eds) *Procedia manufacturing*, pp 11–18. Elsevier
3. Aziz NA, Adnan NAA, Wahab DA, Azman AH (2021) Component design optimisation based on artificial intelligence in support of additive manufacturing repair and restoration: current status and future outlook for remanufacturing. *J Clean Prod* 296(5):2–20
4. Kanishka K, Acherjee B (2023) A systematic review of additive manufacturing-based remanufacturing techniques for component repair and restoration. *J Manuf Process* 89(3):220–283
5. Swetha TA, Bora A, Mohanrasu K, Balaji P, Raja R, Ponnuchamy K, Muthusamy G, Arun A (2023) A comprehensive review on polylactic acid (PLA) synthesis, processing and application in food packaging. *Int J Biol Macromol* 234(4):1–10
6. Li X, Lin Y, Liu M, Meng L, Li C (2023) A review of research and application of polylactic acid composites. *J Appl Polym Sci* 140(2):1–22
7. Letcher T, Waytashek M (2014) Material property testing of 3D-printed specimen in PLA on an entry-level 3D printer. In: *Proceedings of the ASME 2014 international mechanical engineering congress and exposition-IMECE2014*, pp 1–8. ASME, Montreal, Quebec, Canada

8. Torres J, Cole M, Owji A, DeMastry Z, Gordon AP (2016) An approach for mechanical property optimization of fused deposition modeling with polylactic acid via design of experiments. *Rapid Prototyping J* 22(2):387–404
9. Dey A, Yodo N (2019) A systematic survey of FDM process parameter optimization and their influence on part characteristics. *J Manuf Mater Process* 3(3):1–30
10. Benamira M, Benhassine N, Ayad A, Dekhane A (2023) Investigation of printing parameters effects on mechanical and failure properties of 3D printed PLA. *Eng Fail Anal* 148(6):2–12
11. Kim MK, Lee IH, Kim HC (2018) Effect of fabrication parameters on surface roughness of FDM parts. *Int J Precis Eng Manuf* 19(1):37–142
12. Sandanamsamy L, Mogan J, Rajan J, Harun WSW, Ishak I, Romlay FRM, Samykano M (2023) Effect of process parameter on tensile properties of FDM printed PLA. *Mater Today Proc*
13. Sandhu GS, Boparai KS, Sandhu KS (2022) Effect of slicing parameters on surface roughness of fused deposition modeling prints. *Mater Today Proc* 48(1):1339–1345
14. Jatti VS, Sapre MS, Jatti AV, Khedkar NK, Jatti VS (2022) Mechanical properties of 3D-printed components using fused deposition modeling: optimization using the desirability approach and machine learning regressor. *Appl Syst Innov* 5(6):1–15
15. Patil P, Singh D, Raykar SJ, Bhamu J (2021) Multi-objective optimization of process parameters of Fused Deposition Modeling (FDM) for printing Polylactic Acid (PLA) polymer components. *Mater Today Proc* 45(1):4880–4885
16. Ali D, Huayier AF, Enzi A (2023) Parametric prediction of FDM process to improve tensile properties using Taguchi method and artificial neural network. *Adv Sci Technol Res J* 17(4):130–138
17. Kudryashova O, Toropkov N, Lerner M, Promakhov V, Vorozhtsov A, Mironov E (2023) Mathematical modeling of high-energy materials rheological behavior in 3D printing technology. *Heliyon* 9(1):1–12
18. Shi LK, Li PC, Liu CR, Zhu JX, Zhang TH, Xiong G (2024) An improved tensile strength and failure mode prediction model of FDM 3D printing PLA material: theoretical and experimental investigations. *J Build Eng* 90(4):1–16
19. Zhai C, Wang J, Tu Y, Chang G, Ren X, Ding C (2023) Robust optimization of 3D printing process parameters considering process stability and production efficiency. *Addit Manuf* 71(6):1–13
20. Moradi M, Karamimoghadam M, Meiabadi S, Casalino G, Ghaleeh M, Baby B, Ganapathi H, Jose J, Abdulla MS, Tallon P, Shamsborhan M, Rezayat M, Paul S, Khodadad D (2023) Mathematical modelling of fused deposition modeling (FDM) 3D printing of poly vinyl alcohol parts through statistical design of experiments approach. *Mathematics* 11(13):1–14
21. ISO 21920-2:2021 homepage. <https://www.iso.org/standard/72226.html>. Accessed 2 June 2024
22. Afshari H, Taher F, Alavi SA, Afshari M, Samadi MR, Allahyari F (2024) Studying the effects of FDM process parameters on the mechanical properties of parts produced from PLA using response surface methodology. *Colloid Polym Sci* 302(6):955–970
23. Lanzotti A, Grasso M, Staiano G, Martorelli M (2015) The impact of process parameters on mechanical properties of parts fabricated in PLA with an open-source 3-D printer. *Rapid Prototyping J* 21(5):604–617
24. Giri J, Chiwande A, Gupta Y, Mahatme C, Giri P (2021) Efect of process parameters on mechanical properties of 3d printed samples using FDM process. *Mater Today Proc* 47(1):5856–5861
25. Pujiyanto E, Rosyidi CN, Hisjam M, Liquddanu E (2022) Sustainable multi-objective optimization of a machining parameter model for multi-pass turning processes. *Cogent Eng* 9(1):2–7

Predicting Sustainability in SMEs Through Knowledge Factors Using Decision Tree Analysis



Amelia Kurniawati , Artamevia Salsabila Rizaldi , and Mia Amelia

Abstract This research aims to understand the factors influencing sustainability in Small and Medium Enterprises (SMEs) by applying the decision tree method. Three machine learning algorithms, ID3, C4.5, and CART, are compared to evaluate their effectiveness in sustainability data classification. The results show that the C4.5 algorithm has the highest accuracy at 84%, followed by CART at 81% and ID3 at 71%. Decision tree analysis measures knowledge factors such as appropriation of knowledge output, connective capacity, inventive capacity, and innovative capacity to support sustainability in SMEs. The results are that SMEs' ability to access knowledge from external partners (CCp1) and use knowledge to solve problems (ICc3) is critical to achieving sustainability. Organizations with high capabilities in these two aspects tend to meet sustainability criteria. Organizational age also plays a role, with younger organizations with high problem-solving capacity tending to be more sustainable than older ones. This research suggests that SMEs must increase access to external knowledge, utilize knowledge for innovation and problem-solving, and optimize resource use efficiency to achieve sustainability.

Keywords C4.5 algorithm · Decision tree · SMEs · Sustainability

1 Introduction

Sustainability is vital for the long-term success and resilience of Small and Medium Enterprises (SMEs). Research has highlighted the importance of SMEs adopting sustainable practices to ensure their competitiveness and positively impact the environment and society [1]. Despite the challenges SMEs face, such as lack of awareness, limited resources, and skills, implementing sustainability is essential to adapt to changing regulatory frameworks, market trends, and consumer preferences [2].

A. Kurniawati (✉) · A. S. Rizaldi · M. Amelia
Department of Industrial Engineering, Telkom University, Bandung 40257, Indonesia
e-mail: ameliakurniawati@telkomuniversity.ac.id

Sustainable growth not only ensures the survival of SMEs but also positions SMEs for success in a rapidly evolving business landscape [2]. Research has shown that SMEs play an important role in sustainable economic development globally [3]. Min et al. [4] research on sustainability practices in SMEs shows significant gaps, especially in developing countries. Most studies on sustainability practices are conducted in developed countries, with only a tiny proportion focusing on developing countries. In this context, SMEs in developing countries often ignore social and environmental aspects of sustainability practices. Sustainability practices in SMEs are generally still informal, unstructured, and not considered part of a comprehensive business strategy [4]. To address this gap, SMEs must integrate environmental and social sustainability strategies into their operations [5]. Implementing sustainable practices benefits the environment and improves business performance [4].

In facing the challenges of the transition to sustainability, SMEs can take advantage of open innovation supported by knowledge factors. By adopting open innovation, SMEs can obtain and integrate external knowledge from various sources, such as research institutes, universities, and government organizations. Knowledge factors such as appropriation of knowledge output, connective capacity, inventive capacity, and innovative capacity play an essential role in the open innovation process [6–8]. Open innovation facilitates cleaner production in batik SMEs by enabling them to access and integrate external knowledge and technology. This approach helps reduce environmental impacts through improved waste management and environmentally friendly dyes. A study by Rumanti et al. [9], which mapped the conditions of open innovation in Indonesian batik SMEs, highlighted that a conducive open innovation climate could result in significant waste reduction and increase cleaner production processes.

Understanding an SME's sustainability position enables SMEs to make informed decisions regarding resource allocation, investment in sustainable practices, and strategic partnerships [4]. By predicting their sustainability position, SMEs can prioritize initiatives significantly impact their sustainability performance, resulting in long-term success and resilience [4]. In addition, predicting SMEs' sustainability positions is essential to attracting investors, customers, and other stakeholders who value sustainability [10]. Demonstrating commitment to sustainability through predictive measures can increase SMEs' credibility and integrity, fostering trust and confidence among stakeholders [10]. Additionally, estimating SMEs' sustainability position can help develop tools and methodologies for impact measurement and verification, enabling SMEs to assess their sustainability initiatives in environmental, social, and economic impacts [10]. This predictive approach provides a structured framework for evaluating the effectiveness of sustainability projects and investments, ensuring transparency and accountability in sustainable finance [10].

2 Methodology

2.1 Data Collection

In the data collection process, 203 respondents from written Batik SMEs located in Surakarta City, Rembang Regency, and Madura Island were surveyed. This area has been known as a written batik-producing area since the sixteenth century. The selected respondents were SME leaders because they had comprehensive information about operational and managerial activities. Respondents were asked to fill in statements regarding appropriation of knowledge output, connective, inventive, and innovative capacity.

There are two indicators related to the appropriation of knowledge output. First, the organization being able to understand the value of the knowledge it has and documenting it (AKw1). Second, the organization can prevent leakage of internal expertise to competitors and registering intellectual property (AKw2). The assessment rubrication can be seen in Table 1.

There are two indicators related to the connective capacity. First, the organization having the ability to access knowledge from external partners (CCp1). Second, the organization can identify new knowledge possessed by external partners and document it (CCp2). The assessment rubrication can be seen in Table 2.

In the inventive capacity indicator, the organization can improve its knowledge if something is incorrect and immediately implement best practices (ICp1), the organization can identify internal knowledge that is no longer relevant and replace it

Table 1 Appropriation of knowledge output (AKw) assessment rubrication

	High	Medium	Low
AKw1	Organizations fully understand the valuable knowledge they possess and have complete documentation regarding that knowledge	The organization understands valuable knowledge, but the documentation is incomplete	Organizations do not know what their knowledge is worth and do not have adequate documentation
AKw2	Organizations have strong countermeasures in by registering Intellectual Property Rights (IPR) or other formal measures to protect their knowledge	The organization has some countermeasures to prevent knowledge leaks, but there are no formal efforts. Prevention is carried out informally, such as only providing knowledge to nuclear family members or trusted people in the organization	The organization does not have adequate countermeasures to prevent knowledge leakage to competitors

AKw1—The organization being able to understand the value of the knowledge it has and documenting it

AKw2—The organization can prevent leakage of internal expertise to competitors and registering intellectual property

Table 2 Connective capacity (CCp) assessment rubrication

	High	Medium	Low
CCp1	Organizations have the ability to access knowledge from external partners through a variety of different collaborations	Organizations can access external partners' knowledge, but this access is not always consistent and sometimes experiences delays or obstacles	Organizations have difficulty accessing external partners' knowledge and do not have adequate mechanisms or networks to obtain this information when needed
CCp2	Organizations are able to identify new knowledge held by external partners and promptly update their documentation	The organization was able to identify new knowledge held by external partners, but did not promptly update their documentation	Organizations have a low ability to identify new knowledge possessed by external partners

CCp1—The organization having the ability to access knowledge from external partners

CCp2—The organization can identify new knowledge possessed by external partners and document it

with relevant ones (ICp2), and the organization can create the rate of new knowledge through experience and research (ICp3), can be seen in Table 3.

Table 3 Inventive capacity (Icp) assessment rubrication

	High	Medium	Low
ICp1	Organizations can improve their knowledge when something is incorrect and immediately apply the best practices found	Organizations are able to identify errors or gaps in their knowledge, but are not yet fully able to make improvements	The organization has not been able to improve the knowledge it has even though there are errors or deficiencies
ICp2	Organizations can identify internal knowledge that is no longer relevant and immediately replace it with newer and more relevant knowledge	The organization is already aware of irrelevant internal knowledge but has not yet found a replacement	Organizations do not know if their internal knowledge is no longer relevant
ICp3	Organizations can create new knowledge independently through experience and internal research processes	Organizations can create new knowledge through experience and internal research with support from external parties	Organizations can only able to create new knowledge through experience

ICp1—The organization can improve its knowledge if something is incorrect and immediately implement best practices

ICp2—The organization can identify internal knowledge that is no longer relevant and replace it with relevant ones

ICp3—The organization can create the rate of new knowledge through experience and research

Table 4 Innovative capacity (ICc) assessment rubrication

	High	Medium	Low
ICc1	The organization has used all its knowledge to develop products independently	The organization has used some of its knowledge to develop products independently	The organization is not yet fully able to use its knowledge to develop products
ICc2	Organizations can use all their knowledge to make improvements to managerial processes and production processes	Organizations can use all their knowledge to make improvements to managerial processes or production processes	Organizations can use some of their knowledge to make improvements to managerial processes or production processes
ICc3	Organizations can use their knowledge to solve all problems independently	Organizations can use their knowledge to solve some problems independently	Organizations can use their knowledge to solve some problems with external help

ICc1—The organization has used its knowledge to develop products

ICc2—The organization can use its knowledge to improve managerial processes and production processes

ICc3—The organization can use its knowledge to solve all problems

In the innovative capacity indicator, the organization has used its knowledge to develop products (ICc1), the organization can use its knowledge to improve managerial processes and production processes (ICc2), and the organization can use its knowledge to solve all problems (ICc3), which can be seen in Table 4.

Furthermore, the sustainability indicator (Sust) as the dependent variable (Y) is measured based on the planetary (environmental) concept regarding materials, energy, and water used very efficiently. Materials are fully recycled, renewable energy is utilized optimally, and water is used without waste through an efficient recycling system. The garbage produced does not pollute the environment because it is processed using environmentally friendly technology [11].

2.2 Decision Tree

Decision trees are a supervised classification method that utilizes a tree-like structure to assist decision-making by representing decisions and outcomes visually through branch and leaf diagrams [12]. In this method, each node in the tree represents an attribute, with branches indicating the attribute value and leaves indicating the class [13]. Decision trees are favoured for their easy-to-understand nature, resembling the human decision-making process, which helps in extracting concise and credible logical rules from data [14]. The decision tree model can predict whether SMEs will have high or low sustainability. Utilizing the decision tree model can be a tool for analyzing various factors that influence sustainability performance [15, 16].

Decision tree algorithms include a wide variety, with notable examples being ID3, C4.5, and CART. Introduced by Quinlan in 1986, ID3 is a classification algorithm that uses a greedy approach to build a decision tree by selecting the best attributes at each stage. On the other hand, C4.5 is an advancement of ID3 that can handle missing data and continuous values, thus increasing its applicability in various data sets [17]. CART, which stands for Classification and Regression Trees, is a versatile algorithm capable of handling both classification and regression tasks [18]. ID3, C4.5, and CART have been studied and compared extensively in various contexts. For example, a study explored this algorithm and the IQ algorithm to determine the decision tree algorithm with the highest execution efficiency [19]. Another study compared the effectiveness and accuracy rates of the C4.5, ID3, and CART algorithms in classifying diseases, highlighting the practical implications of these algorithms in real-world scenarios [20]. Additionally, the CART algorithm has been applied in diagnosing hepatitis, demonstrating its usefulness in health care applications [20].

3 Results and Discussion

The three machine learning algorithms compared are ID3, C4.5, and CART. From the results obtained, the C4.5 algorithm shows the best performance, with an accuracy of around 84%, followed by CART with an accuracy of around 81% and ID3 with an accuracy of around 71% (See Fig. 1).

This difference in accuracy shows that C4.5 is more effective in data classification than CART and ID3. Therefore, the C4.5 algorithm may be a better choice in applications where accuracy is critical.

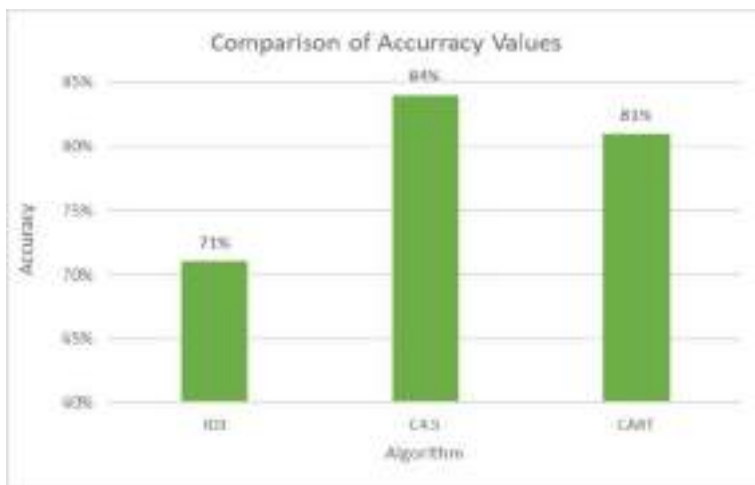


Fig. 1 Comparison of accuracy values

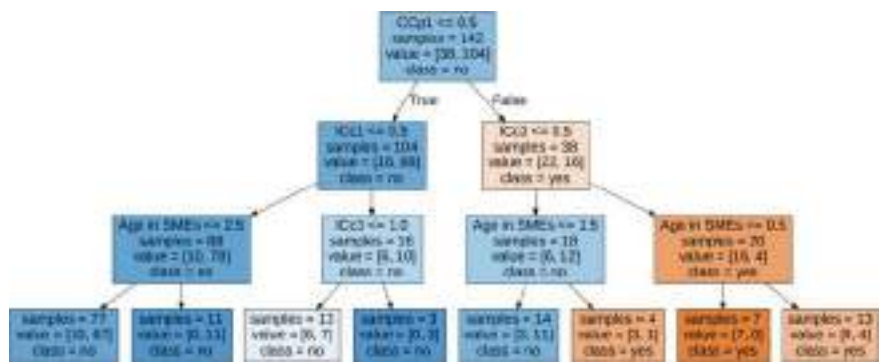


Fig. 2 Decision tree algorithm C4.5

Based on the decision tree analysis provided, we can understand how various factors influence whether an organization meets the sustainability criteria (Sust) or not. This sustainability indicator is measured based on the planet (environmental) concept, which includes efficient use of materials, energy and water, and environmentally friendly waste management (See Fig. 2).

In decision tree analysis, the root node is CCp1, which shows the organization’s ability to access knowledge from external partners. Organizations with a CCp1 score ≤ 0.5 indicate a low ability to access knowledge from external partners and tend not to meet sustainability criteria. This suggests that a lack of access to external knowledge limits an organization’s ability to implement best practices in environmental efficiency. In contrast, organizations with a CCp1 (the organization having the ability to access knowledge from external partners) score > 0.5 can access knowledge from external partners and proceed to further analysis. This suggests collaboration and knowledge exchange are important in supporting sustainability practices and improving organizational environmental efficiency.

On the left branch of the decision tree with CCp1 (the organization having the ability to access knowledge from external partners) ≤ 0.5 , organizations with a low score on ICc1 (use of knowledge for product development) further strengthen their tendency not to meet sustainability criteria. This shows that using knowledge in product innovation is also very important, besides access to knowledge. Younger organizations, ≤ 2.5 years old, in the SME category are less likely to meet sustainability criteria, possibly due to a lack of experience and mature systems to support environmentally friendly practices. In contrast, even though they are older, organizations older than 2.5 years still need to improve their ability to use knowledge for innovation to meet sustainability criteria.

On the right branch of the decision tree with CCp1 (the organization having the ability to access knowledge from external partners) > 0.5 , organizations that can use their knowledge to solve problems (ICc3 ≤ 0.5) tend to meet the sustainability criteria. This shows that good problem-solving skills and the application of knowledge-based solutions are crucial for sustainability practices. Organizations that

are very young (≤ 1.5 years old) but have high problem-solving capabilities tend to meet the sustainability criteria. This may reflect the rapid adoption of best practices and environmental innovation. In contrast, older organizations with good problem-solving capabilities also tend to meet sustainability criteria, indicating that combined experience and problem-solving capabilities support environmentally friendly practices. Furthermore, organizations that score higher on ICc3 (the organization can use its knowledge to solve all problems) and are older (Age in SMEs ≤ 0.5) are less likely to meet sustainability criteria. This shows that even newly established organizations with a high capacity to use knowledge to solve problems have a great chance of meeting sustainability criteria.

The decision tree analysis shows that organizations that want to improve their sustainability must focus on several factors. First, access and collaboration with external knowledge are essential. Organizations that can access knowledge from external partners can better implement sustainable practices, so strengthening external networks and partnerships is crucial. Second, the ability to use knowledge in product development and problem-solving is a key factor. Organizations need to increase their capacity to utilize knowledge for product innovation and problem-solving through training, continuous learning, and investment in research and development. Third, the age of the organization also plays a role, as younger organizations may lack mature systems, but with high problem-solving capabilities, they can still meet sustainability criteria. Older organizations need to improve their use of knowledge to remain sustainable continually. Finally, resource use efficiency is an essential indicator of sustainability. Organizations that meet sustainability criteria tend to be more efficient in using materials, energy and water and better at managing waste. By focusing on these areas, organizations can increase their chances of achieving sustainability, supporting more environmentally friendly and sustainable business practices in the long term.

4 Conclusion

This research uses the decision tree method to analyze the factors that influence the sustainability of Small and Medium Enterprises (SMEs). Decision trees were chosen because of their ability to identify relationships between various variables and final results in a visual and easy-to-understand manner. The algorithm chosen was C4.5 because it has the highest accuracy value between the CART and ID3 algorithms. From the results obtained, SMEs must focus on increasing access to external knowledge, using knowledge for innovation, problem-solving, and efficient use of resources to achieve sustainability. With this strategy, SMEs can support business practices that are more environmentally friendly and sustainable in the long term. Suggestions for further research are to expand the research to other sectors outside Batik and to different geographical locations to identify whether the same findings apply in various industrial and regional contexts.

References

1. Awongua KF, Nwankwo EE, Oladapo JO, Okoye CC, Odunaiya OG, Scholastica UC (2024) Driving sustainable growth in SME manufacturing: the role of digital transformation, project, and capture management. *Int J Sci Res Arch* 11:2012–2021. <https://doi.org/10.30574/ijrsra.2024.11.1.0270>
2. de Santos AM, Becker AM, Ayala NF, Sant'Anna ÂMO (2024) Industry 4.0 as an enabler of sustainability for small and medium enterprises. *Academia Revista Latinoamericana de Administracion* 37:204–226. <https://doi.org/10.1108/ARLA-07-2023-0118>
3. Prasanna RPIR, Jayasundara JMSB, Gamage SKN, Ekanayake EMS, Rajapakshe PSK, Abeyrathne GAKNJ (2019) Sustainability of SMEs in the competition: a systemic review on technological challenges and SME performance. <https://doi.org/10.3390/joitmc5040100>
4. Min HL, Tambunan TTH, Santosa B (2023) Sumiyarti: the drivers of sustainability practices in SMEs and the impact on business performance. *J Econ Manage Trade* 29:1–16. <https://doi.org/10.9734/jemt/2023/v29i121172>
5. Eweje G (2020) Proactive environmental and social strategies in a small- to medium-sized company: a case study of a Japanese SME. *Bus Strategy Environ* 29:2927–2938. <https://doi.org/10.1002/bse.2582>
6. Fisher GJ, Qualls WJ (2018) A framework of interfirm open innovation: relationship and knowledge based perspectives. *J Bus Indus Market* 33:240–250. <https://doi.org/10.1108/JBIM-11-2016-0276>
7. Shin K, Kim E, Jeong ES (2018) Structural relationship and influence between open innovation capacities and performances. *Sustainability (Switzerland)* 10. <https://doi.org/10.3390/su10082787>
8. Kurniawati A, Sunaryo I, Wiratmadja II, Irianto D (2022) Sustainability-oriented open innovation: a small and medium-sized enterprises perspective. *J Open Innov Technol Market Complex* 8. <https://doi.org/10.3390/joitmc8020069>
9. Rumanti AA, Sunaryo I, Wiratmadja II, Irianto D (2021) Cleaner production through open innovation in Indonesian batik small and medium enterprises (SME). *TQM J* 33:1347–1372. <https://doi.org/10.1108/TQM-04-2020-0086>
10. Oyewole AT, Adeoye OB, Addy WA, Okoye CC, Ofodile OC (2024) Enhancing global competitiveness of U.S. SMEs through sustainable finance: a review and future directions. *Int J Manage Entrepreneurship Res* 6:634–647. <https://doi.org/10.51594/ijmer.v6i3.876>
11. Hammer J, Pivo G (2017) The triple bottom line and sustainable economic development theory and practice. *Econ Dev Q* 31:25–36. <https://doi.org/10.1177/0891242416674808>
12. Rochmawati N, Hidayati HB, Yamasari Y, Yustanti W, Rakhmawati L, Tjahyaningtjias HPA, Anistyasari Y (2020) Covid symptom severity using decision tree. In: *Proceeding—2020 3rd international conference on vocational education and electrical engineering: strengthening the framework of society 5.0 through innovations in education, electrical, engineering and informatics engineering, ICVEE 2020*. Institute of Electrical and Electronics Engineers Inc. <https://doi.org/10.1109/ICVEE50212.2020.9243246>
13. Gupta B, Uttarakhand P, Rawat IA (2017) Analysis of various decision tree algorithms for classification in data mining
14. Wang L, Sun M, Cao C (2014) How to mine information from each instance to extract an abbreviated and credible logical rule. *Entropy* 16:5242–5262. <https://doi.org/10.3390/e16105242>
15. Mikučionienė R, Martinaitis V, Keras E (2014) Evaluation of energy efficiency measures sustainability by decision tree method. *Energy Build* 76:64–71. <https://doi.org/10.1016/j.enbuid.2014.02.048>
16. Patalas-Maliszewska J, Łosyk H, Rehm M (2022) Decision-tree based methodology aid in assessing the sustainable development of a manufacturing company. *Sustainability (Switzerland)* 14. <https://doi.org/10.3390/su14106362>

17. Hssina B, Merbouha A, Ezzikouri H, Erritali M (2014) A comparative study of decision tree ID3 and C4.5. In: IJACSA, International journal of advanced computer science and applications, Special issue on advances in vehicular ad hoc networking and applications, pp 13–19
18. Vega FA, Matías JM, Andrade ML, Reigosa MJ, Covelo EF (2009) Classification and regression trees (CARTs) for modelling the sorption and retention of heavy metals by soil. *J Hazard Mater* 167:615–624. <https://doi.org/10.1016/j.jhazmat.2009.01.016>
19. Liu B, Sun Z (2022) Global economic market forecast and decision system for IoT and machine learning. *Mob Inf Syst*. <https://doi.org/10.1155/2022/8344791>
20. Sathyadevi G (2011) Application of CART algorithm in hepatitis disease diagnosis. In: International conference on recent trends in information technology: ICRTIT 2011, pp 1283–1287. IEEE

The Improvement of Procurement Process for Promotional Goods Using Value Stream Mapping and Multi-Criteria Decision Making



Sekar Zaneta Amirul Putri , Wakhid Ahmad Jauhari ,
and Cucuk Nur Rosyidi

Abstract As one of the Fast-moving Consumer Goods (FMCG) companies operating in the cosmetics sector, a company must engage in promotional activities through print or social media and offer attractive package. To support competitive advantage in procurement process requires a careful yet effective selection of suppliers by implementing lean concepts. Value Stream Mapping (VSM) and improvement through the ECRS method will focus on efficiency without compromising process effectiveness by enhancing value-added operations and reducing waste. By reducing time wastage and simplifying the supplier selection process, production lead times become faster while maintaining the same level of value-added activities. To realize time waste reduction while ensuring effectiveness, a decision-making method is needed to accommodate subjective evaluations, unclear demands, and redundancy in bid requests and evaluation quantification. Therefore, this research applies Multi-Criteria Decision Making (MCDM) to identify the best supplier based on 8 criteria. The Best–worst Method (BWM) utilized to determine the weight of each criterion and sub-criterion, which will then be used to rank suppliers using the Technique for Order Preference by Similarity to Ideal Solution (TOPSIS). From the result of the determination of alternative ranking, it can be seen that the most fulfilling alternative is Alternative/Supplier 4 because it has the highest score of similarities.

Keywords Waste · Supplier selection · Value stream mapping · ECRS · BWM · TOPSIS

S. Z. A. Putri (✉) · W. A. Jauhari · C. N. Rosyidi
Universitas Sebelas Maret, Surakarta, Indonesia
e-mail: masayusekar@gmail.com

© The Author(s), under exclusive license to Springer Nature Singapore Pte Ltd. 2025
M. R. Mohamad Yasin et al. (eds.), *Proceedings of the 7th Asia Pacific Conference on Manufacturing Systems and 6th International Manufacturing Engineering Conference—Volume 2*, Lecture Notes in Mechanical Engineering,
https://doi.org/10.1007/978-981-96-5690-5_16

159

1 Introduction

Due to intense competition in the retail industry, particularly among companies selling Fast-moving Consumer Goods (FMCG) products, it is important for companies to not only focus on product quality but also ensure effective communication of information to consumers. According to Swasta and Handoko [1], several factors influence purchase decisions, including strategic location of sellers, good service, salesperson competence, promotion, and product classification. As one of the FMCG companies operating in the cosmetics sector, it actively promotes its products through various means. Currently, promotional activities are conducted through print or social media and attractive package. With enticing and extraordinary package, consumers are stimulated to make purchase decisions.

Therefore, selecting promotional item suppliers is also an important element in a company's promotional activities because it is crucial to find suppliers capable of providing goods/services according to evaluation criteria. Additionally, supplier selection involves many decision-makers, whose will review all aspects of the supply chain operations to choose the best supplier and achieve efficient supply-chain network performance. Especially in the procurement of goods with more complex specifications such as sewing goods, there are many time wastages caused by subjective assessment, demand uncertainty, as well as redundancy in bid requests.

The lean approach focuses on efficiency without compromising process effectiveness by improving value-added operations and reducing waste [2]. According to Langerak and Hultink [3], accelerating activities and tasks as well as simplifying organizational structures also increase the speed of development and improve company performance. Value Stream Mapping (VSM) is one of the continuous improvement tools that can produce products that are cheaper, better, and faster. VSM focuses on efficiency without compromising process effectiveness by improving value-added operations, reducing waste, and meeting customer needs [4]. By reducing waste, leadtime process will decrease, so with the same value-added activities, production time becomes faster. This is because of the reduction in time spent on non-value-added activities. According to Prasetyo et al. [5], there are seven wastes in manufacturing companies, namely defect, inventory, motion, over-production, over-processing, transportation, and waiting. Work method improvements can be made using various methods, one of which is the ECRS (Eliminate, Combine, Rearrange, Simplify) method. ECRS is a work method improvement by eliminating unnecessary or non-value-added work elements, combining tasks, rearranging tasks, or simplifying tasks [6].

To realize a reduction in time wastage while still considering effectiveness, a well-documented decision-making method is needed among decision-makers to accommodate subjective assessments, demand uncertainty, redundancy in bid requests and evaluation quantification. Besides reducing time wastage, a well-documented decision-making method can provide clear information to all parties involved in the procurement process. Therefore, the application of decision-making, commonly known as multi-criteria decision-making (MCDM), is implemented to select the

best supplier with several consideration criteria [7]. Through MCDM, companies will identify suppliers through qualitative and quantitative factors with the highest potential to consistently meet company needs while still considering Supply Chain Management (SCM) concepts.

2 Methodology

To achieve an efficient and effective procurement process, this research goes through several steps. The first step that needs to be taken is identifying the procurement process flow obtained from direct observations and interviews with procurement personnel. This is followed by classifying each work element according to VA, NNVA, and NVA classifications, enabling the identification of waste to eliminate or reduce non-value-added elements using the ECRS method. In addition, this research applies Multi-Criteria Decision Making (MCDM) to select the best supplier based on several consideration criteria.

2.1 Value Stream Mapping

According to Jannah and Siswanti [8], Value Stream Mapping (VSM) is a process mapping tool designed to identify the flow of materials and information in the production process from raw materials to finished products. VSM was first introduced by Rother and Shook [9]. As per Rosanto [10], VSM differs from simple recording techniques because it gathers comprehensive information on each process, including cycle times, resource utilization, lead times, working within available processes, labor requirements, and the flow of information from raw materials to completion. This information also encompasses value-added and non-value-added tasks. In [4], Hines and Taylor proposed a classification of activities in the production line, which can be divide into three categories: Value Added Activity (VA), Necessary but Non Value Added (NNVA), and Non Value Added (NVA). Improvements in a line with waste can be made using the ECRS method (Eliminate, Combine, Rearrange, Simplify). ECRS is a concept for improving work methods by eliminating tasks deemed unnecessary, combining tasks, rearranging tasks, and simplifying tasks [11].

2.2 Best–Worst Method (BWM)

Common methods in MCDM are divided into two types: AHP (Analytic Hierarchy Process) and ANP (Analytic Network Process). The resolution of both methods involves using pairwise comparison, wherein if the obtained comparisons are inconsistent, decision-making cannot be achieved. Pairwise comparisons using AHP tend

to be more forceful without considering other values of one criterion compared to another.

Hence, a new method called the Best–Worst Method (BWM) emerged. Based on BWM, the best criteria (e.g., most desired, most relevant) and the worst criteria (e.g., least desired, least relevant) are identified first by decision-makers. Pairwise comparisons are then made between these two criteria (best and worst) and the other. According to Rezaei et al. [12], there are several prominent features of the BWM method compared to other methods, namely requiring fewer comparative data and producing more consistent comparisons.

2.3 Technique for Order Preference by Similarity to Ideal Solution (TOPSIS)

The efficient utilization of multi-criteria decision-making methods not only reduces risks in procurement processes but also enables the evaluation of suppliers, thereby fostering good relationships between suppliers and buyers. TOPSIS is one of the multi-criteria decision-making methods that can provide a solution from several possible alternatives by comparing each best and worst alternative with others pairwise. This method is employed to determine a solution where the best alternative is closest to the positive ideal solution and furthest from the negative ideal solution [13]. The TOPSIS method is used to rank supplier alternatives as procurement solution alternatives.

3 Result and Discussion

This research was conducted in an FMCG company specializing in cosmetics. Apart from manufacturing cosmetic products, the company needs to procure promotional goods. The company in question, searches for various suppliers to provide suitable promotional goods, particularly those with detailed specifications such as sewn goods, efficiently and effectively. This research focuses on the procurement of promotional goods, specifically sewn goods, such as leather wallets. It began with an analysis of the waste present in procurement with value stream mapping (VSM) and continued with the application of the ECRS method to eliminate non-value-added activities. Subsequently, criteria and sub-criteria were determined to serve as the basis for determining the weight of each criterion using the BWM method. Following with supplier evaluation and ranking were conducted using the TOPSIS method.

3.1 Analysis Waste with Value Stream Mapping

After collecting data on process time and classifying VA, NNVA, and NVA activities, it was found that the classification results for each work element in the procurement process for promotional goods, particularly sewn goods, still contain many NNVA and NVA activities. NNVA and NVA activities are considered as contributing waste to the procurement process and thus should be eliminated or minimized as they do not add value to the process. Therefore, it is necessary to map the current procurement process flow to identify the spread and extent of waste in the procurement process for sewn promotional goods.

Based on the mapping results depicted in Fig. 1, it can be seen that there are still NNVA and NVA activities that need to be minimized or eliminated to achieve an efficient and effective procurement process. Therefore, improvements are made using the ECRS method to reduce or eliminate activities that do not add value while retaining value-added activities by eliminating tasks considered unnecessary, combining tasks, rearranging tasks, and simplifying tasks.

With the ECRS method, the overall procurement process can achieve a total process time reduction from 1243 h to 1083 h. The Value Added Activity (VA) category remains with the same work elements, but there has been a change in the total process time from 865 to 985 h. These work elements include the user sending PR sourcing to procurement, procurement sourcing vendors, procurement negotiating with vendors, procurement preparing and sending Purchase Orders (PO) document to vendors, vendors producing goods, vendors sending goods according to allocated time, vendors preparing and sending full invoices to finance, and finance making payments.

The Necessary but Non-Value Added Activity (NNVA) category also consists of the same work elements, but there has been a change in total process time from 258 to 98 h. These work elements include procurement receiving PR document, procurement requesting sample production, vendors producing samples, vendors sending samples, users receiving and evaluating samples, procurement receiving and reviewing quotations, users signing quotations taking, vendors receiving Purchase Order (PO) documents, DC receiving and checking goods, and finance receiving full invoices. The total time changes in VA and NNVA activities, despite having the same number of activities, occurred due to changes in the delivery process. Originally, vendors were supposed to deliver to National Distribution Center (NDC) for subsequent delivery to regions based on allocation set by distribution, but this was changed to direct vendor delivery to regions as allocated. For Non-Value Added Activity (NVA), the time has been reduced to 0 h, indicating there are no longer activities without added value in the procurement process for promotional sewn goods.

3.2 *Determining the Weight Criteria Using the Best–Worst Method (BWM)*

In the procurement process carried out by this company, 8 main criteria and 8 sub-criteria are selected to be considered as the basis for assessing and evaluating suitable suppliers. The determination of criteria and sub-criteria used is adjusted to the company's needs and identified based on previous research conducted (Table 1).

This is followed by determining the best and worst criteria in general, which will be compared pairwise using the Saaty Scale, which involves assessing on a scale from 1 to 9. For example, DM 1 considered C1 to be best main criteria, two times as important as C2. The example, Table 2 shows only the pairwise comparisons for the main criteria.

Likewise, each decision maker was tasked with assessing the other criteria against the worst criteria. The weights for all criteria and sub-criteria are established using identical procedures. The mean rating across all seven decision-makers regarding the primary criteria is then derived by averaging the overall weights assigned by each decision-maker. The calculation results are presented in Table 4 (Table 3).

The global weight of the sub-criteria is calculated by multiplying the main criteria weight with the local weight of the sub-criteria. It can be concluded that the most crucial criteria are price (C1) and lead time (C2). This is followed by legality (C8), product condition (Q1) and product conformity (Q2) sub-criteria under the quality

Table 1 A literature review on the selection of suppliers for promotional goods such as sewn goods

Criteria	Sub-criteria	References
Price	–	Manik [14] Sulistyoningarum et al. [15]
Lead time	–	Tavana et al. [16]
Flexibility	Demand flexibility	Jariyah [17]
	Sample flexibility	Rizqika and Zuraidah [18]
	Payment flexibility	Djatna [19] Sulistyoningarum et al. [15]
Quality	Product condition	Lin et al. [20] Tavana et al. [16]
	Product conformity	Lin et al. [20]
Production capacity	–	Tsai et al. [21] Yikici and Özçelik [22]
Track record	–	Zhong et al. [23]
Communication	Spesification information	Guarnieri and Trojan [24] Lin et al. [20]
	Order status information	Lin et al. [20]
	Problem responses	Lin et al. [20]
Legality	–	Lin et al. [20]

Table 2 Best to others vectors main criteria

DM	Best	Others							
		C1	C2	C3	C4	C5	C6	C7	C8
1	C1	1	2	4	2	8	5	6	7
2	C4	2	2	4	1	5	6	6	8
3	C2	2	1	4	2	5	3	6	8
4	C1	1	2	3	3	7	6	5	8
5	C4	2	2	2	1	4	3	3	2
6	C4	3	2	6	1	4	4	2	2
7	C8	6	4	2	4	5	4	4	1

Table 3 Others to worst vectors main criteria

DM	1	2	3	4	5	6	7
Worst	C5	C8	C8	C8	C5	C3	C1
C1	8	7	7	8	3	4	1
C2	7	6	8	7	3	5	3
C3	5	5	5	6	3	1	5
C4	7	8	7	6	4	6	3
C5	1	3	4	2	1	3	2
C6	4	2	6	3	2	3	3
C7	3	2	3	4	2	4	3
C8	2	1	1	1	3	4	6

Table 4 Global weights and rankings of criteria and sub-criteria

Criteria	Weight	Sub-criteria	Weight		Ranking
			Local	Global	
C1	0.182	–		0.182	1
C2	0.176	–		0.176	2
C3	0.108	F1	0.413	0.045	8
		F2	0.368	0.041	9
		F3	0.219	0.024	11
C4	0.199	Q1	0.500	0.100	4
		Q2	0.500	0.100	5
C5	0.062	–		0.062	7
C6	0.082	–		0.082	6
C7	0.084	K1	0.494	0.039	10
		K2	0.269	0.022	12
		K3	0.237	0.019	13
C8	0.108	–		0.108	3

criteria (C4), track record (C6), production capacity (C5), demand flexibility (F1) sub-criteria under the flexibility criteria (C3), sample flexibility (F2) sub-criteria under the flexibility criteria (C3), specification information (K1) sub-criteria under the communication criteria (C7). The smallest global weight is held by payment flexibility (F3) sub-criteria under the flexibility criteria (C3), order status information (K2) sub-criteria under the communication criteria (C7), and problem response (K3) sub-criteria under the communication criteria (C7).

3.3 *Supplier's Ranking Determination Using TOPSIS Method*

The determination of alternative rankings is carried out to assess and evaluate the selection of suppliers to choose the one that best fits the company's needs. The ranking determination will utilize the weighting results previously calculated using the BWM method. In this study, the ranking determination will employ the TOPSIS method, which will utilize the closest distance to the ideal positive solution and the farthest distance from the ideal negative solution.

The initial stage of TOPSIS involves constructing a normalized decision matrix derived from the evaluations provided by the decision-makers. Subsequently, a weighted normalized matrix is formed by multiplying this matrix with the weight assigned to each criteria. Following this, distances are compute from both the ideal positive and negative solution matrices. These distances indicate the relative proximity of each alternative, serving as the performance score for each supplier. Finally, the scores are arrange in descending order to ascertain the ranking of the suppliers (Table 5).

It can be concluded that alternative/supplier 4 is the best choice for fulfilling the leather wallet procurement, followed by alternative/supplier 3, alternative/supplier 2, and alternative/supplier 1. By employing this method, supplier selection is no longer solely reliant on the company's historical data but rather on measurable factors. Furthermore, the evaluation outcomes of bids can serve as a reference for the company's routine evaluations of promotional items such as sewn goods in the procurement process.

Table 5 TOPSIS calculation ranking

Alternative	C_i^*	Normalized C_i^*	Ranking
Alternative 1	0.1138526	0.0704076	4
Alternative 2	0.1550227	0.0958676	3
Alternative 3	0.3481785	0.2153171	2
Alternative 4	0.9999963	0.6184077	1

4 Conclusions

This research employs Value Stream Mapping to chart the procurement process of promotional goods such as sewn goods, to analyze the time distribution categorized into three categories: VA, NNVA, and NVA. To reduce or eliminate non-value-added activities, the ECRS method is utilized to improve the procurement process flow, aiming for an efficient and effective process flow. Additionally, to support an efficient and effective procurement process, the BWM and TOPSIS methods are employed to address supplier selection issues. Eight criteria and eight sub-criteria are used to find suppliers that align with the company's requirements, followed by determining the weights of these criteria and sub-criteria using the BWM method. Meanwhile, the TOPSIS method is utilized to determine the ranking and evaluation basis for each supplier. According to the case study in the procurement process of promotional goods such as sewn goods, the total process time has decreased from 1243 h to 1083 h overall, indicating the elimination of non-value-added activities in the procurement process. Additionally, it was found that alternative/supplier 4 is the suitable choice for leather wallet procurement.

The company needs to evaluate and consider the procurement process flow of pro-motional items in this research so that it can be applied and further developed as a reference for the company to achieve an effective and efficient process flow. And also, in further research, it would be advisable to consider volume discount or any other discount scheme offered when purchasing in specific quantities.

References

1. Swasta B, Handoko H (2010) *Manajemen Pemasaran: analisa dan perilaku konsumen*. BPFE. Yogyakarta
2. Jouris Devitami A (2017) Analisis waste Dengan Pendekatan lean manufacturing Menggunakan Metode Wam Dan Valsat Pada proses Produksi veneer Pt Muroco Jember
3. Langerak F, Hultink EJ (2005) The impact of new product development acceleration approaches on speed and profitability: lessons for pioneers and fast followers. *IEEE Trans Eng Manage* 52(1)
4. Hines P, Taylor D (2000) Going lean. *Lean Enterprise Research Centre Cardiff Business School* 1, Cardiff, UK, pp 528–534
5. Prasetyo I, Septianawati G, Utomo NA (2023) Identifikasi Dan Eliminasi Pemborosan Dalam Proses Penerimaan Persediaan Medis. *Juremi Jurnal Riset Ekonomi* 3(1)
6. Saputra AR (2020) *Perbaikan Metode Kerja Di Ukm Tempe Nusantara*, PhD dissertation. Universitas Atma Jaya Yogyakarta
7. Yucesan M, Mete S, Serin F, Celik E, Gul M (2019) An integrated best-worst and interval type-2 fuzzy TOPSIS methodology for green supplier selection. *Mathematics* 7(2)
8. Jannah M, Siswanti D (2017) Analisis penerapan lean manufacturing untuk mereduksi over production waste menggunakan value stream mapping dan fishbone diagram. *Sinteks Jurnal Teknik* 6(1)
9. Rother M, Shook J (1999) *Learning to See: Value-Stream Mapping to Create Value and Eliminate Muda*. Lean Enterprise Institute

10. Rosanto O (2022) Peningkatan Produktivitas Grand Piano dengan Menurunkan Inventory dan Lead Time Melalui Perbaikan Kaizen Dibagian 1 Regulation Grand Piano Assembly (Studi Kasus Departemen Grand Piano Assembly PT. Yamaha Indonesia), PhD dissertation. Universitas Islam Indonesia
11. Amran TG, Wibowo NC (2018) Perbaikan Proses Produksi Sistem Pengereman Kendaraan Bermotor dengan Metode ECRS-Base Line Balancing. In Prosiding Seminar Nasional Pakar, pp 193-204
12. Rezaei J (2016) Best-worst multi-criteria decision-making method: some properties and a linear model. *Omega* 64:126–130
13. Lestari AI, Sudarwati W, Rani AM (2021) Pemilihan Alternatif. Supplier Alat kesehatan Dengan Pendekatan AHP dan TOPSIS. Prosiding Semnastek
14. Manik MH (2023) Addressing the supplier selection problem by using the analytical hierarchy process. *Heliyon* 9(7)
15. Sulistyoningarum R, Rosyidi CN, Rochman T (2019) Supplier selection of recycled plastic materials using best worst and TOPSIS method. *J Phys Conf Ser* 1367(1):012041. IOP Publishing
16. Tavana M, Shaabani A, Di Caprio D, Bonyani A (2021) An integrated group fuzzy best-worst method and combined compromise solution with Bonferroni functions for supplier selection in reverse supply chains. *Clean Logist Supply Chain* 2
17. Jariyah AA (2022) Analisis Strategi Prioritas Pemilihan Supplier Menggunakan Metode AHP (analytical hierarchy process) Studi Kasus Pt. Dari Timur Indonesia, PhD dissertation. Universitas Hasanuddin
18. Rizqika RP, Zuraidah E (2022) Sistem Penunjang Keputusan Pemilihan Supplier Terbaik Dengan Metode Analythical Hierarchy Process Pada PT. Konten Indomedia Pratama. *Resolusi Rekayasa Teknik Informatika dan Informasi* 2(4)
19. Djatna T (2020) Dynamic supplier selection strategy towards negotiation process in beef industry using K-means clustering. *IOP Conf Ser Earth Environ Sci* 443(1):012003. IOP Publishing
20. Lin G-H, Chuang C-A, Tan CL, Yeo SF, Wu F-Y (2023) Supplier selection criteria using analytical hierarchy process (AHP)-based approach: a study in refractory materials manufacturers. *Indus Manage Data Syst* 123(6)
21. Tsai P-H, Tang J-W, Chen C-J (2022) Partnerships that go places: how to successfully market products from vendor partners at retail stores from the vendors' perspective. *J Retail Consum Serv* 64
22. Yikici Ö, Özçelik TÖ (2023) Investment project selection with multi criteria decision making techniques in FMCG industry. *Int J Eng Manage Res* 13(3)
23. Zhong S, Singh SK, Goh M (2020) Efficient supplier selection: a way to better inventory control. *Optim Invent Manage*
24. Guarnieri P, Trojan F (2019) Decision making on supplier selection based on social, ethical, and environmental criteria: a study in the textile industry. *Resour Conserv Recycl* 141

The Compressive Strength and Failure Behaviours of the Alporas Foam—Effect of Different Geometric Sizes



A. N. Md Idriss, S. Kasolang, M. A. Maleque, and M. A. Mohd Azhari

Abstract An experimental work was conducted to determine the compressive strength and failure behaviours of Alporas aluminum foam with different thickness to width (t/w) ratio. The single plate at 40 mm × 40 mm × 12 mm, 30 mm × 30 mm × 12 mm and 20 mm × 20 mm × 12 mm giving the t/w of 0.3, 0.4 and 0.6 were compressed at the static load of 1 mm/min. Under the same testing condition the smallest single plate (20 mm × 20 mm × 12 mm) was compared with another largest combined of two pieces at 40 mm × 40 mm × 24 mm. The ductile property possessed by the structure was evident from the dominant of progressive deformation and crackings. Of all the single plates, the smallest 0.6 t/w one developed the highest specific compressive strength and specific plateau strength of 1.96 MPa/g and 1.55 MPa/g respectively. The lowest recorded specific compressive and plateau strengths were with the largest combined of 2 plates showing both at about 0.19 MPa/g. The specific compressive strength of the smallest single plate sample was 10 times higher than that the largest combined of two plates. The least contained structural defects with the smallest single plate sample size was explained to develop the highest strengths than other samples. The progressive failure averagely between 13 and 58 strain percentages responsible for plateau strength development evidence the Alporas is suitable candidate to be used for safety impact devices combating fatalities or injuries during collision.

Keywords Alporas · Sizes · Strength · Defects · Failure behaviour

A. N. M. Idriss (✉) · M. A. Maleque

Department of Manufacturing and Material Engineering, International Islamic University Malaysia, P.O. Box 10, 50728 Kuala Lumpur, Malaysia
e-mail: ahmednazrin@gmail.com

S. Kasolang

Faculty of Mechanical Engineering, Universiti Teknologi MARA, 40450 Shah Alam, Selangor, Malaysia

M. A. M. Azhari

Faculty of Manufacturing and Mechatronic Engineering Technology, Universiti Malaysia Pahang Al Sultan Abdullah, 26600 Pekan, Pahang, Malaysia

1 Introduction

The aluminum foams are made by expanding their metal volume by introducing distributed pores at various content, shapes and sizes. Generally, they can be classified as open, close or hybrid of which between the close and open structures. Because of the pores being incorporated the foams are several times lighter than that of the solid aluminum alloys [1, 2]. Fuel consumption is reduced to mobilize vehicle because of the reduced weight. Safety devices made of foam such as crash absorbers, crash box, mounting, laminated hood are ideal to progressively decelerate the shock impact and lower the risk of human injuries during collision [3–6]. Either they are reliable or fit to be used for such applications are assured mainly by the structural strengths. Using the static compression test, research showed that the strength of the aluminum foams were influenced by the porosity contents and their sizes [7], porosity shapes [8] type of used alloy or material [9, 10], relative density [11] sample shapes [12] and sample sizes [13].

Ultimate compressive strengths were between about 200 and 400 MPa for treated solid aluminum than open cell and close cell both up to 18 MPa [11, 14, 15]. Increasing the relative density of the aluminum foam, increases the compressive strength [11]. Adding boron carbide increases the compressive and plateau strengths of the foam [9]. The compressive strength of the cast A 356 aluminum foam alloy was about 4–5 times higher than the pure aluminum foam [10]. Plateau strengths were seen to prolong with increased of porosity content. Porosity affect the buckling behaviours [16] Point of defects were the reason for strength reduction and explained more with bigger than smaller sample sizes [7]. The low density regions, defects and weak link made failures to initiate and developed. Their large quantities were with high thickness to width ratio samples which brought strength to the lowest values [13]. In a work, square shaped aluminum foam experienced the highest compressive strength of 20 MPa than the cylinder and triangular shaped of only 12 MPa and 10 MPa respectively. This was followed by the plateau strength which was the greatest with the square shape than that of the cylinder and the least with the triangular [12]. AlSi12 foam developed greater compressive strength of 7.5 MPa than zinc foam at 5.2 MPa [17].

Size is an important parameter as it occupies spaces and increases weight when larger components are used. Our investigation found little information available in the literature of sizes affecting the strength and failure behaviours under the static load. No work was found to deter the compressive strength of alporas aluminum foam at sizes. This experimental work examines the compressive strength and failure behaviour of single plate Alporas between 0.6 and 0.3 thickness to width (t/w). The extracted result from the single plate at the t/w of 0.6 was compared with combined of two plates of the same 0.6 t/w . The t/w values were dimensions from 20 mm \times 20 mm \times 12 mm to 40 mm \times 40 mm \times 24 mm. The relative density, porosity content, strengths and failure behaviours of the used samples were reported.

Table 1 The thickness to width (t/w) ratio and weight of the samples

Number	Condition	Dimension (mm)	Thickness to width (t/w)	Weight (g)
1	Single	40 × 40 × 12	0.3	4.49
2	Single	30 × 30 × 12	0.4	2.77
3	Single	20 × 20 × 12	0.6	1.27
4	Stacked	40 × 40 × 24	0.6	7.82

2 Experimental Work

In this work the as received alporas aluminum foam with the thickness of 12 mm was cut to the dimensions of 20 mm × 20 mm, 30 mm × 30 mm and 40 mm × 40 mm using the Mach 100 flow waterjet machine. Later, the samples were cleaned under the running water to remove the trapped Garnett 80 abrasive particles followed by the drying process. The t/w ratio was calculated by dividing the thickness over the width distance while the weight was by weighing using digital weighing scale. Table 1 shows the calculated thickness to width ratio and weight values for all sample used in the experimental work.

The sample density, relative density and porosity content were calculated using several simple equations used in the previous works [18, 19]. The density of the Alporas was at 0.25 g/cm³. The relative density was at 0.093 while the porosity content was at 90.62%. The distances taken to measure the wall thickness is shown in Fig. 1 while Fig. 2 showed a distance took to measure the pore diameter. The DINO handheld microscope was used to measure the wall thickness and the diameter of the pore. The wall thickness was at 0.18 mm while the pore size was at 4.3 mm. AG-IS Shimadzu universal testing machine was used to compress each used sample at the speed of 1 mm/min until the occurrence of total failure. Trapezium—2 computer software attached to the testing machine was used to monitor and record the strength values. The specific compressive and plateau strengths were calculated strength values over the weight of the respective sample. An example of a compressed sample before and after the test is shown in Fig. 3. The failure morphology of a sample was determined using the JEOL-IT 100 scanning electron microscope. Figure 4 shows the simplified process flow to describe the process. No standard testing method was employed to conduct this experimental work. It was decisions made from discussions and literature reviews.

3 Result and Discussion

This experimental work used the Alporas foam that has been cut using the abrasive water jet cutting machine at different sizes. The compressive strength and plateau strength with their respective specific values of the tested single plate samples between 0.3 and 0.6 t/w were compared. Another experiment was conducted to

Fig. 1 Macrograph showing measured distance for a wall thickness

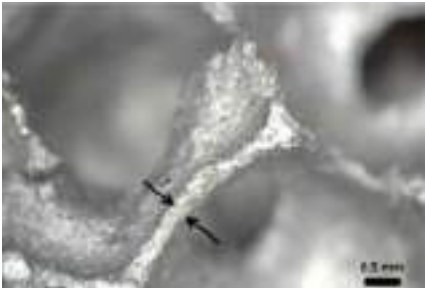


Fig. 2 Micrograph showing measured distance for a pore size

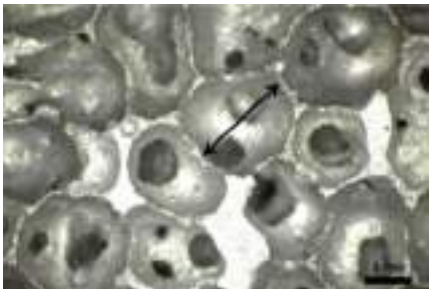


Fig. 3 The morphology of the top view with 20 mm × 20 mm × 12 mm (i) before and (ii) after the compression test

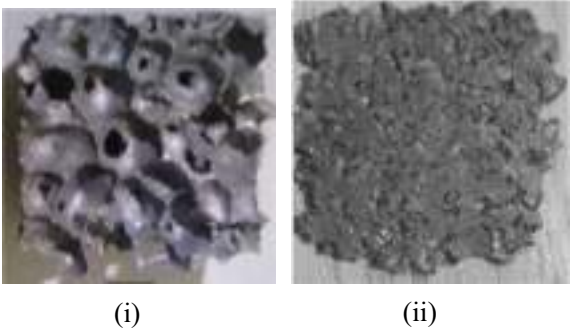


Fig. 4 The flow of the experimental work

compare the strengths of the single 20 mm × 20 mm × 12 mm sample against combined of two samples at 40 mm 40 mm × 24 mm both giving 0.6 t/w. During the experimental work all sample was visibly monitored to determine the fracture behavior while under compression. An image observed using scanning electron microscope was included to evident the fracture mode.

The compressive strength and specific compressive of the single plate alporas against t/w ratio from 0.3 to 0.6 was shown in Fig. 5. It is worth noting that the smallest 20 mm × 20 mm × 12 mm corresponded to 0.6 t/w while 30 mm × 30 mm × 12 mm and 40 mm × 40 mm × 12 mm sample were with 0.4 and 0.3 ratios respectively The figure showed the general trend of strength increment was associated with reduced of sample sizes from the single plate t/w ratio of 0.3 to 0.6. All sample failed because of their resistance against the impeded compression forces during testing evident from strength development at 1.59 MPa of 0.3 t/w ratio to 2.49 MPa with 0.6 t/w. The samples failed through deformations and crackings. The strain produced to develop the compressive strengths during this investigation was below than 13.23%. The specific compressive strength showed gradual increased from 0.36 MPa/g at 0.3 t/w ratio to 1.96 MPa/g of 0.6 t/w. Figure 6 showed the plateau strength and specific plateau strength values of the single plate Alporas from 0.3 to 0.6 of t/w ratio. The plateau and specific plateau strength development followed the same increment behaviour than their respective compressive strength (Figs. 5 and 6). The lowest plateau strength was with the single Alporas at 0.3 t/w ratio giving 1.42 MPa (Fig. 6). It roses to 2.05 MPa when the smallest at 0.6 t/w ratio used during the experimental work. With the specific plateau strength, the heaviest sample (0.3 t/w) suffered the lowest 0.89 MPa/g. The crushing stage gave the single Alporas to the moderate value of 1.08 MPa/g with 0.4 t/w. Following to this, the lightest sample with of 0.6 t/w showed the highest specific plateau of 1.55 MPa/g (Fig. 6).

The result from this investigation showed the single Alporas compressive and plateau strengths in relation to their specific values were influenced by the severally t/w ratios. The compressive strength for the 0.3 t/w was 1.6 times lower than the 0.6 as shown in Fig. 5. Remarkably, the specific compressive strength differences exaggerated to 5.53 times less with the 0.3 t/w ratio than the 0.6 t/w. Similar scenario was also seen on those plateau and specific plateau strengths as shown in Fig. 6. The

Fig. 5 Graph showing the alporas compressive and specific compressive strengths against t/w ratio from 0.3 to 0.6

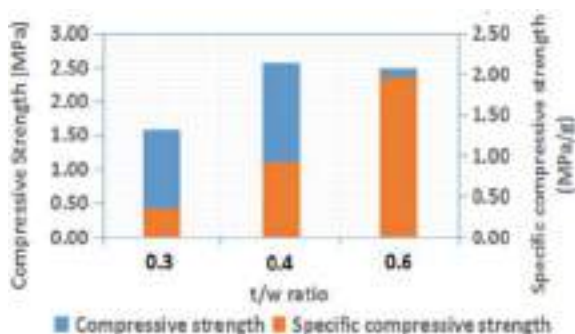
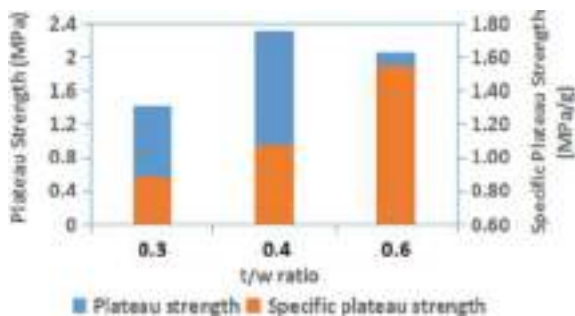


Fig. 6 Graph showing the alporas plateau and specific plateau strengths against t/w ratio from 0.3 to 0.6



plateau strength was 1.44 times lower when 0.3 t/w was compared with the 0.6 single t/w and worsened at 1.74 times of the specific plateau strength seeing increasing the size as dominance for the reduction of strength. Large samples are associated with more of defect points such as poor wall or struts interconnectivity, inclusions, very low density regions and crackings which lead to the poor development of strength [7, 13]. This is why in this work, the largest sample at 0.3 t/w had reasonably lowest strengths values compared to the others. Points of defect made the structure less possible to retain high strength as they are the best spot which favours failure to initiate and progresses. It suggests that the load carrying capacity of the foam reduces as the sample sizes were increased. As a result, the smallest and lightest sample at 0.6 t/w ratio prevailed the strongest of all.

To verify the results an experimental work using combined of two samples each at 40 mm × 40 mm × 12 mm were stacked and tested at the compression speed of 1 mm/min. No adhesive was used to join the two mating surfaces forming a single structure of 24 mm thick. Because of the greater width and thickness, this gave similar 0.6 t/w to that of the single 20 mm × 20 mm × 12 mm. Just like all single plate samples, the largest one failed exquisitely via deformation associated with crackings. The compressive strengths and plateau strengths with their respective specific values of both 0.6 t/w were compared and presented in Figs. 7 and 8.

Fig. 7 Graph showing the compressive and specific compressive strengths of two alporas sizes each at 0.6 t/w

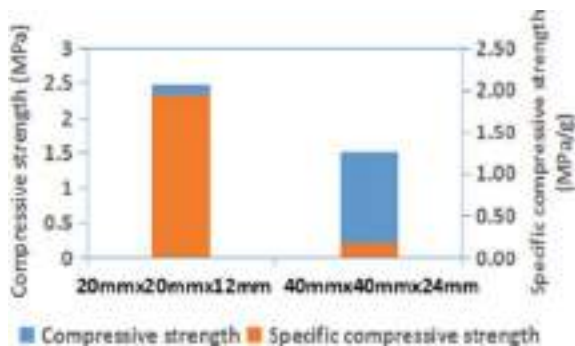
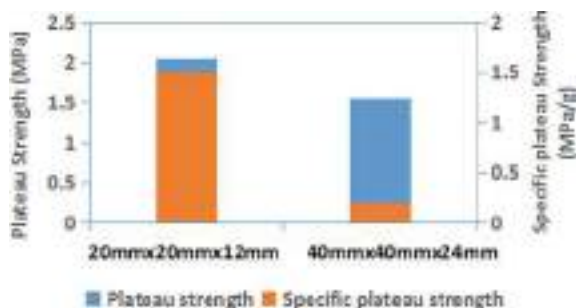


Fig. 8 Graph showing the plateau and specific plateau strengths of two alporas sizes each at 0.6 t/w



The compressive strength of the 40 mm × 40 mm × 24 mm was at 1.51 MPa. Remarkably, the specific compressive strength was far below at 0.19 MPa/g. The 20 mm × 20 mm × 12 mm had greater compressive and specific compressive strengths at 2.49 MPa and 1.96 MPa/g. In Fig. 8, the plateau values of the 40 mm × 40 mm × 24 mm thick was seen lower than the 20 mm × 20 mm × 12 mm thick. At 11 times bigger with the combined of two sample, the compressive strength and specific compressive strength were 1.65 and 10 times lower than that of the single plate as shown in Fig. 7. Further, the reduction of the compressive strengths trend in Fig. 7 were similar with the plateau values as in Fig. 8. With the single plates, the strength reduction was caused by defects such as poor strut interconnection, inclusions, low density regions and crackings. Since the 24 mm thick was the biggest, it can be said that this sample possessed the most populated of the explained defects which had imminently brought the recorded strength to the lowest compared to the others. Another possible reason for strength reduction was the disconnected struts at the mating surfaces. Because no adhesive was used to join for a sturdy structure, their existence was thought as additional points of defect with the combined of two samples. Apparently this character was absent with those the single plates. These disconnected struts do not provide support to raise the strengths. Rather, became failure to easily occur spanned across the surface as compaction load rises. Nevertheless, these were the defects that lead to the lowest load carrying capacity either for the single or combined of two samples. That the combined of two sample was considered having the most ductile structure because of the strain percentage gradually climbed to 29% to reach only 1.51 MPa than other single plate samples below than 13% strain to the maximum strength. While this explained the reason for strength development, The sample or cell sizes, alloying content, phases, testing conditions, porosity content, density, material types affect the strength values. The above result showed that the compressive and plateau strengths corresponding to their specific values by can be tailored by selective sizes adhering to any impact strength applications.

Figure 9 shows the single (20 mm × 20 mm × 12 mm) and combined of two (40 mm × 40 mm × 24mm) percentages of thickness reduction. These were the differences measured before and after the compression test. Figure 10 shows a severe cracked surface notified on a strut. Failure exerted by the testing machine reduced the thicknesses which initially were at 12 mm and 24 mm to 1.2 mm and 3.1 mm

resulting 90% and 87% reduction respectively. Because of the size was small at 20 mm × 20 mm × 12 mm, the lesser metal volume possessed by this sample was low in resistant towards the impediment force by the machine upon densification. It has lead to the easiness of the walls or struts to deform and crack leading the structure to be highly compacted. This is why the single sample retained 90% thickness reduction compared to the larger one of 3% lower at 87%. More metal volume with the larger one (40 mm × 40 mm × 24 mm) appeared to make deformation slightly difficult for failures. Since the combined of two pieces do not use adhesive to mate the two surfaces for a structure, the struts failure was thought through protrusion and crossed against the opposing piece. This explains for the close thickness reduction to 87% than at 90%. It is worth to note that applying more compaction forces would raise the 87% thickness equal to that of 90% possessed by the single sample. Though the combined of two sample had the lowest strengths of all (Figs. 4, 5, 6 and 7), this specimen took the time to progressively crush at 20.9 min while the single thinner 12 mm sample at 10.8 min. Figure 10 showed a severe cracked surface notified on a strut consisting many dimples that evidence ductile failure took place during compaction. Of course with high strength and prolong failure time are two characters beneficial for hampering severe impact. Hampering impact is considered negligible when all pores collapsed with excessive struts deformation.

Fig. 9 The thickness of 0.6 t/w samples before and after the test

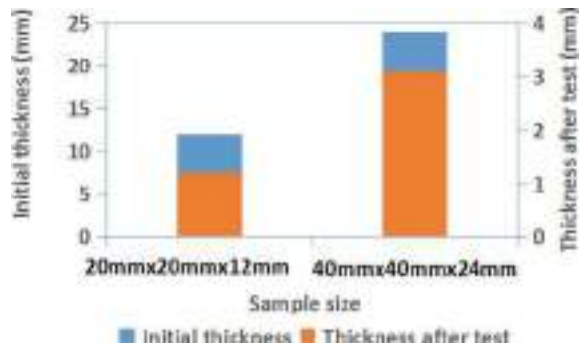
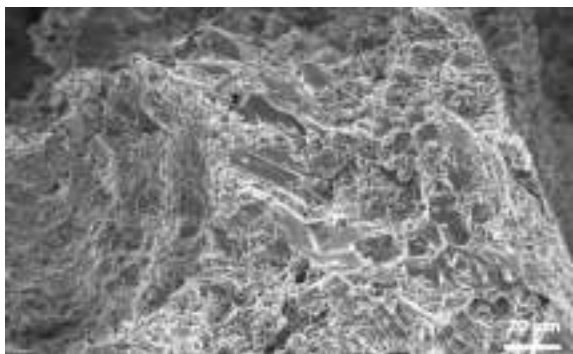


Fig. 10 A crack surface consisting of many dimples on a strut indicating ductile fracture



4 Conclusion

The experimental work to determine the compressive strength and the failure behaviours of the produced sample between the 0.3 and 0.6 t/w ratios were successfully conducted. Failure was through extreme deformation associated with cracking. The single piece of 20 mm × 20 mm × 12 mm sample size gives the specific compressive strength of 1.96 MPa/g, while the largest combined of two at 40 mm × 40 mm × 24 mm shows 0.19 MPa/g. At 11 times bigger, coexistence of the highest structural defect and the disconnected struts at the mating surface are poor to transmit load during compaction giving the lowest strength. The 40 mm × 40 mm × 24 mm sample receives 87% thickness reduction while the 20 mm × 20 mm × 12 mm has a modest higher of 90% both of the same 0.6 t/w. Less thickness reduction is associated with the high amount of pillar struts of the large sample which is beneficial to resist the forcing load. Extreme deformation is inevitable when little struts available with the small sample. The produced strength from 1.42 MPa to 2.49 MPa and from 1.55 MPa/g to 0.19 MPa/g shows that the strength can be tailored by selective sample sizes.

Acknowledgements The authors would like to thank to Ibrahim Razali@Maarof from the Department of Manufacturing and Materials Engineering, International Islamic University of Malaysia, Abdul Halim Saad from the Pusat Pengajian Kejuruteraan Mekanikal, UiTM Permatang Pauh, Penang and Arzuan Kasim from the College of Engineering, UiTM Shah Alam, Selangor for their relentless experimental assistance toward the completion of the work.

References

1. Parveez B, Jamal NA, Maleque MA, Yusof F, Jamadon NH, Adzila S (2021) Review on advances in porous Al composites and the possible way forward. *J Market Res* 15:2017–2038
2. Md Idriss AN, Kasolang S (2022) The dry sliding wear behaviour of open cell aluminum foam against mild steel. *IOP Conf Ser Mater Sci Eng* 1244(1):012009
3. Banhart J (1999) Foam metal—the recipe. *Europhysics News*. January/February
4. Banhart J (2007) Metal foam—from fundamental research to application. *Front Des Mater* 279
5. CYMAT. <http://www.cymat.com/>. Accessed 19 Apr 2020
6. Duocel. <http://www.ergaerospace.com/index.html>. Accessed 19 Apr 2020
7. Koza E, Leonowicz M, Wojciechowski S, Simancik F (2003) Compressive strength of aluminum foam. *Mater Lett* 58:132–135
8. Gaillard C, Despois JF, Mortensen A (2004) Processing of NaCl powder of controlled size and shape for the microstructural tailoring of aluminum foam. *Mater Sci Eng A* 374(1–2):250–262
9. Sunar T, Cetin M (2018) An experimental study on boron carbide reinforced open cell aluminum foam produced via infiltration technique. *Eng Technol Appl Sci Res* 8(6):3640–3645
10. Fadhil HA, Laftah RM, Abdulwahab QT (2024) Mechanical characteristic and energy absorption behaviour of closed-cell and A356 alloyed aluminum foams during compression. *Basrah J Eng Sci* 24(1):1–11
11. Zhao YY, Sun DX (2001) A novel sintering dissolution process for manufacturing Al foams. *Scripta Mater* 44:105–110
12. Kováčik J, Jerz J, Gopinathan A, Šimančík F, Marsavina L (2023) Effect of sample shape on compression behaviour of aluminum foam. *Mater Today Proc* 78:308–313

13. Xia X, Zhao W, Wei Z, Wang Z (2012) Effects of specimen aspect ratio on the compressive properties of MG alloy foam. *Mater Des* 42:32–36
14. Adesola AO, Odeshi AG, Lanke UD (2013) The effect of aging treatment and strain rates on damage evolution in AA 6061 aluminum alloy in compression. *Mater Des* 45:212–221
15. Castro G, Nutt SR, Wenchen X (2013) Compressive and low velocity impact behaviour of aluminum syntactic foam. *Mater Sci Eng A* 578:222–229
16. Yang CC, Nakae H (2000) Foam structure effect on the compression behaviour of foamed aluminum alloy. *ISIJ Int* 40(12):1283–1286
17. Kováčik J, Šimančík F (2004) Comparison of zinc and aluminum foam behaviour. *Kovové Materiály* 42:79–90
18. Md Idriss AN, Kasolang S (2022) The permeability of palm oil through open cell aluminum foam under the influence of gravity. In: *The Proceeding of the 3rd Malaysian international tribology conference. Lecture notes in mechanical engineering*, pp 220–229. Springer (2022)
19. Azizan MA, Ismail MH, Mohd Salleh NA, Natarajan DV (2017) Sound absorption properties at high sound frequency of open cell aluminum foam. *J Mech Eng SI* 2(1):161–173

Autonomous Mobile Robot for Obstacle Avoidance with Vision System



Yoganraj Ravi, Mohd Rais Hakim Bin Ramlee,
and Ismail Mohd Khairuddin 

Abstract Autonomous mobile robots are designed to navigate independently without human intervention. As the demand for these robots increases, new techniques and algorithms are continuously being developed. However, the use of ultrasonic sensors in vision-based obstacle avoidance systems has limitations. One significant disadvantage is their limited range compared to other sensor types, making it difficult to detect objects at longer distances or from wider angles, which may result in blind spots. Additionally, environmental conditions influence item identification accuracy because soft or absorbent surfaces can absorb ultrasonic waves. When many ultrasonic sensors operate simultaneously, there is a possibility of crosstalk or interference, which can result in inaccurate distance readings and obstacle detection. This research aims to develop an autonomous mobile robot capable of avoiding collisions using vision-based methods. The methodology includes capturing approximately 1609 images with a mobile robot-mounted camera, processing these images with the You Only Look Once (YOLO) algorithm for object detection, and converting the results into steering commands. Techniques such as labeling and data augmentation, including flipping and adjusting the brightness, were employed to enhance the dataset. The data was divided into training, validation, and testing sets with a 70:20:10 ratio split for classification. The integration of the YOLO algorithm achieved a detection success rate of approximately 93.3%. This study provides insights into the effectiveness of combining deep learning methods for real-time obstacle avoidance in mobile robotics, highlighting the importance of carefully considering the individual application and environment when selecting sensors for vision-based techniques.

Keywords Vision-based techniques · Deep learning · YOLO · Object detection · Autonomous mobile robot

Y. Ravi · M. R. H. B. Ramlee · I. M. Khairuddin (✉)

Faculty of Manufacturing and Mechatronic Engineering Technology, Universiti Malaysia Pahang
Al-Sultan Abdullah, 26600 Pekan, Pahang, Malaysia

e-mail: ismailkhair@ump.edu.my

1 Introduction

Robots have become essential in everyday life, helping with tasks like rescue operations, cleaning, medical assistance, military support, hazardous work, and autonomous driving. A robot is an automated machine designed to perform tasks usually done by humans or to accomplish tasks beyond human capabilities. They range from simple, single-purpose devices to complex systems with advanced sensory, cognitive, and motor functions. Many tasks require robots to navigate unknown environments and avoid collisions with stationary or moving obstacles.

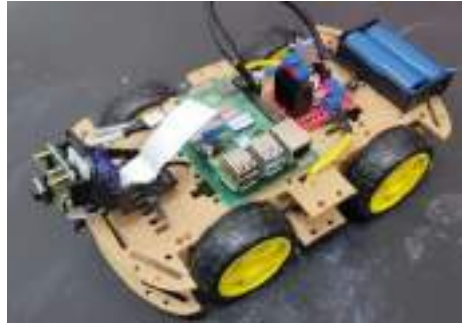
Autonomous mobile robots are designed to manoeuvre independently without human intervention. With the rising demand for these robots, new techniques and algorithms are continually being developed. A recent study revealed that the primary concern for most developers is ensuring the robot navigates without collisions [1–3]. To monitor the surrounding environment and guide the robot, various sensors can be mounted on it. However, the reliability and efficiency of these robots are affected by several factors. Integrating sensor fusion systems, which combine data from multiple sensors like cameras, can address these challenges by providing more comprehensive and reliable information.

Vision techniques used in autonomous mobile robots encompass various methods for visually sensing and processing their surroundings. Cameras, for instance, capture images of the environment, which are then analysed to detect obstacles that the robot needs to avoid. Convolutional neural networks (CNNs) are trained using these images to classify the environment ahead as either “blocked” or “free” in specific instances. This classification helps the robot decide how to navigate and avoid obstacles. The effectiveness of the CNN-based obstacle classifier depends on the quality and diversity of the training data, as well as the architecture of the CNN itself [4–7].

Obstacle avoidance is a crucial aspect of autonomous navigation for mobile robots. Various technologies, such as sonars, infrared sensors, laser scanners, and cameras, have been developed to address this challenge. Sonar devices are cost-effective for obstacle detection but are prone to errors due to reflections. Laser scanners offer high accuracy but face difficulties in unfamiliar environments. Cameras, however, provide detailed scene information, making them a favoured choice for vision-based navigation [8–10].

In developing an autonomous mobile robot that can navigate without colliding, it is essential to consider the limitations ultrasonic sensors, which may have restricted detection ranges and be affected by environmental factors like soft surfaces or interference. A vision-based system for obstacle avoidance, involves using camera images to enhance the autonomous navigation capabilities of robots and UAVs. These systems rely on Convolutional Neural Networks (CNNs) for depth estimation and obstacle detection, which allows for real-time processing and decision-making. For example, in mobile robots, techniques like potential fields and Image-Based Visual Servoing (IBVS) are employed to approach targets while avoiding obstacles. Similarly, for UAVs, monocular cameras are used to ensure safety during flight by estimating depth and implementing obstacle avoidance algorithms [11–14].

Fig. 1 Robot framework with component



To address these challenges, this project aims to create an autonomous mobile robot capable of manoeuvring independently using vision-based techniques. The objectives include designing the robot to operate in environments without collisions, developing a vision algorithm for object detection, and evaluating the effectiveness of this algorithm in guiding the robot's navigation. By integrating these elements, the project seeks to enhance the robot's reliability and efficiency in avoiding obstacles and navigating complex environments [15–17].

2 Methodology

2.1 Development of Mobile Robot

To properly fit these components inside the robot's architecture, this thorough integration procedure demands careful design and structural planning. The Raspberry Pi 4 Model B serves as the robot's basic controller, managing its functions, while the Raspberry Pi Camera Module 3 provides visual perception and detection of objects. The L298 Motor Driver makes it easier to control and operate the motors, which are essential for the robot's mobility, while the Li-Ion battery provides the necessary to power the system. Figure 1 shows the integration of the hardware components on the mobile robot.

2.2 Data Acquisition

Data acquisition is the process of capturing images or video from various sources. This is the initial step in any vision algorithm, where raw visual data is collected for further processing. The camera continuously captures images of obstacles within the lab environment which will be analyzed in subsequent steps of the vision algorithm. Realtime images can be captured through the camera and processed directly through

deep learning system. Three scenarios of dataset were taken from the IMAMS lab environment, resulting in a total of 1609 images. Each image has a file size of approximately 1400 KB, leading to a cumulative dataset size of 1,376,200 KB, or roughly 1.376 GB.

The dataset was split into training, validation, and testing sets. Specifically, the first dataset of 75 images was divided with 70% for training, 20% for validation, and 10% for testing. The second dataset of 551 images and the third dataset of 983 images followed the same split ratio: 70% for training, 20% for validation, and 10% for testing. This structured division ensured a comprehensive evaluation of the model's performance.

2.3 Data Pre-processing

Data pre-processing involves cleaning, transforming, and preparing the raw data to ensure it is suitable for analysis and model building. In computer vision tasks, this includes image labelling and augmentation. For labelling, the Roboflow software was utilized to annotate the images with bounding boxes around the detected objects. This step was crucial for training the YOLOv8 models.

2.4 Data Labelling and Augmentation

A tool for labelling images is employed to mark the images within the gathered dataset. As implied, this labelling tool is utilized to identify object within the images. Its core objective is to enable users to pinpoint or capture an object depicted in the image. The labelling of datasets for all three YOLOv8 models are carried out using Roboflow software. Figure 2 indicates the labels include bounding boxes around objects, which become visible during model testing. Subsequently, these files are stored in the assigned directory within the software.

2.5 Model Configurations

Model training for YOLOv8 involves teaching the model to recognize objects in images by feeding it a pre-processed dataset and allowing it to learn patterns over multiple iterations. Using Google Colab with free GPU resources, the process includes loading a pre-trained YOLOv8 model, setting hyperparameters like learning rate, batch size, and number of epochs, and running a training loop where the model processes images, makes predictions, and adjusts based on errors.

Model 1 was trained for 100 epochs, Model 2 for 300 epochs, and Model 3 for 100 epochs, with a batch size of 16. Images were resized to 320×320 pixels, and the



Fig. 2 Image labelling

learning rate was set to ensure effective learning. A patience parameter of 50 epochs was used, meaning training would stop if no improvement was seen after 50 epochs.

Both YOLOv8s (small) and YOLOv8n (accuracy version) models were used to balance speed and accuracy. The YOLOv8s model is optimized for fast inference with fewer layers and smaller filters, while the YOLOv8n model, with deeper networks and larger filters, prioritizes accuracy at the cost of slightly slower inference times.

2.6 Performance Measure

Precision measures the accuracy of the positive predictions made by a model, defined as the ratio of correctly predicted positive observations (true positives) to the total predicted positives (true positives plus false positives).

$$Precision = \frac{True\ Positives(TP)}{True\ Positives(TP) + False\ Positives(FP)} \quad (1)$$

Recall measures a model's ability to correctly identify all actual positive instances. Recall indicates how many of the actual obstacles are detected by the model.

$$Recall = \frac{True\ Positives(TP)}{True\ Positives(TP) + False\ Negatives(FN)} \quad (2)$$

The F1 score is a metric that combines precision and recall into a single value to provide a balance between the two. It is particularly useful when the class distribution is imbalanced, and both false positives and false negatives are important to consider.

$$F1\ Score = 2 \times \frac{(Precision \times Recall)}{(Precision + Recall)} \quad (3)$$

3 Result and Discussions

3.1 Performance Metrics

Figure 3 shows the evaluation metrics for all three models. The first model achieves a precision of 0.865, indicating that when it predicts an object, it is correct 86.5% of the time. In comparison, the second model exhibits a slightly lower precision of 0.840, suggesting it accurately identifies objects 84.0% of the time. Conversely, the third model demonstrates the highest precision among the three, achieving a precision score of 0.906, meaning it correctly predicts objects with an accuracy of 90.6%.

The first model achieves a recall of 0.865, indicating that it correctly identifies 86.5% of all relevant objects in the dataset. In contrast, the second model demonstrates a higher recall of 0.918, suggesting it captures a larger proportion of relevant objects compared to the first model. Similarly, the third model also shows a high recall of 0.915, indicating it performs similarly to the second model in correctly identifying relevant objects. A higher recall is important as it ensures that fewer relevant objects are missed during detection, highlighting the effectiveness of these models in capturing objects across various scenarios in image data.

The confusion matrices for all three models are displayed as Fig. 4. The first model has a mAP50 score of 0.859, indicating 85.9% precision at this IoU threshold. The second model improves with a mAP50 of 0.887, and the third model performs best with a mAP50 of 0.933, indicating the highest precision in object detection. For mAP50-95, the first model scores 0.468, the second 0.577, and the third 0.656, showing that the third model excels across a broader range of IoU thresholds.

Regarding the F1-score, the first model achieves 0.840, the second 0.880, and the third 0.915, demonstrating the best balance between precision and recall in the third



Fig. 3 Evaluation metrics

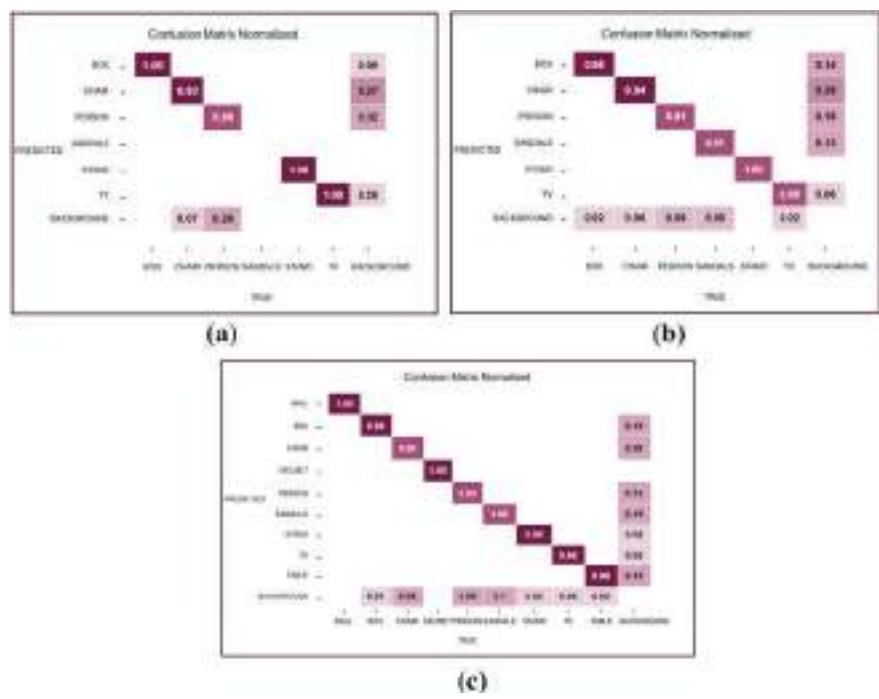


Fig. 4 Normalized confusion matrix: **a** first model, **b** second model, **c** third model

model. The normalized confusion matrix simplifies comparisons across classes, with diagonal values representing true positives and off-diagonal values showing false positives and negatives. The third model consistently outperforms the others in these metrics, making it the most reliable for object detection.

3.2 Detection Result

The third model in the Fig. 5 demonstrated its effectiveness when integrated with an autonomous mobile robot for obstacle avoidance. Initially, the robot moves forward, and upon detecting an obstacle, it stops for two seconds before turning in the appropriate direction based on center-based detection. If the obstacle is detected on the left (x-coordinate of the obstacle center is less than 320), the robot turns right by adjusting the motor directions; if on the right, it turns left. After turning for one second, the robot resumes moving forward. This implementation showcases the third model’s high accuracy and effective performance in real-world applications, significantly enhancing the autonomous robot’s obstacle avoidance capabilities. By leveraging the YOLOv8n architecture and achieving the highest accuracy of 93.3%, the



Fig. 5 Obstacles detected by mobile robot: **a** lab environment objects, **b** ball, **c** stand, **d** helmet

third model outperformed the others, demonstrating superior detection and decision-making in dynamic environments. Figures below demonstrate the obstacles that have been detected by the mobile robot.

4 Conclusions

The project focused on creating an autonomous mobile robot capable of navigating and interacting in its environment. Key to its functionality was a sophisticated vision algorithm based on the YOLO deep learning model, achieving an accuracy rate of 93.3%. This algorithm enabled precise detection of various objects in real-time scenarios, allowing the robot to autonomously maneuver and avoid obstacles. The successful integration demonstrated the algorithm’s robustness and practical utility in real-world applications.

Enhancing the object detection accuracy of the YOLO-based vision algorithm beyond its current 93.3% involves several strategic approaches. Fine-tuning model parameters such as layer configurations, filter sizes, and learning rates allows for precise adjustments based on performance metrics, thereby optimizing the model's ability to detect and classify objects accurately across diverse environments. Exploring different YOLO architectures, offers insights into balancing accuracy, speed, and computational efficiency, crucial for tailoring the model to specific application needs.

Acknowledgements The authors extend their sincere appreciation to the Faculty of Manufacturing and Mechatronic Engineering Technology at Universiti Malaysia Pahang Al-Sultan Abdullah for their generous support, facilities, and opportunities provided throughout this project.

References

1. Gaya JO, Goncalves LT, Duarte AC, Zanchetta B, Drews P, Botelho SSC (2016) Vision-based obstacle avoidance using deep learning. In: 2016 Xiii Latin American robotics symposium and IV Brazilian robotics symposium (Lars/Sbr). <https://doi.org/10.1109/Lars-Sbr.2016.9>
2. Tan H, Qin L, Jiang Z, Wu Y, Ran B (2018) A hybrid deep learning based traffic flow prediction method and its understanding. *Transp Res Part C Emerg Technol* 90(January):166–180. <https://doi.org/10.1016/j.trc.2018.03.001>
3. Dang T-V, Bui N-T (2023) Obstacle avoidance strategy for mobile robot based on monocular camera. *Electronics* 12(8):1932. <https://doi.org/10.3390/Electronics12081932>
4. Chuixin C, Hanxiang C (2019) AGV robot based on computer vision and deep learning. In: 2019 3rd international conference on robotics and automation sciences (ICRAS). <https://doi.org/10.1109/Icras.2019.8808970>
5. Dai X, Mao Y, Huang T, Qin N, Huang D, Li Y (2020) Automatic obstacle avoidance of quadrotor UAV Via CNN-based learning. *Neurocomputing* 402:346–358. <https://doi.org/10.1016/J.Neucom.2020.04.020>
6. Sleaman WK, Hameed AA, Jamil A (2023) Monocular vision with deep neural networks for autonomous mobile robots navigation. *Optik* 272:170162. <https://doi.org/10.1016/J.Ijleo.2022.170162>
7. Pinzon-Arenas JO, Jimenez-Moreno R (2020) Obstacle detection using faster R-CNN oriented to an autonomous feeding assistance system. In: 2020 3rd international conference on information and computer technologies (ICICT). <https://doi.org/10.1109/Icict50521.2020.00029>
8. Khatab E, Onsy A, Varley M, Abouelfarag A (2021) Vulnerable objects detection for autonomous driving: a review. *Integration* 78:36–48. <https://doi.org/10.1016/J.Vlsi.2021.01.002>
9. Liu C, Zheng B, Wang C, Zhao Y, Fu S, Li H (2017) CNN-based vision model for obstacle avoidance of mobile robot. *Matec Web Conf* 139:00007. <https://doi.org/10.1051/Mateconf/201713900007>
10. Ma L, Xie W, Huang H (2020) Convolutional neural network based obstacle detection for unmanned surface vehicle. *Math Biosci Eng* 17(1):845–861. <https://doi.org/10.3934/Mbe.2020045>
11. Ran T, Yuan L, Zhang JB (2021) Scene perception based visual navigation of mobile robot in indoor environment. *ISA Trans* 109:389–400. <https://doi.org/10.1016/J.Isatra.2020.10.023>

12. Rocchi A, Wang Z, Pan Y-J (2023) A practical vision-aided multi-robot autonomous navigation using convolutional neural network. In: 2023 IEEE 6th international conference on industrial cyber-physical systems (ICPS). <https://doi.org/10.1109/Icps58381.2023.10128041>
13. Sinha H, Patrikar J, Dhekane EG, Pandey G, Kothari M (2018) Convolutional neural network-based sensors for mobile robot relocalization. In: 2018 23rd international conference on methods & models in automation & robotics (MMAR). <https://doi.org/10.1109/Mmar.2018.8485921>
14. Szegedy C, Liu W, Jia Y, Sermanet P, Reed S, Anguelov D, Erhan D, Vanhoucke V, Rabinovich A (2015) Going deeper with convolutions. In: 2015 IEEE conference on computer vision and pattern recognition (CVPR). <https://doi.org/10.1109/Cvpr.2015.7298594>
15. Takashima Y, Watanabe K, Nagai I (2019) Target approach for an autonomous mobile robot using camera images and its behavioral acquisition for avoiding an obstacle. In: 2019 IEEE international conference on mechatronics and automation (ICMA). <https://doi.org/10.1109/Icma.2019.8816199>
16. Zhang Z, Xiong M, Xiong H (2019). Monocular depth estimation for UAV obstacle avoidance. In: 2019 4th international conference on cloud computing and internet of things (CCIOT). <https://doi.org/10.1109/Cciot48581.2019.8980350>
17. Khan M, Parker G (2019) Vision based indoor obstacle avoidance using a deep convolutional neural network. In: Proceedings of the 11th international joint conference on computational intelligence. <https://doi.org/10.5220/0008165104030411>

Knowledge Management for Developing Disability-Friendly Criteria in SME



Luciana Andrawina , Mia Amelia , and Artamevia Salsabila Rizaldi

Abstract Developing Small and Medium Enterprises (SME) in Indonesia plays an essential role in the national economy by creating jobs, increasing Gross Domestic Product (GDP) growth, and promoting export development. However, certain groups, such as people with disabilities, face challenges in accessing the benefits of the sector, such as job opportunities, skills training, and access to adequate facilities. This study aims to develop disability-friendly criteria for SME by implementing Knowledge Management (KM) using the SECI (Socialization, Externalization, Combination, Internalization) model. The resource persons involved three SME. Data were collected through in-depth interviews and direct observation. The findings highlight several key challenges, including inadequate facilities, limited access to relevant training programs, and lingering social stigma. Solutions are identified and documented in a structured manner, and practical strategies are developed to address these issues. The study concludes that integrating KM and the SECI model significantly improves inclusivity and support in the business environment for people with disabilities. This research provides comprehensive insights and practical recommendations for SME policymakers and practitioners to create a more inclusive and supportive ecosystem for individuals with disabilities.

Keywords Difable · Small and medium enterprise · Knowledge management

1 Introduction

The development of Small and Medium Enterprises (SME) in Indonesia is significant for the country's economy, and SME have been recognized as the backbone of the national economy [1]. SME are essential in job creation, Gross Domestic Product (GDP) growth, and export development [2]. Although SME are very important for

L. Andrawina (✉) · M. Amelia · A. S. Rizaldi
Department of Industrial Engineering, Telkom University, Bandung 40257, Indonesia
e-mail: luciana@telkomuniversity.ac.id

© The Author(s), under exclusive license to Springer Nature Singapore Pte Ltd. 2025
M. R. Mohamad Yasin et al. (eds.), *Proceedings of the 7th Asia Pacific Conference on Manufacturing Systems and 6th International Manufacturing Engineering Conference—Volume 2*, Lecture Notes in Mechanical Engineering,
https://doi.org/10.1007/978-981-96-5690-5_19

191

people with disabilities, it is difficult to face challenges in accessing the benefits of this sector, such as job opportunities, skills training, and access to adequate facilities. To address the gap in employment opportunities, skills training, and adequate facilities in the SME sector, the concept of disability-friendly SME emerged to ensure active participation and equality of benefits for persons with disabilities in the SME ecosystem. Several studies highlight relevant issues related to people with disabilities. Among them research by Martoyo et al. [3]. Discuss the government's efforts to provide job opportunities for people with disabilities by involving corporations and the government. In addition, research by Negara [4] The study highlights that although people with disabilities have equal rights, they often face discrimination that hinders their independence. To meet the needs of life and achieve independence, they are encouraged to work and improve their social skills. However, due to the limited availability of jobs, many choose to pursue a career in the business sector that suits their abilities.

To meet the living needs and independence of people with disabilities, disability-inclusive business development requires a holistic approach, from physical accessibility to supportive policies. In Indonesia, the disability-friendly SME strategy includes improving physical and technological accessibility to make businesses accessible to all, including people with disabilities [5]. Second, training and empowerment for persons with disabilities are needed to provide the necessary skills and knowledge to manage their businesses [6]. Third, policy support from the government is critical in creating an environment conducive to inclusive business development [7]. Finally, changes in the attitude of the community and business actors towards people with disabilities are also a crucial factor in ensuring sustainability and inclusive business success [8]. In addition, implementing SME social responsibility can also be an effective alternative in supporting the development of micro-businesses, including disability-friendly businesses [9]. This shows that collaboration between the private and public sectors can be essential in creating an inclusive business environment. In addition, inclusive education also plays a vital role in ensuring that all individuals, including people with disabilities, have equal access to education and training opportunities [10].

In Indonesia, the participation of persons with disabilities in SME encourages social inclusion and provides broader economic opportunities. The Ministry of Cooperatives and SME has introduced several policies to support inclusive SME development. However, the effective implementation of these policies faces various challenges. These obstacles include inadequate facilities, limited access to relevant training programs, and social stigma that is still inherent in people with disabilities [11–13]. In addressing these challenges and increasing the participation of persons with disabilities in SME, it is essential to combat stigma and encourage inclusive practices. Research emphasizes the importance of creating a disability-friendly workplace by providing facilities such as necessary training and support and changing people's attitudes toward individuals with disabilities [14, 15]. By creating a more inclusive environment and offering tailored support, SME can harness the potential of individuals with disabilities, leading to increased social integration and economic empowerment [13].

As a strategic step to create a more inclusive environment for SME, implementing Knowledge Management (KM) is crucial. Knowledge Management helps SME define, shape, organize, and disseminate knowledge to work more efficiently, use best practices, and minimize costs [16]. Knowledge Management is the management of knowledge in an organized manner to create business value and generate competitive profits [17, 18].

In this study, Knowledge Management (KM) plays a vital role in expanding understanding and increasing the use of concrete approaches in knowledge management related to developing criteria for disability-friendly facilities in SME [19, 20]. The main focus of the research is on information management and documentation, where SME collect, store, and access information related to the specific needs of persons with disabilities, such as relevant accessibility regulations and standards [21]. This research aims to develop disability-friendly criteria for SME in Indonesia by implementing Knowledge Management (KM) using the SECI (Socialization, Externalization, Combination, Internalization) model.

Various studies have used knowledge management methods to develop inclusive criteria in SMEs and other sectors. Some researchers applied the SECI model to manage and transform tacit knowledge into explicit knowledge to support inclusive business policies. For example, Apriliadi (2019) in Bandung found that knowledge management significantly improved SMEs' performance in the aspects of finance, internal processes, and customer satisfaction [22]. Similarly, Hamdani (2018) used the SECI model to improve the competitiveness of batik SMEs by transforming tacit knowledge into explicit knowledge, highlighting the importance of technology and entrepreneurial orientation in knowledge creation [23]. Kusnindar et al. (2023) further explored how the SECI model facilitates the conversion of tacit knowledge into explicit knowledge through formal and informal interactions in SMEs [24]. Research by Nurhaeni et al. (2024) in similar cases uses qualitative methods with a descriptive approach to analyze penta helix collaboration in the development of social inclusion for people with disabilities in Surakarta. Data was collected through observation, Focus Group Discussion (FGD), and in-depth interviews with the five elements of the penta helix. This method is relevant as it highlights the importance of cross-sector collaboration and stakeholder engagement in creating an inclusive environment, which is similar to the context of this research in developing disability-friendly criteria through a knowledge management approach [25].

This research approach uses case studies on several SME that have applied the principle of inclusiveness, with the SECI (Socialization, Externalization, Combination, Internalization) method, developed by Nonaka and Takeuchi (1995) [26], providing a valuable framework for developing criteria for disability-friendly facilities in SME. This model facilitates the conversion of tacit knowledge into explicit knowledge, allowing for systematic utilization in policymaking and business practices [27]. The SECI model is a structured approach that will assist SME in developing criteria for disability-friendly facilities, encouraging inclusivity and sustainable practices. This study fills the gap in implementing Knowledge Management (KM) in developing disability-friendly criteria in SME, which previously only focused on technical or policy aspects without thorough integration. The novelty of this research

lies in using the SECI model to systematically capture, document, integrate, and internalize knowledge, as well as incorporate technical aspects, training, facility design, and technology integration.

2 Methodology

2.1 Research Design

This study uses the SECI model (Socialization, Externalization, Combination, Internalization) to develop criteria for disability-friendly facilities in SME, focusing on three case study objects, namely, Cemara Paper, Batik Laweyan, and Difabelzone. The SECI model provides a structured approach to managing and converting *tacit* knowledge into explicit knowledge, which is essential for creating inclusive and sustainable business practices. Cemara Paper, Batik Laweyan, and Difabelzone were chosen as the study objects because each of these SME has shown an initial commitment to empowering people with disabilities and has a variety of business types, scales, and inclusivity approaches that provide a rich and diverse perspective for this research.

This research used the SECI model through several stages. The initial stage is socialization, where tacit knowledge is collected from SME owners, employees, and individuals with disabilities through in-depth interviews and direct observation. Next, the externalization stage transforms the tacit knowledge into explicit knowledge that is documented and integrated in the combination stage with regulations and standards related to disability-friendly facilities. At the internalization stage, this explicit knowledge is implemented through training programs to help SME employees internalize and apply the new practices in their daily operations. Thus, this research not only identifies the needs and challenges faced by SMEs with disabilities, but also produces comprehensive criteria and guidelines for creating a more inclusive and disability-friendly business environment.

To ensure the sustainability and effectiveness of this process, the Knowledge Management Cycle is used as a systematic framework for managing the collected knowledge. The KM Cycle begins with the **Create** stage, where new knowledge is created from interactions and experiences in the field. The next stage is **Capture**, where the knowledge that has been created is captured and documented systematically. **Refine** is the stage at which the captured knowledge is processed and refined to ensure relevance and accuracy. Next, knowledge is stored in the **Store** stage to ensure that knowledge can be accessed in the future. In the **Manage** stage, the stored knowledge is organized and maintained to keep it up-to-date and relevant. **Dissemination** is the final stage, where the knowledge that has been organized is shared throughout the organization for implementation. Through this cycle, SME can ensure that knowledge about disability-friendly facilities is collected, documented, and used effectively to improve the inclusivity and sustainability of their businesses.

2.2 Data Collection

This study uses the SECI model (Socialization, Externalization, Combination, Internalization) to develop criteria for disability-friendly facilities in SME. The first stage in using the SECI model is socialization, where tacit knowledge is collected through direct interaction with SME. This research involves in-depth interviews with SME owners, employees, and individuals with disabilities in the three SME. This interview is designed to explore their experiences, needs, and challenges. In addition, direct observation of the day-to-day operations in SME is carried out to understand the informal processes and practices that support inclusivity. This interaction gave insights into how the three SME operate and adapt to become more inclusive toward people with disabilities.

After the socialization stage, the tacit knowledge that has been collected is converted into explicit knowledge through the externalization stage. The insights gained from interviews and observations are documented as detailed reports. This documentation covers various aspects of SME operations, including the role of the government, cooperation with the business sector and academia, and the role of the media in supporting SME with disabilities.

The combination stage involves gathering and integrating existing explicit knowledge to develop comprehensive criteria and guidelines for disability-friendly facilities in SME. This study collects and analyzes documents, regulations, and standards for disability-friendly facilities and accessibility. Explicit knowledge gained from the externalization stage is integrated with existing information to form a more complete and structured understanding. This process involves grouping, categorizing, and rearranging information to create criteria that can be applied in SME.

The final stage in data collection is internalization, where the explicit knowledge that has been developed is converted back into tacit knowledge through hands-on practice and experience. In this study, the internalization process will be carried out through Focus Group Discussion (FGD) in the three SME (Cemara Paper, Batik Laweyan, and Difabelzone) to help employees internalize new knowledge and practices. This FGD will include presentations on the new criteria and guidelines. Employees are encouraged to implement new criteria and guidelines in their day-to-day operations and provide feedback on their effectiveness. Expected outcomes of this study include comprehensive criteria and guidelines for developing disability-friendly SME, increased awareness and understanding of the needs of individuals with disabilities among SME owners and employees, and increased accessibility and inclusivity in SME, which in turn will lead to greater participation of individuals with disabilities in the workforce and economic activities. Thus, this research is expected to significantly contribute to social inclusion and economic empowerment of individuals with disabilities in Indonesia.

3 Result and Discussion

In this section, we present and discuss the findings from our study on the integration of the SECI Model and the Knowledge Management Cycle in developing disability-friendly criteria for three SME, namely SME 1 (Cemara Paper), SME 2 (Batik Toeli Laweyan), and SME 3 (Disabled Zone) (see Fig. 1). By addressing the specific needs and challenges faced by these three SME, we aim to provide comprehensive insights and practical recommendations to create an inclusive and supportive business environment for individuals with disabilities.

3.1 Socialization

The SECI method requires resource persons to obtain tacit knowledge about disability-friendly criteria in SMEs. The Socialization stage was conducted through in-depth interviews with three resource persons, namely from SME 1, SME 2, and SME 3. There were 32 people who became the sample of this study, with details further explained in Table 1.

3.2 Externalization

In the externalization stage, tacit knowledge acquired during socialization is transformed into documented explicit knowledge. The Capture and refine process then ensures that this knowledge is organized and refined to be used effectively. *The following is Table 2, which illustrates the results of externalization for the three SME in developing disability-friendly criteria.*

Fig. 1 SECI model with KM cycle approach



Table 1 Explanation of the resource person

SME	Description
SME 1 (Cemara paper)	Engage people with disabilities in producing products such as fans, envelopes, and tissue boxes and provide training. In this community, people with disabilities use waste for goods that have economic value
SME 2 (Batik Toeli Laweyan)	It has a batik community that explicitly facilitates people with disabilities. The purpose of this community is to provide opportunities for people with disabilities to be independent, self-employed, and generate income. Currently, three disabled workers are all deaf and are in the process of creating a particular location so that more people with disabilities can be facilitated in the future
SME 3 (Difabelzone)	As a place for people with disabilities, volunteers contribute to environmental care actions, such as making shopping bags with a call for environmental love. Production is carried out daily to be distributed to several stores, and orders are placed if there is a custom order

3.3 Combination

In the Combination stage, the knowledge documented from the Externalization stage is integrated with the KM Triad concept from Wickramasinghe and Mills [28] (see Fig. 2).

The KM Triad, which consists of the elements of people, processes, and technologies, is the basis for developing the parameters for this study. People need to improve staff understanding and skills to meet the needs of people with disabilities and develop appropriate training and awareness programs. Processes include convenience, usability, and policies supporting knowledge implementation. Technology facilitates access to information, provides assistive devices, and utilizes digital platforms for product marketing.

In the Combination stage, the integrated knowledge identified barriers and solutions for the three SME in developing disability-friendly criteria. *Table 3 illustrates the results of the Combination in the form of new knowledge obtained from the externalization stage related to the obstacles faced by the three SME in developing disability-friendly criteria.*

This stage focuses on disseminating the combined knowledge across the organization and related parties to ensure that the knowledge can be used effectively.

3.4 Internalization

In the internalization stage, the three SME apply the knowledge documented in the combination stage regarding obstacles and solutions in daily practices. Employees and management across the three SME implemented the identified solutions, such as starting to conduct marketing and sales training through digital platforms, improving

Table 2 Externalization results (capture and refine)

Parameter	Indicator	Information
Uses	Business activities	Business activities carried out by people with disabilities are related to production, but in the three SME, it is still difficult to do marketing and sales
	Non-business activities	The three SME still need to carry out non-business activities, such as training, skill development, and other social activities
Facilities	Business infrastructure	Facilities used to support business activities, such as workspaces and technology, need to be improved in the three SME
	Supporting infrastructure	Additional facilities that support the overall operation of SME, such as rest areas, disability-friendly toilets at SME 1
	Space design	The design and layout of the space have not met the needs of people with disabilities in the three SME to ensure comfort in working
	Physical accessibility	Ease of entry and exit from SME, including access to public facilities around SME
	Information accessibility	Third, SME still need help obtaining the necessary information through disability-friendly technology
Policy	Inclusive policy	Perceptions of inclusive policies that support people with disabilities in the workplace are still unplanned
	Skills program	Lack of implementation of awareness programs in improving understanding of knowledge and skills for people with disabilities
Collaboration	Business	Third, SME cooperate to produce custom goods for several companies
	Academy	SME 1 There is training provided by the university, and SME 2 and 3 establish research cooperation with the university
	Media	Mass media publishes the three SME
	Community	There is a level of cooperation with community organizations and communities in the three SME
	Government	The government's role in supporting SME with disabilities is minimal or even non-existent in all three SME
Technology	Assistive devices	There is a need for the availability and effectiveness of assistive devices that support accessibility
	Communication technology	Requires communication technology that supports sign language and hearing aids
Evaluation	Regular supervision	Requires routine supervision
	Periodic evaluation	Third, SME must improve in implementing periodic evaluations and adjustments to meet disability-friendly facilities

Fig. 2 KM triad

business and supporting facilities, and designing and implementing inclusive policies. Regular training programs and workshops are held to ensure that all employees understand and can apply new knowledge regarding physical and information accessibility. In addition, mentorship and mentoring programs are implemented to guide new or needy employees, ensuring they can adapt to new knowledge and practices. Regular evaluations and feedback from employees are collected to ensure the effectiveness of the implementation of the solution, and the values of inclusivity and accessibility are instilled as part of the organization's culture through internal campaigns and joint activities. Thus, documented knowledge becomes tacit knowledge internalized in individuals and organizational culture, creating a more inclusive and disability-friendly work environment.

Table 3 Combination result

Parameter	Obstacles	Solution
Uses	Difficulties in marketing and sales	Conducted marketing and sales training for people with disabilities and utilized digital platforms to expand market reach
Facilities	There needs to be more adequate business and supporting facilities	Develop and improve business and supporting facilities, including disability-friendly technology and infrastructure
	The design of the space does not meet the needs of people with disabilities	Repairs and adjustments to workspace designs to ensure comfort and safety for people with disabilities
	Physical accessibility and information are still lacking	Repairs and adjustments to workspace designs to ensure comfort and safety for people with disabilities
Policy	Unplanned inclusive policies	Design and implement inclusive policies that support people with disabilities in the workplace
	Lack of awareness and skills programs	Conduct awareness and skills training programs regularly to improve the understanding and ability of persons with disabilities
Collaboration	Lack of involvement and support from the government	Increase advocacy and cooperation with the government to get more significant support for developing SME with disabilities
	Cooperation with business, academia, media, and communities still needs to be improved	Strengthen and expand cooperation with the business sector, academia, media, and communities to support the development of SME with disabilities
Technology	The availability and effectiveness of assistive devices and communication technology still need to be improved	Identify the need for technology and assistive devices and conduct training on using such technology to support accessibility
Evaluation	Lack of regular supervision and periodic evaluation	Implement a routine monitoring system and periodic evaluation to ensure that disability-friendly facilities are constantly maintained and upgraded as needed

4 Conclusion

Implementing Knowledge Management (KM) can develop disability-friendly criteria in SME. Using the SECI model, the study successfully identified the main challenges SME face in creating an inclusive work environment: inadequate facilities, limited access to training programs, and social stigma. Through the stages of Socialization, Externalization, Combination, and Internalization, the accumulated knowledge is integrated and applied as practical solutions that include improving facilities, regular

training, and developing inclusive policies. Implementing KM not only improves employees' understanding and skills of the needs of people with disabilities but also creates a more inclusive and supportive organizational culture. The results of this study provide comprehensive guidance and practical recommendations for policy-makers and SME actors in building a disability-friendly business ecosystem, thereby increasing active participation and equality of benefits for persons with disabilities in the SME sector.

References

1. Widnyana IW, Wijana IMD, Almontasir A (2021) Financial capital, constraints, partners, and performance: an empirical analysis of Indonesia SMEs. *JEMA J Ilm Bid Akunt dan Manaj* 18:210. <https://doi.org/10.31106/jema.v18i2.11318>
2. Tambunan TTH (2011) Development of small and medium enterprises in a developing country: the Indonesian case. *J. Enterpr Commun* 5:68–82. <https://doi.org/10.1108/17506201111119626>
3. Martoyo M, Herlan H, Sukanto S, Sikwan A, Elyta E, Vayed D (2023) Al: Justifikasi Kebijakan Pemerintah Kota Pontianak Dalam Memberikan Peluang Pekerjaan Bagi Penyandang Disabilitas. *J Ilmu Sos dan Ilmu Polit* 12:283–293. <https://doi.org/10.33366/jisip.v12i3.2661>
4. Istifarroh I, Nugroho WC (2019) Perlindungan Hak Disabilitas Mendapatkan Pekerjaan Di Perusahaan Swasta Dan Perusahaan Milik Negara. *Mimb Keadilan* 12:1–23
5. Sadiawati D, Dirkareshza R, Dwi M. AB, Mintarsih M, Apriandhini M, Agustanti RD (2023) Peningkatan Perekonomian Penyandang Disabilitas Melalui Pendaftaran Hak Cipta Dan Pendaftaran Badan Hukum Perorangan Dalam Mendukung Sustainable Development Goals. *JMM (Jurnal Masy Mandiri)* 7:3128. <https://doi.org/10.31764/jmm.v7i4.15572>
6. Army Y, Nilasari AP, Bharata RW, Prasetyanto PK, Lubis RK (2023) Peningkatan Kapasitas UMKM Disabilitas Kota Magelang Melalui Pendampingan Pendirian Koperasi Disabilitas Kota Magelang. *Surya Abdimas* 7:177–182. <https://doi.org/10.37729/abdimas.v7i1.2480>
7. Septiani BA, Chandraderia D, Arini TA, Pratomo Y (2020) Peran Usaha Maju Sukses Bersama (Msb) Dalam Mendukung Pertumbuhan Ekonomi Inklusif. *J Ilm Ekon Bisnis* 25:169–185. <https://doi.org/10.35760/eb.2020.v25i2.2500>
8. Lauba N, Bahtiar B, Supiyah R (2022) Efektivitas Pelatihan Keterampilan Menjahit Dan Salon Penyandang Disabilitas Tuna Rungu Wicara Moehai Kendari. *Welvaart J Ilmu Kesejaht Sos* 3:71–82. <https://doi.org/10.52423/welvaart.v3i1.27389>
9. Oktaria ET, Yusda DD (2020) Efektivitas Penerapan Tanggung Jawab Sosial Perusahaan terhadap Pengembangan Usaha Mikro. *Ekombis Sains J Ekon Keuangan dan Bisnis* 5:37–44. <https://doi.org/10.24967/ekombis.v5i1.601>
10. Suryadi I (2023) Dampak Pendidikan Inklusif Terhadap Partisipasi dan Prestasi Siswa dengan Kebutuhan Khusus. *J Pendidik West Sci* 1:517–527. <https://doi.org/10.58812/jpdws.v1i08.597>
11. Serpian ER, Hadi EN (2021) Reducing stigma of people with disabilities: a systematic review. *J Med Heal Stud* 2:31–37. <https://doi.org/10.32996/jmhs.2021.2.2.3>
12. Handoyo R, Ali A, Scior K, Hassiotis A (2022) A qualitative exploration of stigma experience and inclusion among adults with mild to moderate intellectual disability in an Indonesian context. *J Intellect Disabil* 26:293–306. <https://doi.org/10.1177/17446295211002349>
13. Barbareschi G, Carew MT, Johnson EA, Kopi N, Holloway C (2021) “When they see a wheelchair, they’ve not even seen me”—factors shaping the experience of disability stigma and discrimination in Kenya. *Int J Environ Res Public Health* 18. <https://doi.org/10.3390/ijerph18084272>

14. Silván-Ferrero P, Recio P, Molero F, Nouvilas-Pallejà E (2020) Psychological quality of life in people with physical disability: the effect of internalized stigma, collective action and resilience. *Int J Environ Res Public Health* 17. <https://doi.org/10.3390/ijerph17051802>
15. Lindsay S, Leck J, Shen W, Cagliostro E, Stinson J (2019) A framework for developing employer's disability confidence. *Equal Divers Incl* 38:40–55. <https://doi.org/10.1108/EDI-05-2018-0085>
16. Dalkir K (2011) Book knowledge management in theory and practice. <http://site.ebrary.com/lib/unimannheim/docDetail.action?docID=10476096>
17. Tiwana A (2000) Knowledge management toolkit: the practical techniques for building a knowledge management system
18. Amelia M, Septiningrum L, Rumanti AA (2023) The design of cultural tourism potential indicators at Rembang regency using SECI method. In: *Proceedings of the 6th iMEC-APCOMS 2022*, pp 151–159. Springer, Singapore. https://doi.org/10.1007/978-981-99-1245-2_15
19. Alosaimi M (2018) The role of knowledge management approaches for enhancing and supporting education. *Univ Panthéon-Sorbonne - Paris I* 397
20. Wiig KM (2012) People-focused knowledge management: how effective decision making leads to corporate success. <https://doi.org/10.4324/9780080479910>
21. Othman A, Al Mutawaa A, Al Tamimi A, Al Mansouri M (2023) Assessing the readiness of government and semi-government institutions in Qatar for inclusive and sustainable ICT accessibility: introducing the MARSAD tool. *Sustain* 15. <https://doi.org/10.3390/su15043853>
22. Apriliadi A (2019) The impact of knowledge management on SMEs performance in the city of Bandung. *Int J Recent Technol Eng* 8:550–557. <https://doi.org/10.35940/ijrte.c1123.1083s219>
23. Hamdani NA (2018) Building knowledge-creation for making business competition atmosphere in SMEs of batik. *Manag Sci Lett* 8:667–676. <https://doi.org/10.5267/j.msl.2018.4.024>
24. Kusnindar A, Ambya A, Ahadiat A, Widiniarsih D (2023) Knowledge management peculiarities in MSMEs. *Int Conf Econ Business Entrep*. <https://doi.org/10.4108/eai.13-9-2023.2341183>
25. Nurhaeni IDA, Putri IS, Mulyadi AWE, Sudibyo DP (2024) Penta Helix collaboration in developing social inclusion for persons with disabilities. *J Contemp Gov Public Policy* 5:19–32. <https://doi.org/10.46507/jcgpp.v5i1.105>
26. Nonaka I, Takeuchi H (1995) *The knowledge-creating company: how Japanese companies create the dynamics of innovation*. Oxford University Press, New York
27. Žatuchin D (2024) Beyond SECI: advancing knowledge transformation through digital innovation in MBA education. *Res Sq* 1:0–16
28. Wickramasinghe N, Mills GL (2001) Knowledge management systems: A healthcare initiative with lessons for us all. *Proceedings of the 9th European Conference on Information Systems (ECIS)*, pp 1058–1067

Solving Sustainable Supplier Selection Problems Based on FAHP and FTOPSIS for Textile Industry



Feri Ancen Pakpahan , Mohammad Mi'radj Isnaini ,
Abdul Hakim Halim , and Shih-Che Lo

Abstract The textile industry significantly contributes to Indonesia's Gross Domestic Product, accounting for 7.1% of the non-oil and gas sector in 2019, which declined to 5.8% in 2023. This industry encompasses upstream (fiber-making and spinning), midstream (weaving, knitting, printing, dyeing), and downstream (garment production) segments. The capital-intensive yarn spinning sector is crucial, with raw materials and energy comprising 58.1% and 18.5% of costs, respectively. Effective supplier selection can reduce these costs and enhance market competitiveness. Beyond price and quality, supplier selection now prioritizes sustainability, in alignment with the United Nations' Sustainable Development Goals. This shift is essential for enhancing competitiveness and addressing climate change challenges. This study employs a combined Fuzzy Analytic Hierarchy Process (FAHP) and Fuzzy Technique for Order of Preference by Similarity to Ideal Solution (FTOPSIS) to assess sustainable supplier selection (SSS) criteria in the textile industry. The FAHP results indicate that the economy is the most important criterion among the three (economy, environmental, and social). Product quality is the most important among the sub-criteria, while social responsibility is considered the least important. FTOPSIS identifies Supplier B as the best supplier of all supplier alternatives. The findings offer a deeper understanding of SSS dynamics within the textile industry.

Keywords Sustainable supplier selection · Multi-criteria decision-making · Fuzzy AHP · Fuzzy TOPSIS

F. A. Pakpahan · M. M. Isnaini (✉) · A. H. Halim
Department of Industrial Engineering, Bandung Institute of Technology, Bandung 40132,
Indonesia
e-mail: isnaini@itb.ac.id

S.-C. Lo
Department of Industrial Management, National Taiwan University of Science and Technology,
Taipei 106335, Taiwan

1 Introduction

The textile industry plays a significant role in Indonesia's economy, contributing 7.1% to the non-oil and gas GDP in 2019, which has declined to 5.8% by 2023 [1]. This sector encompasses various processes from fiber-making to garment production. Notably, the yarn spinning segment, which is capital-intensive and technologically advanced, faces substantial costs for raw materials (58.1%) and energy (18.5%) [2, 3]. Consequently, supplier selection, which has traditionally focused on price and quality, is now increasingly integrating sustainable practices aligned with the Sustainable Development Goals (SDGs), which are essential for competitiveness and climate change mitigation [4].

The origins of thread spinning date back 8000 years, with archaeological evidence suggesting its practice around 6000 BC. The mechanization of yarn production began with the introduction of the spinning wheel in 1300 AD and continued evolving through various innovations until the adoption of cap spinning and later ring spinning in the 1960s [5]. Today, synthetic fibers dominate the global fiber market, projected to reach 142 million tons by 2030 [6].

Sustainable Supplier Selection (SSS) and the textile industry are central themes in SSS Management [7]. Research on SSS in the textile industry offers valuable insights; for instance, Wang et al. [8] utilized a fuzzy Multi-Criteria Decision-Making (MCDM) approach in Vietnam's garment industry, while Rahman et al. [9] developed an MCDM framework for Bangladesh's textile dyeing industry, prioritizing criteria such as chemical quality, cost, and delivery timeliness, and ranking one of the suppliers as being the most sustainable.

Businesses worldwide are adopting sustainable supplier selection practices to meet environmental imperatives, integrating economic, environmental, and social factors as emphasized by the World Economic Development Commission (WCED). Using Multi-Criteria Decision-Making (MCDM) techniques like TOPSIS and AHP, companies evaluate suppliers based on environmental impact, social responsibility, and economic viability, aligning business practices with global sustainability principles [10, 11].

Despite a noticeable gap in research, particularly in the yarn spinning sector, there is a significant opportunity for further investigation. This study focuses on sustainable supplier selection (SSS) within yarn spinning industry, aiming to enhance operational efficiency, address environmental concerns, and promote social responsibility across the textile supply chain. Utilizing FAHP and FTOPSIS techniques, the study seeks to develop a robust methodology tailored to the unique challenges faced by the yarn spinning sector, such as rising raw material and energy costs. The research is specifically limited to the yarn spinning sector in Indonesia, with insights gathered from experts within these companies. By leveraging industry expertise, the study aims to address complex decision-making requirements in SSS and contribute to a more sustainable and resilient textile industry.

Table 1 Search keywords and results

Search keywords	Database	Results
Sustainable supplier selection AND textile OR yarn OR weaving OR knitting OR garment	Scopus	39
Sustainable supplier selection AND textile	WoS	33
Green supplier selection textile AND yarn AND weaving AND knitting AND garment	Scopus	20
Green supplier selection AND textile	WoS	19

2 Research Methodology

2.1 Criteria Development

To identify criteria for SSS in the textile industry, a structured literature review was conducted using the Scopus and Web of Science databases, as detailed in Table 1. These databases were chosen because they are among the most widely utilized in academic research. Initially, 111 papers were identified, and refined to 69 unique papers after duplicate removal. A rigorous screening process, focused on relevant titles and abstracts, narrowed the selection to 40 research papers. Subsequent full-text reviews confirmed sustainable selection criteria in 10 papers, unveiling primary criteria—economic, environmental, and social—each further segmented into six sub-criteria, detailed in Table 2. The hierarchy structure of criteria and sub-criteria is illustrated in Fig. 1.

2.2 Questionnaire

This study involved collaboration with seasoned professionals from the Indonesian textile industry, particularly those specializing in yarn spinning, to assess SSS practices. The examination was focused on the five foremost synthetic fiber manufacturers, pivotal entities within the realm of yarn spinning. Employing two distinct questionnaires, the FAHP questionnaire was utilized to ascertain the weighting of economic, environmental, and social criteria, alongside 18 sub-criteria, through expert-driven pairwise comparisons. Concurrently, the FTOPSIS questionnaire aimed to discern the optimal sustainable supplier by soliciting expert evaluations of each supplier's performance across these 18 sub-criteria. This methodological approach facilitated an intricate evaluation of supplier performance and sustainability initiatives.

Table 2 Explanation of sub-criteria

Criteria	Sub-criteria	Explanation	Reference
Economy	Competitive pricing and logistics costs (EC1)	The ability of suppliers to offer competitive prices and efficiency in logistics costs	Ali and Zhang [12], Fadara and Wong [13]
	Product quality (EC2)	Evaluates the consistency of product quality according to industry standards and customer needs	Ali and Zhang [12], Fadara and Wong [13], Güner Gören and Şenocak [14]
	Delivery reliability (EC3)	Assessing the supplier's ability to deliver goods on time as agreed upon schedule	Ali and Zhang [12], Tong et al. [15], Sivaprakasam et al. [16]
	Order flexibility (EC4)	Supplier's ability to adapt to changes in orders and specific requests from the company	Tong et al. [15], Celik et al. [17]
	Payment method flexibility (EC5)	Availability of various payment options to meet the company's preferences and financial conditions	Celik et al. [17], Rodrigues et al. [18]
	Supplier financial stability (EC6)	Evaluate the supplier's financial strength in maintaining operations and fulfilling long-term commitments	Celik et al. [17], Kusi-Sarpong et al. [19], Yang and Wang [20]
Environmental	Environment standards compliance (EV1)	Evaluate supplier's compliance level with environmental standards, such as ISO 14001	Ali and Zhang [12], Tong et al. [15], Sivaprakasam et al. [16]
	Pollution reduction (EV2)	Supplier's efforts to reduce carbon emissions and other pollutants from their production processes	Ali and Zhang [12], Sivaprakasam et al. [16], Fallahpour et al. [21]
	Waste management (EV3)	Supplier's ability to effectively manage waste, including reduction, processing, and utilization of waste	Sivaprakasam et al. [16], Celik et al. [17], Fallahpour et al. [21]
	Energy and resource efficiency (EV4)	Evaluate supplier's efficiency in using energy and natural resources	Celik et al. [17], Yang and Wang [20]
	Contribution to environmental conservation (EV5)	Recognition of suppliers actively participating in environmental conservation efforts, both through internal activities and external collaborations	Tong et al. [15], Yang and Wang [20]
	Innovation in sustainability (EV6)	Evaluate supplier's investment in developing new materials and technologies that support environmental goals	Sivaprakasam et al. [16], Kusi-Sarpong et al. [19], Yang and Wang [20]

(continued)

Table 2 (continued)

Criteria	Sub-criteria	Explanation	Reference
Social	Work welfare and safety (SO1)	Assessment of the supplier’s efforts to ensure the safety and health of workers	Celik et al. [17], Rodrigues et al. [18], Fallahpour et al. [21]
	Fair labor practices (SO2)	Evaluation of the supplier’s labor practices, including fairness in recruitment, career development opportunities, and non-discrimination policies	Tong et al. [15], Fallahpour et al. [21]
	Human resources development (SO3)	Assessment of the supplier’s investment in developing its human resources	Rodrigues et al. [18], Kusi-Sarpong et al. [19]
	Stakeholder relationship management (SO4)	Supplier’s effectiveness in managing relationships with stakeholders	Güner Gören and Şenocak [14], Rodrigues et al. [18]
	Responsiveness to stakeholders (SO5)	Evaluate the supplier’s ability to respond quickly and effectively to feedback, needs, and expectations from various stakeholders	Yang and Wang [20], Fallahpour et al. [21]
	Social responsibility (SO6)	Supplier support for local communities, as well as participation in philanthropic and social activities	Sivaprakasam et al. [16], Celik et al. [17], Rodrigues et al. [18]

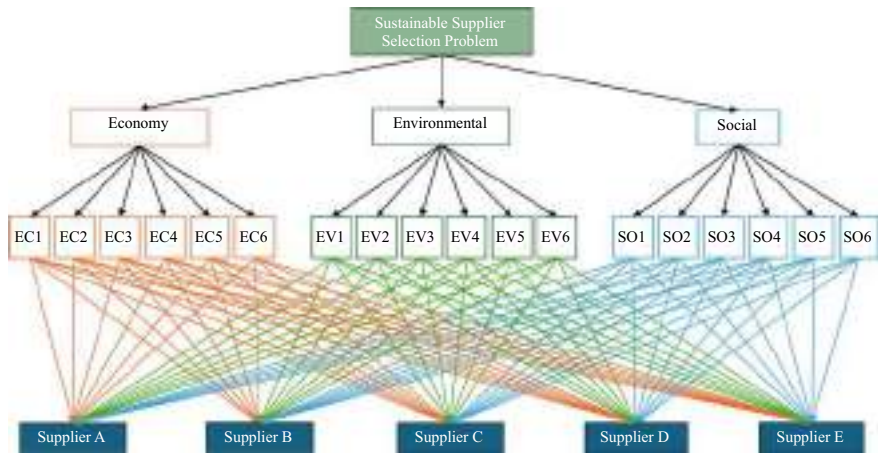


Fig. 1 Hierarchy structure of criteria and sub-criteria

2.3 Fuzzy Analytic Hierarchy Process Method

The FAHP represents a refined iteration of the AHP, tailored to enhance decision-making in contexts fraught with uncertainty and subjective assessments. While AHP adeptly dissects complex decisions into manageable hierarchies, its effectiveness can wane when confronted with the inherent vagueness or uncertainty of human judgment. FAHP mitigates these shortcomings by integrating fuzzy logic, thus capturing the intricacies of real-world decision-making more comprehensively [22]. By employing fuzzy numbers, such as Triangular Fuzzy Numbers (TFNs), FAHP allows decision-makers to express preferences linguistically rather than solely numerically, fostering a more nuanced representation of subjective judgments. Consequently, FAHP contributes a refined methodology that not only accommodates imprecision but also offers a more accurate depiction of decision-maker preferences, thus enriching the decision-making process.

This study aims to explore how industry practitioners prioritize criteria for selecting a sustainable supplier. Utilizing the FAHP, this research assigns weights to each criterion through several steps. Initially, industry respondents complete a questionnaire that includes pairwise comparisons of criteria and sub-criteria, adhering to a TFN scale like that described in Table 3. For example, $\tilde{a}_{ij} = 2$ in important scale, which is mean $\tilde{a}_{ij} = (1, 2, 3)$. Subsequently, the data gathered from the questionnaire informs the calculation of weights and relative importance for each criterion and sub-criterion. Here are the FAHP's several key steps:

- **Hierarchy Structuring:** The problem is structured into a hierarchy, breaking down the decision into criteria and sub-criteria.
- **Pairwise Comparisons:** Criteria and sub-criteria are compared in pairs using linguistic scales, which are converted into TFNs.
- **Fuzzy Synthesis:** Fuzzy numbers are aggregated to determine fuzzy weights for each criterion and sub-criterion.
- **Defuzzification:** The fuzzy weights are converted to crisp values using methods such as the centroid method to rank the criteria.
- **Consistency Check:** The consistency ratio is computed to ensure the reliability of the judgments using Saaty's consistency ratio (CR) in the following manner:

$$CR = CI/RI \quad (1)$$

Table 3 The fuzzy AHP conversion scale

Importance scale	Linguistic value	TFN
1	Both criteria are equally important	(1, 1, 1)
2	One criterion is slightly more important than the other	(1, 2, 3)
3	One criterion is clearly more important than the other	(2, 3, 4)
4	One criterion is strongly more important than the other	(3, 4, 5)
5	One criterion is overwhelmingly more important than the other	(5, 5, 5)

$$CI = (\lambda_{\max} - n)/(n - 1)$$

(2)

where CR is consistency ratio, RI is random index, CI is consistency index, λ_{\max} is the max eigenvalue of the comparison matrix, and n is the number of criteria. Readers intrigued by the procedural intricacies of the FAHP calculation process are encouraged to check out Liu et al. [22] for further elucidation.

2.4 Fuzzy TOPSIS Method

The TOPSIS stands as a widely embraced method within MCDM. Renowned for its user-friendly nature, computational efficiency, and robust mathematical framework, TOPSIS has become a favored approach across diverse decision-making domains. FTOPSIS emerges as a natural extension of the conventional method, integrating fuzzy logic to accommodate uncertainty and imprecision prevalent in MCDM contexts. By harnessing fuzzy numbers and linguistic variables, FTOPSIS endeavors to capture the subtle nuances of subjective judgments and preferences, thus enriching the decision-making process [23, 24].

After the respondents answered the pairwise comparison questionnaire, they were asked again to answer the questionnaire to rate the performance of 5 suppliers based on the 18 sub-criteria using a scale of 1–5 as depicted in Table 4. For example, $x_{ij} = 2$ in performance scale, it means $x_{ij} = (1, 2, 3)$. Using the weight derived from the FAHP, the performance of alternative suppliers will be calculated using FTOPSIS. Here is the FTOPSIS process:

- Constructing the Decision Matrix: Alternatives are evaluated across criteria, with performance ratings expressed as fuzzy numbers.
- Normalizing the Decision Matrix: Performance ratings are normalized for comparability.
- Weighting the Normalized Matrix: The normalized ratings are multiplied by the FAHP-derived weights.
- Determining Ideal and Negative-Ideal Solutions: The ideal solution represents the best performance, while the negative-ideal solution represents the worst.

Table 4 The fuzzy TOPSIS conversion scale

Performance scale	Linguistic value	TFN
1	Very poor: does not meet criteria/severe problem	(1, 1, 1)
2	Poor: below average performance	(1, 2, 3)
3	Average: standard performance	(2, 3, 4)
4	Good: good performance, few areas need improvement	(3, 4, 5)
5	Very good: meets/exceeds criteria, outstanding performance	(5, 5, 5)

- **Calculating the Distance to Ideal Solutions:** The distance of each alternative from the ideal and negative-ideal solutions is calculated using fuzzy distance measures.
- **Closeness Coefficient Calculation:** The closeness coefficient is computed for each alternative to determine its ranking.

Readers intrigued by the procedural intricacies of the FTOPSIS calculation process are referred to NÄdÄban et al. [23] for further elucidation. The conclusive phase of the FTOPSIS method relies on the closeness coefficient. The alternative exhibiting the highest closeness coefficient is deemed the optimal supplier alternative.

3 Experiment Result

3.1 Respondents Demographics

This paper encompasses 31 participants from 22 companies within the yarn spinning industry, embodying a spectrum of roles and departments. Their roles span 6 managers, 17 supervisors, and 8 staff members, highlighting a diverse professional landscape. Educationally, participants range from high school diplomas to master's degrees, blending practical expertise with academic depth. Experience-wise, they range from under five years to over twenty, offering a comprehensive perspective on SSS practices. This demographic breadth enhances the research's applicability and relevance across diverse facets of the textile industry.

3.2 FAHP Result and Analysis

As depicted in Table 5, the FAHP analysis identified economic criteria as the most significant factor in sustainable supplier selection for Indonesia's yarn spinning industry, with a weight of 0.451. Product quality and competitive pricing are the top sub-criteria within this category, with local weights of 0.246 and 0.245, respectively. This prioritization underscores the industry's focus on cost-effectiveness and maintaining high-quality standards, reflecting the importance of these factors in global supply chain management as highlighted in previous studies by Wang et al. [8] and Rahman et al. [9]. The emphasis on economic criteria indicates the industry's need to balance competitive pricing with superior product quality to remain viable and competitive in the market.

Environmental criteria follow closely with a weight of 0.302, demonstrating a strong commitment to sustainability. Key sub-criteria include environmental standards compliance and waste management, with local weights of 0.232 and 0.184, respectively, highlighting efforts to minimize environmental impact. This aligns with

Table 5 Overall ranking of sub-criteria

Criteria	Sub-criteria	Criteria weight	Local weight	Local rank	Global weight	Global rank
Economy	Competitive pricing and logistics costs	0.451	0.245	2	0.11152	2
	Product quality		0.246	1	0.11153	1
	Delivery reliability		0.157	3	0.07069	3
	Order flexibility		0.123	5	0.05532	9
	Payment method flexibility		0.126	4	0.05648	6
	Supplier financial stability		0.103	6	0.04585	11
Environment	Environment standards compliance	0.302	0.232	1	0.07005	4
	Pollution reduction		0.183	3	0.05532	8
	Waste management		0.184	2	0.05548	7
	Energy and resource efficiency		0.161	4	0.04870	10
	Contribution to environmental conservation		0.123	5	0.03727	14
	Innovation in sustainability		0.116	6	0.03501	15
Social	Work welfare and safety	0.247	0.246	1	0.06003	5
	Fair labor practices		0.179	2	0.04398	12
	Human resources development		0.169	3	0.04179	13
	Stakeholder relationship management		0.139	4	0.03465	16
	Responsiveness to stakeholders		0.133	5	0.03319	17
	Social responsibility		0.124	6	0.03120	18

Table 6 Ranking of suppliers

Supplier	D+	D−	CCI	Rank
Supplier A	0.5362	0.0048	0.0088	5
Supplier B	0.0002	0.4948	0.9995	1
Supplier C	0.0538	0.2399	0.8169	4
Supplier D	0.0534	0.2972	0.8477	2
Supplier E	0.0537	0.2610	0.8295	3

global trends toward environmentally responsible practices, as noted by Yang and Wang [20]. Social criteria rank third with a weight of 0.247, emphasizing work welfare and safety as the most critical social sub-criterion, with a local weight of 0.246. Among all sub-criteria, product quality has the highest global weight at 0.11153, while social responsibility ranks lowest at 0.03120. These results indicate the industry's prioritization of economic and environmental factors, with a significant yet lesser emphasis on social aspects. The low consistency ratio (CR) of 0.026 confirms the reliability of these assessments. These results also underscore the need for a balanced approach in supplier selection to achieve sustainability.

3.3 FTOPSIS Result and Analysis

Employing FTOPSIS, the study assesses five raw material suppliers within Indonesia's yarn spinning industry using 18 sub-criteria to determine the optimal sustainable supplier. The results are detailed in Table 6.

The results show that Supplier B is the top performer, with a closeness coefficient index (CCI) of 0.9995, indicating its strong alignment with the ideal supplier profile. This makes Supplier B the optimal choice for raw material supply in Indonesia's yarn spinning industry. In contrast, Supplier A is the worst performer, with the lowest CCI of 0.0088.

4 Conclusion and Future Research

This study evaluates sustainable supplier selection (SSS) in Indonesia's textile industry using FAHP and FTOPSIS methodologies. Economic criteria are paramount, with a weight of 0.451, emphasizing product quality and competitive pricing. Environmental criteria, weighted at 0.302, underscore the commitment to sustainability through compliance and waste management. Social criteria, though less emphasized at 0.247, prioritize work welfare and safety. FTOPSIS analysis ranks Supplier B as the most ideal supplier with a CCI of 0.9995, indicating strong alignment with sustainable practices. Supplier A ranks lowest, highlighting areas for improvement.

This study offers a comprehensive SSS framework for the yarn spinning industry, providing a structured approach to sustainable supplier selection. The findings highlight the industry's prioritization of economic and environmental criteria while underscoring the need for greater attention to social factors. Future research should compare SSS criteria across different textile sectors, such as weaving, knitting, and dyeing, to develop a comprehensive framework and make a case study to evaluate the whole textile industry. Another direction is to identify barriers to implementing SSS practices within the textile industry and propose strategies to enhance sustainability and supply chain resilience.

Acknowledgements The authors gratefully acknowledge the support from the Ministry of Industry of the Republic of Indonesia and the Master's Dual Degree Program between Bandung Institute of Technology and National Taiwan University of Science and Technology.

References

1. BPS-Statistic Indonesia Website: Distribution of GDP at current market prices by industry (2010=100) (Percent), <https://www.bps.go.id/en/statistics-table/2/MTA2IzI=/seri-2010--distribusi-pdb-menurut-lapangan-usaha-seri-2010-atas-dasar-harga-berlaku--persen-.html,%20last>. Accessed 25 May 2024
2. Ministry of Industry website: Mendorong Kinerja Industri Tekstil dan Produk Tekstil, <https://kemenperin.go.id/download/28303>. Accessed 20 May 2024
3. Dewi RG, Parinderati R, Hendrawan I, Dewantoro MWB, Bayuwega WD (2019) Energy efficiency monitoring in textile industries to achieve GHG emissions reduction target in Indonesia. In: IOP conference series: earth and environmental science. Institute of Physics Publishing
4. Rahardjo B, Wang FK, Lo SC, Chou JH (2023) A hybrid multi-criteria decision-making model combining DANP with VIKOR for sustainable supplier selection in electronics industry. Sustainability (Switzerland) 15
5. Texcoms Textile Solutions: Textile spinning: textile technology knowledge series, volume II. <https://www.scribd.com/document/472230456/Textile-Spinning-pdf>. Accessed 20 May 2024
6. BPS-Statistic Indonesia website: National export import data. <https://www.bps.go.id/en/exim>. Accessed 20 May 2024
7. Lis A, Sudolska A, Tomanek M (2020) Mapping research on sustainable supply-chain management. Sustainability (Switzerland) 12
8. Wang CN, Yang CY, Cheng HC (2019) A fuzzy multicriteria decision-making (MCDM) model for sustainable supplier evaluation and selection based on triple bottom line approaches in the garment industry. Processes 7
9. Rahman MM, Bari ABMM, Ali SM, Taghipour A (2022) Sustainable supplier selection in the textile dyeing industry: an integrated multi-criteria decision analytics approach. Resour Conserv Recycl Adv 15
10. Karakoç Ö, Memiş S, Sennaroglu B (2024) A review of sustainable supplier selection with decision-making methods from 2018 to 2022
11. Khulud K, Masudin I, Zulfikarijah F, Restuputri DP, Haris A (2023) Sustainable supplier selection through multi-criteria decision making (MCDM) approach: a bibliometric analysis
12. Ali H, Zhang J (2023) A fuzzy multi-objective decision-making model for global green supplier selection and order allocation under quantity discounts. Expert Syst Appl 225
13. Fadara TG, Wong KY (2023) A decision support system for sustainable textile product assessment. Text Res J 93:1971–1989

14. Güner Gören H, Şenocak AA (2018) Macbeth based Taguchi loss functions approach for green supplier selection: a case study in textile industry. *Text Apparel*
15. Tong L, Wang J, Yi J (2021) Sustainable textile and apparel enterprise supplier selection research. *AATCC J Res* 8:46–53
16. Sivaprakasam R, Selladurai V, Sasikumar P (2015) Implementation of interpretive structural modelling methodology as a strategic decision making tool in a Green Supply Chain Context. *Ann Oper Res* 233:423–448
17. Celik E, Yucesan M, Gul M (2021) Green supplier selection for textile industry: a case study using BWM-TODIM integration under interval type-2 fuzzy sets. *Environ Sci Pollut Res*
18. Rodrigues LVS, Casado RSGR, de Carvalho EN, Silva MM, e Silva LC (2020) Using FITradeoff in a ranking problem for supplier selection under TBL performance evaluation: an application in the textile sector. *Production* 30:1–14
19. Kusi-Sarpong S, Gupta H, Khan SA, Chiappetta Jabbour CJ, Rehman ST, Kusi-Sarpong H (2023) Sustainable supplier selection based on industry 4.0 initiatives within the context of circular economy implementation in supply chain operations. *Prod Plann Control* 34:999–1019
20. Yang Y, Wang Y (2020) Supplier selection for the adoption of green innovation in sustainable supply chain management practices: a case of the Chinese textile manufacturing industry. *Processes* 8:1–24
21. Fallahpour A, Wong KY, Rajoo S, Fathollahi-Fard AM, Antucheviciene J, Nayeri S (2021) An integrated approach for a sustainable supplier selection based on Industry 4.0 concept. *Environ Sci Pollut Res*
22. Liu Y, Eckert CM, Earl C (2020) A review of fuzzy AHP methods for decision-making with subjective judgements
23. Nădăban S, Dzitac S, Dzitac I (2016) Fuzzy TOPSIS: a general view. In: *Procedia computer science*, pp 823–831. Elsevier B.V.
24. Palczewski K, Sałabun W (2019) The fuzzy TOPSIS applications in the last decade. In: *Procedia computer science*, pp 2294–2303. Elsevier B.V.

Vendor Managed Inventory Model Considering Degree of Component Commonality and Quality Inspection Policies



Yosi Agustina Hidayat  and Nadin Fadilla

Abstract In this paper, Vendor Managed Inventory (VMI) model is combined with quality inspection policy according to defect fraction. This condition is found in a product with degree of component commonality of its raw materials. Calculation of optimal inventory policy will be carried out by considering the degree of commonality of the component and the presence of defective fractions in the ordering lot. We develop 5 (five) inventory policy models that represent the raw material quality inspection methods: (a) without inspection; (b) 100% inspection with replacement of defective raw materials; (c) 100% inspection without replacement; (d) acceptance sampling with replacement; and (e) acceptance sampling without replacement. The objective function of the five models is to minimize the combined total cost of VMI inventory and quality inspection. Based on the result, the optimum policy is the acceptance sampling without replacement. This policy results in 20.90% holding-cost saving, 57.51% shortage-cost saving, 53.08% quality inspection-cost saving, and 98.26% ordering-cost increasing compared to existing costs. This cost saving is obtained because the VMI supply chain system considers the component commonality, which is possible for a shorter lead time to occur which reduces inventory costs in the form of decreasing the cost of safety stock and the possibility of shortages of raw materials.

Keywords VMI · Component commonality strategy · Quality inspection policy · Defect fraction

Y. A. Hidayat (✉)

Industrial Engineering Department, Faculty of Industrial Technology, Institut Teknologi Bandung (ITB), Bandung 40132, Indonesia

e-mail: yosi@itb.ac.id

The Center for Logistics and Supply Chain Studies (CLoCS), Institut Teknologi Bandung (ITB), Bandung 40132, Indonesia

N. Fadilla

Engineering Management Department, Faculty of Industrial Technology, Institut Teknologi Bandung (ITB), Bandung 40132, Indonesia

1 Introduction

The intensity of market competition in the globalization era brings a challenge for a company to manage its own supply chain (SC) system. This transformation and uncertainty regarding the state of market development become essential and the company's focus to clearly understand its procurement system. In recent years, firms in many industries have experienced the need to offer increasing levels of product variety [1]. While the length of the product life cycle during which profits can be earned is becoming shorter due to rapid technological advances [2], the cost of developing and offering products has been rising sharply due to the increasing complexity of product variety. One major source of complexity faced by firms is the proliferation of components and component suppliers, which leads to higher product development and component quality costs. Besides, a different production system (i.e., made to order (MTO) or made to stock (MTS)) has different supplier selection criteria [3]. The more complicated the SC network is, the more combination of MTO and MTS strategy should be considered [3]. The production system has an impact on the supplier selection, and the existing suppliers can affect the selection of the production system reciprocally. The supplier with a long delivery time may change the production mode from MTO to MTS since the supplier cannot quickly respond to the market. Due to this situation, Wang et al. [4] investigated coordination mechanisms for cases in which the SC is decentralized. One of the decentralization strategies is Vendor Managed Inventory (VMI).

In this paper, the product studied is solar water heater (SWH) produced by renewable energy company. SWH is an energy-based product by utilizing sunlight as energy source. This product was chosen because it provides the largest percentage of product sales to the company. The company experienced a decrease in sales of this product. As a solution, the company's engineering division develops the raw material of SWH panels by considering the strategy of using common components in the structure of the raw material for the product, known as the component commonality concept. The company also experienced problems related to the arrival of raw materials by suppliers. Even though the inspection process has been conducted, there are still defective fractions of components that are passed in the production process, so that the quality of the final product does not meet company standards, and it can reduce customer satisfaction.

One approach to solve the problem is through coordination within SC using VMI. According to [5], VMI represents a strategy in SC that have short replenishment time with frequency and on-time delivery so that it can reduce the delivery cost. VMI has a role in reducing inventory cost and simultaneously ensuring the availability inventory level [6]. In the VMI system, buyer inventory is monitored and controlled by supplier. Suppliers will be responsible for making the raw material delivery with the right amount and at the right time to prevent stock out that can impact on customer service level at buyer level. The successful implementation of VMI can be achieved with

good collaboration between the two parties as well as trust to share information with each other. In this paper, VMI model is combined with quality inspection policy according to defect fraction in a product with component commonality of its raw materials.

2 Literature Study and Model Development

VMI is one form of relationship between two companies with different echelons (buyer and seller). VMI was developed in the late 1980s and is currently one of the most popular models to improve the SC integration [7]. VMI becomes complex because there is acquisition in reorder and inventory management by the vendor. In other words, to determine when the purchasing order is being issued by the vendor and how much the amount is based on the material usage history. For VMI to run smoothly, buyers should share the information about their procurement business process and material usage history, while the vendor should share their information about procurement and how they do the material delivery.

The component commonality concept is a strategy for using the same component in producing a variety of products. Commonality is an approach where two or more different components for different final products are replaced by common component that can perform the function it replaces [8]. This strategy can be applied in the company's SC to face business challenges, especially to fulfill customer preferences that are growing more complex. These challenges encourage the company to become more innovative in designing product development strategies (product proliferation) to provide a variety of products with efficient cost.

In this paper, there is also quality inspection for raw materials to produce product SWH. The VMI will be implemented to overcome uncertainty from suppliers, such as delays in the arrival of raw materials and the quality of raw materials provided by suppliers. The VMI will also consider the concept of component commonality. Too many variations tend to have a negative impact on production operations because they increase complexity and production costs and have an impact on the difficulty of estimating fluctuations in demand and controlling inventory.

The characteristics of demand for raw materials are uncertain and there are fluctuations in demand for raw materials production. In this paper, the lead time is considered as a decision variable to determine the optimum time for procuring raw materials. The characteristics of the raw material inventory obtained from suppliers also contain a defective fraction in each lot that arrives, so an inspection process needs to be carried out before the raw materials are used in the production process. The size of the defect fraction in each lot is uncertain, where the distribution pattern of the defect fraction will be determined based on the company's historical data. Quality inspection policy in the form of the type of quality inspection is also a decision variable.

There are several recent studies that prove the success of VMI approach. Salas-Navarro et al. [9] proposed a joint optimization model considering VMI for deteriorating items at three level SC (multiple suppliers, manufacturers, and retailers) in dairy industry. Aligned with this paper which uses uncertainty demand, their model can reduce the deterioration rates and generate more profit for the SC. Their model also uses the cost of quality inspection which in this paper we use this cost component to calculate total cost. With the same objective, that is cost minimization, study by Golpîra [10] and Khatun et al. [11] shows that the implementation of VMI can reduce the total cost.

Model development was carried out with the aim of accommodating study systems that do not yet exist in the reference model. The reference model used is a combination of model development between [12] which accommodates the determination of quality inspection policies and model development in [13] and complemented by model development by Hidayat et al. [14] in accommodating the calculation of the optimum degree of commonality of components. The model formulated in [13] have not been able to fully answer several problems faced by companies such as the need for a more responsive SC so that it can be mutually beneficial, the development of raw materials for product SWH that consider the degree of component commonality, and the presence of a defect fraction in the order lot size. The model in [13] did not accommodate the optimum quality inspection policy in their inventory policy calculations, so development was carried out by adding a quality inspection cost component to the cost component.

The reference model related to quality inspection policies used is the model formulated in [12] which integrates optimal inventory and quality inspection policy selection models. In the reference model, the components of quality costs are the costs of receiving defective products, replacement costs, and inspection costs, all of which are expenses that must be borne by the buyer. However, in the model developed, with the VMI inventory system there is a division of responsibility for the components of quality inspection costs, namely replacement costs are the responsibility of the supplier, inspection costs and receiving defective products are the responsibility of the buyer. Apart from that, the reference model also does not consider the costs that arise because of the inspection without replacement policy, that is the costs of disposing of defective raw materials.

2.1 Model Notation

All notations are provided from Tables 1, 2, 3 and 4.

Table 1 Index notation of the developed model

Notation	Description	Unit
i	The number of final product produced ($i = A, B, \dots, N$)	Unit
j	The total number of components (unique and common) ($j = a, b, c, \dots, n$)	Unit
j_{un}	The number of unique component ($j_{un} = a, c, \dots, n_{un}$)	Unit
j_{com}	The number of common component ($j_{com} = b, \dots, n_{com}$)	Unit

Table 2 Parameter notation of the developed model

Notation	Description	Unit
D_i	The average buyer demand for final product i	Unit
S_i	The standard deviation buyer demand for final product i	Unit
P_{ij}	The order per unit of component j for final product i	IDR/unit
AS_{ij}	The supplier's ordering cost of component j for final product i	IDR/order
AB_{ij}	The buyer's ordering cost of component j for final product i	IDR/order
h_{ij}	The buyer's holding cost of component j for final product i	IDR/ unit-time
π_{ij}	The shortage cost of component j for final product i	IDR/unit
α_{ij}	The proportion of component j for final product i that remains unmet from the VMI supply chain stock	%
C_i	The inspection cost per unit	IDR/unit
C_d	The cost of accepting defect product	IDR/unit
C_r	The cost of replacing defect product	IDR/unit
\bar{p}	The average fraction of defects in product	%

Table 3 Variable notation of the developed model

Notation	Description	Unit
ss_{ij}	The safety stock of component j for final product i	Unit
N_{ij}	The expected inventory shortage of component j for final product i	Unit
TC'	The total inventory cost in VMI supply chain	IDR/time
KB'	The buyer's inventory cost	IDR/time
KS'	The supplier's inventory cost	IDR/time
O_b	The cost of purchasing component j for final product i	IDR/time
O_p	The cost of ordering component j for final product i	IDR/time
O_s	The supplier's holding cost of component j for final product i	IDR/time
O_k	The shortage cost of component j for final product i	IDR/time
O_{ss}	The supplier's set-up cost of component j for final product i	IDR/time
O_Q	The expected quality cost over the planning horizon	IDR/time

Table 4 Decision variable of the developed model

Notation	Description	Unit
e'_{ijun}	The degree of commonality, i.e., the percentage of unique component j_{un} for final product i produced using common component	–
Q'_{ij}	The order lot size of component j for final product i	Unit
L'_{ij}	The lead time of component j for final product i	Time
r'_{ij}	The reorder point of component j for final product i	Unit

2.2 Model Formulation

By combining the VMI inventory system and the five choices of quality inspection methods, there are five developed model, namely the VMI inventory model (a) without inspection; (b) 100% inspection with replacement of defective raw materials; (c) 100% inspection without replacement; (d) acceptance sampling with replacement; and (e) acceptance sampling without replacement. The performance measure of this inventory system is minimizing the combined expected total cost of inventory and quality inspection. The expected total cost is obtained by totalizing the buyer's inventory cost and supplier's inventory cost as shown in Eq. (1).

$$TC' = KB' + KS' = \sum_{i=1}^N (O_{bi} + O_{pi} + O_{si} + O_{ki} + O_{ssi} + O_{qi}) \tag{1}$$

Without Inspection. In this model, there is no inspection carried out when all the raw materials are received by the buyer. Therefore, the components of quality costs that will be borne by the buyer are the costs of receiving defective products and disposal costs.

$$TC' = \sum_{i=1}^N [P_{ijun}(1 - e_{ijun})D_i + P_{ijcom}e_{ijun}D_i + C_{dijun}(1 - e_{ijun})D_i\bar{p} + C_{dijcom}e_{ijun}D_i\bar{p} + C_{bijun}(1 - e_{ijun})D_i\bar{p} + C_{bijcom}e_{ijun}D_i\bar{p}]$$

$$\begin{aligned}
& \left[\frac{AB_{ijun}(1 - e_{ijun})D_i}{Q'_{ijun}} + \frac{AB_{ijcom}e_{ijun}D_i}{Q'_{ijcom}} \right. \\
& \quad + h_{ijun} \left\{ \frac{1}{2}Q'_{ijun} + Z_\alpha S_i(1 - e_{ijun})\sqrt{L'_{ijun}} \right\} \\
& \quad + h_{ijcom} \left\{ \frac{1}{2}Q'_{ijcom} + Z_\alpha S_i e_{ijun}\sqrt{L'_{ijcom}} \right\} \\
& \quad + \frac{\pi_{ijun}(1 - e_{ijun})^2 D_i S_i \beta \sqrt{L'_{ijun}}}{Q'_{ijun}} + \frac{\pi_{ijcom}(e_{ijun})^2 D_i S_i \beta \sqrt{L'_{ijcom}}}{Q'_{ijcom}} \\
& \quad \left. + \frac{AS_{ijun}(1 - e_{ijun})D_i}{Q'_{ijun}} + \frac{AS_{ijcom}e_{ijun}D_i}{Q'_{ijcom}} \right] \\
& + \sum_{i=1}^N \quad (2)
\end{aligned}$$

With 100% Inspection and Replacement. The raw materials received will be completely inspected by the buyer and when defective raw materials are found, the supplier must replace them with new raw materials of good quality. Therefore, the quality costs in this model consist of inspection costs and replacement costs. Inspection costs are the responsibility of the buyer and replacement costs are the responsibility of the supplier.

$$\begin{aligned}
TC' = & \sum_{i=1}^N [P_{ijun}(1 - e_{ijun})D_i + P_{ijcom}e_{ijun}D_i + C_{ijun}(1 - e_{ijun})D_i + C_{ijcom}e_{ijun}D_i] \\
& + \sum_{i=1}^N \left[\frac{AB_{ijun}(1 - e_{ijun})D_i}{Q'_{ijun}} + \frac{AB_{ijcom}e_{ijun}D_i}{Q'_{ijcom}} \right] \\
& + \left[h_{ijun} \left\{ \frac{1}{2}Q'_{ijun} + Z_\alpha S_i(1 - e_{ijun})\sqrt{L'_{ijun}} \right\} + h_{ijcom} \left\{ \frac{1}{2}Q'_{ijcom} + Z_\alpha S_i e_{ijun}\sqrt{L'_{ijcom}} \right\} \right] \\
& + \left[\frac{\pi_{ijun}(1 - e_{ijun})^2 D_i S_i \beta \sqrt{L'_{ijun}}}{Q'_{ijun}} + \frac{\pi_{ijcom}(e_{ijun})^2 D_i S_i \beta \sqrt{L'_{ijcom}}}{Q'_{ijcom}} \right] \\
& + \left[\frac{AS_{ijun}(1 - e_{ijun})D_i}{Q'_{ijun}} + \frac{AS_{ijcom}e_{ijun}D_i}{Q'_{ijcom}} \right] + C_{rijun}(1 - e_{ijun})D_i \bar{p} + C_{rijcom}e_{ijun}D_i \bar{p} \quad (3)
\end{aligned}$$

100% Inspection and without Replacement. In this model, the quality inspection policy is used to inspect all raw materials received by the company, but any raw materials found to be defective will not be replaced with good quality raw materials. This policy will cause a difference between the number of raw materials stored temporarily before the production process takes place and the raw materials ordered. The magnitude of this difference is influenced by the average fraction of defects found in the order lot when the inspection is carried out. The quality inspection policy for this model is the responsibility of the buyer.

$$\begin{aligned}
TC' = & \sum_{i=1}^N \left[P_{ij_{un}} (1 - e_{ij_{un}}) D_i + P_{ij_{com}} e_{ij_{un}} D_i + \frac{C_{iij_{un}} (1 - e_{ij_{un}}) D_i}{1 - \bar{p}} + \frac{C_{iij_{com}} e_{ij_{un}} D_i}{1 - \bar{p}} \right. \\
& \left. + \frac{C_{bij_{un}} (1 - e_{ij_{un}}) D_i \bar{p}}{1 - \bar{p}} + \frac{C_{bij_{com}} e_{ij_{un}} D_i \bar{p}}{1 - \bar{p}} \right] \\
& + \sum_{i=1}^N \left[\frac{AB_{ij_{un}} (1 - e_{ij_{un}}) D_i}{Q'_{ij_{un}} (1 - \bar{p})} + \frac{AB_{ij_{com}} e_{ij_{un}} D_i}{Q'_{ij_{com}} (1 - \bar{p})} \right] \\
& + \left[h_{ij_{un}} \left\{ \frac{1}{2} Q'_{ij_{un}} (1 - \bar{p}) + Z_{\alpha} S_i (1 - e_{ij_{un}}) \sqrt{L'_{ij_{un}}} \right\} \right. \\
& \left. + h_{ij_{com}} \left\{ \frac{1}{2} Q'_{ij_{com}} (1 - \bar{p}) + Z_{\alpha} S_i e_{ij_{un}} \sqrt{L'_{ij_{com}}} \right\} \right] \\
& + \left[\frac{\pi_{ij_{un}} (1 - e_{ij_{un}})^2 D_i S_i \beta \sqrt{L'_{ij_{un}}}}{Q'_{ij_{un}} (1 - \bar{p})} + \frac{\pi_{ij_{com}} (e_{ij_{un}})^2 D_i S_i \beta \sqrt{L'_{ij_{com}}}}{Q'_{ij_{com}} (1 - \bar{p})} \right] \\
& + \left[\frac{AS_{ij_{un}} (1 - e_{ij_{un}}) D_i}{Q'_{ij_{un}} (1 - \bar{p})} + \frac{AS_{ij_{com}} e_{ij_{un}} D_i}{Q'_{ij_{com}} (1 - \bar{p})} \right] \tag{4}
\end{aligned}$$

Sampling Inspection with Replacement. In this model, n items of raw materials received will be taken for inspection by the buyer and when defective raw materials are found, the supplier must replace them with new raw materials of good quality. Inspection costs and costs for receiving defective products are the responsibility of the buyer and costs for replacing defective products are the responsibility of the supplier.

$$\begin{aligned}
TC' = & \sum_{i=1}^N \left[P_{ij_{un}} (1 - e_{ij_{un}}) D_i + P_{ij_{com}} e_{ij_{un}} D_i + D_i (1 - e_{ij_{un}}) \left[C_{iij_{un}} + \varphi(n, c) - \frac{n\varphi(n, c)}{Q'_{ij_{un}}} \right] \right. \\
& \left. + D_i e_{ij_{com}} \left[C_{iij_{com}} + \varphi(n, c) - \frac{n\varphi(n, c)}{Q'_{ij_{com}}} \right] \right] \\
& + \sum_{i=1}^N \left[\frac{AB_{ij_{un}} (1 - e_{ij_{un}}) D_i}{Q'_{ij_{un}}} + \frac{AB_{ij_{com}} e_{ij_{un}} D_i}{Q'_{ij_{com}}} \right] \\
& + \left[h_{ij_{un}} \left\{ \frac{1}{2} Q'_{ij_{un}} + Z_{\alpha} S_i (1 - e_{ij_{un}}) \sqrt{L'_{ij_{un}}} \right\} + h_{ij_{com}} \left\{ \frac{1}{2} Q'_{ij_{com}} + Z_{\alpha} S_i e_{ij_{un}} \sqrt{L'_{ij_{com}}} \right\} \right] \\
& + \left[\frac{\pi_{ij_{un}} (1 - e_{ij_{un}})^2 D_i S_i \beta \sqrt{L'_{ij_{un}}}}{Q'_{ij_{un}}} + \frac{\pi_{ij_{com}} (e_{ij_{un}})^2 D_i S_i \beta \sqrt{L'_{ij_{com}}}}{Q'_{ij_{com}}} \right] \\
& + \left[\frac{AS_{ij_{un}} (1 - e_{ij_{un}}) D_i}{Q'_{ij_{un}}} + \frac{AS_{ij_{com}} e_{ij_{un}} D_i}{Q'_{ij_{com}}} \right] \\
& + D_i (1 - e_{ij_{un}}) \left[C_{rij_{un}} \bar{p} - \sum_{y=0}^c C_{rij_{un}} m_n(y) P_n(y) \left(1 - \frac{n}{Q'_{ij_{un}}} \right) \right]
\end{aligned}$$

$$+ D_i e_{ijun} \left[C_{rijcom} \bar{p} - \sum_{y=0}^c C_{rijcom} m_n(y) P_n(y) \left(1 - \frac{n}{Q'_{ijcom}} \right) \right] \quad (5)$$

Sampling Inspection without Replacement. Every lot that comes from the supplier will be sampled for inspection and there will be two conditions. If an order lot is accepted, it means that the number of defective products in the sample does not exceed the acceptance limit. There remains the possibility of the lot still containing defective raw materials. Therefore, it is possible to have costs for receiving defects from the lot that is not inspected. If an order lot is rejected, it means that the number of defective products in the sample exceeds the acceptance limit so that a 100% inspection of the lot size will then be carried out.

$$\begin{aligned} TC' = & \sum_{i=1}^N [P_{ijun} (1 - e_{ijun}) D_i + P_{ijcom} e_{ijun} D_i] \\ & + \frac{D_i (1 - e_{ijun}) \left[Q'_{ijun} (C_{iijun} + C_{bijun} \bar{p} + \varphi(n, c)) - \frac{n\varphi(n, c)}{Q'_{ijun}} \right]}{Q'_{ijun} [1 - \bar{p} + \lambda(n, c)] - n\lambda(n, c)} \\ & + \frac{D_i e_{ijcom} \left[Q'_{ijcom} (C_{iijcom} + C_{bijcom} \bar{p} + \varphi(n, c)) - \frac{n\varphi(n, c)}{Q'_{ijcom}} \right]}{Q'_{ijcom} [1 - \bar{p} + \lambda(n, c)] - n\lambda(n, c)} \\ & + \sum_{i=1}^N \left[\frac{AB_{ijun} (1 - e_{ijun}) D_i}{Q'_{ijun} (1 - \bar{p} + \lambda(n, c)) - n\lambda(n, c)} + \frac{AB_{ijcom} e_{ijun} D_i}{Q'_{ijcom} (1 - \bar{p} + \lambda(n, c)) - n\lambda(n, c)} \right] \\ & + \left[h_{ijun} \left\{ \frac{Q'_{ijun} (1 - \bar{p} + \lambda(n, c))}{2} - n\lambda(n, c) + Z_\alpha S_i (1 - e_{ijun}) \sqrt{L'_{ijun}} \right\} \right. \\ & \quad \left. + h_{ijcom} \left\{ \frac{Q'_{ijcom} (1 - \bar{p} + \lambda(n, c))}{2} - n\lambda(n, c) + Z_\alpha S_i e_{ijun} \sqrt{L'_{ijcom}} \right\} \right] \\ & + \left[\frac{\pi_{ijun} (1 - e_{ijun})^2 D_i S_i \beta \sqrt{L'_{ijun}}}{Q'_{ijun} (1 - \bar{p} + \lambda(n, c)) - n\lambda(n, c)} + \frac{\pi_{ijcom} (e_{ijun})^2 D_i S_i \beta \sqrt{L'_{ijcom}}}{Q'_{ijcom} (1 - \bar{p} + \lambda(n, c)) - n\lambda(n, c)} \right] \\ & + \left[\frac{AS_{ijun} (1 - e_{ijun}) D_i}{Q'_{ijun} (1 - \bar{p} + \lambda(n, c)) - n\lambda(n, c)} + \frac{AS_{ijcom} e_{ijun} D_i}{Q'_{ijcom} (1 - \bar{p} + \lambda(n, c)) - n\lambda(n, c)} \right] \quad (6) \end{aligned}$$

3 Results and Analysis

There are three types of raw materials that compose the SWH product (panel glass, pipe rise, and seal glass). Based on Table 5, the acceptance sampling inspection model without replacement provides the cheapest total costs based on components of SWH product. Therefore, this model is then proposed as selected model. The differences between ordering costs, holding costs, shortage costs and supplier set-up costs are

Table 5 Comparison of total inventory cost in IDR

VMI inventory policy	Panel glass	Pipe riser	Seal glass
Without inspection	2,705,578,524	4,904,817,847	1,710,772,457
100% inspection with replacement	2,721,963,370	4,993,389,989	1,703,879,594
100% inspection without replacement	2,670,038,102	4,904,817,777	1,682,377,221
Sampling inspection with replacement	2,718,102,993	4,879,995,739	1,699,819,361
Sampling inspection without replacement	2,660,518,007	4,752,545,526	1,667,139,980

Table 6 Improvement to proposed policy model

Cost component	Existing policy	Proposed policy	Improvement (%)
Ordering cost	IDR 14,166,279	IDR 28,086,000	−98.26
Holding cost	IDR 132,273,880	IDR 104,633,297	20.90
Shortage cost	IDR 59,053,798	IDR 25,091,898	57.51
Quality cost	IDR 697,946,260	IDR 327,484,693	53.08

not significantly different from one model to another. So, it can be concluded that the difference in total costs between one model and another is caused by costs related to the quality of the raw materials.

The implementation of VMI has resulted in a shift in cost components that were originally the responsibility of the buyer and are now the responsibility of the supplier. These cost components are ordering costs, holding costs, shortage costs, and quality costs. In this section, the performance evaluation of the proposed model and existing conditions will be reviewed only on the four cost components presented in Table 6. As shown in Table 6, the proposed policy model will result in an increase in the ordering cost. This happens because the proposed model orders are made for 2 (two) types of components (unique and common components). The increase in the number of raw materials ordered will be directly proportional to the ordering costs incurred. Increasing the frequency of orders means that ordering costs also increase.

On the other hand, there are significant savings in other cost components. Savings in the holding cost occur because in the VMI SC system, procurement lead times will be shorter and even possible there will be no lead time. Short lead times have an impact on the small amount of safety stock that must be stored, which then causes a decrease in the resulting holding costs. This result can validate the literature that VMI provides a solution to the inefficiencies caused by long delivery times in a decentralized supply chain by improving inventory management and reducing lead times, which enables companies to better balance the trade-offs between MTO and MTS. For the same condition, shortage cost also can be improved because the shorter lead time, the higher the replenishment rate that occurs so that the expected amount of raw material shortages that may occur is small. Quality cost also can be improved, considering that in the VMI supply chain suppliers have an obligation to provide raw

materials of good quality to buyers. With good trust between the two actors, the cost components in the quality inspection policy can be minimized.

4 Conclusion

VMI inventory policy is determined for the raw materials that composed the product SWH using a mathematical model that considers the optimum degree of commonality of components and considers defective fractions. Based on the result, the optimum policy is the acceptance sampling without replacement. This policy results in 20.90% holding-cost saving, 57.51% shortage-cost saving, 53.08% quality inspection-cost saving, and 98.26% ordering-cost increasing compared to existing costs. The implementation of a VMI, as one of decentralization strategies in procurement systems, causes a shift in responsibility for quality inspection components. The shift in responsibility occurs in the inventory cost components, such as holding costs, ordering costs and shortage costs that become the responsibility of the supplier. Overall, the VMI system considering commonality component and defect fraction will create good coordination between the company and suppliers in the SC so that it can reduce total inventory costs. For further research, this study can be extended by (1) considering product deterioration and probabilistic demand with lead time acceleration or lead time decision within VMI system. By accelerating lead time, the company can reduce the risk of deterioration and balance the trade-offs between MTO and MTS, especially in industries where product quality and shelf life are critical. (2) The integrated work in this paper can be improved computationally by designing a decision support system that can accommodate the VMI-based inventory model that has been developed.

References

1. MacDuffie JP, Sethuraman K, Fisher ML (1996) Product variety and manufacturing performance: evidence from the international automotive assembly plant study. *Manage Sci* 42:350–369
2. Nevens TM, Summe GL, Uttal B (1990) Commercializing technology: what the best companies do. *Harv Bus Rev* 68:154–163
3. Sun XY, Ji P, Sun LY, Wang YL. Positioning multiple decoupling points in a supply network. *Int J Prod Econ*
4. Wang C, Huang R, Wei Q (2015) Integrated pricing and lot-sizing decision in a two-echelon supply chain with a finite production rate. *Int J Prod Econ* 161:44–53
5. Simchi-Levi D, Kaminsky P, Simchi-Levi E (2000) *Designing and managing the supply chain concepts, strategies, and case studies*. McGraw-Hill, New York
6. Taleizadeh AA, Shokr I, Konstantaras I, VafaeiNejad M (2020) Stock replenishment policies for a vendor-managed inventory in a retailing system. *J Retail Consum Serv* 55:1–18
7. Ghasemi E, Lehoux N, Rönqvist M (2024) A multi-level production-inventory-distribution system under mixed make to stock, make to order, and vendor managed inventory strategies: an application in the pulp and paper industry. *Int J Prod Econ* 271:1–22

8. Ma S, Wang W, Liu L (2002) Commonality and postponement in multistage assembly systems. *Eur J Oper Res* 142:523–538
9. Salas-Navarro K, Romero-Montes JM, Acevedo-Chedid J, Ospina-Mateus H, Florez WF, Cárdenas-Barrón LE (2023) Vendor managed inventory system considering deteriorating items and probabilistic demand for a three-layer supply chain. *Expert Syst Appl* 218:1–20
10. Golpîra H (2020) Optimal integration of the facility location problem into the multi-project multi-supplier multi-resource Construction Supply Chain network design under the vendor managed inventory strategy. *Expert Syst Appl* 139
11. Khatun A, Islam S, Garai A (2023) Enhanced environmental and economic sustainability of VMI-CS agreement-based closed-loop supply chain for deteriorating products. *Results Control Optim* 13
12. Ben-Daya M, Noman SM (2008) Integrated inventory and inspection policies for stochastic demand. *Eur J Oper Res* 185:159–169
13. Hidayat YA, Anna ID, Khrisnadewi A (2011) The application of vendor managed inventory in the supply chain inventory model with probabilistic demand. In: *IEEE international conference on industrial engineering and engineering management*, pp 252–256. IEEE, Singapore
14. Hidayat YA, Simatupang T, Sebrina, Ariansyah MN, Sembada WJ (2017) Vendor managed inventory on Two echelon inventory system with optimum accelerated lead time and component commonality. In: *IEEE international conference on industrial engineering and engineering management*, pp 1382–1386. IEEE, Singapore

A Hybrid Multi-Criteria Decision-Making Model for Evaluating Energy Efficiency Practices in Indonesia's Textile Industry



Mulia Hendra, Muhammad Akbar , Shi-Woei Lin ,
and Dradjad Irianto

Abstract Energy plays a crucial role in the socioeconomic development of nations, especially in manufacturing sectors like the textile industry. Energy consumption directly impacts production costs and market competitiveness, making energy efficiency essential. However, selecting and implementing the most appropriate energy efficiency measures are complex management problems due to numerous influencing factors should be considered. This study aims to develop a framework for evaluating energy efficiency in the textile industry by establishing criteria and using a hybrid multi-criteria decision-making (MCDM) model that considers the interrelationships among these criteria. Expert opinions were gathered using the Delphi method to validate criteria from literature. Furthermore, a hybrid MCDM model by combining Decision-Making Trial and Evaluation Laboratory (DEMATEL) and Analytic Network Process (ANP) to identify interrelationships and assigned weights of the criteria. The study found that technical and economic factors are most critical. Key technical criteria include ‘Technical applicability’ and ‘Technology accessibility,’ while ‘Potential of economic savings’ is the most critical economic factor. Other important economic criteria are ‘Implementation cost’ and ‘Operation and maintenance cost.’ This framework can be applied as a decision-making tool across various sectors, with the advantage of accounting for interrelationships among criteria, enhancing practical applicability.

M. Hendra (✉) · M. Akbar · D. Irianto
Industrial Engineering Department, Institut Teknologi Bandung, Bandung, Indonesia
e-mail: mulia.hendra@gmail.com

M. Akbar
e-mail: muhammad@itb.ac.id

M. Hendra · S.-W. Lin
Department of Industrial Management, National Taiwan University of Science and Technology,
Taipei City, Taiwan

Keywords Energy efficiency · Textile industry · Delphi method · DEMATEL · ANP

1 Introduction

Energy is crucial for socioeconomic development of the nation, especially in manufacturing sectors like the textile industry. Energy costs can significantly affect product prices and competitiveness, ranging from 5 to 10% of total operating expenses in countries such as Brazil, China, India, Italy, Korea, Turkey, and the USA. In Indonesia, these costs are higher at 15–45% [1]. Implementing energy-saving measures in textile industry can reduce energy consumption and emissions up to 35% [2].

Selecting the most appropriate energy efficiency practices are complex management problems involving multiple factors such as social, technological, economic, and environmental. Multi-Criteria Decision-Making (MCDM) methods can be effective for integrating benefits, costs, and stakeholder perspectives, making them useful for energy planning and evaluating efficiency practices in manufacturing [3].

Previous studies have applied MCDM methods across industries. Ozturk et al. used a mix of CWM, WSM, and SRM for selecting techniques in the woolen textile industry [2]. Richter et al. applied PROMETHEE II to prioritize energy efficiency measures [3]. Banadkouki used Entropy Weight Method (EWM) and fuzzy TOPSIS for selecting strategies in the ceramic industry [4]. Mokhtar et al. combined AHP and TOPSIS for selecting measures in cement production [5]. Demirel et al. used PROMETHEE for selecting energy-saving measures in steam boilers [6].

Classical MCDM methods have their strengths but often struggle in complex scenarios. Combining these methods can overcome their limitations, enhancing decision-making efficiency [7]. A powerful hybrid approach is integrating the Decision-Making Trial and Evaluation Laboratory (DEMATEL) with the Analytic Network Process (ANP), forming DANP. DEMATEL helps in weighing interrelated criteria by visualizing and analyzing complex causal relationships, identifying critical factors within a system. When paired with ANP, this method effectively addresses weighting challenges involving interdependent criteria. DANP has been successfully applied in fields such as energy system analysis and low-carbon energy planning, showcasing its effectiveness in complex decision-making situations [8].

2 Methods

The framework of this study consists of three stages. First, developing evaluation criteria by literature review and expert judgement using Delphi method. Second, determining interrelationship and influence among the criteria by using the DEMATEL method. Finally, generating the weights of the criteria by integrating the DEMATEL and ANP method.

2.1 Delphi Method

This study involved a panel of five experts from three textile industries in Indonesia, utilizing a two-round Delphi method to validate evaluation criteria for energy efficiency practices [9]. In the first round, experts were given a questionnaire to rate each criterion on a 5-point Likert scale, from “1 = very irrelevant” to “5 = very relevant” [10], and were also encouraged to suggest additional criteria not listed in the questionnaire. The results from the first round were recorded and incorporated into the second-round questionnaire. In the second round, experts re-evaluated the criteria based on the feedback from the first round, including any newly suggested criteria. This process aimed to refine expert opinions and achieve consensus among the panel. In this study, consensus was defined as having an average expert rating of at least 4, or 80% agreement, for each criterion. This threshold was set to screen and validate the criteria effectively [11].

2.2 Integrating DEMATEL-ANP

DEMATEL

The DEMATEL method is applied to observe the interrelations between criteria [12]. The DEMATEL process can be outlined in the following steps:

1st step—Determine the average direct influence matrix.

The average direct influence matrix is used to capture the consensus among experts about the direct influences between criteria. Each expert evaluates the direct influence of one criterion on another using a rating system from ‘0 = no influence’ to ‘4 = very high influence’ [13]. This matrix is derived by averaging the evaluations of multiple experts, providing a balanced view of the direct relationships. These values are aggregated into an average matrix A , as shown in the following equations:

$$A = \begin{bmatrix} a_{11} & \cdots & a_{1j} & \cdots & a_{1n} \\ \vdots & & \vdots & & \vdots \\ a_{i1} & \cdots & a_{ij} & \cdots & a_{in} \\ \vdots & & \vdots & & \vdots \\ a_{n1} & \cdots & a_{nj} & \cdots & a_{nn} \end{bmatrix} \quad (1)$$

2nd Step, Determine the initial influence matrix.

Normalize the average matrix A by computing the aggregate all rows and columns in the initial average matrix, then identify the maximum sum value among all rows and columns. Finally, divide each element in the matrix by the maximum sum value to obtain the normalized direct-relation matrix X using Eqs. 2 and 3, ensuring that all diagonal elements are set to zero.

$$X = s \cdot A \quad (2)$$

$$s = \min \left[1/\max_i \sum_{j=1}^n a_{ij}, 1/\max_i \sum_{i=1}^n |a_{ij}| \right]. \quad (3)$$

3rd step—Generate the total influence matrix.

The total influence matrix is derived from the normalized direct-relation matrix. The total influence matrix T is calculated using the formula:

$$T = +X^2 + \cdots + X^k = X(I - X)^{-1} \quad (4)$$

where X is the normalized direct-relation matrix and I is the identity matrix.

Then, a threshold value is set to screen out negligible influences. Only values above this threshold are considered significant relationship.

4th step—Obtain the impact relation digraph.

By calculating sum of row and sum of column for the total matrix T , then obtain the impact relation digraph of the cluster and criteria.

$$R = (R_i)_{n \times 1} = \left[\sum_{j=1}^n t_{ij} \right]. \quad (5)$$

$$C = (C_i)_{n \times 1} = (C_j)_{1 \times n}' = \left[\sum_{i=1}^n t_{ij} \right]_{1 \times n}' \quad (6)$$

R_i denotes the sum of the i th row of matrix T , representing the total direct and indirect impact that criterion i has on other criteria. Similarly, C_i represents the sum of the j th column of matrix T , showing the total direct and indirect impact received by criterion j from other criteria. When $i = j$, the combined value of $(R_i + C_i)$ serves as an index of the total influence a criterion exerts and receives, indicating its central importance in the network. If $(R_i - C_i)$ is positive, it suggests that factor i is predominantly influenced by other factors.

Analytic Network Process (ANP)

ANP method as an extension of the Analytical Hierarchy Process (AHP) designed to overcome the limitations of a strict hierarchical structure in MCDM. The method would be explained as followed.

5th step—Determine the unweighted supermatrix of ANP.

The experts asked to rate the pairwise comparison matrix using a scale from “1 = equal importance” to “9 = extremely importance” [14], to determine the relative importance values among the criteria. The expert judgments aggregated into geometric mean by using Microsoft Excel. The geometric mean values input into the ANP network design based on total influence matrix of DEMATEL by using Super Decision software to generate the unweighted supermatrix of ANP as illustrated in Eq. 7. The consistency ratio (C.R.) of all the pairwise comparison also checked with Super Decision software and the results is below than 0.1 indicting consistent judgment.

$$W = \begin{bmatrix} W_{11} & W_{12} & \cdots & W_{1n} \\ W_{12} & W_{22} & \cdots & W_{2n} \\ \vdots & \vdots & \ddots & \vdots \\ W_{n1} & W_{n2} & \cdots & W_{nn} \end{bmatrix} \quad (7)$$

Integrating DEMATEL-ANP

6th step—Determine the weighted supermatrix of DEMATEL.

In this study, the θ -cut matrix is generated by applying a threshold value θ to the total influence matrix T . The threshold θ is calculated by averaging all elements of matrix T . Elements in matrix T that are below θ are set to zero, indicating a reduced influence on other criteria. The resulting matrix is known as the θ -cut matrix of the total influence matrix T_θ , as illustrated in Eq. 8.

$$T_\alpha = \begin{bmatrix} t_{11}^\alpha & \cdots & t_{ij}^\alpha & \cdots & t_{1n}^\alpha \\ \vdots & & \vdots & & \vdots \\ t_{i1}^\alpha & \cdots & t_{ij}^\alpha & \cdots & t_{in}^\alpha \\ \vdots & & \vdots & & \vdots \\ t_{n1}^\alpha & \cdots & t_{nj}^\alpha & \cdots & t_{nn}^\alpha \end{bmatrix} \quad (8)$$

where if $t_{ij} < \alpha$, then $t_{ij}^\alpha = 0$, or else $t_{ij}^\alpha = t_{ij}$, and t_{ij} within the total influence matrix, T . Then, normalize the θ -cut total influence matrix, T_α , by dividing by Eq. 9.

$$d_i = \sum_{j=1}^n t_{ij}^\alpha. \quad (9)$$

Thus, the θ -cut total-influence matrix could be normalized and represented as T_s .

$$T_s = \begin{bmatrix} t_{11}^\alpha/d_1 & \cdots & t_{ij}^\alpha/d_1 & \cdots & t_{1n}^\alpha/d_1 \\ \vdots & & \vdots & & \vdots \\ t_{i1}^\alpha/d_i & \cdots & t_{ij}^\alpha/d_i & \cdots & t_{in}^\alpha/d_i \\ \vdots & & \vdots & & \vdots \\ t_{n1}^\alpha/d_n & \cdots & t_{nj}^\alpha/d_n & \cdots & t_{nn}^\alpha/d_n \end{bmatrix} = \begin{bmatrix} t_{11}^s & \cdots & t_{ij}^s & \cdots & t_{1n}^s \\ \vdots & & \vdots & & \vdots \\ t_{i1}^s & \cdots & t_{ij}^s & \cdots & t_{in}^s \\ \vdots & & \vdots & & \vdots \\ t_{n1}^s & \cdots & t_{nj}^s & \cdots & t_{nn}^s \end{bmatrix}. \quad (10)$$

This research employs the normalized θ -cut total-influence matrix, T_s , and the unweighted supermatrix W in conjunction with Eq. 11, to obtain the weighted supermatrix W_w .

$$W_w = \begin{bmatrix} t_{11}^s \times W_{11} & t_{21}^s \times W_{12} & \cdots & \cdots & t_{n1}^s \times W_{1n} \\ t_{12}^s \times W_{21} & t_{22}^s \times W_{22} & & \vdots & \vdots \\ & \vdots & \cdots & t_{ji}^s \times W_{ij} & \cdots & t_{ni}^s \times W_{in} \\ & \vdots & & \vdots & & \vdots \\ t_{1n}^s \times W_{n1} & t_{2n}^s \times W_{n2} & \cdots & \cdots & t_{nn}^s \times W_{nn} \end{bmatrix}. \quad (11)$$

7th step—Limiting the supermatrix.

Raise the weighted supermatrix to successive powers until the matrix stabilizes and changes between iterations become negligible using Eq. 12. This process captures the long-term influences among elements. Then, the global priority vectors, also known as weights are generated.

$$\lim_{k \rightarrow \infty} W_w^k. \quad (12)$$

3 Results

3.1 The Expert Panel

This study involves five selected experts with extensive knowledge and experience in implementing energy efficiency practices in Indonesia’s textile industry. These experts work at three different textile companies in Bandung, West Java. Profile of the experts can be shown I Table 1.

Table 1 Profile of the experts

No	Position	Education	Experience	Company
1	Energy manager	Diploma degree	More than 20 years	Integrated textile company <ul style="list-style-type: none">– Fiber making– Yarn spinning– Fabric making (weaving, non-woven, knitting, dyeing and finishing)
2	Compliance manager	Master degree	More than 15 years	
3	Manager of environment, social, & governance (ESG) department	Bachelor degree	More than 25 years	Fabric making textile company <ul style="list-style-type: none">– Weaving– Dyeing and finishing
4	Manager of engineering department	Bachelor degree	More than 20 years	
5	Manager of utility and maintenance department	Bachelor degree	More than 10 years	Textile company <ul style="list-style-type: none">– Dyeing and finishing fabric– Garment

3.2 Evaluation Criteria

The evaluation criteria based on two rounds Delphi method are shown in Table 2.

Table 2 Evaluation criteria for evaluating energy efficiency practices

Cluster	Criteria	References
A. Energy	A1. Potential energy savings	[3, 5, 6]
	A2. Energy consumption reduction	[2, 4]
B. Economy	B1. Potential of economic saving	[2, 6]
	B2. Implementation cost	[2–6]
	B3. Operation and maintenance cost	[3, 6]
	B4. Payback period	[3, 5, 6]
	B5. Energy price	Expert opinion
C. Environmental	C1. Reduction of emission	[3]
	C2. Reduction of waste	[3]
	C3. Environmental benefit	[3]
D. Technical	D1. Technical applicability	[2, 3, 5, 6]
	D2. Technology accessibility	[6]
	D3. Adjustment level with existing equipment	[4, 5]
	D4. Implementation time	[4, 5]
	D5. Monitoring system	Expert opinion

3.3 Interrelationship Among the Criteria

Impact Relation Diagram

Based on Fig. 1, which shows the causal-effect relationships between clusters, the energy and technical clusters are the causing clusters with positive ($R_i - C_i$) values. On the other hand, the economy and environmental clusters are the affected clusters with negative ($R_i - C_i$) values. Figure 2 shows that technology accessibility (D3) and implementation time (D4) are the main causing criteria, while potential economic savings (B1), implementation/investment cost (B2), and payback period (B4) are the most affected criteria.

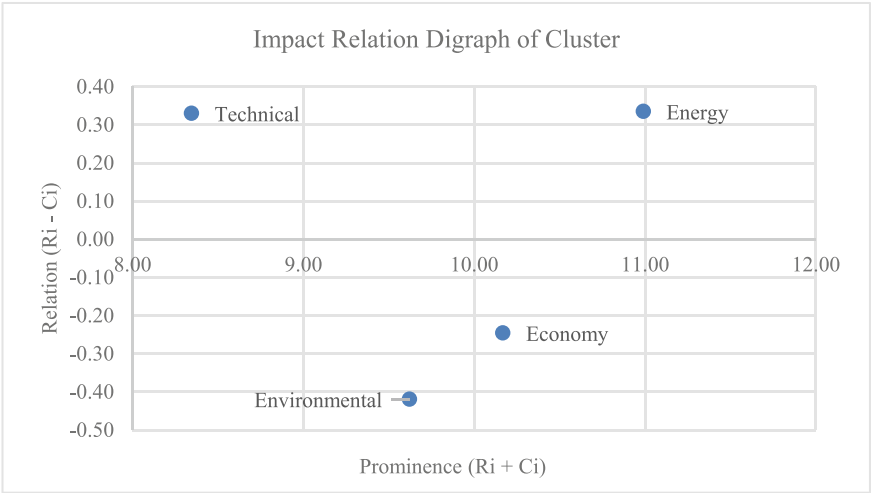


Fig. 1 Impact relation digraph of cluster

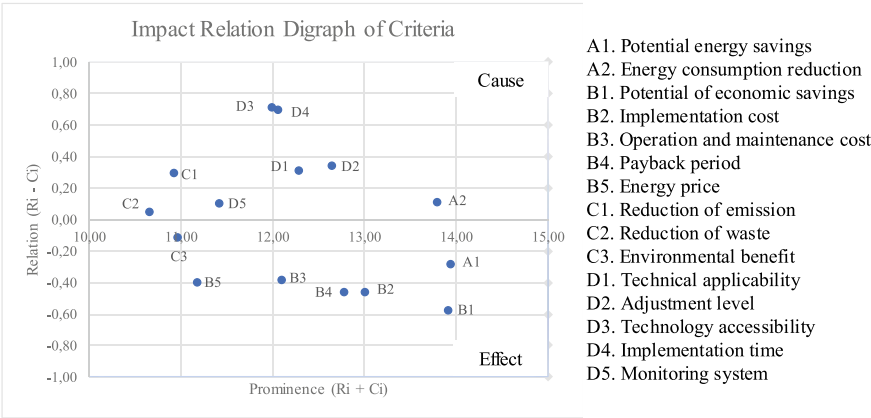


Fig. 2 Impact relation digraph of criteria

3.4 Weights of the Criteria

The weights of the criteria generated by integrating DEMATEL-ANP method as shown in Table 3. The results show a detailed prioritization of the clusters and criteria within an assessment framework. Technical factors emerge as the most critical, commanding the highest cluster weight of 0.3830. Among the technical criteria, ‘Technical applicability,’ ‘Technology accessibility,’ and ‘Implementation time’ are notably significant, ranking sixth, fifth, and fourth overall, respectively. Economic factors follow closely, with a cluster weight of 0.3340, underscoring their substantial

Table 3 The weights of cluster and criteria

Cluster	Weight	Criteria	Weight
A. Energy	0.1629	A1. Potential of energy savings	0.08148
		A2. Energy consumption reduction	0.08138
B. Economy	0.3340	B1. Potential of economic savings	0.08099
		B2. Implementation cost	0.07707
		B3. Operation and maintenance cost	0.07180
		B4. Payback period	0.06406
		B5. Energy price	0.04004
C. Environmental	0.1202	C1. Reduction of emission	0.04016
		C2. Reduction of waste	0.04004
		C3. Environmental benefit	0.03995
D. Technical	0.3830	D1. Applicability	0.07702
		D2. Adjustment level	0.07585
		D3. Technology accessibility	0.07902
		D4. Implementation time	0.07926
		D5. Monitoring system	0.07188

influence. Within this cluster, the ‘Potential of economic savings’ stands out as the most critical economic criterion and the third most important overall.

4 Discussion

The results highlight the weights of clusters and criteria within the assessment framework, identifying technical and economic factors as the most critical, with weights of 0.3830 and 0.3340, respectively. Key technical criteria include ‘Technical applicability,’ ‘Technology accessibility,’ and ‘Implementation time,’ underscoring the importance of robust technical capabilities and innovations for enhancing energy efficiency. Economic factors also play a significant role, with ‘Potential of economic savings’ being the most critical criterion, followed by ‘Implementation cost’ and ‘Operation and maintenance cost,’ emphasizing the financial aspects of adopting energy efficiency practices.

These findings align with Richter et al. (2023), who also identified economy and technical aspects as significant factors, highlighting ‘payback period’ and ‘cost of implementation’ as crucial economic criteria, and ‘ease of implementation’ and ‘probability of success/acceptance’ as key technical criteria [3]. Similarly, Banadkoui (2023) found that the ‘cost of implementation’ is essential for energy efficiency measures [4]. Given the high importance of technical and economic factors, there is a clear need for government support. Policies and incentives, such as funding for

research and development, subsidies for energy-efficient technologies, and financial incentives for companies achieving significant energy savings, can facilitate the implementation of energy efficiency measures.

5 Conclusions

Evaluating energy efficiency practices in the industry is a complex challenge due to multi-dimensional and often conflicting criteria. This study identified common evaluation criteria from literature, and through expert judgment using the Delphi method, a final list of 15 criteria was developed, providing decision-makers in the textile industry with a comprehensive and validated tool to enhance energy efficiency.

The study also explored the interrelationships among these criteria using expert perceptions to reflect real-world scenarios. By employing the DEMATEL method, the study mapped the relationships and influences among the criteria, creating a network relation map. Criteria within the clusters of energy, economy, and technical aspects showed significant interrelations and feedback, while the environmental cluster mainly interacted with the energy cluster, influencing potential energy savings in the economy cluster but not significantly interacting with the technical cluster.

In the final step, the study aimed to generate weights for the criteria to identify the most critical factors for implementing energy efficiency practices in the textile industry. By integrating DEMATEL and ANP methods, the relative importance of each criterion was determined based on expert judgments. The results highlighted that the potential for energy savings, reduction in energy consumption, and economic savings were the top three most important criteria, while energy price, waste reduction, and environmental benefits were the least important.

6 Future Research

Despite the rigorous methods used in this study, some limitations should be addressed in future research. Firstly, the expert panel was composed of professionals with practical experience in energy efficiency within the textile industry. Including a more diverse panel with members from academia, research institutions, or energy conservation consultancy could broaden perspectives and enhance evaluation objectivity. Secondly, the study heavily relied on expert opinions, which can be influenced by incomplete information and inherent uncertainty. Future research could incorporate fuzzy concepts or a fuzzy linguistic scale to better capture and represent this subjective uncertainty.

References

1. Dewi RG, Parinderati R, Hendrawan I, Dewantoro MWB, Bayuwega WD (2019) Energy efficiency monitoring in textile industries to achieve GHG emissions reduction target in Indonesia. In: IOP conference series: earth and environmental science, vol 363, no 1. IOP Publishing, p 012019
2. Ozturk E, Cinperi NC, Kitis M (2020) Improving energy efficiency using the most appropriate techniques in an integrated woolen textile facility. *J Clean Prod* 254:120145
3. Richter B, Marcondes G, Monteiro N, Costa SE, Loures E, Deschamps F, Lima E (2023) Industrial energy efficiency assessment and prioritization model-an approach based on multi-criteria method PROMETHEE. *Int J Sustain Energy Plan Manag* 37:41–60
4. Banadkouki MRZ (2023) Selection of strategies to improve energy efficiency in industry: a hybrid approach using entropy weight method and fuzzy TOPSIS. *Energy* 279:128070
5. Mokhtar A, Nasooti M (2020) A decision support tool for cement industry to select energy efficiency measures. *Energy Strat Rev* 28:100458
6. Demirel YE, Simsek E, Ozturk E, Kitis M (2021) Selection of priority energy efficiency practices for industrial steam boilers by PROMETHEE decision model. *Energy Effic* 14(8):89
7. Esmael Nezhad A, Nardelli PH (2022) Multiple-Criteria Decision-Making (MCDM) applications in optimizing multi-objective energy system performance. In: *Handbook of smart energy systems*, pp 1–32.
8. Lin R, Ren J (2021) Overview of multi-criteria decision analysis and its applications on energy systems. In: *Energy systems evaluation. Multi-criteria decision analysis*, vol 2. Springer International Publishing, Cham, pp 1–26
9. Clemen RT, Winkler RL (1999) Combining probability distributions from experts in risk analysis. *Risk Anal* 19:187–203
10. Krosnick JA, Fabrigar LR (1997) Designing rating scales for effective measurement in surveys. In: *Survey measurement and process quality*, pp 141–164; Gustafson DH, Shukla RK, Delbecq A, Walster GW (1973) A comparative study of differences in subjective likelihood estimates made by individuals, interacting groups, Delphi groups, and nominal groups. *Organ Behav Hum Perform* 9(2):280–291
11. Diamond IR, Grant RC, Feldman BM, Pencharz PB, Ling SC, Moore AM, Wales PW (2014) Defining consensus: a systematic review recommends methodologic criteria for reporting of Delphi studies. *J Clin Epidemiol* 67:401–409
12. Tzeng GH, Huang JJ (2011) *Multiple attribute decision making: methods and applications*. CRC Press
13. Liou JJ, Tzeng GH, Chang HC (2007) Airline safety measurement using a hybrid model. *J Air Transp Manag* 13(4):243–249
14. Saaty TL (2008) The analytic hierarchy and analytic network measurement processes: applications to decisions under risk. *Eur J Pure Appl Math* 1(1):122–196

Barrier Model Development for Industry 4.0 Technologies Adoption in Small-to-Medium Food and Beverage Industry in Indonesia



Arif Nurrahman, Nur Faizatus Sa'idah, Hui-Chih Hung,
and Iwan Inrawan Wiratmadja

Abstract Adopting Industry 4.0 technology is anticipated to enhance industry efficiency, productivity, and product customization. Nevertheless, this transition may induce significant alterations to corporate systems, presenting numerous challenges that industries must navigate during implementation, especially for small-to-medium industries. Hence, this study examines the interrelationships among barriers and identify the critical obstacles to implementing Industry 4.0 in small-to-medium industries within the food and beverage sector in Indonesia. To achieve this, an integrated methodology combining the Delphi Method, Interpretive Structural Modeling (ISM), and Matrix Impact with Cross Multiplication Applied to Classification (MICMAC) analysis is employed. The barriers to Industry 4.0 implementation are conceptualized using the Technology-Organization-Environment (TOE) framework. This study found that the MICMAC analysis supports the model derived from the ISM results. Insufficient government support, the need for investment, insufficient Industry 4.0 training, and insufficient standardization efforts are critical barriers that are located in the independent cluster according to the MICMAC analysis and are positioned at high levels in the ISM model.

Keywords Barrier · Industry 4.0 · Delphi method · Interpretive Structural Modeling (ISM) · MICMAC analysis

A. Nurrahman (✉) · N. F. Sa'idah · I. I. Wiratmadja
Institut Teknologi Bandung, Bandung, West Java, Indonesia
e-mail: rahman.arifn@gmail.com

H.-C. Hung
National Yang Ming Chiao Tung University, Hsinchu City, Taiwan

1 Introduction

The Indonesian government has prioritized enhancing industrial productivity and efficiency by adopting Industry 4.0 technologies. To this end, Indonesia has formulated a strategic initiative known as “Making Indonesia 4.0,” which serves as a comprehensive roadmap for navigating the complexities of the Fourth Industrial Revolution [1]. This initiative aims to equip Indonesia with the capabilities necessary to leverage the transformative opportunities of Industry 4.0. Notably, the food and beverage sector, predominantly comprising small-to-medium industries, is identified as a key priority sector for the implementation of Industry 4.0 technologies. However, this sector encounters significant challenges, including elevated logistics costs and inadequate cold chain infrastructure, which contribute to food spoilage and loss [1]. Moreover, the industry is burdened by the short shelf life of raw materials and products and is highly vulnerable to hygiene-related issues during production processes [1].

Implementing Industry 4.0 has the potential to significantly improve productivity, maintain competitive value, enhance knowledge, facilitate work collaboration, improve cost-effectiveness, preserve flexibility and speed, and uphold or enhance quality [2]. Nonetheless, its application will lead to significant alterations in the industry’s operational systems. As a result, industries will encounter numerous challenges during its implementation especially for small-to-medium industries. Small-to-medium industries struggle to implement Industry 4.0 because of the challenges in complexity for combining human workers and these new technologies effectively [3]. Lack of stakeholder support and inadequate managerial support are significant factors overlooked by small-to-medium industries in India [4].

Previous studies have provided empirical evidence regarding the challenges that hinder the adoption of Industry 4.0 technologies in small-to-medium industries [5]. However, the reliance on a narrow methodological framework, particularly the use of Focus Group Discussions, may introduce biases. These biases can arise from the influence exerted by the moderator or the dominance of certain participants, potentially leading to skewed findings. Furthermore, the intricate interrelationships among the factors impeding Industry 4.0 adoption have not been thoroughly explored. Although several studies have attempted to establish hierarchical relationships within the Indian manufacturing sector [6, 7], they often fail to distinguish between large industries and small-to-medium industries, which may result in different obstacles being identified. Moreover, these studies are not industry-specific, limiting the generalizability of their findings to other environmental contexts [8].

Further studies have explored the integration of sustainability and Industry 4.0 within barrier and interaction models for small-to-medium industries in the automotive industry [9]. However, these studies did not employ a comprehensive adoption theory framework, such as the Technology-Organization-Environment (TOE) framework. Consequently, the systematic examination of technological, organizational, and environmental factors influencing the adoption of Industry 4.0 may be constrained. Traditional adoption models, such as the Technology Acceptance Model (TAM) and the Theory of Reasoned Action (TRA), predominantly focus on

the technological factors affecting an organization's structure and behavior [10]. In contrast, the TOE framework underscores the significance of social and environmental factors, providing a more holistic perspective that enhances the understanding of an organization's overall context and technological attributes [11].

Therefore, this research is designed to identify the interrelationships among the barriers and determine the critical barrier to Industry 4.0 implementation for small-to-medium industries in the food and beverage sector, utilizing the TOE framework. In this study, integration of multi criteria decision-making methods such as the Delphi method, ISM method (Interpretive Structural Modeling) and MICMAC (Matrix Impact of Cross Multiplication Applied to Classification) analysis are employed.

2 Literature Review

2.1 Technology Adoption Using TOE Framework

Adoption theory framework provides comprehensive perspective on the challenges and factors affecting an organization's adoption processes by including environmental constructs. Technology-Organization-Environment framework (TOE) is aimed at studying technological innovation in the context of organizations [10]. The technological context refers to the technological advancements that are significant for industry, including the technologies that are already available in the market. The organizational context refers to the internal characteristics and resources of a firm. Environmental context encompasses the external factors that have the potential to influence the firm's adoption of technology.

2.2 Barrier Model Development

Barrier is defined as a significant obstacle that hinders or obstructs the process of technology adoption to the extent that it significantly hampers or disrupts it [12]. Barrier factors from Elhusseiny and Crispim work [13], Senna et al. work [10] are utilized to determine the barriers for this research. The barrier factors from Elhusseiny and Crispim work [13] are included as basic model because it represents small-to-medium industries barriers to implementing Industry 4.0 in developing countries using PRISMA for a systematic review of quantitative information. The additional barrier factors from Senna et al. work [10] are utilized because to their thorough coverage of environmental barriers and some extra barriers that are not addressed in other models. Additionally, Portugal Industries are dominated by small-to-medium industries, which is similar to the manufacturing condition in Indonesia.

3 Research Methodology

The methodology employed to examine the obstacles to Industry 4.0 adoption in manufacturing organizations involves several distinct stages, as illustrated in Fig. 1. The study employed a two-stage questionnaire process. The first stage, using the Delphi method in two iterations, aimed to identify and refine the barrier factors. The second stage focused on determining the interrelationships and identifying critical barrier factors through ISM-MICMAC analysis.

3.1 Data Collection

Experts selected for the Delphi method and ISM-MICMAC analysis were required to have a minimum of five years of experience in the manufacturing sector and

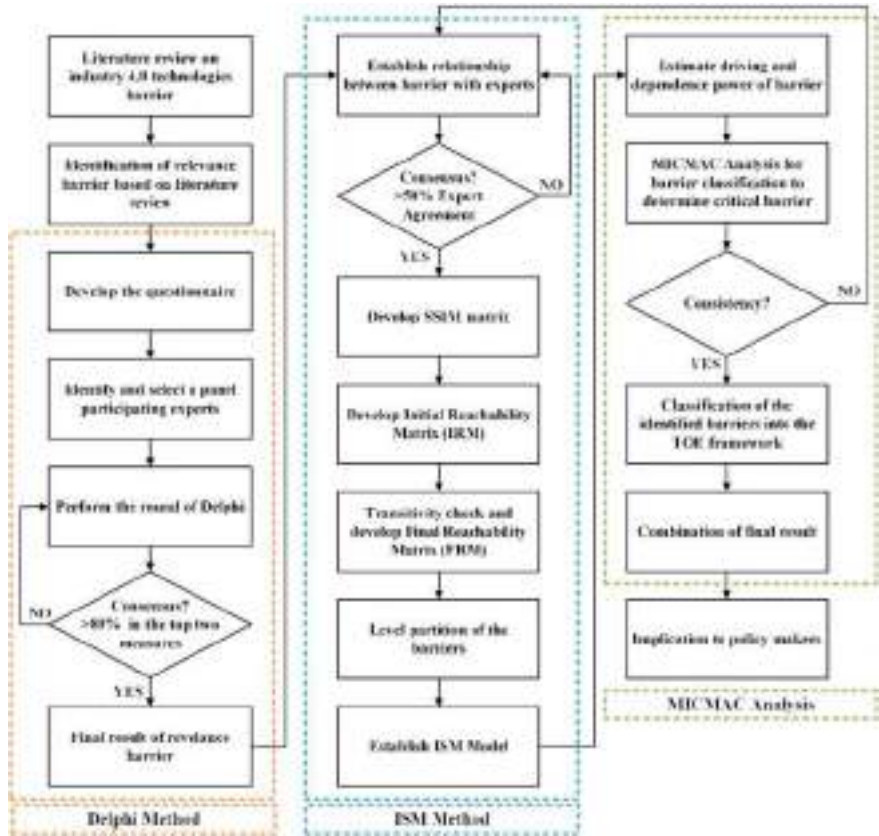


Fig. 1 Research methodology

substantial knowledge of Industry 4.0 concepts, demonstrated through engagement in seminars, research, or other relevant activities. The Delphi method involved 7 experts, while the ISM-MICMAC analysis included 11 experts, representing small-to-medium food and beverage industries, government, and technology consultants.

3.2 Delphi Method for Determining Barrier Factors

The Delphi method, a structured group technique, was chosen for its ability to achieve consensus among diverse experts. This approach involves anonymous feedback, multiple rounds of questioning, and the option for participants to revise their opinions based on the input of others [14].

Initially, 19 barrier factors for implementing Industry 4.0 are chosen for this research. Moreover, some experts were done to verify the relevance level of barrier factors using 5 Likert scale. Furthermore, they were allowed to add or remove some barrier whom they thought did not relate to the study. Barrier with more than 80% on the 5-Point Likert scale in the top two measures (relevant and very relevant) is considered to have consensus, warranting further discussion in the second phase of the Interpretive Structural Modeling (ISM) questionnaire [15].

According to the Delphi method results, 12 barriers were identified as follows:

- Technological barrier include insufficient knowledge of management systems and data knowledge (B1), risks to cybersecurity in industry 4.0 deployments (B2), inadequate incorporation and compatibility of technologies (B3).
- Organizational barrier include lack of qualified talent (B4), need for investment (B5), absence of a digital roadmap (B6), insufficient research and improvement efforts (B7), insufficient industry 4.0 training (B8).
- Environmental barrier include insufficient Government support (B9), insufficient standardization effort (B10), insufficient digital infrastructure (B11), insufficient legal and contractual guarantees (B12).

3.3 ISM-MICMAC Methodology for Determining the Interrelation Among Barrier and Critical Barrier

Interpretive Structural Modeling (ISM) is a tool that help visualize the connections between different factors involved in a complex issue [10]. The process includes the following steps based on Senna work [10]. Final Reachability Matrix shown in Table 1.

Examining a set of factors or elements based on their driving and dependency strengths is typically conducted using MICMAC (Matrix Impact of Cross Multiplication Applied to Classification) analysis [10]. A driving-dependency power chart is created based on Final Reachability Matrix and classify barrier factors into four

Table 1 Final Reachability Matrix (FRM)

		B[j]												Driving power
		12	11	10	9	8	7	6	5	4	3	2	1	
B[i]	1	1*	1*	0	0	0	1	1	0	1*	1*	1*	1	8
	2	0	0	0	0	0	0	0	0	0	0	1	0	1
	3	0	0	0	0	0	1	1*	0	0	1	0	1	4
	4	1*	1*	0	0	0	1	1	0	1	1	1	1	8
	5	1	1	1	0	1	1	1	1	1	1	1	1	11
	6	1	1	0	0	0	1	1	0	1	1	1	1	8
	7	0	0	0	0	0	1	0	0	0	0	0	0	1
	8	1	1*	0	0	1	1	1	0	1	1	1	1	9
	9	1	1	1	1	1	1	1	1	1	1	1	1	12
	10	1	1	1	0	0	1	1	0	1*	1	1	1	9
	11	1*	1	0	0	0	1	1	0	1*	1	1	1	8
	12	1	1*	0	0	0	1	1	0	1*	1	1	1*	8
Dependence power		9	9	3	1	3	11	10	2	9	10	10	10	87

distinct groups, which are represented by the autonomous, dependent, linkage, and independent groups. The autonomous group and the dependent group typically manifest at a low level in the model of ISM. Conversely, the linkage and independent groups typically arise at the high level from model of ISM.

4 Result and Discussion

The ISM-based model was formed by organizing the 12 barriers based on the findings of level partitioning and linking them according to the Final Reachability Matrix. Figure 2 describes the barriers at different levels in the ISM model, offering valuable insights into their influence on the adoption of Industry 4.0 technology. The model of ISM consists of six distinct levels of obstacles. Barrier factors at lower levels represent outcomes that are impacted by various factors identified at higher levels. Some of the barriers in the environment group are situated at higher levels which have higher importance and relevance to the implementation of Industry 4.0 technologies. Barriers from the organization group are present at almost every level except level 6, indicating that the organizational barrier significantly influences this ISM model. Barriers from the technology group are positioned at lower levels, specifically at levels 1 and 2, indicating a high dependence on other barriers.

Based on the ISM model, the insufficient government support (B9), which is an environmental barrier, is significant in terms of its influence on drive and dependency power. This finding supports previous research [10], which indicates that barriers

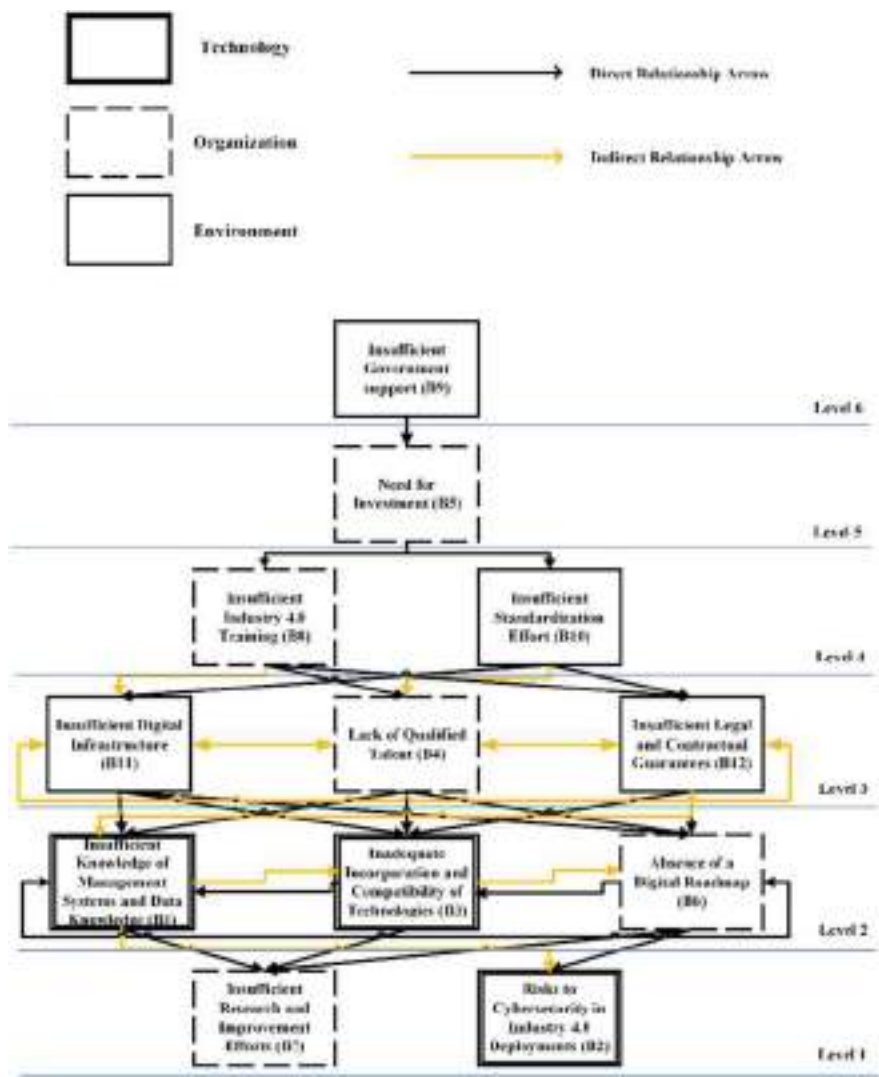


Fig. 2 ISM's model of barriers on adopting Industry 4.0 technologies

from the environment group hold the highest importance due to their low dependency and high driving power. The barrier factor at the highest level, which is level 6, needs to be solved first. Following this, the barrier factors in level 5, which represent the need for investment (B5), and level 4, which represent insufficient industry 4.0 training (B8) and insufficient standardization effort (B10), also need to be addressed as they are at high levels. To identify the critical barrier that needs to be prioritized and addressed initially in the implementation of Industry 4.0 technologies, the MICMAC analysis chart was created based on Final Reachability Matrix as shown in Fig. 3.

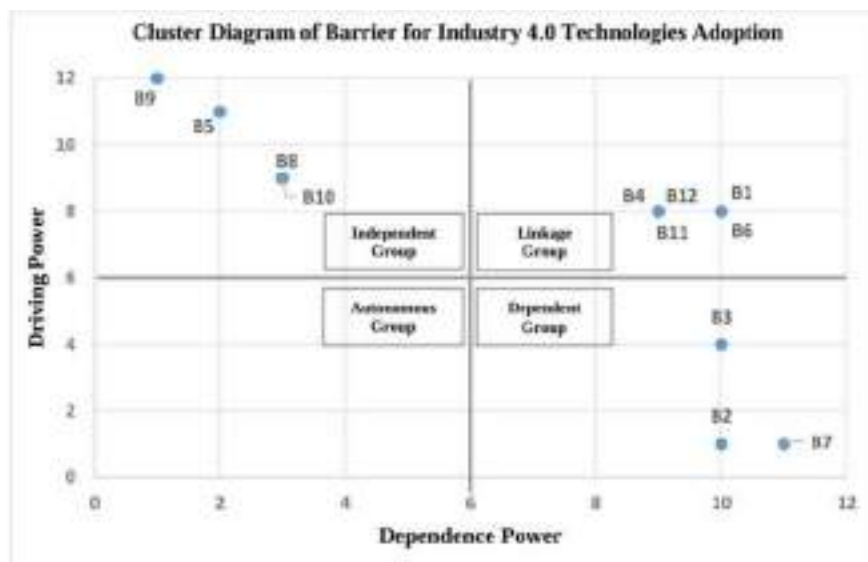


Fig. 3 MICMAC analysis chart result

There are no barriers present within the autonomous group which is distinguished by its low driving and dependence power. This suggests that all barriers have a substantial impact on one another, and none exist in isolation inside the system. This finding also strengthens the Delphi method's results, which identify relevant barriers for Industry 4.0 implementation. There are four barriers in an independent group which are considered as critical barriers. Based on the ISM-MICMAC methodology, MICMAC analysis results support the model from ISM result. Insufficient government support (B9), need for investment (B5), insufficient Industry 4.0 training (B8), and insufficient standardization effort (B10) are critical barriers, that are in the independent group (high driving power, low dependency) in cluster diagram from MICMAC analysis and positioned at high levels (level 6, level 5, level 4) in the ISM model. The study contributed to the existing body of literature by enhancing and expanding the understanding of the emerging role of Industry 4.0 within small-to-medium industries, through the development of a framework addressing the adoption barriers of Industry 4.0 technologies [4, 9, 10, 16].

Government support such as incentive and policy plays a crucial role as barrier for small-to-medium industries toward Industry 4.0. In a similar vein, the insufficient governmental assistance as a significant obstacle hindering the India small-to-medium industries ability to embrace Industry 4.0 in a sustainable manner [4, 9]. This finding aligns with research from Rahman [16], which concluded that high investment costs have significantly hindered the adoption of Industry 4.0 technologies in the food and beverage industry in Bangladesh. The adoption of Industry 4.0 technologies by small-to-medium industries is heavily dependent on the availability of funds to invest in new technologies, conduct research and development in digitalization,

and educate individuals with digital skills [16]. Insufficient training highlights the need for management to carefully develop, implement, and plan strategies that guide decisions related to workforce resources and hiring, in order to support the digital transformation of small-to-medium industries. This conclusion aligns with previous studies by Kumar [9]. Regarding to insufficient of standardization, small-to-medium food and beverage industries face challenges due to insufficient preparation in information technology and operations technology, specifically in terms of the absence of standardized information technology and operational technology systems, as well as the absence of integrated back-end systems [10].

According to the ISM-MICMAC results, several recommendations have been developed to overcome barriers to implementing Industry 4.0 technologies for small-to-medium industries in the food and beverage sector in Indonesia. The recommendations are specifically for Ministry of Industry of Republic of Indonesia as follows:

- Providing incentives for small-to-medium industries (such as tax reduction, technology subsidy) and facilitate digital infrastructure improvements.
- Collaborating with academic institutions to enhance education and research initiatives tailored specifically for small-to-medium industries.
- Promoting the establishment of standards for Industry 4.0 technologies by involving industries and third parties or technical bodies, such as consultants or technology providers.

5 Conclusion and Future Research

The findings of this study conclude that strategic priorities for small-to-medium industries food and beverage industries in Indonesia, particularly those facing environmental barriers such as inadequate government support and insufficient standardization efforts, as well as organizational barriers like the need for greater investment and training in Industry 4.0, are crucial for effectively overcoming technological challenges. However, this study specifically focuses on small-to-medium industries, and the barriers identified may differ from those encountered in other sectors. The scope of this study could be extended to explore the feasibility of implementing Structural Equation Modeling with an increased sample size within the Indonesian context, thus statistically validating the developed model.

Acknowledgements The author expresses gratitude for the financial support provided by the Ministry of Industry of the Republic of Indonesia through a scholarship. We would like to express our gratitude to the small-to-medium concrete pole industries and other relevant parties who participated in this study.

References

1. Ministry of Industry of Republic Indonesia: Making Indonesia 4.0 (2018) https://bsn.go.id/uploads/download/making_indonesia_4.0_-_kementerian_perindustrian.pdf. Accessed 20 Dec 2023
2. Costa F, Freccasetti S, Rossini M, Portioli-Staudacher A (2023) Industry 4.0 digital technologies enhancing sustainability: applications and barriers from the agricultural industry in an emerging economy. *J Clean Prod* 408:137208
3. Ushada M, Trapsilawati F, Amalia R, Putro NAS (2024) Modeling trust decision-making of Indonesian food and beverage SME groups in the adoption of Industry 4.0. *Cybern Syst* 55:534–550
4. Goel P, Kumar R, Banga HK, Kaur S, Kumar R, Pimenov DY, Giasin K (2022) Deployment of interpretive structural modeling in barriers to Industry 4.0: a case of small and medium enterprises. *J Risk Financ Manag* 15
5. Orzes G, Rauch E, Bednar S, Poklemba R (2019) Industry 4.0 implementation barriers in small and medium sized enterprises: a focus group study. In: *IEEE international conference on industrial engineering and engineering management*, December 2019, pp 1348–1352
6. Kumar P, Bhamu J, Sangwan KS (2021) Analysis of barriers to Industry 4.0 adoption in manufacturing organizations: an ISM approach. *Procedia CIRP* 98:85–90
7. Kamble SS, Gunasekaran A, Sharma R (2018) Analysis of the driving and dependence power of barriers to adopt industry 4.0 in Indian manufacturing industry. *Comput Ind* 101:107–119
8. Dutta G, Kumar R, Sindhwani R, Singh RK (2020) Digital transformation priorities of India's discrete manufacturing SMEs – a conceptual study in perspective of Industry 4.0. *Compet Rev* 30:289–314
9. Kumar S, Raut RD, Aktas E, Narkhede BE, Gedam VV (2023) Barriers to adoption of industry 4.0 and sustainability: a case study with SMEs. *Int J Comput Integr Manuf* 36:657–677
10. Senna PP, Ferreira LMDF, Barros AC, Bonnín Roca J, Magalhães V (2022) Prioritizing barriers for the adoption of Industry 4.0 technologies. *Comput Ind Eng* 171
11. Awa HO, Ukoha O, Emecheta BC (2016) Using T-O-E theoretical framework to study the adoption of ERP solution. *Cogent Bus Manag* 3:1–23
12. Justy T, Pellegrin-Boucher E, Lescop D, Granata J, Gupta S (2023) On the edge of big data: drivers and barriers to data analytics adoption in SMEs. *Technovation* 127
13. Elhusseiny HM, Crispim J (2021) SMEs, barriers and opportunities on adopting Industry 4.0: a review. *Procedia Comput Sci* 196:864–871
14. Clyne B, Sharp MK, O'Neill M, Pollock D, Lynch R, Amog K, Ryan M, Smith SM, Mahtani K, Booth A, Godfrey C, Munn Z, Tricco AC (2024) An international modified Delphi process supported updating the web-based “right review” tool. *J Clin Epidemiol* 170:111333 (2024)
15. von der Gracht HA (2012) Consensus measurement in Delphi studies. Review and implications for future quality assurance. *Technol Forecast Soc Change* 79:1525–1536
16. Rahman M, Emon MEH, Antor MH, Haque SA, Talapatra S (2024) Identification and prioritization of barriers to Industry 4.0 adoption in the context of food and beverage industries of Bangladesh. *Benchmarking*

Study of Sintering Effects on Grain Size of Al-Doped ZnO/Graphene Nanoparticles via Microwave-Assisted Sol–Gel Method



Karthikraj A. L. Nithyanantham, Suraya Sulaiman,
Wan Fahmin Faiz Wan Ali, Izman Sudin, and Ramli Junid

Abstract The advancement of thermoelectric materials is vital for efficient energy conversion. However, reducing thermal conductivity and maintaining the electrical properties is still challenging and limits the overall thermoelectric material's efficiency. This study investigates the impact of the sintering effect on the grain size of Al-doped ZnO/Graphene nanoparticles via the microwave-assisted sol–gel method. The composition of the materials was confirmed using X-ray diffraction (XRD) and energy-dispersive X-ray spectroscopy (EDX), including the successful integration of Graphene. Field emission scanning electron microscopy (FESEM) revealed the critical role of sintering at 1100 °C, which reduced the particle sizes of Zinc Oxide to 392.987 nm and Aluminum to 48.57 nm. This reduction in particle size is essential for decreasing thermal conductivity and optimizing the figure of merit (ZT) values. Furthermore, this approach not only enhances thermoelectric properties but also preserves the stable morphology of Graphene, ensuring consistent electrical conductivity. These findings suggest that this method promises improved performance and higher ZT values, marking a significant step forward in thermoelectric material development. Future applications may benefit from these enhanced properties, leading to more efficient energy conversion systems.

Keywords Al-doped ZnO · ZnO nanoparticles · Nanostructuring · Sol–gel synthesis

K. A. L. Nithyanantham · S. Sulaiman (✉) · R. Junid
Faculty of Manufacturing and Mechatronic Engineering Technology, Universiti Malaysia Pahang
Al-Sultan Abdullah, Pekan, Pahang, Malaysia
e-mail: surayas@ump.edu.my

S. Sulaiman · W. F. F. W. Ali · I. Sudin
Faculty of Mechanical Engineering, University Teknologi Malaysia, Skudai, Johor, Malaysia

1 Introduction

Thermoelectric materials represent a pivotal technology in the realm of sustainable energy, enabling the direct conversion of waste heat into electrical power—a process vital for reducing energy losses and enhancing overall efficiency in various industrial and domestic applications. Central to the functionality of these materials is the dimensionless figure of merit, ZT , which quantifies their thermoelectric efficiency [1].

However, several challenges hinder thermoelectric performance, including material development, structural improvements, temperature management, heat transfer efficiency, contact resistance, and geometric constraints [2, 3]. Current technologies, such as electrochemical supercapacitors, struggle with low specific surface area and inadequate electrical conductivity of materials like zinc oxide, limiting their effectiveness in thermoelectric applications. Additional hurdles include low efficiency, high production costs, thermal limitations, toxicity concerns, and resource scarcity [3].

While abundant and economical, zinc oxide (ZnO) has historically exhibited limitations in achieving high thermoelectric efficiencies, typically falling below 0.52 at 1100 K [1]. To overcome these challenges, recent research has focused on enhancing ZnO by doping it with aluminium [4] and integrating graphene [1], strategies aimed at boosting its ZT value. Aluminium doping optimises the charge carrier concentration and mobility within the material, thereby enhancing its electrical conductivity and thermoelectric efficiency [5]. Meanwhile, the incorporation of graphene not only stabilizes the material's structure but also contributes to improved thermal and electrical transport properties, increases electron density and reduces lattice thermal conductivity [1, 6, 7].

Nanostructuring and doping are effective strategies for enhancing the thermoelectric properties of ZnO materials by manipulating their crystalline structure and particle size. Reducing the grain size through nanostructuring techniques can reduce thermal conductivity by increasing phonon scattering at grain boundaries [8]. Doping techniques, particularly aluminium enhance thermoelectric materials by increasing electrical conductivity and reducing thermal conductivity [8, 9]. This approach involves application introducing impurities into the material lattice to alter its electronic properties. These approaches collectively optimise ZnO-based materials for efficient thermoelectric applications, particularly in high-temperature waste heat recovery [9, 10].

The sintering process is a crucial step in fabricating Al-doped ZnO/graphene bulk samples. This step enhances the relative density, increases electrical conductivity, decreases thermal conductivity and reduces porosity [1]. Proper sintering conditions ensure a finer and denser material that improves the charge carrier mobility and reduces phonon scattering, leading to higher ZT values [11].

This study specifically investigates the synthesis and sintering effects of Al-doped ZnO/graphene nanoparticles to enhance thermoelectric performance. This study aims to synthesize Al-doped ZnO/graphene nanostructures using microwave irradiation

and calcination conditions to achieve high crystallinity and phase purity. Investigations continue to assess the impact of sintering temperature and duration on the microstructure, densification, and phase stability of the synthesized composites. This research aims to provide valuable insights for enhancing ZnO-based thermoelectric materials, thereby advancing the development of more efficient energy conversion technologies.

2 Experimental Methods

The study aims to enhance the thermoelectric properties of zinc oxide (ZnO) by incorporating 0.02 at% aluminium and 1.5 wt% graphenes. The synthesis method involves a sol-gel process followed by microwave irradiation heating, calcination and sintering process. Zinc acetate dihydrate was dissolved in ethanol under continuous stirring at room temperature. Next, aluminium acetate is added to the solution and stirred until dissolved. Sodium hydroxide is added to adjust pH 6–6.5, aiding in the formation of thick gels. These gels were irradiated at 800 W for 2 min to form a precursor powder. The resulting powder was crushed, sieved and calcinated at 800 °C for 1 h. After that, Al-doped ZnO powder was pelletized and sintered at temperatures 950, 1100, and 1150 °C. Figure 1 shows the schematic diagram of the synthesis procedure and the properties of the materials used are summarized in Table 1. The synthesized Al-doped ZnO/Graphene powders were characterized using X-ray Diffraction (XRD), Field Emission Scanning Electron Microscopy (FESEM) and Energy-Dispersive X-ray Spectroscopy (EDX).

The hydrolysis and condensation of zinc acetate dihydrate, aluminium acetate and sodium hydroxide to form Al-doped ZnO is shown in Eq. (1). Zinc acetate dihydrate and aluminium acetate reacts with sodium hydroxide to form zinc hydroxide and aluminium hydroxide which decomposes into zinc oxide and aluminium oxide

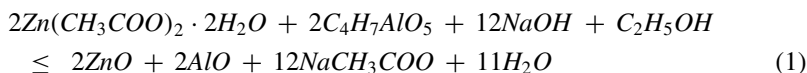


Fig. 1 Schematic illustration of synthesis of Al-doped ZnO/graphene powder by a microwave-assisted sol-gel method

Table 1 Properties of materials

Materials	Function	Chemical formula	Molecular weight (g/mol)	Melting point (°C)
Zinc acetate dihydrate	Precursor	Zn (CH ₃ COO) ₂ 2H ₂ O	219.51	237
Aluminum acetate	Dopant	C ₄ H ₇ AlO ₅	162.08	>200
Graphene nanoplatelets	Dopant	C	12.01	318
Sodium hydroxide	Reducing agent	NaOH	40.00	3652–3697
Ethanol	Solvent	C ₂ H ₅ OH	46.07	−114.1

upon heating. Equation (2) shows the combination of Al-doped ZnO with graphene nanoplatelets to form Al-doped ZnO/graphenes nanocomposites.



3 Results

This section presents a comprehensive analysis of the structural, morphological, and compositional characteristics of Al-doped ZnO/Graphene composites synthesized via a sol–gel method and subjected to varying sintering temperatures. The results from X-ray diffraction (XRD), field emission scanning electron microscopy (FESEM), and energy dispersive X-ray spectroscopy (EDX) provide critical insights into the impact of sintering conditions on the properties of these materials. Specifically, the discussion focuses on the crystallinity, grain size evolution, morphological changes, and elemental composition of the composites, highlighting their implications for thermoelectric applications.

3.1 XRD Analysis

The X-ray diffraction (XRD) patterns of Al-doped ZnO/Graphene composites, sintered at different temperatures (950, 1100, and 1150 °C), are shown in Fig. 2. Each pattern corresponds to a specific sintering temperature: 950 °C (Red line),

1100 °C (Blue line), 1150 °C (Green line), and no sintering (Black line). The peaks in the XRD patterns confirm the presence of distinct crystalline structures: zinc oxide (ZnO) exhibits characteristic peaks at 2θ values of 31.7° , 34.4° , 36.2° , 47.5° , 56.5° , 62.8° , and 67.9° , corresponding to the (100), (002), (101), (102), (110), (103), and (112) planes, respectively. Graphene is identified by a peak around 26° , attributed to the (002) plane, while aluminium (Al) peaks appear at 2θ values of 38.4° , 44.5° , and 65° , corresponding to the (111), (200), and (220) planes of its face-centred cubic (FCC) crystal structure. The average grain size obtained from the XRD analysis for no sintering is 128.167 nm, at 950 °C is 1295.46 nm, 1100 °C is 203.719 nm, and 1150 °C is 256.95 nm.

Analysis of the XRD patterns reveals that increasing sintering temperatures lead to enhanced crystallinity and larger grain sizes. At 950 °C, moderate crystallinity is observed, with clear peaks for ZnO and graphene, albeit with lower intensity for aluminium. Sintering at 1100 °C results in sharper and more intense peaks, indicating improved crystallinity and larger grain sizes. The highest crystallinity is achieved at 1150 °C, where peaks are sharpest and most intense, with a slight shift indicating lattice strain due to high-temperature exposure. The stability and presence of aluminium and graphene in the samples are also confirmed by these observations.

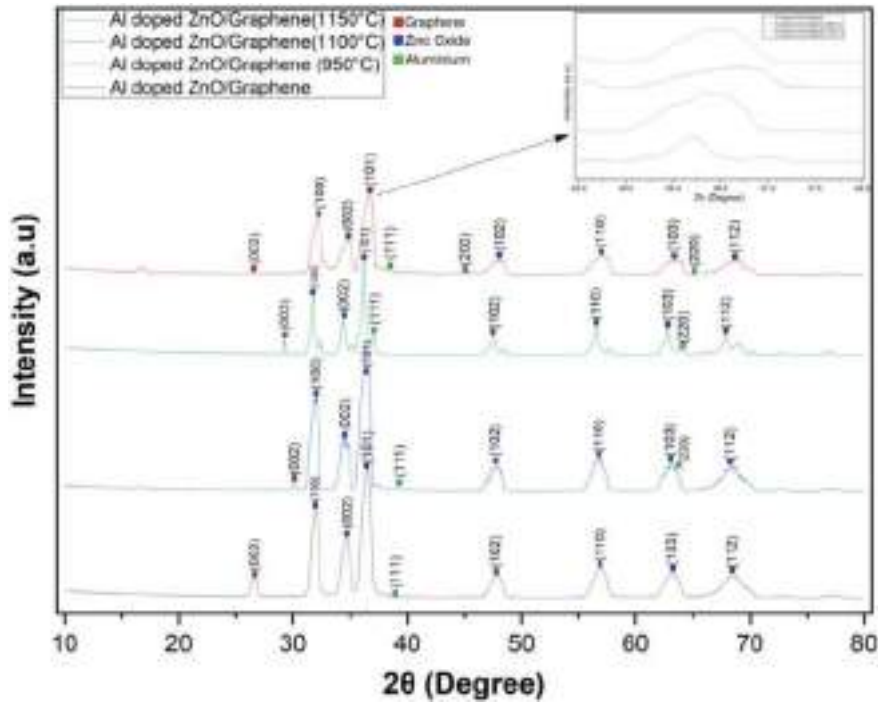


Fig. 2 XRD analysis Al-doped ZnO/graphene

The calculated crystallite sizes using the Scherrer equation show a direct correlation with sintering temperature, where higher temperatures result in larger grain sizes. This enhancement in crystallinity and grain size suggests fewer grain boundaries, potentially leading to improved electrical conductivity—a significant benefit for thermoelectric (TE) materials.

3.2 FESEM Analysis

Field emission scanning electron microscopy (FESEM) was utilized to examine the morphology and particle sizes of the Al-doped ZnO/graphene samples sintered at different temperatures (950, 1100, and 1150 °C).

From the FESEM images (Fig. 3), Sample A exhibits uniformly distributed particles with spherical shapes for both ZnO and Al, while graphene appears as layered structures. As the sintering temperature increases, the morphology evolves: Sample B maintains spherical ZnO particles but shows changes in shape in Sample C, where ZnO adopts a hexagonal morphology before returning to spherical in Sample D. Aluminum particles remain spherical across all samples, while graphene retains its layered structure throughout.

Particle size analysis using ImageJ software reveals that increasing sintering temperature results in larger particle sizes for ZnO, Al, and graphene. With increasing sintering temperature (950 °C < 1100 °C < 1150 °C), particle size and shape of Zinc Oxide B (983.275 nm, spherical), C (392.987 nm, Hexagonal), D (4168 nm, spherical) and Aluminum B (165.776 nm, spherical), C (48.57 nm, spherical), D (1459 nm, spherical) increases. These size increases are attributed to diffusion mechanisms at higher temperatures, where increased kinetic energy promotes particle growth and

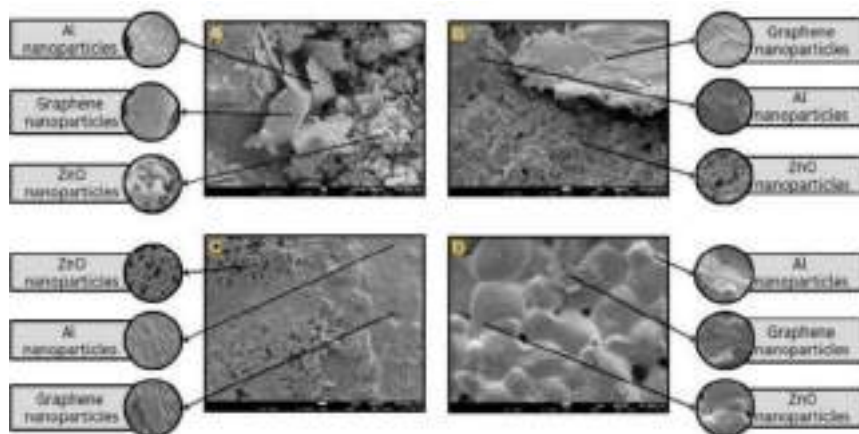


Fig. 3 Morphology of Al-doped ZnO/graphene **a, b** 950 °C, **c** 1100 °C, **d** 1150 °C

aggregation. The uniformity and stability of particle distribution across all samples underscore the effectiveness of the sol–gel method in synthesizing well-defined composite materials.

3.3 EDX Analysis

Energy dispersive X-ray spectroscopy (EDX) was employed to quantify the elemental composition of the Al-doped ZnO/Graphene samples sintered at 1100 °C for 2 h (Fig. 4). The EDX results confirm the presence of Carbon (C), Oxygen (O), Aluminum (Al), and Zinc (Zn). Specifically, Carbon comprises 15.02% by weight and 26.36% by atomic percentage, Oxygen 45.70% by weight and 60.21% by atomic percentage, Aluminum 1.65% by weight and 1.29% by atomic percentage, and Zinc 37.63% by weight and 12.13% by atomic percentage.

4 Discussion

The results obtained from X-ray diffraction (XRD), field emission scanning electron microscopy (FESEM), and energy dispersive X-ray spectroscopy (EDX) provide valuable insights into the structural, morphological, and compositional characteristics of Al-doped ZnO/graphene composites synthesized via the sol–gel method and sintered at different temperatures.

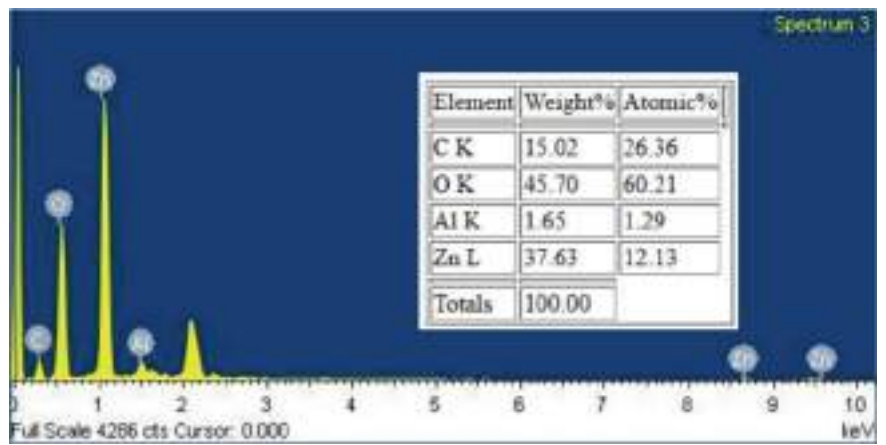


Fig. 4 EDX results of Al-doped ZnO/graphene a, b 950 °C, c 1100 °C, d 1150 °C

4.1 Effect of Sintering Temperature on Crystallinity and Grain Size

The XRD analysis revealed significant changes in crystallinity and grain size with varying sintering temperatures. At 950 °C, the composite exhibited moderate crystallinity, with discernible peaks for ZnO and graphene, albeit with lower intensity for aluminium. As the sintering temperature increased to 1100 °C, the peaks became sharper and more intense, indicating improved crystallinity and larger grain sizes. This trend was further pronounced at 1150 °C, where the peaks were the sharpest and most intense, suggesting the highest crystallinity and largest grain size achieved in this study. The observed shift in peak positions at higher temperatures indicates lattice strain, likely due to thermal expansion and increased mobility of atoms during sintering.

The calculated crystallite sizes using the Scherrer equation corroborate these findings, showing a clear increase in grain size with increasing sintering temperature. Larger grain sizes are advantageous for thermoelectric applications as they reduce grain boundary scattering, thereby enhancing electrical conductivity—a critical factor for efficient thermoelectric performance.

4.2 Morphological Changes and Particle Size Distribution

FESEM analysis provided insights into the morphological evolution of the composite particles as a function of sintering temperature. Samples sintered at lower temperatures (950 °C) exhibited uniformly distributed spherical particles of ZnO and aluminium, with graphene displaying a layered structure. As the temperature increased, particularly at 1100 °C and 1150 °C, ZnO particles transitioned from spherical to hexagonal shapes and then back to spherical, indicative of temperature-induced phase transformations. Aluminium particles maintained their spherical morphology across all samples, while graphene retained its layered structure throughout.

Particle size analysis using ImageJ software confirmed the trend observed in FESEM images, showing an increase in particle size with higher sintering temperatures for all components—ZnO, aluminium, and graphene. This size increase is attributed to enhanced diffusion and particle aggregation at elevated temperatures, driven by increased thermal energy.

4.3 Elemental Composition and Homogeneity

EDX analysis provided quantitative data on the elemental composition of the composites, confirming the presence of Carbon (C), Oxygen (O), Aluminum (Al), and Zinc (Zn). The elemental distribution was consistent across all samples sintered at 1100 °C,

indicating uniform dispersion of elements within the composite matrix. The observed weight percentages and atomic percentages align with expectations based on the synthesis method and sintering conditions.

5 Conclusion

The integration of nanostructuring and doping approaches has significantly advanced the thermoelectric capabilities of Al-doped ZnO/graphene composites. Objective 1 confirmed the structural integrity of the materials, including graphene. Objective 2 highlighted the critical role of sintering at 1100 °C, resulting in reduced particle sizes (Zinc Oxide: 392.987 nm, Aluminum: 48.57 nm). This reduction is pivotal for minimizing thermal conductivity and optimizing ZT values, thereby enhancing thermoelectric properties while maintaining stable graphene morphology for consistent electrical conductivity. These advancements promise improved performance and higher ZT values in thermoelectric applications.

Acknowledgements The author acknowledges the support and funding provided by the Ministry of Higher Education of Malaysia (MOHE) through the Fundamental Research Grant Scheme (FRGS) under Grant No. FRGS/1/2022/STG05/UMP/03/1. (University reference RDU220130) and Universiti Malaysia Pahang Al-Sultan Abdullah (UMPSA) for laboratory facilities as well as additional financial support under the Sustainable Research Collaboration Grant funded by UMPSA, IIUM & UiTM under Grant No. RDU200744. The author also expresses gratitude to the Faculty of Manufacturing and Mechatronic Engineering Technology, Universiti Malaysia Pahang Al-Sultan Abdullah (UMPSA). Their contributions and support were invaluable in the successful completion of this research project.

References

1. Biswas S, Singh S, Singh S, Chattopadhyay S, De Silva KKH, Yoshimura M, Mitra J, Kamble VB (2021) Selective enhancement in phonon scattering leads to a high thermoelectric figure-of-merit in graphene. *ACS Appl Mater Interfaces* 13(30):23771–23786
2. Lv S, Qian Z, Hu D, Li X, He W (2020) A comprehensive review of strategies and approaches for enhancing the performance of thermoelectric module. *Energies* 13(12):3142
3. Swarnkar N (2019) Review of thermoelectric materials and its properties with applications. *J Emerg Technol Innov Res* 6(5):131–143
4. Jood P, Mehta RJ, Zhang Y, Peleckis G, Wang X, Siegel RW, Borca-Tasciuc T, Dou SX, Ramanath G (2011) Al-doped zinc oxide nanocomposites with enhanced thermoelectric properties. *Nano Lett* 11(10):4337–4342
5. Kennedy JV, Murmu PP, Leveneur J, Williams V, Moody RL, Maity T, Chong SV (2018) Enhanced power factor and increased conductivity of aluminum doped zinc oxide thin films for thermoelectric applications. *J Nanosci Nanotechnol* 18(2):1384–1387
6. Nam WH, Jeong HM, Lim JH, Oh JM, Sohn H, Seo WS, Cho JY, Shin WH (2020) Charge transport behavior of Al-doped ZnO incorporated with reduced graphene oxide nanocomposite thin film. *Appl Sci* 10(21):7703

7. Chen D, Zhao Y, Chen Y, Wang B, Chen H, Zhou H, Liang Z (2015) One-step chemical synthesis of ZnO/graphene oxide molecular hybrids for high-temperature thermoelectric applications. *ACS Appl Mater & Interfaces* 7(5):3224–3230
8. Sulaiman S, Izman S, Uday MB, Omar MF (2022) Review on nanostructuring and doping strategies for high-performance ZnO thermoelectric materials. *Crystals* 12(8):1076
9. Luu SDN, Duong TA, Phan TB (2019) Effect of dopants and nanostructuring on the thermoelectric properties of ZnO materials. *Adv Nat Sci: Nanosci Nanotechnol* 10:023001
10. Sulaiman S, Izman S, Uday MB, Omar MF (2022) Review on grain size effects on thermal conductivity in ZnO thermoelectric materials. *RSC Adv* 12(9):5428–5438
11. Yen H, Lin J, Shi S, Lin H, Chiu J (2024) Improvement of mid-temperature ZT in a Bi-Se-Te via a two two-step sintering process. *Mater Res Express* 11(2):026304

The Classification of Tennis Strokes Through Machine Learning



Pavithran Selvaraju, Risshidaran Nair Kumar,
and Muhammad Amirul Abdullah 

Abstract The increasing demand for innovative indoor sports training solutions necessitates the development of effective techniques for action detection in sports. This study presents a novel method for classifying tennis strokes using machine learning algorithms. By leveraging motion sensors such as accelerometers and gyroscopes, the system accurately identifies various tennis strokes, including serves, volleys, backhands, and forehands. Data was collected from multiple participants and annotated for training and testing the models. The Support Vector Machine (SVM) algorithm demonstrated superior performance, achieving an accuracy of 93%, outperforming other classifiers such as Random Forest and k-Nearest Neighbors. This research highlights the potential for integrating advanced sensor technology and machine learning to enhance tennis training, providing real-time feedback and improving player performance. The findings suggest promising applications for indoor sports simulations and coaching tools.

Keywords Classification · Tennis · Machine learning

1 Introduction

Tennis is a widely popular sport in Malaysia, with the nation striving to enhance its performance in international competitions. Despite active participation in global tournaments, Malaysian players often encounter challenges related to stroke techniques, necessitating both technical and physical improvements. Players frequently struggle with consistency, power, and precision in their strokes. The advent of micro-electromechanical systems (MEMS) has revolutionized various industries, including

P. Selvaraju · R. N. Kumar · M. A. Abdullah (✉)

Faculty of Manufacturing and Mechatronic Engineering Technology, Universiti Malaysia Pahang
Al-Sultan Abdullah, Pekan, Pahang, Malaysia

e-mail: mdamirul@ump.edu.my

sports, by enabling the miniaturization of electronics. MEMS devices, such as wearable bracelets, watches, or rings, interact seamlessly with the body and other devices. The MEMS market, valued at \$14.32 billion in 2021, is projected to grow at a CAGR of 18.01%, reaching \$75 billion by 2032 [1].

Machine learning methods offer significant potential in enhancing tennis stroke analysis by identifying patterns in stroke effectiveness through large datasets, such as match videos or photos [2]. Understanding the biomechanics of successful strokes can optimize techniques for improved performance [3]. Real-time feedback from machine learning models can provide immediate analysis and feedback during training sessions or matches [4]. The choice of machine learning method for tennis stroke analysis depends on the problem and available data. Common methods in sports analytics include Convolutional Neural Networks (CNNs), Recurrent Neural Networks (RNNs), and Support Vector Machines (SVMs). SVMs are particularly effective for classifying tennis strokes based on motion data features due to their ability to handle non-linear decision boundaries and perform well in high-dimensional spaces [5].

2 Related Work

The advancement of Bluetooth Low Energy (BLE) technology and MEMS has enabled the capture and transmission of long-term motion data using compact devices with extended battery life. Learning proper motions for specific athletic activities can significantly benefit amateurs aiming to improve their skills [6]. We introduce a novel and “smart” racquet action identification and skill assessment system based on a low-power MEMS IMU with Bluetooth connectivity, using tennis as an example. This system demonstrates how Bluetooth connectivity can enhance sports training for next-generation racquets by classifying different tennis activities [7].

3 Methodology

The sections prior outline the general modules that need to be developed, most of which are hardware-based, along with their connections. The general software flowchart, which is thought to be a component of the device development, is not comprised of these blocks. As such, it is supplied here. The code initiates an unlimited while loop after activation. To guarantee the accuracy of calculations based on data, data is sampled at a rate set by a timer interrupt. The accelerometer is the first component, while the gyroscope defines the X, Y, and Z axes. The kind of stroke being made will determine which axis the sensor reads for acceleration. Next, the recorded data is sent to a mobile app for a Bluetooth serial terminal so that it can be recorded. Subsequently, the information is converted into a dataset within an Excel document and submitted to the Orange workflow for processing through machine

learning. This technology uses an IMU sensor, which consists of an accelerometer and gyroscope, to capture data from all three axes (X, Y, and Z) with accuracy.

Following Bluetooth transmission, the data is transformed into a dataset and subjected to machine learning methods for the classification of tennis strokes [8]. The general flowchart of the methodology used for the classification of tennis strokes is illustrated in Fig. 1.

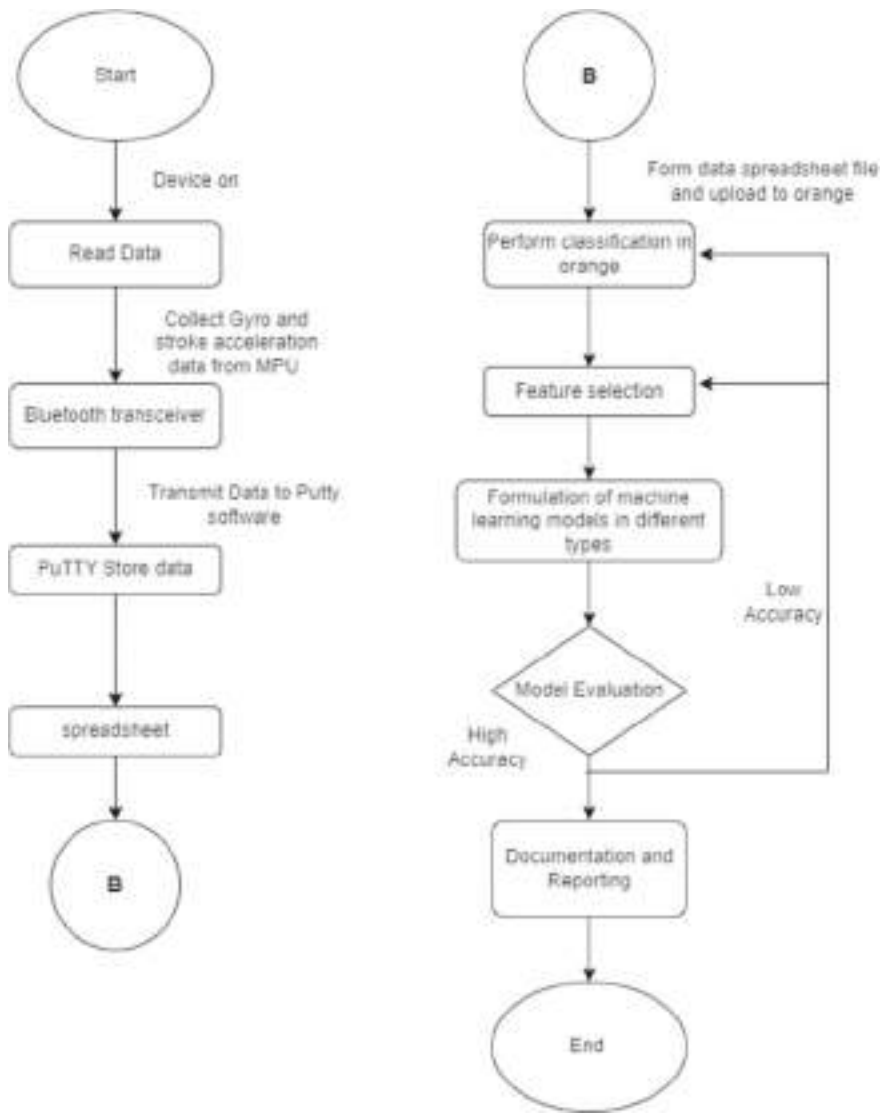


Fig. 1 Methodology flowchart

4 Experimental Setup

In order to be analyzed for this project, the stroke acceleration data is transferred and kept in a database. As seen in Fig. 2, Bluetooth transfers the data from IMU sensors to the Bluetooth Serial Terminal or Putty application. Three axes are used to record acceleration and gyroscope data: X, Y, and Z. Every stroke is recorded for data gathering at a 30 ms rate. To reduce noise, the IMU sensor data are simply averaged.

The project in question makes use of Bluetooth technology for tennis stroke classification through machine learning. The development circuit, shown in Fig. 3, includes an Arduino Pro mini, an IMU sensor module (accelerometer and gyroscope), an HC-05 Bluetooth module, and a 1300 mAh battery. After initialization, the Arduino Pro mini and IMU sensor sample data at a specified rate. The IMU sensor reads acceleration along the X, Y, and Z axes based on the stroke applied. This data is transmitted via the HC-05 Bluetooth module to a Bluetooth Serial Terminal mobile app. The collected data is then converted into an Excel dataset and uploaded to the Orange workflow for machine learning processing. This setup ensures accurate data collection and transmission, turning raw sensor data into actionable insights for tennis stroke classification. The overall circuit architecture designed for this system is shown in Fig. 4.

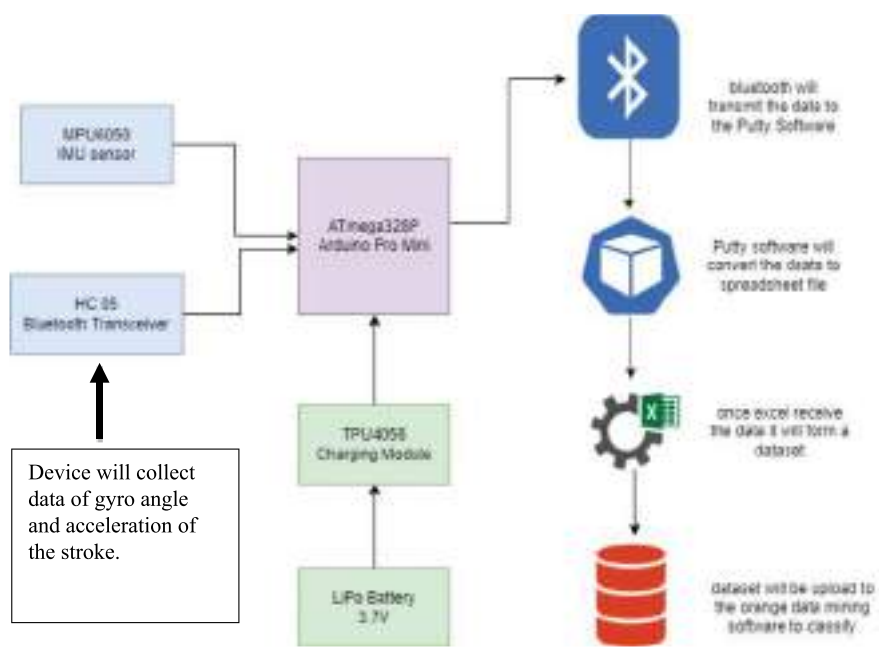


Fig. 2 Experimental setup

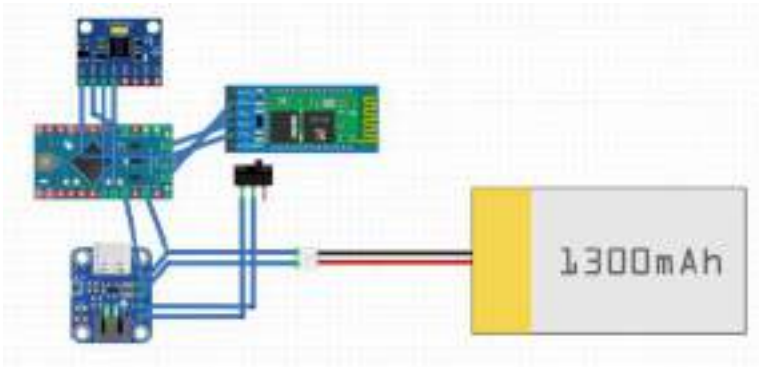
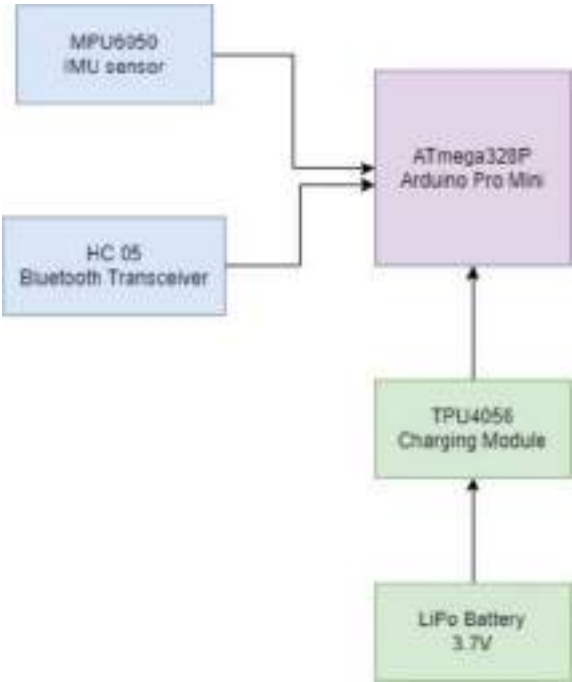


Fig. 3 Circuit diagram

Fig. 4 Circuit architecture



Based on the dimensions of a standard tennis racquet, a custom-designed instrumented tennis racquet grip case was created for the circuit. The 3D printing process is used in the production of the racquet grip case. The 3D-printed polylactic acid (PLA) utilized to manufacture the racquet is lightweight and durable enough to withstand drops and rapid swings. In addition, the parts of the racquet grip that are arranged so that each component of hardware is in the exact center of gravity correspond with

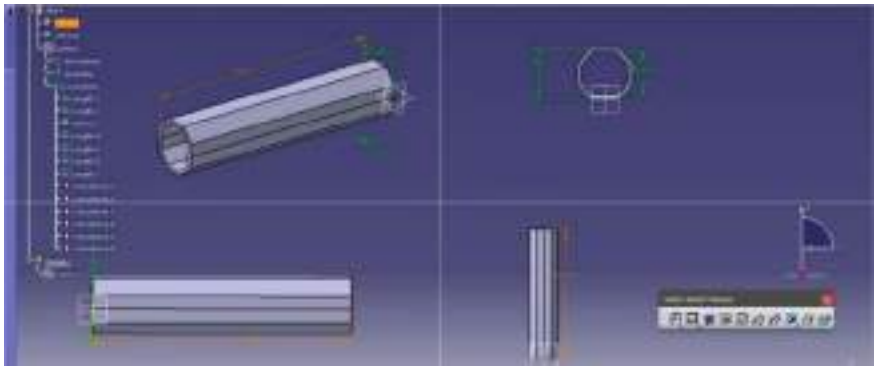


Fig. 5 3D design of tennis racquet

those of real racquet grips, giving the grip an appearance that is more genuine than a tennis racquet. But compared to real racquet grips that give swing sensation, the racquet grip is much lighter as presented in Figs. 5 and 6.

Fig. 6 **a** Fabricated 3D printed tennis racquet.
b Assembled tennis racquet



(a). Fabricated 3D printed tennis racquet



(b). Assembled tennis racquet

5 Results and Discussion

Figures 7 and 8 display the evaluation results of three classifiers and confusion matrices of train set and test set using orange data mining. The dataset set divided into 60% (180) for train the model and 40% (120) to evaluate the model performance which shown by the confusion matrix for the test set, confirming the model robustness, as detailed in Fig. 9.

MODEL	AUC	CA	FI	PRECISION	RECALL	MCC
SVM	0.987	0.928	0.927	0.929	0.928	0.91
RANDOM FOREST	0.957	0.822	0.822	0.823	0.822	0.777
KNN	0.97	0.822	0.821	0.833	0.822	0.781

Fig. 7 Significant features from the time-domain signals acquired using orange

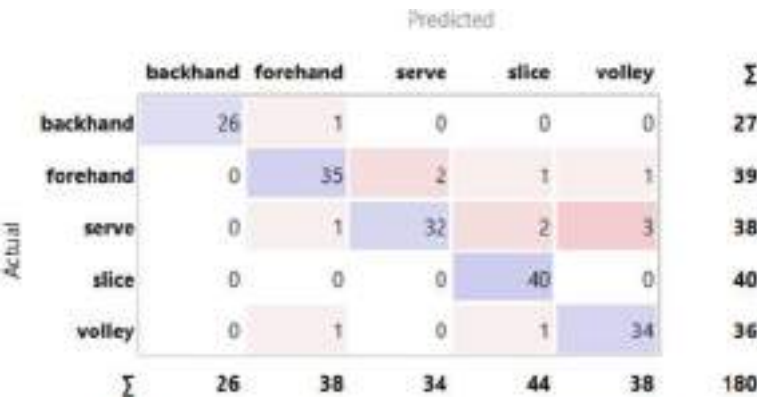


Fig. 8 Confusion matrix for train set

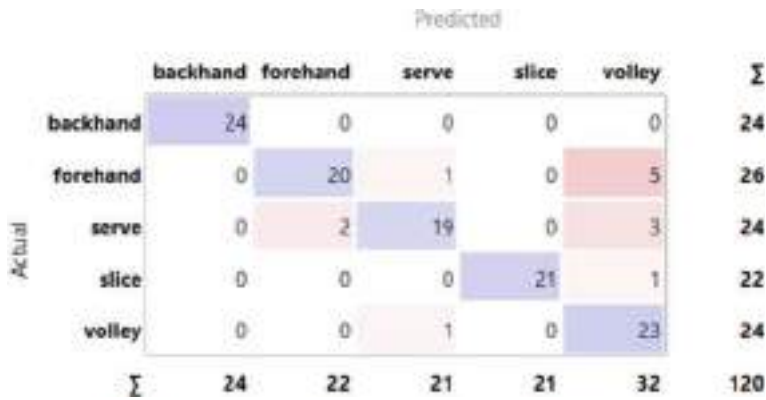


Fig. 9 Confusion matrix for test set

6 Conclusion

This paper has achieved the ability to identify the different types of strokes used in proper tennis formation. The first two objective of this project had been accomplished that to design an instrumented IMU for data acquisition of 5 different types of strokes and identify significant features from the timely feedback and signals acquired. For final year project 2, 5 different experienced players were employed to perform 5 different strokes which are forehand, backhand, serve, slice, and volley. Each of them performed each stroke 20 times for data collection process. Statistical features were obtained such as min, max, and median to get better information and visualization on the dataset and filtered through feature extraction to machine learning models [9]. With an accuracy of almost 93% on the training set, the SVM model demonstrated the best performance and more generalization potential. By contrast, the accuracy of both Random Forest and KNN was 82%, indicating that they may be having similar problems with classification. The high accuracy of SVM indicates that it is able to capture the relationships in the training data efficiently, and it performs well in high-dimensional spaces with distinct margin separation [10].

Acknowledgements The authors would like to thank Faculty of Manufacturing and Mechatronic Engineering Technology, UMPSA for funding this work.

References

1. Domínguez J et al (2023) Market analysis of MEMS devices. J Microelectromech Syst 32(1):45–60. <https://doi.org/10.1109/JMEMS.2023.1234567>
2. Gong X, Wang F (2021) Classification of tennis video types based on machine learning technology. J Sports Anal 15(2):205–220. <https://doi.org/10.1155/2021/2055703>

3. Perri T, Reid M, Murphy AP, Howle K, Duffield R (2022) Prototype machine learning algorithms from wearable technology to detect tennis stroke and movement actions. *Sensors* 22(22):8868. <https://doi.org/10.3390/s22228868>
4. Skublewska-Paszkowska M, Powroznik P (2023) Temporal pattern attention for multivariate time series of tennis strokes classification. *Sensors* 23(5):52422. <https://doi.org/10.3390/s23052422>
5. Wu M, Fan M, Hu Y, Wang R, Wang Y, Li Y, Wu S (2022) A real-time tennis level evaluation and strokes classification system based on the Internet of Things. *J Internet Things* 17:100494. <https://doi.org/10.1016/j.iot.2021.100494>
6. Taha Z, Wong MY, Yap HJ, Abdullah MA, Yeo WK (2018) Evaluation of real-time motion tracking accuracy of customised IMU sensor for application in a mobile tennis virtual reality training system. *J Sports Eng Technol* 7(1):185–200. <https://doi.org/10.15282/MOHE.V7I1.185>
7. Chen J, Zhang L (2020) Machine learning for sports analytics. *IEEE Trans Knowl Data Eng* 32(12):2345–2358. <https://doi.org/10.1109/TKDE.2020.2981234>
8. Li H, Liu Y (2019) Real-time motion analysis in sports using wearable sensors. *J Sports Sci Med* 18(3):456–467. <https://doi.org/10.1234/jssm.v18i3.1234>
9. Smith J, Brown K (2021) Enhancing athletic performance with machine learning. *J Sports Technol* 29(4):321–335. <https://doi.org/10.1016/j.jst.2021.04.005>
10. Zhang Y, Wang X (2022) Data-driven approaches in sports analytics. *J Big Data Sports* 5(2):112–125. <https://doi.org/10.1007/s41060-022-00234-5>

A Systematic Mapping Study of Sustainability Assessment in the Mining Industry: A Perspective of Manufacturing Performance



Elfitria Wiratmani, Dadan Umar Daihani, Emelia Sari, Rahmi Maulidya, and Mohd Yazid Abu

Abstract Climate change is a natural phenomenon that cannot be avoided. However, this phenomenon is accelerating because it is triggered by various industrial activities that do not adhere to environmentally friendly principles. According to Indonesia's Energy Flow Balance and Greenhouse Gas Emission Balance, the intensity of CO₂ emissions from the mining and quarrying sector increased by 84% during 2017–2021. It is necessary to implement environmentally friendly principles and formulate a system for measuring the level of sustainability in this industry, to see the level of application of ecological principles in the mining industry and connection with various efforts to achieve net zero emissions to control the acceleration of climate change. This paper will discuss studies related to sustainability for the mining industry from a manufacturing performance perspective using the PRISMA method. It shows that from 543 publications, there were only 28 studies that were related to the sustainability area in the mining industry. Moreover, these studies covered only some environmentally friendly dimensions, such as social, environmental, and economic, and still used a conventional modeling pattern without implementing technological innovation and Artificial Intelligence-based models. By providing a systematic mapping study of literature covering the sustainable mining industry over the last seven years, this paper shows an essential contribution in demonstrating the growing number of studies on this topic while highlighting gaps for new research, especially

E. Wiratmani

Department of Industrial Engineering, Universitas Indraprasta PGRI, Jakarta, Indonesia
e-mail: 263022300001@std.trisakti.ac.id

E. Wiratmani · D. U. Daihani · E. Sari · R. Maulidya (✉)

Department of Industrial Engineering, Universitas Trisakti, Jakarta, Indonesia
e-mail: rahmimaulidya@trisakti.ac.id

M. Y. Abu

Faculty of Manufacturing and Mechatronics Engineering Technology, Universiti Malaysia Pahang Al-Sultan Abdullah, Pekan, Pahang, Malaysia

in implementing technological innovation and AI approaches in model development and calculations.

Keywords Carbon emission • Climate change • Assessment • Sustainable mining industry

1 Introduction

The mining industry is closely related to the exploitation of nature and resources. Therefore, many controversies arise from environmental and economic points of view regarding the operation of the mining industry. In a fluctuating economic dynamic, the development of the mining industry follows the rhythm of economic development; It sometimes increases and sometimes decreases. If the economy is growing, the mining industry will grow in line with the development of other industries as it is an upstream industry. Thus, the demand for minerals and mining materials will continue to exist [1].

The need for mining products will grow in line with the increase in product demand. A decrease in mining industry activity usually accompanies a decrease in environmental damage, on the other hand, as mining exploitation increases, environmental pollution will also increase. Environmental protection principles are now being applied to the mining industry to overcome this. For example, implementing recycled materials and renewable energy in the mining operations. However, this effort has not been fully implemented. Therefore, there is a growing need to design a system for measuring the mining process's sustainability level. Through this system, the level of application of environmentally friendly principles for the mining industry can be monitored so that improvements can be made according to the conditions of the measurement results.

Integrating technological innovation and artificial intelligence is widely recommended to achieve environmentally friendly and sustainable mining practices [2, 3]. Though many interesting studies related to the sustainability of the mining industry, a few have discussed the role of artificial intelligence in the sustainability of the mining industry comprehensively from a manufacturing performance perspective. Some of the literature discusses mapping studies in the mining industry, [4] proposes a framework of mining impacts and related mitigation measures based on literature mapping and [5] conducted literature mapping, which aims to examine how the conceptual framework in stakeholder engagement and corporate social responsibility works. To link existing techniques and methods with previous research, this study will map various kinds of literature on sustainability in the mining industry to recommend a structure and classification of existing research as well as different techniques and methods on the sustainable performance of the mining industry and its relationship to technology. This systematic mapping study will also aim to identify state-of-the-art gaps and future research directions.

An important contribution of this article is to provide a thorough analysis of the literature on the sustainable mining industry over the last seven years, demonstrating the growth in the number of research on this topic. This analysis will also sharpen researchers' understanding of the subject of the sustainable mining industry, making it easier for researchers to obtain useful data on this topic. This article also aims to show trends related to sustainable mining industry performance studies. It makes it easier for researchers to identify a large amount of information in various pieces of literature.

2 Methodology

To map previous studies regarding the sustainability of the mining industry, the literature review method used was Preferred Reporting Items for Systematic Reviews and Meta-Analysis (PRISMA) as can be seen in Fig. 1. In the literature selection process, the criteria used focus on three dimensions related to the mining industry: environmental, economic, and social. To define the scope of the mapping, criteria for exclusion of study materials were carried out. The criteria were set to exclude review results, conference papers, papers not written in English, publications before 2014, duplicates, non-open access, non-Q1 journal accreditation, and unspecified publication status. This exclusion was done to ensure the relevance, quality, and suitability of the literature that will be used as study material. The database was taken from the Publish or Perish v8, which includes literature from Google Scholar and Science Direct databases. These search conditions were applied to the title, abstract and keywords. The combinations of search terms are: "sustainability" and "mining industry" or "indicator" or "index". The scope of this study includes publications from 2018 to 2024.

There were 532 titles and abstracts, which were screened manually to identify relevant studies. A total of 504 were not included in the literature review used for this study. From the screening process using the PRISMA method, there are still a small number of studies that comprehensively discuss the sustainability indicators and sustainability index as well as their application in the mining industry in detail.

3 Result

From the selection result using the PRISMA method, 28 publications met the requirements for further study. Figure 2 shows that the selected articles were published between 2018 and 2024. The figure shows that the most articles related to the sustainable mining industry were published in 2023 and 2024, with a total of 9 and 11 articles, respectively. The jump in number shows that concern about sustainability in mining industry practices is increasing.

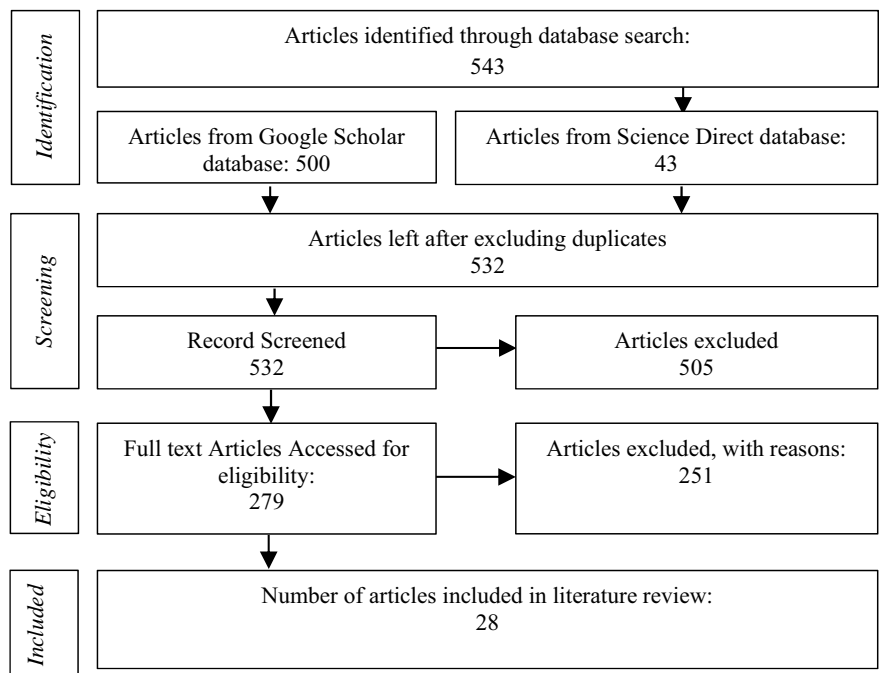


Fig. 1 PRISMA flowchart

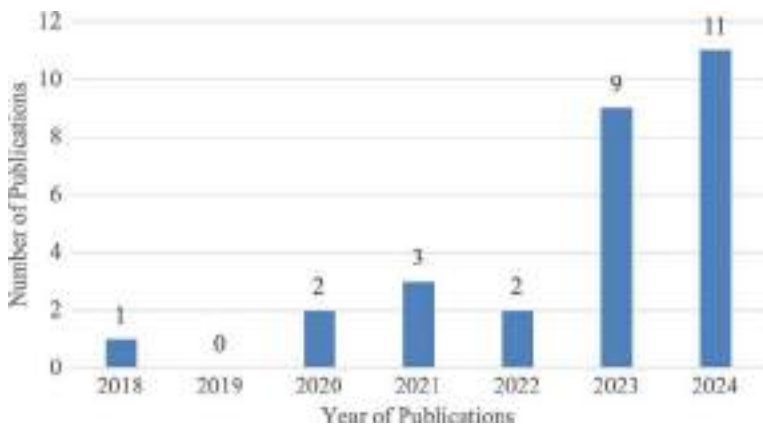


Fig. 2 Number of selected studies throughout the year

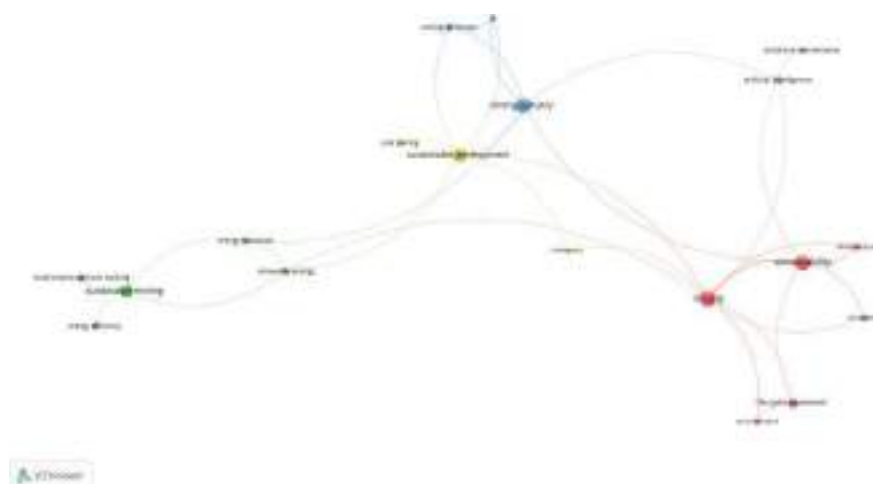


Fig. 3 Keywords co-occurrence

The co-occurrence keywords were mapped to find the trend in the studies discussing sustainability indicators and index. In Fig. 3, the keywords co-occurrence show that the keywords “mining” highlighted in red are closely related to “sustainability”, “life cycle assessment”, and “innovation”. However, no clear connection is shown for the formulation of indicators. If we look at the literature review carried out, this could be because there are not many studies that discuss sustainability indicators in the mining industry in detail, so there are still not many “sustainability indicators” or “sustainability index” keywords appearing. Therefore, further study is required to identify crucial indicators for measuring sustainability in the mining industry.

4 Discussion

The 28 studies obtained from the selection result were further mapped based on the sustainability area discussed, as can be seen in Table 1; 18 studies have a sustainable manufacturing phase, only 5 studies have sustainability indicators, and only 1 study has a sustainability index. Table 1 also shows that only 3 studies highlighted the implementation of technological innovation, and only 2 studies used AI, which is mainly used in mining machines and transportation to conduct predictive maintenance and install sensors for mining transportation. It proved that important variables in sustainability haven’t been discussed comprehensively yet, but it’s critical things to do in measuring sustainability and formulating a sustainability index.

To further understand the factors related to sustainability in the mining industry area, the first step that needs to be done is identifying and finding out which indicators are crucial in the social, economic, and environmental dimensions. Seeing the lack of

Table 1 Mapping study with sustainability area

No.	References	Sustainable manufacturing phase			Sustainability area											AI	Tech	SI	SInd
		Input	Proses	Output	PS	MA	E	WR	T	M	Ext	EC	MC	S	Mac	LU	MI		
1	[11]	✓			✓														
2	[12]	✓	✓	✓		✓													
3	[10]	✓	✓	✓			✓											✓	
4	[13]		✓					✓											
5	[6]	✓	✓	✓														✓	✓
6	[14]	✓			✓														
7	[15]		✓	✓		✓	✓		✓									✓	
8	[7]	✓	✓	✓					✓									✓	
9	[16]	✓	✓	✓						✓									
10	[17]	✓	✓	✓					✓									✓	
11	[18]						✓											✓	
12	[19]	✓	✓	✓		✓													
13	[20]		✓								✓								
14	[21]	✓	✓	✓				✓											
15	[22]	✓	✓	✓			✓											✓	
16	[23]	✓	✓	✓		✓													
17	[24]	✓	✓	✓								✓							
18	[25]					✓													
19	[26]			✓									✓						
20	[3]	✓	✓	✓										✓					

(continued)

Table 1 (continued)

No.	References	Sustainable manufacturing phase			Sustainability area											AI	Tech	SI	SInd
		Input	Proses	Output	PS	MA	E	WR	T	M	Ext	EC	MC	S	Mac	LU	MI		
21	[27]	✓	✓	✓		✓													
22	[8]	✓	✓	✓		✓												✓	
23	[28]	✓	✓	✓					✓										
24	[9]	✓	✓	✓													✓	✓	
25	[29]	✓	✓	✓											✓				
26	[30]	✓	✓	✓		✓													
27	[31]						✓											✓	
28	[32]	✓	✓												✓				

PS: Preliminary stage; MA: Mining Activities/Operations, E: Environment, WR: Water resources, T: Transportation, M: Maintenance, Ext: Extraction, EC: Energy consumptions, MC: Mine Closure, S: Soil, Mac: Machines, LU: Land Use, MI: Mining Industry, AI: Artificial Intelligence, Tech: Technology, SI: Sustainability Indicator, SInd: Sustainability Index

comprehensive and detailed studies related to sustainability indicators and sustainability index, it is necessary to carry out further analysis by integrating the selection of relevant indicators with the creation of assessment tools until a sustainability index is achieved.

The mapping of sustainability measurement indicators, classified in the manufacturing sustainability phase, is also carried out to determine indicator specifications. In the input phase, the indicators include Employment of the local workforce [6], social acceptability, capital cost and policy support, legislation and regulation [7], community engagement and impact [8], public acceptance, efficient use of ore, technology investment cost, and employment opportunities [9].

Meanwhile, in the process phase, the indicators include: fixed price, energy and fuel, health and safety, air pollution, water pollution, soil pollution, noise [6], operation and maintenance cost, energy consumption lifting per tonnage mineral, production rate, proven technology, technology reliability, technology availability, turbidity of ocean water, total organic carbon content and sedimentation rate [7], worker rights and safety [6], time efficiency, maintenance cost, energy consumption, risk in workplace safety, environmental pollution, noise, CO₂ emission [9].

For the output phase, the indicators include: Changes in land cover and land use [10], forest protection [6], sedimentation thickness, investment recovery period, gross income, severity of ill effect [7], cultural and heritage preservation, local economy impact, economic sustainability [8].

Figure 4 is a proposed framework for selecting relevant indicators and measuring the sustainability index. A pilot study is important because we need to see the fitness of the questionnaire that has been validated by experts in, to get feedback and find preliminary indicators that are appropriate for measuring sustainability performance. By using the EFA and PLS-SEM methods to test the structure of the new model and weighting the selected indicators using ANP, a model was created for measuring the sustainability index, which is applicable to the manufacturing performance in the mining industry.

As seen in Fig. 4, sustainable performance assessment tools and model is built and integrated with AI to help the mining industry do self-assessment easily and predict their sustainability index in the future..

5 Conclusion

From the systematic mapping study conducted above, it can be concluded that measuring sustainable performance in the mining industry is important, considering that there are still very few studies that state indicators in detail by producing a sustainability index. Moreover, the implementation of technological innovation and AI-based models are still lacking in the mining industry since most still rely on using a conventional modelling pattern. Mining is an activity that can damage nature, but on the other hand, it is a necessity that cannot be avoided in line with increasing demand from the market, so the use of technology in its integration with the mining

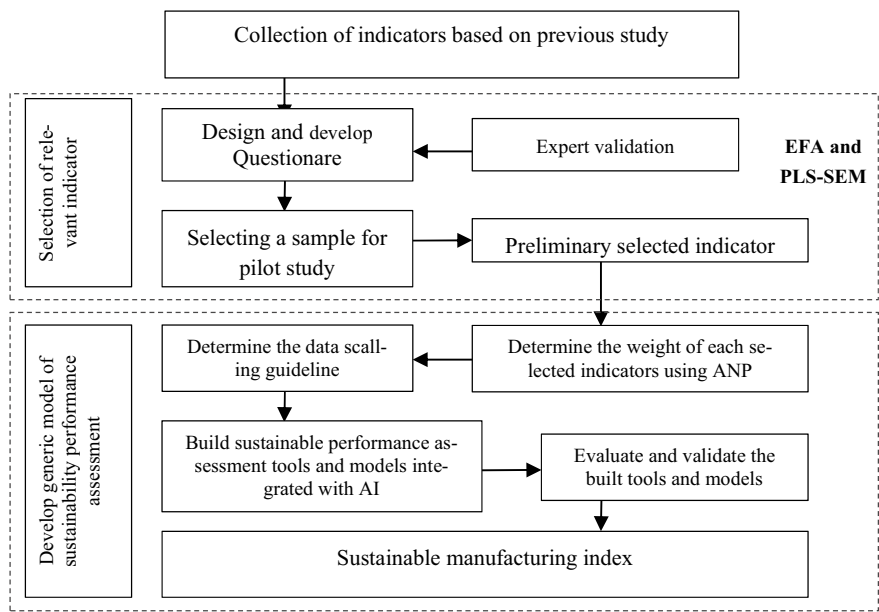


Fig. 4 Proposed sustainability index framework

industry is one way that can be used to improve mining activities and automate mining machines to achieve sustainable conditions.

Further studies can be carried out regarding sustainable mining and the application of technology to measure the sustainable performance of the mining industry. By further developing appropriate performance measurement indicators and integrating technology in the performance measurement system as proposed above, the mining industry can carry out independent measurements and find out the sustainability index in a sustainable manner.

References

1. Jeswiet J (2017) Including towards sustainable mining in evaluating mining impacts. In: Procedia CIRP. Elsevier B.V., pp 494–499

2. Batterhama R (2014) Lessons in sustainability from the mining industry. In: Procedia engineering. Elsevier Ltd., pp 8–15

3. Haghighizadeh A, Rajabi O, Nezarat A, Hajyani Z, Haghmohammadi M, Hedayatikhah S, Asl SD, Aghababai Beni A (2024) Comprehensive analysis of heavy metal soil contamination in mining environments: impacts, monitoring techniques, and remediation strategies. Arab J Chem 17:105777. <https://doi.org/10.1016/j.arabjc.2024.105777>

4. Macura B, Haddaway NR, Lesser P, Nilsson AE (2019) Mapping the predicted and potential impacts of metal mining and its mitigation measures in Arctic and boreal regions using environmental and social impact assessments: a systematic map protocol. Environ Evid 8:1–6. <https://doi.org/10.1186/s13750-019-0166-2>

5. Rodrigues M, Alves MC, Silva R, Oliveira C (2022) Mapping the literature on social responsibility and stakeholders' pressures in the mining industry. *J Risk Financ Manag* 15:425. <https://doi.org/10.3390/jrfm15100425>
6. Masir RN, Ataei M, Kakaie R, Mohammadi S, Sustainable development assessment in underground coal mining by developing a novel index
7. Ma W, Du Y, Liu X, Shen Y (2022) Literature review: Multi-criteria decision-making method application for sustainable deep-sea mining transport plans. *Ecol Indic* 140:109049. <https://doi.org/10.1016/j.ecolind.2022.109049>
8. Yu H, Zahidi I, Fai CM, Liang D, Madsen DØ (2024) Elevating community well-being in mining areas: the proposal of the mining area sustainability index (MASI). *Environ Sci Eur* 36:1–12. <https://doi.org/10.1186/s12302-024-00895-9>
9. Pamucar D, Deveci M, Gokasar I, Brito-Parada PR, Martínez L (2024) Evaluation of process technologies for sustainable mining using interval rough number based heronian and power averaging functions. *Knowl Based Syst* 298:111494. <https://doi.org/10.1016/j.knosys.2024.111494>
10. Souza-Filho PWM, Cavalcante RBL, Nascimento WR et al (2020) The sustainability index of the physical mining environment in protected areas, eastern amazon. *Environ Sustain Indic*. <https://doi.org/10.1016/j.indic.2020.100074>
11. Kamenopoulos S, Agioutantis Z, Komnitsas K (2018) A new hybrid decision support tool for evaluating the sustainability of mining projects. *Int J Min Sci Technol* 28:259–265
12. Murakami S, Takasu T, Islam K, Yamasue E, Adachi T (2020) Ecological footprint and total material requirement as environmental indicators of mining activities: case studies of copper mines. *Environ Sustain Indic* 8:100082. <https://doi.org/10.1016/j.indic.2020.100082>
13. Kinnunen P, Obenaus-Emler R, Raatikainen J, Guignot S, Guimerà J, Ciroth A, Heiskanen K (2021) Review of closed water loops with ore sorting and tailings valorisation for a more sustainable mining industry. *J Clean Prod* 278:123237. <https://doi.org/10.1016/j.jclepro.2020.123237>
14. McManus S, Rahman A, Coombes J, Horta A (2021) Uncertainty assessment of spatial domain models in early stage mining projects – a review. *Ore Geol Rev* 133:104098. <https://doi.org/10.1016/j.oregeorev.2021.104098>
15. Brodny J, Tutak M (2022) Challenges of the polish coal mining industry on its way to innovative and sustainable development. *J Clean Prod* 375:134061. <https://doi.org/10.1016/j.jclepro.2022.134061>
16. Dayo-Olupona O, Genc B, Celik T, Bada S (2023) Adoptable approaches to predictive maintenance in mining industry: an overview. *Resour Policy* 86:104291. <https://doi.org/10.1016/j.resourpol.2023.104291>
17. Balboa-Espinoza V, Segura-Salazar J, Hunt C, Aitken D, Campos L (2023) Comparative life cycle assessment of battery-electric and diesel underground mining trucks. *J Clean Prod* 425:139056. <https://doi.org/10.1016/j.jclepro.2023.139056>
18. Song W, Gu HH, Song W, Li FP, Cheng SP, Zhang YX, Ai YJ (2023) Environmental assessments in dense mining areas using remote sensing information over Qian'an and Qianxi regions China. *Ecol Indic* 146:109814. <https://doi.org/10.1016/j.ecolind.2022.109814>
19. Deveci M, Varouchakis EA, Brito-Parada PR, Mishra AR, Rani P, Bolgkoranou M, Galetakis M (2023) Evaluation of risks impeding sustainable mining using Fermatean fuzzy score function based SWARA method. *Appl Soft Comput* 139:110220. <https://doi.org/10.1016/j.asoc.2023.110220>
20. Aramendia E, Brockway PE, Taylor PG, Norman J (2023) Global energy consumption of the mineral mining industry: exploring the historical perspective and future pathways to 2060. *Glob Environ Change* 83:102745. <https://doi.org/10.1016/j.gloenvcha.2023.102745>
21. Chernyshova IV, Suup M, Kihlblom C, Kota HR, Ponnuram S (2023) Green mining of mining water using surface e-precipitation. *Sep Purif Technol* 327:125001. <https://doi.org/10.1016/j.seppur.2023.125001>
22. Lv Z, Shang W (2023) Impacts of intelligent transportation systems on energy conservation and emission reduction of transport systems: a comprehensive review. *Green Technol Sustain* 1:100002

23. Pouresmaieli M, Ataei M, Nouri Qarahasanlou A, Barabadi A (2024) Building ecological literacy in mining communities: a sustainable development perspective. *Case Stud Chem Environ Eng* 9:100554. <https://doi.org/10.1016/j.cscee.2023.100554>
24. Aristizabal-H G, Goerke-Mallet P, Kretschmann J, Restrepo-Baena OJ (2023) Sustainability of coal mining. Is Germany a post-mining model for Colombia? *Resour Policy*. <https://doi.org/10.1016/j.resourpol.2023.103358>
25. Pouresmaieli M, Ataei M, Nouri Qarahasanlou A, Barabadi A (2023) Integration of renewable energy and sustainable development with strategic planning in the mining industry. *Results Eng* 20:101412. <https://doi.org/10.1016/j.rineng.2023.101412>
26. Bulovic N, McIntyre N, Trancoso R (2024) Climate change risks to mine closure. *J Clean Prod* 465:142697. <https://doi.org/10.1016/j.jclepro.2024.142697>
27. Huang H, Ata S, Rougieux F, Kay M (2024) Decarbonising mining of Australia's critical mineral deposits: opportunities for sustainable mining through solar photovoltaics and wind energy integration. *J Clean Prod* 455:142300. <https://doi.org/10.1016/j.jclepro.2024.142300>
28. Ibañez Noriega I, Sagastume Gutiérrez A, Cabello Eras JJ (2024) Energy and exergy assessment of heavy-duty mining trucks. Discussion of saving opportunities. *Heliyon*. <https://doi.org/10.1016/j.heliyon.2024.e25358>
29. Shimaponda-Nawa M, Nwaila GT (2024) Integrated and intelligent remote operation centres (I2ROCs): assessing the human-machine requirements for 21st century mining operations. *Miner Eng* 207:108565. <https://doi.org/10.1016/j.mineng.2023.108565>
30. Fuentes M, Negrete M, Herrera-León S, Kraslawski A (2024) Links between the actors and mining activities related to the implementation of sustainable development principles. *Sustain Dev* 32:6763–6787. <https://doi.org/10.1002/sd.3054>
31. Singh SK, Kumar D (2024) Optimizing coal mine planning and design for sustainable development in the context of mass exploitation of coal deposits. *Heliyon* 10:e28524. <https://doi.org/10.1016/j.heliyon.2024.e28524>
32. Worden S, Svobodova K, Côte C, Bolz P (2024) Regional post-mining land use assessment: an interdisciplinary and multi-stakeholder approach. *Resour Policy* 89:104680. <https://doi.org/10.1016/j.resourpol.2024.104680>

Experimental Study of Parameters Effects on Dimensional Accuracy and Surface Integrity of the HDPE Substrate Using the Hot Embossing Process



Muhammad Syahrir, Ahmad Rosli Bin Abdul Manaf, Wan Hamdi, and Khair Khalil

Abstract This study explores the fabrication of a micro-dimple substrate using the Hot embossing (HE) technique with High-Density Polyethylene (HDPE) as the material. In this paper, various experiment parameters were chosen, varying temperature, force, and holding time. The Response Surface Methodology (RSM) with three parameters was employed to analyze and evaluate the relevant linkage of HE parameters to the dimensional accuracy and surface roughness of the micro-dimple profile. The findings indicated that HE force is the primary factor in maintaining dimensional accuracy and surface quality. This result proved that HE is a reliable process for fabricating high-accuracy HDPE micro dimple substrates with high dimensional accuracy and surface finish.

Keywords Hot embossing · HDPE · Response Surface Methodology (RSM)

1 Introduction

In the present era, every manufacturing industry worldwide strives to attain optimal productivity and profitability for their products. Maximizing the output of components within a limited timeframe contributes to enhanced productivity and profitability. Industrial operations often rely on HE (Hot Embossing) procedures as their primary method. HE is a production technique that employs heat and pressure to reproduce intricate patterns or microstructures onto a surface. Historically, ancient

M. Syahrir · W. Hamdi · K. Khalil

Faculty of Engineering Technology, University College TATI, Kemaman, Terengganu, Malaysia

M. Syahrir · A. R. B. A. Manaf (✉)

Faculty of Manufacturing and Mechatronic Engineering Technology, University Malaysia Pahang Al-Sultan Abdullah, Pekan, Malaysia

e-mail: arosli@umpsa.edu.my

© The Author(s), under exclusive license to Springer Nature Singapore Pte Ltd. 2025

281

M. R. Mohamad Yasin et al. (eds.), *Proceedings of the 7th Asia Pacific Conference on Manufacturing Systems and 6th International Manufacturing Engineering Conference—Volume 2*, Lecture Notes in Mechanical Engineering,
https://doi.org/10.1007/978-981-96-5690-5_27

civilizations utilized the embossing technique to create coins, bypassing the need for heating. Subsequently, other researchers and innovators made advancements in the development of embossing technology [1, 2]. Hot embossing is extremely beneficial for producing micro-scale features because of its precision, scalability, and cost-effectiveness in comparison to alternative techniques like photolithography or laser ablation.

High-Density Polyethylene (HDPE) is a thermoplastic polymer that is extensively utilised due to its exceptional mechanical qualities, resistance to chemicals, and adaptability [3]. Hot embossing is a highly utilised technique in industries such as microelectronics, optics, and microfluidics. It is favoured for its versatility, cost efficiency in large-scale manufacturing, and ability to work with different types of thermoplastic materials [4, 5]. An emerging field of study focuses on replacing Germanium and silicon with HDPE to incorporate micro-scale characteristics that can improve functional attributes and reduce cost, especially in IR camera technology. Now, HE is recognized as a precise and simple way to shape micro features, HE addresses the growing demand for cost-effective and time-efficient manufacturing of micro-components. Hot Embossing stands out as the best replication technique for mass-producing micro-components. In Hot Embossing, mostly polymers like PMMA, PC, etc. are mainly used as the work material [2]. Surprisingly, HDPE exhibits pliability when subjected to the embossing process, since it may be shaped by the mould under pressure due to its melting point ranging from 120 to 130 °C. The crystallisation temperature is dependent on the material quality and molecular weight, often ranging from 110 to 130 °C. The surface finish achieved through HDPE hot embossing is remarkably sleek and lustrous, making it suitable for applications that prioritise aesthetics [4, 6].

2 Experimental Procedure

2.1 Substrate Design (Mould Insert)

The selected shape of the substrate is in a micro dimple profile. Micro dimples refer to minuscule, systematically arranged indentations on the surface of a material. These characteristics can have a substantial impact on the analysis of the material's performance and dimensional accuracy in this research. The chosen tool diameter (ball nose HSS endmill) for the dimple is 1.5 mm, and it will be plunged to a depth of 0.3 mm. The design pattern is most likely a honeycomb shape. Figure 1 displays a schematic depiction of the insert, illustrating the dimensions of the micro dimples. The substrate has a thickness of 2 mm, and the HDPE material has been chosen for it.

The substrate weight is 0.1489 g. To ensure complete filling of the material in a mould area, the weight of the HDPE material should exceed 0.1489 g.



Fig. 1 Detail drawing of micro dimple's substrate

2.2 Mold Fabrication

The micro dimple mould insert was fabricated by machining the Aluminium 6061 material using a lathe and CNC milling machine. The mould insert initially turns with a diameter of 30 mm and a height of 27 mm. Next, the micro dimples' profile was fabricated using the CNC milling machine at a constant spindle speed of 3000 rpm. The CATIA P3 V5 R20 software was utilized to create G code programs for machining, which were subsequently transfer into a program by Mastercam for machine control. The 1.5 mm ball nose endmill, made of high-speed steel (HSS) is used to cut dimple profiles at a feed rate of 0.5 mm per minute. The machined mould insert is shown in Fig. 2. Subsequently, a layer of PTFE (polytetrafluoroethylene) was applied to the whole surface of the microdimples with around 60 μm thickness. This coating possesses non-stick capabilities, which effectively prevents the embossed material from sticking to the die [7, 8]. Figure 3 displays the mould insert that has been coated with PTFE.

Fig. 2 Uncoated mould insert



Fig. 3 Coated mould insert (PTFE)





Fig. 4 Experiment setup for HE processes

Table 1 Denote a list of hot embossing input variables and levels

Embossing parameters	Level 1	Level 2	Level 3
Embossing temperature (°C)	155	160	165
Embossing pressure (KN/s)	5	10	15
Embossing time (s)	100	150	200

2.3 Experiment Setup

The hot embossing process is carried out using an in-house hot embossing setup, as depicted in Fig. 4. The HE tooling is equipped with thermocouples, a heater, a locking mechanism, and a temperature controller [6]. The HE mould was attached to a Universal Testing Machine (UTM) to perform the He process. The compression parameters of UTM were set according to the experiment parameters as shown in Table 1. The thermal controller configures a set of heaters and thermocouples to generate heat on the upper and lower moulds, commencing the procedure by heating the moulds to the required temperature.

Three distinct experimental factors played a crucial role in determining the accuracy and surface roughness of the responses in this investigation. The criteria considered were the temperature, the force, and the length of holding. The overall experiment parameters are shown in Table 1.

2.4 Substrate Evaluation

Once the demoulding process was finished, the microstructure of the substrates was examined using a three-dimensional (3D) laser microscope known as LEXT OLS5000 Olympus. To evaluate the precision of replication and the integrity of the surface, we conducted measurements of the Sag height and diameter for each microdimple and documented the data for every sample. The research identified

differences between the height of the mould Sag and the Sag height of the replicated substrate. These differences were recognized as shrinkage that occurred during the cooling process and the presence of trapped air during the pressing process.

3 Results and Discussion

This research study utilises two primary statistical techniques: Analysis of Variance (ANOVA) and Response Surface Methodology (RSM). The Design Expert v13 software is utilised as a statistical tool to assess the differences between two or more means [9, 10]. ANOVA is used to assess if there are statistically significant differences between the means. With the FCD approach, there are three (3) responses ($n = 3$) and six (6) central points ($n_0 = 6$), the total number of runs generated is 20.

An investigation was carried out to assess the impact of temperature, force, and holding time on the dimensional accuracy and surface roughness. Table 1 demonstrates that the temperature, force, and holding time have a substantial effect on the dimensional accuracy and surface roughness of the HDPE substrate. Equation 1 is utilised to compute the replication accuracy of an embossed microchannel.

$$\text{Replication Accuracy} = \frac{\text{Size of micro dimples substrate}}{\text{Size micro dimples insert}} \times 100 \quad (1)$$

3.1 Data Analysis—Normality Test

These results are subsequently employed to formulate an equation representing the responses. The normal probability plot must be measured and evaluated for range of residuals that should be near or close to the mean line for any ANOVA analysis [9, 10]. To validate the outcomes, a normality test is conducted to determine if a data set is well-modelled by a normal distribution and the results are presented in Fig. 5a and Fig. 5b as a normal probability plot. This graphical representation facilitates a comparison between the predicted and achieved values for the design matrix. Referring to Fig. 5a and b, it can be observed that the mean line, which represents the average responses of this experiment fits well with all the responses. This alignment indicates that the residuals, which are the discrepancies between anticipated and actual values, are minor and closely match the mean line. This approach is designed to ensure that the experimental findings are reliable and accurate.

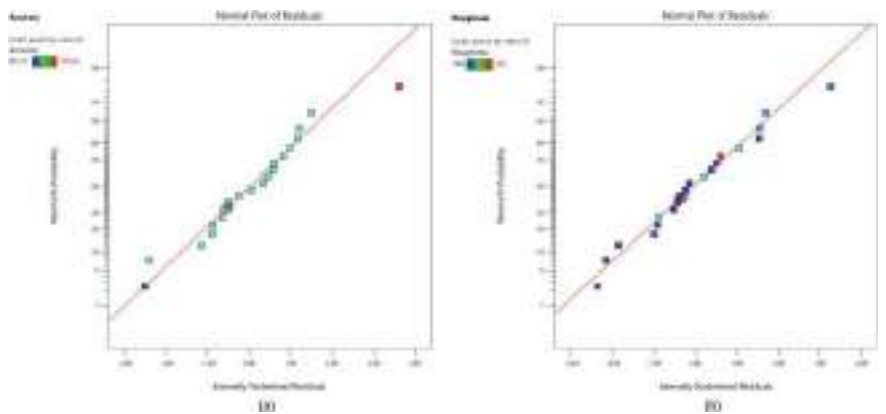


Fig. 5 Normal probability plot. **a** Accuracy, **b** roughness

3.2 *Impact of Hot Embossing Parameters on Dimensional Accuracy*

The analysis of variance (ANOVA) for dimensional accuracy and surface roughness, as well as the predicted regression coefficients, are shown in Tables 2 and 3, respectively. The model selection is determined by the presence of insignificant lack of fits. The Design Expert software suggests using a linear model for analysis during this test [1].

The ANOVA findings for the reduced quadratic model (Table 2) indicate that there is a statistically significant overall effect on Accuracy as the response variable, with an

Table 2 Summary ANOVA of result accuracy response in the reduced quadratic model

Source	Sum of squares	df	Mean square	F-value	p-value	
Model	26.01	7	3.72	3.22	0.0365	Significant
A-temperature	3.10	1	3.10	2.69	0.1270	
B-force	3.71	1	3.71	3.21	0.0982	
C-time	1.76	1	1.76	1.53	0.2399	
AB	3.25	1	3.25	2.82	0.1191	
AC	4.29	1	4.29	3.72	0.0777	
BC	4.84	1	4.84	4.19	0.0632	
A ²	5.05	1	5.05	4.38	0.0584	
Residual	13.85	12	1.15			Not significant
Lack of fit	8.00	7	1.14	0.9761	0.5299	
Pure error	5.85	5	1.17			
Cor total	39.85	19				

Table 3 Summary ANOVA of result surface roughness response in the reduced quadratic model

Source	Sum of squares	df	Mean square	F-value	p-value	
Model	19,967.60	10	1996.76	15.78	0.0002	Significant
A-temperature	1368.90	1	1368.90	10.82	0.0094	
B-force	1464.10	1	1464.10	11.57	0.0079	
C-time	5382.40	1	5382.40	42.53	0.0001	
AB	3003.13	1	3003.13	23.73	0.0009	
AC	2485.13	1	2485.13	19.64	0.0016	
BC	1830.13	1	1830.13	14.46	0.0042	
A ²	8.20	1	8.20	0.0648	0.8047	
B ²	164.20	1	164.20	1.30	0.2841	
C ²	481.14	1	481.14	3.80	0.0830	
ABC	2415.13	1	2415.13	19.08	0.0018	
Residual	1138.95	9	126.55			Not significant
Lack of fit	760.11	4	190.03	2.51	0.1703	
Pure error	378.83	5	75.77			
Cor total	21,106.55	19				

F-value of 3.22 and a p-value of 0.0365. Nevertheless, upon examining the individual predictor variables (A-Temperature, B-Force, C-Time, AB, AC, BC, and A²), none of them exhibit a significant impact on explaining the variability in Accuracy (all p-values > 0.05). The Lack of Fit analysis demonstrates that the model fits well. While the model is generally significant, a more streamlined version may offer a more meaningful representation of the relationship between predictor variables and Accuracy.

The ANOVA findings indicate that the predictor variable “B-Force” has a p-value of 0.0982, which is slightly below the customary significance level of 0.05. However, this result is not sufficient to establish statistical significance. When comparing the two variables, “A-Temperature” has a p-value of 0.1270 and “C-Time” has a p-value of 0.2399. While the p-value of “B-Force” is lower compared to the other variables, it does not definitively prove statistical significance. Thus, one may tentatively argue that “B-Force” appears to be more suggestive of importance when compared to “A-Temperature” and “C-Time”.

The analysis of variance (ANOVA) reveals a significant interaction between specific parameters and the temperature during hot embossing. Figure 6a and b demonstrates the effects of hot embossing temperature and force on the accuracy of the micro-dimple's substrate [11]. The accuracy of the micro-dimple profile is enhanced when the hot embossing temperature is increased within the range of 150–170 °C, and similarly when the force is increased between 5 and 15 kilonewtons. As a result, the accuracy value increases from 97.12 to 105.29%. The improvement is due to the reduction in the viscosity of the polymer material as the temperature increases, resulting in better filling of the HDPE material into the cavities.

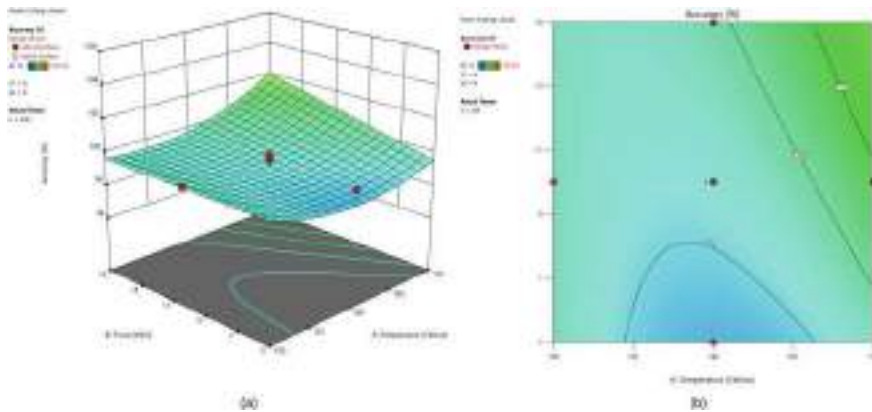


Fig. 6 Graph of temperature versus force on accuracy of HDPE substrate. **a** 3D surface, **b** contour plot

3.3 Impact of Hot Embossing Parameters on Surface Integrity

The ANOVA findings for the Reduced Cubic model (Table 3) demonstrate that the model successfully accounts for variations in Roughness. The Model F-value of 15.78 and the low p-value of 0.0002 indicate that there is a very low probability (0.02%) that the observed results are affected by random noise. The variables A (Temperature), B (Force), and C (Time), along with their interactions, have a considerable impact on Roughness. However, the squared values of A, B, and C (A^2 , B^2 , and C^2) do not have a significant impact on Roughness. The Lack of Fit analysis reveals a statistically insignificant lack of fit (F-value 2.51, p-value 0.1703), suggesting that the model adequately fits the data. The residual analysis (Residual Sum of Squares 1138.95, 9 degrees of freedom) provides insights into unexplained variability. In summary, the results guide interpretation, emphasizing significant factors affecting Roughness and suggesting potential model improvement by identifying non-significant terms. Factor Coding and Type III—Partial Sum of Squares enhance understanding of how factors are represented in the analysis.

The significance of Temperature, Force, and Time factors in our Analysis of Variance (ANOVA) can be gauged through their p-values. A lower p-value indicates stronger evidence against the null hypothesis, highlighting greater significance. In our analysis, Temperature, Force, and Time have p-values of 0.0094, 0.0079, and 0.0001, respectively. Among these factors, Time (C) is the most impactful on Roughness, with the smallest p-value. This suggests a high level of confidence that Time's effects on Roughness are not random. Consequently, in the Reduced Cubic model, HE time appears to be the most influential factor in determining the Roughness response, followed by force, and then temperature.

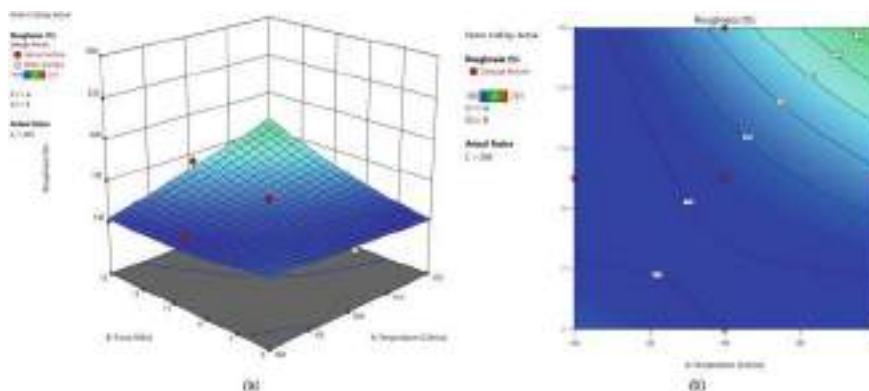


Fig. 7 Graph of temperature and force on roughness of HDPE substrate. **a** 3D surface, **b** contour plot

According to the analysis of variance (ANOVA), there is a significant interacting effect observed between the hot embossing temperature and the other factors. As the temperature for hot embossing increases, the value of surface roughness decreases, eventually matching or even reaching the roughness of the mould surface. The primary cause of this phenomenon is the influential function of temperature in determining surface roughness during hot embossing. An increase in temperature during the procedure leads to a decrease in surface roughness (R_a) [12]. The elevated temperature also amplifies the viscosity of the mould [13, 14]. The correlation between temperature, force, and surface roughness is represented in Fig. 7. The curvature of the graphs in Fig. 7a indicates the interplay among these factors. An increase in temperature and force results in a significant decrease in surface roughness. Optimal temperature conditions enhance the flow of polymer material, allowing it to effectively fill gaps or imperfections in the mould, resulting in a more polished surface [15].

4 Conclusion

In summary, this research has effectively designed a hot embossing technology specifically for producing micro dimples in HDPE. Consequently, the investigation reaches the following conclusion:

1. The study found that temperature, force, and embossing time have a substantial impact on the quality of the microdimples.
2. From analysis we can conclude that the force is the primary factor that influenced the dimensional accuracy of the micro-dimpled HDPE substrate structure, and the holding time is the primary factor that influenced the surface roughness of the micro-dimpled HDPE substrate structure.

3. The contour plot for ANOVA demonstrates that the precision in dimensions of micro dimples on HDPE substrate rises from 97.12 to 105.29 with an elevation in hot embossing temperature, moving from 150 to 170 °C.
4. The surface roughness percentage experienced a decline from 225 to 104 as the temperature rose from 150 to 170 °C. This reduction in surface roughness percentage indicates an improvement in the substrate's surface quality.

Acknowledgements The authors gratefully acknowledge the University Malaysia Pahang Al-Sultan Abdullah and University College TATI for their tremendous cooperation in completing this study.

References

1. Datta S, Deshmukh SS, Kar T, Goswami A (2023) A review on modelling and numerical simulation of micro hot embossing process: fabrication, mold filling behavior, and demolding analysis, 01 March 2023. Institute of Physics. <https://doi.org/10.1088/2631-8695/acc1c1>
2. Deshmukh SS, Goswami A (2020) Hot embossing of polymers – a review. *Mater Today Proc.* <https://doi.org/10.1016/j.matpr.2019.12.067>
3. Sangnal Matt Durandhara Murthy V, Vaidya U (2019) Improving the adhesion of glass/polypropylene (glass-PP) and high-density polyethylene (HDPE) surfaces by open air plasma treatment. *Int J Adhes Adhes* 95:102435. <https://doi.org/10.1016/j.ijadhadh.2019.102435>
4. Rosli A, Yan J (2015) Press molding of Si-HDPE hybrid lens substrate for infrared optical applications,” In: Proceedings of the 8th international conference on leading edge manufacturing in 21st century, LEM 2015. https://doi.org/10.1299/jsmelem.2015.8._2508-1_
5. Manaf ARA, Sugiyama T, Yan J (2017) Design and fabrication of Si-HDPE hybrid Fresnel lenses for infrared imaging systems. *Opt Express* 25(2):1202. <https://doi.org/10.1364/oe.25.001202>
6. Bin Ahmad MS, Manaf ARBA (2024) Hot embossing of micro grating and its replication accuracy. *J Adv Res Appl Mech* 113(1):118–137. <https://doi.org/10.37934/aram.113.1.118137>
7. Chen J, Chi W, Dang K, Xie P, Yang W (2021) Improving appearance quality of injection molded microcellular parts through mold coating of PTFE and zirconia. *J Appl Polym Sci* 138(33):50828. <https://doi.org/10.1002/app.50828>
8. Li J, Yu W, Zheng D, Zhao X, Choi CH, Sun G (2018) Hot embossing for whole Teflon superhydrophobic surfaces. *Coatings* 8(7):227. <https://doi.org/10.3390/coatings8070227>
9. Redhwan AAM, Azmi WH, Najafi G, Sharif MZ, Zawawi NNM (2019) Application of response surface methodology in optimization of automotive air-conditioning performance operating with SiO₂/PAG nanolubricant. *J Therm Anal Calorim* 135(2):1269–1283. <https://doi.org/10.1007/s10973-018-7539-6>
10. Khalil K, Mohd A, Mohamad COC, Faizul Y, Zainal Ariffin S (2021) The optimization of machining parameters on surface roughness for AISI D3 steel. *J Phys Conf Ser* 1874(1):012063. <https://doi.org/10.1088/1742-6596/1874/1/012063>
11. Schirmeister CG, Hees T, Licht EH, Mülhaupt R (2019) 3D printing of high density polyethylene by fused filament fabrication. *Addit Manuf* 28:152–159. <https://doi.org/10.1016/j.addma.2019.05.003>
12. Abdul Manaf AR, Yan J (2017) Improvement of form accuracy and surface integrity of Si-HDPE hybrid micro-lens arrays in press molding. *Precis Eng* 47:469–479. <https://doi.org/10.1016/j.precisioneng.2016.10.002>

13. Zou W, Sackmann J, Striegel A, Worgull M, Schomburg WK (2019) Comparison of hot embossing micro structures with and without ultrasound. *Microsyst Technol* 25(11):4185–4195. <https://doi.org/10.1007/s00542-019-04469-1>
14. Sun J et al (2019) Development and application of hot embossing in polymer processing: a review. *ES Mater Manufact* 6:3–17. <https://doi.org/10.30919/esmm5f605>
15. Xiong H, Wang L, Wang Z (2019) Chalcogenide microlens arrays fabricated using hot embossing with soft PDMS stamps. *J Non Cryst Solids* 521:119542. <https://doi.org/10.1016/j.jnoncrysol.2019.119542>

Sustainable Value Stream Mapping Application in the Furnace Process at a Large Nickle Company



Cristin Angel , Cucuk Nur Rosyidi , and Wakhid Ahmad Jauhari

Abstract This study aims to improve productivity in the skimming furnace process of a Large Nickle Company by applying the Sustainable Value Stream Mapping (Sus-VSM) method. This company focuses on the exploration and processing of nickel ore in Indonesia with an average production of 75,000 tonnes per year. By considering environmental, social, and economic aspects, the research aims to identify and eliminate waste that becomes a bottleneck in the production of nickel matte. The research used the American Productivity Center (APC) method to measure current productivity, while the Line Balance Ratio (LBR) assessed production imbalance. The cause of the problem was analyzed using fishbone analysis, and waste was corrected using the lean concept. The results show that the application of Sus-VSM can increase the productivity and efficiency of the furnace skimming process by reducing the duration of NVA (Non-Value Added) in the close to open skimming process by 21.27 min, determining the standard time to perform close to open skimming work for 164 min, improving operator working conditions by implementing the use of ear protection devices in the form of helmet mounted earmuffs, and designing modifications to the automatic rosebud tool equipped with hydraulic. Thus, the Sus-VSM method can be a sustainable solution to improve productivity and production balance in the nickel mining industry. The proposed improvements depicted in the future continuous value stream mapping can increase the time efficiency of the close to open skimming process by 5%.

Keywords Lean manufacturing · Sustainable value stream mapping · Productivity · Waste · Nickel

C. Angel (✉) · C. N. Rosyidi · W. A. Jauhari
Industrial Engineering Departement, Faculty of Engineering, Sebelas Maret University, Surakarta, Indonesia
e-mail: Cristinangl30@student.uns.ac.id

1 Introduction

The rapid development of the mining industry and the high demand for nickel encourage companies to increase productivity and competitiveness, one of which is through the application of lean manufacturing concepts. Lean manufacturing is a systematic approach that aims to eliminate waste and improve efficiency in the production process [1]. Its philosophy focuses on continuous improvement and eliminating non-value-added activities. The implementation of lean manufacturing in various industries has been proven effective, one of which is in a timing belt supplier company that experienced a 19.1% increase in productivity through a cycle time study [2], as well as a garment company that recorded a productivity increase of 16.66% [3].

This research focuses on the implementation of sustainable lean manufacturing with the Sustainable Value Stream Mapping (Sus-VSM) method at Nickel Company, which is the largest multinational company in nickel production in Indonesia. The production process at Nickel Company includes dryer, reduction furnace, smelting in electric furnace, and refining in converter. Based on observations, in the nickel ore processing process there is a problem in the form of accumulation of matte and slag products in the furnace (bottleneck). This problem is caused by inefficient use of time in the close to open skimming work process, resulting in non-value-added activities in the form of waiting time of 21.27 min. This causes the furnace process to not run efficiently and effectively, which will have an impact on the amount of production output and productivity. In addition, current global issues such as employee health and welfare and environmental sustainability are also behind this research. Thus, companies are required to care and be responsible for the environment and social. This is in accordance with the rules set by the government in Law No. 32 of 2009 and Law No. 46 of 2007 regarding social and environmental responsibility that must be implemented by companies.

This research extends the use of traditional VSM by incorporating sustainability metrics to create Sus-VSM, which has proven effective in various manufacturing case studies. As such, this research makes a significant contribution to the implementation of sustainable lean manufacturing in the mining industry, specifically in order to improve the productivity and long-term efficiency of the nickel production process at Nickel Company. This research aims to produce improvement proposals in the form of Future Sus-VSM on environmental, social, and economic aspects, which can be used to increase productivity in the skimming furnace process at Large Nickel Company. The proposed improvements are obtained from the results of waste elimination, noise control, workload minimization, and potential hazards that exist in the skimming furnace process environment.

2 Research Methodology

The research method used in this study is sustainable value stream mapping to improve productivity. This method considers the assessment of three important aspects including environmental, social, and economic. The aspect assessment is based on the sustainable value stream mapping matrix [4]. The selection of the assessment metrics is done by observation, interview, and document study. Thus, the assessment metrics for environmental aspects are noise measurements. The noise measurement metric aims to determine the noise level that exists in the furnace process, namely whether it is in the noise threshold range or not. The assessment metrics for social aspects are Physical Load Index (PLI) and Work Environment Risk. This metrics aims to determine the workload and potential hazards that exist in the furnace station work environment that can affect productivity. The assessment metrics for economic aspects are waste identification and elimination at close to open skimming process used kaizen [5] and time motion study [6]. This metric aims to increase time efficiency in order to increase productivity. In an effort to increase productivity, the American Productivity Center model is used to calculate the company's current productivity level, while the line balance rate (LBR) method is used to calculate the balance value of the production line.

3 Results and Discussion

3.1 American Productivity Center (APC) Calculation

APC is used to determine the current productivity level based on the productivity index, profitability index, and price improvement index [7]. The productivity level can be calculated using Eq. 1.

$$IPF = IP \times IPH \quad (1)$$

This calculation uses the company's output and input data in 2022 and 2023. The results of the productivity index calculation in Fig. 1 show that in 2023 the company's productivity increased by 10% because the amount of output increase was greater than the amount of input. The input that has the greatest influence is labor by 24%, so it is concluded that the company is able to increase labor productivity. The calculation of the profitability index in Fig. 2 shows that the company's profitability has decreased by 8% with the smallest profitability index being capital input. This happened because in 2023 the capital profitability index decreased by 23% due to the addition of quite a lot of fixed assets in that period. The calculation of the price improvement index in Fig. 3 shows that the highest price improvement index is energy at 0.937%. Meanwhile, the lowest price improvement index is capital input at 0.699%. Based on Eq. (1), the profitability index is directly proportional to the

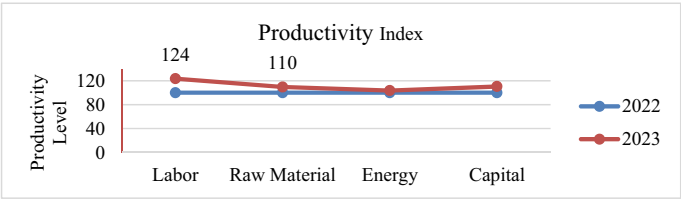


Fig. 1 Productivity index graph

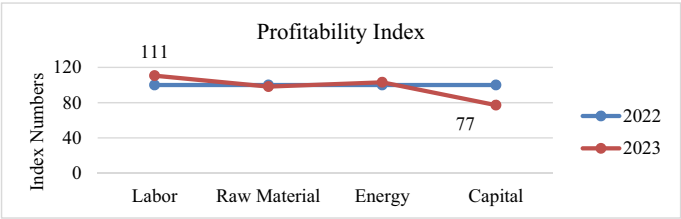


Fig. 2 Provitability index graph

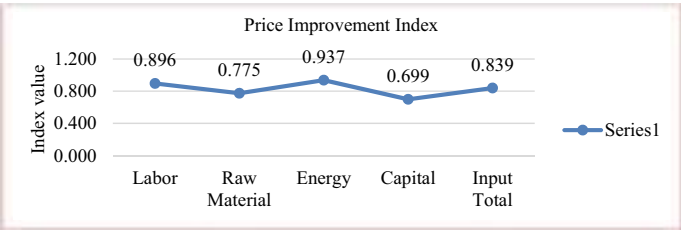


Fig. 3 Graph of price improvement index

productivity index but inversely proportional to the price improvement index. The higher the price improvement, the lower the profitability. Meanwhile, the higher the productivity development, the higher the profitability. Therefore, in this condition, increasing profitability can be done by improving the productivity of the company by focusing on improving labor input, capital input, and raw material input.

3.2 Line Balance Rate (LBR) Calculation

Line balance ratio is used to calculate the current level of balance in the nickel ore processing process [8]. The data used in this study are production output data and operating time of each work station. The calculation results in Fig. 4 show that the furnace process station has the lowest output amount with the highest total operating

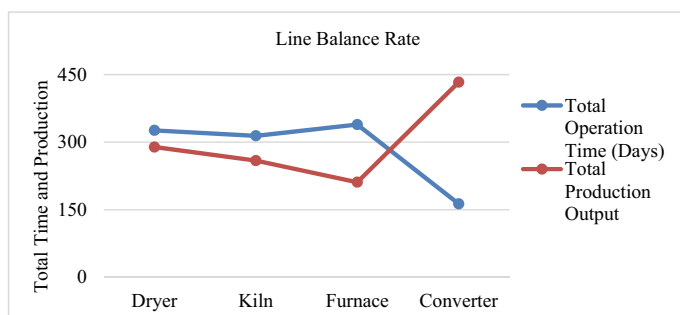


Fig. 4 Line balance rate

time, so it is concluded that there is a buildup of material (bottleneck) in the furnace process which causes unbalanced production.

3.3 *Economic Metrics*

Assessment of economic metrics of sustainable value stream mapping in the form of waste identification. Waste identification is carried out using the time and motion study method in the close to open skimming furnace process. Current Sus-VSM can help the waste identification process at the process station shown in Table 1. Shows the results of the time and motion study that consists of value-added (VA), necessary-non-value-added (NNVA) and non-value-added (NVA) activities that hinder the efficiency and effectiveness of the skimming and tapping process. Therefore, improvements are given to eliminate the non-value added.

3.4 *Social Metrics*

Social metrics explain the workload using the physical load index (PLI) and the work environment hazards to operators using work environment risk [9]. The workload is obtained from the results of the PLI questionnaire and interviews conducted in all furnace processes on shifts 1 and 2 shown in Table 2. The total PLI in the furnace process is 85.66. Based on the workload assessment range, this value represents that the work in the furnace process provides an average load with the strength of the pressure having a moderate impact on the operator. The work environment risk measurement shown in Table 3 produces three hazard factors that have the highest value, namely electrical systems, the use of chemicals and materials, and pressurized systems. Proposed improvements to social metrics are shown in Table 6.

Table 1 The results of time and motion study

Activity	Description	Average duration (min)
Close skimming	VA	1.05
Waiting for the haulmaster	NVA	3.70
Preparing the ladle (water pot)	VA	1.52
Picking up and positioning the hose	NVA	1.63
Flushing the launder	VA	4.12
Picking up the jack hammer	NVA	1.02
Cleaning the tilting	VA	12.64
Cleaning the launder	VA	35.40
Waiting for the loader	NVA	13.42
Moving the ladle (water pot)	NNVA	6.48
Waiting for CRO (Control Room Operator)	NNVA	77.50
Initial drilling on skimming	VA	9.74
Picking up and positioning the bar	NVA	0.90
Picking up and positioning the rosebud	NVA	0.60
Open skimming	VA	1.64

3.5 *Environmental Metrics*

The environmental metric assessment of sustainable value stream mapping is the measurement of the noise level in the furnace process. The results of the noise level calculation shown in Table 3 were measured using a sound level meter at each measurement point. The selection of measurement points considers areas that are representative of noise sources and affected areas. Based on the measurement results, measurement points 1 and 2 have noise levels above the threshold with a maximum exposure of 3.03 and 1.62 h. If workers do not use APT when exceeding the maximum exposure limit, it will cause hearing loss, so noise control needs to be done (Table 4).

3.6 *Current Value Stream Mapping (Sus-VSM)*

Current value stream mapping describes the current business process based on data collection conducted at the company. Figure 5 shows the information flow, material flow, lead time and cycle time created using Lucidchart software. The maximum lead time is found in the furnace process in the form of the calcsine material melting process. Based on the results of the time and motion study, the total NVA in the furnace skimming process is 21.27 min, the total NNVA is 83.98 min, and the total VA is 66.10 min. In addition, the current Sus-VSM figure also explains the results

Table 2 Physical Load Index (PLI)

Activity	Workload	PLI score	Description
Body position	Slight hunchback	4	Operator close skimming
	Hunchbacked once	0.4	Pick up and operate tools
	Entangled	0	
	Hunchback picking up	0.3	Picking up tools
Arms	One arm above shoulder	2	Lift bar
	Both arms above the shoulder	0	
Feet	Squat	3	Flushing the launderer
	Kneel	0	
	Walk	4	Doing work
A load that is lifted/brought down perpendicularly	Light load (<10)	1	Pick up equipment
	Medium load (10–20 kg)	0	
	Heavy load (>20 kg)	0	
Loads that are lifted/brought down in a bent manner	Light load (<10)	0	Remove rosebuds and bars
	Medium load (10–20 kg)	0	
	Heavy load (>20 kg)	4	
Total PLI		18.66	

Table 3 Work environment risk

Hazard factors	Value
Electrical system (E)	3
Chemical/Material usage (H)	3
Pressurized system (P)	3
High-speed component (S)	1

Table 4 Calculation result of noise level in furnace process

Measurement Point	Noise level (dB)	Maximum exposure limit (h)
Point 1 (skimming)	89.2	3.03
Point 2 feedbin)	84.1	9.62
Point 3 (transformer)	91.9	1.62

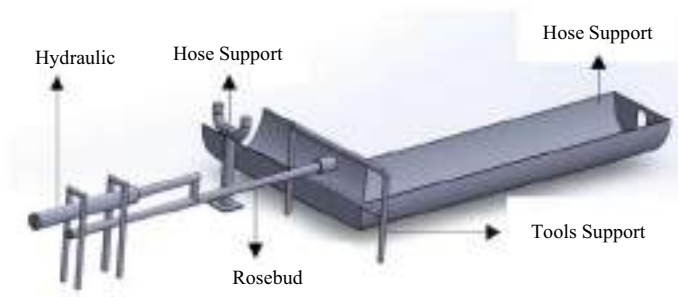


Fig. 5 Recommendations for proposed improvements to social aspects

of measuring the noise level in the furnace process. measurement point 1 has a noise level of 89 db, point 2 is 84 db, and point 3 is 90 db. This can have a negative impact on the operator’s health because the noise level exceeds the threshold. In addition to the noise level, workload and potential risks of the work environment can also affect the comfort and safety of operators while working. According to the image that the total PLI value has a value of 19 and the total average work environment value of 3 means that the strength and risk has the medium impact for worker.

3.7 Improvement Recommendation

See Table 5 and 6.

Table 5 Recommendations for proposed improvements in economic aspects

No.	Waste	Recommendation proposal economic aspects
1	Waiting for haulmaster and loader	Improving the communication system between operators and operations management
2	Waiting for hose collection	Set up hose storage tools, prepare equipment to be used before close skimming
3	Waiting for jack hammer retrieval	Designing a tool storage layout that is close to Launder and Tilting
4	Waiting for bar and rosebud positioning	Prepare the rosebud and bar tools to be used before open skimming. Store the tools in an organized manner after use
5	Waiting for CRO command to <i>open skimming</i>	Improve equipment maintenance system, using a drying system or the use of hot air to speed up the drying process drying, and training on proper equipment operation for operators

Table 6 Recommendations for proposed improvements in environmental and social aspects

Proposed improvements for environmental aspects	Proposed improvements for social aspects
Engineering control by designing a silencer	Controlling hazards caused by electrical systems by providing warning signs on each insulating equipment, using rubberized coatings on electrical cables in the metal floor area, testing and inspecting insulation and equipment, and using standard personal protective equipment from electrical hazards
Administrative control by creating a work rotation system	Control hazards caused by the use of chemicals by providing warning signs in the area, and using standard personal protective equipment regularly
Use of <i>moulded earmuff helmet</i>	Control hazards caused by system pressure by conducting regular inspection and maintenance of machines, providing safety training such as safe use of machines, and using standard personal protective equipment that has been set

3.8 Future Value Stream Mapping

Future value stream mapping represents the results of proposed improvements to increase productivity in nickel ore processing. Proposed improvements include waste elimination, use of personal protective equipment, tool design and modification. The proposed Future Sus-VSM is shown in Fig. 7. The implementation of the proposed improvements results in time efficiency to complete the close to open skimming process of 164 min with a noise level minimization of 30 db (Fig. 6).

4 Conclusions

This research applies the Sustainable Value Stream Mapping (Sus-VSM) method to improve productivity, efficiency, and operator welfare in the skimming furnace process at Nicle Company. Through the elimination of wastes such as delays and tool inefficiencies, the process time was cut from 171 to 164 min, increasing efficiency of the close to open skimming process by 5%. Social aspects were improved by reducing physical workload and hazard risk through modification of laundering tools and design of auxiliary tools to support worker safety and comfort. Environmental aspects were improved by controlling the impact of noise using ear protection equipment in the form of moulded earmuff helmets. The results of these improvements allow operators to work more safely and comfortably, supporting increased productivity and profitability of the company as well as operator welfare. For future research, it is recommended to cover the entire nickel processing process, and consider various environmental aspects.

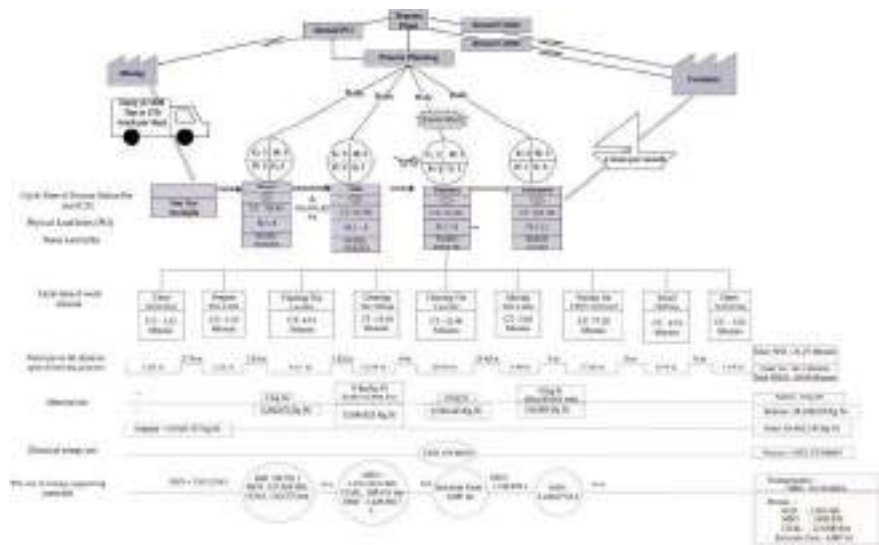


Fig. 6 Current sustainable value stream mapping

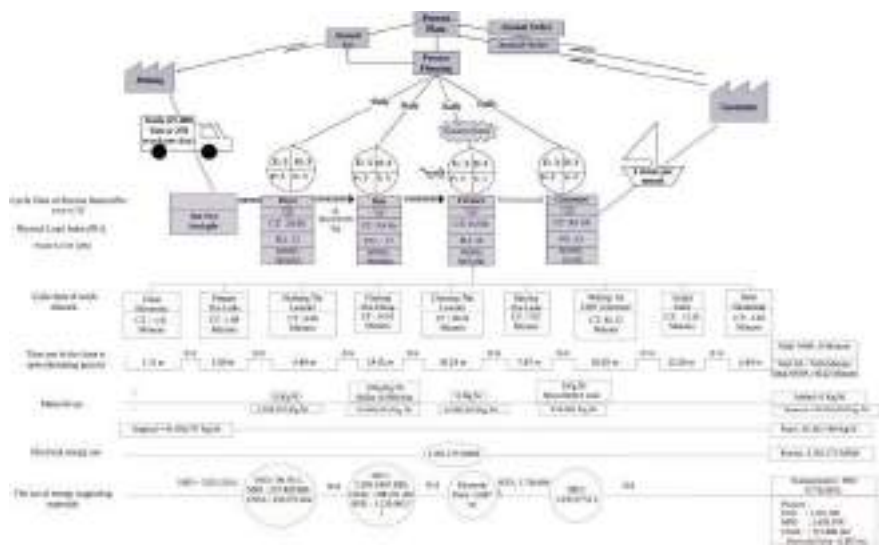


Fig. 7 Future sustainable value stream mapping

References

1. Batwara A, Sharma V, Makkar M, Giallanza A (2024) Impact of smart sustainable value stream mapping fuzzy PSI decision making framework. *Sustain Futures* 7:100–201. <https://doi.org/10.1016/j.sfr.2024.100201>

2. Edwin Joseph R, Kanya N, Bhaskar K, Francis Xavier J, Sendilvelan S, Prabhahar M, Kanimozhi N, Geetha S (2020) Analysis on productivity improvement, using lean manufacturing concepts. *Mater Today: Proc* 45:7176–7182. <https://doi.org/10.1016/J.Matpr.2021.02.412>
3. Mulugeta L (2020) Productivity improvement through lean manufacturing tools in Ethiopian garment manufacturing company. *Mater Today: Proc* 37(Part 2):1432–1436. <https://doi.org/10.1016/J.Matpr.2020.06.599>
4. Hartini S, Cipto Mulyono U, Anityasari M, Sriyanto M (2020) Manufacturing sustainability assessment using a lean manufacturing tool: a case study in the Indonesian wooden furniture industry. *Int J Lean Six Sigma* 11(5):957–985. <https://doi.org/10.1108/Ijls-12-2017-0150>
5. Santos E, Lima TM, Gaspar PD (2023) Optimization of the production management of an upholstery manufacturing process using lean tools: a case study. *Appl Sci (Switz)* 13(17). <https://doi.org/10.3390/App1317997>
6. Cury PHA, Saraiva J (2018) Time and motion study applied to a production line of organic lenses in Manaus industrial hub. *Gestao E Producao* 25(4):901–915. <https://doi.org/10.1590/0104-530x2881-18>
7. Ahmudi, Mahachandra M, Handayani NU (2019) Productivity evaluation through American productivity center approach at PT Sejahtera Furnindo. *IOP Conf Ser: Mater Sci Eng*. <https://doi.org/10.1088/1757-899X/598/1/012074>
8. Teshome MM, Meles TY, Yang C-L (2024) Productivity improvement through assembly line balancing by using simulation modeling incase of Abay garment industry Gondar. *Heliyon* 10:e23585. <https://doi.org/10.1016/j.heliyon.2023.e23585>
9. Hollmann S, Klimmer F, Schmidt KH, Kylian H (1999) Validation of a questionnaire for assessing physical work load. *Scand J Work Environ Health* 25(2):105–114. <https://doi.org/10.5271/Sjweh.412>

Green Strategy Implementation and Innovativeness in SMEs: A Pathway Towards Sustainable Development Goals



Iwan Inrawan Wiratmadja, Fandi Achmad, and Afrin Fauzya Rizana

Abstract Environmental sustainability has emerged as a critical global concern driven by climate change, biodiversity loss, and pollution. Small and Medium Enterprises (SMEs), which constitute approximately 90% of businesses and over 50% of jobs worldwide, encounter significant challenges in implementing sustainable practices due to limited resources and knowledge. This study investigates how SMEs can integrate green strategies and innovative practices to achieve sustainability goals within the Sustainable Development Goals (SDGs) framework. Therefore, The research aims to develop a conceptual model that combines green business strategies, green competencies, green innovation, and green manufacturing practices to enhance SMEs' sustainable performance. The study employs an exploratory–descriptive approach, analyzing literature to identify key themes and relationships between variables. The proposed model highlights the importance of green competencies, including knowledge, skills, and attitudes, in fostering green innovation and manufacturing practices. The findings suggest that green strategies can improve SMEs' operational efficiency, reduce environmental impacts, and enhance competitiveness. This research contributes to the literature by focusing on SMEs' role as change agents in achieving global sustainability and offers practical recommendations for implementing green strategies effectively.

Keywords Green business strategies · Green competencies · Green innovation · Green manufacturing practice · Sustainability performance

I. I. Wiratmadja · A. F. Rizana (✉)
Bandung Institute of Technology, Bandung, Indonesia
e-mail: afrinfauzya@telkomuniversity.ac.id

F. Achmad · A. F. Rizana
Telkom University, Bandung, Indonesia

1 Introduction

Environmental sustainability has become a pressing global issue due to climate change, biodiversity decline, and pollution [1, 2]. Industries face pressure to reduce their ecological footprint while maintaining profitability. Sustainability entails the ability to fulfill present needs without compromising future generations' ability to fulfill their own needs [2, 3]. This highlights the importance of sustainability-focused business strategies. Small and Medium-sized Enterprises (SMEs) significantly contribute to the global economy but often lack the resources to implement sustainable practices [3]. This is exacerbated by rising consumer expectations for environmentally friendly products and services, creating an urgent need for innovative approaches to help SMEs become sustainable and competitive [3–5]. SMEs make up about 90% of businesses and over 50% of jobs worldwide [6]. They face challenges like limited access to financial resources, technology, and knowledge for sustainable practices. In developing countries, SMEs are vital to local economies, and their adoption of sustainability principles has broad implications for economic and social development [3, 7]. This study examines how SMEs can integrate green strategies and innovative practices to achieve sustainability goals. Within the framework of the Sustainable Development Goals (SDGs), particularly goals 8 (decent work and economic growth), 9 (industry, innovation, and infrastructure), and 12 (responsible consumption and production), it is crucial to develop policies that support environmental sustainability. Sustainable practices in SMEs can reduce environmental impacts and enhance their global market position. Integrating SDG principles into SME operations is essential for inclusive and sustainable development, supporting long-term economic resilience and societal well-being.

SMEs contribute significantly to economic development but also cause considerable environmental problems, generating about 70% of global pollution. In Asia, SMEs exacerbate resource consumption and environmental issues, leading to climate change and frequent natural disasters. The raw material used per GDP unit in Asia is double that of other regions, causing significant environmental impacts and resource scarcity. Despite recognizing sustainability's importance, SMEs face obstacles in implementing green strategies, primarily due to a lack of understanding and skills in practical sustainability. Caldera et al. [8] highlight that many SMEs prioritize short-term profits over long-term sustainable benefits. Structural barriers, like limited access to green technologies and financial support, along with regulatory limitations, further hinder SMEs' sustainability efforts [9, 10]. These challenges necessitate improved resource utilization to align economic development with environmental preservation [11, 12].

In facing the challenges of implementing green strategies, several key factors can influence the success of SMEs in adopting sustainable practices. One of them is the development of green competencies, which include the knowledge, skills, and attitudes needed to implement environmentally friendly business practices [11]. In addition, adopting a green business strategy that is integrated with the organization's goals is also an essential factor. This strategy should improve operational efficiency, reduce

waste, and minimize environmental impacts while focusing on profitability. Green technology and product innovation also play a crucial role in supporting sustainable practices [5]. These technologies not only help reduce emissions and waste but also increase the competitiveness of products and services in the market [12–14]. Another influencing factor is support from external stakeholders, including the government, consumers, and local communities. This support can be through financial incentives, establishing a supportive regulatory framework, and increasing consumer awareness and demand for green products. By identifying and utilizing these factors, SMEs can more easily transition to sustainable business practices.

Previous research [7, 12, 14–16] has shown that implementing green strategies can provide significant benefits to organizations, including improved reputation, reduced operating costs, and improved environmental performance. Adopting green technologies can improve energy efficiency, reduce greenhouse gas emissions, and help companies cope with pressure from regulators and consumers to adopt sustainable practices. However, these studies often focus on large companies, while SMEs are often overlooked. In the context of SMEs, limited resources and knowledge are significant barriers to adopting sustainable practices, but support from the government and community can help overcome these challenges. This study aims to fill the literature gap by focusing on SMEs' role in implementing green strategies and innovation. This study focuses on SMEs as change agents in achieving the Sustainable Development Goals. By highlighting the role of SMEs, this study offers a new perspective on the contribution of small organizations to global sustainability. This study aims to develop a model that integrates green strategy, green manufacturing practice, and green innovation to support SMEs' sustainability. This study aims to identify and analyze the factors that influence the adoption of green strategies and innovation in SMEs and their impacts on business performance, the environment, and society. This study also provides practical recommendations for SMEs in implementing green strategies effectively, with the hope of making significant contributions to academic literature and industry practices and facilitating SDG achievement through innovative and sustainable approaches.

2 Method

This study aims to design a new conceptual model related to the role of green business strategy and green competencies towards green innovation and the role of green innovation towards green manufacturing practice, which ultimately impacts sustainable performance in SMEs. This model seeks to provide an overview for SMEs on how they can develop green strategies, the capabilities needed for successful green manufacturing practices, and how synergies between strategies and capabilities can drive SME innovation for green manufacturing and lead to sustainability. This study uses an exploratory, descriptive approach to develop a model based on a literature review. The relationship between the exploratory descriptive research method and the theoretical analytical approach can be described in Fig. 1.

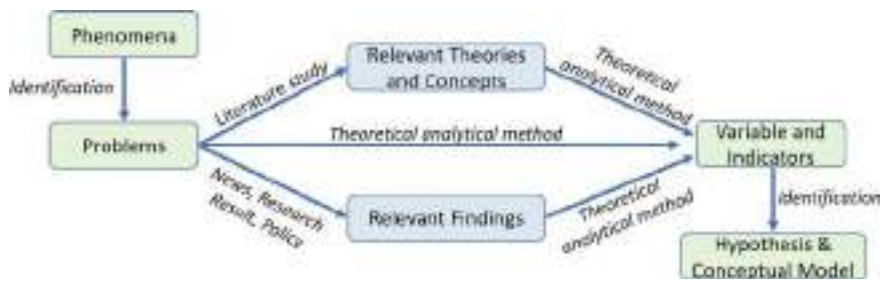


Fig. 1 Research steps

The data obtained from the literature review were analyzed qualitatively to identify key themes and relationships between the variables studied. The results of the analysis were used to develop a comprehensive and in-depth model. The research model built in this study consists of five main variables: green business strategy, green competencies, green innovation, green manufacturing practice, and SMEs sustainability performance.

3 Result and Discussion

SMEs are one sector that contributes greatly to extraordinary resource consumption, waste and environmental problems, so discussions regarding the achievement of sustainability performance in the context of SMEs need to be carried out. Sustainability in SMEs is considered a critical topic that requires great efforts to achieve. This research proposes a conceptual model that integrates green strategy, green manufacturing practice, and green innovation in encouraging sustainability in SMEs. Simultaneously with the development of the conceptual model, this research also proposes 4 hypotheses. The proposed conceptual model is shown in Fig. 2.

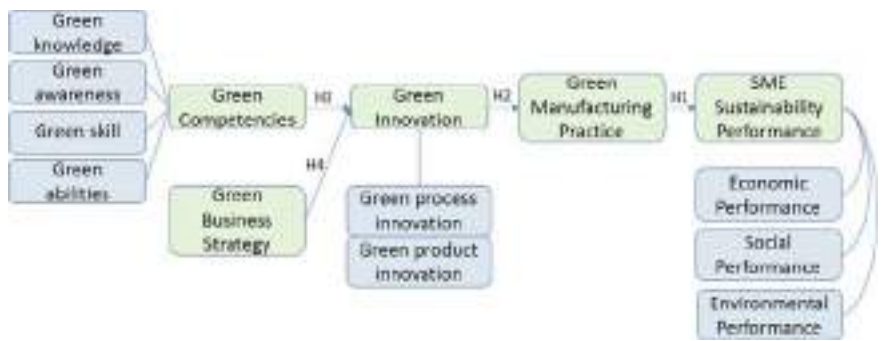


Fig. 2 Proposed conceptual model

Table 1 Definition of variable

Variable	Definition
Green competencies	Set of abilities, skills, knowledge, and commitment, which enable an organization to work efficiently
Green business strategy	The proactive integration of environmental concerns into the strategic plans of various departments within a firm
Green innovation	Ability to develop ideas, products, and processes that can minimize the environmental impact generated by the company's operational processes
Green manufacturing Practice	An approach aimed at minimizing the negative environmental consequences of production by reducing toxics, waste, pollution, and optimizing use of raw material and energy
SMEs sustainable performance	The ability of SMEs to be able to meet current needs and at the same time strive to ensure that future generations can continue to meet their needs by balancing the achievement of economic performance with environmental and social aspects

The designed research model includes all relevant variables and relationships. Table 1 defines the concepts used in this study.

3.1 *SME Sustainability*

The terms sustainable, sustainable development, and sustainability are often used interchangeably, with all three terms emphasizing the relationship between social justice, economic productivity, and environmental quality. Sustainable development is rooted in environmental awareness, which emerged in the 1970s. The concepts of sustainability and sustainable development began to be recognized and became the starting point for discussions by various parties since the World Commission on Environment and Development (WCED) held a conference in Brussels and published a Report entitled *Our Common Future* [16]. Several researchers have shown various interpretations of sustainability, so there is no universally accepted and agreed definition of sustainability [17, 18]. In the context of organizations, most discussions about sustainability focus on the triple bottom line (TBL) concept introduced by Elkingtons in 1997, which consists of economic, environmental, and social dimensions [11, 17]. SMEs still have difficulty understanding and implementing sustainable practices due to the complexity of sustainability issues, limited understanding of sustainability, and limited resources [11]. Several previous studies have attempted to study sustainability for SMEs in general [11], manufacturing SMEs [12], and service SMEs [3]. In general, these studies emphasize the importance of competence, innovation, strategy, green practice, green culture, and the role of stakeholders in realizing sustainability in SMEs.

3.2 Green Manufacturing Practice and SME Sustainability

Green manufacturing is defined as an approach aimed at minimizing the negative environmental consequences of production by reducing toxics, waste, pollution, and optimising use of raw material and energy [19, 20]. The term green manufacturing was created to represent the emerging manufacturing approach that incorporates a range of green strategies in order to enhance ecological efficiency. Green manufacturing practice assists organization, including small, medium, and large enterprises, to understand what has to be done to mitigate the negative impacts of manufacturing processes on the environment. Green manufacturing practice encompass the development of goods and systems that minimize the consumption of materials and energy, substituting non-toxic materials for toxic ones, using renewable materials instead of non-renewable ones, decreasing unwanted output, and transforming outputs into usable inputs through recycling [20]. Green manufacturing practice has significant potential for reducing emissions, managing energy, and improving resource efficiency [19]. Green manufacturing practice consists of practice related to reduce, reuse, recover, redesign, remanufacture, recycle and lean manufacturing practices [12]. Green practice can be applied in all manufacturing stream such as green procurement practice, green design, green process, green packaging, green marketing, green transportation, and reverse logistic [20]. Green manufacturing practice play a crucial role in providing guidance to both small and large enterprises on how to effectively address and mitigate their negative environmental consequence [21]. responsible for developing environmentally sustainable products that have no negative impact on the environment at any point of their life cycle, including manufacturing, usage, and disposal [21]. Organizations are forced to shift from traditional to environmentally-friendly practices in order to adapt and thrive in response to the increasing environmental issues. Organizations can attain sustainable performance by implementing green practices [7]. Green practice, such as green supply chain management practices enables firms to effectively meet their economic and environmental objectives and promote sustainability [7]. Organization that prioritize green supply chain goals consistently emphasize the need of their suppliers adopting environmentally friendly practices in order to achieve their performance-related objectives. Thus, this study propose the following hypotheses:

H1: Green manufacturing positively influences SME sustainability performance.

3.3 Green Innovation and Green Manufacturing Practice

Green innovation or technology innovation are two terms often used interchangeably, referring to a company's ability to develop ideas, products, and processes that can reduce the environmental consequences produced by the company's operational activities [12]. Green innovation includes adopting innovations in technology, products, processes, organizational structures, or management methods carried out by companies to achieve sustainable development [12]. Green innovation is related to reducing pollution, resource efficiency, minimizing waste, and reducing waste

[22]. Green innovation is generally categorized into two types: process innovation and product innovation [14]. Green product innovation involves a comprehensive approach to the product life cycle, from manufacturing to disposal, focusing on improvements in product durability, reducing and selecting environmentally healthier raw material, and eliminating hazardous substances, thereby promoting sustainability [14]. Meanwhile, green process innovation seeks to minimize energy usage in the manufacturing process and the conversion of waste into a valuable product. Green innovation allows enterprises to reduce the negative environmental impacts of their operations and gain a competitive advantage [23]. It can promote new manufacturing process and products that are less harmful to the ecosystem and natural environment [23]. Thus, this study propose the following hypotheses:

H2: Green innovation positively influences green manufacturing.

3.4 Green Competencies and Green Innovation

Competencies are the set of abilities, skills, knowledge, and commitment, which enable an organization to work efficiently [15, 24]. Green competencies refer to knowledge, abilities, and attitudes necessary to enable the minimization of negative impacts on the environment as well as initiating and implement action in accordance with the principles of sustainable development [25]. It is important for organization to possess basic knowledge of the environment, demonstrate awareness of environmental concerns, and have the necessary skills in order to address environmental challenges [15]. Green competences have been previously characterized as the combination of green knowledge, green awareness, green skills, and green abilities [15]. Beside those four factors, Cabral & Dhar, [24] added green attitude and green behavior as the components of green competencies. Green knowledge refers to the understanding of the facts, concepts, and linkages associated with the natural environment and the entire ecosystem [15, 24]. Green knowledge focuses on acquiring knowledge about environmental challenges and solution to address these issues by promoting environmentally friendly attitudes and behaviors [24]. Green awareness refer to the consciousness or perception of environmental issues and challenges caused by the organisation [26]. Green awareness allows organizations to assess the consequences of their actions to the environment and encourages organizations to be mindful of environmental degradation, leading to reduced energy consumption and improved energy efficiency [26]. Green skill refer to the specific skill needed to perform environmentally strategy and create green products and services [15]. Green skills are crucial for promoting sustainable development and enhancing pro-environmental initiatives, ensuring the positive effects of establishing an environmental management system [24]. Green abilities refer to capacity to combine theoretical knowledge and practical expertise in the natural environment to address real environmental issues, either naturally or acquired [24]. Organization can achieve green innovation by effectively acquiring, integrating, and implementing environmental knowledge, which enhances their ability to address the environmental challenges [15]. Previous study indicates that green competences are a crucial requirement for achieving green innovation [15]. Competencies serve as the

fundamental basis of motivation and capacity for firms to engage in innovation. The success of product or process innovation is mostly determined by the role played by competencies. Therefore, green competencies have become an essential aspect of organizations' green innovation. Thus, this study propose the following hypotheses:

H3: Green competencies positively influences green innovation.

3.5 Green Business Strategy and Green Innovation

In today business, implementing a green business strategy is widely recognized as a good approach to attain financial expansion and mitigate environmental degradation [27]. Green Business Strategy, refers to the proactive integration of environmental concerns into the strategic plans of various departments within a firm [15]. This term defined as the acknowledgment and integration of environmental issues into the development of company strategies across all functional areas, including human resource management, supply chain, manufacturing, marketing, and finance [27]. The implementation of green business strategy become essential due to a growing need and pressure from various stakeholder for businesses to protect the environment [27]. Companies that actively pursue green strategy can reap numerous advantages beyond financial gains [28]. Companies that lack a well-defined green strategy in their business will face difficulties to fulfill their environmental commitments, resulting to become uncompetitive and unresponsive to ecological well-being [27]. According to Yasir et al. [28], the generic strategic planning process consists of six step including: (1) setting the mission and goals; (2) situation analysis; (3) strategi choice; (4) strategy formulation; (5) implementation; and (6) evaluation. Implementing green business strategy enables the firm to comprehend and acknowledge innovative ideas, hence facilitating the alignment of strategies with the development of environmentally friendly products, services, and overall company expansion [29]. Green Business Strategies significantly impact an organization's creative side, aiding in the development of new green products and services. However, the success of these strategies depends on aligning green innovation strategies with the firm's strategic plans [15]. Thus, this study propose the following hypotheses:

H4: Green business strategy positively influences green innovation.

Our conceptual model offers a more holistic and integrated approach than previous models, which often focus on a single aspect like green innovation or manufacturing practices. This model uniquely combines green competencies, innovation, and manufacturing practices into one comprehensive framework. Notably, it highlights the often-overlooked role of green competencies as a foundational element influencing the effectiveness of green strategies. Additionally, it emphasizes the direct link between green manufacturing practices and sustainability performance, including economic, social, and environmental outcomes for SMEs.

4 Conclusion

This study highlights the importance of implementing green strategies and innovation in SMEs to achieve environmental sustainability. SMEs play a vital role in the global economy but need more resources and knowledge to adopt sustainable practices. By developing a conceptual model that integrates green business strategies, green competencies, and green innovation, this study shows that SMEs can improve their sustainability performance. Green competencies, which include the knowledge, skills, and attitudes required to carry out environmentally friendly business practices, are shown to be critical in driving green innovation and manufacturing practices. The results show that implementing green strategies improves operational efficiency, reduces environmental impacts, and enhances SMEs' competitiveness in the global market. In addition, support from external stakeholders, including government, consumers, and local communities, plays a significant role in facilitating SMEs' transition to sustainable practices. This study makes a significant contribution to the literature by highlighting the role of SMEs as agents of change in achieving sustainable development goals. SMEs contribute significantly to the SDGs, as they are often more innovative in sustainable practices than large industries, although resource constraints can limit their impact. However, their contribution remains vital, especially in local communities and developing regions. The findings of this study are enlightening, offering practical recommendations for SMEs in implementing green strategies effectively. Thus, this study is expected to encourage policies that support environmental sustainability and improve economic and social welfare in the long term.

References

1. Kolawole AS, Iyiola AO (2023) Environmental pollution: threats, impact on biodiversity, and protection strategies. In: Sustainable utilization and conservation of Africa's biological resources and environment, pp 377–409
2. Bakos J, Siu M, Orenge A, Kasiri N (2020) An analysis of environmental sustainability in small & medium-sized enterprises: patterns and trends. *Bus Strateg Environ* 29(3):1285–1296
3. Achmad F, Prambudia Y, Rumanti AA (2023) Sustainable tourism industry development: a collaborative model of open innovation, stakeholders, and support system facilities. *IEEE Access* 11:83343–83363
4. Rodrigues M, Franco M (2023) Green innovation in small and medium-sized enterprises (SMEs): a qualitative approach. *Sustainability* 15(5):4510
5. Achmad F, Wiratmadja II (2024) Driving Sustainable performance in SMEs through frugal innovation: the nexus of sustainable leadership, knowledge management, and dynamic capabilities. *IEEE Access* 12:103329–103347
6. Gherghina ȘC, Botezatu MA, Hosszu A, Simionescu LN (2020) Small and medium-sized enterprises (SMEs): the engine of economic growth through investments and innovation. *Sustainability* 12(1):347
7. Alraja MN, Imran R, Khashab BM, Shah M (2022) Technological innovation, sustainable green practices and SMEs sustainable performance in times of crisis (COVID-19 pandemic). *Inf Syst Front* 24(4):1081–1105

8. Caldera HTS, Desha C, Dawes L (2019) Evaluating the enablers and barriers for successful implementation of sustainable business practice in 'lean' SMEs. *J Clean Prod* 218:575–590
9. Rizos V, Behrens A, Van der Gaast W, Hofman E, Ioannou A, Kafyke T, Topi C (2016) Implementation of circular economy business models by small and medium-sized enterprises (SMEs): Barriers and enablers. *Sustainability* 8(11):1212
10. Achmad F, Prambudia Y, Rumanti AA (2023) Improving tourism industry performance through support system facilities and stakeholders: the role of environmental dynamism. *Sustainability* 15(5):4103
11. Kiranantawat B, Ahmad SZ (2023) Conceptualising the relationship between green dynamic capability and SME sustainability performance: the role of green innovation, organisational creativity and agility. *Int J Organ Anal* 31(7):3157–3178
12. Al-Hakimi MA, Al-Swidi AK, Gelaidan HM, Mohammed A (2022) The influence of green manufacturing practices on the corporate sustainable performance of SMEs under the effect of green organizational culture: a moderated mediation analysis. *J Clean Prod* 376:134346
13. Javaid M, Haleem A, Singh RP, Suman R, Gonzalez ES (2022) Understanding the adoption of Industry 4.0 technologies in improving environmental sustainability. *Sustain Oper Comput* 3:203–217
14. Xie X, Huo J, Zou H (2019) Green process innovation, green product innovation, and corporate financial performance: a content analysis method. *J Bus Res* 101:697–706
15. Yahya S, Khan A, Farooq M, Irfan M (2022) Integrating green business strategies and green competencies to enhance green innovation: evidence from manufacturing firms of Pakistan. *Environ Sci Pollut Res* 29(26):39500–39514
16. Ruggerio CA (2021) Sustainability and sustainable development: a review of principles and definitions. *Sci Total Environ* 786:147481
17. Amui LBL, Jabbour CJC, de Sousa Jabbour ABL, Kannan D (2017) Sustainability as a dynamic organizational capability: a systematic review and a future agenda toward a sustainable transition. *J Clean Prod* 142:308–322
18. Lankoski L (2016) Alternative conceptions of sustainability in a business context. *J Clean Prod* 139:847–857
19. Bendig D, Kleine-Stegemann L, Gisa K (2023) The green manufacturing framework—a systematic literature review. *Clean Eng Technol* 13:100613
20. Toke LK, Kalpande SD (2019) Critical success factors of green manufacturing for achieving sustainability in Indian context. *Int J Sustain Eng* 12(6):415–422
21. Omar A, Al-shari A, Shah SHA, Erkol Bayram G, Zameer Rahman E, Valeri M (2024) Green manufacturing practices and SMEs' sustainable performance: a moderated mediation mechanisms of green innovation and managerial discretion. *Eur Bus Rev* 36(4):588–609
22. Le TT (2022) How do corporate social responsibility and green innovation transform corporate green strategy into sustainable firm performance? *J Clean Prod* 362:132228
23. Shahzad M, Qu Y, Rehman SU, Zafar AU (2022) Adoption of green innovation technology to accelerate sustainable development among manufacturing industry. *J Innov Knowl* 7(4):100231
24. Cabral C, Dhar RL (2019) Green competencies: construct development and measurement validation. *J Clean Prod* 235:887–900
25. Graczyk-Kucharska M (2022) Achieving sustainable manufacturing and green organizations: preliminary research on green competencies. *Manag Prod Eng Rev* 13
26. Cabral C, Dhar RL (2021) Green competencies: insights and recommendations from a systematic literature review. *Benchmark Int J* 28(1):66–105
27. Begum S, Ashfaq M, Asiaei K, Shahzad K (2023) Green intellectual capital and green business strategy: the role of green absorptive capacity. *Bus Strateg Environ* 32(7):4907–4923
28. Yasir M, Majid A, Qudratullah H (2020) Promoting environmental performance in manufacturing industry of developing countries through environmental orientation and green business strategies. *J Clean Prod* 275:123003
29. Ashraf SF, Li C, Wattoo MU, Murad M, Mahmood B (2024) Green horizons: unleashing green innovation through green business strategies and competencies. *Bus Strateg Environ*

Development Model of Organizational Learning, Innovation and Performance: A Case Study on Disabled MSMEs in Bandung



Hanifah Widyarani Sinatrya, Luciana Andrawina, and Sri Martini

Abstract This study examines the development model of organizational learning, innovation, and performance within Micro, Small, and Medium Enterprises (MSMEs) owned by individuals with disabilities in Bandung. MSMEs play a vital role in economic growth and social inclusion, yet disabled MSMEs face unique challenges that hinder their development. Utilizing a mixed-methods approach, including qualitative interviews and quantitative data analysis through PLS-SEM, the research reveals that organizational learning positively influences innovation and performance, with path coefficients of 0.566 and 0.357, respectively. Furthermore, the study highlights the critical roles of government, academic institutions, and associations in supporting disabled MSMEs by providing resources, training, and collaborative opportunities. The findings emphasize the necessity for targeted interventions and strategic support to enhance the sustainability and competitiveness of disabled MSMEs, ultimately contributing to broader goals of economic equity and social inclusion. This research aims to provide actionable insights for policymakers, educators, and stakeholders to foster a more inclusive entrepreneurial landscape for individuals with disabilities.

Keywords Organizational learning · Innovation · Performance · Disabled MSMEs

1 Introduction

Micro, Small, and Medium Enterprises (MSMEs) play a vital role in driving economic growth and innovation globally, particularly in Indonesia, where they account for 99% of all enterprises and contribute over 61% to the national GDP [1]. Among these, disabled MSMEs, which are owned or operated by individuals with disabilities, are essential for promoting social and economic inclusion. There are

H. W. Sinatrya (✉) · L. Andrawina · S. Martini
Industrial Engineering, Telkom University, Bandung, Jawa Barat, Indonesia
e-mail: hanifahsinatrya@gmail.com

© The Author(s), under exclusive license to Springer Nature Singapore Pte Ltd. 2025
M. R. Mohamad Yasin et al. (eds.), *Proceedings of the 7th Asia Pacific Conference on Manufacturing Systems and 6th International Manufacturing Engineering Conference—Volume 2*, Lecture Notes in Mechanical Engineering,
https://doi.org/10.1007/978-981-96-5690-5_30

315

271,000 disabled MSME actors in West Java alone [2], reflecting a significant potential for economic contribution. However, these businesses face various challenges, such as social stigma, marketing, resources, limited access to capital, bureaucratic hurdles, and inadequate business knowledge [3, 4]. Despite the growth of MSMEs, the employment rate among persons with disabilities remains low, with only 55.5% employed as of August 2020 [5]. Therefore, interventions are needed to scale up their businesses and foster a more inclusive economic environment.

This study explores the relationship between organizational learning, innovation, and performance in disabled MSMEs, emphasizing the need for tailored support to address their specific challenges and opportunities. By collaborating with government, academics, and associations, this study aims to develop an actionable model to improve the performance and sustainability of disabled MSMEs, ultimately contributing to broader economic growth and social equality goals, as well as ensuring no one is left behind in the pursuit of sustainable development. The developed model can contribute to the achievement of SDGS 8 by increasing productivity and innovation among disabled MSMEs. By improving their access to new knowledge and skills, disabled MSMEs can develop more competitive products and services, thereby increasing their income and creating new jobs.

2 Literature Review

2.1 *Person with Disabilities*

There are various terms used to refer to individuals with disabilities, among which “persons with disabilities” and “differently abled” are commonly used. Disabilities are individuals with physical, intellectual, mental, and sensory limitations for an extended period and experience obstacles and difficulties to participate fully and effectively with other citizens based on equal rights but can still do things in different ways [6, 7]. Disabilities can include physical health impairments, sensory impairments, cognitive impairments, and mental health conditions [8, 9].

2.2 *Disabled MSMEs*

Micro, Small, and Medium Enterprises (MSMEs) are businesses operated by individuals, groups, small enterprises, or households. As a developing country, Indonesia views MSMEs as the foundation of the economic sector, fostering self-sufficiency in community economic growth [10]. Disabled MSMEs are businesses that involve individuals with disabilities, whether as owners, workers, or partners. They have at least two employees, including at least one person with a disability. These businesses operate across various sectors, such as fashion, crafts, culinary, and services,

and cater to individuals with diverse disabilities, including physical, mental, sensory, and intellectual impairments.

2.3 *Learning Organization*

Learning organizations refer to a type of organization, whereas organizational learning is the activity or process of learning within the organization. Therefore, learning organizations require effort, while organizational learning can occur without deliberate effort [11]. Organizational learning is the process by which organizations acquire, retain, and transfer knowledge to enhance performance and competitive advantage. This involves creating, preserving, and disseminating knowledge within the organization, enabling entities to adapt and innovate based on past experiences and insights [12]. The model of organizational learning represents a concept of continuous learning processes undertaken by organizations to create positive changes in performance and adaptation to their environment [13–15]. This process involves changes in the organizational model that allow the organization to maintain and improve its performance [13]. The concept underscores the importance of organizations continually learning independently to respond to changes quickly and effectively [15]. In organizational learning, developing new knowledge and insights from the experiences of individuals within the organization can influence behavior and enhance the company's capabilities [16].

2.4 *Innovation*

Innovation in organizational learning is a crucial driver of organizational success and adaptability. It involves implementing new learning methods, such as different learning models, using technology in education, or developing innovative learning strategies [17]. Innovation can also be linked to the development of organizational innovation as a mediator between organizational learning and organizational performance [18]. In MSMEs, innovation can be measured through three main dimensions: product innovation, process innovation, and management system innovation [19]. Product innovation includes developing new products or improvements to existing products to meet evolving market needs, while process innovation focuses on changes in how MSMEs conduct operational or production activities to enhance efficiency and quality. Management system innovation encompasses the management of resources, business processes, and strategies to achieve better business objectives. MSMEs actors must be capable of innovating to adapt to changes in the business environment [19].

2.5 Performance

Performance is a crucial indicator for achieving business success and objectives, encompassing various factors such as financial inclusion, financial literacy, financial management, human resource competence, marketing strategies, and market orientation [20–24]. The measurement of MSME's performance can include financial and non-financial aspects, such as innovation, employee management, customer relations, and return on investment [20, 21]. Financial literacy, organizational culture, and risk management practices can significantly influence MSMEs' efficiency and overall performance [25]. Furthermore, social capital, knowledge transfer, and organizational learning capabilities contribute to organizational performance [26, 27].

2.6 Government, Academic, and Associations

MSMEs play a vital role in economic growth and job creation, particularly for individuals with disabilities. The government significantly contributes to MSME development by providing policies, resources, and support to help these enterprises navigate various challenges. Research indicates that government support positively influences innovation and performance among MSMEs, enhancing their overall impact on the national economy and employment rates [28]. Academic also play a crucial role in strengthening MSMEs through innovation, business consulting, and establishing business incubators. Their contributions enhance the competitiveness of MSMEs by providing essential training and financial guidance, especially for those operated by individuals with disabilities [29].

Additionally, academic institutions can facilitate community partnership programs that improve the capacities of these enterprises, ensuring they are better equipped to thrive in the marketplace [3]. Associations further support MSMEs by serving as platforms for knowledge sharing, legal protection, and advocacy. These organizations help disabled entrepreneurs develop their businesses by providing motivation, guidance, and networking opportunities, which are crucial for accessing broader markets and enhancing product competitiveness [4, 30].

3 Research Method

This research uses a qualitative-quantitative method with qualitative data collection techniques in the form of interviews with disabled MSMEs, Sentra Wyata Guna, and CidCo (Creative Business of Disabled Community). In contrast, quantitative data collection is carried out by distributing questionnaires to disabled MSMEs in Bandung. Determining the number of respondents with a minimum sample of 5–10

times the dimension. This study has 9 dimensions and uses a minimum sample of 6 times the dimension, so a minimum of 54 respondents is required. This research aims to determine the relationship between variables based on previous research. This research is designed as cross-sectional, which means that data is collected within a certain period and analyzed, and conclusions are drawn based on the data.

The research methodology is structured into four key stages. The introductory stage begins with identifying the background of the problem, focusing on MSMEs run by individuals with disabilities in Bandung. This involves literature studies and observations to gather relevant data, theories, and insights. Based on these findings, the research problem is formulated, leading to the establishment of objectives and defining the scope of the study, which centers on three variables: organizational learning, innovation, and performance. Next, the research model is developed in the data collection and processing stage, and hypotheses are formulated based on previous studies. Data collection involves primary data obtained through questionnaires and secondary data from existing literature and reports. The data is processed using PLS-SEM, which includes creating a model construct, conducting validity and reliability tests, and ensuring the accuracy and consistency of the collected data. Structural model testing follows, allowing for an examination of the relationships among the identified constructs. Finally, during the analysis stage, the results from the model testing are interpreted to derive hypothesis testing outcomes. This stage culminates in the closing stage, where conclusions are drawn, the overall analysis results are summarized, and recommendations are provided to enhance future research endeavors. This comprehensive methodology ensures a thorough exploration of the interplay between organizational learning, innovation, and the performance of MSMEs operated by individuals with disabilities.

4 Results and Discussion

The research sample consists of 57 respondents who are owners or workers of 27 disabled MSMEs in Bandung, covering various types of disabilities such as physical, intellectual, and sensory, at least 17 years old, and come from multiple business sectors such as fashion, culinary, and craft. There are both disabled and non-disabled respondents because not all owners or workers of disabled MSMEs are disabled. Reliability and AVE (Average Variance Extracted) can be seen in Table 1, the research instrument shows good reliability. The Cronbach's Alpha value of all items is above 0.6 and Composite Reliability is above 0.7. In addition, the AVE value for all constructs is greater than 0.5. These results indicate that the research instrument can measure constructs reliably and validly. Furthermore, the path coefficients can be seen in Table 2, there is a positive and statistically significant relationship between the research variables.

Table 1 Reliability and AVE

	Cronbach's alpha	rho_A	Composite reliability	AVE
Efficiency	0.674	0.679	0.859	0.754
Experiment	0.833	1.267	0.878	0.646
Innovation	0.817	0.834	0.873	0.581
Product innovation	0.792	0.806	0.865	0.617
Process innovation	0.662	0.834	0.802	0.579
Interaction	0.677	0.726	0.815	0.597
Knowledge interpretation	0.800	0.834	0.908	0.832
Finance	0.881	0.886	0.914	0.680
Performance	0.859	0.868	0.894	0.553
Operational	0.688	0.698	0.827	0.615
Organizational learning	0.790	0.799	0.858	0.551
Risk taking	0.677	0.794	0.854	0.746

Table 2 Path coefficients

	Original sample	Sample mean	Standard deviation	T statistics	P values
Innovation \leq performance	0.292	0.285	0.153	1.915	0.055
Organizational learning \leq innovation	0.566	0.569	0.105	5.379	0.000
Organizational learning \leq performance	0.357	0.367	0.157	2.271	0.023

4.1 Organizational Learning Positively Affects Innovation

The PLS-SEM analysis results in Table 2 indicate that organizational learning positively influences innovation, with a path coefficient of 0.566. This suggests that as the level of organizational learning increases, so does the level of innovation produced. The T-statistics value of 5.379 is greater than 1.96, indicating a statistically significant relationship, while the P-value of 0.000 provides strong evidence to support the hypothesis. Dimensions affecting organizational learning include interaction, experimentation, risk-taking, and knowledge interpretation, with each dimension having indicators.

The interaction dimension measures how often and effectively disabled MSMEs exchange information and ideas with their external environment, fostering innovation. Interviews reveal that these MSMEs engage in various activities such as visits, research, and training to enhance this exchange. The experimentation dimension shows how disabled MSMEs find new ways to operate, adapting their marketing strategies and utilizing digital tools. Additionally, the risk-taking dimension highlights their willingness to innovate despite limitations in their workforce. Finally, the

knowledge interpretation dimension assesses how well these MSMEs understand and apply new knowledge, as indicated by their structured approaches to sharing information and documenting their processes. These findings align with prior research confirming the positive relationship between organizational learning and innovation.

4.2 Organizational Learning Positively Affects Performance

The PLS-SEM analysis in Table 2 indicates that organizational learning positively influences performance, evidenced by a path coefficient of 0.357. This implies that as the level of organizational learning increases, so does the level of performance achieved. The T-statistics value of 2.271 exceeds the threshold of 1.96, confirming the statistical significance of the relationship, while the P-value of 0.023 is less than 0.005, providing substantial evidence to support the hypothesis. Several dimensions affect performance, including financial, operational, and efficiency, with each dimension having indicators.

The financial dimension evaluates how well-disabled MSMEs manage their finances to enhance profitability and financial stability. Interviews revealed that not all disabled MSMEs experience continuous income and profit growth; however, they strive to improve their financial situation through various means, such as attending product-related training, engaging in digital marketing training to expand their reach, participating in community monitoring and support, learning from past mistakes, leveraging technology, and sharing knowledge with external parties. The operational dimension assesses the effectiveness of disabled MSMEs in their operations to enhance efficiency and productivity. To improve operational efficiency, these MSMEs consider customer feedback, seek skilled workers in their business sector, and prioritize motivated employees. Lastly, the efficiency dimension measures how effectively disabled MSMEs utilize resources to minimize costs and increase profitability. Strategies for enhancing efficiency include leveraging technology, providing ongoing training and support to workers, and considering innovations based on employee capabilities. These findings are consistent with previous research indicating a positive relationship between organizational learning and performance.

4.3 Innovation Positively Affects Performance

The PLS-SEM analysis results in Table 2 reveal that innovation positively impacts performance, indicated by a path coefficient of 0.292. This suggests that higher levels of innovation correlate with improved performance outcomes. The T-statistics value of 1.915 is slightly below the critical threshold of 1.96, indicating that the relationship between innovation and performance is statistically significant. Moreover, the P-value of 0.055 is less than 0.005, providing adequate evidence to support the

hypothesis. Several dimensions influence innovation, including product innovation and process innovation, with each dimension having indicators.

The product innovation dimension assesses how frequently disabled MSMEs introduce new or enhanced products, aiming to attract new customers, increase market share, and boost profitability [31]. Interviews indicated that while disabled MSMEs strive to introduce new products, not all do so regularly. Some MSMEs have dedicated teams for product innovation, enabling disabled workers to follow the team's direction. However, some MSMEs encourage disabled workers to innovate independently, even though product innovations may not always align with customer needs due to the workers' capabilities. The process innovation dimension evaluates how often disabled MSMEs implement improved processes to enhance efficiency, reduce costs, and improve product or service quality [32]. The interviews revealed that all disabled MSMEs are trying to innovate processes through various means, such as attending training sessions, incorporating customer feedback, collaborating with external partners, and researching industry practices. These findings align with previous research indicating a positive relationship between innovation and performance.

4.4 Government, Academic, and Associations Can Influence the Relationship Between Organizational Learning, Innovation, and Performance

This study investigates the impact of government, academic, and associations on organizational learning, innovation, and performance within disabled MSMEs. Data was collected through interviews, focusing on the roles and forms of collaboration between these entities and the businesses they support, as well as an analysis of prior research.

The government is crucial in supporting disabled MSMEs through various programs and policies. One of them is at the Sentra Wyata Guna, an organization under the Ministry of Social Affairs of the Republic of Indonesia that focuses on rehabilitation and training for the independence of disabled individuals. It provides educational services, training, mentoring, internship programs at Cafe More, and facilities for starting businesses within the center. The education, training, and mentoring aim to empower disabled individuals to become financially independent, with earnings approaching the regional minimum wage (UMR). After achieving independence, Sentra Wyata Guna offers these entrepreneurs business capital and monitoring. Interviews with participants under the Sentra Wyata Guna program reveal significant benefits, indicating that these services help them attain financial independence and enhance their business success. Furthermore, training and mentoring promote innovation to improve performance and business quality. However, feedback from other disabled MSMEs indicates that Sentra Wyata Guna's services and other government programs have not reached all disabled MSMEs. Many feel a lack

of government collaboration and assert that policies often tend to be general and not focused on the specific needs of disabled MSMEs. Consequently, these entrepreneurs hope for government-targeted programs and policies that address the unique challenges disabled MSMEs face. Previous studies support these findings, indicating that effective government policies and programs can significantly enhance MSMEs' organizational learning, innovation, and performance [27, 31, 33].

Academic institutions also play a vital role in supporting disabled MSMEs. One is at the Widyatama University in Bandung, which contributes to disabled individuals through the Art Therapy Center, a hub for scientific contributions and support for disabled individuals. The center has various programs and activities, including a disabled business community called CidCo, which promotes financial independence by producing and marketing creative products. CidCo is currently part of a program under the Department of Cooperatives and MSMEs in Bandung to assist with marketing and development. Additionally, several disabled MSMEs collaborate with universities for research on their products, such as UMKM Madu Raden Ibrahim working with ITB to test honey quality. Moreover, some MSMEs welcome research conducted by students from various universities, which positively impacts their ability to enhance product quality and competitiveness. Prior research also indicates that academic involvement in MSME development can improve organizational learning, innovation, and performance [28, 31, 34].

Associations support disabled MSMEs by enhancing their organizational learning, innovation, and performance. Interviews reveal that disabled MSMEs often collaborate more with associations than government entities or academic institutions. Associations like Setara Berdaya, Alunjiva, Rumah Cintara, Biruku Indonesia, House of Hope, Dilans, and Bilic provide various services to assist disabled MSMEs, including mentoring, training, grants, promotional support through websites and bazaars, seminars, packaging assistance, and help with business licenses and halal certificates. Associations also facilitate forums for sharing information, knowledge, and experiences among disabled MSME practitioners, fostering relationships that enhance competitiveness and business development. Entrepreneurs have expressed appreciation for the support received from these associations. Previous research corroborates these findings, showing that MSME associations can significantly improve their members organizational learning, innovation, and performance [31, 35].

The results of the research model can be seen in Fig. 1.

5 Conclusion

This study highlights the significance of organizational learning, innovation, and performance in the context of MSMEs owned by individuals with disabilities in Bandung. The analysis results indicate that organizational learning significantly impacts innovation and performance, with path coefficients of 0.566 and 0.357, respectively. This suggests that enhancing organizational learning contributes to

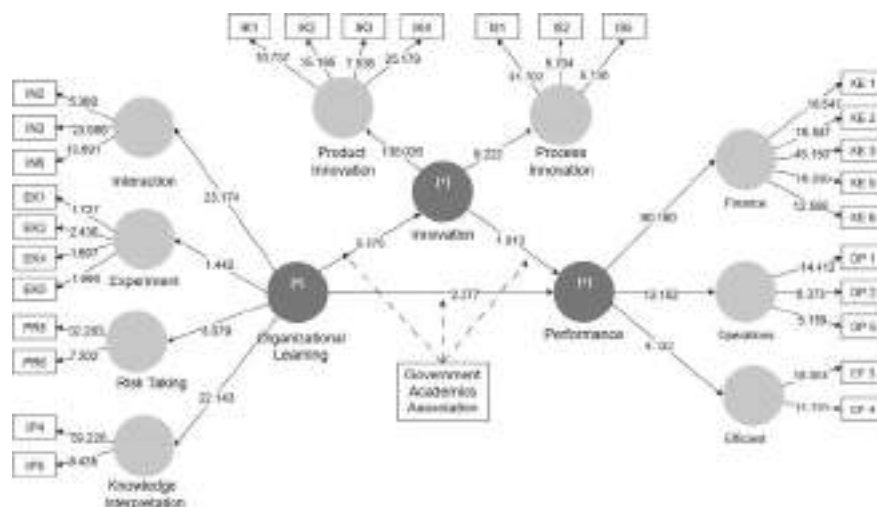


Fig. 1 Research model

improvements in innovation and performance, serving as a foundation for developing actionable strategies that address the unique challenges disabled MSMEs face. Furthermore, the roles of government, academia, and associations are crucial in supporting these enterprises by providing resources, training, and networking opportunities, ultimately fostering an inclusive environment that promotes the economic empowerment of individuals with disabilities. The findings underscore the need for targeted interventions and collaborative efforts to enhance the sustainability and growth of disabled MSMEs, ensuring that they can effectively participate in the broader economic landscape.

References

1. Kementerian Koperasi dan UKM (2023) The contribution of MSMEs to the national economy. Report on MSME development
2. Rezqiana R (2021) Disabled MSMEs in West Java: opportunities and challenges. *Econ Rev West Java* 10(2):75–89
3. Army A, Gunawan A, Mauliansyah R (2023) The role of government and academic institutions in supporting disabled MSMEs. *Journal of Economic Development* 25(3):67–81
4. Sawitri D, Indahsari R, Sari P (2021) The role of social capital in the development of disabled MSMEs. *Int J Commun Empower* 12(1):45–57
5. Fajri A, Nurhadi A, Supriyadi R (2021) Employment rates among persons with disabilities: a case study in Indonesia. *Sociol Work J* 11(3):134–145
6. Law No. 8 of 2016 (2016) Law No. 8 of 2016 on persons with disabilities
7. Maftuhin M (2016) Understanding the term “differently abled.” *J Disab Stud* 8(1):14–20
8. Okoro E, Fadeyi O, Orji U (2018) Health conditions and their impact on employment among persons with disabilities. *Int J Public Health* 63(2):123–135

9. Andrews R, James S, Kim T (2019) Understanding disabilities: a review of terminology and definitions. In: Smith J, Brown K (eds) 5th international conference on disability studies, vol 12345. LNCS. Springer, Heidelberg, pp 10–25
10. Vinatra A (2023) The role of MSMEs in the economic landscape of Indonesia. *J Econ Dev* 30(1):100–110
11. Ortenblad A (2001) On differences between organizational learning and learning organization. *Learn Organ* 8(3):125–133
12. Argote L, Miron-Spektor E (2011) Organizational learning: from experience to knowledge. *Organ Sci* 22(5):1123–1137
13. Simarmata J, Almaududi A (2019) Organizational learning: a framework for improving performance. *Int J Manag Sci* 20(3):120–135
14. Sultan F (2022) Adapting to change: the importance of organizational learning. *J Bus Res* 27(1):67–78
15. Taufik M, Nugroho A (2020) Learning organizations: strategies for enhancing performance. *Int J Organ Stud* 14(2):88–100
16. Jiménez-Jiménez D, Sanz-Valle R (2011) Innovation and organizational learning: the role of knowledge management. *Innov Manag* 5(2):145–162
17. Handayani R, Mardani A, Sari N (2020) Innovation in organizational learning: a review of recent studies. *Manag Sci* 15(1):12–28
18. Sulistyani R, Lathifah A (2020) Organizational learning and its impact on innovation and performance in MSMEs. *J Bus Innov* 15(4):330–342
19. Ariescy L, Cania A, Susdiani S (2022) Measuring innovation in MSMEs: dimensions and indicators. *Int J Bus Manag* 14(4):112–128
20. Kusuma H, Salim A, Dwi R (2022) Financial literacy and its impact on MSME performance. *J Field Actions* 19(1):78–90
21. Islami R, Sari Y, Azzahra N (2017) The importance of human resource competence in MSME success. *J Hum Resour Manag* 29(3):233–245
22. Mahastanti S, Utoyo S (2022) Market orientation and MSME performance: the mediating role of innovation. *Bus Res Q* 18(4):289–302
23. Hermawati H, Rindiani R, Puspita W (2020) Marketing strategies in MSMEs: a study of customer relations. *J Mark Res* 27(4):110–124
24. Saharsini A (2022) The impact of marketing strategies on MSME performance. *J Mark Stud* 11(3):210–222
25. Hadyan M, Rakhman M, Fadhlila D (2022) Financial management practices and their impact on MSME performance. *J Financ Stud* 20(2):44–58
26. Li S, Luo Y (2011) The role of social capital in enhancing organizational performance. *J Bus Strateg* 22(3):112–125
27. Ashtari R, Salehi-Sadaghiani M (2014) The impact of knowledge transfer on organizational performance. *J Knowl Manag* 18(1):45–56
28. Fauziyah R, Setyawan A, Sutrisno A (2020) Government support and its impact on innovation in MSMEs. *J Bus Res* 32(2):23–34
29. Gunawan A, Khotimah A, Budi R (2021) Enhancing MSME competitiveness through academic collaboration. *Int J Entrep* 9(1):56–72
30. Indahsari R (2021) Role of associations in empowering disabled MSMEs. *Int J Commun Dev* 5(2):95–106
31. Zahra SA, George G (2002) Absorptive capacity: a review, reconceptualization, and extension. *Acad Manag Rev* 27(2):185–203
32. Romer P (1994) Endogenous technological change. *J Polit Econ* 98(5):S71–S102
33. Porter, M.: Competitive Advantage: Creating and Sustaining Superior Performance. *Harvard Business Review Press* (1990).
34. Perkins, R., D. M., & Xu, S.: The Role of Academia in SME Development: A Review. *Journal of Small Business Management* 48(2), 223–243 (2010).
35. Tholib M, Shidiq A, Dwi S (2023) The influence of associations on MSME performance: a case study. *Int J Bus Stud* 10(1):56–70

Health Diagnostics for Lithium-Ion Batteries Using Convolutional Neural Network Model



Ikhsan Romli, Mohammad Mi'radj Isnaini, Rachmawati Wangsaputra, and Bermawi Priyatna Iskandar

Abstract Accurate health diagnostics are crucial for ensuring battery reliability in critical applications, preventing potential malfunctions, and reducing the risk of accidents. This research proposes a Data-Driven approach using Convolution Neural Network (CNN) model to diagnose battery health. Lithium-ion batteries (LIB) are a type of battery that is widely used in many industries. Battery datasets from NASA are used as training and testing datasets to build the proposed model. This study proposes SoH diagnostics based on data pre-processing method and CNN model. In data pre-processing, the capacity degradation data is visualized, highly related features are selected by Pearson Correlation Coefficient (PCC). Then, all features are normalized by the min-max feature scaling method, which will speed up the training process in achieving the minimum cost function and then data splitting is performed. After pre-processing, all selected features are incorporated into the CNN model. There are four main features in this study **i.e.** cycle (t), voltage (V), current (I), and temperature (T) as input data. The layering structure is configured by referring to Multi-Channel-CNN (MC-CNN) and LeNet-5. The output for predicting the battery uses State of Health (SoH). The proposed CNN show better results compare with MC-CNN, has result RMSE (Root Mean Square Error) as 1.58%.

Keywords SoH · CNN · Lithium-ion · Health diagnostics

I. Romli (✉) · M. Mi'radj Isnaini · R. Wangsaputra · B. P. Iskandar
Department of Industrial Engineering and Management, Faculty of Industrial Technology, Institut Teknologi Bandung, Bandung, Indonesia
e-mail: 33421004@mahasiswa.itb.ac.id

I. Romli
Department of Industrial Engineering, Universitas Pelita Bangsa, Bekasi, Indonesia

1 Introduction

Health diagnostics of the equipment have been applied to address potential problems in various industrial domains, such as manufacturing [1], aircraft [2], energy [3], and others. Proactive steps can be made to ensure dependable system performance once it is possible to forecast when damage will occur. Diagnostics can simplify standardized maintenance models by predicting component degradation in advance. Lithium-ion batteries (LIBs) are crucial for energy storage due to their long cycle life, high energy, and high power density, making their health diagnostics essential to prevent significant losses and dangers from potential failures [4]. To ensure optimal performance and longevity of LIB in various applications, it's essential to monitor their State of Health (SoH) by tracking impedance increase and capacity decrease [5]. This diagnostic process involves analyzing data such as voltage, current, and temperature to detect potential failures and ensure battery reliability [6].

Recent research aims to develop advanced methods for accurately assessing SoH of LIB. Effective diagnostic techniques are essential for enhancing battery reliability, safety, and overall system performance by enabling early detection of potential issues [7]. Researchers use different methods for State of Health (SoH) estimation, which are classified into three main categories: Physical-Based Models (PBM), Hybrid Models (HM), and Data-Driven Models (DDM). PBM is further divided into Conventional, Observer-Based, and Filter-Based Methods, while DDM includes Rule-Based, Classification and Regression, Probabilistic, Feed Forward Neural Networks (FFNN), and Recurrent Neural Networks (RNN). PBM techniques, such as electrochemical and equivalent circuit models, rely on physical principles and are discussed in [8, 9]. Although they are reasonably accurate, they struggle with adapting to battery degradation and usage changes, leading to efforts to combine PBM with DDM to enhance accuracy.

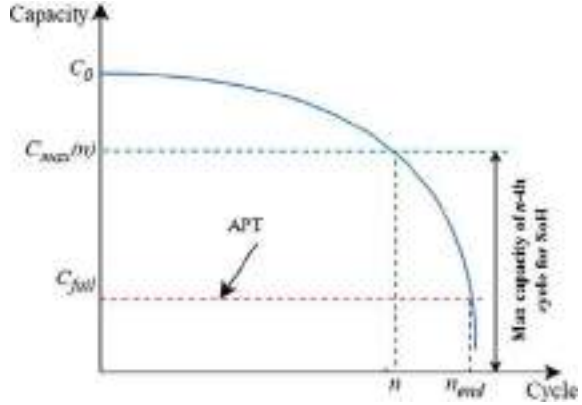
The empirical model with a back-propagation neural network (BPNN) has a mean absolute error (MAE) of about 2%. HM techniques offer higher accuracy and resilience but are complex, while DDM methods are simpler and cheaper [10].

One of the powerful DDMs that can extract features on its own is Deep Learning (DL). CNN is one of DL that can deliver rapid computational speeds on mobile devices or vehicles because they utilize a series of convolutional and matrix multiplication operations that can be processed in parallel [11], but need improved accuracy with multi-channel charging profiles [12].

One type of CNN that is simple and performs well is LeNet-5. LeNet-5 has not traditionally been used for NASA LIB SoH estimation, the model is commonly used for classification tasks. LeNet-5, a convolutional neural network released in 1998 by Yann LeCun and collaborators, was among the first used for digit recognition. It has 60 k parameters across 7 layers and initially recognized handwritten digits in the MNIST dataset and bank cheques, inspiring modern CNNs despite limited adoption due to computing constraints at the time [13].

The purpose of this study is to improve accuracy over baseline models by developing a SoH estimation model for LIB utilizing the DDM approach. Using

Fig. 1 Capacity variation over cycles [15]



multi-channel charging profile data, such as cycle (t), voltage (V), current (I), and temperature (T), it develops an effective CNN architecture that extends the DDM approach.

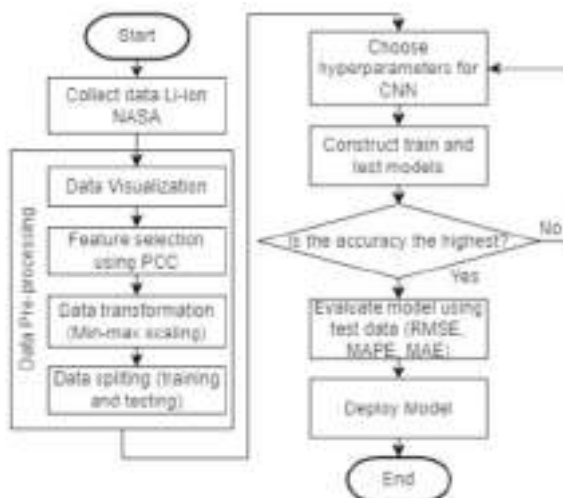
2 Definition of Battery Health Diagnostics

A battery is often regarded as being close to the end of its useful life when its actual capacity drops below the Acceptable Performance Threshold (APT) [14]. APT typically ranges from 70 to 80% of rated capacity. Base on Zhang et al. [13], SoH can be calculated by using Eq. 1. $C_{max}(n)$ is the measured max capacity at the n th cycle and $C(0)$ is the measured capacity of the battery at the beginning of its life. Battery deterioration is indicated by the SoH, which tends to decrease during the cycle. As the battery capacity at full charge drops 20–30% of its nominal capacity or rated capacity, the battery is often considered to have reached failure. Each of them $C(0)$ and $C_{max}(n)$ has units of Ampere-hour (Ah) [15]. The relations of these variables are depicted in Fig. 1.

$$SoH = \frac{C_{max}(n)}{C(0)} \leq 100\% \quad (1)$$

3 Research Method

The proposed research methodology depicted in Fig. 2. Data involves collecting LIB datasets from NASA for training and testing the model. The process includes data pre-processing with feature selection using the Pearson Correlation Coefficient

Fig. 2 Proposed method

(PCC) and all features are normalized by the min–max feature scaling method, which will speed up the training process in achieving the minimum cost function and then data splitting is performed into 70% training data and 30% testing data. After setting and selecting CNN parameters, the model is trained and tested using these features. The model’s performance is evaluated using RMSE, MAPE, and MAE metrics, and then the model is deployed.

4 Data Visualizations

The LIB charge and discharge experimental data set from the National Aeronautics and Space Administration (NASA) was the source of the experimental data. The LIB data used in this study is a collection of rechargeable cylindrical LIB aging data with the file name is BatteryAgingARC-FY08Q4, the cell chemistry is Lithium Cobalt Oxide (LiCoO_2), with type 18,650, capacity 2.1 Ah [16]. The data collection contains four battery numbers: B0005, B0006, B0007, and B0018. The batteries are all 18,650 models with a rated capacity of 2 Ah. Every experiment is conducted at 24 °C, room temperature.

The charging experiment was charged in two stages: first, in constant voltage mode until the current dropped to 20 mA, and subsequently, in constant current mode until the voltage hit 4.2 V. A steady current of 2 A was used during the discharge process until the voltage dropped to 2.7 V (B0005), 2.5 V (B0006), 2.2 V (B0007), and 2.5 V (B0018), in that order.

In every charging and discharging cycle, the charging and discharging processes begin at time 0, and data related to these processes, including voltage, current, temperature, and actual capacity, are recorded. The experiment came to an end when the

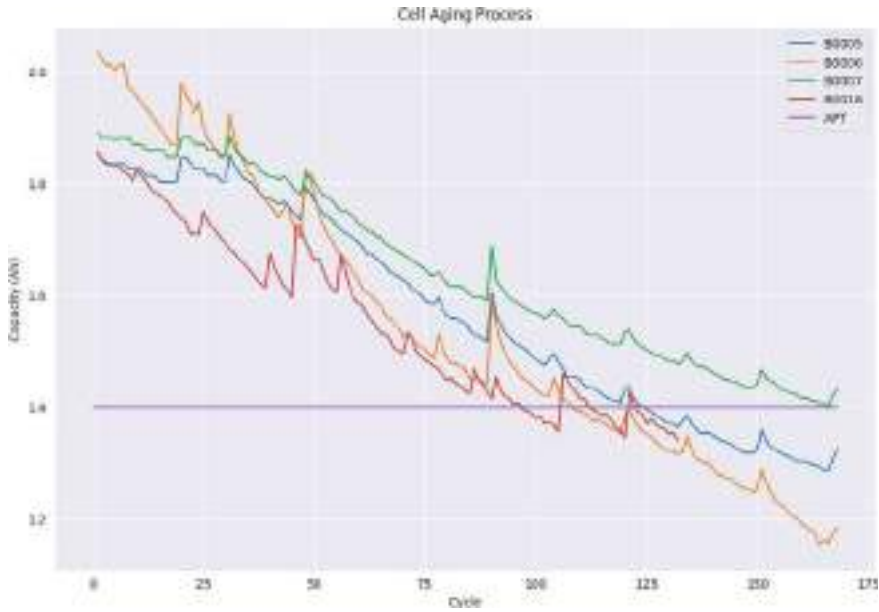


Fig. 3 Actual capacity deterioration curve for lithium-ion batteries from NASA

measured actual capacity fell below the 70% rated capacity (APT). In Fig. 3, the actual capacity deterioration curve of four batteries is displayed.

5 Feature Selection

The Pearson Correlation Coefficient (PCC) analysis is one method for quantifying the linear relationship between two variables. It is the product of the standard deviations and covariance of two variables, per reference [14]. The PCC is calculated using the Eq. 2. The sample's x -variable values are indicated by z_i , its y -variable values are indicated by q_i , and its y -variable mean is indicated by \bar{q} . The correlation coefficient ranges from -1.0 to 1.0 , indicating the strength and direction of a linear relationship between two variables. A value of 1.0 signifies a perfect positive linear relationship, -1.0 signifies a perfect negative linear relationship, and 0 indicates no linear relationship.

$$PCC = \frac{\sum_{i=1}^n (z_i - \bar{z})(q_i - \bar{q})}{\sqrt{\sum_{i=1}^n (z_i - \bar{z})^2} \sqrt{\sum_{i=1}^n (q_i - \bar{q})^2}} \quad (2)$$



Fig. 4 PCC analysis for six features

PCC analysis is used to choose the input for the SoH model. Five features-cycle (t), rated voltage (V), rated current (A), rated temperature ($^{\circ}\text{C}$), and time (s)-are taken from each usage cycle, except capacity, which is used as the target.

The linear dependency of these features on each other is then quantitatively assessed using different dependent distributed scales, with higher values indicating a stronger relationship, and vice versa. The indicated integers have an absolute value, meaning that their representation is the same regardless of sign. As shown in Fig. 4, the seven traits can be permuted to yield a total of 36 correlation coefficients.

Using battery capacity as the predictive goal in representing SoH, PCC analysis revealed that battery capacity has a closer relationship with cycle (0.99), voltage (0.14), current (-0.13), and temperature (-0.14). The cycle, voltage, current, and temperature was used as the four input features of the prediction model to estimate battery SoH by the aforementioned PCC analysis. The subsampled data that retains the changes observed during the charging interval is used in this study because, although the BMS setup indicates that there are many data points during the charging process, it is inefficient to use all the data due to the sensitivity of the data and the complexity in estimating it. The extracted features, obtained by uniformly sampling the raw battery data, serve as input data for the suggested model. Specifically, in the charging profile, there are features of cycle, voltage, current, and temperature, each of which is taken as ten samples, the number being determined based on the results of experiments that have been conducted on varying the number of samples (Table 1), so that the result of combining the samples forms an input matrix organized as a vector with 40 elements. To avoid further oscillations, the data is averaged over the sample interval using normalization.

All features in the dataset were normalized into the interval $[0, 1]$ using the feature scaling approach after feature selection. This will aid model optimization processes in reaching the least cost function more quickly and enhance the effectiveness of

Table 1 Variation of number of samples data

No. sample	MAPE (%)	MAE (%)	RMSE (%)
5	5.9	4.7	5.6
10	1.9	1.6	2.1
15	2.1	1.8	2.4
20	6.2	5	5.9

model training. In this instance, the employed feature scaling approach is the max–min scaling method. The PCC is calculated using the Eq. 3. The raw data is denoted by x_i , the scaled data by x_{scaled} , and the lowest and maximum values of the raw data are indicated by x_{min} and x_{max} , respectively [17].

$$x_{scaled} = \frac{x_i - x_{min}}{x_{max} - x_{min}} \quad (3)$$

6 SoH Diagnostics Based on CNN Model

In this investigation, a 2-dimensional CNN was employed. CNN is a popular deep learning technique that CNN employs in at least one of its layers in place of generalized matrix multiplication [18]. The 2-dimensional convolution operation is calculated using the Eq. 4. W is the filter or kernel matrix size and X is the input matrix. Convolution, pooling, flattening and fully-connected layers make up the conventional CNN architecture [19].

$$S(i, j) = (X \leq W)(i, j) = \sum_{m=-k}^k \sum_{n=-k}^k X(i - m, j - n) W(m, n) \quad (4)$$

The activation function receives the output from the convolution operation, which is carried out in the convolution layer to extract features. The pooling layer offers reliable learning outcomes for input data and can be used to shrink the spatial size of the feature map. After that, the output signal is forwarded to the following layer. It is possible to extract global features from input data by going through several stages of convolution and pooling layers. The regression task for SoH estimation is ultimately completed through the fully connected layer, which is the final layer of the CNN model.

Google Collaboratory carried out the training to the proposed lightweight CNN model in general, which provided a GPU with 25 GB of RAM. Table 2 shows the adjusted settings and parameters, and Table 3 shows the configuration of the CNN model. This CNN configuration model is inspired by MC-CNN [12] and model LeNet-5 [13]. In this study, MC-CNN is used the principle of using input data with

multi-channel (t, V, I, T) as well as a baseline for comparison. LeNet-5 can be adapted for LIB, leveraging their capability to extract features from time-series or sensor data related to battery health diagnostics. Therefore, the configuration of the CNN model is organized based on the layer arrangement of LeNet-5 with adjustments to its settings and parameters.

Based on the configuration in Table 3, the CNN architecture was built and shown in Fig. 5.

To evaluate the estimation accuracy, the mean absolute percentage error (MAPE) was used as the error index. In addition, mean absolute error (MAE) and root mean square error (RMSE) were also calculated. The SoH estimation of the proposed method is plotted per cycle in Fig. 6, in the case of battery B0005, it can be seen that the CNN CNN performs better by using a multi-channel charging profile, it is shown that the error estimation value is smaller than that performed by [12].

Table 4 shows the comparison of accuracy results between the baseline model and the proposed model. In this study, dropout for regularization was not performed because during the experiment it resulted in reduced accuracy. Based on the performance evaluation results, the proposed CNN model has shown better performance than Multi Channel—CNN (MC-CNN) and even outperforms Multi Channel—Long Short-Term Memory (MC-LSTM) which is said to be the best in the comparison conducted by [12], with smaller RMSE and MAE values.

Table 2 Settings and adjusted parameters for the CNN model

	Setting	Parameter
Trainable layer	Pooling layer	Maxpooling 2D
	Connected layer	Layer depth = 7 Activation function = LeakyReLU, $\alpha = 0.1$
	Dense layer	Activation function = linear
Learning optimizer	Adam optimizer	Learning rate = 0.001
Training	NASA LIB 10 × 4, data segmentation	Number of epochs = 1000 Batch size = 50 step per epoch = training sample

Table 3 The configuration of the CNN model

No. of layer	Species	Dimension	Parameter
1	2D Conv. layer C1	$1 \times 37 \times 32$	160
2	Max. pooling layer S1	$1 \times 37 \times 32$	0
3	2D Conv. layer C2	$1 \times 10 \times 32$	2064
4	Max. pooling layer S2	$1 \times 7 \times 16$	0
5	Flatten layer	32	0
6	Fully connected layer	1	33
7	Fully connected layer	1	2

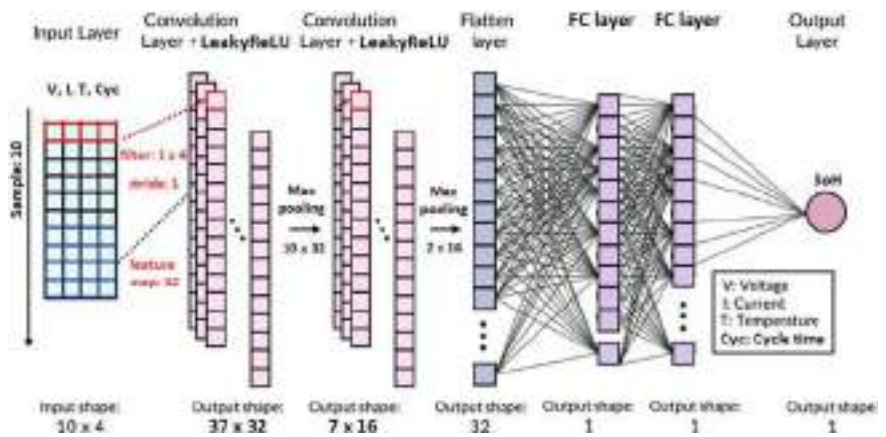


Fig. 5 CNN architecture for SoH diagnostics

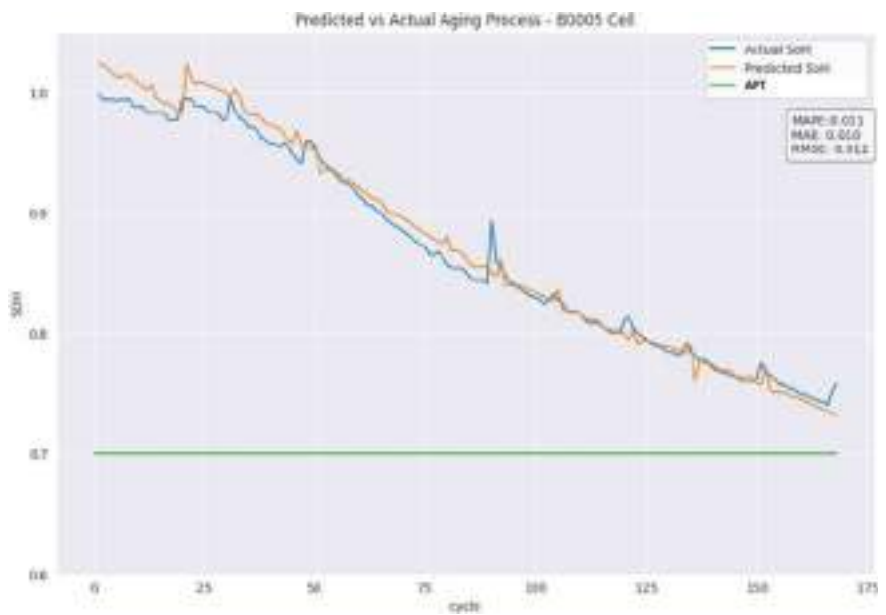


Fig. 6 Battery SoH diagnostics for B0005

Table 4 Comparison of estimation error of the baseline and the proposed model

Model	Structure	MAPE (%)	MAE (%)	RMSE (%)
MC-CNN [12]	Input-Conv1-Dropout-Conv2-FC-Output Filter: Conv1($1 \times 2@10$), Conv2($1 \times 2@5$) Stride: Conv1(1,1), Conv2(1,1)	2.89	4.43	5.84
CNN (proposed)	Input-Conv1-Conv2-FC1-FC2-Output Filter: Conv1($1 \times 4@32$), Conv2($1 \times 4@16$) Stride: Conv1(1,1), Conv2(1,1)	1.60	1.37	1.58

7 Conclusion

In this paper, a health diagnostic model for LIB based on CNN was developed with multi-channel V, I, T input data with adjustments to the configuration of parameter settings and layer structure. By utilizing the LIB from NASA, estimation results from the perspective of error index have been performed. Numerical results show that for the case of time series data, proper parameter setting and layer structure will result in high accuracy, and the addition of layers and dropouts as regularization will not necessarily result in better accuracy. The proposed CNN method has outperformed the method done by [12] with input data of voltage, current strength, and temperature. In future research, the proposed method can be extended by considering the k-cross validation method and updating the internal parameters.

Acknowledgements This research is funded by: (i) the Ministry of Education, Culture, Research and Technology (Kemdikbudristek) of the Republic of Indonesia through The Indonesia Endowment Funds for Education (LPDP) and Agency for the Assessment and Application of Technology Indonesia (BPPT) that is managed by Puslapdik (Pusat Layanan Pembiayaan Pendidikan) Kemdikbudristek, (ii) research grant under Institut Teknologi Bandung—Mitsubishi Corporation collaboration under contract 782/IT1.B07/KS.00/2023 Mitsubishi Corporation Grant Tahun 2024, (iii) P2MI—ITB internal grant.

References

1. Gao G, Zhou D, Tang H, Hu X (2021) An intelligent health diagnosis and maintenance decision-making approach in smart manufacturing. *Reliab Eng & Syst Saf* 216:107965
2. Kordestani M, Orchard ME, Khorasani K, Saif M (2023) An overview of the state of the art in aircraft prognostic and health management strategies. *IEEE Trans Instrum Meas* 72:1–15
3. Islam MM, Lee G, Hettiwatte SN (2018) A review of condition monitoring techniques and diagnostic tests for lifetime estimation of power transformers. *Electr Eng* 100:581–605 Springer
4. Meng J, Ricco M, Luo G, Teodorescu R (2019) A simplified model-based state-of-charge estimation approach for lithium-ion battery with dynamic linear model. *IEEE Trans Indus Electron* 66(10):7717–7727
5. Xiong R, Li L, Tian J (2018) Towards a smarter battery management system: a critical review on battery state of health monitoring methods. *J Power Sources* 405:18–29

6. Zhao J, Feng X, Wang J, Lian Y, Ouyang M, Burke AF (2023) Battery fault diagnosis and failure prognosis for electric vehicles using spatio-temporal transformer networks. *Appl Energy* 352:121949
7. Ruan H, Wei Z, Shang W, Wang X, He H (2023) Artificial Intelligence-based health diagnostic of Lithium-ion battery leveraging transient stage of constant current and constant voltage charging. *Appl Energy* 336:120751
8. Singh P, Chen C, Tan CM, Huang S-C (2019) Semi-empirical capacity fading model for SoH estimation of li-ion batteries. *Appl Sci* 9(15):3012. <https://doi.org/10.3390/app9153012>. Art. no. 15
9. Montaru M, Fiette S, Koné J-L, Bulte Y (2022) Calendar ageing model of Li-ion battery combining physics-based and empirical approaches. *J Energy Stor* 51:104544
10. Jiang Y, Zhang J, Xia L, Liu Y (2020) State of health estimation for lithium-ion battery using empirical degradation and error compensation models. *IEEE Access* 8:123858–123868
11. Chemali E, Kollmeyer PJ, Preindl M, Fahmy Y, Emadi A (2022) A convolutional neural network approach for estimation of li-ion battery state of health from charge profiles. *Energies* 15(3):1185
12. Choi Y, Ryu S, Park K, Kim H (2019) Machine learning-based lithium-ion battery capacity estimation exploiting multi-channel charging profiles. *IEEE Access* 7:75143–75152
13. LeCun Y, Bottou L, Bengio Y, Haffner P (1998) Gradient-based learning applied to document recognition. In: *Proceedings of the IEEE*. IEEE Xplore
14. Xu H, Peng Y, Su L (2018) Health state estimation method of lithium ion battery based on NASA experimental data set. In: *IOP conference series: materials science and engineering*. IOP Publisher
15. Zhang Y, Li Y-F (2022) Prognostics and health management of lithium-ion battery using deep learning methods: a review. *Renew Sustain Energy Rev* 161:112282. <https://doi.org/10.1016/j.rser.2022.112282>
16. Saha B, Goebel K (2007) Battery data set. NASA Ames PCoE, Moffett Field, CA, USA. <https://ti.arc.nasa.gov/tech/dash/groups/pcoe/prognostic-data-repository/>
17. Bao LN, Le D-N, Nguyen GN, Bhateja V, Satapathy SC (2017) Optimizing feature selection in video-based recognition using Max-Min Ant System for the online video contextual advertisement user-oriented system. *J Comput Sci* 21:361–370
18. Goodfellow I, Bengio Y, Courville A (2016) *Deep Learning*. MIT Press
19. Choi H, Ryu S, Kim H (2018) Short-term load forecasting based on ResNet and LSTM. In: *Proceedings of IEEE international conference on communication, control, computing technologies for smart grids (SmartGridComm)*, Oct. 2018. IEEE, Aalborg, Denmark

Design and Fabrication of a New Replaceable Nozzle for Abrasive Water Jet Application



Nuraini Lusi, Mebrahitom Gebremariam, Abdur-Rasheed Alao,
Kushendarsyah Saptaji, and Azmir Azhari

Abstract Nozzles are critical to the quality of the cuts produced during abrasive waterjet machining. The quality of the results of AWJ machining depends on the focus of the nozzle, which increases over time due to the aggressiveness of the abrasive particles that wear the inner wall of the nozzle. The purpose of this study is to explore fundamentally new terms to increase the wear resistance of the nozzle for the abrasive jet machine and increase its durability. This study mainly dealing with the designing and fabrication of a new replaceable nozzle. Compared to the traditional nozzle, which needs to be replaced regularly, this new replaceable nozzle offers a special feature in terms of recyclability. The new interchangeable parts, manufactured using additive manufacturing, consist of two parts: 50% of the inlet and 50% of the outlet of the entire nozzle length, using a screw thread mechanism. Accelerated wear test conducted to study the wear progression. The result showed that the exit diameter increased by more than 50% compared to the initial diameter and had a linear relationship with time. Weight loss measurement indicate a powerful tool in nozzle wear characterization.

N. Lusi · A. Azhari (✉)

Faculty of Manufacturing and Mechatronic Engineering Technology, Universiti Malaysia Pahang
Al-Sultan Abdullah, Pekan, Pahang, Malaysia
e-mail: azmir@umpsa.edu.my

N. Lusi

Department of Mechanical Engineering, Politeknik Negeri Banyuwangi, Banyuwangi, East Java, Indonesia

M. Gebremariam

College of Engineering and Built Environment, Birmingham City University, Birmingham, UK

A.-R. Alao

Faculty of Engineering, Universiti Teknologi Brunei, Gadong, Brunei Darussalam

K. Saptaji

Department of Mechanical Engineering, Faculty of Engineering and Technology, Sampoerna University, Jakarta, Indonesia

Keywords Accelerated wear test · Outlet diameter · Abrasive waterjet · Nozzle wear

1 Introduction

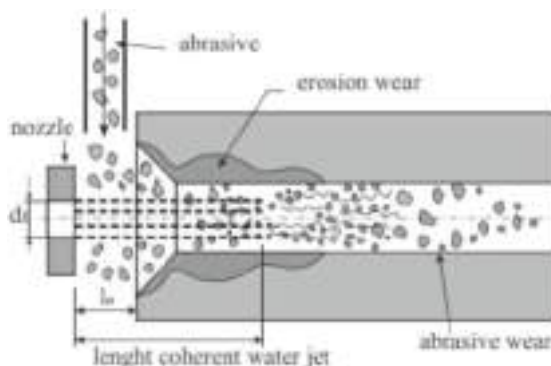
Abrasive waterjet (AWJ) technology is widely used due to the advantages such as environmental friendliness, no chemicals, no heat affected zone (HAZ), and no thermal process that affects the deformation of the workpiece [1]. The industry has used AWJ machining technology for more than 40 years for a variety of operations including cutting, milling, grooving, trimming and turning [2]. AWJ can effortlessly cut through both metallic and non-metallic materials, including composites, glass, steel, ceramics and other advanced materials [3]. The primary mechanism of AWJ creates a high-velocity stream of water by accelerating abrasive particles through an orifice using high-pressure water which passes through a mixing chamber. The abrasive particles experience combined inertial forces, causing them to collide with the nozzle walls, which is the primary cause of nozzle wear. Nozzle degradation has a direct impact on the accuracy, efficiency and cost-effectiveness of the AWJ. One of the main problems is damage to the inner diameter of the nozzle, which ultimately limits the range of use. Wear that occurs on the nozzle affects the cutting results, in particular increasing the surface roughness and the kerf width on the workpiece [4].

Nozzle erosion is a dynamic and complex phenomenon that depends on a number of factors such as: material, geometry related to design and AWJ system parameters [5]. The worn nozzle may not experience a uniform wear with equal increase of internal diameter. In most cases, the erosion is severer near the nozzle inlet than the outlet [6]. Sometimes, the region near the outlet experiences minimal or no erosion at all [7]. However, the worn has to be replaced as a whole although there is no erosion in some part of it. Worn nozzles will be thrown away like worn cutting tools in other traditional machining processes. In addition, replacing the nozzle may result in higher processing costs due to the short life of the nozzle. Consequently, it is crucial to create a new nozzle that can be reused in order to extend the tool's lifespan. In this study, the new design of replaceable nozzle was produced by selective laser melting. The purpose of this study is to investigate the wear characteristic of replaceable nozzle through the nozzle exit diameter, middle diameter, and nozzle weight loss. The accelerated wear test applied to investigate the wear performance of the replaceable nozzle using hard abrasive Aluminium Oxide (Al_2O_3).

2 Wear Characteristic of the Focusing Tube

The development of nozzles made of materials that are exceptionally hard and resistant to wear and erosion was crucial in order to effectively use AWJ in precision cutting. In the conical inlet and upper area, where particles mixed with water and

Fig. 1 The focus tube wear fundamental model [9]



air cause erosion at different impact angles, the inner walls of the focusing tubes are susceptible to impact wear from coarse abrasive particles. Abrasive sliding wear also occurs in the lower section of the tube as a result of the energy transfer between the air and the high-velocity water jet, which fractures particles into micros and submicron fragments [6]. The fundamental model of focus tube wear is shown in Fig. 1.

A number of issues are covered by the term “wear” on the nozzle, such as increases in outlet diameter, wear patterns developing along the internal surface, and nozzle weight loss [7, 8]. Weight loss of the focusing tube can be used to determine when it first starts to show signs of wear. Erosion of the inner wall of the tube results in wear patterns along its inner surface and weight loss. Extended utilization of the focusing tube results in modifications to the exit geometry, particularly the opening eccentricity. The ratio of the largest to smallest dimensions at the exit is known as eccentricity [9]. Accelerated wear tests were designed to screen potential mixing tube materials and quickly identify wear trends using less wear-resistant mixing tubes made of steel or harder abrasives like silicon carbide and aluminum oxide. To observe wear performance under industrial operating conditions, actual-condition wear tests used real materials and parameters [10].

3 Materials and Experimental Procedures

3.1 Material and Sample Fabrication

The replaceable nozzle made from the metal powder SS316L on the 3D printer machine RenAM 500E. SS316L is commonly utilised as a structural material due to its exceptional functional characteristics, including high resistance to corrosion and oxidation, significant mechanical strength, and excellent formability. It is widely used in several fields, such as biomedical industry, onshore and offshore marine applications, food processing industries, and automotive applications. The replaceable nozzle fabricated using additive manufacturing (AM) technology laser powder bed

fusion (LPBF). Table1 shows the list of LPBF parameters that used to manufacture nozzles.

The current conventional nozzle based on industrial used in AWJ was taken as an initial model, and a few design changes were made. The design of replaceable serve as prototype. The nozzle is composed of two merged parts, as shown in Fig. 2. Only the first section closest to the inlet that has the most erosion needs to be replaced if the nozzle is worn. Consequently, it is necessary to reuse the second part close to the outlet that has little to no erosion and attach it to a new inlet part. The reusability of this innovative nozzle design prolongs the tool’s lifespan and safeguards the environment.

Table 1 Laser powder bed fusion parameters

LBF parameters	
Layer thickness	0.05 mm
Hitch distance	0.11 mm
Stripe width	5 mm
Strip overlap	0.06 mm
Scanning rotation between subsequent layers	90°
Scanning strategy	Stripe
Laser diameter	75 μm
Powder particle diameter	50 μm
Other parameters or manufacturing pre-and-post-process	Argon purging less than 1000 ppm oxygen
Laser power	240 W
Point distance	0.05 mm
Exposure time	0.00008

Fig. 2 The new design of replaceable nozzle



3.2 Experimental Set up

An accelerated wear test was developed to conduct the studies on nozzle wear quickly and cost effectively [10, 11]. The test employed standard operating parameters and uses hard abrasive Al_2O_3 # 80 as erodent particle. In order to examine and understand the characterize of nozzle wear, a test method was designed. The primary technique used for monitoring the condition of the focusing tube is by observing the diameter of its exit tube. Several scholars have uncovered a direct proportionality between the exit diameter and the duration of time [12]. A weight loss measurement was performed by initially measuring the weight of the focusing tube at the beginning of the operation and thereafter continuously monitoring its weight throughout the machining phase. A digital scale was used to compute the mass of the focusing tubes. The test lasted thirty minutes, with measurements made every ten minutes. A video measuring system was used to observe the nozzle exit diameter and was measured three times.

The wear test was carried out on the self-developed CNC water jet cutting machine as shown in Fig. 3, which has a pump that can generate water pressure up to about 100 MPa. The type of pump used is an air driven liquid pump. A computer numerical control (CNC) system governs the operation of the machine. The motion of the table is regulated along dual axes (X and Y) together with the movement of the nozzle in the Z-axis (depth).

Fig. 3 The self-developed CNC AWJ machine [13]



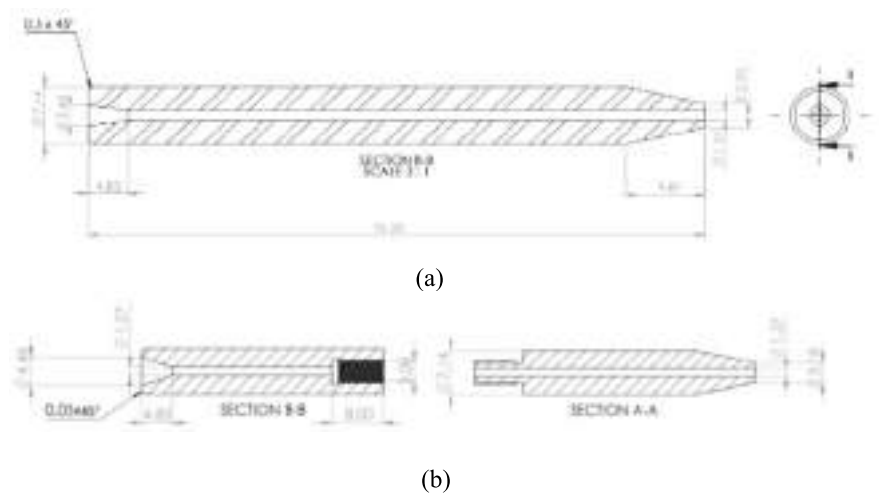


Fig. 4 The **a** initial industrial nozzle **b** new design 50%;50% nozzle

Table 2 Nozzle dimensions

Outside diameter (mm)	Internal diameter (mm)	Length (mm)
7.14	1.27	76.2

4 Result and Discussion

4.1 CAD Modeling of a Newly Developed Replaceable Nozzle

The first stage was designed the replaceable nozzle using software. The design of the replaceable nozzle was drawn using SolidWork software, as shown in Fig. 4. The new design nozzle is having 50% each for inlet and outlet parts respectively. The dimensions of the nozzle are listed in Table 2.

4.2 Manufactured Replaceable Nozzles

The fabricated replaceable nozzles and cross-sectional view of a waterjet nozzle is shown in Fig. 5. The entire nozzle does not need to be discarded after it has worn out, as it is designed with separate components. The outlet component is easily installed using a screw thread mechanism and can be repurposed. The operator of an abrasive waterjet machine is only required to maintain an inventory of reusable parts. Additionally, this novel reusable nozzle design has the potential to minimize waste, thereby promoting environmental conservation.

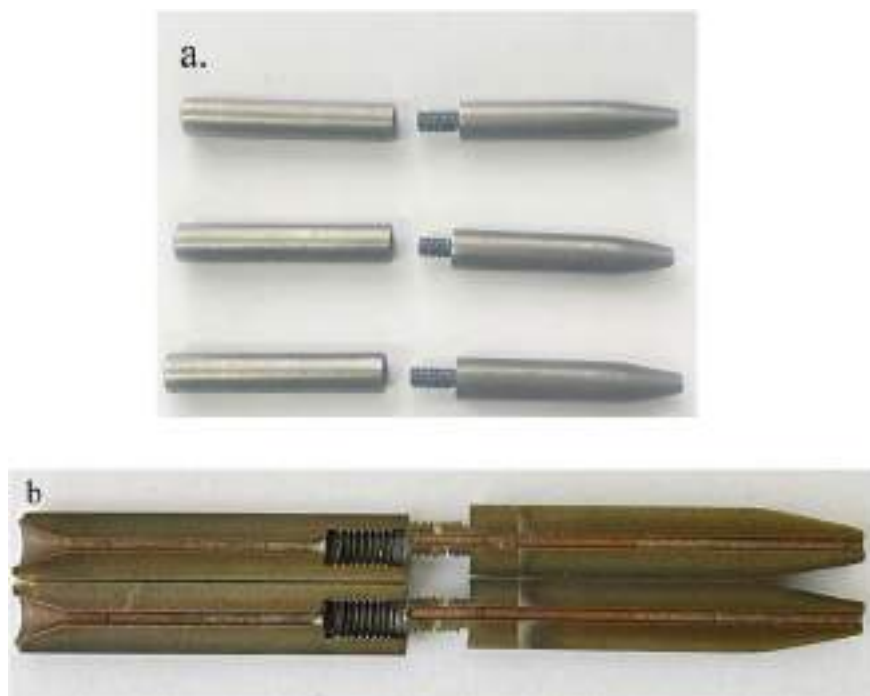


Fig. 5 3D printed consisting both inlet and outlet parts (a) cross section of printed nozzles (b)

The new design replaceable nozzle is compatible to be used in all commercial waterjet machines. It can conveniently fit to any commercial abrasive waterjet machines which uses a commercial nozzle. Furthermore, the life of the nozzle of the outlet part can be extended since it will be reused by replacing the nozzle with a new inlet part. Figure 6 shows the nozzle installation in AWJ cutting head.

4.3 Nozzle Wear Tests

The wear test was performed with a water jet pressure of 69 MPa, an abrasive flow rate of 0.5 g/s, and an orifice diameter of 0.1016 mm. The outlet diameter of the nozzle was determined by designating three locations on the inner edge of the nozzle, from which the software subsequently computed the radius. The results of the nozzle exit diameter variation with the operation time are shown in Fig. 7. In this diagram, the outlet diameter variations are plotted versus the time of operation. As shown in the figure, the longer duration of the wear tests the wider diameter of the outlet. It can be seen that the outlet diameter increases rapidly up to 20 min, and within further 30 min operation it almost remains constant. Furthermore, through this replaceable nozzle, the middle diameter of nozzle can be measured directly without the need

Fig. 6 The installation of the new replaceable nozzle



for a cross section through the nozzle. It is interesting to notice that the wear that occurred in the middle diameter was bigger than the outlet diameter. At the middle nozzle, a few abrasive particles will make contact with the nozzle wall then will be expelled evenly to the outlet diameter.

The correlation between the mass loss of the focusing tube and the operation time is illustrated in Fig. 8. After the maximum test duration of 30 min, there was a weight loss exceeding 1.5 g. It is clear that weight loss data can be used to predict nozzle performance because nozzle weight loss is almost exactly linear throughout the test. The stability of the accelerated wear test is indicated by the linearity of the data, which also shows excellence repeatability and control [11].

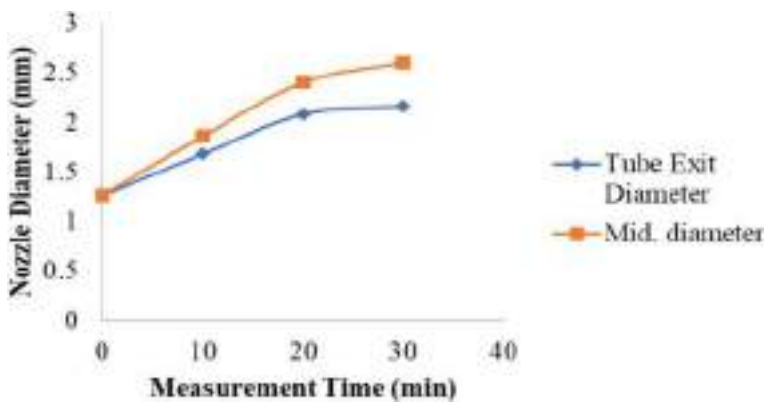


Fig. 7 The enlargement of the nozzle diameter

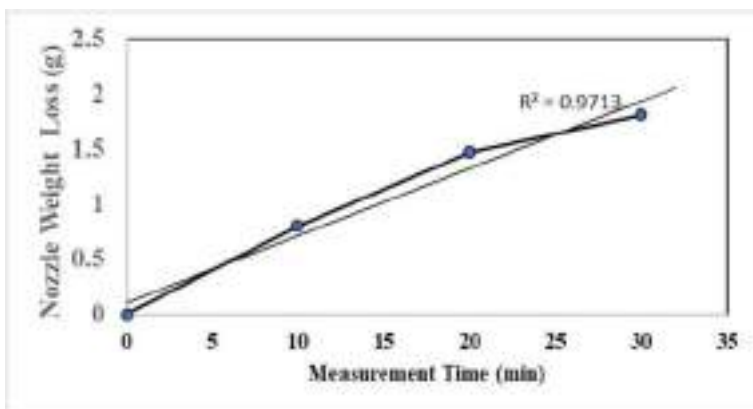


Fig. 8 The cumulative weight loss of nozzles

In Figs. 9 and 10, the outlet and middle profiles are visualized before and after thirty minutes of operation. The images reveal that the hole is nearly perfectly round when the nozzle is new. However, as the wear increases, the roundness gradually diminishes. Consequently, the jet becomes more unstable and loses its efficiency. Prolonged use of the focusing tube leads to transformations in the exit geometry, specifically the occurrence of opening eccentricity [7].

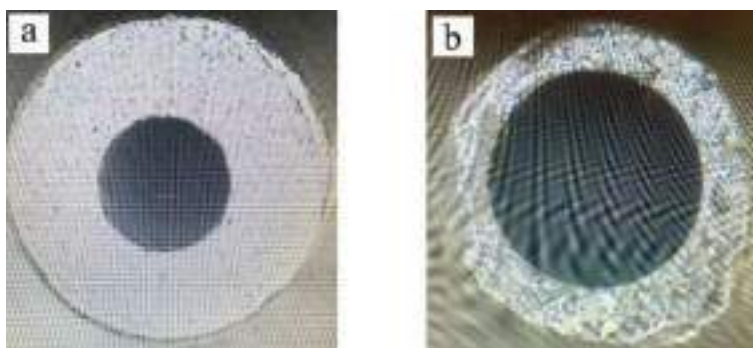


Fig. 9 Nozzle outlet profiles of **a** before operation and **b** worn nozzle after 30 min operation

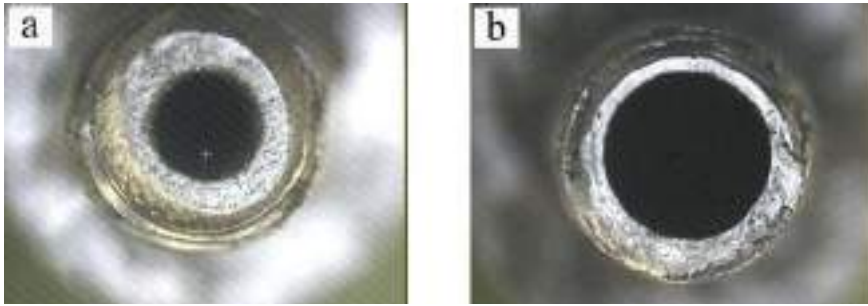


Fig. 10 Nozzle middle diameter profiles of **a** before operation and **b** worn nozzle after 30 min operation

5 Conclusion

In conclusion, the replaceable nozzle for waterjet machining application has been successfully fabricated. The findings of the prototype, which are the main subject of this paper, indicate that the idea of new replaceable nozzle is viable for implementation in industrial activities. Some machining parameters especially at a higher impact energy may result in severe erosion of the nozzle thus makes it not possible to reuse the outlet part. Hence, the whole nozzle body needs to be replaced with a new one. Therefore, a further study is required to determine recommended machining parameters for optimum reusability of the nozzle.

Acknowledgements The authors gratefully acknowledge the technical and financial supports from the Universiti Malaysia Pahang Al-Sultan Abdullah through PGRS 230327 and Vice Chancellor Scholarship (VCS) and under Ministry of Higher Education Malaysia through PRGS/1/2024/TK10/UMP/02/1 (RDU240802).

References

1. Nguyen T, Wang J (2019) A review on the erosion mechanisms in abrasive waterjet micromachining of brittle materials. *Int J Extrem Manuf* 1(1):12006
2. Abrasive HM, Machining W (2024) *Materials* (Basel). 17(13):3273
3. Natarajan Y, Murugesan PK, Mohan M, Liyakath Ali Khan SA (2020) Abrasive water jet machining process: a state of art of review. *J Manuf Process* [Internet] 49:271–322. <https://doi.org/10.1016/j.jmapro.2019.11.030>
4. Azmir MA, Ahsan AK (2009) A study of abrasive water jet machining process on glass/epoxy composite laminate. *J Mater Process Technol* 209(20):6168–6173
5. Mardi KB, Dixit AR, Pramanik A, Basak AK (2021) Tribology in (abrasive) water jet machining: a review [Internet]. In: *Machining and tribology: processes, surfaces, coolants, and modeling*. Elsevier Inc, 113–125p. <https://doi.org/10.1016/B978-0-12-819889-6.00004-6>
6. Bourgeois L, Fabbri E, Fastre P, Kremer J, Koesters R (2005) New tungsten carbide material with nanoscale grain size for focusing tubes. In: *Proceedings of WJTA American waterjet conference*, Houston, Texas, USA, pp 21–23

7. Jelena B, Bogdan N, Vlatko M (2008) Focusing tube wear and quality of the machined surface of the abrasive water jet machining. *Tribol Ind.* 30(3&4):55
8. Perec A, Pude F, Grigoryev A, Kaufeld M, Wegener K (2019) A study of wear on focusing tubes exposed to corundum-based abrasives in the waterjet cutting process. *Int J Adv Manuf Technol* 104(5–8):2415–2417
9. Nedić B, Baralić J (2010) The wear of the focusing tube and the cut-surface quality. *Tribol Ind.* 32(2):38–48
10. Hashish M (1994) Observations of wear of abrasive-waterjet nozzle materials. *J Tribol* 116(3):439–444
11. Nanduri M, Taggart DG, Kim TJ (2000) A study of nozzle wear in abrasive entrained water jetting environment. *J Trib* 122(2):465–471
12. Prijatelj M, Jerman M, Orbanic H, Sabotin I, Valentinλil J, Lebar A et al (2017) Determining focusing nozzle wear by measuring AWJ diameter. *J Mech Eng* 63:597–605
13. Murugan M, Gebremariam MA, Hamedon Z, Azhari A (2018) Performance analysis of abrasive waterjet machining process at low pressure. In: *IOP conference series: materials science and engineering*. IOP Publishing, p 12051

Measurement of Operational Risk Management Using the AS/NZS ISO 31000:2009 in the Outsourcing Start-Up Company



Tiena Gustina Amran, Annisa Dewi Akbari, Ellyana Amran, Adinda Aniza, Emelia Sari, and Mohd Yazid Abu

Abstract The decision to outsource by a company is influenced by numerous factors, including cost reduction, enhanced productivity, and improved performance quality. Outsourcing firms, as service providers, enable their clients to concentrate on core business functions, such as the information technology (IT) operations of the organization. However, IT outsourcing activities are susceptible to various risks, including resource shortages that impede client satisfaction, challenges in employee training, and human errors leading to system malfunctions. This research aims to conduct an operational risk management assessment utilizing the AS/NZS ISO 31000:2009 framework. The risk management process initiates with the identification of risks, their sources, and their potential impacts; proceeds with an evaluation of these risks based on their likelihood and potential consequences; and culminates in an analysis of the underlying causes and the formulation of strategies to mitigate these risks. The processes of risk identification and assessment are conducted by individuals recognized as experts within the company. Data for this research were gathered using the expert judgment approach, with respondents including the CEO, COO, GA, Finance and Accounting Manager, Sales Manager, and PMO. The implementation and evaluation of this research were carried out through a comprehensive review of the company's operational activities, grounded in the AS/NZS ISO 31000:2009 framework and the risk management methodologies articulated by Cooper et al. This study identified 140 risk impacts, comprising 82 internal risks and 58 external

T. G. Amran · A. D. Akbari (✉) · A. Aniza · E. Sari
Faculty of Industrial Technology, Department of Industrial Engineering, Universitas Trisakti,
Jakarta, Indonesia
e-mail: Annisa.dewi@trisakti.ac.id

E. Amran
Faculty of Economics and Business, Universitas Trisakti, Jakarta, Indonesia

M. Y. Abu
Faculty of Manufacturing and Mechatronic Engineering Technology, Universiti Malaysia Pahang
Al-Sultan Abdullah, Pekan, Pahang, Malaysia

risks. The findings indicate a reduction in risk severity compared to the initial conditions. Initially, 39 risks were classified as high (22.11% of the 140 identified risks). Following the calculation of residual risks, 8 risks remained categorized as high (5.71% of the 140 identified risks), while 31 risks were downgraded to low or moderate levels.

Keywords Risk management · Priority risk · Residual risk · Monitoring hierarchy · Start-up · IT · AS/NZS · ISO · Outsourcing

1 Introduction

Celerates is an outsourcing company that develops IT talents in the form of IT workforce training and distributes them to companies who want to outsource IT functions in their company. IT is the most frequently outsourced function and has a high demand. These IT functions include application development and support, information system integration, and Outsourcing training in the IT field also known as ITES-BPO or Information Technology Enabled Services—Business Process Outsourcing [1]. IT outsourcing cannot be separated from risks. Operational performance in outsourcing is related to risks such as unavailability of manpower to meet client needs, slow software, and loss of work equipment. Celerates as a start-up company must be adaptive to the conditions of its business environment and be able to anticipate the risks that will be faced.

A method that can help companies to face risks is risk management [2]. Currently, Celerates does not have a risk management analysis that complies with risk management standards in the global market. In this study, risk management was made using the US/NZS ISO 31000: 2009 standard because it is suitable for research on the operational performance of outsourcing companies. The purpose of this study is to design an operational risk management strategy in the Celerates outsourcing start-up company. Risk management that is carried out is the company's operational performance because the company's operational activities are related to external parties which makes the company need to have a risk handling strategy for the impacts of the risks that will be faced.

2 Literature Review

Risk management is a method that a company needs to prepare in facing possible risks that will threaten the company's existence or activities while carrying out its business activities [3]. Risk management is an approach taken to understand, identify and evaluate risks in a project or organization [4]. The main objective of risk management is to recognize risks in a project or company and develop strategies to

minimize and avoid risks. There are several risk management standards and frameworks including AS/NZS ISO 31000:2009, British Standards BS 31100, and COSO ERM [5]. In this study, the risk management standard used was the US / NZS ISO 31000: 2009 standard because this standard can be applied to any business and is suitable for companies from small to large scale, this standard can be applied to a start-up company like Celerates.

3 Research Methodology

Figure 1 is a flowchart of the research methodology conducted on this study.

4 Result and Discussion

4.1 Determination of the Risk Context

Risk identification is carried out based on the operational performance of Celerates and its supporting activities. This research is based on making a model to determine the risk context, risk analysis, and risk evaluation [6]. The determination of the risk context is carried out with an ISO 31000 approach, which is to collect the context of all possible risk factors into a mapping. This risk context is divided into an internal risk context and an external risk context. Furthermore, this mapping is carried out as a basis for initial risk identification. The determination of the risk context in Celerates is as Fig. 2.

Risk management research requires expert respondents as assessors or appraisers. The selection criteria for expert respondents refer to O'Hagen et al. [7]. Expert respondents will fill out three questionnaires, namely the risk identification questionnaire, the risk assessment questionnaire, and the remaining risk assessment questionnaire. The expert respondents in this study are the people who have the highest authority in the company and who best understand the overall operational performance of the company. Identification is also carried out on external risks. Although external risks are beyond Celerates' control, Celerates still needs to prepare a strategy to anticipate disruptions in the company's operational activities. This study required six expert respondents who filled out three questionnaires, namely the risk identification questionnaire, the risk assessment questionnaire, and the remaining risk assessment questionnaire. The expert respondents in this study are the people who have the highest authority in the company and understand the overall operational performance of the company. Here are six of those respondents. Respondents consisted of CEO, COO, GA, Sales Manager, and Project Management Officer.

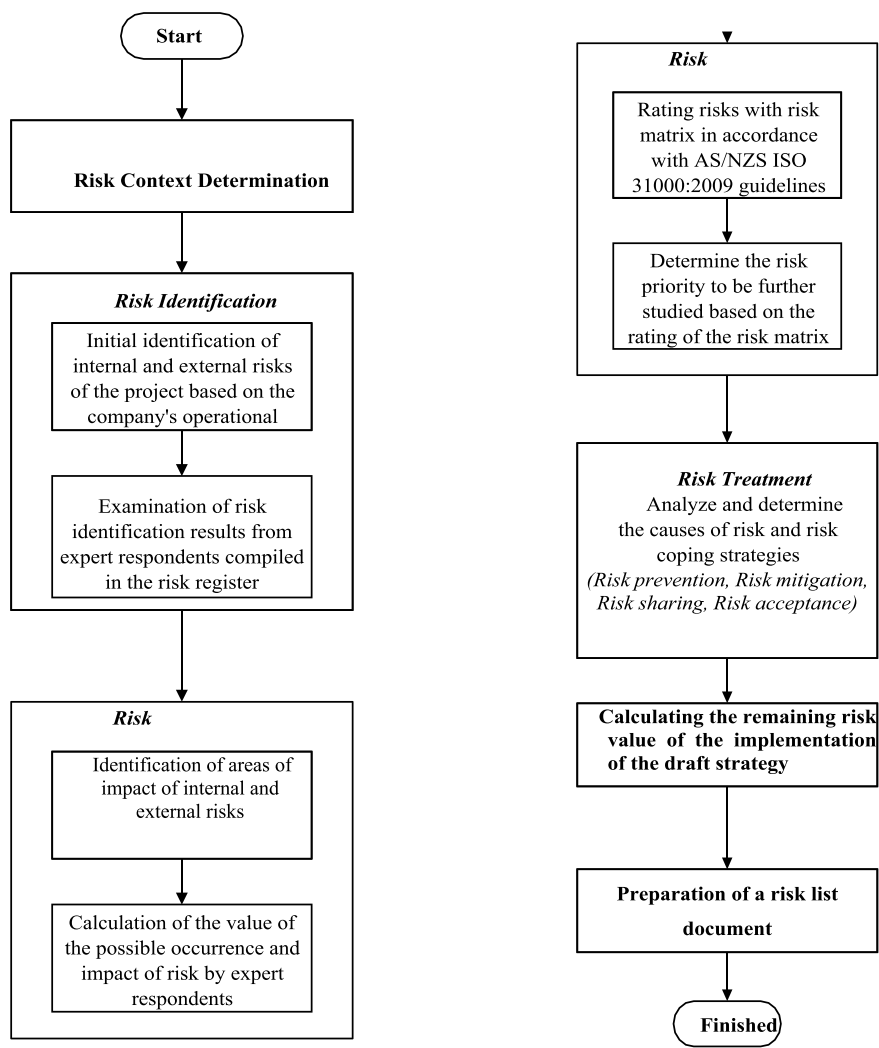


Fig. 1 Flowchart of data processing methodology

4.2 Risk Identification

Risk identification is carried out twice. The first risk identification is risk identification referring to the determination of the risk context and risk source from mapping at the risk context determination stage which refers to the scope and business activities of the company. The second risk identification was carried out by distributing a questionnaire with the examination of risk results to six expert respondents.

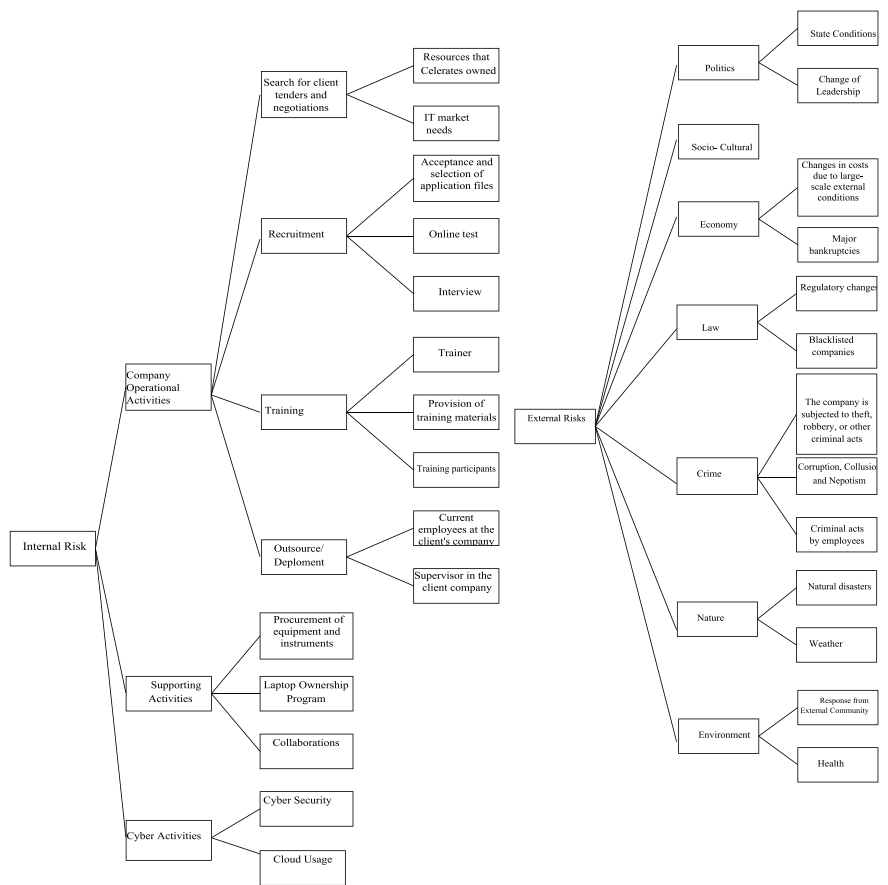


Fig. 2 Identification of internal and external risk context

Examination of the results of risk identification was carried out by distributing questionnaires to six expert respondents. The result of the risk identification examination is a list of risks that will then be assessed at the risk assessment stage. The resulting list of internal risks consists of 18 sources of risk, 82 risks, and 132 impact risks in Celerates, Identification of external risks shows that there are 7 sources of risk, 24 risks, and 58 impact risks.

4.3 Risk Assessment

Identify Risk Impact Areas

Identification of the areas of impact affected by each risk was carried out by conducting a literature study survey, and interviews with expert respondents. Table 1 is the results of the identification of areas of impact of internal and external risks of the company.

Calculation of Possible Events and Risk Impacts Assessment

In this questionnaire, expert respondents will provide an assessment of the risks that have been identified in Celerates. The assessment is carried out by determining the value of the possible occurrence of the risk (probability of occurrence), and the impact caused by the identified risk. Then, the average value of the possible event value and the impact value is calculated. The provision of values is given according to the risk scale according to the theory on the study of literature. Risks with a dangerous level that means risks that may interfere with the activities or work of Celerates will be analyzed at a later stage. An assessment for a possible event is filled in for each risk number, while an impact assessment is filled in for each risk impact area. Herewith Scale of assessment of possible risk events very low (possible occurrences < 2%), Low ($2\% < x < 10\%$), Medium ($10\% < x < 50\%$), High ($50\% < x < 80\%$), Very High ($>80\%$) [8].

4.4 Risk Evaluation

Risk Rating Mapping

Risk mapping is carried out using a risk matrix. Table 2 is the risk matrix based on AS/NZS ISO 31000:2009.

The combination of the value of the probability of the event with the value of the impact of the risk will converge at one point, that point is the risk rating for that risk. The average of the respondents' values for possible risk events R1 is 3, and the average of the impact values for the risk impact areas is 3. When viewed on the risk matrix, the combination of a probability of event scale of 3 with an impact scale of 3 converges at one point, that is, a moderate risk rating. Then the risk rating is medium. Risk evaluation for internal risks is that there is 1 risk impact that has a low rating, 97 is medium rating, 34 is high rating, and no risk has a very high rating. As for external risks. There are 50 risk impacts that have a moderate rating, and 8 high ratings. Risk analysis and strategy design were carried out for high and very high risk ratings [9].

Table 1 Identify areas of impact of internal risks

No.	Sources of risk	No.	Risks	Risk impact field	
1	Search for client tenders	R1	Client needs do not match the capabilities and availability of employees and the company	Financial	The company must find other ways to earn income while not having clients
				Employee	Employees are unemployed while waiting for the placement period
				Technology	Companies need to make adjustments to fill the skill gap
		R2	Have not acquired clients until the specified time	Financial	The company must find other ways to earn income while not having clients
				Employee	Employees are unemployed while waiting for the placement period
		R3	Negotiations with the client did not find a point of agreement	Financial	The company must find other ways to earn income as long as it has not yet gained clients
				Employee	Employees are unemployed while waiting for the placement period
		R4	The client cannot be contacted in the middle of the negotiation period or the client's PIC has changed	Financial	The company must find other ways to earn income while not having clients
				Employee	Employees are unemployed while waiting for the placement period
				Job performance	Vagueness in one client reduces the time and focus of the company's salespeople to acquire other clients
		R5	Client needs can be met, but currently celerates do not have enough resources	Financial	Sudden increments to meet client needs in a short period of time

(continued)

Table 1 (continued)

No.	Sources of risk	No.	Risks	Risk impact field	
				Technology	Companies need to make adjustments to technology capabilities and HR adjustments
		R6	There are clients who are directly willing to hire Celerates employees without going through Celerates	Employee	The possibility of employees to receive offers from clients
		R7	Clients are slow to sign	Financial	The company must find other ways to obtain income as long as it has not yet obtained a client, it has been incurred costs to carry out planning
				Employee	Employees are unemployed during the waiting period

Table 2 Risk matrix map

			Impact				
			1	2	3	4	5
			Very low	Low	Medium	High	Very high
Possible occurrences	5	Very high	Medium	High	High	Very high	Very high
	4	High	Medium	Medium	High	High	Very high
	3	Medium	Low	Medium	Medium	High	High
	2	Low	Low	Medium	Medium	Medium	High
	1	Very low	Low	Low	Low	Medium	Medium

Determining Risk Priority

The risks that prioritized are those that belong to high and very high ratings. In this study, neither internal risks nor external risks had a high rating. There were 25 internal risks identified and 5 external risks had high ratings. The risk consists of 31 internal risk impacts and 8 external risk impacts. Furthermore, these risks will be analyzed for the causes of the risks and the strategies needed to deal with these risks. Table 3 is a portion of the risk priority table in Celerates.

Table 3 Selected priority risks

Risk no.	Risks	Risk impact field		Initial risk value		
				KK	D	Risk rating
R1	Client needs do not match the capabilities and availability of employees and the company	Technology	Companies need to make adjustments to fill the skill gap	3	4	High
R2	Not acquiring clients until the specified time	Financial	The company must find other ways to earn income as long as it has not yet gained clients	3	4	High
R5	Client needs can be met, but currently Celerates does not have enough resources	Financial	Sudden increments to meet client needs in short time	4	3	High
		Technology	Companies need to make adjustments to technology capabilities and HR adjustments		3	High

4.5 Risk Treatment

Risk Prevention Strategy Planning

Each identified risk has this high rating will be made an analysis of the causes of the risk and an analysis of the risk prevention strategy. Table 6 is a portion of the risk cause analysis table.

After the cause of the priority risk is known, a risk prevention strategy is designed based on the identified risk causes. Referring to the AS/NZS ISO 31000:2009 and the journal “Evaluating Risks in Construction Projects Based on International Risk Management Standard AS/NZS ISO 31000:2009”, there are four alternative risk prevention strategies used in this study, namely Risk Prevention, Risk Sharing, Risk Mitigation, and Risk acceptance [10]. Table 4 is an example of causes of risk and risk management strategy.

Calculation of the Remaining Risk Values

The implementation of the risk mitigation strategy will make the value of possible events and the impact of risk decrease. The remaining value of the decrease is residual risk. The calculation of the remaining risk value was carried out by filling out the

Table 4 Risk management strategy

Risks no.	Risks	Causes of risk	Risk management strategy
R1	Client needs do not match the capabilities and availability of employees and the company	Changes in the scope of IT needs in the market	Risk Mitigation: 1. Providing alternative offers and approaches to continue using the services of Celerates Risk Acceptance: 1. Continue to maintain communication to cooperate in the future
		Lack of market research	
		New trends emerge in IT operations in target companies	
R2	Have not acquired clients until the specified time	No client has yet suited Celerates' needs and capabilities	Risk mitigation 1. Apply for a contract extension with a client whose project is in progress 2. Apply for employee rotation to clients whose projects are ongoing so that employees who have not been placed are not idle 3. Applying for services for different projects in the client's company that is in the contract period 4. Apply for additional employees in the client company who are in the contract period 5. Continue to conduct training, internal projects, or provide case studies for employees who have not been placed 6. Re-research the current demand for IT operations Risk acceptance 1. Carrying out other plans to earn money other than by outsourcing. This can be in the form of providing training in other places, system repair services or programming for one call, and software or hardware installation
		The competencies are relevant, but there are disagreements on cost, time, equipment	
		Not many companies were in need of IT talent at that time	

remaining risk assessment questionnaire by six expert respondents. In this questionnaire, the risk management strategies that have been made are listed. After calculating the residual risk, the results were obtained that there was 1 risk impact having a low rating, 23 medium ratings, and 7 high ratings. As for external risks, there are 7 risk impacts that have a moderate rating, and 1 risk impact that has a high rating. This shows that there is a decrease in the impact of risk after a risk management strategy is implemented. Table 5 are the full results of the remaining risk values.

4.6 Risk Rating Analysis

This study discusses risk management strategies for priority risks. Risks that have low and medium ratings are considered to be within the limits of the company's tolerance so that no deeper analysis is carried out, then only focus on high risks. Table 6 shows the summary of risk management strategy for this research.

Table 5 Value of remaining internal risks

Risk	Risk impact field		Initial risk rating		Prevention strategies	Value of remaining risks			
			Average	Risk Rating		Average	Risk rating		
								KK	D
R1	Client needs do not match the capabilities and availability of employees and the company	Technology	Companies need to make adjustments to fill the skill gap	3	4	High	Risk mitigation 1. Providing alternative offers and approaches to continue using the services of Celerates Risk acceptance 1. Continue to maintain communication to cooperate		
R2	Not acquiring clients until the specified time	Financial	The company must find other ways to earn income as long as it has not yet gained clients	3	4	High	Risk mitigation 1. Apply for a contract extension with a client whose project is in progress 2. Apply for employee rotation to clients whose projects are ongoing so that employees who have not been placed are not unemployed 3. Apply for employee rotation to clients whose projects are ongoing so that employees who have not been placed are not unemployed 4. Applying for services for different projects in the client's company that is in the contract periodMengajukan penambahan karyawan di perusahaan klien yang sedang dalam masa kontrak 5. Continue to conduct training, internal projects, or provide case studies for employees who have not been placed 6. Re-research the current demand for IT operations Risk acceptance 1. Carrying out other plans to earn money other than by outsourcing. This can be in the form of providing training in other places, system repair services or programming for one call, and installation of software or hardware		

(continued)

Table 5 (continued)

Risk	Risk impact field		Initial risk rating				Prevention strategies		Value of remaining risks		
			Average		Risk Rating				Average		Risk rating
			KK	D	KK	D					
R5	Client needs can be met, but currently Celerates does not have enough resources	Financial	4	3	High	Risk mitigation 1. Provide alternative offers and approaches to continue using the services of Celerates at the moment, at the same time preparation of resources and equipment to be started as soon as possible 2. Continue to maintain communication to cooperate in the future	2	2	Medium		
		Technology		3	High					3	Medium
R6	There are clients who are directly willing to hire Celerates employees without going through Celerates	Employee	4	3	High	Risk mitigation 1. Make contract points with employees regarding the rules, terms and conditions of quitting employment or changing jobs with the client company for ongoing client projects 2. Regarding quitting and transferring work to a client company that still has not entered into a contract or is in the negotiation stage, follows the terms and conditions applicable to the contract between Celerates and the employee 3. Negotiating prices so that clients continue to use Celerates' services and do not recruit directly	3	2	Medium		

(continued)

Table 5 (continued)

Risk	Risk impact field	Initial risk rating				Prevention strategies		Value of remaining risks		
		Average		Risk Rating			Average		Risk rating	
		KK	D				KK	D		
R8	The budget prepared is far different from what turns out to be needed	3	4	High			Risk mitigation 1. Conduct price research periodically prices, prices of equipment and software needed to be continuously monitored for changes in prices that may exist. The prices monitored are the current price and the historical price 2. Financial planning is carried out by the most expert people 3. Make preparations for unexpected costs 4. Intensive coordination and communication between divisions so that financial planning is integrated and does not collide or double 5. Intensive coordination and communication with clients 6. In the budget related to the client, making financial planning and the insurer, and having obtained an agreement between the Celerates party and the client. If there is a budget change caused by changes and additions by the client that is not in accordance with the contract, then the change is the responsibility of the client	3	2	Medium
R9	Limited initial data information needed for program design that causes inaccuracies in preliminary design base	3	4	High	Risk mitigation 1. Intensive communication and coordination with clients regarding the data needed to make designs from Celerates 2. Conduct regular meetings or coordination to integrate the design that has been made by Celerates and ensure that there is no unconvayed information between the two parties. Periodic coordination of this draft is carried out before the start of the project referring to the contract 3. Research and design are carried out, or monitored by the most skilled people in Celerates	2	2	Medium		
			4	High			2	Medium		

(continued)

Table 5 (continued)

Risk	Risk impact field		Initial risk rating				Prevention strategies		Value of remaining risks		
			Average		Risk Rating				Average		Risk rating
			KK	D	KK	D			KK	D	
R 10	Design changes with new additions or corrections	Job performance	The project or work suffers a setback in the execution time of the original plan	3	4	High	Risk mitigation 1. conduct periodic meetings or coordination to integrate the draft already made by Celerates and ensure that there is no un conveyed information between the two parties to avoid unilateral changes beyond expectations Periodic coordination of this draft is carried out before the start of the project referring to the contract 2. Research and design is carried out, or monitored by the most skilled people in Celerates Make a contract point that significant changes outside the contract that may cause changes to budgets, resources, and plans will be borne by the client	2	2	Medium	
R 11	There is not yet a sufficient number of applications until the specified time	Job performance	The project or work suffers a setback in the execution time of the original plan	4	3	High	Risk prevention 1. Entering into a contractual agreement only if Celerates already has at least 50% of the employees of the total required amount Risk mitigation 1. Share and re-upload job ads 2. Make job offers with word of mouth, and still follow the applicable procedures 3. Apply for an extension of the project start time 4. Conduct unpaid training and offer to take part in interview selection for the most qualified training participants who have not worked elsewhere 5. Continue to run the project according to the predetermined time with the number of employees currently owned, but with the alternative of overtime that will be paid by Celerates Risk acceptance 1. Allocate unforeseen costs from the original draft to pay for overtime or other losses resulting from project setbacks	4	3	High	

(continued)

Table 5 (continued)

Risk	Risk impact field		Initial risk rating			Prevention strategies	Value of remaining risks			
			Average		Risk Rating		Average		Risk rating	
			KK	D			KK	D		
R12	Characteristics and skills of candidates do not match the needs	Job performance	The project or work suffers a setback in the execution time of the original plan	4	4	High	Risk prevention 1. Provide descriptions, specifications, and requirements that are as clear as possible and in accordance with those required by the company 2. Ensure that job advertisements are right on target and in accordance with the keywords that may be searched referring to SEO Risk mitigation 1. Offer an alternative role that can be given if the candidate is judged to be a good potential 2. Offer can be done before the start of the interview stage Risk acceptance 1. Continue to accept potential candidates to participate in the next stage, and provide more intensive training if the candidate is accepted	2	2	Medium
R15	Managers or people who are not directed or untrained to perform file selection	Job performance	The passing of candidates who turn out not to be in accordance with their abilities will hinder the work or project	3	4	High	Risk prevention 1. Ensure that there is no miscommunication and misinformation between divisions in the company 2. Ensure that user needs have been conveyed properly to the file selector Application file selection is only carried out by, or under the supervision of people who are experts and experienced in screening and file selection	2	1	Low
R18	The number of candidates who pass the online test does not reach the required quota	Job performance	The project or work suffers a setback in the execution time of the original plan	4	3	High	Risk prevention 1. The questions to be given to candidates are first tested internally in Celerates Risk acceptance 1. Re-posting job ads Lowering the standard of passing the online test accompanied by the provision of intensive training	2	2	Medium
(continued)										

(continued)

Table 5 (continued)

Risk	Risk impact field		Initial risk rating			Prevention strategies		Value of remaining risks		
			Average		Risk Rating			Average		Risk rating
			KK	D				KK	D	
R20	Online test cannot necessarily be the standard for a candidate ready to enter Celerates (not standardized)	Job performance	The passing of candidates who turn out not to be in accordance with their abilities will hinder the work or project	4	3	High	Risk prevention 1. Online tests should only be made by users, or people who are very skilled about the functions to be performed by candidates 2. Online test is made referring to existing references, which may be used as learning material by candidates Risk mitigation 1. Providing more intensive training for candidates who are not in accordance with their needs	2	2	Medium
R34	Trainers are not directed to achieve training goals	Job performance	Employees do not obtain the expected skills and outputs that affect job performance at the client company	3	4	High	Risk prevention 1. Filter trainers based on reputation and experience teaching the material to be delivered 2. Ensure that the needs of each division are well coordinated 3. Conduct in-depth briefings on the objectives of trainings, which are expected to be obtained by employees after going through training, an overview of the work that employees will do in the client company 4. The PIC of Celerates first knows the syllabus or training material that will be delivered by the trainer at least 3 days in advance. The material in question can be in the form of powerpoint slides, videos, program listings, and others Risk mitigation 1. Provide a brief deepening of the material if the training that has been carried out is considered ineffective Risk sharing 1. Make an agreement with the trainer containing that if more than 50% of the training participants do not pass the exam at the end of the training, the trainer (external) is required to provide free retraining	2	2	Medium

(continued)

Table 5 (continued)

Risk	Risk impact field		Initial risk rating			Prevention strategies	Value of remaining risks		
			Average		Risk Rating		Average	Risk rating	
			KK	D				KK	D
R36	Trainer prices are too expensive	Financial	4	3	High	Risk mitigation 1. Negotiating prices Risk acceptance 1. Allocate unexpected costs to cover the difference in payment budget	3	2	Medium
R42	Insufficient training time	Job performance	4	3	High	Risk acceptance 1. Apply for an extension of the project start time to the client 2. Keep starting the project according to the promised time. Employees start working at client companies but employees still do training on weekends. Celerates bears transport costs as an overtime count 3. Allocate unexpected costs for losses that has been caused	4	3	High
R43	Training participants (employees) do not have basic knowledge to take part in the training	Job performance	4	3	High	Risk mitigation 1. The company makes equality training that aims to generalize the abilities of employees so that employees who do not have basic knowledge can have supplies before conducting material training for work preparation	2	2	Medium
R45	Employees do not pass the selection in the client company	Job performance	4	4	High	Risk prevention 1. Making preparations in the form of a selection simulation at the client company Risk acceptance 1. Applying for other employees to be selected	2	2	Medium

(continued)

Table 5 (continued)

Risk	Risk impact field	Initial risk rating			Prevention strategies			Value of remaining risks		
		Average		Risk Rating				Average		Risk rating
		KK	D					KK	D	
	Financial	The presence of expenses, cost overruns outside of planning		4	High				3	Medium
R47	Employee	Decreased employee satisfaction or trust	4	3	High	Risk prevention 1. Take into account the cost of transportation of employees to the client's workplace when placing employees in the client's premises Risk mitigation 1. Provide certain incentives for employees whose residence and place of work in the client company are more than 15 km away	2		3	Medium
	Company's reputation	Client satisfaction or trust in the company decreases		4	High				2	Medium
R49	Employee	Decreased employee satisfaction or trust	4	3	High	Risk prevention 1. The management level ensures that there are no changes and additions to the work outside the contract 2. The management level routinely follows-up with employees regarding the work done up to the first month to find out whether the work given is outside the contract Risk acceptance 1. Any significant changes of work made during the life of the project, submitted to the executive level for negotiation	2		2	Medium
	Company reputation	Client satisfaction or trust in the company decreases		3	High				3	Medium
	Technology	Companies need to make adjustments to fill the skill gap		4	High				2	Medium

(continued)

Table 5 (continued)

Risk	Risk impact field		Initial risk rating			Prevention strategies	Value of remaining risks			
			Average		Risk Rating		Average	Risk rating		
			KK	D				KK	D	
		Company reputation	Client satisfaction or trust in the company decreases	4	High			2	Medium	
R58	Work bottlenecks due to planning and quality control of work that relies on client project managers	Job performance	A project or work suffers a setback in the implementation or completion time of the original plan	4	3	High	Risk mitigation 1. Define and agree on detailed schedules and deadlines for work on tasks and project work 2. Create a task work SOP that lists the number of changes/ revisions, the maximum number of additions and changes 3. Coordinate and communicate well with supervisors and project managers	4	3	High
R65	The client has not paid in accordance with the agreement	Job performance	The project or work has a deterioration in the implementation or completion time of the original plan, the work is not optimal	4	3	High	Risk mitigation 1. Intensive coordination with clients ahead of the agreed payment date 2. Set detailed schedules and deadlines for payment processing during negotiations and contracts 3. Establish late fees if payment is made past the deadline 4. Intensive coordination with clients who do not pay	3	4	High
		Financial	The presence of expenses, cost overruns outside of planning		4	High			2	Medium
(continued)										

(continued)

Table 5 (continued)

Risk	Risk impact field	Initial risk rating			Prevention strategies	Value of remaining risks		
		Average		Risk Rating		Average		Risk rating
		KK	D	KK		D	KK	D
R71	Employees resign in the middle of the laptop payment installment period	4	4	High	Risk mitigation 1. Require employees to leave important documents in Celerates 2. Resigned employees must leave the laptop at Celerates if the installment payment is still below 70%, and the installment payment continues For employees who have paid installments above 70% can bring a laptop, and still have to leave important documents until the installment payment has been paid off	3	2	Medium
R79	Human error that causes system errors	3	4	High	Risk prevention 1. Enforce strict rules regarding the maximum time of basic working hours and overtime 2. Software installation, hardware purchase, cloud use requires coordinated admin approval in the financial and operational fields 3. The supervisor ensures that the employees under him are aware of the risks that may result from misuse of the software or cloud, and the losses that have been caused 4. Ensure employees in charge of using the cloud know the limits of cloud usage clearly and as early as possible Risk mitigation 1. Contact the service system from the cloud, or bank to make usage withdrawals, cancellation of bills if possible Risk sharing 1. Communication and coordination of compensation cost sharing with clients Risk acceptance 5. 1. Allocating unexpected costs to pay damages	3	4	High

(continued)

Table 5 (continued)

Risk	Risk impact field		Initial risk rating			Prevention strategies	Value of remaining risks		
			Average		Risk Rating		Average		Risk rating
			KK	D			KK	D	
R8 5	Country conditions that cause internet access blocking	Job performance	3	4	High	Risk mitigation 1. Review the internet access blockade policy for essential business processes for the wider community Contact clients and parties dealing with Celerates regarding the condition, and coordinate work delays	3	3	Medium
R8 9	Changes in IDR exchange rates	Financial	3	4	High	Risk mitigation 1. Salary or bonus deduction Adjust the financial plan	3	3	Medium
R9 1	Increased labor costs	Financial	4	4	High	Risk mitigation 1. Re-develop priorities in the financial plan and reevaluate the financial plan with new conditions	3	4	High
(continued)									

(continued)

Table 5 (continued)

Risk	Risk impact field		Initial risk rating			Prevention strategies	Value of remaining risks				
			Average		Risk Rating		Average	Risk rating			
			KK	D					KK	D	
R1 01 The occurrence of corruption, collusion, nepotism or bribery in one's own company or client	Employee	Conditions that cause the company to be forced to lay off, causing employee satisfaction and trust to decrease	3	4	High	Risk prevention 1. Internal transparency regarding draft fees, income, expenses, tax payments, and recruitment Risk mitigation 1. Obtaining legal aid Risk sharing 1. Losses resulting from KKN actions by the client will be fully borne by the client			3	Medium	
	Financial	Financial losses due to KKN; expenses for obtaining legal assistance		4	High						
	Company reputation	Client satisfaction or trust, potential clients towards the company decline, and a bad image in the eyes of society		4	High						
									2	3	Medium
										4	Medium

(continued)

(continued)

Table 5 (continued)

Risk	Risk impact field	Initial risk rating				Prevention strategies	Value of remaining risks		
		Average		Risk Rating			Average		Risk rating
		KK	D	KK	D				
R1 02	The occurrence of criminal violations by employees of the company	Company reputation	3	4	High	Risk prevention 1. Make very strict regulations regarding employees who commit criminal acts, do not tolerate in any form Risk Mitigation 1. Obtaining legal assistance for the company if any employee commits a criminal act. Legal aid as a representation of Celerates, not employees who commit criminal act Contacting connections, and relationships to straighten out distorted news if needed	1	5	Medium
		Client satisfaction or trust, potential clients towards the company decline, and a bad image in the eyes of society							
		Regulation		4	High				
		Violation of regulations						5	Medium

Table 6 Summary of risk management strategy

	Risk aspects					
	Job performance	Financial	Employee	Company's reputation	Technology	Regulation
Number of risks affected	15	11	4	4	3	1
Risk management strategies in general	Risk mitigation coordination between top management and clients or prospective clients regarding	Risk mitigation in the form of coordination of budgeting between divisions, and risk acceptance in the form of the use of unexpected costs	Risk mitigation in the form of coordination between top management and clients or prospective clients regarding	Risk mitigation is in the form of coordinating with the client to overcome mistakes on the part of Celerates	Risk mitigation for periodic research on market trends, or acceptance of risk by communicating with potential clients to use existing resources	Risk mitigation for obtaining legal assistance

4.7 Risk Register Analysis

This document was created to provide details about the identified risks, areas of risk impact, probability of a risk occurrence, value of risk impact, causes of risk, and risk management strategies. In addition, the remaining risk assessment is also made to show the influence of predetermined handling strategies. In the risk register, there is also a PIC filling to be done in the future so that risk handling is right on target. Furthermore, risk monitoring can be done with three types of monitoring, namely continuous monitoring, monitoring by top management, and monitoring by third parties. This monitoring hierarchy is long-term for monitoring risk documents and risk management strategies. This study is in line with research conducted by Suyasa and Legowo (2019), which analyzes the risk of risk management information systems, especially in financial technology, which is based on the level of risk that is occurring and also measures the level of maturity that has been implemented whether it is in accordance with the expected target of one of the state-owned banks. This study successfully identified the level of risk faced by Bank XYZ [11]. The application of risk management in an organization is a process of actions and activities carried out continuously to provide confidence in achieving organizational goals through effective and efficient activities [12].

5 Conclusions

The AS/NZS ISO 31000:2009 risk management standard serves as a robust framework for operational risk management within companies. This study identifies seven key areas of risk impact: financial, facilities, job performance, employees, technology, regulation, and company reputation. Internal risk identification reveals 18 sources of risk, 82 risks, and 132 risk impacts within the company. External risk identification highlights 7 sources of risk, 24 risks, and 58 risk impacts.

This study focuses on risk management strategies for high-priority risks, as risks with low or medium ratings are considered within the company's tolerance levels and do not require in-depth analysis. Initially, 39 risks were classified as high (22.11% of the 140 identified risk impacts). After further validation, 8 risks remained high (5.71% of the 140 risk impacts), while 31 risks were downgraded to low or medium ratings.

Financial risks primarily result in overspending and sudden cost overruns. The mitigation strategy includes accepting risks through contingency funds and coordinating budgeting across company divisions. Job performance risks generally lead to project delays or deterioration in project completion times. Strategies to address these risks involve negotiations and communication with stakeholders to ensure project continuity within the predetermined timeline, despite limited resources, and the use of contingency funds to cover losses.

Employee-related risks affect employee satisfaction, particularly in client-facing roles or outsourced contracts. These risks are managed through coordination with clients regarding project needs and employee work contracts. Technology risks necessitate adjustments in technological resources to meet client demands or bridge skill gaps. Risk mitigation involves periodic market trend analysis and engaging with clients to utilize existing resources effectively.

Reputational risks impact client trust and public perception. The mitigation strategy includes coordinating with clients to address errors and restore confidence. Regulatory risks involve potential legal violations related to external factors. The management strategy includes risk mitigation through legal consultation.

The calculation of residual risk values serves as a validation method to determine the effectiveness of risk reduction efforts. For risks that do not decrease, the company regularly monitors and reviews them using a risk register, which consolidates risks and management strategies. In the IT outsourcing domain, significant sources of risk include resource qualifications, contractual complexities, technology trends, unexpected costs, and IT talent challenges. Implementing a comprehensive risk management system is essential to achieving business goals and ensuring sustainability. This research offers valuable insights for both discrete and continuous manufacturing organizations, as well as service providers, particularly start-ups, in maintaining long-term viability.

References

1. Charles W (2009) 21st century management. SAGE Publications, Singapore
2. Dhar S, Balakrishnan B (2006) Risks, benefits, and challenges in global IT outsourcing. *J Glob Inform Manag* 14:59–89
3. Nduwimfura P, Zheng J (2015) A review of risk management for information system outsourcing. *Int J Bus Humanit Technol* 5(4)
4. Yacov H (2016) Risk modelling, assessment, and management, 4th edn. Wiley, Hoboken
5. Ruzaini S, Habibah N, Mohamed A (2008) Conceptual framework on risk management in IT outsourcing projects. *WSEAS Trans Inform Sci Appl* 5(4):816–831
6. Wahyudi S, Awalul M (2014) Manajemen Risiko dalam Proses Memilih Vendor menggunakan ISO 31000 dan Analisis Laporan Keuangan. Universitas Sebelas Maret, pp 2579–6429
7. Beaudrie C, Kandlikar M (2016) Expert judgment for risk assessment. University of British Columbia, Vancouver
8. Renault BY, Agumba JN, Ansary N (2016) A theoretical review of risk identification. In: 5th applied research conference, vol 773–782
9. Wisnuwardhana A (2012) Penilaian dan Perlakuan Risiko Berbasis AS/NZS 4360:2004 pada Proyek Fase Pengembangan Migas Blok A PT Medco E&P Indonesia, Tesis MT, Teknik Industri, Bandung, Institut Teknologi Bandung
10. Thao H, Van Tiep N, Linh D (2014) Evaluating risks in construction projects based on international risk management standard AS/NZS ISO 31000:2009. *Infrastruct Univ Kuala Lumpur Res J* 2(1)
11. Suyasa GWA, Legowo N (2019) The implementation of system enterprise risk management using framework ISO 3100. *J Theor Appl Inform Technol* 97(10):2669–2683
12. Sumiyati, Hadiningrum K, Hazma, Susanti I, Bakthi KY (2020) The role of risk management in achieving organization's goals. *Int J Arts Soc Sci* 3(4)

The Reliability and Effectiveness of Sensors in IoT-Enabled Solar Drying System



Thevanesveeran Aso Kumar, Nur Najmiyah Jaafar , Sarah 'Atifah Saruchi , Nafrizuan Mat Yahya , and Suraya Sulaiman

Abstract Interest in using solar energy for a variety of purpose has increased due to the growing need for environmentally friendly and energy-efficient solutions. The creation and evaluation of an Internet of Thing (IoT) enabled solar drying system for agricultural usage is the main goal of this project. The principle aim of this study is to examine the effectiveness of the sensors that are incorporated into the system. The methodology involved designing an IoT-enabled solar dryer equipped with sensors for temperature, humidity, and voltage, connected to a microcontroller for data processing and remote controlling via the Blynk app. Time series and correlation analyses were conducted to assess system performance. Results indicates stable voltage patterns, effective moisture removal at higher temperatures, and strong correlations between solar panel output and battery efficiency. This study concludes that integrating IoT improves the drying process by optimizing conditions and reducing manual intervention help for sustainable food preservation.

Keywords Solar Dryer · Sensors · Internet of Thing (IoT) · Agriculture · Energy

1 Introduction

The need for food production and preservation is rising as a result of the world's population growth. Extending shelf life and minimizing food deterioration are important goals of traditional food preservation techniques like drying. Specifically, solar drying uses sunlight to extract moisture from food goods, which makes it an economical and environmentally friendly method for both home and agricultural use.

Solar drying is a sustainable method that aligns with the principles of utilizing resources efficiently, reducing waste, and employing eco-friendly technologies. This

T. A. Kumar · N. N. Jaafar (✉) · S. 'Atifah Saruchi · N. M. Yahya · S. Sulaiman
Faculty of Engineering Technology Manufacturing and Mechatronics, Universiti Malaysia Pahang
Al Sultan Abdullah, Pekan, Pahang, Malaysia
e-mail: najmiyah@umpsa.edu.my

innovative technology not only saves costs but also helps in preserving food nutrients effectively, that provides solution for sustainable food preservation. However, traditional solar drying methods often face challenges such as inconsistent drying times and difficulty in maintaining optimal drying conditions.

To address these issues, advancements in Internet of Things (IoT) technologies have been integrated with solar dryers. IoT technologies enable real-time process automation and monitoring, improving the consistency and efficiency of the drying process. In other words, as an analogy to understand this concept is thinking of IoT as a network of interconnected sensors and devices that work together to optimize the drying conditions, similar to how a smart home system controls temperature and lighting for energy efficiency. Therefore, the integration of IoT with solar drying systems aims to optimize drying conditions, and similar to how a smart home system controls temperature and lighting for energy efficiency.

Recent studies have highlighted the growing application of IoT sensors in solar drying systems. This demonstrating significant improvements in efficiency, monitoring, and automation. For example, a low cost IoT-enabled semi spherical solar dryer was developed by [1] for Arabica coffee beans using DHT22 sensors. This sensors used to measure temperature and humidity, and load cells to track the drying mass, which allowed for remote monitoring and control through cloud server, enhancing the overall drying process.

This study aims to investigate the effectiveness of various sensors in an IoT-enabled solar drying system. By evaluating the sensors' responsiveness, precision, and reliability under different environmental conditions, the research seeks to enhance the system's overall efficiency and performance. The ultimate goal is to develop a more effective and reliable solar drying solution that can be used in agricultural and residential settings.

2 Related Work

Food drying is one of the oldest methods of food preservation, with traditional techniques such as air drying, sun drying, and smoking. Although these methods have been effective, however these techniques have limitations such as prolonged drying times, contamination risks, and dependency on weather conditions.

Alternative technique of food drying is solar dryer, a machine for drying used solar-powered energy. Solar dryers can be categorized into three main types: passive, active, and hybrid. Passive solar dryers rely solely on natural convection and sunlight for drying. While, active solar dryers incorporate mechanical components like fans to enhance air circulation and improve drying efficiency [2]. Third category is hybrid solar dryers where they combine elements of both passive and active systems, using solar energy during sunny periods and alternative energy sources when sunlight is insufficient. These can provide economic benefits and improving the shelf life of perishable goods [3–5].

Besides, solar dryers play an important role in agriculture not only efficient in preserving food but also reduce post-harvest losses. They are particularly beneficial in areas with abundant sunlight and limited access to conventional energy sources [6]. By extending the shelf life of perishable goods, solar dryers contribute to food security and provide economic benefits to farmer [7].

The integration of Internet of Things (IoT) technology into solar drying systems has revolutionized their operation, enabling precise control and monitoring of drying conditions. IoT technology uses sensors, actuators, and connectivity solutions to monitor soil conditions, crop health, and environmental with real-time data that can be used to optimize the drying process.

Various sensors are used in IoT applications to collect data on environmental and operational parameters [8]. Sensors which commonly used in these applications include humidity sensors, temperature sensors, moisture sensors, and light sensors to ensure product quality and improving overall system efficiency [9, 10]. The integration of solar drying systems with IoT applications can assist for automation processes, good drying conditions, and enable remote monitoring, thereby reducing the need for manual intervention and minimizing errors [9].

Previous studies have demonstrated the numerous benefits of integrating IoT with solar drying systems. According to [9] IoT-based systems improved drying efficiency by maintaining optimal temperature and humidity levels and able to enhance product quality through precise monitoring. While [10] highlighted that the automation of drying parameters using IoT led to improve accuracy and reduced errors compared to manual methods. Additionally, [11] discussed various techniques to enhance solar dryer performance. It is shown that IoT plays a key role in optimizing drying process and achieving consistent results. These studies collectively indicate that IoT integration can significantly enhance the performance of solar dryers, providing better control and improved energy efficiency.

Despite these advancements, challenges such as system complexity, data accuracy, sensor reliability, and data accuracy continue to be areas of ongoing investigation. Furthermore, the integration of IoT technologies can increase the complexity of the systems, requiring specialized knowledge for installation, maintenance, and operation, which may pose barriers to adoption in rural or resource-constrained settings [12].

In summary, integrating IoT with solar drying system enhances drying efficiency, reduce energy consumption, and improves product quality through real-time data and automation. Ongoing research is needed to address these issues and fully harness the potential of IoT-enable solar drying technologies.

3 Methodology

The research began with detailed project planning, identifying key objectives, required components, and expected outcomes. The focus was on designing an IoT-enabled solar drying system that could monitor and control drying parameters in real-time to enhance the drying process's efficiency and reliability.

Figure 1 illustrates the process flowchart for this research. The solar panel absorbs sunlight and will charge up the battery which will be coordinated by the solar charge controller. The battery will power up the ESP32 which will be connected to the two DHT22 sensors that will record the temperature and the humidity in the chamber. The ESP32 is also connected to the ACS712 current sensor which will get the voltage reading from the battery so that the charging up of the battery can be monitored. All of these data will be sent to the Blynk app and through this app, users can control the temperature and humidity by controlling the fan.

The system comprised with several essential components as shown in Table 1.

The IoT solar dryer system was designed to optimize the drying process through continuous monitoring and control. The system's architecture included sensor nodes, a central processing unit, solar power generation, and an IoT interface for remote access. The wiring diagram for the IoT-enabled solar dryer illustrates (see Fig. 2) how various components are interconnected to create a functional system. This system consists of a solar panel, a solar charge controller, a battery, multiple DC

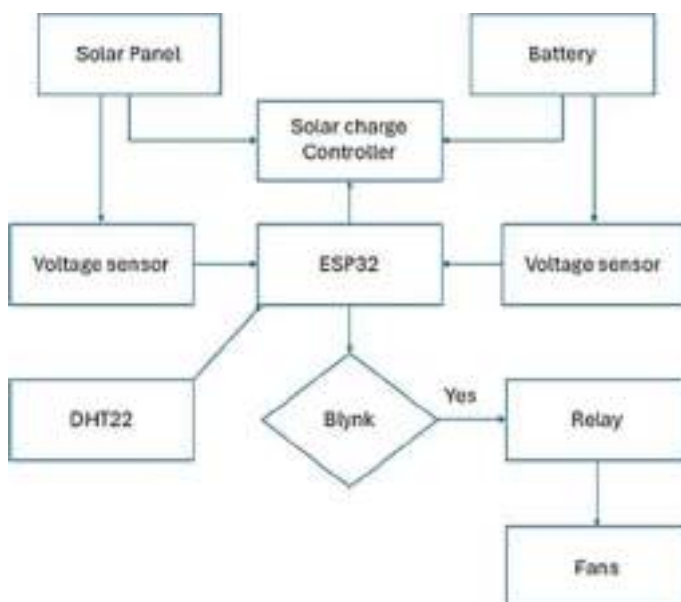


Fig. 1 IoT-enabled solar dryer process flowchart

Table 1 IoT enable solar dryer components

Component	Instruments	Function
Sensors	DHT22	Temperature and humidity, voltage sensors
Microcontrollers	ESP32	Data processing and communication
Solar panel (manufacture: iDorNation)		Provide renewal source energy for drying system
IoT platform	Blynk App	Real-time monitoring and data visualization
Battery		Power storage

fans with heatsinks and Peltier, a ventilator fan, voltage sensors, a DHT22 sensor, a microcontroller, and the Blynk app for remote monitoring and control.

The solar panel is responsible for converting sunlight into electrical energy. The positive and negative terminals of the solar panel are connected to the input terminals of the solar charge controller. The solar charge controller regulates the voltage and current from the solar panel to prevent overcharging the battery. It has input terminals

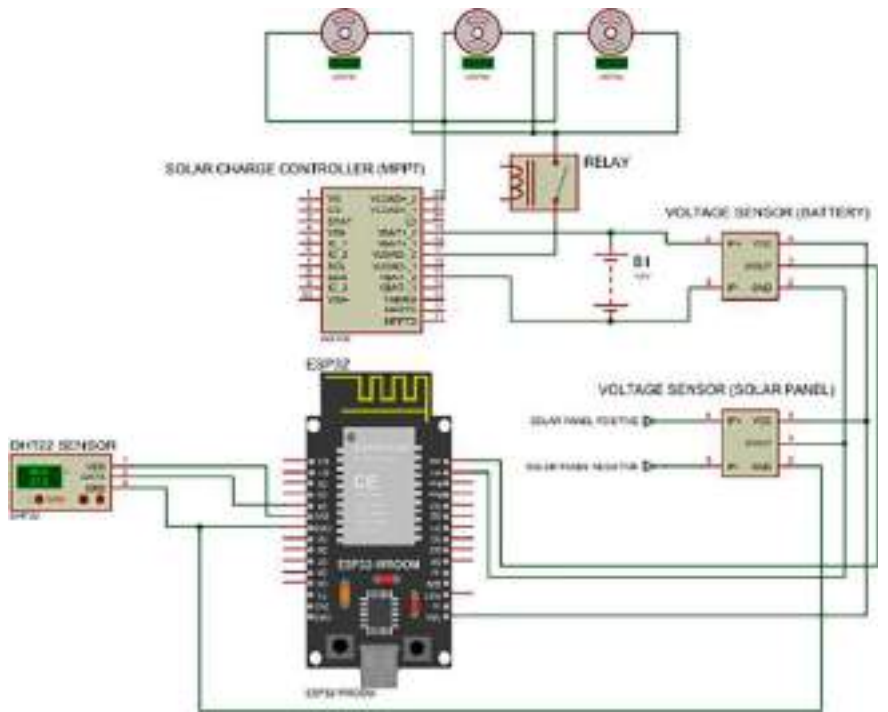


Fig. 2 The wiring diagram of IoT- enabled Solar Dryer Machine

connected to the solar panel, battery terminals connected to the battery, and load terminals connected to the drying system components.

The battery stores the electrical energy generated by the solar panel. Its positive and negative terminals are connected to the corresponding terminals on the solar charge controller. The system includes multiple DC fans that circulate air within the drying chamber to ensure uniform drying. These fans are connected in parallel to the load terminals of the solar charge controller. Heatsinks with Peltier are mounted on the DC fans to enhance heat dissipation.

Additionally, there is a ventilator fan that provides ventilation to remove moisture-laden air from the drying chamber. Similar to the other fans, it is connected to the load terminals of the solar charge controller. To monitor the voltage levels of the battery and the solar panel, voltage sensors are connected to the positive and negative terminals of the battery and solar panel. The sensor outputs are connected to the microcontroller for data logging and monitoring.

The DHT22 sensor measures temperature and humidity inside the drying chamber. It has three pins: VCC, GND, and Data. VCC is connected to the 5 V output of the microcontroller, GND is connected to the ground, and the Data pin is connected to a digital input pin of the microcontroller. The microcontroller ESP32 collects data from the sensors and controls the operation of the fans. It is connected to the load terminals of the solar charge controller for power supply. The sensors are connected to the microcontroller for data collection, and output pins of the microcontroller are connected to relays or transistors that control the fans' on/off state.

Finally, the Blynk app provides a user interface for remote monitoring and control of the solar dryer. It communicates with the microcontroller via Wi-Fi or Bluetooth. The microcontroller sends data to the Blynk app for visualization and receives commands to control the fans.

The wiring diagram ensures that all components are correctly connected, allowing for efficient operation of the solar dryer with real-time monitoring and control capabilities through the Blynk app. This setup optimizes drying parameters and validates the reliability of the sensors and IoT applications, making the solar dryer system more effective and user-friendly.

The programming involved coding the microcontrollers to read sensor data and transmit it to the IoT platform. The Blynk application was configured to display the data and provide control functionalities. Software tools used included Arduino IDE for coding and Blynk for IoT integration.

A controlled testing environment was set up to evaluate the system's performance under various conditions. The environment simulated different weather conditions to test the sensors' responsiveness and reliability.

4 Results and Discussions

The collected data were visualized using graphs and charts, showing trends in temperature, humidity, and moisture levels. This visualization helped in understanding the drying process’s dynamics and the sensors’ performance.

4.1 Time Series Analysis

The time series analysis of solar panel voltage reveals distinct daily cycles, reflecting the panel’s response to varying sunlight availability, with higher voltages observed during daylight hours and drops at night. This pattern aligns with findings in solar photovoltaic (PV) systems, where solar irradiance significantly influences voltage stability and performance, particularly under fluctuating weather conditions [13].

The absence of a significant long-term trend suggests that the solar panel maintains consistent performance over time. Anomalies in voltage readings during the day should be monitored to ensure the solar panel is functioning optimally and not obstructed (see Fig. 3).

Battery voltage also shows distinct daily cycles, corresponding to charging during the day and discharging at night. Voltage levels are higher during the day when the solar panel is actively charging the battery and lower at night when the battery is discharging. There is no significant long-term trend in battery voltage, indicating stable performance of the battery over the observed period. Sudden drops in voltage readings may indicate periods of high energy consumption or insufficient sunlight for charging. The cyclical patterns confirm that the battery is effectively charged by

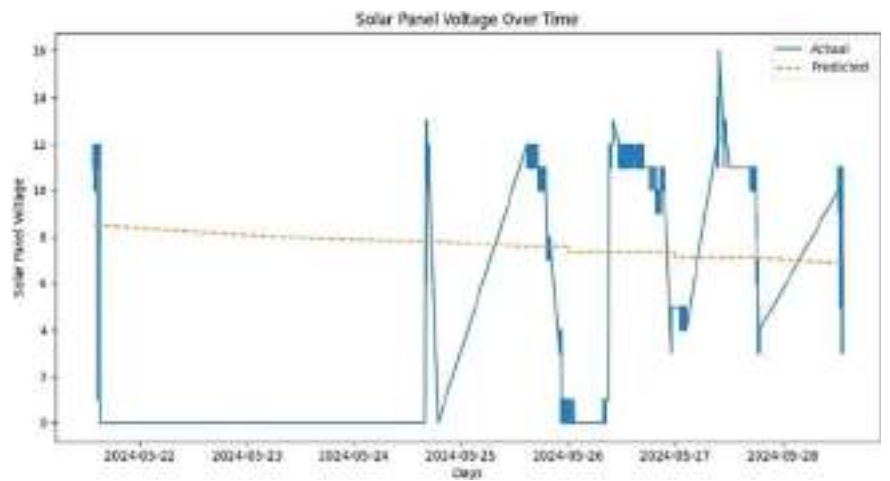


Fig. 3 Solar panel voltage over time

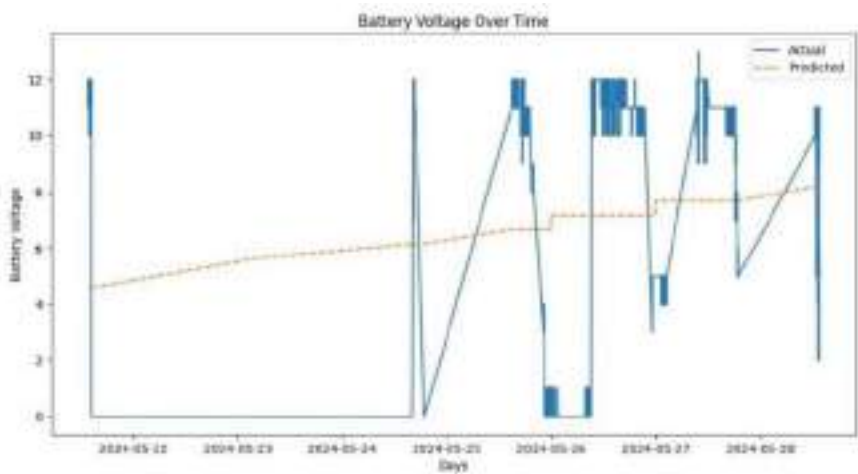


Fig. 4 The battery voltage over time

the solar panel during the day and used to power the dryer at night. The absence of a significant long-term trend suggests that the battery maintains its capacity well over time, indicating good health and stability. Anomalies in voltage readings should be monitored to ensure the battery is not over-discharged or under-charged, which could affect its longevity and performance (see Fig. 4).

4.2 Correlation Matrix

The correlation matrix is a table showing correlation coefficients between variables. Each cell in the matrix represents the correlation between two variables. Correlation coefficients range from -1 to 1 , where:

- 1 indicates a perfect positive correlation.
- -1 indicates a perfect negative correlation.
- 0 indicates no correlation.

The strong negative correlation between temperature and humidity (-0.89) aligns with findings in solar drying studies, indicating that higher temperature drives moisture out, reducing humidity levels within the drying chamber, which is crucial for effective drying processes [14]. The moderate positive correlations between temperature and both solar panel voltage (0.44) and battery voltage (0.46) suggest that increased sunlight boosts solar power generation, heating the dryer while also enhancing battery charging efficiency, a relationship observed in systems utilizing photovoltaic thermal collectors [15].

Conversely, the moderate negative correlations between humidity and both solar panel voltage (-0.59) and battery voltage (-0.63) indicate that high humidity often associated with overcast or humid conditions, diminished solar efficiency and battery performance, a challenge also reported in studies on the environmental impact on solar systems by [16].

Lastly, the strong positive correlation (0.94) between solar panel voltage and battery voltage highlights the direct impact of solar power generation on battery charging efficiency (see Fig. 5).

These correlations provide valuable insights into the interactions between environmental conditions (temperature and humidity) and the performance of the solar dryer system (solar panel and battery voltages). Understanding these relationships helps in optimizing the drying process, ensuring efficient energy use, and maintaining the reliability of the sensors and overall system.

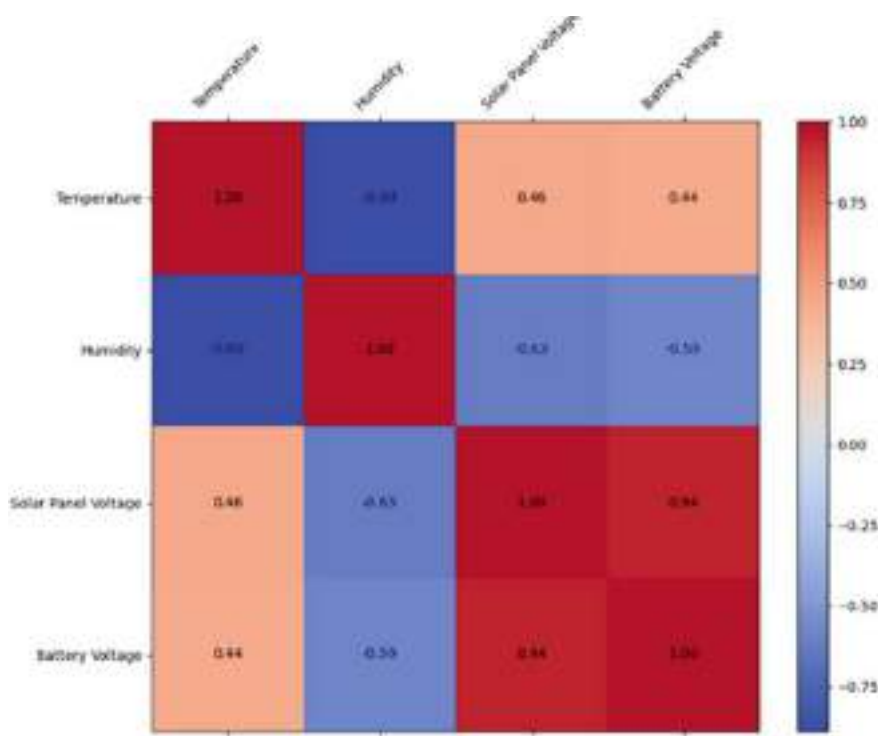


Fig. 5 Correlation matrix of the variables

5 Conclusion

The integration of IoT technologies into solar drying systems especially in food industry application enhances the efficiency, reliability and performance of the drying process. The time series analysis of solar panel voltage revealed distinct daily cycles with voltage peaking around 12–14 V during daylight and dropping to 0 V at night, indicating effective energy capture and usage patterns consistent with solar irradiance. The analysis also showed that there was no significant long-term trend, conforming stable performance over the observation period. In the correlation matrix, the strong negative correlation between temperature and humidity (-0.89) aligns with the expected drying dynamics, where higher temperatures drive moisture out of the drying chamber. Additionally, the strong positive correlation (0.94) between solar panel voltage and battery voltage emphasizes the direct impact of solar power generation on battery charging efficiency. These findings highlight the importance of continuous monitoring and IoT integration to optimize drying conditions, reduce energy consumption, and ensure consistent product quality. Expanding these studies to include economic analyses will help to understand the cost–benefit implication IoT technologies in solar drying on a larger scale.

References

1. Pramono E, Karim M, Fudholi A, Bulan R, Lapcharoensuk R, Sitorus A (2022) Low-cost telemonitoring technology of semispherical solar dryer for drying arabica coffee beans. *INMATECH Agric Eng*
2. Tiwari S, Tiwari GN, Al-Helal IM (2016) Performance analysis of photovoltaic–thermal (PVT) mixed mode greenhouse solar dryer. *Sol Energy* 133:421–428
3. Kathiresan R, Janani M, Naveen KM, Narashimabalaji E, Rasiga R (2023) Solar energy based smart irrigation system using IoT. *J ISMAC*
4. Abhinaya A, Anusha R, Arpitha K M, Jaishwal A, More M (2021) Solar powered irrigation system with IOT-connectivity and farm monitoring. *Int J Adv Res Comput Sci* 12:72–77
5. Ciftcioglu G, Kadirgan F, Kadirgan M, Kaynak G (2020) Smart agriculture through using cost-effective and high-efficiency solar drying. *Heliyon* 6
6. Udomkun P et al (2020) Review of solar dryers for agricultural products in Asia and Africa: an innovation landscape approach. *J Environ Manag* 268:110730
7. Hananda N et al (2023) Solar drying in Indonesia and its development: a review and implementation. *IOP Conf Ser Earth Environ Sci* 1169(1):012084
8. Al-Fuqaha A, Guzani M, Mohammadi M, Aledhari M, Ayyash M (2015) Internet of things: a survey on enabling technologies, protocols, and applications. *IEEE Commun Surv Tutor* 17(4):2347–2376
9. Miano J, Nabua M, Gaw A, Alce A, Ecleo C, Repulle J, Omar J (2023) Optimizing drying efficiency through an IoT-based direct solar dryer system: integration of web data logger and SMS notification. *Int J Adv Comput Sci Appl*
10. Paes J, Ramos V, Oliveira M, Pinto M, Lovisi T, Souza W (2022) Automation of monitoring of drying parameters in hybrid solar-electric dryer for agricultural products. *Revista Brasileira de Engenharia Agrícola e Ambiental*
11. Sandali M, Boubekri A, Mennouche D (2019) Improvement of the thermal performance of solar drying systems using different techniques: a review. *J Sol Energy Eng*

12. Desa W, Fudholi A, Yaakob Z (2020) Energy-economic-environmental analysis of solar drying system: a review. *Int J Power Electron Drive Syst (IJPEDS)*
13. Olarewaju R, Ogunjuyigbe A, Ayodele T, Mosetlhe T, Yusuff A (2023) Assessing the voltage stability of power system in the presence of increasing solar PV penetration. In: 2023 IEEE AFRICON, pp 1–6
14. Das M, Alic E, Akpinar E (2020) Numerical and experimental analysis of heat and mass transfer in the drying process of the solar drying system. *Eng Sci Technol Int J*
15. Arslan E, Aktas M (2020) 4E analysis of infrared-convective dryer powered solar photovoltaic thermal collector. *Sol Energy* 208:46–57
16. Mustafa R, Gomaa M, Al-Dhaifallah M, Rezk H (2020) Environmental impacts on the performance of solar photovoltaic systems. *Sustainability*

Thermodynamic Analysis of Microstructural Evolution in Aluminum Alloys



Mohamad Rusydi Mohamad Yasin  and Dongke Liu 

Abstract The utilization of mathematical modeling and simulation has become essential in the advancement of die casting alloys. The current study centers on the utilization of thermodynamic numerical analysis to predict the phase evolution of die casting alloys based on aluminum. The analysis enables the examination of crucial matters, including the regulation of morphology and the enhancement of the solidification range in the alloy design. The analysis can also be employed to depict the maximum solubility of the constituents in the alloy system. The modeling process utilizes advanced simulation software, specifically Computherm Pandat software. The suggested model is designed to forecast the solidification trajectory of the die casting alloy. The simulation principally relies on the solidification profiles, while tracing it on the aluminum alloys quaternary phase diagram. The findings from the simulations of solidification conducted on aluminum-based alloys are given and contrasted with existing experimental data. Considering the overall progress, it seems that the suggested method is a feasible foundation for creating a powerful computational tool for simulating the solidification process of die casting aluminum alloy.

Keywords Alloy · Solidification · Die casting · Simulation

1 Introduction

Aluminum alloy ingots commonly have a high concentration of impurities when utilized in the metal casting industry. Some of the most prevalent impurities found in aluminum alloy include θ -AlMnFeSi, θ -AlFeSi, and Al-Fe. Iron (Fe) is consistently

M. R. M. Yasin (✉)

Universiti Malaysia Pahang Al-Sultan Abdullah, Pekan, Pahang, Malaysia
e-mail: rusydi@umpsa.edu.my

D. Liu

Southeast University, Nanjing, Jiangsu, China

included in aluminum silicon alloys to provide increase in the strength of the alloys [1]. However, iron (Fe) is considered a harmful element in aluminum alloys due to its role in the production of impurities [2, 3]. Due to the low solubility limit of iron (Fe) in aluminum (Al) alloys ($<0.05\%$), the formation of intermetallic compounds such as AlFe and AlFeSi is a typical occurrence. The high Fe level in the alloy will negatively affect its mechanical characteristics, leading to a significant loss in ductility once the Fe content exceeds a critical threshold [4, 5]. A multitude of researchers have been investigating various approaches to mitigate the adverse impact caused by the presence of θ -AlFeSi. The presence of θ -AlFeSi phases significantly reduces the mechanical quality of Aluminum-Silicon die-casting alloys. This is mostly due to the shape of the phase that has sharp edge and needle-like structure, which creates areas of concentrated stress inside the alloy matrix. Nevertheless, the process of extracting the Fe element from the alloy is both expensive and challenging, particularly when the Fe level drops below a specific threshold percentage. Thus, it is uncommon to get an Al-Si alloy that is completely devoid of iron [6]. Controlling the proportion and structure of the AlFeSi phase, particularly the θ -AlFeSi phase, is a crucial method for enhancing the strength of Al-Si die casting alloys. A rigorous approach for doing thermal study on the solidification process of aluminum alloys has been described by Backerud et al. [7]. The study conducted comprehensive experimental investigations on various commercially available wrought aluminum alloys and cast aluminum alloys. This was accomplished through the use of differential thermal analysis (DTA), optical metallography (OM), and scanning electron microscopy (SEM) with energy dispersive analysis of X-ray (EDX). The experimental research is characterized by an idealized laboratory setup, yet it may be time-consuming and not cost-effective for the industry [8].

Recently, the die casting industry has shown a growing interest in accurately simulating both the macroscopic heat transfer and mold filling processes during casting, as well as predicting the microstructures of the final component. Thermodynamic simulation using commercial software can now predict the phase formation sequence, including intermetallic phases, during solidification, thanks to advancements in phase diagram calculations. The simulation conducted in this work can be utilized in the process of alloy development to mitigate the creation of brittle and undesired θ -AlFeSi inter-metallics. This can be achieved by strategically determining the ideal solidification path for the alloy. This paper presents a systematic study on the simulation of θ -AlFeSi intermetallics production in die-casting aluminum alloy. The study utilizes the PanAluminum database in the Computherm Pandat thermodynamic simulation software. Thermal dynamic simulation is a cost-effective method for guiding the design of die-casting alloys. The prediction of the phase formation sequence during solidification in ternary alloys is simple as the phase diagrams of the ternary system is common. In practical industrial settings, alloys having more than three elements, known as higher order alloys, are commonly employed due to their significantly enhanced mechanical capabilities. Unfortunately, there is a scarcity of dependable liquidus projections for these alloys. This research aims to simulate the solidification trajectory of a quaternary alloy system in order to forecast the production of different phases. Thermodynamic modeling can be used to analyze the

solidification path and reduce the occurrence of undesirable intermetallic phase in the design of die-casting aluminum alloys.

2 Thermodynamic Calculation Design

The equilibrium phase diagram of aluminum die casting alloys was calculated using the Pandat software, utilizing the built-in database Pan Aluminum. The database is specially tailored for the Aluminum casting alloys. This study specifically studied the Al-Fe-Mn-Si system. The iron and manganese content in each specified die-casting alloy with a specific silicon percentage significantly influence the mechanical properties of the resulting material. Consequently, it is particularly important to examine the formation of phases that contain both iron (Fe) and manganese (Mn) by precipitation. The compositions of the alloys under analysis are documented in Table 1. The phase diagram data for multicomponent die casting aluminum alloys are integrated with a solidification profile to forecast the trajectory during solidification process. The quaternary liquid projections were computed and solidification routes of the chosen die-casting alloys are graphed on the Al-Mn-Fe-Si quaternary phase diagram. The series of reactions that occur throughout the solidification process are subsequently compared with the solidification path in order to ascertain the creation of phases along the solidification path.

Table 1 Commercially available Al-Si DC alloy composition

Alloy	Composition (wt%)						
	Si	Fe	Mn	Cu	Mg	Zn	Ni
A360	9.5	1.3	0.3	0.6	0.5	0.5	0.5
B360	9.5	0.4	0.3	0.6	0.5	0.2	0.1
D380	8.5	1.3	0.5	3.5	0.2	1.0	0.5
F380	8.5	0.4	0.3	3.5	0.2	1.0	0.1
381	9.5	1.3	0.5	3.5	0.13	3.8	0.5
A381	9.5	0.4	0.3	3.5	0.13	3.8	0.1
A383	10.5	1.3	0.5	2.5	0.2	3.0	0.3
C383	10.5	0.4	0.3	2.5	0.2	3.0	0.1
C384	11.25	1.3	0.5	3.5	0.2	3.0	0.5
D384	11.25	0.4	0.3	3.5	0.2	3.0	0.1

3 Results and Discussion

Figure 1 depicts the liquidus projection of the Al-Fe-Si system, with a manganese (Mn) component of 0%. The projection indicates that the development of the primary Al-Fe-Si phase does not occur when the Fe component is below 0.5%. Line (a) serves as the boundary line where the production of both intermetallic phases of θ -AlMnFeSi and θ -AlFeSi takes place. This line is crucial because it defines the constraints on the Si and Fe composition in the alloy, hence determining the order of phase formation during the solidification of the alloy.

Figure 2 depicts the composition of A360, with the solidification path illustrated by the blue line. The solidification path commences at the θ -AlFeSi region, hence the formation of θ -AlFeSi takes place at the onset of the solidification process. Line (i) represents the creation of θ -AlFeSi, which continues until the boundary between the θ -AlFeSi and θ -AlFeSi phases is reached. In this stage, the amount of Fe is decreased in order to produce θ -AlFeSi, while the amount of Si remains constant. The reaction proceeds by the creation of secondary θ -AlFeSi and θ -AlFeSi along the boundary line (ii) until the composition of the ternary eutectic is achieved. The phase consumes fractions of Fe, Mn, and Si. The solidification process progresses as Al, Si, and θ -AlFeSi are formed in the ternary eutectic at point (iii). The whole nucleation sequence of A360 is displayed in Table 2. The formation sequence commences with the formation of θ -AlFeSi and θ -AlFeSi, which is then succeeded by the formation of Al, and ultimately Si.

Figure 3 illustrates the composition of B360, with the green line indicating its solidification course. B360 shares the same composition as A360, with the exception

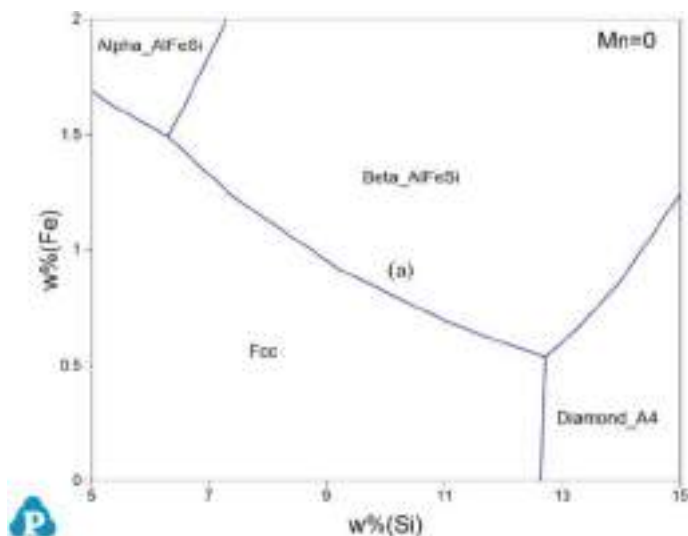


Fig. 1 Al-Fe-Si liquidus projection

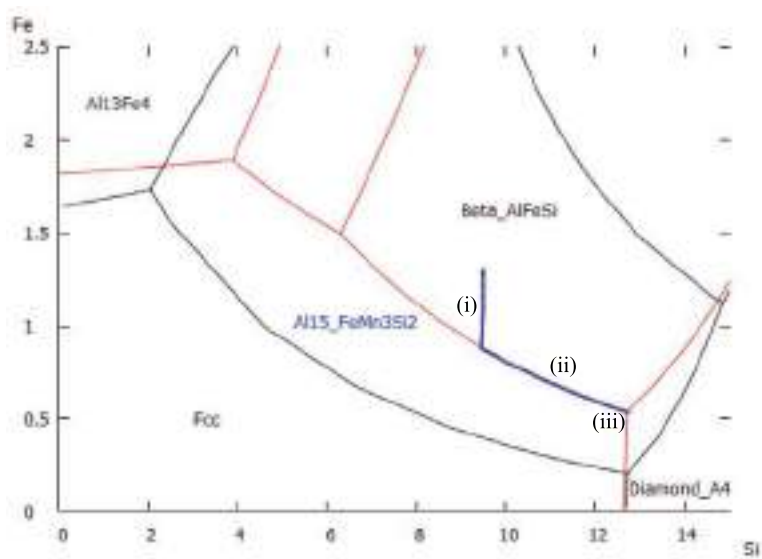


Fig. 2 A360 alloy solidification path

Table 2 Reaction during A360 alloy solidification

Temp (K)	Reactions during SOLIDIFICATION
906.8	$\text{Liq} \leq \theta\text{-Al}_{15}\text{FeMn}_3\text{Si}_2$
881.0	$\text{Liq} \leq \theta\text{-Al}_{15}\text{FeMn}_3\text{Si}_2 + \theta\text{-AlFeSi}$
871.4	$\text{Liq} \leq \theta\text{-Al}_{15}\text{FeMn}_3\text{Si}_2 + \text{Al} + \theta\text{-AlFeSi}$
848.6	$\text{Liq} \leq \theta\text{-Al}_{15}\text{FeMn}_3\text{Si}_2 + \text{Si} + \text{Al} + \theta\text{-AlFeSi}$

of having a reduced iron (Fe) percentage. The process of solidification begins within the region of $\theta\text{-AlFeMnSi}$, making the creation of the $\theta\text{-AlFeMnSi}$ phase more prevalent. Line (iv) demonstrates the creation of $\theta\text{-AlFeMnSi}$ and Al until the point where the connection between $\theta\text{-AlFeMnSi}$ and Si is established. In this phase, the proportion of Si is decreased to produce $\theta\text{-AlFeMnSi}$, while the proportion of Fe remains unchanged. The reaction proceeds via the creation of secondary $\theta\text{-AlFeMnSi}$, Al, and Si along the boundary line (v) until the composition of the ternary eutectic is achieved. During this phase, the fractions of Al and Mn are depleted while the fraction of Si remains constant, resulting in a rise in the percentage of Fe. The solidification process progresses as $\theta\text{-AlFeSi}$ forms in the ternary eutectic at point (vi). Table 3 displays the nucleation sequence of B360 alloy. The formation sequence commences with the creation of $\theta\text{-AlFeSi}$ and Al, succeeded by Si, and ultimately $\theta\text{-AlFeSi}$.

The Fe reduction can cause a change from the $\theta\text{-AlFeSi}$ phase to the $\theta\text{-AlFeMnSi}$ phase. The inclusion of Fe above the boundary line between $\theta\text{-AlFeMnSi}$ and $\theta\text{-AlFeSi}$ introduces the $\theta\text{-AlFeSi}$ phase at the beginning of the solidification process, resulting in its significant presence within the solidified aluminum alloy. On the

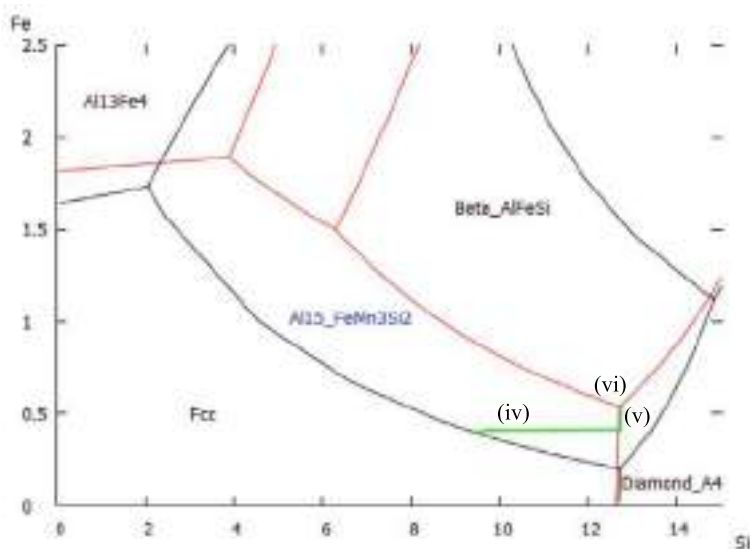


Fig. 3 B360 alloy solidification path

Table 3 Reaction during B360 alloy solidification

Temp (K)	Reactions during solidification
871.9	$\text{Liq} \leq \theta\text{-Al}_{15}\text{FeMn}_3\text{Si}_2$
871.8	$\text{Liq} \leq \theta\text{-Al}_{15}\text{FeMn}_3\text{Si}_2 + \text{Al}$
848.8	$\text{Liq} \leq \theta\text{-Al}_{15}\text{FeMn}_3\text{Si}_2 + \text{Si} + \text{Al}$
848.6	$\text{Liq} \leq \theta\text{-Al}_{15}\text{FeMn}_3\text{Si}_2 + \theta\text{-AlFeSi} + \text{Si} + \text{Al}$

contrary, the creation of $\theta\text{-AlFeSi}$ occurs towards the conclusion of the solidification process, resulting in limited occurrence. In comparison, the modeling results indicate that the fraction of $\theta\text{-AlFeSi}$ generated is 2.95% for A360, whereas for B360, which has a lower Fe content, the fraction of $\theta\text{-AlFeSi}$ is decreased to 0.53%.

The solidification path for the chosen die-casting alloys is depicted on the Al-Si-Fe-Mn quaternary liquidus projection, as illustrated in Fig. 4. The alloys demonstrate analogous route patterns to A360 and B360, where the presence of Fe influences the production of $\theta\text{-AlFeSi}$. Based on the $\theta\text{-AlFeSi}$ percent calculation, it is evident that D380 has the highest formation of $\theta\text{-AlFeSi}$, followed by A360, 381, A383, and C384. The production of $\theta\text{-AlFeSi}$ occurs along the boundary line between $\theta\text{-AlFeSi}$ and $\theta\text{-AlFeSi}$. It may be inferred that a longer path over this boundary line results in a higher fraction of $\theta\text{-AlFeSi}$ phase formation. As an illustration, the A360 alloy, which takes a longer route along the boundary line, has a $\theta\text{-AlFeSi}$ fraction of 2.95%, whereas the A383 alloy, which takes a shorter route along the boundary line, has a $\theta\text{-AlFeSi}$ fraction of 2.54%. Meanwhile, the simulation results indicate that the use of die-casting alloys with a lower percentage of Fe results in a significantly reduced

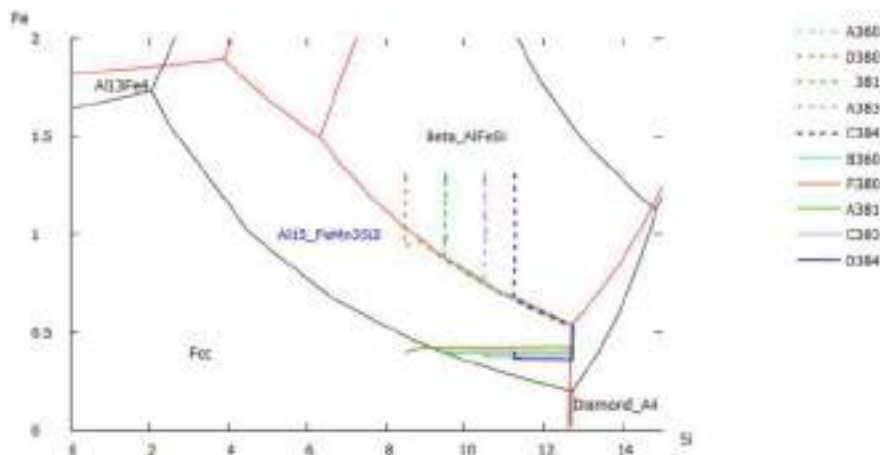


Fig. 4 Solidification path of DC alloys by thermodynamic simulation

formation of θ -AlFeSi. The A383 alloy consists of 2.54% of the θ -AlFeSi percent, but the C383 alloy, which has a lower Fe content, only consists of 0.52% of the θ -AlFeSi fraction. The decrease in the θ -AlFeSi fraction is directly proportional to the decrease in the Fe content in all the die-casting alloys under analysis.

Figure 5 illustrates the comparison of the θ -AlFeSi phase fraction obtained from the simulation results with the Quality Index (QI) of the die casting alloys studied by Donahue [9]. The comparison is made for three different die casting alloy pairings. The Quality Index increases as the production of the θ -phase decreases for each alloy pair [10]. As an illustration, B360 has less iron (Fe) than A360, leading to a decrease in the fraction of θ -AlFeSi phase by 81.2%. The Quality Index has subsequently experienced a 29% boost. Therefore, it can be inferred that minimizing the formation of the θ -AlFeSi phase has a beneficial impact on the Quality Index of the alloy, consequently enhancing its mechanical qualities.

4 Conclusions

This study examines the use of thermal dynamic modeling to forecast the production of the θ -AlFeSi and θ -AlFeSi phases in an aluminum die-casting alloy. The study presents the finding that the inclusion of iron (Fe) in the alloy's composition promotes the creation of the θ -AlFeSi phase. The proportion of θ -AlFeSi production is determined by whether the composition is higher or lower than the border line between θ -AlFeSi and θ -AlFeSi. If the iron (Fe) content exceeds the threshold, the θ -AlFeSi phase increases in size because it is created at the beginning of the solidification process. The θ -AlFeSi phase consistently arises following the θ -AlFeSi phase. Decreasing the iron level in the alloy has a more significant effect on reducing the

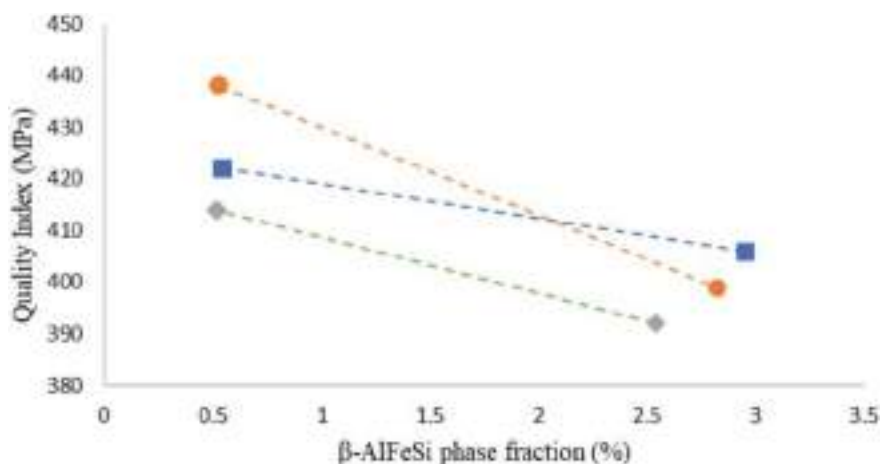


Fig. 5 Graph of Quality Index (QI) versus θ -AlFeSi phase fraction

fraction of the θ -AlFeSi phase compared to the θ -AlFeSi phase. The fraction of θ -AlFeSi phase production increases as the solidification path through the θ -AlFeSi and θ -AlFeSi boundary line becomes longer. By minimizing the production of the θ -AlFeSi phase, the Quality Index of the alloy is enhanced.

Acknowledgements The author expresses gratitude to the University of Malaysia Pahang provided financial support for this research effort through grant RDU Number RDU220317 and Tabung Persidangan Dalam Negara (TPDN). Additionally, author expresses gratitude to the Ministry of Higher Education Malaysia for their support of the study through the Fundamental Research award Scheme (FRGS), with the award number FRGS/1/2022/TK0/UMP/02/67.

References

1. Donahue RJ, Cleary TM, Anderson KR (2010) U.S. Patent No. US 6923935 B1. U.S. Patent and Trademark Office, Washington, DC
2. Green J (2007) Aluminum recycling and processing for energy conservation and sustainability. ASM International, Materials Park
3. Mazlan MS, Yasin MRM (2022) A comparative review of effect of ultrasonic shot peening on LCF behavior of the alloys. In: Innovative manufacturing, mechatronics & materials forum 2022, pp 105–110
4. Khalifa W, Samuel F, Gruzleski H (2003) Iron intermetallic phases in the Al corner of the Al-Si-Fe system. *Metall Mater Trans A* 34(13):807–825
5. Yasin MRM, Mazlan MS, Hamran NNN (2024) Optimizing DC alloy properties: impact of T6 heat treatment at high solution temperatures on θ -AlFeSi phase transformation. In: Intelligent manufacturing and mechatronics 2023, Springer proceedings in materials, vol 40, pp 309–318
6. Crepeau PN (1995) Effect of iron in Al-Si casting alloys: a critical review. *Trans Am Foundrymen's Soc* 103:361–366
7. Backerud L, Chai G, Tamminen J (1990) Solidification of characteristics of aluminum alloys, vol 2. AFS Skanalumium

8. Ruben S, Yasin MRM (2024) Simulation on effect of ultrasonic shot peening velocity on VMS of aluminum A380 die-casting alloy. In: Intelligent manufacturing and mechatronics 2023. Lecture notes in networks and systems, vol 850, pp 463–472
9. Donahue RJ (2016) Designing better structural Al DC alloys. In: Presented at 2016 Chrysler casting symposium, Kokomo IN
10. Yasin MRM, Abdul Razak SNA (2021) Effect of high temperature solution heat treatment time on quality index and morphology of A356 DC alloy. Mater Today Proc 48:1924–28

Studies on pH Effects on ZnO Nanoparticles via Microwave-Assisted Sol–Gel Method



Suraya Sulaiman , Wan Fahmin Faiz Wan Ali , Izman Sudin ,
Muhammad Firdaus Omar , and Nadhrah Md. Yatim 

Abstract This study investigates the effect of pH on the synthesis of zinc oxide (ZnO) nanoparticles through a sol–gel method. The nanoparticles were synthesized at pH values of 9, 11, and 13, employing microwave irradiation at 600 Watts and subsequent calcination at a temperature of 700 °C for one hour. XRD analysis confirms the significant decrease in crystallite size with an increase in the pH levels of the medium. The smallest size of crystallites was 27.4280 nm at pH 13. FESEM analysis also showed that ZnO nanoparticles synthesized at pH 13 were more uniform and smaller particle sizes, with a rounded morphology and a size range of 76.1–156.0 nm. EDX confirmed the high purity of the nanoparticles, as the Zn and O composition closely matched with the theoretical values. The results revealed that the pH value of 13 is optimal for producing high-purity ZnO nanoparticles with the smallest and most uniform sizes, making them ideal for advanced technological applications.

Keywords Microwave heating · ZnO nanoparticles · Nanostructure · Crystallinity · Particle size

S. Sulaiman (✉)

Faculty of Manufacturing and Mechatronic Engineering Technology, Universiti Malaysia Pahang
Al-Sultan Abdullah, Pekan, Pahang, Malaysia

e-mail: surayas@ump.edu.my

S. Sulaiman · W. F. F. W. Ali · I. Sudin

Faculty of Mechanical Engineering, Universiti Teknologi Malaysia, Skudai, Johor, Malaysia

M. F. Omar

Physics Department, Faculty of Science, Universiti Teknologi Malaysia, Skudai, Johor, Malaysia

N. Md. Yatim

Faculty Science and Technology, Universiti Sains Islam Malaysia, Nilai, Negeri Sembilan,
Malaysia

© The Author(s), under exclusive license to Springer Nature Singapore Pte Ltd. 2025

M. R. Mohamad Yasin et al. (eds.), *Proceedings of the 7th Asia Pacific Conference on Manufacturing Systems and 6th International Manufacturing Engineering Conference—Volume 2*, Lecture Notes in Mechanical Engineering,
https://doi.org/10.1007/978-981-96-5690-5_36

399

1 Introduction

Due to the constantly expanding daily need for energy by all populations globally, the globe is fast becoming a global village, and the Earth as such cannot change. The requirement for energy and associated services for the social and economic pleasure of people. A significant challenge arises from waste heat generated during fuel combustion or chemical reactions, which is often released into the environment without being utilized effectively [1, 2]. To address this issue, researchers are exploring ways to recycle and convert waste heat into electricity, which could offer a promising solution to global warming and climate change. Thermoelectric waste heat recovery systems have been developed to convert large amounts of waste heat into electrical power, offering a promising solution to the worldwide energy shortage and ecological issues. However, these systems currently operate with an efficiency of only about 7–10% [3, 4].

Recent years have seen a surge in research on conventional thermoelectric materials, such as bismuth telluride (Bi_2Te_3) for waste heat recovery systems. Thermoelectric materials have attracted significant interest due to their potential to effectively convert waste heat from industrial processes into usable energy. However, conventional thermoelectric materials encounter notable challenges, such as poor stability at high temperatures, high toxicity, and dependence on costly or rare elements, which diminish their practical appeal and feasibility [5]. Much of the recent literature focuses on enhancing oxide materials, particularly zinc oxide (ZnO), by doping with various elements (Al, Ni, Bi, Sn, Graphene) at elevated temperatures [3]. Despite these efforts, achieving the desired figure of merit ($ZT > 2$) remains challenging [2]. Additionally, research on how pH affects the properties of ZnO nanoparticles is still limited. This study aims to address this gap by evaluating both the purity and grain size of zinc oxide powder synthesized through a microwave-assisted sol–gel method, which also examines the influence of pH on the microstructure of pure ZnO using the same method.

Thermoelectric materials play a crucial role in converting thermal energy into electrical energy via the Seebeck effect, where temperature gradients generate an electric voltage. The effectiveness of these materials is determined by their figure of merit (ZT), with a higher ZT value indicating more efficient energy conversion. A ZT value of 1 or greater is typically desired to achieve a conversion efficiency exceeding 10% [3, 6–8]. To maximize thermoelectric performance, materials must possess high electrical conductivity, low thermal conductivity, and a substantial Seebeck coefficient [9]. Among the various thermoelectric materials, n-type ZnO has been widely studied due to its potential for power generation at elevated temperatures. Various approaches, such as doping and co-doping with different elements, have been explored to enhance the power generation capacity of ZnO. However, despite these efforts, most studies report ZT values below 1. The highest ZT values recorded are 0.44 at 1000 K for Al-doped ZnO [10] and 0.52 at 1100 K for ZnO doped with 1 at% Al and 1.5 wt% reduced graphene oxide (RGO) [11]. Consequently, additional

strategies, including nanostructuring, are required to further enhance the performance of thermoelectric materials [3, 12].

The nanostructuring technique emphasizes the development and growth of ultra-fine, pure, and uniform grains. By reducing grain sizes, researchers can enhance the properties of the material. Specifically, smaller grain sizes are effective in lowering thermal conductivity, as they increase phonon scattering at the grain boundaries, which in turn reduces the material's thermal conductivity. As grain sizes approach the nanoscale, phonon scattering intensifies, leading to a significant decrease in lattice thermal conductivity. This reduction is beneficial for thermoelectric materials because lower thermal conductivity helps maintain lower operational temperatures [3, 13]. Moreover, nanostructuring promotes energy filtering and electron confinement, which boosts the Seebeck coefficient and further decreases thermal conductivity through enhanced phonon scattering at interfaces. These advancements contribute to a higher figure of merit (ZT) compared to conventional thermoelectric materials. Additionally, the morphology of ZnO, including its shape and size, can be influenced by the pH level during synthesis. The balance between H^+ and OH^- ions plays a critical role in determining the morphology of the synthesized ZnO. Research has indicated that at pH 6, a high concentration of H^+ ions and a low concentration of OH^- ions can hinder the effective formation of the ZnO structure [14, 15].

2 Experimental Procedure

ZnO nanoparticles were synthesized using a microwave-assisted sol-gel method. Initially, a zinc acetate solution was prepared by dissolving 48 g of zinc acetate dihydrate ($Zn(CH_3COO)_2 \cdot 2H_2O$) in 360 ml of ethylene glycol, stirring continuously until a clear solution was achieved, as described by the chemical reaction in Eq. (2). Separately, a 1 M sodium hydroxide (NaOH) solution was prepared by dissolving 40 g of NaOH in 1 L of distilled water. The pH of the zinc acetate solution was carefully adjusted to 9, 11, and 13 by incrementally adding the 1 M NaOH solution, with the pH being monitored using a pH meter. The pH-adjusted solution was then subjected to magnetic stirring and heated at 80 °C on a hot plate until gel formation occurred, involving the reactions described in Eqs. (4) and (5). The formed gel was subsequently dried in a microwave oven at 600 Watts for 3 min, with intermittent stirring. The dried gel was then crushed and calcined at 700 °C for 1 h, a process represented by Eq. (6). A schematic diagram of the ZnO nanoparticles synthesis procedure is shown in Fig. 1, while Fig. 2 provides an overview of the methodology flowchart. The properties of the materials used are summarized in Table 1. The ZnO nanoparticles were characterized using X-ray diffraction (XRD) for phase analysis, field-emission scanning electron microscopy (FESEM), and energy-dispersive X-ray spectroscopy (EDX) to assess their morphology and composition. The particle size, anticipated to be below 100 nm, along with the average crystallite size, was determined using the Debye-Scherrer equation as described in Eq. (1).

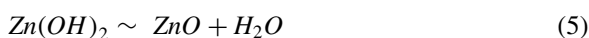
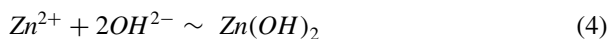
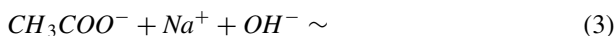
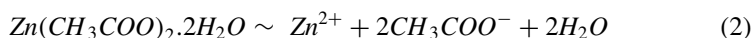


Fig. 1 Schematic illustration of synthesis of ZnO nanoparticles by a microwave-assisted sol-gel method at microwave heating (Power: 600 W time: 3 min)

$$D = \frac{K\lambda}{\beta \cos \theta} \quad (1)$$

where D is the crystallite size, κ is the Scherrer constant (0.9), λ is the X-ray wavelength, θ is the FWHM of the XRD peak, and θ is the Bragg angle.

The chemical reactions leading to the formation of ZnO can be summarized as follows:



3 Results and Discussion

This section presents a comprehensive analysis of the structural, morphological, and compositional characteristics of ZnO nanoparticles synthesized via a sol-gel method and subjected to varying pH at 9, 11, and 13 and microwave irradiation heating power at 600 Watts. The results obtained from X-ray diffraction (XRD),

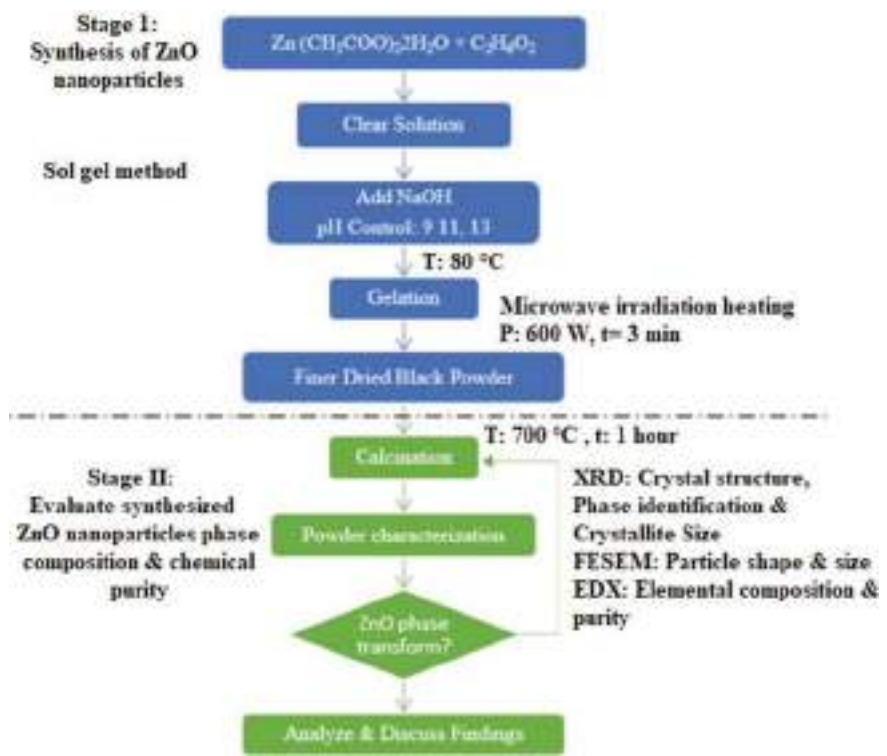


Fig. 2 Overview of methodology flowchart

Table 1 Properties of materials

Materials	Function	Chemical formula	Purity (%)	Molecular weight (g/mol)	Melting point (°C)
Zinc acetate dihydrate	Precursor	$Zn(CH_3COO)_2 \cdot 2H_2O$	≤98	219.51	237
Ethylene glycol	Solvent	$C_2H_6O_2$	≤99.8	62.068	>200
Sodium hydroxide	pH controller	NaOH	≤97	39.997	3652–3697

field emission scanning electron microscopy (FESEM), and energy-dispersive X-ray spectroscopy (EDX) offer valuable insights into the influence of microwave irradiation on these nanoparticles. The discussion focuses on the crystallinity, grain size evolution, morphological changes, and elemental composition of the nanoparticles, highlighting their potential implications for thermoelectric applications.

3.1 XRD Analysis

Figure 3 illustrates the XRD patterns of ZnO powders synthesized at different pH values (9, 11, and 13) using microwave heating at 600 Watts, scanned over a range of 10° – 80° . The results confirm that the ZnO samples exhibit a wurtzite hexagonal crystal structure, with diffraction peaks corresponding to the (100), (002), (101), (102), (110), (103), (112), and (201) planes. The patterns align well with standard ZnO data, specifically matching the space group P63mc (JCPDS card no 36-1451), indicating the formation of pure ZnO with a polycrystalline nature.

The highest intensity peak for all samples was observed at the (101) plane, with 2θ values of 36.50714° , 36.44329° , and 36.46341° for pH 9, 11, and 13, respectively (Table 2). The average crystallite size (D), calculated using the Debye–Scherrer equation, revealing sizes of 29.7780, 29.6165, and 27.4280 nm for pH 9, 11, and 13, respectively, under microwave heating at 600 W (Table 2). Notably, the smallest crystallite size of 27.4280 nm was observed at pH 13. The crystallite size decreases progressively with increasing pH, showing a 0.54% reduction from pH 9 to pH 11 and a more significant decrease of 7.89% from pH 11 to pH 13. This trend is attributed to the highly alkaline environment at higher pH, which enhances hydrolysis and promotes the formation of smaller particle sizes.

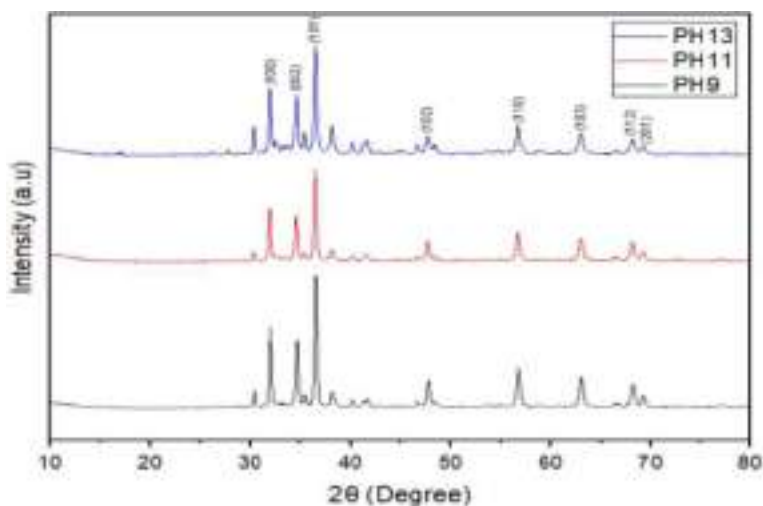


Fig. 3 XRD analysis ZnO nanoparticles at pH 9, 11 and 13 for microwave irradiation heating at 600 Watts

Table 2 Crystallite size of ZnO nanoparticles

Power (W)	pH	2 θ (°)	FWHM	Crystallite size (Nm)
600	9	36.50714	0.28092	29.7780
	11	36.44329	0.28240	29.6165
	13	36.46341	0.30495	27.4280

3.2 FESEM Analysis

Field emission scanning electron microscopy (FESEM) was utilized to examine the morphology and particle sizes of the ZnO powders synthesized under varying pH conditions and microwave heating powers. The observations revealed significant variations in particle morphology and size distribution influenced by both pH and microwave power settings.

At 600 Watts of microwave heating, the FESEM images as shown in Fig. 4a and b show that ZnO nanoparticles synthesized at pH 9 exhibit non-uniform shapes, deviating from the commonly reported spherical morphology. This irregularity may be attributed to the transition from a neutral pH to an alkaline sol, affecting particle formation. The particle size distribution for pH 9 ranged widely from 144.6 to 3270.1 nm, indicating significant agglomeration or non-uniform growth during synthesis. For ZnO nanoparticles synthesized at pH 11 under the same microwave power as shown in Fig. 4c and d, the morphology remained globular, with a more consistent particle size range of 229.2–459.3 nm. This finding aligns with previous studies that reported a morphological transition from rod-like structures to globular forms under specific synthesis conditions [16]. The presence of glycerol in the reaction medium likely acted as an agglomeration inhibitor, helping to stabilize the nano-sized particles. At pH 13, the ZnO nanoparticles displayed a more rounded morphology as shown in Fig. 4e and f, with a significantly smaller particle size distribution ranging from 76.1 to 156.0 nm. This result suggests that higher pH conditions, coupled with moderate microwave power, favor the formation of smaller and more uniform ZnO nanoparticles.

3.3 EDX Analysis

An energy dispersive X-ray (EDX) spectroscopy analysis was performed to determine the chemical composition of the synthesized substance. The analysis revealed Zn and O weight percentages of 66.96, 60.72, 64.70 and 33.04, 39.28, 35.30% for pH levels 9, 11, and 13, respectively, as shown in Fig. 5. These results indicate the formation of pure ZnO across different pH levels, with the surface of the ZnO nanoparticles displaying elements of both Zn and O. This confirms the high purity of the ZnO nanoparticles. Similar findings have been reported in previous studies, where the mass percentages of Zn and O were found to be 73.9 and 26.1%, respectively

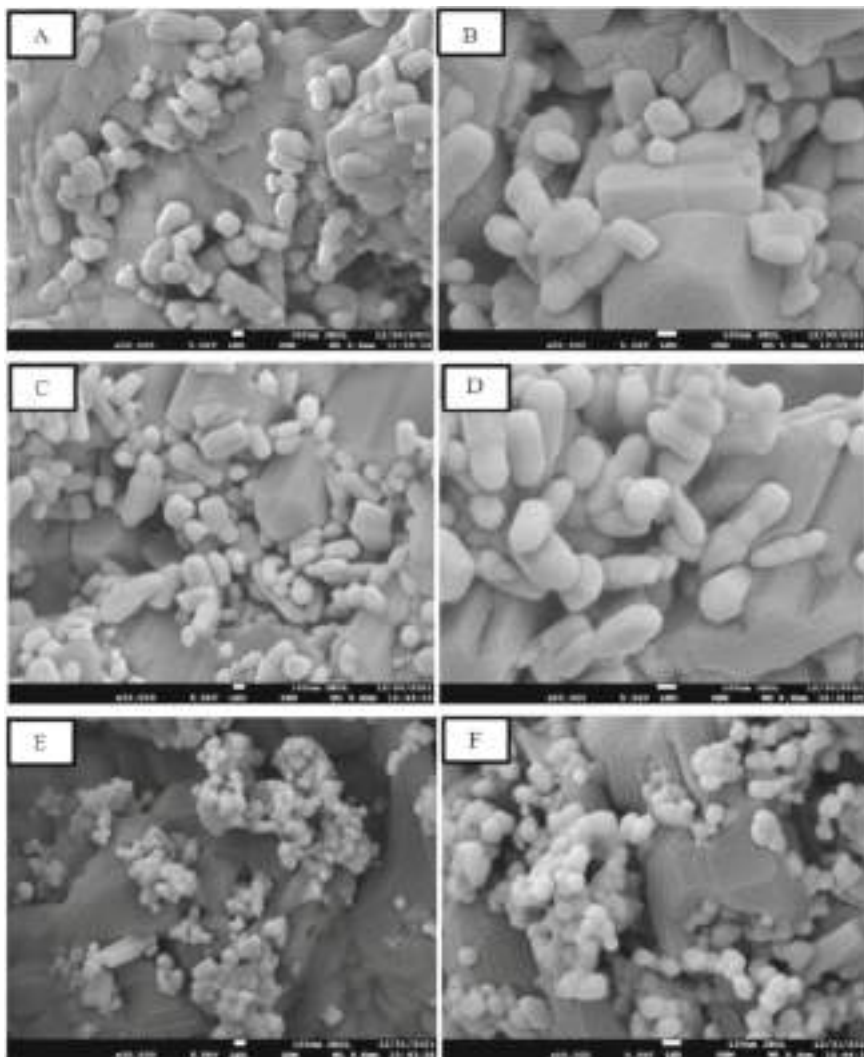


Fig. 4 Morphology of ZnO nanoparticles at 600 W **a** pH 9, 30 kx magnifications, **b** pH 9, 50 kx magnifications, **c** pH 11, 30 kx magnifications, **d** pH 11, 50 kx magnifications, **e** pH 13, 30 kx magnifications, **f** pH 13, 50 kx magnifications

[17, 18]. It is also noted that the theoretical mass percentages of Zn and O are 80.3 and 19.7%. Thus, the EDX analysis confirms that the synthesized ZnO nanoparticles possess high purity, with a composition rich in Zn and O elements. These findings are consistent with the XRD data.

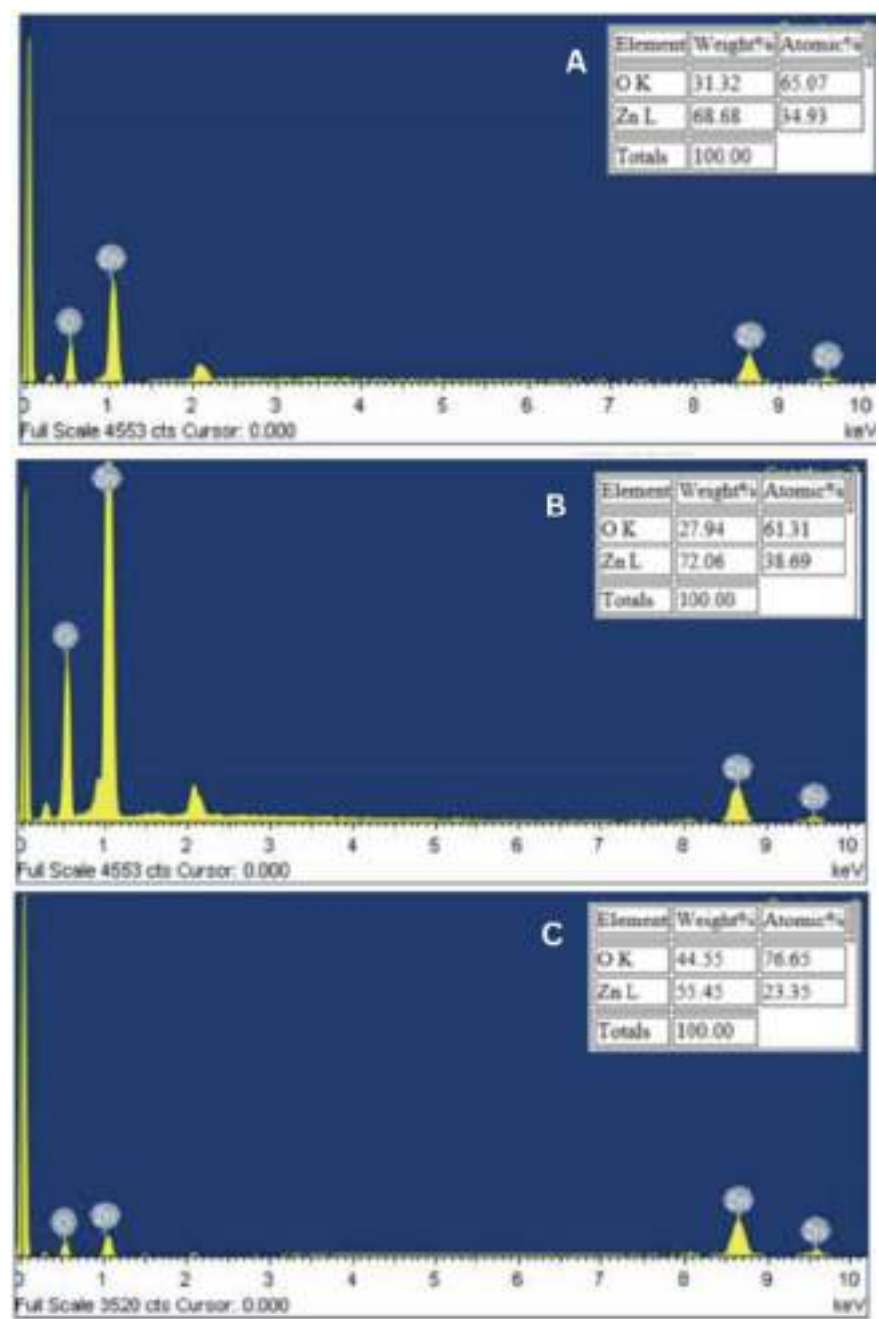


Fig. 5 Morphology of Al doped ZnO/Graphene **a**, **b** 950 °C, **c** 1100 °C, **d** 1150 °C

4 Conclusion

This study successfully met its objectives by offering valuable insights into the synthesis of ZnO nanoparticles through the microwave-assisted sol-gel method, specifically examining the influence of pH on their microstructural properties. The findings confirm that this synthesis technique is effective in producing high-purity ZnO nanoparticles with a hexagonal wurtzite structure. The research demonstrated that pH levels significantly influence both crystallite and particle sizes, with an increase in pH resulting in smaller particles. Notably, at pH 13, the smallest crystallite size was observed at 27.4280 nm, alongside the most uniform and rounded morphology. The EDX analysis confirmed the high purity of the ZnO nanoparticles, with Zn and O present in proportions consistent with high-quality synthesis. In conclusion, this study underscores the crucial role of pH in optimizing the microstructure of ZnO nanoparticles synthesized via microwave-assisted methods. These results contribute to the broader understanding of how synthesis parameters can be fine-tuned to enhance the properties of nanomaterials, particularly for their application in advanced technological fields.

Acknowledgements The author gratefully acknowledges the support and funding provided by the Ministry of Higher Education of Malaysia (MOHE) through the Fundamental Research Grant Scheme (FRGS) under Grant No. FRGS/1/2022/STG05/UMP/03/1 (University reference RDU 220130). Additional thanks are extended to Universiti Malaysia Pahang Al-Sultan Abdullah (UMPSA) for providing laboratory facilities and financial assistance through the Sustainable Research Collaboration Grant funded by UMPSA, IIUM, and UiTM under Grant No. RDU200744. The author also extends sincere appreciation to the Faculty of Manufacturing and Mechatronic Engineering Technology at Universiti Malaysia Pahang Al-Sultan Abdullah (UMPSA) for their invaluable contributions and support, which were instrumental in the successful completion of this research project.

References

1. Orr B, Akbarzadeh A, Mochizuki M, Singh R (2016) A review of car waste heat recovery systems utilising thermoelectric generators and heat pipes. In: *Applied thermal engineering*, vol 101. Elsevier Ltd., pp 490–495
2. Singh R, Dogra S, Dixit SS, Vatin NI, Bhardwaj R, Sundramoorthy AK, Perera HCS, Patole SP, Mishra RK, Arya S (2024) Advancements in thermoelectric materials for efficient waste heat recovery and renewable energy generation. *Hybrid Adv* 5:100176
3. Sulaiman S, Sudin I, Al-Naib UMB, Omar MF (2022) Review of the nanostructuring and doping strategies for high-performance ZnO thermoelectric materials. *Crystals* 12(8):1076
4. Jouhara H, Khordehgah N, Almahmoud S, Delpech B, Chauhan A, Tassou SA (2018) Waste heat recovery technologies and applications. *Therm Sci Eng Prog* 6:268–289
5. Ren G, Lan J, Zeng C, Liu Y, Zhan B, Butt S, Lin YH, Nan CW (2015) High performance oxides-based thermoelectric materials. *JOM* 67(1):211–221
6. Sulaiman S, Izman S, Udaya MB, Omar MF (2022) Review on grain size effects on thermal conductivity in ZnO thermoelectric materials. *RSC Adv* 12:5428–5438

7. Choi M, An J, Lee H, Jang H, Park JH, Cho D, Song JY, Kim SM, Oh M-W, Shin H, Jeon S (2024) High figure-of-merit for ZnO nanostructures by interfacing lowly-oxidized graphene quantum dots. *Nat Commun* 15:1996
8. Kusumawati AD, Suprayogi T, Diantoro M, Dasna I, Subakti (2018) New simple synthesis, crystal system and physical properties of ZnS₂ compound. *J Phys: Conf Ser* 1120:012083
9. Zahra R, Mahmood K, Ali A, Rehman U, Amin N, Arshad MI, Hussain S, Mahmood MHR (2019) Growth of Zn₂GeO₄ thin film by thermal evaporation on ITO substrate for thermoelectric power generation applications. *Ceram Int* 45(7):9262–9268
10. Jood P, Mehta RJ, Zhang Y, Peleckis G, Wang X, Siegel RW, Borca-Tasciuc T, Dou SX, Ramanath G (2011) Al-doped zinc oxide nanocomposites with enhanced thermoelectric properties. *Nano Lett* 11(10):4337–4342
11. Biswas S, Singh S, Singh S, Chattopadhyay S, Silva KKHD, Yoshimura M, Mitra J, Kamble VB (2021) Selective enhancement in phonon scattering leads to a high thermoelectric figure-of-merit in graphene oxide-encapsulated ZnO nanocomposites. *ACS Appl Mater Interfaces* 13(20):23771–23786
12. Norouzi M, Kolahdouz M, Ebrahimi P, Ganjian M, Soleimanzadeh R, Narimani K, Radamson H (2016) Thermoelectric energy harvesting using an array of vertically aligned Al-doped ZnO nanorods. *Thin Solid Films* 616:1–6
13. Kinemuchi Y, Mikami M, Kobayashi K, Watari K, Hotta Y (2010) Thermoelectric properties of nanograined ZnO. *J Electron Mater* 39(9):2059–2063
14. Ashraf R, Riaz S, Hussain SS, Naseem S (2015) Effect of pH on properties of ZnO nanoparticles. *Mater Today: Proc* 2(10):5529–5536. Elsevier Ltd.
15. Alias SS, Ismail AB, Mohamad AA (2010) Effect of pH on ZnO nanoparticle properties synthesized by sol-gel centrifugation. *J Alloy Compd* 499(2):231–237
16. Wang Z, Li H, Tang F, Ma J, Zhou X (2018) A facile approach for the preparation of nano-size zinc oxide in water/glycerol with extremely concentrated zinc sources. *Nanoscale Res Lett* 13:32
17. Brintha SR, Ajitha M (2015) Synthesis and characterization of ZnO nanoparticles via aqueous solution, sol-gel and hydrothermal methods. *IOSR J Appl Chem* 8(11):66–72
18. Hasnidawani JN, Azlina HN, Norita H, Bonnia NN, Ratim S, Ali ES (2016) Synthesis of ZnO nanostructures using sol-gel method. *Procedia Chem* 19:211–216

Real Time Simulation of Optimal Control-Based Flow Control for Continuous Production System



Rachmawati Wangsaputra and Fariz Muharram Hasby

Abstract Optimal control is a powerful method for addressing the challenges posed by dynamic systems, such as those found in continuous production. However, many real-world optimization tasks involve solving non-convex optimization problems, which is usually very time-consuming. In previous study, the time consuming problem tackled by an Adaptive Resonance Theory-2 Neural Network (ART-2 NN) employed as a solution technique of optimal control problem. This study investigates the behavior of real-time, optimal control-based production systems in response to two disturbances: changes in demand and variations in the available machine composition. LABVIEW is used to create a real-time simulation. The results demonstrate that the optimal control model exhibits a fast transition time before reaching new states.

Keywords Optimal control · Real time simulation · Continuous production control · ART-2 NN

1 Introduction

It is obvious that in the 4.0 industry environment with CPS, IoT and AI in Intelligent Manufacturing System especially in control, the technology offers by IMCS the capability to control the system continuously and in a real time manner need more advanced methods. Real time system control mention 3 (three) things: (i) record and

R. Wangsaputra (✉) · F. M. Hasby
Institut Teknologi Bandung, Bandung, Jawa Barat, Indonesia
e-mail: rwangsap@itb.ac.id

R. Wangsaputra
Department of Logistics, Institut Teknologi Bandung, Ganesha 10, Bandung 40132, Indonesia

F. M. Hasby
Department of Industrial Engineering, Institut Teknologi Bandung, Ganesha 10, Bandung 40132, Indonesia

monitor all system status especially changes happen, (ii) assess the system output compare with the target and (iii) make fast—good response to the changes [1]. This research aims to study the behavior of an optimal control-based production system in responding in a real time manner due to changes of internal and external condition. Maimon case study is used in this study. The solution technique following the result of Wangsaputra [2] research which is approaching solution for optimal control problems using Adaptive resonance Theory-2 Neural Network. The simulation using LABVIEW. There are 2 (two) scenarios of disturbance: (i) demand changes and (ii) machine breakdown. The purpose of this research is: (i) to test the model and to prepare for the development of the physical systems.

2 Problem Formulation

To compare the results fairly, Maimon coffee production cell study is used again in this study. The production cell consists of individual machines with sequence-dependent setup (Fig. 1a). The coffee production cell characteristic's is *make-to-order*, a group of individual machines, sequence-dependent setup and multilevel *bill of material* (BOM). There are 4 (four) types of end product: mellow, sustain, perk and turbo mix and denoted as product $i = 1, 2, 3$ and 4 respectively. The raw material for producing these 4 (four) ends products is light, medium and dark beans. The raw materials are first blended using 3 (three) blender machines ($k = 1, 2, 3$) and then packaged using 2 (two) packaging machine ($k = 4, 5$). The buffers for mellow, sustain, perk and turbo are indexed as product $i = 5, 6, 7$ and 8. The three kinds of raw material which are light, medium and dark beans are indexed as $k = 9, 10$ and 11. $X_i(t)$ denotes the buffer level for product i at time t .

The cell has a total of 5 (five) machines ($k = 1, 2, 3, 4, 5$); blender A ($k = 1$) for all sorts of mixture ($i = 1, 2, 3, 4$); blender B ($k = 2$) for only mellow, sustain and perk mixtures ($i = 1, 2, 3$); blender C ($k = 3$) for mellow, sustain and turbo ($i = 1, 2, 4$). This machine-product relationships is indexed as j , the machine state, for each machine. For example, Blender C ($k = 3$) has 3 (three) states, $j = 1, 2$ and 4. The number in a small box in each machine represents the maximum production rate for a certain mixture using that machine, v_{ijk} . For example, $v_{833} = 75$ shows that the maximum capacity of machine $k = 3$ at state $j = 3$ for product $i = 8$ is 75 units per day.

In general the production system consisting of K machines, where each individual machine $k = 1, 2, \dots, K$ can be set up in a number of states $j = 1, 2, \dots, J(k)$, one state at a time, which corresponds to the production of an item $i = 1, 2, \dots, I$. Every machine k in state j is characterized by its maximum production capacity or maximum consumption capacity. Maximum production capacity is denoted by a positive magnitude of v_{ikj} , while maximum consumption capacity is the opposite.

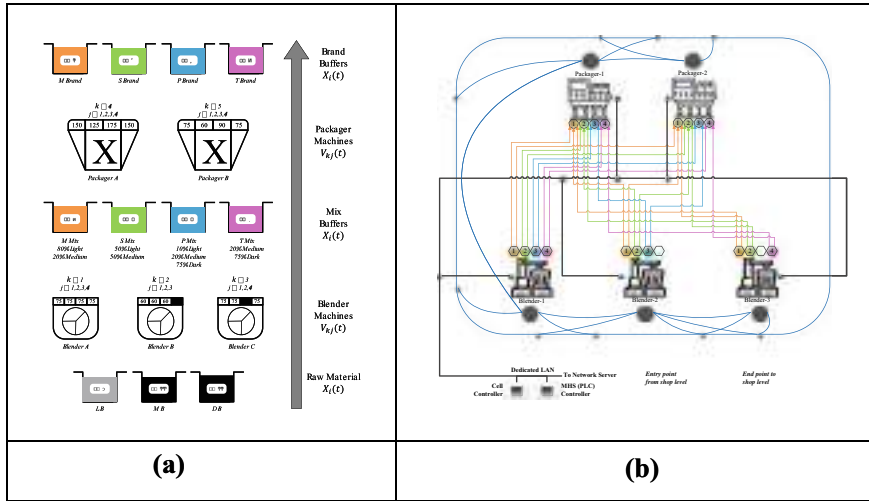


Fig. 1 **a** The structure of the production system. **b** The diagrammatic of the production system

2.1 Production Process

The production process is modeled as a continuous flow of products through its buffer. The current products flow through a buffer, $X_i(t)$, is modeled as a difference between total production of a product, $\sum_{kj} u_{kj}(t)v_{ikj}$, and its demand, $d_i(t)$, as shown in Eq. (1):

$$\dot{X}_i(t) = \sum_{kj} u_{kj}(t)v_{ikj} - d_i(t) \quad (1)$$

2.2 Setup Process

The setup process is characterized by setup speed which is notated by a variable $w_{kij'}(t)$. Here, the index j is always smaller than j' . If the setup process is to change machine states from state j to state j' then $0 \rightarrow w_{kij'}(t) \rightarrow T_{kij'}^{-1}$, on the other side, if setup process is to change machine states from j' to j , then $0 \infty w_{kij'}(t) \infty -T_{kij'}^{-1}$. By defining $w_{kij'}(t)$ whose j is always smaller than j' , the number of control variables associated with machine k , $w_{kij'}(t)$, is reduced from $J(k)^2$ to $J(k)[J(k) - 1]/2$.

Let $V_{kj}(t)$ be state j variable of machine k and be normalized to vary between zero and one. The sequence-dependent setup process is modeled by the dynamics of state variable $V_{kj}(t)$ (see Eq. 2).

$$\dot{V}_{kj}(t) = \sum_{j>j'} w_{kj'j}(t) - \sum_{j'>j} w_{kjj'}(t) \quad (2)$$

2.3 Constraints

Production and setup processes are limited by a set of constraints. Equations (1) and (2) are constrained by its initial conditions. The initial condition of Eq. (1) is its buffer level at point $t = 0$.

$$X_i(0) = X_{0i} \quad (3)$$

The initial condition of Eq. (2) is the status of machine state at point $t = 0$ (see Eq. (4))

$$\sum_j V_{kj}(0) = 1 \quad (4)$$

The machine state $V_{kj}(t)$ cannot be smaller than zero. This is modeled by applying equality as in Eq. (5).

$$V_{kj}(t) \geq 0 \quad (5)$$

The Eqs. (4) and (5) guarantee that each machine cannot be set to more than one state at a time. The production control variables, $u_{kj}(t)$, and setup rate control variables, $w_{kjj'}(t)$ are constrained as follows:

$$u_{kj}(t) \geq 0, -T_{kj'j}^{-1} \rightarrow w_{kjj'}(t) \rightarrow T_{kjj'}^{-1} \quad (6)$$

The production process on a machine is permitted only if it is in a production state not in a setup state. This fact is considered by imposing a mixed constraint on both $u_{kj}(t)$ and $V_{kj}(t)$ as in Eq. (7).

$$u_{kj}(t) \rightarrow \Theta[V_{kj}(t) - 1] \quad (7)$$

Function $\Theta[V_{kj}(t) - 1]$ is a step function which has a value of zero when $V_{kj}(t) - 1 \rightarrow 0$ and a value of one when $V_{kj}(t) - 1 > 0$. This step function $\Theta[V_{kj}(t) - 1]$ is not compatible with the canonical form of optimal control theory; therefore, the step function is approximated by a continuous function that is close enough to the step function. This paper approximates the step function by a function shown in Eq. (8).

$$f_n[V_{kj}(t)] = \frac{1}{\pi} \tan^{-1} \{n[V_{kj}(t) - 1]\} + \frac{1}{2} \quad (8)$$

The higher the value of parameter n , the closer the function $f_n[V_{kj}(t)]$ to the step function $\Theta[V_{kj}(t) - 1]$.

2.4 Performance Measurement

The performance, the objective function, is measured based on the cost of the production process consists of the buffer carrying cost and the shortage cost. This objective function is called a functional in optimal control terminology. Equation (9) shows this functional.

$$\frac{1}{2} \int_0^T \sum_i p_i[X_i(t)] [X_i(t) - X_i^S]^2 \Rightarrow \min \quad (9)$$

The variable X_i^S denote the safety stock level. The value $p_i[X_i(t)] = p_i^1$ if $X_i(t) \geq X_i^S$ whereas $p_i[X_i(t)] = p_i^2$ if $X_i(t) < X_i^S$. The parameters p_i^1 and p_i^2 denote the buffer carrying cost and penalty cost respectively.

2.5 Maximum Principle

The derivation of maximum principle by Maimon et al. (1998), Khmelnitsky (1994–2002) and Kogan (1994–2001) is as follows: For example, a trajectory $[X^*(t), u^*(t)]$ and $[V^*(t), w^*(t)]$ are an optimal solution, with $X(t)$ is a production state variable vector with I dimension, $u(t)$ is a machine load control variable vector with $(K \times J)$ dimension, $V(t)$ is state setup variable vector with $(K \times J)$ dimension, and $w(t)$ is a setup rate control variable vector with $(K \times J - 1 \times J - 1)$ dimension, then, there exists a co-state production variable $\Psi^X(t)$ with I dimension and co-state setup variable vector $\Psi^V(t)$ with $(K \times J)$ dimension which is piece-wise continuous; Lagrange multiplier $H(t)$ with $(K \times J)$ dimension which is differentiable at each t ; performance measure $dM(t)$ with $(K \times J)$ dimension; such that the following conditions apply:

Non-negativity

$$\eta_{kj}(t) \geq 0, d\mu_{kj}(t) \geq 0 \quad (10)$$

Maximum principle

The optimal control strategy is achieved by maximizing the Hamiltonian (H) at each t , as:

$$H = -\frac{1}{2} \sum_i p_i [X_i(t)] [X_i(t) - X_i^S]^2 + \sum_{kj} \psi_{kj}^V(t) \left[\sum_{j>j'} w_{kj'j}(t) - \sum_{j'>j} w_{kjj'}(t) \right] \\ + \sum_i \psi_i^X(t) \left[\sum_{kj} u_{kj}(t) v_{ikj} - d_i(t) \right]$$

Subject to:

$$u_{kj}(t) \propto 0, \quad -T_{kj'j}^{-1} \rightarrow w_{kjj'}(t) \rightarrow T_{kjj'}^{-1} \quad (11)$$

$$u_{kj}(t) \rightarrow \Theta [V_{kj}(t) - 1] \quad (12)$$

Co-state system

The co-state equation system for dynamic FMS scheduling with sequence-dependent setup is determined as follow:

$$\dot{\psi}_i^X(t) = p_i [X_i(t)] [X_i(t) - X_i^S]; \quad \psi_i^X(T) = 0; \quad (13)$$

$$d\psi_{kj}^V(t) = -\eta_{kj}(t) f'_n [V_{kj}(t)] dt - d\mu_{kj}(t); \quad (14)$$

$$\psi_{kj}^V(T+0) = 0; \quad (15)$$

with $\eta_{kj}(t) = \sum_i \psi_i^X(t) v_{ikj}$,

Complementary slackness:

$$\eta_{kj}(t) \{u_{kj}(t) - f_n [V_{kj}(t)]\} \equiv 0; \quad (16)$$

$$\int_0^T V_{kj}(t) d\mu_{kj}(t) = 0 \quad (17)$$

3 Maximum Principle Analysis

The total model for dynamic scheduling with sequence-dependent setup can be summarized as follows.

The Pontryagin maximum principle for finding optimal solution is:

$$\begin{aligned}
 & \text{Minimize } \frac{1}{2} \int_0^T \sum_i p_i [X_i(t)] [X_i(t) - X_i^S]^2 \\
 & \text{subject to:} \\
 & \dot{X}_i(t) = \sum_{kj} u_{kj}(t) v_{ikj} - d_i(t); \\
 & X_i(0) = X_{0i}; \\
 & \dot{V}_{kj}(t) = \sum_{j>j'} w_{kj'j}(t) - \sum_{j'>j} w_{kjj'}(t) \\
 & \sum_j V_{kj}(0) = 1; \quad V_{kj}(t) \geq 0; \\
 & u_{kj}(t) \geq 0; \quad -T_{kj'j}^{-1} \rightarrow w_{kjj'}(t) \rightarrow T_{kjj'}^{-1} \\
 & u_{kj}(t) \rightarrow \Theta [V_{kj}(t) - 1] \\
 & \text{with} \\
 & i = 1, 2, \dots, I; \quad k = 1, 2, \dots, K; \\
 & j = 1, 2, \dots, J(k)
 \end{aligned} \tag{18}$$

Given:

Hamiltonian:

$$\begin{aligned}
 H = & - \sum_{kj} \psi_{kj}^V(t) \left[\sum_{j>j'} w_{kj'j}(t) - \sum_{j'>j} w_{kjj'}(t) \right] + \\
 & \sum_i \psi_i^X(t) \left[\sum_{kj} u_{kj}(t) v_{ikj} - d_i(t) \right]
 \end{aligned}$$

Co-state system:

$$\begin{aligned}
 \dot{\psi}_i^X(t) &= p_i [X_i(t)] [X_i(t) - X_i^S]; \quad \psi_i^X(T) = 0; \\
 d\psi_{kj}^V(t) &= -\eta_{kj}(t) f_{ij'} [V_{kj}(t)] dt - d\mu_{kj}(t);
 \end{aligned}$$

$$\psi_{kj}^V(T+0) = 0;$$

$$\text{with: } \eta_{kj}(t) = \sum_i \psi_i^X(t) v_{ikj}$$

Necessary condition for optimal solution:

$$\begin{aligned} H[\psi_i^X(t), X_i^*(t), u_{kj}^*(t), t] &= \underset{u_{kj}(t) | g[X_i^*(t), u_{kj}(t), t] = 0}{\operatorname{argmax}} H[\psi_i^X(t), X_i^*(t), u_{kj}(t), t] \\ H[\psi_{kj}^V(t), V_{kj}^*(t), w_{kjj'}^*(t), t] &= \underset{w_{kjj'}(t) | g[V_{kj}^*(t), w_{kjj'}(t), t] = 0}{\operatorname{argmax}} H[\psi_{kj}^V(t), V_{kj}^*(t), w_{kjj'}(t), t] \end{aligned} \quad (19)$$

Three optimal production regimes for each machine state are determined because of the maximization of the Hamiltonian as a function of production rates $u_{kj}(t)$:

- (i) full production regime $u_{kj}(t) = f_n[V_{kj}(t)]$, when $\sum_i \psi_i^X(t) v_{ikj} > 0$
- (ii) partial production regime $u_{kj}(t) \in [0, f_n[V_{kj}(t)]]$, when $\sum_i \psi_i^X(t) v_{ikj} = 0$
- (iii) idle regime $u_{kj}(t) = 0$, when $\sum_i \psi_i^X(t) v_{ikj} < 0$.

While the maximization of Hamiltonian as a control function setup rate $w_{kjj'}(t)$ leads necessary condition setup as in Eq. (20): with t_s as an starting time *setup* from state j to j' .

Maimon et al. [3] proposed methods in solving the problem in general, which is solving the optimization of the process production and setup process. The first step in Maimon's model is finding the sequence of the machine state change. In doing this, all the machines in the system is assumed works at the maximum load condition, then based on the co-state setup equation the sequence of machine state change is found. Next, once the sequence is known, the optimal load is found for each machine as well as the timing.

4 Real Time Simulation

Figure 2 shows the flow in preparing the simulation and in conducting the experiment in order to study the behavior of the real time optimal control system. Unfortunately, the development of the real time simulation system, was not explained in this paper due to space limit. First, the preparation of ART-2 NN Optimizer.

In step-[a], the Neural Network (NN) Optimizer developed is an ART-2 NN. Previous research shows that analytical methods encounter difficulty in finding solutions which are very time consuming [4]. Wangsaputra and Sesaro suggested an improvement of numerical methods, while reducing the time in finding solution but still time consuming. In research in 2011 between Wangsaputra and Hasby, help from

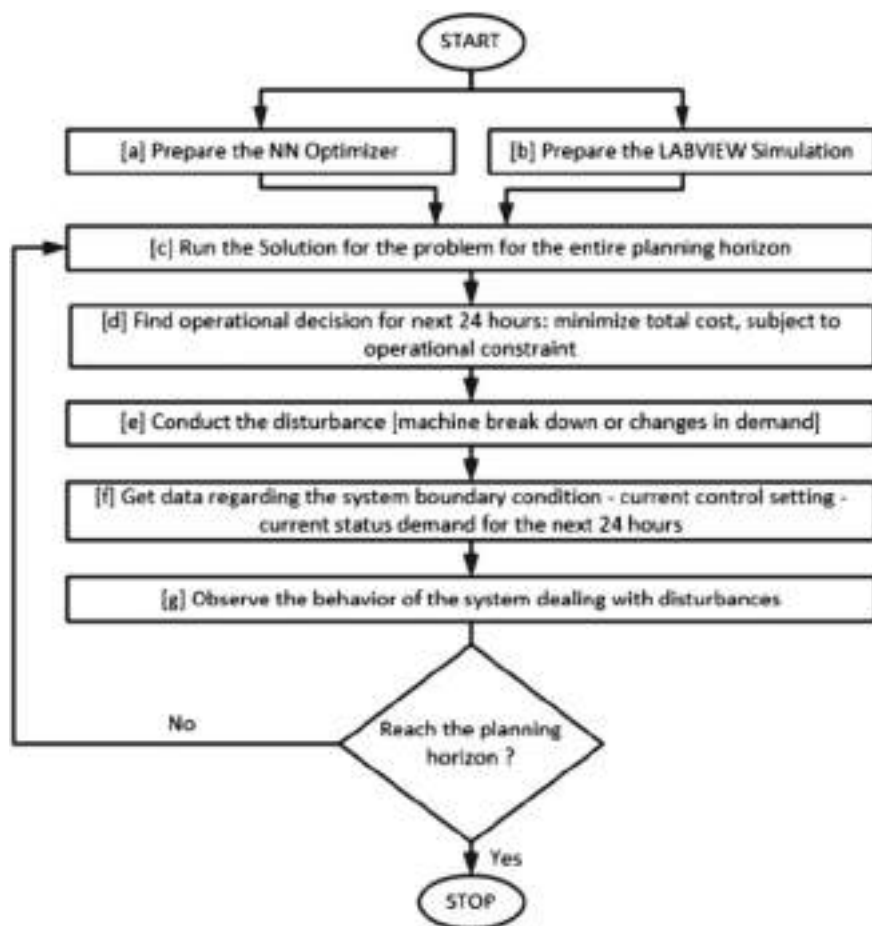


Fig. 2 The simulation plan

TOMLAB-MATLAB application was used but still encountered limitations in developing large problems [5]. In 2010 Wangsaputra developed the ART-2 NN approach in finding solution of optimal control, and it is good enough to reach the minimum cost while the time getting solution is relatively fast [6]. In step-[b] this research hasn't been implemented in a real system, instead we run it in a LABVIEW simulation. As we know, a real-time simulation refers to a computer model of a physical system that can execute at the same rate as actual "wall clock" time, commonly in computer gaming; it is important in the industrial market for operator training and off-line controller tuning. Due to space limit, the development of the real time simulation using LABVIEW is not explained in the paper. It utilized several principles explained in [1, 7–9] to build a real time simulation. Once we have already set the data, we conduct step-[c]. Once we have already set the solution, we run the

Table 1 Scenario of real-time simulation

Step	Description	T [h]
a	Initial optimal solution	
b	Real-time simulation	
c	Run the solution	
d	Operational Decision [next 24 h]	
e	First disturbances	10
f	Data of status systems	
g	Observation during disturbance	
c	Finding new solution	
d	Operational Decision [next 24 h]	
e	Second disturbances [demand changes]	15
f	Data of status systems	
g	Observation during disturbance	
c	Finding new solution	

simulation, step-[d]. Then in step-[e] we start the scenario, which is first change the condition of the machine composition. Step-[f] is a very crucial step, where we get new status that triggers changes in the systems. In step-[g], observation is conducted, consist of the transition time needed before reaching new state.

5 Experiment

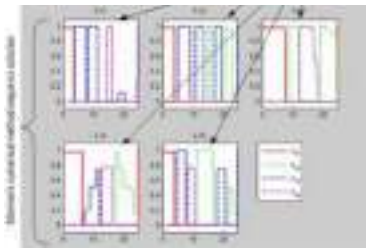
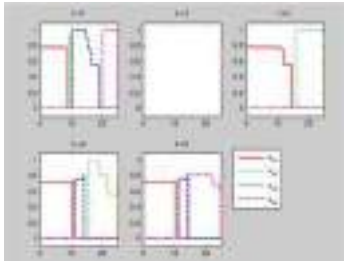
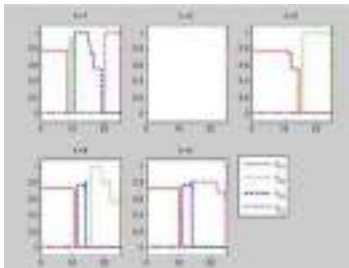
Following steps in Fig. 2, the planning horizon is 25 h, and in the hours of 10, machine A breaks down; therefore, only 1 (one) machine works. When it occurs, the system gathers all the system status, and with new status, the optimizer tries to find new solution. When it is already running steady again suddenly, the demand changes when a product is stopped, and the other product was doubled (Table 1).

The result of the experiment is shown in Table 2.

6 Analysis

It is very important that for real time system, the computation time in getting solution needs to be fast, regarding that the response need to be given is in order of minutes even seconds, the use of neural network for this problem is very important.

Table 2 The Disturbances in t=10 and t=20

No.	Decision variables	Results
		
	t = 10; machine k = 2 breakdown with D remain the same	
	t = 15; the D change to double	

7 Conclusion

There are 4 (four) conclusions in this study: (i) the optimal control model for the production system discussed, can response fast due to the changes in demand dan machine breakdown, (ii) the calculation of the new solution need to be below the response required for the system, (iii) real time simulation helps a lot in analyzing the model.

Acknowledgements This work was supported by funded by P2MI—ITB 2024 internal grant.

References

1. Zhang Z, Qu T, Huang GQ, Zhao K, Zhang K, Li M, Zhang Y, Liu L, Zhong H (2024) Digital twin and blockchain-enabled trusted optimal-state synchronized control approach for distributed smart manufacturing system in social manufacturing. *J Manuf Syst* 76:385–410
2. Wangsaputra R, Hasby FM (2011) Behavior of optimal control based real time scheduling. In: Proceeding seminar Nasional Teknik Industri & Kongres BKSTI VI, pp 1–154
3. Mughal AM (2016) Real time modeling, simulation and control of dynamical systems, 1st edn. Springer, Cham
4. Kang D (2014) Real-time optimal control of water distribution systems. *Procedia Eng* 70:917–923
5. Li J, Jiang Z, Zhao Y, Feng X, Zheng M (2024) An optimal load distribution and real-time control strategy for integrated energy system based on nonlinear model predictive control. *Energy* 308:132878
6. Magrini L, Rosenzweig P, Bach C et al (2021) Real-time optimal quantum control of mechanical motion at room temperature. *Nature* 595:373–377
7. Wang K, Lu F, Chen Z, Li J (2024) Real-time optimal control for attitude-constrained solar sailcrafts via neural networks. *Acta Astronaut* 216:446–458
8. Wangsaputra R (2010) Adaptive resonance theory-2 neural network approach for solution technique of optimal control model study case: a real time scheduling model. In: Asia Pacific industrial engineering and management systems conference 2010 (APIEMS 2010). Melaka, Malaysia
9. Wangsaputra R, Sesaro AW, Yanuardy R (2009) Implementation of optimal control based dynamic scheduling in syrup production systems. In: 1st Asia Pacific conference on manufacturing systems (APCOMS). Jogjakarta, Indonesia
10. Aghili J, Mula O (2024) An optimal control framework for adaptive neural ODEs. *Adv Comput Math* 50:52
11. Hasby FM, Wangsaputra R (2012) Study of optimal control based real-time scheduling model on single and two machine systems. In: Proceedings of the Asia Pacific industrial engineering & management systems conference 2012 (APIEMS). Phuket, Thailand
12. Kosaka N, Chida Y, Tanemura M, Yamazaki K (2023) Real-time optimal control of automatic sewing considering fabric geometric shapes. *Mechatronics* 94:103005

Solving the Capacitated Vehicle Routing Problem (CVRP) with the Simulated Annealing Method: A Case Study



Parwadi Moengin , Elvania Rivanda Dantjie, and Fani Puspitasari

Abstract Product distribution is still an important problem for a company, where companies usually use intuitive methods to distribute products. This paper discusses the use of the capacitated vehicle routing problem (CVRP) model to help companies. In this paper, CVRP is solved using the Simulated Annealing method to get the shortest route. The simulated annealing method itself is one of the metaheuristic methods that can fulfil the integration and optimization process. This CVRP model is applied to a medium-sized company located in Jakarta. The results of implementing this model can reduce distribution routes by around 7.3%, thereby saving distribution costs.

Keywords Capacitated Vehicle Routing Problem (CVRP) · Metaheuristic · Simulated annealing · Transportation · Distribution

1 Introduction

Product distribution is carried out to distribute products that have been produced to the customers, therefore the distribution must be done correctly in order to avoid waste in transportation costs. In product distribution, it can incur considerable costs, one of which is transportation costs. Transportation costs are one of the highest expenses in logistics distribution, because distribution is a major part of logistics activities and is the main part between industry and customers in the supply chain [1]. The implementation of a good distribution route is one of the motives to minimize expenses for companies in an effort to find the best way to solve problems and improve transportation efficiency [2].

The problem that needs to be solved is to find the shortest route to optimize distribution and reduce transportation costs. With this problem, the company has a

P. Moengin (✉) · E. R. Dantjie · F. Puspitasari
Department of Industrial Engineering, Universitas Trisakti, Jakarta, Indonesia
e-mail: parwadi@trisakti.ac.id

problem related to the vehicle routing problem (VRP). VRP itself is a problem that occurs a lot in real life, especially in the distribution of goods and in supply chain management. VRP aims to design a set of best routes with minimum cost starting from one depot and ending at one depot. Each route can be visited once, therefore the total customer demand on each route does not exceed the vehicle capacity [3]. Therefore, this research focuses on problems related to the capacity of vehicles used in the distribution process. The problem in question is CVRP or Capacitated Vehicle Routing Problem which is a problem in finding the shortest route with low costs and certain capacities that are known in advance [4–6].

2 Method

2.1 *Metaheuristic*

Metaheuristic methods have been widely used in solving vehicle routing problems, often finding optimal solutions to NP-hard problems such as routing, scheduling and others [7]. NP-hard problems (Non Polynomial Problems) are problems that are considered difficult to solve in polynomial time [8]. The more routes to be solved, the time required does not increase linearly, but will increase polynomially, so metaheuristic methods are used. These methods consist of differential evolution algorithm, simulated annealing, tabu search, ant colony optimization, artificial bee colony, particle swarm optimization, and genetic algorithm [9]. In this research, one of the methods of metaheuristics will be used, called the simulated annealing method to solve the vehicle routing problem, specifically the CVRP (Capacitated Vehicle Routing Problem).

2.2 *Vehicle Routing Problem (VRP)*

Vehicle Routing Problem (VRP) is a problem in determining the route of NP-hard basic combinatorial optimization [10]. This VRP is a classic routing problem aimed at finding the least-cost route for a set of homogeneous vehicles located at a depot to geographically dispersed customers. VRP involves delivery of goods, pick-up and drop-off of students or pick-up of packages as well as express mail delivery [11]. There are several variations of VRP, including:

- Capacitated Vehicle Routing Problem (CVRP). In CVRP, vehicles have a certain capacity and the total demand from customers must not exceed the capacity of the vehicle.
- Vehicle Routing Problem with Time Windows (VRPTW). In VRPTW, customers can only be served by one vehicle at a certain time interval in the planning horizon [12].

- Capacitated Vehicle Routing Problem with Time Windows (CVRPTW). CVRPTW belongs to the VRP type, where there is a limit or capacity limitation and also has a time window of each demand point.
- Vehicle Routing Problem with Pick-Up and Delivering (VRPPD). In VRPPD, customers can pick up products and send them back to the depot.

2.3 Capacitated Vehicle Routing Problem (CVRP)

Capacitated Vehicle Routing Problem (CVRP) is one of the variations of VRP. In CVRP, vehicles have a certain capacity and the total demand from customers cannot exceed the vehicle capacity [6]. CVRP has the main objective of serving each customer by reducing the aggregate travel distance and cannot exceed the vehicle capacity. Each vehicle starts from the same depot, delivers products to customers and returns to the initial depot. The mathematical model of CVRP is explained further below [4]:

Notations

d_{ij} = distance from node (customer) i to (customer u) j

n = number of customers

D_j = number of demands sent to customers $j \in J$

Q_k = vehicle capacity k

K = group of vehicles, $K = \{1, 2, \dots, k\}$

J = group of customers, $J = \{1, 2, \dots, n\}$

J_0 = group of nodes including depot, $J_0 = \{0, 1, 2, \dots, N\}$

x_{ij} and y_j = a variable used to avoid subtour, can be interpreted as the position of nodes (customers) $i, j \in J_0$ in a route.

Decision variable

$$x_{ijk} = \begin{cases} 1, & \text{if there is a visit from point } i \text{ to point } j \text{ by vehicle } k \\ 0, & \text{if there are no visits from point } i \text{ to point } j \text{ by vehicle } k \end{cases}$$

Objective function

$$\text{Min } Z = \sum_{k \in K} \sum_{i \in J} \sum_{j \in J_0} d_{ij} x_{ijk} \quad (1)$$

Constraints

Each customer is visited exactly once by one vehicle.

$$x_{ijk} = 1, i \in J_0 \quad (2)$$

The total demand of all points on a route does not exceed the capacity of the vehicle.

$$D_j x_{ijk} \leq Q_k, k \sim K \quad (3)$$

Every route starts from depot.

$$x_{0jk} = 1, k \sim K \quad (4)$$

Every vehicle that visits a point will inevitably leave that point.

$$x_{ijk} - x_{ijk} = 0, k \sim K \quad (5)$$

Each route ends at the depot.

$$x_{i0k} = 1, k \sim K \quad (6)$$

The variable x_{ijk} is a binary integer variable.

$$x_{ijk} \sim \{0, 1\}, (i, j \sim J_0, k \sim K) \quad (7)$$

2.4 Simulated Annealing

This simulated annealing method is one of the metaheuristic methods that is sufficiently simple and flexible to be used in finding optimal or near optimal solutions [13]. This method can be applied in a problem, especially distribution problems, which can fulfill the integration and optimization process. The advantage of using this method is that it allows finding the lowest value of the objective function in complex searches efficiently [5]. The simulated annealing method was developed from an analogy to the cooling process of molten metal in crystal formation, called annealing. Annealing is a metallurgical science that uses the science of scheduling the cooling process to produce efficiency in the optimal use of energy to produce metal [3]. The temperature decrease gradually is called the annealing process, which will be used in this study to solve the CVRP problem so as to obtain an optimal solution. In solving the CVRP problem, the distribution points to be arranged are analogous to atoms that move freely, and by analogizing the temperature value as the number of iterations to be carried out [14]. The steps to solve the problem with this method are:

- Initial Solution

The initial solution is the first step in solving this method which will be initialized as S1. The initial solution can be generated randomly which will produce a distribution route with the shortest distance criteria. The distribution route starts from the depot, then looks for the area closest to the depot, then will continue by determining the other closest areas [14]. This initial solution generation can be done using a program such

as the MATLAB software by generating as many random numbers as the number of points to be traversed.

- New Solution

The distribution points in the initial solution will be evaluated by the calculation process with respect to vehicle capacity. To produce a new solution or S2 will be formed by experiencing transposition or exchanging places. The route will be cut and small routes will be formed according to the capacity of the vehicle used.

- Evaluation

Evaluation is the process of calculating the total distance to be travelled by each vehicle in the route that has been generated by considering capacity constraints and depot locations.

- Metropolis

This simulated annealing method implements the metropolis criterion as the probability of acceptance or rejection of the new solution or S2 in the simulated annealing algorithm. There are several criteria in metropolis, the first is S2 will be accepted if the value of the difference between the total distance S2 and the total distance S1 or referred to as ΔC is smaller than 0. The second criterion is to accept S2 if the $\exp\left[-\frac{\Delta C}{T_0}\right]$ value bigger than the random number value [0, 1] or a random value with limits of 0–1 [8]. If the generated value of the two criteria is not sufficient, the accepted solution is the initial solution or S1 as the solution that will be used in this research. The Fig. 1 shows the simulated annealing method used in this research [15].

3 Numerical Example

A company operating in the food and beverage industry (FNB), is used as a case study in this paper. In addition to producing products, the company delivers or distributes products to other agents or to the intended customers. The company distributes products to different places and locations that are not close to each other until the vehicle fleet returns to the depot. At the time of product distribution, the route used in each fleet is different and the capacity of the vehicle fleet is also different. The vehicle fleet used in this study is two ankle trucks that deliver at least 14 delivery points per day around Jakarta.

The method that will be used is the simulated annealing method. This simulated annealing method is one of the metaheuristic methods that can fulfil the integration and optimization process. The advantage of using this method is that it allows finding the lowest value of the objective function in complex searches efficiently [5]. This method is widely used to solve difficult optimization problems, such as VRP problems. In a company's logistics system, transportation is important to connect every element in the supply chain, but it can generate the greatest costs [6]. By using the

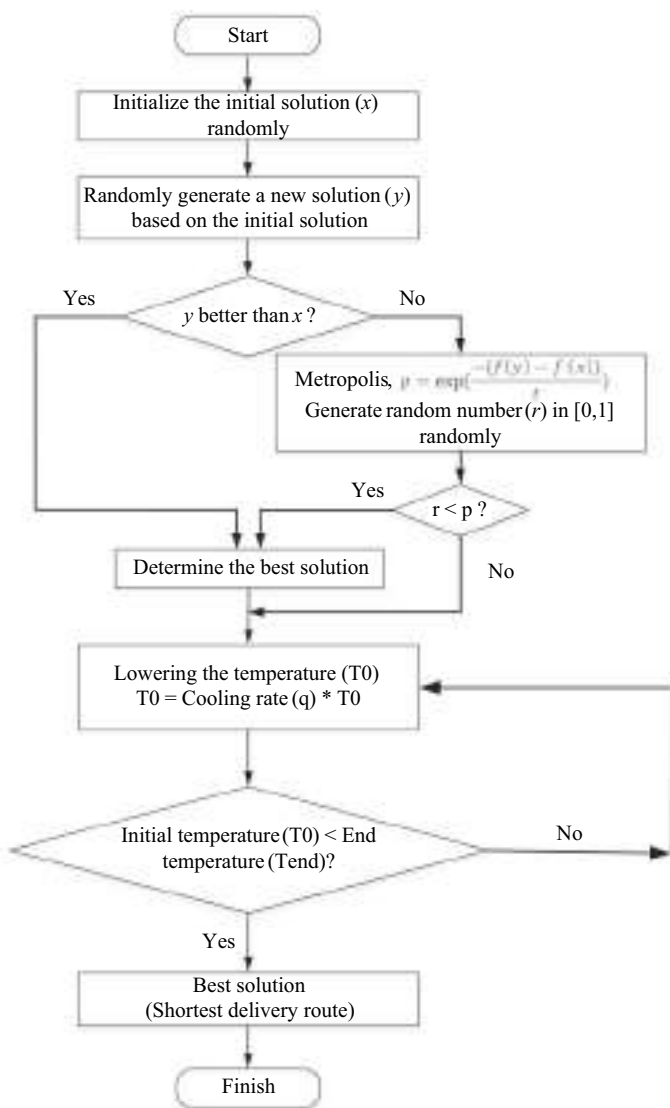
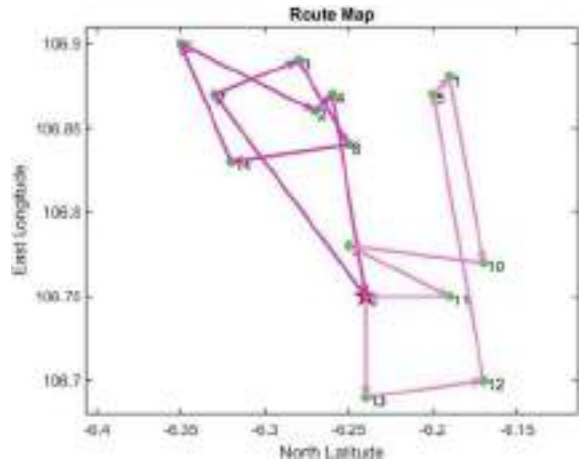


Fig. 1 Flowchart of simulated annealing method

simulated annealing method, this research is expected to solve the CVRP problem in product distribution at the company to be more optimal and can be able to reduce transportation costs.

From the resulting output, it can be seen that there is an elapsed time which shows the time required for the running process in the MATLAB software to produce the output. From the output above, the resulting load rate is 100%, which means that

Fig. 2 Graph of distribution route



each ankle truck car loads 100% of the available capacity. The soy sauce distribution route is also depicted as in Fig. 2 in the form of a route graph as follows:

The comparison between the total distance before and the total distance after improvement in solving CVRP with the simulated annealing method using MATLAB software is contained in Table 1.

Sensitivity Analysis

Sensitivity analysis was conducted in this study with the aim of seeing the changes that occur and the effect of the results obtained if the parameter values in this simulated annealing method change [16]. Table 2 shows a comparison of the count values generated if the q value changes. Changes in the q value affect and cause differences in the number of counts, namely if the q value is getting smaller, fewer counts can be produced. This happens because it shows that the temperature is decreasing faster so that it can reach the final temperature faster. Conversely, if the q value is larger, the more counts will be generated. However, the change in q value does not affect the total distance generated, the total distance at each change in q value has the same result, which is 224.6 km. Therefore, changes in the q value only affect the number of counts.

Table 1 Comparison of before and after evaluation results

Vehicle	Initial route	Initial distance (km)	New route	New distance (km)
Ankle truck 1	0–1–2–3–4–5–6–7–0	118.5	0–7–3–8–14–6–2–4–0	120.7
Ankle truck 2	0–8–9–10–11–12–13–14–0	123.9	0–13–12–5–1–10–9–11–0	103.9
Total		242.4		224.6

Table 2 Sensitivity analysis for *q* value

q	Count	Total distance (km)
0.9	66 times	224.6
0.7	20 times	224.6
0.5	10 times	224.6
0.3	6 times	224.6
0.1	3 times	224.6

4 Conclusion

From the results of calculations and evaluations that have been carried out manually and with the help of MATLAB software with a maximum iteration of 1 time, an optimal route or route with the shortest distance is obtained in the distribution of soy sauce products for 2 ankle trucks. The improvement in this study has decreased the total distance from 242.4 km so that there is a difference of 17.8 km with a decrease in distance of 7.3%. In addition to improving the distribution route, an improvement was also made to the system for providing gasoline costs, which a decrease in gasoline costs by 7.2% per day. It can be concluded that solving CVRP using the simulated annealing method can produce the shortest route and minimum cost.

References

1. Andriansyah RN, Sentia PD (2020) Simulated annealing algorithm for heterogeneous vehicle routing problem (case study). *Jurnal Teknologi Informasi Dan Ilmu Komputer (JTIIK)* 7(5). <https://doi.org/10.25126/jtiik.202072018>

2. Darina S, Wibowo AT, Ridwan M (2021) Penggunaan algoritma simulated annealing Untuk Menyelesaikan Masalah Vehicle Routing Pada Rute Distribusi Supermarket. *Netw Eng Res Oper* 6(2):99. <https://doi.org/10.21107/nero.v6i2.223>

3. Mar'I F, Mahmudy WF, Santoso PB (2018) An improves simulated annealing for the capacitated vehicle routing problem (CVRP). Department of Computer Science Brawijaya University Malang, Indonesia, 65145 Department of Industrial Engineering 9(3)

4. Ihan (2021) An improved simulated annealing algorithm with crossover operator for capacitated vehicle routing problem. *Swarm Evol Comput* 64:100911. <https://doi.org/10.1016/j.swevo.2021.100911>

5. Iswari T, Asih AMS (2018) Comparing genetic algorithm and particle swarm optimization for solving capacitated vehicle routing problem. *IOP Conf Ser: Mater Sc Eng* 337(1):012004. <https://doi.org/10.1088/1757-899X/337/1/012004>

6. Kristina S, Sianturi RD, Husnadi R (2020) Application of the capacitated vehicle routing problem (CVRP) model using Google OR-tools to map drug delivery routes to pharmaceutical wholesale companies. *Jurnal Telematika* 15(2):101–106

7. Kristina S, Sianturi RD, Husnadi R (2020) Application of the capacitated vehicle routing problem (CVRP) model using Google OR-tools to map drug delivery routes to pharmaceutical wholesale companies (Penerapan model capacitated vehicle routing problem (CVRP) Menggunakan Google OR-tools Untuk Penen). *Jurnal Telematika* 15(2):101–106

8. Mohammed MA, Ghani MKA, Hamed RI, Mostafa SA, Ahmad MS, Ibrahim DA (2017) Solving vehicle routing problem by using improved genetic algorithm for optimal solution. *J Comput Sci* 21:255–262. <https://doi.org/10.1016/j.jocs.2017.04.003>
9. Panggabean HP (2005) Algoritma simulated annealing Untuk Pembentukan Sel Mesin Dengan Dua Tipe Fungsi Objektif Dan Dua Cara Pembatasan Sel. *Jurnal Teknik Industri* 6(1):10–24. <https://doi.org/10.9744/jti.6.1.10-24>
10. Redi AANP, Maula FR, Kumari F, Syaveyenda NU, Ruswandi N, Khasanah AU, Kurniawan AC (2020) Simulated annealing algorithm for solving the capacitated vehicle routing problem: a case study of pharmaceutical distribution. *Jurnal Sistem Dan Manajemen Industri* 4(1):41–49. <https://doi.org/10.30656/jsmi.v4i1.2215>
11. Sajid M, Jafar A, Sharma S (2020) Hybrid genetic and simulated annealing algorithm for capacitated vehicle routing problem. In: PDGC 2020 - 2020 6th international conference on parallel, distributed and grid computing, November 2020, pp 131–36. <https://doi.org/10.1109/PDGC50313.2020.9315798>
12. Suprayogi S (2017) Pemecahan Masalah Rute Kendaraan Dengan Trip Majemuk, Jendela Waktu Dan Pengantaran-Penjemputan Simultan Menggunakan Algoritma Genetika. *Jurnal Teknik Industri Undip* 12(2):95. <https://doi.org/10.14710/jati.12.2.95-104>
13. Tavakkoli-Moghaddam R, Safaei N, Kah MMO, Rabbani M (2007) A new capacitated vehicle routing problem with split service for minimizing fleet cost by simulated annealing. *J Frankl Inst* 344(5):406–425. <https://doi.org/10.1016/j.jfranklin.2005.12.002>
14. Wei L, Zhang Z, Zhang D, Leung SCH (2018) A simulated annealing algorithm for the capacitated vehicle routing problem with two-dimensional loading constraints. *Eur J Oper Res* 265(3):843–859. <https://doi.org/10.1016/j.ejor.2017.08.035>
15. Welsh DJA (1989) Simulated annealing: theory and applications. *Bull Lond Math Soc* 21. <https://doi.org/10.1112/blms/21.2.204b>
16. Wirdianto E, Jonrinaldi BS (2007) Penerapan Algoritma Simulated Annealing Pada Penjadwalan Distribusi Produk. *Jurnal Optimasi Sistem Industri* 7(1):7–20

Designing the Flexible Jig and Fixture to Reduce the Production Time of the Excavator Buckets



Rahmi Maulidya , Nora Azmi , Soni Iskandar, and Docki Saraswati

Abstract This paper studies a flexible jig and fixture to support the production of the excavator buckets. In processing the buckets for big excavators, the operator should be equipped with jigs and fixtures to conduct the process of spot welding. The problem occurs when the jig and fixture need more space for the processes and the storage. This paper aims to propose a design of a flexible jig and fixture for processing the buckets that can minimize the production time. Based on the current jigs and fixtures, a flexible jig and fixture is developed to solve problems. The fixture design is equipped with movable pins that can be easily repositioned in the provided holes on the jig, corresponding to the type of bucket being produced. The production time has decreased by 17.65%. This approach can make the most of the limited workspace available.

Keywords Flexible · Jigs and fixtures · Bucket · Design product

1 Introduction

An operator needs jigs and fixtures in manufacturing activities to fulfill the task. The design of an effective jig and fixture depends on the implication of the process plan [1]. The process of joining two or more components needs a jig and fixture to help in positioning the components and supporting the processes [2]. The jigs and fixtures are usually developed for a certain component. After a certain time, there will be more jigs and fixtures to be handled and organized. The storage for keeping the jigs and fixtures is also limited. Most of those jigs and fixtures are obsolete and must be eliminated. The new products launched need another new jig and fixture. This gap led the research to a flexible jig and fixture design.

R. Maulidya · N. Azmi (✉) · S. Iskandar · D. Saraswati
Industrial Engineering Master Program, Universitas Trisakti, Jakarta, Indonesia
e-mail: nora.azmi@trisakti.ac.id

In the production of big excavators, the bucket is also designed to fulfill the customer's needs such as digging, holding, and moving the material [3]. The size of the bucket depends on the capacity targeted for the bucket. The buckets for big excavators can be divided into a family of 125 tons (the size of 5–7 m³) and a family of 200 tons (the size of 11–13 m³). The bucket itself is connected to the arm of the excavator. The demand for this big excavator is fluctuating and usually in small quantities. Therefore, the production of those big excavators needs to result in good final products, especially in producing the buckets.

The demand for buckets of big excavators led to the production being conducted manually. The processes become inefficient and need more time to double-check the results [4]. Another problem with the quality occurs [5], especially when the buckets go to further machining process. The rejection occurs in two types of reject, first, the reject that can be reworked by filling the welding fluid to the Hinge, and second, the reject that makes the Hinge surface on the bucket not exposed to the machining process.

The problem is identified in the production of a bucket for a big excavator that the storage space needed with the additional facilities for transportation back and forth to the storage area. The fact that the number of jigs and fixtures is increasing due to the expansion of the new products, and the maintenance of those jigs and fixtures has also become a problem. The objective of this research is to design a flexible jig and fixture to reduce the production time of the bucket. In this paper, the design of the jig and fixture is set to be flexible based on the research on flexible jigs for drilling [6], and flexible automatic jigs for the base of car manufacturing [7].

Several assumptions are as follows. This research focuses on two bucket families of big excavators, each of which has different sizes of components. A bucket consists of a base bucket, two hinges, and two to four covers. The flexible jig and fixture are designed to support the assembly of the hinge, cover, and base using spot welding. The jig and fixture in this research are for manual operation.

2 Methods

The methodology in Fig. 1 is proposed by comparing the methodology of product design according to [8] and the key indicators for designing the jig and fixture [9]. The method starts with studying the components of a bucket and then setting the center point for the base plate jig using the X-axis and Y-axis [10]. After setting the clamping adjustment, then build the flexible jig and fixture started from Type I to Type V. The fool-proofing arrangement is set to color the different uses of the jigs.

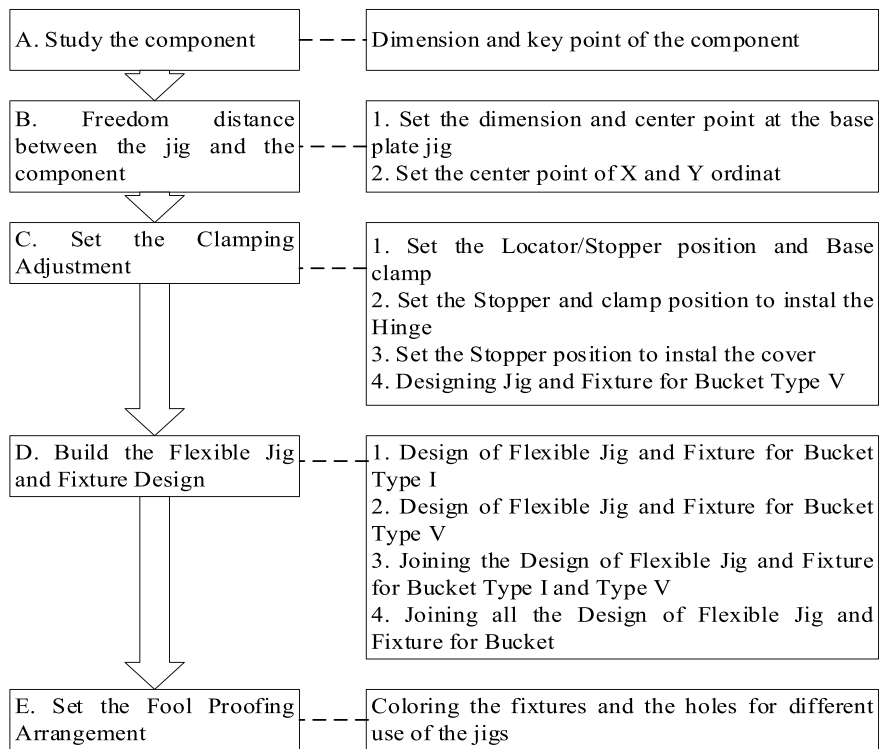


Fig. 1 Build a flexible jig and fixture design for the buckets

3 Result and Discussion

3.1 Study the Component

This paper illustrates the need for a flexible jig and fixture in the spot welding process for the five buckets belonging to big excavators of a family of 125 tons (the bucket size of 5, 6, and 7 m³) and a family of 200 tons (the bucket size of 11 and 13 m³). The key indicators from Fig. 2 are defined for the five types of buckets. Table 1 shows the dimensions for all types of buckets.

There are two concepts of tightening the jig and the fixture such as using nut and bolt [11] and using the pin locator. The concept selection is conducted to select between the reference design concept of using nut and bolt, compared to the use of a pin locator. The criteria of selection are ease of use, ease of setup, accuracy, durability, the number of tools, ease of storage, and ease of manufacture. The score for the concept of pin locator is 4, better than the score for the concept of nut and bolt, −2.

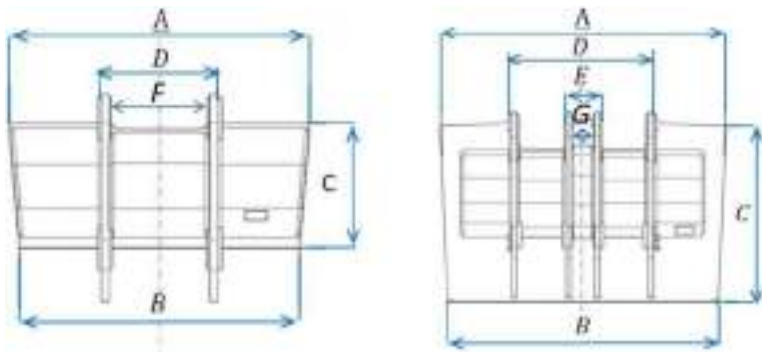


Fig. 2 The bucket of 125 tons (left) and 200 tons (right)

Table 1 The dimensions of the key indicator for the five types of buckets

Type	Type/Model	Dimension (mm)						
		A	B	C	D	E	F	G
I	125 T (5.5 m ³)	2024.3	1891.0	848.7	897.5		703.5	
II	125 T (6.7 m ³)	2177.3	2042.7	856.2	897.5		703.5	
III	125 T (7.5 m ³)	2171.3	2030.3	897.6	897.5		703.5	
IV	200 T (12 m ³)	2453.0	2331.6	1393.4	1322.0	334.0		188
V	200 T (14 m ³)	2577.1	2438.5	1571.4	1322.0	330.0		188

The next step is to generate the design concept for the jig and fixture by studying and analyzing the dimensions and the key indicators for each type.

3.2 Set the Dimensions and the Center Point for the Base Plate Jig

The dimensions for the base plate jig are defined heuristically as the longest and the widest dimensions of all types [12]. It is Type V that is set to be Point A and Point C, each is added with 300 mm. So, the length and the width are obtained. The next step is setting the center point of the base plate jig. The center is based on Point C and divided by 2, and Point A divided by 2. The center represents the X-axis and Y-axis.

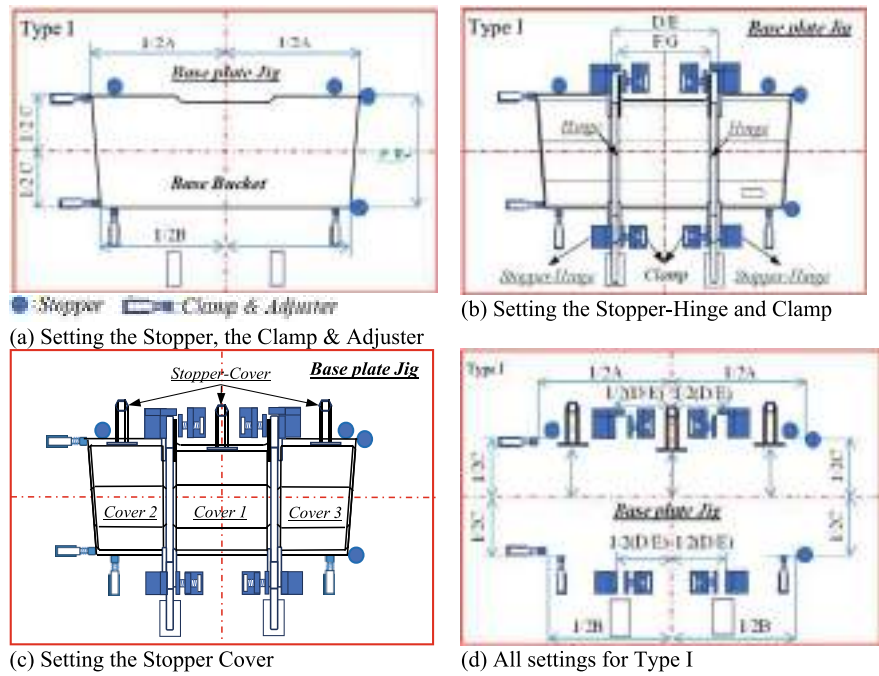


Fig. 3 Setting position for type I

3.3 Setting the Stopper, Clamp, and Adjuster

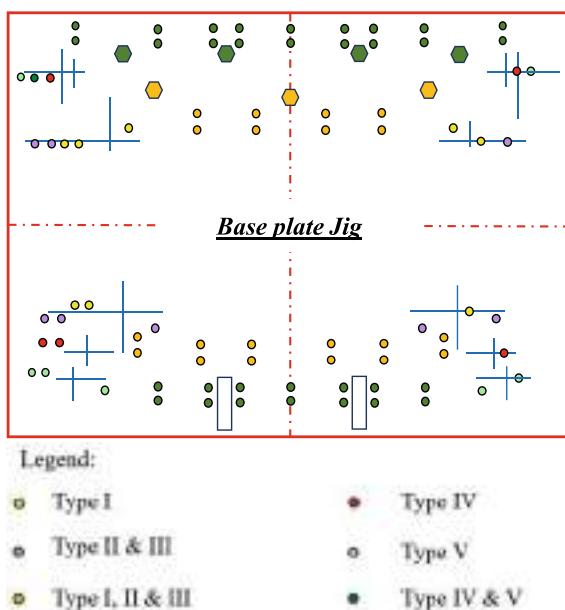
The setting started from Type I (the smallest bucket). Figure 3 shows the setting position for Type I. The steps are (a) setting the Stopper for the base bucket and then setting the Clamp and Adjuster. (b) setting the stopper-hinge and the clamp for the Hinge. (c) setting the stopper cover for the bucket cover. Repeat Fig. 3 for the setting position of Type II to Type V.

3.4 Designing the Flexible Jig and Fixture

After all the stopper, clamp and adjuster for all types are set, then Fig. 4 shows the mapping in the base plate jig. The fool-proofing arrangement can be seen by the colour set for each type. Those holes are equipped with movable pins that can be easily repositioned.

The manual procedure for using the flexible jig and fixture can be seen as follows. The design for Type I is developed in Fig. 5, and for Type V can be seen in Fig. 6. Bucket Type I has two hinges, and Bucket Type V has four hinges. The assembly of

Fig. 4 The design of pin locator for all types



the hinge to the base plate uses spot welding. The jig locks the material and then the welding process can be finished.

Table 2 shows the result for each type after the observation and the result shows the reduction of production time. The flow process chart compares the current and future conditions using the flexible jig and fixture. The activity for the future condition is set by eliminating the setup time of picking the jig and fixture from the storage and place to the area of production, changing with the activity of placing the pins to the hole and loosening the pins based on the color of the jig.

The production time for the five types of buckets can be finished in 4,146.2 min if the production runs continuously from Bucket Type I to Bucket Type V. During production activities, the process of removing parts from the machines takes a lot of time, so a minimal time is required to complete the production process, integrated with an economical production scale [13]. Figure 7 shows the schedule for the production using the flexible jig and fixture, starting from the fastest processing time using Type I. The bar in Fig. 7 is illustrated by the total time that can be seen in Table 2. It is assumed that the process of each type of bucket is one. This activity of setting the process is conducted manually by the operator. So, the setting position is dominated by the work of the operator. There should be other alternatives to speed up the process such as using a pneumatic adjuster and clamping to lock the material. So, the operator can easily adjust the material and do the welding.

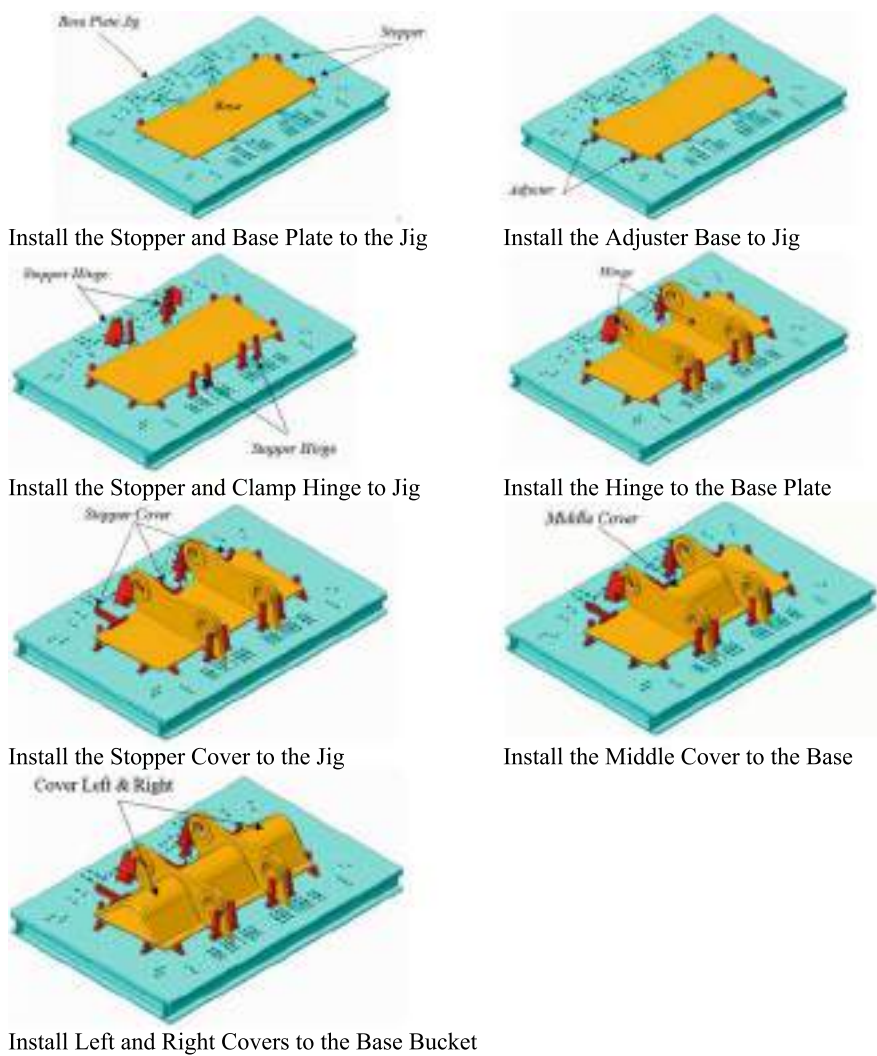


Fig. 5 The flexible jig and fixture for type I

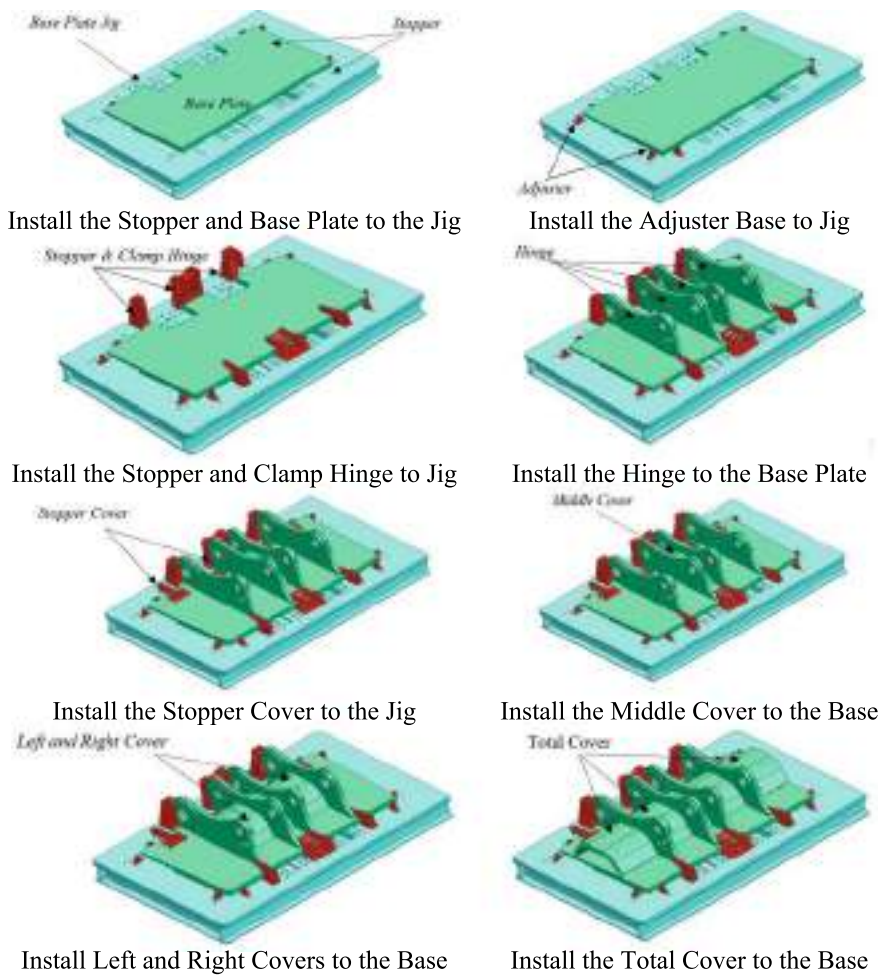


Fig. 6 The flexible jig and fixture for type V

Table 2 The result of the key indicator for the five types of buckets

No.	Description	Observation result (min)				
		I	II	III	IV	V
1	Preparing the base plate	5.7	5.7	5.7	6.7	6.7
2	Marking the hinge position and adjusting the distance between the hinge	32.2	32.2	32.2	64.4	64.4
3	Installing the hinge	8.6	8.6	8.6	17.2	17.2
4	Setting the cover	82.5	82.5	82.5	140.5	140.5
5	Installing the support bar	22.4	22.4	22.4	42.4	42.4
6	Welding the hinge	534.7	539.5	565.1	755.2	773.1
Total time		686.1	690.9	716.5	1026.4	1044.3
Reduction time		146.6	146.6	146.6	228.6	228.6
Performance (%)		17.61	17.50	16.99	18.22	17.96



Fig. 7 Production scheduling started from type I to type V

4 Conclusion

This paper studies a novel of flexible jigs and fixtures designed for a big excavator’s bucket that can reduce production time. The area of storage for those jigs and fixtures is limited which led this research to design one base plate with temporary fixture positions as a multi-dimension jig. This research accommodated a flexible jig and fixture for the five types of bucket production using the selected concept of pin locator, instead of using nuts and bolts. The flexible jig and fixture are designed after each stopper, clamp, and adjuster is defined. The combination of all types is set to map the pin locator on the base plate. Then the design of the flexible jig and fixture is defined. This design should be tested before the mockup is built. Therefore, the activity time shows a reduction of 17.65%.

The next research is developing a flexible jig and fixture with a pneumatic system for adjustment and clamping (pneumatic clamps with a pneumatic cylinder driven by compressed air to lock).

References

1. Falahat M, Chong SC, Liew C (2024) Navigating new product development: uncovering factors and overcoming challenges for success. *Heliyon* 10(1):e23763. <https://doi.org/10.1016/j.heliyon.2023.e23763>
2. Fielder F, Ehrenstein J, Holtgen C, Blondrath A, Schaper L, Goppert A, Schmit R (2024) Jigs and fixtures in production: a systematic literature review. *J Manuf Syst* 72:373–405. <https://doi.org/10.1016/j.jmsy.2023.10.006>
3. Kumar S, Campilho RDSG, Silva FJG (2019) Rethinking modular jigs' design regarding the optimization of machining times. *Procedia Manuf* 876–883. Elsevier B.V. <https://doi.org/10.1016/j.promfg.2020.01.169>
4. Radhwan H, Effendi MSM, Rosli MF, Shayfull Z, Nadia KN (2019) Design and analysis of jigs and fixtures for manufacturing process. *IOP Conf Ser Mater Sci Eng* 551:012028. <https://doi.org/10.1088/1757-899X/551/1/012028>
5. Jones D et al (2024) The prototype taxonomised: towards the capture, curation, and integration of physical models in new product development. *Comput Ind* 155:104059. <https://doi.org/10.1016/j.compind.2023.104059>
6. Rajesh S, Vijaya Ramnath B, Parswajinan C, Vishnu K, Sridhar R (2020) Multi component drill jig for brake lining component. *Mater Today: Proc* 3903–3906. Elsevier Ltd. <https://doi.org/10.1016/j.matpr.2021.02.342>
7. Siddardha B (2018) ScienceDirect Improving the productivity and tool life by fixture modification and renishaw probe technique. www.sciencedirect.com
8. Sibanda V, Murena E (2023) Realisation of design methodologies and tools in modern manufacturing systems. In: *Procedia CIRP*. Elsevier B.V., pp 468–473. <https://doi.org/10.1016/j.procir.2023.03.109>
9. Schuh G, Bergweiler G, Lichtenthäler K, Fiedler F, De La Puente Rebollo S (2020) Topology optimisation and metal based additive manufacturing of welding jig elements. In: *Procedia CIRP*. Elsevier B.V., pp 62–67. <https://doi.org/10.1016/j.procir.2020.04.066>
10. Oberfichtner L, Ahrens A, Fritzsche R, Richter-Trummer V, Todtermuschke M (2022) Solving a multi-dimensional matching problem for grouping clamping points on car body parts. In: *Procedia CIRP*. Elsevier B.V., pp 126–131. <https://doi.org/10.1016/j.procir.2022.02.166>
11. Stebner SC et al (2024) Monitoring the evolution of dimensional accuracy and product properties in property-controlled forming processes. *Adv Indus Manuf Eng* 8:100133. <https://doi.org/10.1016/j.aime.2023.100133>
12. Sun W, Gao Y (2022) The rule-based specification of the datum-based model for geometric dimensioning & tolerancing. In: *Procedia CIRP*. Elsevier B.V., pp 189–196. <https://doi.org/10.1016/j.procir.2022.10.026>
13. Kumar SR, Krishnaa SD, Gowthamaan KK, Mouli DC, Chakravarthi KC, Balasubramanian T (2020) Development of a Re-engineered fixture to reduce operation time in a machining process. *Mater Today: Proc*. Elsevier Ltd., pp 3179–3183. <https://doi.org/10.1016/j.matpr.2020.09.056>

Tensile Properties and Characterization of Tamarind Powder Reinforced Epoxy-Jute Fiber Hybrid Polymer Composites



Dewan Muhammad Nuruzzaman, Noor Mazni Ismail,
A. K. M. Parvez Iqbal, Nayem Hossain, A. K. M. Asif Iqbal,
and Md. Jobaed Hossen

Abstract The aim of this research was to investigate the influence of tamarind seed powder on the tensile properties of epoxy-jute fiber hybrid polymer composite. Interfacial adhesion and elemental distribution of the prepared composite specimen were also studied. In order to do so, epoxy-jute fiber polymer composite reinforced by tamarind seed particle was prepared using hand layup method. Five different compositions of composites were prepared by varying tamarind seed particles as 0, 5, 10, 15 and 20% respectively. In this research, total 6 layers of jute fiber mat were used to prepare each type of composite specimen. Tensile tests were carried out using a universal testing machine at a cross-head speed of 2 mm/min for all types of composite specimens. The obtained results showed that tensile properties such as yield strength, tensile strength, tensile modulus and elongation at break varied significantly for each type specimen depending on the percentage reinforcement of tamarind powder. From the microstructural characterization viewpoint, it was evident that very good interfacial bonding between epoxy matrix and jute fiber was formed for each type composite specimen. It was also observed that tamarind particles were almost uniformly distributed within the epoxy-jute fiber composite structure which means that preparations of all types composite specimens were well executed. In

D. M. Nuruzzaman · A. K. M. Parvez Iqbal · N. Hossain · Md. Jobaed Hossen
Department of Mechanical Engineering, International University of Business Agriculture and Technology, Uttara Model Town, Dhaka, Bangladesh

N. M. Ismail (✉)

Faculty of Manufacturing and Mechatronic Engineering Technology, Universiti Malaysia Pahang Al-Sultan Abdullah, Pekan, Pahang Darul Makmur, Malaysia
e-mail: drmazni@umpsa.edu.my

A. K. M. Asif Iqbal

Department of Mechanical Materials and Manufacturing Engineering, Faculty of Science and Engineering, University of Nottingham Ningbo China, Yinzhou, Ningbo, China

addition, elemental analysis of the composite specimen showed the weight percentages of different components to identify the presence of different chemical elements in the composite structure.

Keywords Epoxy · Jute fiber · Tamarind powder · Tensile properties · Characterization

1 Introduction

Composite material is one of the greatest inventions in modern technology and uses of this material in different applications have been expanding rapidly. These engineered materials possess superior properties and offer a diverse range of advantages over traditional single component materials. In modern constructions, different types composites such as polymer matrix composites (PMC), metal matrix composites (MMC) or ceramic matrix composites (CMC) can be used depending on different types applications in structural elements [1]. Due to the high demand in modern constructions, research is going on in order to design and develop new generation composite material to meet specific functional requirements. Very recent progresses of the development, characterization and applications of different types composite materials have been reported [2–4]. The fiber material (reinforcement) can be obtained from natural resources (animal, plant or mineral) such as sisal, jute, hemp, flax, bamboo, kenaf, wool, silk, coir, wood etc. or synthetic (man-made) fiber such as graphite, glass, Kevlar (aramid), carbon, rayon, nylon etc. [5].

At present time, natural fiber based composites are attaining much attraction and huge popularity because of its high potential as an alternative and environment friendly choice as compared to the synthetic fiber based composites. On the other hand, natural fiber composites are on the point of achieving an integral part of society because of their diverse useful applications. According to world natural fiber production report 2019, jute and related fibers are considered as major part other than cotton [6]. For the past few years, jute fibers have gained considerable attention because of their mechanical, physical, chemical and thermal properties [7, 8]. The mechanical properties such as specific strength and specific modulus of jute fiber are comparable to that of glass fiber. Processing, characterization, performance and application of jute fiber composites have been reported in detail [9]. In addition, some important challenges with natural fibers, particularly jute fibers and possible future directions have been discussed. Tamarind seed is a huge amount of waste or byproduct from tamarind pulp industry. Seed contains the endosperm or kernel (70–80%) and testa or coat (20–30%). The entire seed possesses ample amount proteins (13–20%) while the coat contains considerable amount of fiber (20%). Tamarind kernel powder (TKP) is one of the main raw materials for jute, paper, food, pharmaceutical and textile industries. In view of this, in recent years, collection and utilization of tamarind seeds have been focused. Tamarind seed has the huge potential for numerous applications

in food and non-food products. There is also a huge demand of tamarind seed for industrial applications [10].

The effects of tamarind powder (TP) and palm powder (PP) reinforcements on the strengths and hardness of polyester-TP-PP composites were investigated [11]. Experimental results indicated that tensile strength, impact strength and hardness of composites were influenced depending on the percentage reinforcements of TP and PP combinations. Water absorption, flexural strength, tensile strength and hardness of tamarind shell powder reinforced epoxy composites were investigated [12]. The obtained results revealed that hardness, water absorption, tensile strength and flexural strength are influenced by the percentage composition of tamarind powder reinforcement. Flexural, tensile and impact properties of flax-PLA reinforced epoxy nanocomposites were investigated [13]. The obtained results revealed that due to addition of MgO and Al₂O₃ nanofillers, treated flax/PLA/epoxy composites showed improved bending, tensile and impact strengths as compared to untreated composites. Water absorption and mechanical properties of epoxy-sugarcane-tamarind powder hybrid composites were investigated [14]. The obtained results revealed that capability of water absorption and stress resistance were improved due to addition of tamarind powder and sugarcane powder into epoxy matrix.

Although numerous studies on mechanical properties of jute fiber (JF) based polymer composites and considerable investigations on the properties of tamarind seed particles were carried out, there is a lack of comprehensive research that focuses specifically on the composites containing epoxy resin polymer combining with jute fiber and tamarind seed particles. In this research, the effects of tamarind powder (TP) on the tensile properties of five different compositions of epoxy-JF-TP composites were investigated. The microstructural examinations were carried out to investigate the interfacial interaction between epoxy matrix and jute fiber. In addition, elemental analysis of the composite specimen was carried out to examine different elements of the prepared composite structure.

2 Experimental Procedure

2.1 Specimen Preparation

In preparation of epoxy-JF-TP composite, at first, woven jute fiber mat was collected from local market and was cut according to required size 300 mm × 300 mm for each layer. For each composite sample, 6 layers of jute fiber mat were used. In this research, Lapox B-11 epoxy resin and Lapox K-6 epoxy hardener (curing agent) were used. Each composite sample was meticulously prepared with the ratio of 10:1 solution composition, involving 500 ml of epoxy resin and 50 ml of epoxy hardener. With appropriate measurement, epoxy resin and epoxy hardener were carefully combined in a container and followed by thorough mixing to achieve a well-mixed homogeneous blend in order to create a strong and durable composite structure. Tamarind

seeds were collected locally. Using an oven, the seeds were dried at 70 °C for 2 h to reduce the moisture content inside the seed. Then the seeds were roasted at low temperature for 30 min in order to make the seed brittle. After that, roasted seeds were grinded using a grinding machine and then sieved using 400 mesh strainer to remove course particles. After that, powder of tamarind seed particles, i.e. tamarind powder (TP) was measured as 5, 10, 15 and 20% weight percentages of 6 layers jute fiber mat using a high precision electronic analytical balance (accuracy 0.0001 g). The composites with different compositions were prepared using hand-layup method and for this purpose, a square mold was fabricated with dimension 300 mm x 300 mm. During preparation of composites, all necessary steps were followed properly and meticulously. For all composition of composite parts, the curing process was carried out for 72 h in atmospheric conditions and under static loading of 200 N. After completion of preparation of composite plate size 300 mm x 300 mm, the molded part of composite plate was ejected very carefully. Test specimens of 250 mm x 25 mm x 6 mm in size were cut for 5 different compositions of epoxy-JF-TP composites according to ASTM D3039 standard.

2.2 Tensile Test of Composite Specimen

For tensile testing, a universal testing machine (UTM), SHIMADZU, Made in Japan, maximum load capacity of 300 kN was used. Before application of load, each composite specimen was mounted to the UTM grips and all test procedures were followed according to ASTM standard. During the application of load, test speed or crosshead speed of 2 mm/min was applied for all composite specimens depending on different weight percentages of tamarind seed powder. For different types composite specimens, all tests were carried out under identical conditions until fracture occurred. During tests, important test data such as elastic modulus, yield strength, tensile strength and tensile elongation were recorded.

2.3 Characterisation of Composite Specimen

After tensile tests of epoxy-JF-TP composite specimens, fractured parts of different composite specimens were characterized using an ultra high resolution Schottky Field Emission Scanning Electron Microscope (FESEM) (Model: JEOL JSM-7610F) to investigate the morphology of fractured surfaces. The micrographs evidently clarified the fiber-matrix interaction and distinctively explained the fracture behavior of ruptured surfaces of different types composites. In addition, energy dispersive X-ray spectroscopy (EDS) analytical technique was used to identify the chemical compositions or elemental contents of composite structure.

3 Results and Discussion

For different compositions of Epoxy-JF-TP composite specimens, yielding property i.e., tensile stress at yield point or yield strength (permanent set at 0.2%) is presented in Fig. 1. For each type composite specimen, initial yielding started at low stress level where strain occurred without corresponding increase in stress. Due to the application of continuously increasing load, final yielding of the specimen reached at higher stress level where strain occurred at faster rate without any increase in stress. For each composition of composite, plastic deformation took place at this tensile stress level. For Epoxy + JF + 0%TP composite where no tamarind powder added, final yielding or plastic deformation initiated at 12.26 MPa stress level which is shown in Fig. 1. Due to the addition of 5% tamarind powder, plastic deformation of Epoxy + JF + 5%TP composite started at stress level of 16.06 MPa which is 31% higher than the yielding level of Epoxy + JF + 0%TP composite. In case of 10% addition of tamarind powder, Epoxy + JF + 10%TP composite exhibited increased yield strength 20.43 MPa which is nearly 67% greater than yield strength of composite containing no tamarind powder. The obtained results also showed that due to the increased tamarind powder content to 15%, final yielding of Epoxy + JF + 15%TP composite started at little higher stress level 21.09 MPa which is nearly 72% greater than yield strength of composite without containing tamarind powder. Lastly, figure shows that final yielding or plastic deformation of Epoxy + JF + 20%TP composite started at 21.14 MPa which is significantly higher (about 72.4%) than yield strength of composite with no tamarind powder. On the other hand, due to increased tamarind powder from 15 to 20%, plastic deformation of composite started at slightly higher level and yield strength of composite hardly increased. From figure it is apparent that due to addition of more than 10% tamarind powder, yield strength of composite hardly improved.

Figure 2 shows the tensile modulus or elastic modulus of different compositions of Epoxy-JF-TP composites. Tensile modulus of Epoxy-JF-TP composite is the degree of rigidity against the application of tensile load under the crosshead speed of 2 mm/min. The Epoxy-JF-0%TP composite exhibited less resistance to deformation and resulted in a low modulus 1.1 GPa which is shown in Fig. 2. The Epoxy-JF-5%TP composite showed much improved modulus 2.16 GPa which is nearly 96% higher than the composite with no tamarind powder. With the addition of 10% tamarind powder, Epoxy-JF-10%TP composite revealed further improved modulus 2.8 GPa which is about 154% greater than the composite without tamarind powder. From the figure it can be seen that Epoxy-JF-15%TP composite exhibits significantly higher modulus 3.5 GPa which is 218% greater as compared to that of composite without TP. This indicates that composite with 15%TP shows high rigidity against deformation. Lastly, due to addition of 20% tamarind powder, composite exhibits little higher modulus 3.6 GPa as compared to the modulus of composite with 15%TP. The obtained result indicates that composite with 20%TP possesses high stiffness under the application of tensile load. The numerical values of tensile modulus of

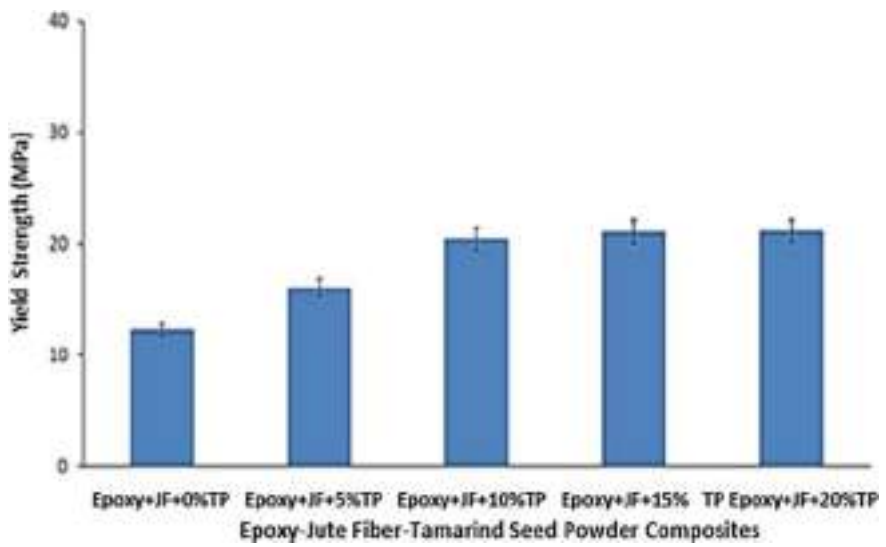


Fig. 1 Yield strength (permanent set at 0.2%) of Epoxy-JF-TP composite specimens

composites are significantly higher as compared to tensile modulus of the composite reported in previous investigation [12].

Ultimate tensile strength (UTS) or tensile strength (TS) is the built-in property of the prepared tamarind powder reinforced Epoxy-JF-TP composites. Tensile strength is maximum stress that can withstand by composite before failure occurred and results

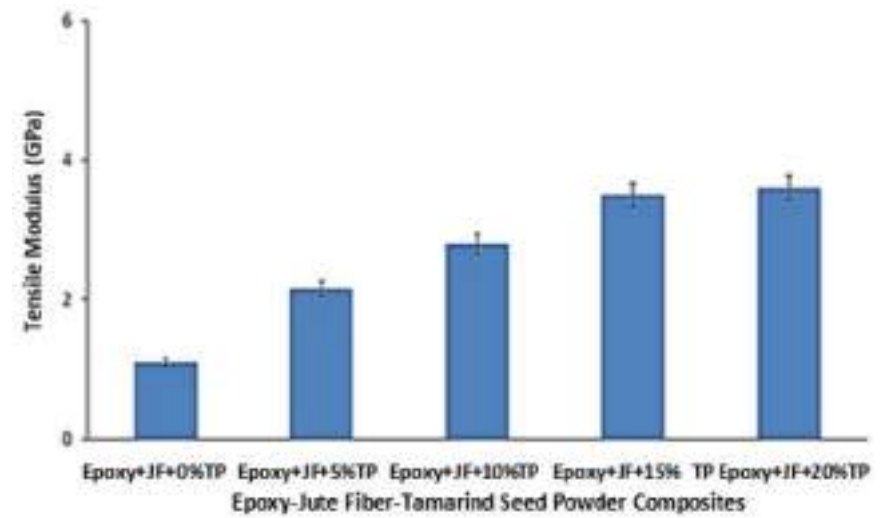


Fig. 2 Tensile modulus of Epoxy-JF-TP composite specimens

for different composites are shown in Fig. 3. Obtained result revealed that composite with no addition of tamarind powder possesses tensile strength 13.1 MPa which is shown in Fig. 3. The Epoxy-JF-5%TP composite showed improved tensile strength 19.63 MPa which is nearly 50% higher than composite with no tamarind powder. With addition of 10% tamarind powder, Epoxy-JF-10%TP composite showed higher tensile strength 22.34 MPa which is about 71% greater than composite without tamarind powder. Figure shows that Epoxy-JF-15%TP composite exhibits further increased strength 25.63 MPa which is almost 96% greater as compared to that of composite without TP. Finally, due to 20% tamarind powder as reinforcement, composite shows much improved strength 28.17 MPa as compared to strength of composite with 15%TP. From figure it is apparent that due to addition of tamarind particles up to 20%, tensile strength of composite shows continuously increasing trend. The values of tensile strength of composites are relatively higher as compared to tensile strength of the composite reported in previous literature [12].

During tensile testing of Epoxy-JF-TP composite, tensile elongation or breaking strain is the total elongation experienced by the composite before failure occurred and the results are shown in Fig. 4. The obtained result showed that without addition of tamarind particles, Epoxy-JF-0%TP composite exhibited less resistance to deformation and resulted in high elongation 7.05 mm before failure occurred and the result is shown in Fig. 4. The Epoxy-JF-5%TP composite showed significantly less elongation 2.11 mm at failure point which is 70% lower than the elongation of composite with no tamarind powder. For 10% tamarind powder addition, Epoxy-JF-10%TP composite revealed further less elongation 1.83 mm until fracture which is about 74% lower than the composite without TP. The obtained result also showed

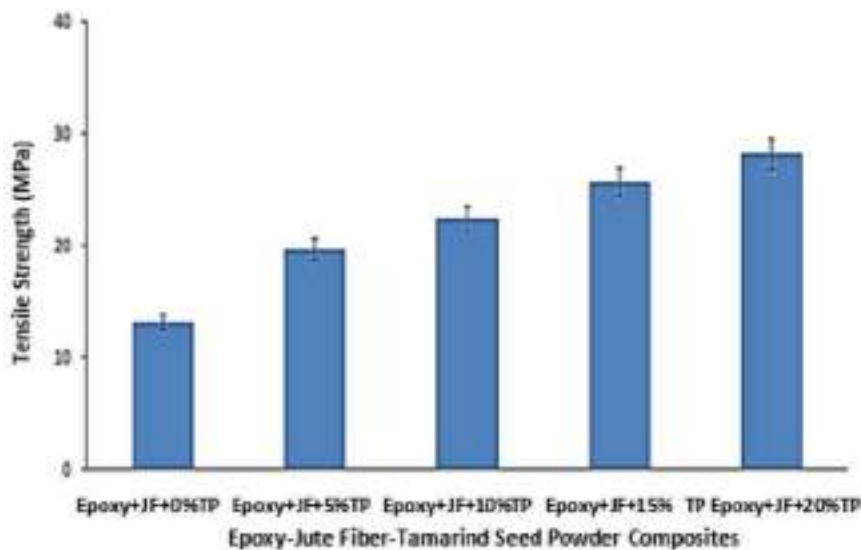


Fig. 3 Tensile strength of Epoxy-JF-TP composite specimens

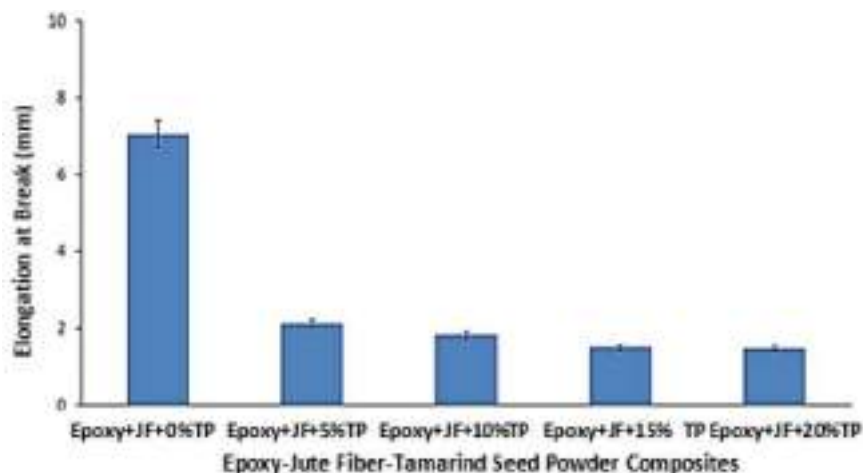


Fig. 4 Elongation at break of Epoxy-JF-TP composite specimens

that Epoxy-JF-15%TP composite revealed high resistance to elongation which is 1.49 mm shown in Figure. Finally, with 20% tamarind powder, composite exhibited somewhat greater resistance to elongation 1.47 mm before failure occurred and this elongation is nearly 80% lower than that of composite without TP. It is noticed that due to addition of more than 10% tamarind powder, strain of composite decreases significantly means that composite contains high rigidity. Characteristics of these results suggest that due to addition of 15–20% tamarind powder, resistance to elongation of composite hardly influenced by tamarind powder which elucidate that composite becomes more stiff and less flexible due to increased reinforcing action of powders or fillers [15, 16].

Figure 5 reveals the micrographs of fractured surface of Epoxy-JF-TP composite specimens using field emission scanning electron microscopy (FESEM). These micrographs distinctly present the ruptured surfaces of different types of composite specimens under tensile loading with crosshead speed of 2 mm/min. As shown in figure, Epoxy-JF-TP composite contains (a) 0% tamarind powder (TP) (b) 5% tamarind powder (TP) (c) 10% tamarind powder (TP) (d) 15% tamarind powder (TP) (e) 20% tamarind powder (TP). From Fig. 5a to e, it is evident that there are protruding fibers of jute and pull-out occurred for each type composite specimen. From the microstructural viewpoint, it is distinct that for each type composite specimen, the nature of fracture is ductile due to long jute fiber pull-out. Moreover, because of strong fiber-matrix interaction, it is apparent that for each type composite structure, jute fiber is completely embedded by the epoxy matrix. The microstructural examination further clarifies that good interfacial bonding occurred means that good preparations were carried out in developing the composite structure.

Energy-dispersive X-ray spectroscopy (EDS) is an analytical technique used to identify the elemental composition or chemical characterization of materials. Field

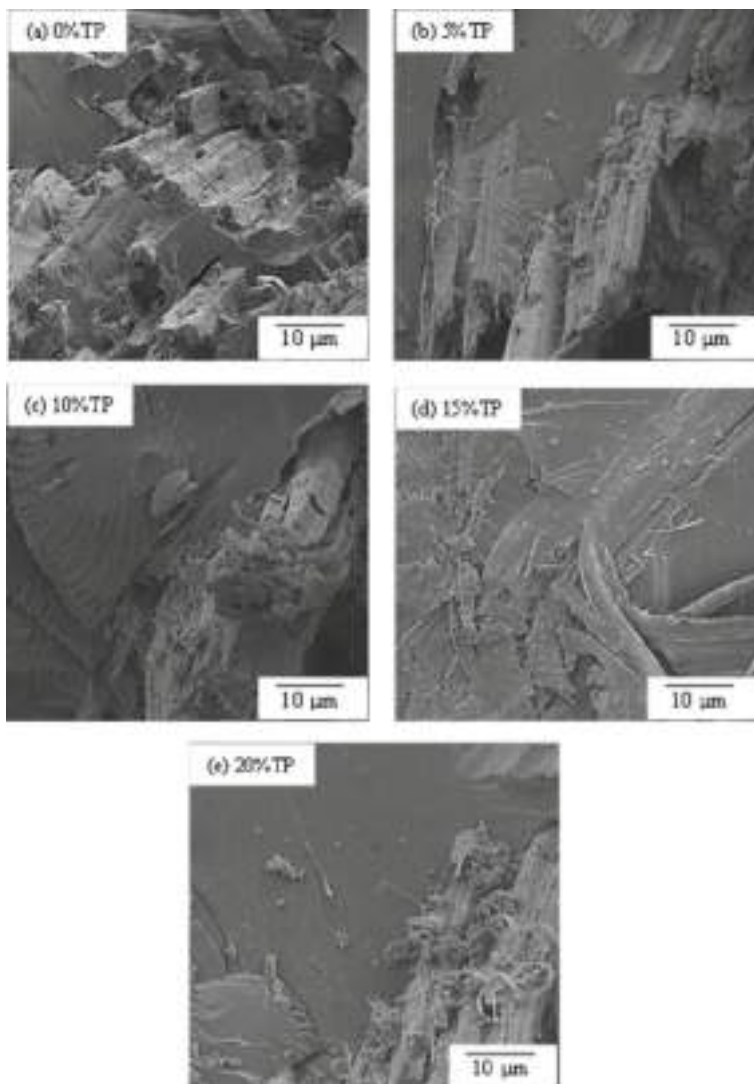


Fig. 5 FESEM Micrograph of fractured surfaces of Epoxy-JF-TP composites under tensile loading **a** 0%TP **b** 5%TP **c** 10%TP **d** 15%TP **e** 20%TP

Emission Scanning Electron Microscope (FESEM) is equipped with EDS system. The data produced by the EDS analysis comprises a spectrum with a peak equal to all elements contained in composite. In addition, EDS system can identify automatically the percentage for each element detected to show quantitative analysis (percentages of individual elemental concentrations). Figure 6 shows EDS test results of composite under acceleration voltage of 15.0 kV. The peak position in the graph leads to identification of each element and peak height serves to quantify the concentration of each

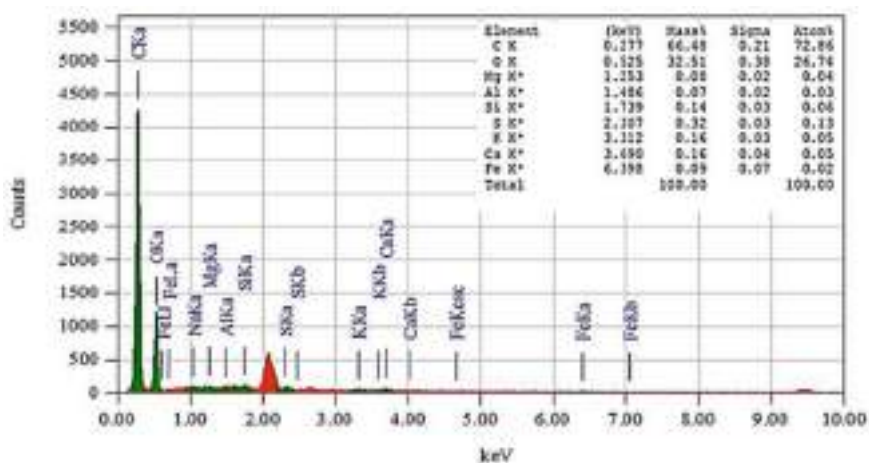


Fig. 6 Elemental distribution of Epoxy-JF-15%TP composite specimen

element in composite sample. These results show chemical elements that are present in the Epoxy-JF-15%TP composite specimen. From the figure we can see the weight percentages of different elements as: Carbon, C (71.39%), Oxygen, O (27.96%), Sodium, Na (0.08%), Magnesium, Mg (0.02%), Aluminum, Al (0.06%), Silicon, Si (0.09%), Sulfur, S (0.16%), Potassium, K (0.03%), Calcium, Ca (0.13%) and Iron, Fe (0.06%) which confirms all elements that present in the composite structure.

4 Conclusions

Influence of tamarind powder reinforcement on the tensile properties of Epoxy-JF-TP polymer composite was investigated. Results showed that strength at yield point, tensile modulus, tensile strength, and elongation at break were significantly influenced depending on the percentage reinforcement of tamarind powder. From the microstructural observation, it was noticed that jute fiber was completely embedded by the matrix and strong matrix-fiber interaction was occurred for each type composite specimen. Microstructural observation also clarified that ductile failure mechanism occurred with jute fiber protruding from the surface for different composites. In addition, elemental distribution of test results showed the presence of different chemical elements in the composite structure.

Acknowledgements The authors acknowledge the financial support of research project from Miyan Research Institute, International University of Business Agriculture and Technology (IUBAT). The authors also acknowledge the assistance by technical staffs of Department of Mechanical Engineering, IUBAT in preparing the composite specimens.

References

1. Pastuszak PD, Muc A (2013) Application of composite materials in modern constructions. *Key Eng Mater* 542:119–129
2. Yang G, Park M, Park SJ (2019) Recent progresses of fabrication and characterization of fibers-reinforced composites: a review. *Compos Commun* 14:34–42
3. Sajan S, Selvaraj DP (2021) A review on polymer matrix composite materials and their applications. *Mater Today: Proc* 47:5493–5498
4. Fan Q, Duan H, Xing X (2024) A review of composite materials for enhancing support, flexibility and strength in exercise. *Alex Eng J* 94:90–103
5. Singh SP, Duttb A, Hirwani CK (2022) Mechanical, modal and harmonic behavior analysis of jute and hemp fiber reinforced polymer composite. *J. Nat. Fibers* 20:1–15
6. Chandekar H, Chaudhari V, Waigaonkar S (2020) A review of jute fiber reinforced polymer composites. *Mater Today: Proc* 26:2079–2082
7. Shahinur S, Hasan M, Ahsan Q, Saha DK, Islam MS (2015) Characterization on the properties of jute fiber at different portions. *Int J Polym Sci* 2015:1–6
8. Biswas S, Ahsan Q, Cenna A, Hasan M, Hassan A (2013) Physical and mechanical properties of jute, bamboo and coir natural fiber. *Fibers Polym* 14:1762–1767
9. Shahinur S, Sayeed MMA, Hasan M, Sayem ASM, Haider J, Ura S (2022) Current development and future perspective on natural jute fibers and their biocomposites. *Polym* 14:1–32
10. Surati BI, Minocheherhomji FP (2018) Benefits of tamarind kernel powder - a natural polymer. *Int J Adv Res* 6:54–57
11. Jeyaprakash P, Moshi AAM, Rathinavel S, Babu AG (2021) Mechanical property analysis on powderized tamarind seed-palm natural fiber hybrid composites. *Mater Today: Proc* 43:1919–1923
12. Baig W, Mushtaq M (2021) Investigation of mechanical properties and water absorption behaviour on tamarind shell fiber- reinforced epoxy composite laminates. *Mater. Today: Proc.* 45:440–446
13. Amjad A, Abidin MSZ, Alshahrani H, Rahman AAA (2021) Effect of fibre surface treatment and nanofiller addition on the mechanical properties of flax/PLA fibre reinforced epoxy hybrid nanocomposite. *Polymers* 13:1–16
14. Jayaraman R, Viknesh M, Girimurugan R (2023) Experimental investigations on mechanical and water absorption properties of epoxy resin matrix treated sugarcane and tamarind shell powder reinforced bio-composites. *Mater Today: Proc* 74:636–641
15. Nuruzzaman DM, Kusaseh NM, Ismail NM, Iqbal AKMA, Rahman MM, Azhari A, Hamedon Z, Yi CS (2019) Influence of glass fiber content on tensile properties of polyamide polypropylene based polymer blend composites. *Mater Today: Proc* 29:133–137
16. Rahman MM, Sultana S, Islam Z, Sarker MKU, Halim ME, Shaikh MAA (2024) Assessment of green biocomposites based on polyvinyl alcohol and grafted biopolymer tamarind kernel powder with polyacrylic acid. *Res Mater* 23:1–9

Microstructure and Hardness Distribution of Seven-Layered Al-Al₂O₃ Graded Composite Material Prepared Through Pressureless Sintering



Maziyana Marzuki, Noor Mazni Ismail,
and Dewan Muhammad Nuruzzaman

Abstract In the present study, different percentages of Aluminium (Al) and Aluminium Oxide (Al₂O₃) were integrated layer by layer for preparation of seven-layered graded composite material. Due to large difference in properties, crack or defect is the main problem for metal-ceramic combination. The prepared graded structure was investigated layer by layer for any defect or crack that might appear in the layer or at the interface. By using a steel die set combination, different layers of different percentages of metal-ceramic were integrated in preparation of the graded composite. After that a pressureless two-step sintering method was used. During the sintering process, a maximum temperature of 630 °C was applied for 3 h sintering duration. Each layer of graded specimen and interfaces of different layers were characterized using Field Emission Scanning Electron Microscopy (FESEM). Vickers microhardness testing was carried out for different layers of composite. The obtained results showed that there is a good distribution of ceramic (Al₂O₃) particles into metallic (Al) matrix when ceramic content up to the 20% (fifth layer). On the other hand, it was also observed that when ceramic content more than 20%, agglomeration occurred for the sixth and seventh layer. Microstructural observations showed that layers boundary and all interfaces are almost parallel. Moreover, it was obvious that no crack was found in the layer or at the interface which confirmed the good preparation process of graded structure.

Keywords Microstructure · Hardness · Seven-layered · Aluminium · Aluminium oxide · Sintering

M. Marzuki · N. M. Ismail (✉)

Faculty of Manufacturing and Mechatronic Engineering Technology, Universiti Malaysia Pahang Al-Sultan Abdullah, Pekan, Pahang Darul Makmur, Malaysia

e-mail: drmazni@umpsa.edu.my

D. M. Nuruzzaman

Department of Mechanical Engineering, International University of Business Agriculture and Technology, Dhaka, Bangladesh

1 Introduction

The new generation graded composite materials are gaining popularity for solving practical problems in various industrial sectors for a range of applications namely automotive, armor, aerospace, biomedical and optoelectronics components. In preparation of graded composite materials, metal and ceramic are incorporated together with varied proportions and applying different methods namely laser sintering, powder metallurgy, centrifugal casting, chemical vapor deposition, physical vapor deposition and thermal spraying. These new graded composite materials are suitable for multiple functions and able to solve practical problems with high performance [1–5]. Functionally graded composite structures are two types, continuous structure and stepwise structure. In continuous structure, microstructure and composition vary in a continuous way with the distance. On the other hand, in stepwise structure, microstructure and composition vary in stepwise way with clear identification of the interface between layers. For the stepwise structure, powder metallurgy is the most suitable method for achieving gradient structure with desired properties while centrifugal force is the suitable method to achieve the continuous structure with required properties [6]. In powder metallurgy method, compaction of powders and sintering, the two most important steps. Because of residual stress and thermal expansion, crack or camber is prevalent in the sintered specimen. To avoid the crack or camber, the parameters need to be controlled during sintering process [7]. The compaction of powder involves the influencing parameters powder density, particle shape and size. Moreover, properties and qualities of powder particles are important factors in controlling compressibility performance of powder. In addition, work hardening of particle is an important factor which influences hardness of green compact. Density of green compact significantly influences porosity and strength of structure [8].

In recent times, aluminium based composites in high demand and these composites showed potential for successful application in industrial sectors for excellent mechanical and tribological properties, good corrosion and oxidation resistance, high stiffness and strength, moderate coefficient of thermal expansion etc. [9]. Aluminium oxide ceramic possesses good strength, high stiffness, good wear resistance, high chemical inertness and high hardness [10]. Multi-layered composites were prepared and obtained results showed that good bonding was formed between two materials of substrate and deposition [11]. Aluminium based composite structure was analysed and obtained results showed that hardness of middle or inner part of composite was lower as compared to that of outer part [12]. The strength of inner part was also lower than that of outer part. Experimental and theoretical investigations of thermo-mechanical deformation of aluminium based composite panels were carried out [13]. Thermo-mechanical response of composite panel was analysed for various loading conditions and the reported results clarified the agreement between theoretical and experimental results. Four-layered Al-Al₂O₃ graded composite material was prepared under pressureless sintering at 620 °C and less porosities were observed in third layer than that of fourth layer [14]. Four-layered Al-Al₂O₃ graded composite

material was investigated and it was noticed that due to increase in ceramic content, hardness steadily increases layer by layer until fourth layer [15].

The objective of research was to prepare seven-layered aluminium-aluminium oxide (Al-Al₂O₃) graded composite specimen through two-step pressureless sintering process considering 0–30% aluminium oxide concentration (with 5% increment). Microstructural investigations were carried out from first layer to seventh layer and at each interface between two adjacent layers. Microvickers hardness of individual layer was also examined in this research study.

2 Experimental Procedure

2.1 Sample Preparation

In preparation for the seven-layered aluminium-aluminium oxide graded composite, Al powders and Al₂O₃ powders were used. According to molecular weight, amount of each powder composition was calculated for individual layer. The powder constituents were sieved and then mixed in order to form each layer. The mixture for each layer was blended for achieving homogeneous mixture. In this research, the percentage compositions of the seven-layered Al-Al₂O₃ graded composite varied as 100:0, 95:5, 90:10, 85:15, 80:20, 75:25 and 70:30 from first layer to seventh layer which is presented in Fig. 1. Mixed powders of varied compositions were stacked very carefully from first layer to seventh layer in cylindrical die of 30 mm diameter. Using a hydraulic press (TOYO: Model TL30, capacity 30 ton), uniaxial pressure was applied very slowly at room temperature and the pressure was increased step by step. After each step of powder compaction process, sufficient time was allowed to settle the powder compact at stable condition and the compaction process was continued until it reached to 30 Ton. After that using the hydraulic press, the seven-layered green compact sample was ejected carefully from the die so that no wear and tear occurred around any surface of specimen.

2.2 Sintering of Green Compact

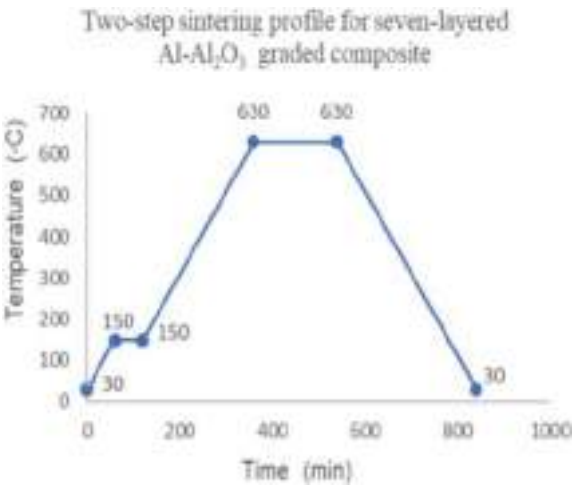
Using a pressureless sintering furnace (Nabertherm; made in Germany), sintering of seven-layered green compact was carried out following two-step sintering cycle [16–18]. The sintering cycle was applied for this research is shown in Fig. 2. In first step of sintering cycle, heating rate 2 °C/min was applied and specimen temperature started to increase from room temperature 30 °C until temperature reached to 150 °C. One hour holding time was maintained at this 150 °C temperature. In sintering cycle for second step, specimen was allowed to heat with identical heating rate up to sintering

Fig. 1 Percentage compositions for each layer of seven-layered Al-Al₂O₃ graded composite



temperature 630 °C. At this temperature 630 °C, sintering time was kept for three hours. Finally, specimen was cooled to room temperature.

Fig. 2 Two-step sintering at sintering temperature 630 °C and 3 h sintering duration



2.3 Characterisation of Specimen

Due to sintering process, the radial shrinkage of specimen was occurred and using a vernier caliper shrinkage was calculated by measuring specimen diameter before and after sintering process [19]. Moreover, weight of the specimen was measured before and after sintering process. In calculating specimen shrinkage and weight, ten measurements were taken and average values were considered. For examining seven-layered Al-Al₂O₃ graded composite structure, at first, specimen was cut along the layers cross section. The cross-sectional surface of the sample was prepared by grinding and polishing operations. In grinding operation, different fine grits of abrasives were used. Polishing operation was continued until fine and smooth surface was obtained for microstructural observations. After that specimen was mounted for cross-sectional surface images of seven-layered composite structure. In order to examine the surface morphology and crack/defect/imperfection (along cross section of composite specimen), field emission scanning electron microscopy (FESEM) was utilized using electron back-scattered mode. All observations were conducted for individual layer and interface between adjacent layers.

2.4 Vickers Microhardness Testing

Vickers microhardness tests were carried out on polished surface of each layer of seven-layered test specimen. Hardness was measured along the cross-sectional surface (longitudinal direction) of specimen and test procedure was followed according to ASTM E-384. In the experimentation, test was performed at every 1 mm interval for individual layer and total 10 test data were recorded for each layer. The average hardness result was considered for every individual layer of seven-layered graded composite structure [20].

3 Results and Discussion

3.1 Effect of Sintering

The radial shrinkage of seven-layered graded composite specimen can be clarified as diameter reduction of green specimen because of sintering process. It was noticed that because of shrinkage during sintering, diameter of green compact decreased. For this seven-layered Al-Al₂O₃ green specimen, the diameter was considered as average diameter which was measured 30 mm and equal to die diameter. After sintering process, specimen diameter decreased to 29 mm resulted in radial shrinkage 1 mm. It is believed that total porosity of specimen was influenced by sintering temperature and sintering time. Moreover, test results showed that specimen lost

weight after sintering. The weight loss occurred due to vaporization of alumina where oxygen diffused out at high temperature. The average weight of seven-layered green specimen was measured 22.67 g and the average weight of sintered specimen was measured 20.40 g, so that weight loss calculated as 2.27 g or 10%. The obtained results suggest that during three hours holding time, decrease in porosities occurred which results in reduction in surface area and contributes to densification of compact and hence weight loss of specimen occurred as reported in previous work [21].

3.2 Microstructural Observation

Microstructural studies were carried out for surface images of seven-layered Al- Al_2O_3 graded composite. Using electron back-scattered mode, FESEM images were captured for each layer and interface between two adjacent layers. Microstructural images of seven-layered composite structure are shown in Fig. 3a–g.

The ceramic element aluminium oxide was recognized as dark area whereas metallic phase aluminium was recognized as light grey area. Moreover, pores were observed as black spots from third layer to seventh layer which are apparently recognized in Fig. 3c–g. Microstructural observations revealed that pores exist clearly in the third layer containing 10% alumina and these pores increased significantly

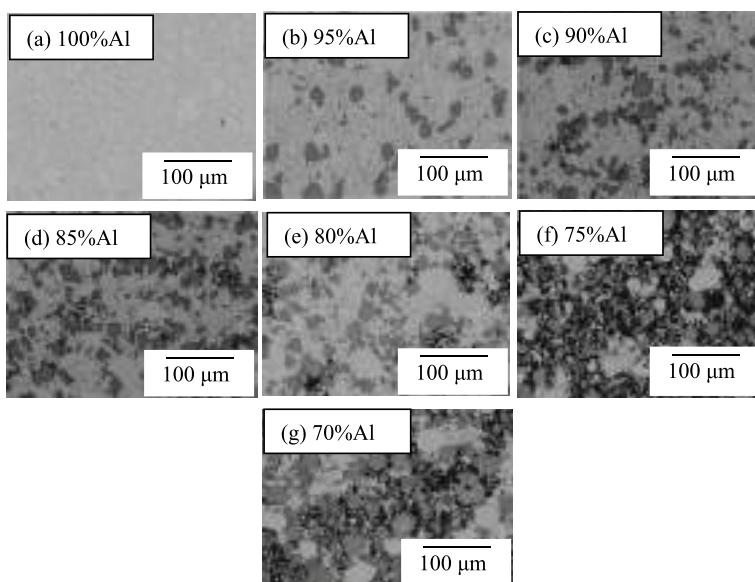


Fig. 3 Microstructures **a** first layer: 100% Al **b** second layer: 95%Al + 5% Al_2O_3 **c** third layer: 90%Al + 10% Al_2O_3 **d** fourth layer: 85%Al + 15% Al_2O_3 **e** fifth layer: 80%Al + 20% Al_2O_3 **f** sixth layer: 75%Al + 25% Al_2O_3 **(g)** seventh layer: 70%Al + 30% Al_2O_3

with the increase in ceramic content up to 30% (seventh layer). The obtained results suggest that with addition of increased ceramic content, air entrapment in the layer increased which in turn contributed to increased porosity significantly in sixth and seventh layers [22]. The microstructure of graded structure also revealed that good distribution of alumina ceramic within aluminium matrix which was observed from second layer to seventh layer. The obtained results showed the existence of ceramic particles which is almost uniformly distributed in second layer (Fig. 3b) and a gradual ceramic increment within matrix proves the stepwise gradation layer by layer up to seventh layer (Fig. 3g) which confirms that preparation of seven-layered composite specimen is well executed.

In Fig. 4, FESEM images of each interface between two adjacent layers of the seven-layered Al-Al₂O₃ graded composite specimen are presented. From these observations, it is understood that first-second, second-third, third-fourth, fourth-fifth, fifth-sixth and sixth-seventh layers are segregated by interface marked by dotted line PP', QQ', RR', SS', TT' and UU' in Fig. 4a-f respectively. In processing of seven-layered graded structure, compaction was carried out in a careful way in order to achieve stepwise gradation and to ensure continuity of structure. On closer viewing of layer by layer, the microstructures revealed that there is no macrocrack or microcrack identified in any layer or at any interface. The findings suggest that there is a good interfacial bonding between metal and ceramic from second layer to seventh layer. The evidence also suggests that gradation of seven-layered composite took place step by step up to the seventh layer. A close inspection of microstructures revealed that each interface was nearly parallel and in line with two adjacent layers which confirmed that powder stacking and compaction processes of seven-layered graded composite were properly implemented. Moreover, there was no sign of split off or delamination of layers at any position from first layer to seventh layer or fracture across any layer confirmed that interfacial bonding was good enough for seven-layered graded composite structure at sintering temperature 630 °C and isothermal holding time of 180 min. Microstructural observations also revealed that porosities in sixth and seventh layers were increased remarkably due to addition of 25 and 30% of ceramic content respectively. The increased porosities in sixth layer and seventh layer might be reduced sufficiently by implementing higher sintering temperature or longer sintering time [23, 24].

3.3 Hardness Distribution

Figure 5 shows the test results of Vickers microhardness along cross-sectional surface of each layer of seven-layered Al-Al₂O₃ graded composite. These results were considered as the average hardness result of ten test data 1 mm apart along the cross-sectional surface for every individual layer. The obtained results show that average hardness at first layer that contains 100%Al is 29.86 HV and average hardness of second layer (5%Al₂O₃) increased to 32.32 HV. Test results reveal that average hardness of third layer increased to 34.18 HV and hardness of fourth layer (15%Al₂O₃)

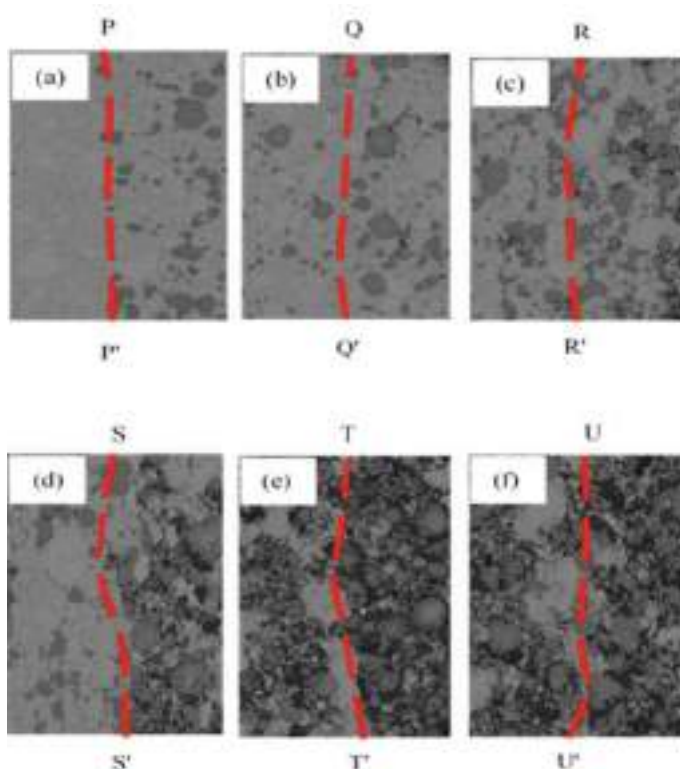
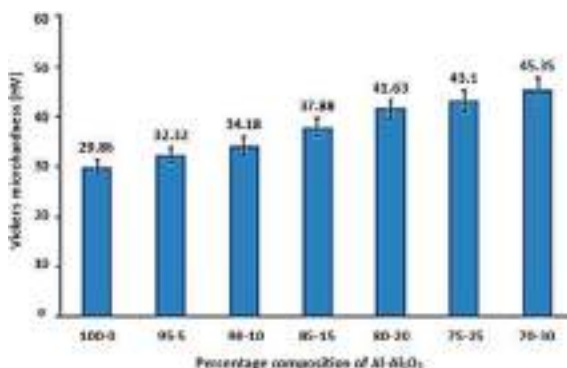


Fig. 4 Seven-layered Al-Al₂O₃ graded composite: Interface between adjacent layers: **a** interface PP' between first–second layers **b** interface QQ' between second–third layers **c** interface RR' between third–fourth layers **d** interface SS' between fourth–fifth layers **e** interface TT' between fifth–sixth layers **f** interface UU' between sixth–seventh layers

further increased to 37.88 HV. The obtained results show that average hardness of fifth, sixth and seventh layer is 41.63 HV, 43.1 HV and 45.35 HV respectively. It is noticed that due to gradual increase in ceramic content (Al₂O₃) for next layer, hardness of graded composite specimen increases layer by layer. It is believed that addition of high hardness ceramic material into soft ductile material contributed to increase in hardness of seven-layered graded composite progressively. It is believed that due to higher sintering temperature and increased number of layers, layer by layer hardness was much improved as compared to previous investigations [14, 15].

Fig. 5 Distribution of hardness in each layer of seven-layered Al-Al₂O₃ graded composite



4 Conclusions

Seven-layered Al-Al₂O₃ graded composite structure was prepared layer by layer using powder metallurgy and two-step pressureless sintering. During sintering process, a maximum temperature of 630 °C was applied for 3 h duration. The microstructure of graded structure showed that there is good distribution of alumina ceramic within aluminium matrix and gradual ceramic increment reveals stepwise gradation layer by layer up to seventh layer. The microstructures also confirmed that there is no macrocrack or microcrack identified in any layer or at any interface. Microstructural observations revealed that each interface was nearly straight and parallel to two adjacent layers which confirmed that all processes during preparation of seven-layered graded composite were properly implemented. There was no sign of delamination of layers at any position from first layer to seventh layer or fracture across any layer proved that interfacial bonding was good enough for composite structure. In addition, tests data showed that hardness of graded composite increases progressively with gradual increase in alumina ceramic up to seventh layer.

Acknowledgements This work was a part of the research work of first author during master program and was supported by fundamental research grant scheme FRGS/1/2018/TK03/UMP/02/14. The authors are grateful for financial support to complete the research work. The authors also acknowledge the assistance by technical staffs of Faculty of Manufacturing and Mechatronic Engineering Technology.

References

1. Watanabe Y, Hattori Y, Sato H (2015) Distribution of microstructure and cooling rate in Al-Al₂Cu functionally graded materials fabricated by a centrifugal method. *J Mater Process Technol* 221:197–204
2. Naebe M, Shirvanimoghaddam K (2016) Functionally graded materials: a review of fabrication and properties. *Appl Mater Today* 5:223–245

3. Jamaludin SNS, Basri S, Hussain A, Alothmany DS, Mustapha F, Nuruzzaman DM (2014) Three-dimensional finite element modeling of thermomechanical problems in functionally graded hydroxyapatite/titanium plate. *Math Probl Eng* 2014:1–20
4. Wu K, Scheler S, Park HS, Porada MW (2013) Pressureless sintering of $\text{ZrO}_2\text{-ZrSiO}_4/\text{NiCr}$ functionally graded materials with a shrinkage matching process. *J Eur Ceram Soc* 33:1111–1121
5. Radhi NS (2018) A review for functionally gradient materials processes and useful application. *J Univ Babylon Eng Sci* 26:42–46
6. Udupa G, Rao SS, Gangadharan KV (2014) Functionally graded composite materials: an overview. *Proc Mater Sci* 5:1291–1299
7. Sun L, Sneller A, Kwon P (2008) Fabrication of alumina/zirconia functionally graded material: from optimization of processing parameters to phenomenological constitutive models. *Mater Sci Eng A* 488:31–38
8. Al-Qureshi HA, Soares MRF, Hotza D, Alves MC, Klein AN (2008) Analyses of the fundamental parameters of cold die compaction of powder metallurgy. *J Mater Process Technol* 199:417–424
9. Erdemir F, Canakci A, Varol T (2015) Microstructural characterization and mechanical properties of functionally graded $\text{Al}_{2024}/\text{SiC}$ composites prepared by powder metallurgy techniques. *Trans Nonferrous Met Soc China* 25:3569–3577
10. Zhang J, Yang S, Chen Z, Wyszomirska M, Zhao J, Jiang Z (2019) Microstructure and tribological behaviour of alumina composites reinforced with SiC graphene core-shell nanoparticles. *Tribol Int* 131:94–101
11. Zhang CH, Zhang H, Wu CL, Zhang S, Sun ZL, Dong SY (2017) Multi-layer functional graded stainless steel fabricated by laser melting deposition. *Vacuum* 141:181–187
12. Radhika N, Raghu R (2016) Development of functionally graded aluminium composites using centrifugal casting and influence of reinforcements on mechanical and wear properties. *Trans Nonferrous Met Soc China* 26:905–916
13. Lin Q, Chen F, Yin H (2017) Experimental and theoretical investigation of the thermo-mechanical deformation of a functionally graded panel. *Eng Struct* 138:17–26
14. Kamaruzaman FF, Nuruzzaman DM, Chowdhury MA, Jamaludin SNS, Basri S, Ismail NM (2019) Characterisation of four-layered $\text{Al-Al}_2\text{O}_3$ functionally graded material prepared through powder metallurgy and pressureless sintering. *Int J Mater Prod Technol* 59:48–62
15. Nuruzzaman DM, Iqbal AKMA, Marzuki M, Chowdhury MA, Ismail NM, Latiff MIA, Rahman MM, Gebremariam MA (2020) Investigation on microstructure and hardness of aluminium-aluminium oxide functionally graded material. *Lecture notes in mechanical engineering*, pp 478–83
16. Nuruzzaman DM, Kamaruzaman FFB (2016) Processing and mechanical properties of aluminium-silicon carbide metal matrix composites. *IOP Conf Ser Mater Sci Eng* 114:1–7
17. Yusefi A, Parvin N (2017) Fabrication of three layered W-Cu functionally graded composite via spark plasma sintering. *Fusion Eng Des* 114:196–202
18. Latiff MIA, Nuruzzaman DM, Basri S, Ismail NM, Jamaludin SNS, Kamaruzaman FF (2018) Preparation and characterization of 6-layered functionally graded nickel-alumina ($\text{Ni-Al}_2\text{O}_3$) composites. *IOP Conf Ser Mater Sci Eng* 342:1–8
19. Shahrjerdi A, Mustapha F, Bayat M, Sapuan SM, Majid DLA (2011) Fabrication of functionally graded hydroxyapatite-titanium by applying optimal sintering procedure and powder metallurgy. *Int J Phys Sci* 6:2258–2267
20. Carvalho O, Buciumeanu M, Madeira S, Soares D, Silva FS, Miranda G (2015) Optimization of AlSi-CNTs functionally graded material composites for engine piston rings. *Mater Des* 80:163–173
21. Xu Z, Hodgson MA, Chang K, Chen G, Yuan X, Cao P (2017) Effect of sintering time on the densification, microstructure, weight loss and tensile properties of a powder metallurgical Fe-Mn-Si alloy. *Metals* 7:1–17
22. Bhattacharyya M, Kumar AN, Kapuria S (2008) Synthesis and characterization of Al/SiC and $\text{Ni/Al}_2\text{O}_3$ functionally graded materials. *Mater Sci Eng A* 487:524–535

23. Almomani MA, Shatnawi AM, Alrashdan MK (2015) Effect of sintering time on the density, porosity content and microstructure of copper - 1 wt. % silicon carbide composites. *Adv Mater Res* 1064:32–37
24. Yuan X, Qu X, Yin H, Feng Z, Tang M, Yan Z, Tan Z (2021) Effects of sintering temperature on densification, microstructure and mechanical properties of Al-Based alloy by high-velocity compaction. *Metals* 11:1–11